# INTERACTIONS MATERIALS – MICROORGANISMS

## Concretes and Metals more Resistant to Biodeterioration

Christine Lors, Françoise Feugeas, Bernard Tribollet

edp sciences

biology | materials

# INTERACTIONS MATERIALS - MICROORGANISMS

## Concretes and Metals more Resistant to Biodeterioration

# INTERACTIONS MATERIALS - MICROORGANISMS

## Concretes and Metals more Resistant to Biodeterioration

**Christine Lors, Françoise Feugeas, Bernard Tribollet**

edp sciences

This handbook is published with the help of the CNRS.

Printed in France.



ISBN (print): 978-2-7598-2200-3 – ISBN (ebook): 978-2-7598-2317-8

# Table of contents

# Theme 4. Biodeterioration of non-metallic materials

# Theme 5. Design and modification of materials

# Preface

Materials interact with their environment and this interaction is responsible for their aging and deterioration. These phenomena of deterioration limit the lifetime of the materials and it is not easy to predict their occurrence, which also makes it difficult to predict the operational lifetime of the structures or their components. While the scientific and technical aspects of these phenomena are important, economic and societal considerations are also important: high costs, damage to the reliability and safety of facilities and people and health risks. Among the various modes of deterioration of materials, that in which the presence of microorganisms present in the environment is liable to induce accelerated deterioration is called biodeterioration. Microorganisms are then in contact with the surface of the material and cause it to deteriorate. The processes involved are complex and require a multidisciplinary approach: chemistry and electrochemistry, surface physico-chemistry, materials science, microbiology.

This book presents a considerable and coherent set of recent data on biodeterioration phenomena, covering different classes of materials, in particular metallic and cementitious materials. Consisting of eighteen chapters and structured into five main themes, it covers the essential aspects of biodeterioration, from understanding the mechanisms of surface reactions to proposing innovative solutions to improve the resistance of materials to biodeterioration, biofilm formation, biocorrosion of metals, alloys and biodeterioration of cementitious materials and concretes.

The authors of the various chapters are recognized specialists in their fields. The coordinators of this book, Christine LORS, Françoise FEUGEAS and Bernard TRIBOLLET, have done an excellent job, the result of which is the publication of this book, which will certainly be a reference text in the field.

This initiative was made possible thanks to the support given by the CNRS to the organization of the BIODEMAT school held in La Rochelle in October 2014 and to the CEFRACOR Committee on Biodeterioration of Materials, whose mission is to strengthen the links between academic and industrial actors in all areas concerned with biocorrosion and biodeterioration as well as the protection of materials against these alterations.

I hope that this collective project, perfectly carried out from the beginning to the end, will serve as an example and as an incentive for other similar projects.

Paris, November 15, 2018

Dr Philippe MARCUS
Director of Research, CNRS - Chimie ParisTech
President of the French Corrosion Society (CEFRACOR)
Past-President of the European Federation of Corrosion

# List of authors

Name: BLOCK
First name: Jean-Claude
Establishment: Université de Lorraine
Address: LCPME, 405 rue de Vandoeuvre, 54600 Villers-lès-Nancy (France)
E-mail: jean-claude.block@univ-lorraine.fr

Name: BOUSTA
First Name: Faisl
Establishment: Laboratoire de Recherche des Monuments Historiques
Address: 29 rue de Paris, 77420 Champs-sur-Marne (France)
E-mail: faisl.bousta@culture.gouv.fr

Name: BOUSTINGORRY
First name: Pascal
Establishment: CHRYSO
Address: 7 rue de l'Europe, 45300 Sermaises (France)
E-mail: pascal.boustingorry@chryso.com

Name: BRIANDET
First name: Romain
Establishment: Institut Micalis, INRA, AgroParisTech, Université Paris-Saclay
Address: Domaine de Vilvert, 78350 Jouy-en-Josas (France)
E-mail: romain.briandet@jouy.inra.fr

Name: DEBIEMME-CHOUVY
First name: Catherine
Establishment: LISE, UMR 8235 CNRS-SU
Address: Sorbonne Université, 4 place Jussieu, 75005 Paris (France)
E-mail: catherine.debiemme-chouvy@sorbonne-universite.fr

Name: DOGHRI
First name: Ibtissem
Establishment: Université de La Rochelle, LIENSs UMR 7266 CNRS-ULR, LIENSs
Address: bâtiment Marie Curie, avenue Michel Crépeau, 17042 La Rochelle Cedex 01 (France)
E-mail: ibtissem.doghri@univ-lr.fr

Name: DUPONT-GILLAIN
First name: Christine
Establishment: Faculté des Bioingénieurs et Institut de la Matière Condensée et des Nanosciences, Université catholique de Louvain
Address: Place Louis Pasteur 1 (Bte L4.01.10), 1348 Louvain-la-Neuve (Belgique)
E-mail: christine.dupont@uclouvain.be

Name: FERON
First name: Damien
Establishment: Den-Service de la Corrosion et du Comportement des Matériaux dans leur Environnement (SCCME) CEA, Université Paris-Saclay
Address: bâtiment 458, PC n° 50, 91191 Gif-sur-Yvette Cedex (France)
E-mail: damien.feron@cea.fr

Name: FEUGEAS
First name: Françoise
Establishment: INSA de Strasbourg
Address: 24 boulevard de la Victoire, 67084 Strasbourg (France)
E-mail: francoise.feugeas@insa-strasbourg.fr

Name: FORET
First name: Christophe
Establishment: KURITA France
Address: Zone Industrielle du Bec, 33810 Ambes (France)
E-mail: christophe.foret@kurita.eu

Name: FRANCIUS
First name: Grégory
Establishment: CNRS
Address: LCPME UMR 7564, 405 rue de Vandoeuvre 54600 Villers-les-Nancy (France)
E-mail: gregory.francius@univ-lorraine.fr

Name: FRATEUR
First name: Isabelle
Establishment: Université Pierre et Marie Curie, LISE/UMR 8235 CNRS-UMPC
Address: 4, place Jussieu, 75252 Paris Cedex 05 (France)
E-mail: isabelle.frateur@upmc.fr

Name: JORAND
First name: Frédéric
Establishments: Université de Lorraine, LCPME UMR 7564 CNRS-UL / ETH Zürich, IBP, *Soil Chemistry Group*
Addresses: 405 rue de Vandœuvre, F-54600 Villers-lès-Nancy (France) / Universitätstrasse 16, 8092 Zürich (CH)
E-mail: frederic.jorand@univ-lorraine.fr

Name: HERISSON
First name: Jean
Establishment: IMERYS Technology Center - Lyon
Address: 1 rue Le Chatelier - Parc Technologique - 38090 Vaulx-Milieu (France)
E-mail: jean.herisson@imerys.com

Name: JEANNIN
First name: Marc
Establishment: Université de La Rochelle, LaSIE UMR 7356 CNRS-ULR
Address: bâtiment Marie Curie, avenue Michel Crépeau, 17042 La Rochelle Cedex 01 (France)
E-mail: mjeannin@univ-lr.fr

Name: LANGUMIER
First name: Mikaël
Establishment: Université de La Rochelle, LIENSs UMR 7266 CNRS-ULR / LaSIE UMR 7356 CNRS-ULR
Address: bâtiment Marie Curie, avenue Michel Crépeau, 17042 La Rochelle Cedex 01 (France)
E-mail: m.langumier@hotmail.fr

Name: LANNELUC
First name: Isabelle
Establishment: Université de la Rochelle, LIENSs UMR 7266 CNRS-ULR
Address: bâtiment Marie Curie, avenue Michel Crépeau, 17042 La Rochelle Cedex 01 (France)
E-mail: ilannelu@univ-lr.fr

Name: LEVI
First name: Yves
Establishment: Université Paris sud, Université Paris Saclay, UMR 8079, CNRS, AgroParisTech
Address: Faculté de Pharmacie, 5 rue Jean Baptiste Clément, 92290 Chatenay-Malabry (France)
E-mail: yves.levi@u-psud.fr

Name: LORS
First name: Christine
Establishment: IMT Lille Douai, Département Génie Civil & Environnemental
Address: 941, rue Charles Bourseul, 59500 Douai (France)
E-mail: christine.lors@imt-lille-douai.fr

Name: MERCHAT
First name: Michèle
Establishment: CLIMESPACE
Address: 3-5 bis boulevard Diderot, 75012 Paris (France)
E-mail: michele.merchat@climespace.fr

Name: NECIB
First name: Sophia
Establishment: ANDRA, Direction Recherche et Développement, Service Colis – Matériaux
Address: Centre de Meuse/Haute Marne, RD 960 55290 Bure (France)
E-mail: Sophia.NECIB@andra.fr

Name: PINEAU
First name: Samuel
Establishment: ACCOAST
Address: 4 rue Bernard Moitessier, 56880 Ploeren (France)
E-mail: samuel.pineau@accoast.fr

Name: REFAIT
First name: Philippe
Establishment: Université de La Rochelle, LaSIE UMR 7356 CNRS-ULR
Address: bâtiment Marie Curie, avenue Michel Crépeau, 17042 La Rochelle Cedex 01 (France)
E-mail: prefait@univ-lr.fr

Name: ROMAINE
First name: Alexandre
Establishment: Vallourec - Centre de Recherche

Address: 60 route de Leval, BP 20149, 59620 Aulnoye-Aymeries (France)
E-mail: alexandre.romaine@vallourec.com

Name: ROUX
First name: Sébastien
Establishment: Institut Jean Lamour (UMR 7198), Université de Lorraine/ IUT Nancy Brabois, Dpt. Génie Civil Construction Durable
Address: Le Montet, rue du Doyen Urion, 54601 Villers-lès-Nancy (France)
E-mail: sebastien.roux@univ-lorraine.fr

Name: SABLE
First name: Sophie
Establishment: Université de La Rochelle, LIENSs UMR 7266 CNRS-ULR
Address: bâtiment Marie Curie, avenue Michel Crépeau, 17042 La Rochelle Cedex 01 (France)
E-mail: ssable@univ-lr.fr

Name: SABOT
First name: René
Establishment: Université de La Rochelle, LaSIE UMR 7356 CNRS-ULR
Address: bâtiment Marie Curie, avenue Michel Crépeau, 17042 La Rochelle Cedex 01 (France)
E-mail: rsabot@univ-lr.fr

Name: SANCHEZ-VIZUETTE
First name: Pilar
Establishment: INRA UMR1319 Micalis
Address: Domaine de Vilvert, 78352 Jouy-en-Josas (France)
E-mail: pilar.sanchez@inserm.fr

Name: SERRES
First name: Nicolas
Establishment: INSA Strasbourg
Address: 24 boulevard de la Victoire, 67084 Strasbourg (France)
E-mail: nicolas.serres@insa-strasbourg.fr

Name: TRIBOLLET
First name: Bernard
Establishment: Université Pierre et Marie Curie, LISE/UMR 8235 CNRS-UPMC
Address: 4, place Jussieu, 75252 Paris Cedex 05 (France)
E-mail: bernard.tribollet@upmc.fr

# Acknowledgements

The coordinators of this book would like to thank the theme leaders for their contribution to the elaboration of this book:

- Françoise FEUGEAS for the theme 1,
- Frédéric JORAND for the theme 2,
- Bernard TRIBOLLET and René SABOT for the theme 3,
- Christine LORS for the theme 4,
- Nicolas SERRES for the theme 5.

Thanks also to the people who reviewed the chapters, in particular Régine BASSEGUY, Essia BELHAJ, Xavier BELLANGER, Jean-Claude BLOCK, Romain BRIANDET, Etienne DAGUE, Denis DAMIDOT, Christine DUPONT, Françoise FEUGEAS, Frédéric GARABETIAN, Suzanne JOIRET, Frédéric JORAND, Bruno LARTIGES, Valérie L'HOSTIS, Christine LORS, Christophe MERLIN, Laurent MOUTEAUX, Sophie SABLE, Nicolas SERRES, Bernard TRIBOLLET.

# Theme 1
# Physico-chemistry of surfaces

The first chapter deals with surface science, which is of paramount importance in many fields of science and technology. Changing adhesion between two materials, making a biocompatible material, developing catalysts, or fighting biocorrosion are all challenges that can only be overcome by relying on surface characterization and modification techniques.

The construction materials, consisting of an aggregation of various mineral phases offering particularly complex surfaces, are presented in chapter 2. The nature of the species obtained by hydration of cements, aluminates or silicates induces a particular behaviour towards the aqueous solutions, depending on their pH or their ionic strength.

Finally, some characteristics of the concrete surfaces explaining their colonization by microorganisms are presented in chapter 3. Parameters influencing the bioadhesion of microorganisms, such as the physico-chemistry of the colonized surface, notably its roughness, but also its chemistry and its more or less hydrophilic nature, are analysed by some experimental techniques to characterize them and to demonstrate their influence on biocolonization. A dynamic contact angle measurement technique is developed as an example.

# 1 Introduction to the physical chemistry of surfaces

**Christine Dupont-Gillain**

## 1.1. Generalities

A surface (or interface) is the area of a biphasic system located at the frontier between the two phases. Surfaces are found between two distinct solid phases (as in alloys), between a solid and a liquid phase, between two immiscible liquids (as in emulsions), or between a solid phase and a gas phase. A transition between the properties of two phases occurs at the interface. Although the surface is often considered as a plane, for reasons related to geometrical description and application of mathematical models, this transition operates over a given thickness, and the surface is actually tridimensional [1].

Surface science is of uttermost importance in many scientific and technological fields. Challenges such as increasing the adhesion between materials, improving the biocompatibility of a material, designing a biosensor, developing a catalyst, or mitigating (bio)corrosion can only be taken up based on surface modification and characterization techniques.

Is there a good reason to consider surfaces apart from other systems and to devote a branch of science to them? Surfaces actually display very peculiar properties, as a result of the discontinuity which characterizes them. In contrast with a molecule (or atom) located in the bulk of a material, a molecule located at the interface may be submitted to very different interactions depending on the direction. Take, for example, the oil-water interface: the interfacial water molecule can only establish hydrogen bonds from the water side. This discontinuity of interactions generates particular phenomena. Surfaces are highly reactive, a feature that is largely exploited in heterogeneous catalysis, for example. They also tend to be modified in contact with the surrounding environment, either through the adsorption of compounds present in one of the two phases, or through the reorganization of one of these phases (surface enrichment or depletion of one constituent or chemical function of this phase).

Surface science is tightly related to colloid science, with colloids being small particles with a size in the range 1-1000 nm. Finely divided materials do indeed develop very large surface areas. Powders made of particles in the nanometer range, or materials with a porosity at this scale, exhibit specific surface areas

of hundreds of square meters per gram. In these materials, the ratio between the developed surface and the volume is very high, and their behaviour is then largely described through concepts of the physical chemistry of interfaces [1, 2]. For example, activated carbon is used in filtration given its large specific surface area which allows the elimination of undesired compounds through their adsorption. This is illustrated in figure 1.1, which shows the discoloration of a food dye solution through its contact with activated charcoal (typically used for purification of water in aquariums). Within a few hours, the dye molecules are adsorbed in the pores of the activated charcoal. The tendency of the surface of the activated carbon to bind dye molecules finds its origin in the high surface energy of the material, which will be reduced after adsorption. The concept of surface energy will be detailed in section 1.2, while adsorption processes will be discussed in section 1.3 of this chapter.

This introductory chapter aims at giving an overview of important concepts in surface science, and at stimulating curiosity regarding this topic. Since the chapter is written for a readership with a diversity of backgrounds, it does not enter into theoretical details, for which the reader is invited to consult more specialized articles or textbooks, as for example those cited in the text.


**FIG. 1.1.** – Solution of a yellow food dye, before (left) and after (right) treatment with activated charcoal particles, which were directly introduced in the solution.

## 1.2. Surface tension and wettability

### *1.2.1. Concepts*

You have certainly observed the following: an insect walking on water, as if there was a kind of superficial skin on top of the latter; that it is possible to fill a water glass above its upper level, ending up with a water dome; you may have seen mercury droplets rolling on a surface, hardly touching it; you may have noted also that the thin water trickle that gets out of a tap breaks down into a series of droplets. These observations are all related to surface tension, or

surface energy, of these liquids. It costs energy to enlarge the surface of a liquid. Therefore, a liquid will spontaneously tend to decrease its surface area, with a view to reducing the total energy of the system [1].

The concept of surface energy, illustrated here above for the case of liquid-air interfaces, may be extended to all kinds of interfaces. The surface tension $\gamma$ is the change in free energy dG related to the increase by one unit of the interfacial area dA:

$$dG = \gamma \, dA \tag{1.1}$$

Since the natural tendency of systems is to reduce their free energy ($dG < 0$), interfacial areas are spontaneously reduced. This explains the spontaneous coalescence of the dispersed phase of an emulsion, or Ostwald ripening, as it is called, observed when solid precipitates are aged.

The surface tensions $\gamma_{LV}$ of a few liquids are given in table 1.1. The notation LV in index underlines the fact that these values are linked to the interface between a liquid (L) phase and a vapour (V) phase. Note that the vapour phase is commonly assimilated to a vacuum. In the case of a liquid - solid (S) interface, surface tension will be noted $\gamma_{LS}$, and so on for other kinds of interfaces. The units of surface tension are given in units of energy per unit of surface area ($J\ m^{-2}$), or in units of force per unit of length ($N\ m^{-1}$). Liquids found in table 1.1 are ranked by order of increasing surface tension. In this way, the link between the value of the surface tension and the nature of intermolecular (or interatomic) interactions does appear. The stronger the interactions within the liquid, the higher the amount of energy needed to create a new unit of surface area, the higher the surface tension. Hence, the low $\gamma_{LV}$ value for hexane is associated to the weak London-van der Waals interactions acting between apolar hexane molecules. The increasing values found for ethanol, 2-aminoethanol and water are reflecting the increasing influence of hydrogen bonds established between these molecules. Finally, mercury atoms are interacting through metallic bonding, which is even stronger. A correlation can actually be established between the boiling temperature of liquids and their surface tension.

**Table 1.1.** – Surface tension $\gamma_{LV}$ of selected liquids [3].

| **liquid** | $\gamma_{LV}$ **(mJ m$^{-2}$)** |
|---|---|
| hexane | 18.4 |
| ethanol | 22.4 |
| 2-aminoethanol | 48.3 |
| water | 72.9 |
| mercury | 486.5 |

Starting from surface tension, it is quite straightforward to assess the work of cohesion and adhesion [1, 4]. Cohesion refers to the attraction between two entities from the same substance, while adhesion is the attraction existing between

different substances, as illustrated in figure 1.2. The work of cohesion $W_{11}$ can be extracted from the balance of lost and created interfaces when trying to separate a material by one unit of surface area:

$$W_{11} = 2\,\gamma_1 = 2\,\gamma_{SV} \tag{1.2}$$

Two units of solid-vacuum surface area are indeed created upon separation. As far as adhesion between solids 1 and 2 is concerned, the same approach allows calculating the work of adhesion $W_{12}$ as follows:

$$W_{12} = \gamma_1 + \gamma_2 - \gamma_{12} \tag{1.3}$$

The separation process indeed leads to the creation of one unit of solid 1 - vacuum surface area and one unit of solid 2 – vacuum surface area, as well as to the loss of one unit of solid 1 - solid 2 interfacial area.

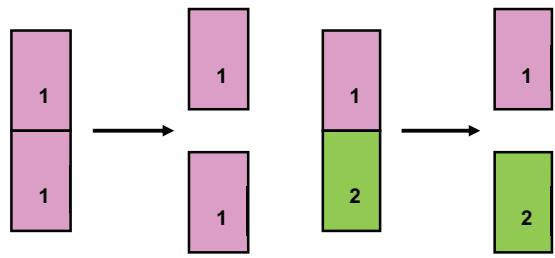


**FIG. 1.2.** – Illustration of the work of cohesion (left) and of adhesion (right). Solids 1 and 2 are placed in an environment that can be assimilated to a vacuum.

When a droplet of liquid is deposited on the surface of a solid material, this droplet takes a shape that depends on the equilibrium between the tendency of the liquid to be cohesive, and its tendency to adhere to the solid. The wettability of a solid can be quantified through the measurement of the contact angle of the liquid on this solid. The contact angle θ is the angle formed between the surface plane and the tangent to the droplet, taken at the contact point between the three phases: solid, liquid and vacuum (or gas), as illustrated in figure 1.3. Hence, mercury has a very high contact angle on most solid substrates, while the contact angle of water is low on polar substrates, which are said to be hydrophilic and higher on more apolar substrates, which are said to be hydrophobic. If water molecules can establish hydrogen bonds with the solid surface, the tendency to adhere on this solid will indeed compensate the high cohesion of water.

The balance between the vectors representing the projections in the horizontal plane of interfacial tensions acting at equilibrium along the contact line between the droplet and the solid (Fig. 1.3) allows Young's equation to be deduced [1, 2]:

$$\gamma_{SV} = \gamma_{SL} + \gamma_{LV}\cos\theta \tag{1.4}$$

This equation links the three interfacial tensions involved. The contact angle θ can be measured directly, based on the analysis of images of the liquid droplet profile. These constitutes fast and low-cost measurements. The information obtained allows solid surfaces to be ranked according to their affinity for a given liquid of interfacial tension $\gamma_{LV}$. This thus constitutes a first-choice experimental approach to evaluate the success of surface modification strategies. It should however be noted that the obtained result depends on both $\gamma_{SL}$ and $\gamma_{SV}$. Methods based on the use of several liquids (*i.e.,* different $\gamma_{LV}$ values) allow $\gamma_{SV}$ to be estimated. Such methods must be used with caution as the hypotheses underlying their use are seldom met (ideal smooth surface not penetrated by the liquid; state of thermodynamic equilibrium; approximations related to the quantification of interactions).

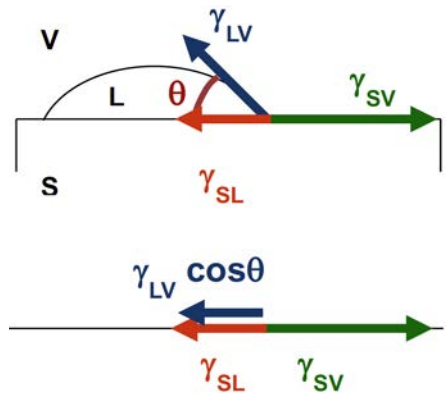


**Fig. 1.3.** – Top: Scheme of a liquid (L) droplet deposited on a solid substrate (S) in an environment assimilated to vacuum (V), illustrating the way the contact angle θ is defined, as well as the action of interfacial tensions. Bottom: Projection of the interfacial tensions on the horizontal plane, allowing Young's equation to be deduced (Eq. (1.4)).

### 1.2.2. Applications

The tendency for systems to reduce their interfacial energy explains the instability of colloidal systems, *i.e.,* small particles tend to aggregate to decrease interfacial areas. It also drives adsorption (Section 1.3), including the surface contamination of solid materials. Materials with a high surface energy have a particularly strong tendency to be contaminated. For a material in contact with air, indeed, the adsorption of rather apolar organic molecules from the atmosphere results in a decrease of the surface energy. Therefore, carbon, for example, is the most abundant element found at the extreme surface of stainless steel, while the metallic elements typical of that material are under-represented at the outermost surface compared to the bulk of the material.

Surface tension and wettability are also key concepts to understand capillary adhesion [4]. This latter is observed when two solid surfaces are contacting each other through a thin film of a liquid that wets these surfaces well (*i.e.,* low value of θ). This is what we experience when we touch sand with wet hands, or less often, when we stick a spoon to our nose (Fig. 1.4a).

Capillary adhesion results from the low pressure created within the liquid film that separates two solid surfaces, as long as the liquid meniscus is concave, which is the case if the surfaces are well wetted by the liquid (Fig. 1.4c). Hence, two glass slides can adhere to each other owing to a thin water film (water contact angle of clean glass is close to zero). Conversely, two polytetrafluoroethylene (PTFE, more commonly named Teflon) plates, with a high water contact angle value of about 110°, do not adhere through a water film. In this case indeed, the liquid meniscus is convex, and the pressure within the liquid film is higher than the atmospheric pressure. This is illustrated in fig. 1.4b and fig. 1.4c. The relationship between the surface tension of the liquid and the pressure across the liquid meniscus is described by Laplace's equation [1], the development of which is however beyond the scope of this introductory chapter.

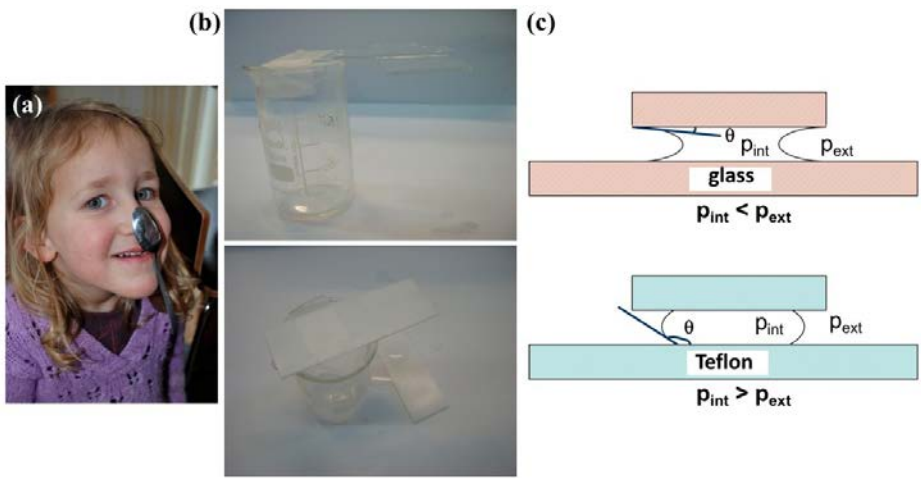


**FIG. 1.4.** – Illustrations (a and b-top) and principle (c-top) of capillary adhesion. (b, c) Top: capillary adhesion between two microscope slides, between which a drop of water was deposited. One slide is immobilized above a beaker; the second one is placed perpendicular below this first slide. (b, c) Bottom: absence of capillary adhesion in the same conditions but using this time two Teflon plates.

Understanding and controlling capillary adhesion opens many perspectives, whether it is to use it or to avoid it. There are building approaches that are based on the use of wet mineral particles, which form robust materials once linked together through the action of capillary forces acting upon drying, as clay plasters,

for example. On the contrary, in industrial processes aiming at producing powders (pigments, drugs, food, *etc.*), capillary forces are generally unwanted, with a view to obtain aggregate-free powders that can easily be dispersed in water. To reach this goal, approaches such as freeze-drying (technically known as lyophilisation) or drying with supercritical $CO_2$ are used. The common aim of these approaches is to prevent capillary adhesion between particles, because this would force the intimate contact between particles and would later hinder their dispersion.

Superhydrophobic surfaces have a water contact angle value higher than 150°. Such surfaces are found in Nature (Lotus, Nasturtium or cabbage leaves) and their properties are actually referred to as "the Lotus effect" [5]. Observing and analysing the surface of these vegetal species has allowed to understand that the very high water contact angle value is resulting from a combination of a particular surface chemical composition (the epicuticular wax is very hydrophobic) and of a similarly particular topography (with the juxtaposition of roughness on the microscale, owing to the presence of vegetal cells, and on the nanoscale, due to wax crystals). Biomimetic approaches, *i.e.*, approaches inspired by Nature, are now used to design superhydrophobic materials [6, 7]. Their main advantage resides in the fact that water droplets have a small contact area with the surface, and are rolling on the material, collecting dust or other fouling particles on their way. Superhydrophobic surfaces are thus self-cleaning, as illustrated in figure 1.5.

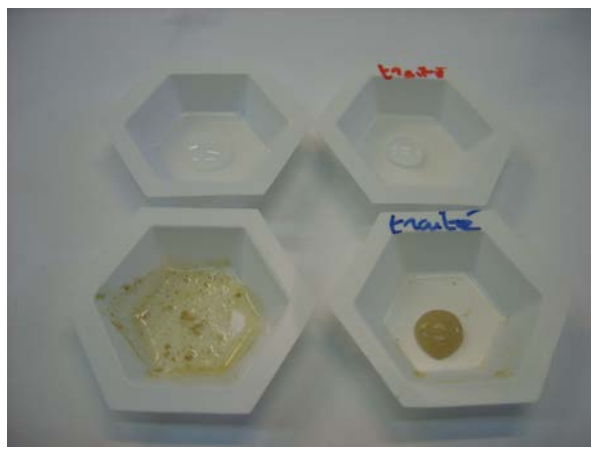

**Fig. 1.5.** – Four polyethylene weighing scoops. Left: weighing scoops as such. Right: weighing scoops treated with a coating that makes them superhydrophobic (Tegotop 105 in spray; commercial product). Top: a water droplet was deposited on the weighing scoop. Bottom: the weighing scoop was fouled with pepper, then a water droplet was deposited and was moved along the surface plane to tentatively collect pepper particles; this was only successful in the case of the superhydrophobic weighing scoop (bottom right image).

## 1.3. Adsorption

In a biphasic system, if one compound present in one of the phases is able to move within this phase (solute in a liquid phase, polymer chain above the glass transition temperature, *etc.*), and if this compound reduces the interfacial tension by establishing favourable interactions with the two phases, then it will accumulate in the surface domain. Adsorption refers to this accumulation of a compound at the interface and must be distinguished from absorption (which designates the penetration of the compound within a phase).

Figure 1.6 presents the concentration profile of a solute that adsorbs at the interface between two immiscible phases α (liquid) and β (liquid, solid or gas). The hatched area represents the amount of solute that can be considered as attached to the interfacial area, in other words, the adsorbed amount or surface excess Γ. This adsorbed amount is evaluated taking into account a position of the interfacial plane that was defined by making sure that the solvent itself does not present any surface excess. Here, the decrease in solvent concentration is linear in the interfacial area, and therefore, the surface plane is localized at the position where the concentration is half the one found in the bulk of phase α [1].

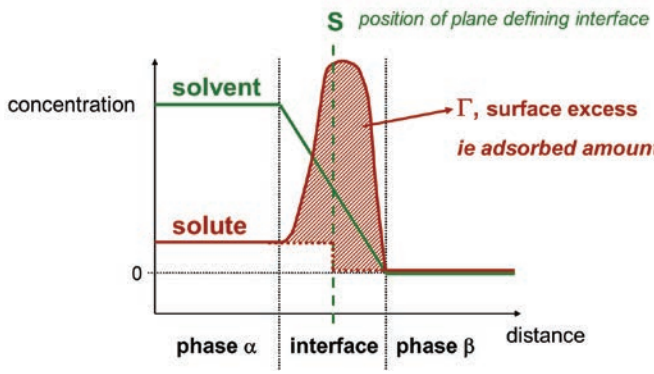


**FIG. 1.6.** – Scheme of concentration profiles of a solvent and a solute both present in a phase α, in contact with a phase β. The interfacial area separating these two phases is depicted. The red hatched area represents the solute surface excess, which is associated to the interface. The broken green line gives the position of the plane defining the frontier between the two phases. By convention, the position of this plane is such that there is no surface excess of the solvent itself.

The preferential occupation of the surface by a compound present in one of the two phases is illustrated in figure 1.7. A drop of detergent (washing-up liquid) was deposited in the middle of a water surface on which pepper had been previously dispersed. The amphiphilic detergent molecules tend to spontaneously accumulate at the interface (*i.e.,* to get adsorbed), pushing the pepper

particles out to the edges of the recipient. This highlights the concept of surface pressure Π, which results from the difference between the surface tension $\gamma_0$ of water (whose molecules are bound through hydrogen bonds) and the surface tension $\gamma$ of a detergent aqueous solution. The latter is lower because of the weaker interactions, of the van der Waals type, that act between the aliphatic chains of the detergent:

$$\Pi = \gamma_0 - \gamma \tag{1.5}$$

This surface pressure provokes the displacement of pepper particles towards the recipient walls. In the same way, a small piece of a floating polymer sheet is propelled on the surface of water if a drop of detergent is placed behind it.

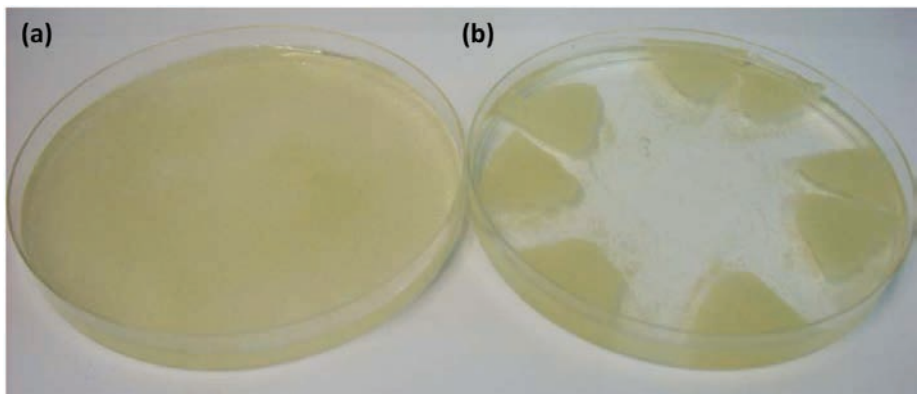


**Fig. 1.7.** – Water surface on which pepper was dispersed, (a) before and (b) after depositing a drop of liquid detergent in the middle of the recipient.

Generally, adsorption finds its origin in weak interactions (van der Waals forces, electrostatic interactions, hydrogen bonds, hydrophobic interactions) acting between the surface and the adsorbate. This process is referred to as physisorption. Adsorption may, however, also result from the formation of covalent bonds between the compound and the surface, which is then called chemisorption. Depending on the case, adsorption may be considered essentially reversible, as for gas molecules on a solid, or may be largely irreversible, as for proteins on a solid. In the first case, desorption, *viz.*, the reverse process, constantly competes with adsorption, in a dynamic equilibrium, while in the second case, desorption is very limited [2].

In the case of reversible adsorption, the process may be described based on the Langmuir model [1]. This model rests on several hypotheses: adsorption is considered fully reversible, and the surface is constituted of a defined number of adsorption sites, which are all equivalent and can each be occupied by an adsorbed moiety. This typically corresponds to the case of chemisorption. Adsorption can then be considered as a chemical equilibrium, leading to the

formation of a particle-site complex (s-p) starting from the free adsorption site (s) and the free particle (p) (ion, molecule):

$$s + p \leftrightarrows s\text{-}p \tag{1.6}$$

An equilibrium constant K can be associated to this chemical equilibrium:

$$K = (s\text{-}p) \,/\, (s)\ (p) \tag{1.7}$$

The fraction $\Theta$ can then be defined by dividing the number of occupied sites ($n_{s\text{-}p}$) to the total number of sites ($n_{total}$), *i.e.,* to the sum of occupied ($n_{s\text{-}p}$) and free ($n_s$) sites:

$$\Theta = n_{s\text{-}p} \,/\, n_{total} = n_{s\text{-}p} \,/\, (n_{s\text{-}p} + n_s) \tag{1.8}$$

Langmuir equation is finally deduced by combining equations 1.7 and 1.8, and by assimilating activities to concentrations:

$$\Theta = C \,/\, ((1/K) + C) \tag{1.9}$$

With C, the equilibrium concentration of the adsorbate in the phase in contact with the surface.

It should be noted that in the case of adsorption onto a solid, with adsorption sites s, from a liquid phase containing the solvent l and the solute p, equation 1.6 is rather written as follows:

$$s\text{-}l + p \leftrightarrows s\text{-}p + l \tag{1.10}$$

Since the activity of the solvent in the liquid phase can be considered constant in a sufficiently diluted regime, the resulting equation will be similar to equation (1.9) [1].

Langmuir equation is represented in figure 1.8 under the form of a graph of the evolution of the fraction $\Theta$ of occupied sites as a function of the concentration C of the adsorbate. At high concentrations ($C \gg 1/K$), $\Theta$ tends asymptotically to 1 (all sites are occupied, or in other words, the maximum adsorbed amount is reached). At low concentrations ($C \ll 1/K$), $\Theta \sim KC$ and the graph can be assimilated to a straight line with a slope equal to K. Moreover, half of the sites are occupied ($\Theta = 0.5$) at a concentration equal to 1/K. Starting from experimental data (adsorption isotherm), the model leads to the determination of the constant K, which gives indication of the tendency to form s-p complexes (Eq. (1.6)), thus describing the affinity of the adsorbate for the interface.

It is tempting to apply the Langmuir model to many situations in which data related to the adsorbed amount were experimentally determined. Quite often, there will be a good, if not excellent, agreement between the mathematical model and the data. As for every modelling approach, hypotheses that were made to develop the model should however be kept in mind. As far as protein adsorption is concerned, the assumption of reversibility is usually not met and applying the Langmuir model is subject to caution. Drawing a plot according

to the Langmuir model is however convenient to compute an apparent affinity, and to highlight a saturation behaviour at high concentration. In the case of the adsorption of ions, the expression can be adapted, taking into account the fact that K varies with the local electrical potential, and thus with the adsorbed amount. There are other models to describe adsorption, whose presentation is however falling outside of the scope of this introduction chapter.

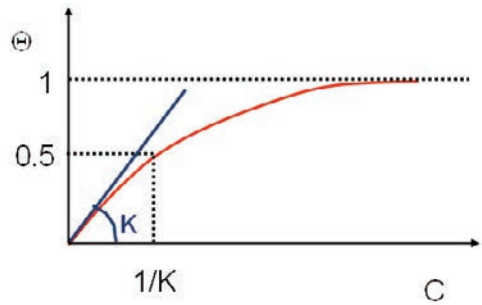


**Fig. 1.8.** – Evolution of the fraction Θ of occupied sites as a function of the equilibrium concentration C of the adsorbate, as described by the Langmuir model. K is the equilibrium constant of the association reaction between the adsorption site and the adsorbed particle.

## 1.4. Charged surfaces

### *1.4.1. Concepts*

Electrostatic interactions play a very important role in many processes and are notably among the weak interactions which are at the origin of physisorption. They find their origin in the presence of electrical charges at interfaces. Almost all surfaces bear electrical charges [1]. This can be attributed to: (i) acid-base reactions at interfaces, with the deprotonation of acidic function that generates negative charges, or to the protonation of basic functions that generates positive charges; (ii) the selective dissolution of an ion constitutive of a salt: there is electro-neutrality within an ionic crystal, but the crystal surface may be enriched in one of its constituting ions if the tendency to be dissolved in the surrounding liquid is not the same for the different constituting ions; (iii) structural defaults of a solid, as is the case for so-called "swelling" clays (smectites), in which substitutions of $Si^{4+}$ by $Al^{3+}$, or of $Al^{3+}$ by $Mg^{2+}$, generate the presence of negative charges at the surface, compensated by mobile alkaline ions between the sheets of these clays; (iv) the preferential adsorption of ions which modify the intrinsic electrical potential of the surface, as illustrated by the accumulation of phosphate ions at the surface of a variety of metals. It should be noted that a surface

can simultaneously bear positive and negative charges. In such case, it is said to be "zwitterionic". This is generally the case for biological surfaces.

With a view to modelling and understanding interactions between two charged surfaces, taking into account the intensity and distance over which electrostatic interactions are at play, the distribution of ions in solution at the proximity of a charged solid surface must be described, as well as the variation of the electrical potential, as a function of the distance to the interface. In a first approach, it can be considered that the surface charges are entirely compensated by opposite sign ions located in the immediate vicinity of the interface. In such case, the potential varies linearly, from a value equal to the intrinsic surface potential $\Psi_0$ at the level of the interface, to a value of zero beyond the plane where the counter-ions are localized. Figure 1.9 illustrates this model, called the Helmholtz model, or the parallel-plate capacitor model [1, 2]. This model can be considered simplistic as it depicts a very ordered and frozen situation, not likely to be compatible with the tendency of systems to be disordered.

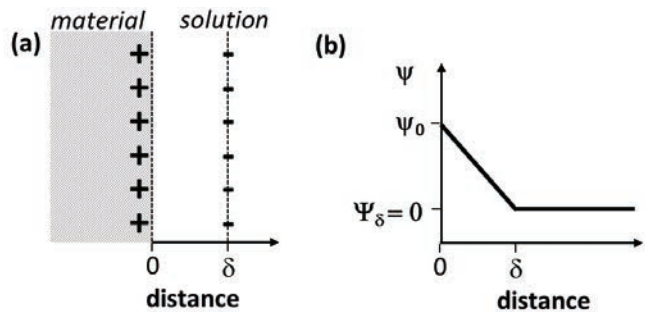


**FIG. 1.9.** – (a) Representation of a charged solid surface in contact with a solution containing ions, according to the Helmholtz model: counter-ions with a sign opposite to the surface charges are aligned at a distance δ along the surface plane to compensate the surface charge. (b) Evolution of the electrical potential Ψ as a function of distance according to the model depicted in (a).

More sophisticated models describing ion distribution close to a charged surface were developed [1, 2]. Gouy-Chapman model, coupled to Debye-Hückel approximation for surfaces with a weak electrical potential, have led to a so-called "diffuse double layer" representation of the interface. Without entering into details, it is considered here that both ions with an opposite and an identical charge compared to the surface can be found at its vicinity, with, however, an overrepresentation of counter-ions, and an underrepresentation of co-ions, compared to the bulk of the solution (Fig. 1.10a and Fig. 1.10b). The evolution of the electrical potential Ψ as a function of distance x is described by the following equation:

$$\Psi = \Psi_d \exp(-x\kappa^{-1}) \qquad (1.11)$$

With $\Psi_d$, the potential at the origin of the diffuse double layer, and $\kappa^{-1}$, the Debye length. This evolution is represented in figure 1.10c. It should be noted that, when $x = \kappa^{-1}$, $\Psi / \Psi_d = \exp(-1) = 0.368$. In other words, the Debye length is the distance from the surface at which only about one third of the initial potential is remaining. The Debye length is inversely proportional to the square root of the ionic strength I of the medium, which is a function of the concentration and the valency of the ions. Hence, the higher the salt concentration, the shorter the distance over which the surface charge is compensated, and the shorter the distance over which electrostatic interactions are effective. Moreover, for a given concentration, a multivalent salt will screen the surface charge over a shorter distance compared to a monovalent salt. Debye lengths typical of aqueous media with different salt concentrations are summarized in table 1.2.

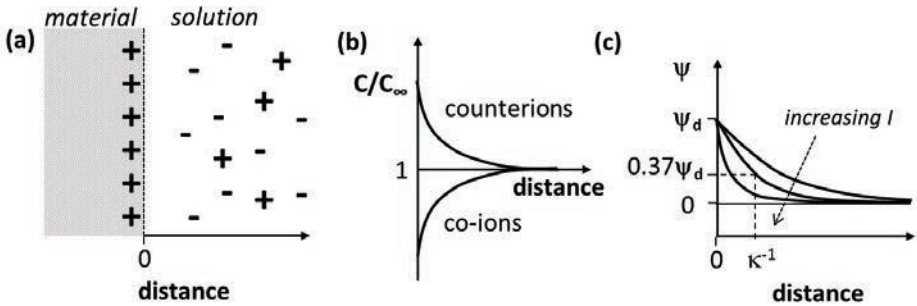


**Fig. 1.10.** – (a) Scheme of a charged solid surface in contact with an ion-containing solution, according to the diffuse double layer model: counter-ions (with a charge opposite to the one of the surface) and co-ions are respectively over- and underrepresented close to the surface in comparison with the solution bulk, as also shown by their concentration C profile in (b), with $C_\infty$ the concentration in the solution bulk. (c) Evolution of the electrical potential $\Psi$ as a function of the distance, according to the model illustrated in (a) and (b), and depicted for increasing ionic strengths I values.

**Table 1.2.** – Debye length in aqueous media with different ionic strengths.

| Ionic strength I (M) | $\kappa^{-1}$ (nm) | Relevant aqueous medium |
|---|---|---|
| 1 | 0.3 | seawater |
| $10^{-1}$ | 1 | culture medium, biological fluid, industrial water |
| $10^{-3}$ | 10 | tap water |
| $10^{-5}$ | 100 | mountain lake |
| $10^{-6}$ | 300 | distilled water |

To both take into account the tendency of systems to be disordered, on the one hand and the peculiar affinity of some ions for surfaces, on the other, charged interfaces will finally be better described based on a global approach which combines Helmholtz model with the double diffuse layer theory. This is illustrated in figure 1.11. A first linear decrease of the potential is provoked by the accumulation of high affinity ions very close to the surface, in the so-called Stern layer. The remaining potential is then screened by ions from the diffuse double layer. In practice, electro-kinetic methods are usually applied to determine the surface electrical potential. The measured potential, called the $\zeta$ potential, corresponds to the potential at the shear plane between the surface and the solution, which is considered to be close to the potential at the origin of the double diffuse layer, *i.e.,* at the level of the Stern layer. A surface with a $\zeta$ potential equal to zero is said to be at its isoelectric point (iep). It should be noted that this does not necessarily corresponds to the point of zero charge (pzc), which is defined by the situation in which $\Psi_0 = 0$ V. Indeed, if ions are adsorbed in the Stern layer, the potential measured at the shear plane may substantially differ from the one intrinsically related to the surface.

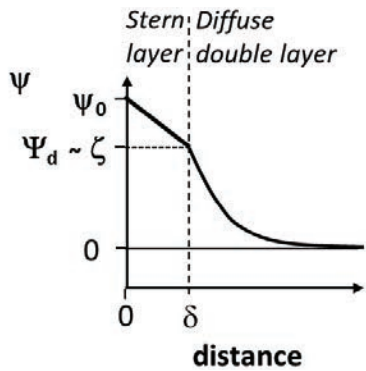


**FIG. 1.11.** – Evolution of the potential with the distance from a solid surface in contact with an ion-containing solution, according to the global model. Ions are found in the Stern layer, then a diffuse double layer screens the remaining charge. The $\Psi_d$ potential at the origin of the diffuse double layer may be assimilated to the $\zeta$ potential which can be determined experimentally based on electro-kinetic methods.

### *1.4.2. Interactions between charged surfaces*

When two charged surfaces get closer to each other, the observed behaviour will depend on the different interactions that may occur, and in particular on electrostatic interactions. For two surfaces of the same kind, thus bearing the same electrical charge, the contribution of electrostatic interaction will be repulsive. Such surfaces will only adhere if other interactions are strong enough

to compensate the effect of electrostatic repulsion. If a suspension of charged particles is considered, this suspension will be stable if electrostatic repulsion outweighs attractive interactions, and in particular if it plays a role at sufficiently long distance to prevent shorter distance forces (such as van der Waals forces) to act. The coagulation of the suspension can be triggered by decreasing the contribution of electrostatic repulsion. On the one hand, a pH change may alter the surface electrical potential. On the other hand, adding salts to the medium may reduce the distance over which electrostatic repulsion is effective. This is illustrated in figure 1.12. A suspension of gold particles was synthesized by reduction of a gold salt in presence of citrate [8]. Such particles are negatively charged. The original suspension at pH 4 is stable and exhibits a red colour, corresponding to particles with a diameter of about 20 nm. There is indeed a direct relationship between the size of gold particles and the suspension colour [9]. The colour is left unchanged when KCl is added to the suspension, which remains stable. In contrast, the addition of $CeCl_3$ provokes an immediate modification of the colour of the suspension, which becomes purple-blue. The estimated diameter of the obtained aggregates is of about 60 nm. Moreover, the suspension is unstable, and a blackish deposit form in a few hours, leaving a totally transparent supernatant. This illustrates the concept of Debye length. In a medium with a low ionic strength, gold particles are repulsive to each other due to the negative charges of the citrate groups. When a trivalent salt is used, the higher ionic strength provokes a contraction of the diffuse double layer (thus a decrease of the Debye length), and electrostatic repulsion between particles becomes restricted to a very short distance. In such case, van der Waals forces can provoke particle aggregation, followed by sedimentation.

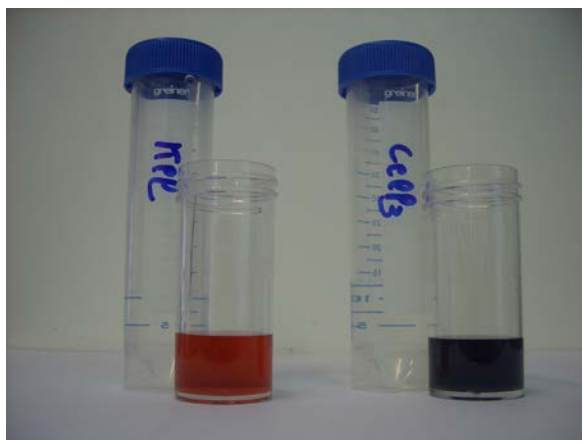


**Fig. 1.12.** – Suspensions of gold colloids bearing citrate groups at their surface, after the addition of a few drops of (left) a KCl solution, (right) a $CeCl_3$ solution. The purple-blue suspension obtained after adding $CeCl_3$ becomes transparent, with a blackish deposit, after a few hours, while the red suspension obtained in presence of KCl is stable. This experiment was performed based on reference [8].

The so-called DLVO theory (named according to its authors: Derjaguin, Landau, Verwey and Overbeek) allows interactions between two surfaces to be predicted, based on both electrostatic and van der Waals interactions [4]. $G_{tot}$, the total free energy of interaction between two particles (or between two flat surfaces, or between a particle and a flat surface) is calculated based on the sum of $G_{electr}$, the free energy attributed to electrostatic interactions, and $G_{vdW}$, attributed to van der Waals interactions:

$$G_{tot} = G_{electr} + G_{vdW} \tag{1.12}$$

For particles or surfaces with the same surface charge, $G_{electr}$ is always positive (*i.e.,* repulsive potential), while $G_{vdW}$ is always negative (*i.e.,* attractive potential). The intensity of these contributions however depends on the distance, and the resulting $G_{tot}$ depends on the evolution of $G_{eletr}$ and $G_{vdW}$ as a function of the distance. This is illustrated in figure 1.13. When the electrostatic repulsion operates at long distance (high value of the Debye length; Fig 1.13a), the repulsive barrier that arises prevents van der Waals forces from acting, and there is no adhesion. In the case of a suspension of particles, this latter will then be stable. If, however, the Debye length is short (Fig. 1.13b), van der Waals forces will be effective and adhesion will be possible. In such case, a suspension of particles will coagulate. Intermediate situations may occur, in which a secondary attractive minimum, however followed at a shorter distance by a repulsive barrier, will maintain particles at a given distance from each other.

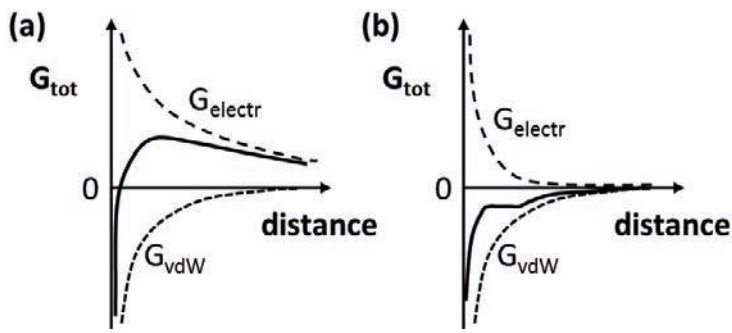


**FIG. 1.13.** – Scheme of DLVO theory applied to two different situations in which electrical repulsion operates (a) at long distance, (b) at short distance.

If DLVO theory appears to be a very good tool to predict and understand adhesion, its limitations should however be recalled. On the one hand, it only applies to ideal surfaces, which are smooth, homogeneous, rigid, and to very short distances between these surfaces. On the other hand, all interactions other than van der Waals and electrostatic ones are neglected by this theory. Hence, repulsion attributed to hydration between hydrophilic surfaces, or attraction between hydrophobic surfaces are not taken into account. Similarly,

all interactions attributed to the presence of macromolecules at interfaces (*i.e.,* steric repulsion, attraction by bridging between macromolecules or between macromolecules and surfaces) are neglected. In the particular case of biofilms, DLVO theory appears to be very simplistic: microorganisms indeed bear many biomacromolecules at their surface and secrete exopolymers that may modify the surface of solid substrates. The reader is thus invited to study the effect of macromolecules, and in particular of charged macromolecules, at interfaces in more depth [4]. Moreover, specific interactions, which are characteristic of biological system, are also possible between microorganisms and adsorbed biomacromolecules [10]. Finally, the effect of a soft layer at the surface of microorganisms, and of the heterogeneity of their surface, was taken into account in more advanced electro-kinetic theories [11].

## 1.5. Characterization and modification of surfaces

At the end of this chapter, the importance of surface characterization tools must be underlined. The surface of a material only represents a very small fraction of that material. Conventional techniques used by material scientists do not generally apply to the study of surfaces. The signal generated from the surface is indeed negligible compared to the one of the bulk of the material. The most common surface analysis techniques include wettability measurements, surface-sensitive spectroscopies (X-ray photoelectron spectroscopy – XPS, ultraviolet photoelectron spectroscopy – UPS, time-of-flight secondary ion mass spectroscopy – ToF-SIMS, surface-sensitive infrared spectroscopies – ATR-FTIR, PM-IRRAS), scanning electron microscopy (SEM) and near-field microscopies (STM, AFM and related techniques). References [12-14] may be used to get familiar with the principle of these techniques and their application to systems at the interface between materials and biological systems. It should be noted that the spatial resolution and the probed depth vary strongly from one technique to another. This must be taken into account when it comes to data interpretation.

The surface properties of solid materials and of microorganisms play a central role in biofilm formation, biocorrosion and biodeterioration. Consequently, mitigation strategies may be based of the modification of the physical and/or chemical surface properties of solid substrates. Two types of approaches can be distinguished for such modifications: (1) the deposition of a coating on the material (for example, the deposition of a thin polymer layer at the surface of a metal alloy); (2) the surface alteration of the existing material (for example, the electro-polishing of a metal alloy). In both cases, the objective is to keep the bulk properties of the material intact (including its mechanical properties), while modifying the interactions of the material with its environment, through alteration of the interfacial area. References [15, 16] give an overview of the main strategies used for surface modification.

## Acknowledgements

I address my warmest acknowledgements to Paul Rouxhet, not only for his critical reading of the manuscript, but as well for transmitting his passion for interfaces and much more. I also thank the organizing committee of the BIODEMAT school, and in particular Isabelle FRATEUR, for the energy successfully spent on this occasion, for the benefit of the scientific community and especially for young research scientists.

## References

[1] Hiemenz P.C., Rajagopalan R. (1997) "Principles of Colloid and Surface Chemistry." Marcel Dekker, New York, USA, 650 p.
[2] Norde W. (2003) "Colloids and Interfaces in Life Sciences." Marcel Dekker, New York, USA, 433 p.
[3] Jasper J.J. (1972) "The surface tension of pure liquid compounds." J. Phys. Chem. Ref. Data, 1, 841-1010.
[4] Israelachvili J.N. (2011) "Intermolecular and Surface Forces." Academic Press, Oxford, UK, 674 p.
[5] Barthlott W., Neinhuis C. (1997) "Purity of the sacred Lotus, or escape from contamination in biological surfaces." Planta, 202, 1-8.
[6] Erbil H.Y. *et al.* (2003) "Transformation of a simple plastic into a superhydrophobic surface." Science, 299, 1377-1380.
[7] Puukilainen E. *et al.* (2007) "Superhydrophobic polyolefin surfaces: controlled micro- and nanostructures." Langmuir, 23, 7263-7268.
[8] Bucak S., Rende D. (2014) "Colloid and Surface Chemistry: a laboratory guide for exploration of the nano world." CRC Press, Boca Raton, USA, 161-166.
[9] Haiss W. *et al.* (2007) "Determination of size and concentration of gold nanoparticles from UV-Vis spectra." Anal. Chem., 79, 4215-4221.
[10] Klemm P., Schembri M.A. (2000) "Bacterial adhesins: function and structure." Int. J. Med. Microbiol., 290, 27-35.
[11] Gaboriaud F., Duval J.F.L. (2010) "Progress in electrohydrodynamics of soft microbial particle interphases." Curr. Opinion Coll. Interface Sci., 15, 184-195.
[12] Vickerman J.C., Gilmore I. (2009) "Surface Analysis: the principal techniques." Wiley, Chichester, UK, 686 p.
[13] Rivière J.C., Myhra S. (2009) "Handbook of Surface and Interface Analysis: methods for problem-solving." CRC Press, Boca Raton, USA, 671 p.

# 2 Construction materials: general description and physical chemistry

**Pascal Boustingorry, Jean Herisson**

## 2.1. General description – cements, mortars and concretes

When reading about construction materials a lot of language misuse may be found in the literature. The authors found it relevant to start this chapter by defining the terms and abbreviations that will be used later in the text.

The word "cement" refers to a powder able to set and harden after mixing with water, even submerged. As mentioned later, the true original name of common grey cement is "Portland cement", though this phrase is seldom used in the common language. Other cements, with different chemical compositions and hardening mechanisms, exist so that "cement" may well be considered as a plural or generic term.

The mixture of a cement, sand and water is called "mortar": the main applications of such materials are façade finishing, sealing, joints, upper layer self-levelling screeds (often with floor heating equipment), *etc.*

For larger volumes, a mixture of cement, water, sand and gravel (stones of up to 20-22 mm diameter) is used, which bears the name of "concrete". The aim here is to occupy as much space as possible with materials cheaper than cement, while ensuring a final strength compatible with the application. The apparent simplicity of this is deceptive, as shown by the abundance of papers or whole books devoted to concrete "mix-design" [1-6], which relies upon principles of particle packing optimization [7-10].

Cements themselves are mineral materials the major elements of which are calcium (Ca), aluminium (Al), oxygen (O), sulphur (S), silicon (Si) and iron (Fe). This elemental composition may be assessed easily for instance by X-Ray fluorescence (XRF), and expressed in oxide equivalents. Cement manufacturers have developed a system of shorthand notation, by attributing a single letter to each oxide, allowing an abridged description of some very complex phases. The correspondence between the shorthand notation and the equivalent oxide phases is given in table 2.1 as a reference. The reader is reminded that the notation is sometimes synonymous of a symbol of an element of the

periodic table, and that they should not be mistaken. The shorthand notation will be used through the remainder of the text.

**TABLE 2.1.** – Correspondence table between cement notation and oxide phases in cements.

| Oxide phase | Cement shorthand notation |
|---|---|
| $CaO$ | C |
| $SiO_2$ | S |
| $Al_2O_3$ | A |
| $Fe_2O_3$ | F |
| $SO_3$ | $\overline{S}$ or \$ |
| $H_2O$ | H |

## 2.1.1. Portland cement

### 2.1.1.1. History and manufacturing

The first reported work about lime cements, mortars and concretes is attributed to the French chemist Louis Vicat starting from 1818, but the British researcher Joseph Aspdin filed a milestone patent in 1824 under the self-explanatory title of *"An Improvement in the Modes of Producing an Artificial stone"*.

The manufacturing process was summarily described at the time, but it is still valid today. A so-called "raw mix" made of clay and limestone is 'interground', then slowly fed into a kiln, a slowly rotating and slightly inclined cylinder which is usually several meters wide and several tens of meters long. The raw mix undergoes a temperature rise to 1450 °C during its gentle fall through the kiln, which induces the chemical transformations described in the next paragraphs.

After quenching at the bottom of the kiln, a greyish stony material is gathered: the *clinker*, which needs an additional grinding before use. Its direct mixing with water produces an uncontrollable hardening in mere minutes, which can be conveniently mitigated by intergrinding with a source of calcium sulphate, modifying the chemical processes of hardening described in section 2.2.4. The final interground mixture of clinker and calcium sulphate is Portland cement.

### 2.1.1.2. Mineral composition and morphology of Portland cement

Portland cement is made of polyphasic grains, more precisely of crystalline inclusions within a surrounding crystalline matrix of a different composition. This texture is easily observed under an optical microscope on polished sections (Fig. 2.1).

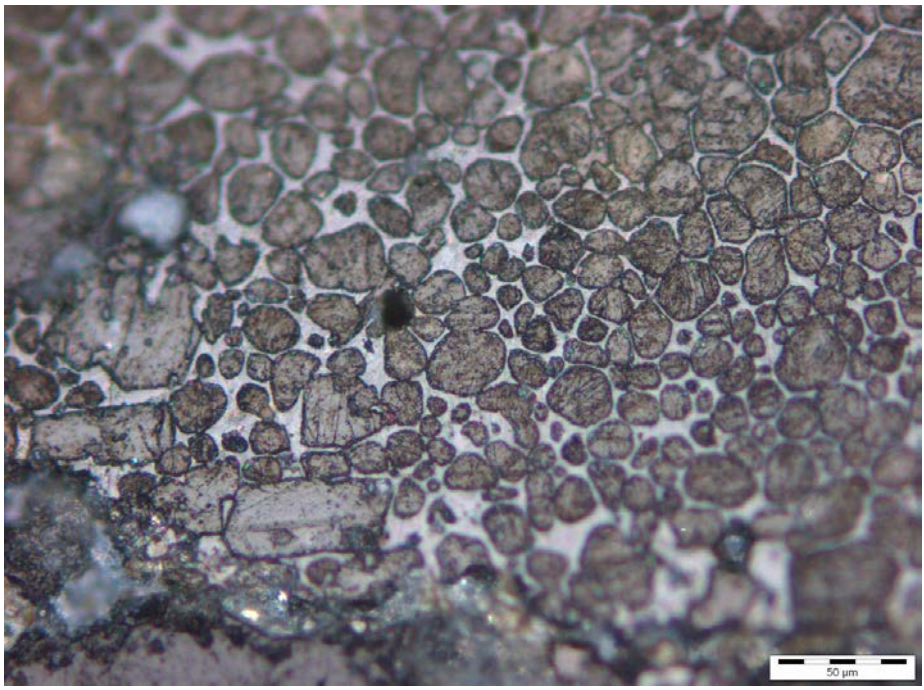


**Fig. 2.1.** – Optical microscope observation of a polished section of a clinker grain – Picture taken in the CHRYSO laboratory by Sylvain Soret (2014).

The shorthand notation of the main phases according to table 2.1 is given in table 2.2.

**Table 2.2.** – Clinker main phases, and their shorthand notations and usual names.

| Phase formula | Theoretical oxide equivalent | Shorthand | Common name |
|---|---|---|---|
| $Ca_3SiO_5$ | $3CaO.SiO_2$ | $C_3S$ | Alite |
| $Ca_2SiO_4$ | $2CaO.SiO_2$ | $C_2S$ | Belite |
| $Ca_3Al_2O_6$ | $3CaO.Al_2O_3$ | $C_3A$ | Tricalcium aluminate |
| $Ca_4Al_2Fe_2O_{10}$ | $4CaO.Al_2O_3.Fe_2O_3$ | $C_4AF$ | Tetracalcium alumino-ferrite |

The transformations in the kiln are well-known and described today and recent excellent reviews are available, among them [11], from which figure 2.2 is inspired.

Limestone is decarbonated around 550-1000 °C which produces a noticeable amount of $CO_2$, and this stage, incidentally, is the main source of $CO_2$ emission of the process. This produces quick lime CaO, supplier of calcium in the

phases forming at later stages. Clay provides aluminates and silicates, though the latter may come from limestone impurities.

Aluminosilicates, possibly containing iron oxides, are calcined into alumina, silica and ferric oxide between 600 and 950 °C. At higher temperatures (600-1280 °C), these compounds will combine with lime through solid-state reactions to yield calcium aluminates and belite $C_2S$. Between 1280 and 1450 °C a crucial stage occurs, the formation of alite $C_3S$ in a melted state. Alite is indeed essential in cement reactivity, as the main source of mechanical strength.

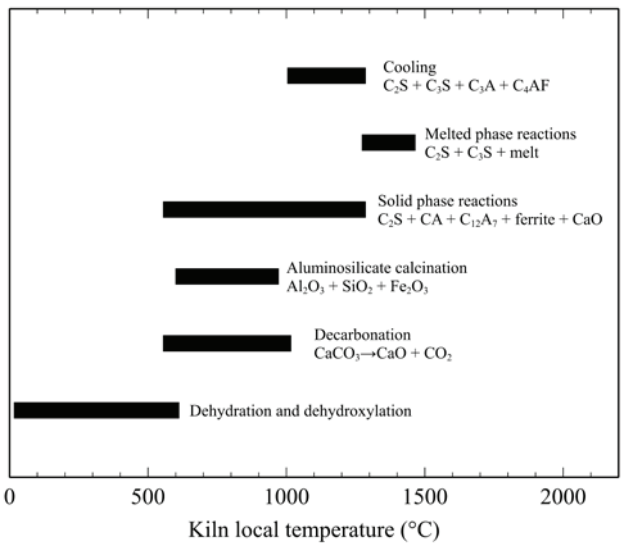


**FIG. 2.2.** – Schematic transformation stages of the raw mix in the kiln during clinker production (inspired by [11]). Materials cross the stages chronologically from the bottom to the top of the diagram.

After cooling, clinker is obtained as a polyphasic material whose composition is given in table 2.3. The proportions of the four main phases change from one cement to the other, because of subtle variations in the raw mix compositions and in process control. The most commonly observed composition ranges are given in table 2.3.

**TABLE 2.3.** – Most often observed clinker main phase compositions.

| Phase | Weight fraction common ranges (%) |
|---|---|
| $C_3A$ | 0 – 16 |
| $C_3S$ | 50 – 75 |
| $C_2S$ | 7 – 30 |
| $C_4AF$ | 4 – 20 |

## 2.1.2. Calcium Aluminate Cements (CAC)

### 2.1.2.1. History and manufacturing

Calcium aluminate cements were initially developed to solve problems linked to the presence of sulphate sources (generally gypsum $CaSO_4.2H_2O$ - *C$H*$_2$* or anhydrite $CaSO_4$ - *C$*) found in the ground near the concrete element. The industrial development of such cements is essentially due to J. Bied (Laboratory Director of the company Pavin de Lafarge at the beginning of the 20th Century), leading to a patent published in 1908 and a first product sold under the name of Ciment Fondu Lafarge in 1918. This cement, still sold under the brand name Ciment Fondu® (from the French for "Melted Cement"), resulted from the melting of a mixture of bauxite (or other low-silicate aluminous and ferrous oxide) with limestone.

The production of CAC is roughly a thousand times less than the Portland cement production worldwide, which makes it a specialty material to be used as it is or blended, in order to take advantage of its particular properties (fast strength acquisition, high temperature resistance/refractory properties, chemical resistance, *etc.*).

The final content of alumina ($Al_2O_3$) will define the process. For low contents (40-55%) the fusion route will be chosen. Bauxite and limestone rocks are fed into a static kiln heated at 1450 °C, then melted into a homogeneous bath subsequently extracted and cooled into a clinker. A final grinding allows obtaining the cement powder. For high alumina amounts (60-80%), CAC is produced in rotary kilns by sintering at 1600 °C, very similarly to the Portland cement process. In order to obtain a high quality sintering, the raw mix is interground and homogenized before feeding. Once again, a final stage of grinding is needed to obtain the cement powder.

### 2.1.2.2. Morphology and mineral composition of calcium aluminate cements

The main component of CAC is monocalcic aluminate $CaO.Al_2O_3$ (CA in shorthand notation), a monoclinic et pseudohexagonal crystal phase [12]. Some other phases of intermediate stoichiometries of CaO and $Al_2O_3$ also exist (Fig. 2.3).


**Fig. 2.3.** – Possibly existing phases in CAC along the $CaO/Al_2O_3$ composition axis.

Depending on the raw mix composition, different secondary oxides enrich the system. Among them are $SiO_2$, $Fe_2O_3$, $TiO_2$, $SO_3$, MgO or alkali sulphates, which give birth to a wealth of secondary materials: gehlenite ($C_2AS$), belite ($C_2S$), ferrite ($C_4AF$), perovskite (a calcium titanate CT) or ye'elimite ($C_4A_3$$). Among these, only ye'elimite is hydraulic at 20 °C, the others being unable to self-hydrate in the presence of water.

### 2.1.3. Modern cements: mixtures of minerals

In areas of the world where the $CO_2$ footprint of human activity is a concern, or wherever productivity increase is needed, a clear trend is observed towards heavy blending of Portland cement with mineral "fillers", mostly coming in as by-products of other industries. The principle is to combine Portland cement with mineral materials which are able to eventually yield hydration reaction products of the same nature and strength. The most commonly used materials, depending on their local availability, are:

- Blast furnace slag: siliceous residue of iron ore melting;
- Fly ash: siliceous residue of coal burning (power plants);
- Limestone.

The use of such materials is however standardized. In Europe, the standard EN 197-1 (2000) defines cement classes as a function of the addition nature and proportion — an excerpt is given in table 2.4 for the most commonly observed blends. The ASTM (American Standard of Testing and Methods) also enforces a classification and blending limits in the USA and other complying countries. In many cases, a loss in initial strength at early age (1-7 days) is observed, which has motivated an abundant research work about the possible underlying mechanisms and workarounds [13-19]. At later ages (28 days and beyond), durability and strength properties at least equal to Portland cement concretes are frequently observed [20-23], making mineral additions a source of added value to modern civil engineering concretes.

**TABLE 2.4.** – Excerpt from EN 197-1 (2000), weight percent compositions of blended cements.

| Code | Notation | Clinker | Slag | Fly ash | Limestone | Minor additions (calcium sulphates) |
|---|---|---|---|---|---|---|
| CEM I | CEM I | 95% | | | | 0-5% |
| CEM II | CEM II/A-V | 80-94% | | 6-20% | | 0-5% |
| | CEM II/B-V | 65-79% | | 21-35% | | 0-5% |
| | CEM II/A-LL | 80-94% | | | 6-20% | 0-5% |
| | CEM II/B-LL | 65-79% | | | 21-35% | 0-5% |
| CEM III | CEM III/A | 35-64% | 36-65% | | | 0-5% |
| | CEM III/B | 20-34% | 66-80% | | | 0-5% |
| | CEM III/C | 5-19% | 81-95% | | | 0-5% |
| CEM V | CEM V/A | 40-64% | 18-30% | 18-30% | | 0-5% |
| | CEM V/B | 20-38% | 31-50% | 31-50% | | 0-5% |

## 2.2. Setting and hardening – fundamental principles of crystallisation

The hardening of "hydraulic" mineral binders does not rely upon a mere drying process; it is indeed possible to observe such a hardening in immersed conditions with concretes of Portland cement.

The hardening of a cement paste is due to several chemical reactions between the pure phases of the cement and the water added in the mixture. Water being a reactant in the process, the whole setting and hardening is called "cement hydration" and the products are called "hydrates". If at first the phenomenon was understood as a progressive transformation of solid cement grains into another solid, the defenders of the theory of in-solution reactions, led by the French chemist Le Chatelier, allowed for a better understanding of the hydration process [24].

Today there is strong experimental evidence that noticeable concentrations of ions may be measured in the water surrounding cement grains, from the very first instants of contact and that these concentrations may change through the course of setting and hardening [26, 27]. This shows that some dissolving first takes place to produce a strongly concentrated solution, and then some consuming mechanism of the dissolved ions takes over.

The whole process relies then upon a dissolution-precipitation mechanism, the constitutive phases of cement dissolving first, producing salts which compose the hydrates. Thermodynamically and kinetically speaking, it is based upon notions of equilibrium and unbalance between an ionic solution and solid crystals, as will be further described in the next paragraph.

### *2.2.1. Notions of solubility equilibrium, undersaturation and supersaturation*

The motor of dissolution or crystallization in an aqueous solution is of a thermodynamic nature and depends on the difference between the initial state of this solution and a "target" equilibrium state, characteristic of the chemical system and depending on pressure and temperature. The moderation principle due to Le Chatelier describes this by stating that any perturbation of a balanced physical or chemical system will trigger an evolution tending to restore the original equilibrium state.

In the very precise case of a solid crystal in equilibrium with a solution of its constitutive ions, the thermodynamic balance is achieved when the chemical potential of all dissolved species is equal to the chemical potential of the same species in the crystal. The laws of thermodynamics show that this state corresponds to the situation where the ion activity product (IAP) of the dissolved species is equal to a constant $K_s$, called "solubility constant", although dependent upon pressure and temperature.

$$K_s = \frac{\prod_{i=1}^{n} a_i^{pi}}{\prod_{i=1}^{m} b_i^{qi}} \tag{2.1}$$

$a_i$: chemical activity of reaction product i
$p_i$: stoichiometric coefficient of reaction product i
$b_i$: chemical activity of reactant i
$q_i$: stoichiometric coefficient of reactant i

The chemical activity of an ion is a value proportional to its concentration, the proportionality factor being the activity coefficient $\gamma_i$ (equal to 1 in the case of an "ideal" solution). This is a correction to concentration to take into account the thermodynamic influence of the other ions present in the solution. The chemical activity of a massive solid phase is always 1 as well as the activity of the solvent. In the following text, the activity coefficients will be supposed to be equal to 1 (*i.e.,* no ionic thermodynamic interaction), for the sake of simplicity.

When ion concentrations are such that the IAP of the solution is exactly equal to $K_s$, the solution is said to be *saturated*. For example, for the dissolution of sodium chloride, $NaCl \rightleftarrows Na^+ + Cl^-$, the solubility constant reads:

$$K_s = \frac{[Na^+][Cl^-]}{1} = [Na^+][Cl^-]$$

its value at 25 °C is roughly 39 mol² L⁻². The solution is then exactly saturated when $[Na^+] = [Cl^-] = \sqrt{39} \approx 6.245$ mol L$^{-1}$, hence around 365 g L$^{-1}$. Such a system is at its equilibrium, and has no reason to evolve whatsoever.

If NaCl crystals are mixed with pure water, the initial state of the solution is IAP = 0, while the thermodynamic equilibrium prescribes IAP = 39 mol² L⁻². The crystals will then dissolve until the concentrations in sodium and chloride ions reach the saturation value of 6.245 mol L$^{-1}$. If the amount of NaCl is too low to reach this point, concentrations will settle to a lower value and all the solid matter will dissolve: the solution is defined as *undersaturated*. In constant conditions of temperature and pressure, this system has no reason to evolve any further: the IAP is too low to induce precipitation of crystals, and there is no solid left to dissolve.

The opposite case of *supersaturation* is also possible: let us consider a 1 mol L$^{-1}$ caustic soda solution, to which enough calcium chloride is added to reach a 0.1 mol L$^{-1}$ calcium concentration. The related dissolution reactions and solubility constants at 25 °C are given below:

$NaOH \rightleftarrows Na^+ + OH^-$ $\quad K_s = [Na^+][OH^-] = 742.56$ mol² L$^{-2}$

$CaCl_2 \rightleftarrows Ca^{2+} + 2Cl^-$ $\quad K_s = [Ca^{2+}][Cl^-]^2 = 180.19$ mol³ L$^{-3}$

The IAPs of each reaction (1 $mol^2\ L^{-2}$ for caustic soda and $10^{-3}\ mol^3\ L^{-3}$ for calcium chloride) show that the solution is undersaturated with respect to both species and that their dissolution will be complete.

But in this case, four ion species are present and all the cation-anion combinations must be taken into account: the solubility equilibria of sodium chloride NaCl and calcium hydroxide $Ca(OH)_2$. As shown earlier, the former will yield an undersaturated solution while sodium and chloride concentrations remain below 6.245 mol $L^{-1}$. Thus, sodium chloride is not expected to precipitate here.

However, the solubility of calcium hydroxide is governed by the reaction:

$$Ca(OH)_2 \rightleftarrows Ca^{2+} + 2OH^- \quad K_s = [Ca^{2+}][OH^-]^2 = 8.00 \cdot 10^{-6}\ mol^3\ L^{-3}$$

And the IAP of our example solution is:

$$[Ca^{2+}][OH^-]^2 = 0.1 \cdot 1^2 = 10^{-1}\ mol^3\ L^{-3}$$

This value is far greater than the $K_s$ of calcium hydroxide. To restore equilibrium, crystals of this salt will then form until calcium and hydroxide concentrations decrease towards such values that the solution will be exactly saturated (IAP = $K_s$ for calcium hydroxide).

That is an example of the *common ion effect*: the simultaneous dissolution of two undersaturated substances produces a supersaturated solution with respect to a third one, which then starts to crystallize. This consumes ions, decreases the IAPs of the original species, which then dissolve further to maintain their equilibrium, which in turn maintains the supersaturation with respect to the third substance, *etc.* This cycle of dissolution-precipitation stages lasts as long as none of the ion source substances is depleted.

The hardening of cement pastes relies on such cycles, the ion sources being the pure anhydrous phases ($C_3A$, $C_3S$, $C_2S$, $C_4AF$ for Portland cement), and ion "consumers" being the hydrate phases, described in section 2.2.5.

Let us take note that predicting dissolution or crystallization conditions may be determined by computing the ratio between the IAP and the solubility constant of a given species:

$$\beta = \frac{\text{IAP}}{K_s} \tag{2.2}$$

If $\beta < 1$, the solution is undersaturated. If $\beta > 1$ it is supersaturated and $\beta$ takes then the name of *supersaturation ratio.*

All those notions describe the equilibrium states towards which any system will try to evolve, either through dissolution or crystallization, depending on the value of $\beta$. But what remains crucial in most systems are the *rates* at which the phenomena occur. In the case of a supersaturated solution, kinetic parameters will decide of the time it takes for crystals to appear and grow in the volume. It is generally recognized that this happens in two stages: first, crystal embryos, or *nuclei*, appear, and then crystal growth begins around these nuclei.

### 2.2.2. Nucleation

Nucleation is considered as an important kinetic process of heterogeneous transformations, among which the apparition of a solid in a liquid solution. The basic assumption is that the atoms, ions or molecules present in solution must first agglomerate before forming the future solid phase. The solid embryo thus formed, also called a *cluster*, must reach a critical size before crystal growth itself may begin. In this sense, nucleation represents an often-critical stage as far as reaction kinetics are concerned.

Most of the following description is based upon the excellent review (in French) by the Ecole des Mines d'Albi (France) [27].

To be accurate, the mechanism described above is only one of the possible nucleation mechanisms, and is called *primary homogeneous nucleation*: the solution is initially devoid of any particle, which is a seldom-met ideal case. Particles of the same chemical nature as the considered substance may also act as pre-existing nuclei, allowing what is called *secondary homogeneous nucleation*. Finally, even particles of a "foreign" chemical nature may constitute nuclei, in which case *heterogeneous nucleation* occurs. The last two mechanisms give way to what is called seeding techniques, where particles are added to accelerate crystallization.

For primary homogeneous nucleation, it is shown that the free energy of formation of a cluster is a non-monotonous function of the number $i$ of elements (atoms, ions, molecules) of the said cluster. The supersaturation ratio β has a very strong influence on this free energy [27]:

$$G_i = kT\left(-i\ln\beta + \Theta i^{2/3}\right) \tag{2.3}$$

Θ is a term describing the contribution of the surface energy of the cluster:

$$\Theta = \frac{s\gamma_{SL}}{kT} \tag{2.4}$$

In equation (2.4) $\gamma_{SL}$ is the liquid-solid interfacial tension and $s$ the cluster outer surface area.

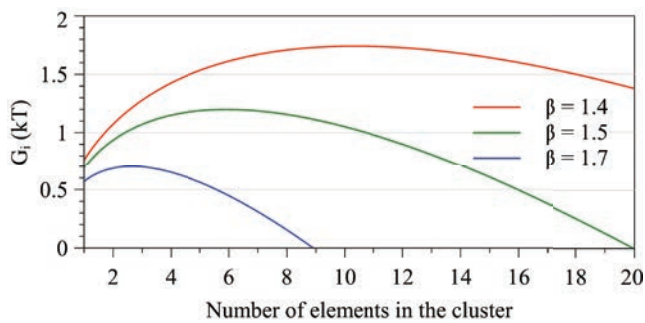


**FIG. 2.4.** – Cluster free energy as a function of the number of elements in the cluster, with the influence of the supersaturation ratio.

Spontaneous growth from the cluster is possible only when $\Delta G_i < 0$, *i.e.* when the cluster is composed by a number of elements greater than a critical value $i^*$ defined by the maximum of free energy, thus by [27]:

$$i^* = \left(\frac{2\Theta}{3\ln\beta}\right)^3 \tag{2.5}$$

The critical cluster size for spontaneous growth is then a decreasing function of the supersaturation ratio, as shown by figure 2.5.

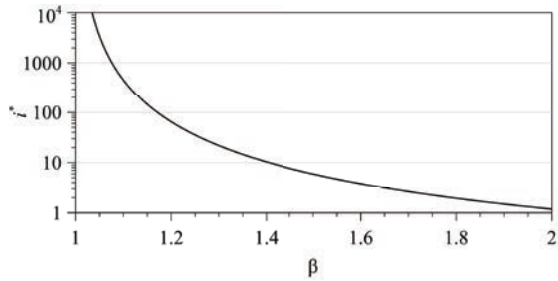


**Fig. 2.5.** – Cluster critical number of elements for spontaneous growth as a function of the supersaturation ratio.

This results in the fact that when the supersaturation ratio increases, it is more probable, thus more frequent, to generate clusters larger than the critical size for spontaneous aggregation. Supersaturation is then a major control parameter for cluster formation kinetics. Another parameter, the surface energy through the term $\Theta$, may also be a control parameter.

Steady state nucleation kinetics have been derived from the aforementioned developments. For primary homogeneous nucleation, the rate of nucleation is given by [28]:

$$B_1 \propto \left(\frac{\Theta}{9\pi}\right)^{1/2} \exp\left[-\frac{4\Theta^3}{27\ln^2\beta}\right] \tag{2.6}$$

This, once again, is an increasing function of the supersaturation ratio:

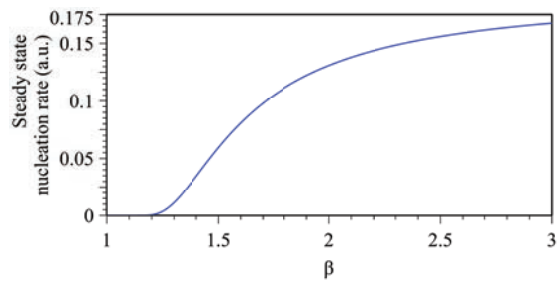


**Fig. 2.6.** – Steady state primary homogeneous nucleation rate as a function of the supersaturation ratio.

Secondary homogeneous nucleation may proceed through the release of crystalline debris, for example, by attrition in sheared or stirred systems. The first crystals formed by primary nucleation may contribute to this mechanism. The steady state nucleation rate takes the following shape, an increasing function of the supersaturation ratio [27]:

$$B_2 \propto \exp\left[-\frac{K}{\ln \beta}\right] \tag{2.7}$$

Heterogeneous nucleation adds a level of complexity because the considered nucleus has to form onto a "foreign" surface and an interfacial tension term must be taken into account. Nevertheless, the energy barrier is very often lower than for homogeneous nucleation, which makes seeding by particles of a different substance an efficient nucleation accelerator [30, 31]. It was also shown that the size ratio between nuclei and the seed particles has a strong influence.

### 2.2.3. Crystal growth

As soon as enough nuclei of a sufficient size are formed, crystal growth may begin and become the controlling kinetic stage. This growth may itself be described as a two-stage process, each one being possibly limiting [28]:

- Diffusion of the constituents from the solution to the growing crystal;
- Integrating of the constituent into the superficial crystal layer, which itself is similar to a diffusing process.

Most diffusing mechanisms follow a kinetic law as a power law of a concentration difference between points in space within the solution. Growth kinetic laws thus often take the following format [28]:

$$G \propto \left(C - C_{eq}\right)^g \tag{2.8}$$

In equation (2.8), $C$ is the solute concentration, $C_{eq}$ its equilibrium concentrating as defined by the solid solubility, and $g$ a generally non-integer power. Equation (2.8) may also be expressed in terms of the supersaturation ratio, which then controls growth as well as nucleation. More complex expressions, designed to take two-dimensional growth or growth around crystal defects into account, may also be found in the literature. They all consider the supersaturation ratio as the main driving parameter.

Finally, let us mention that the crystal structure describing the final solid prescribes the positions of the constituents in space, which implies that some crystal faces may preferentially incorporate the said constituents for minimum energy reasons. Growth rates may then depend on the crystal face considered, creating a broad range of anisotropies and shapes. This effect is illustrated on figure 2.7.

To sum up about this very complex subject, let us simply state that supersaturation, *i.e.,* the fact that crystal component concentrations in solution are

higher than the values prescribed by the solubility equilibrium of the said crystal, defines both the rates of apparition and the relative amounts of the substances that will eventually form the solid material.

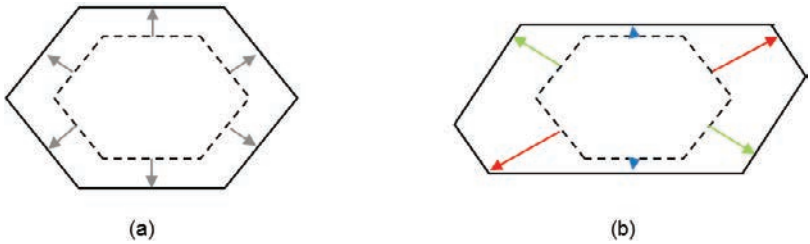


**FIG. 2.7.** – Illustration of the influence of growth rate on the crystal shape. (a) isotropic growth rates, (b) face-dependent growth rates.

## 2.2.4. *Principles of crystallisation applied to Portland cement*

### 2.2.4.1. *Aluminate phase hydration*

The solubility diagram on figure 2.8 shows that several stable hydrate phases may be obtained after dissolving $C_3A$ in water. In the case of Portland cement, the obtained hydroaluminates are of not much use, and their formation must be avoided. First, their growth is very abundant and exothermal, and induces a stiffening of the paste which is too fast to manipulate the material, also known as *flash setting*. Secondly, it has been observed that too large an amount of such hydrates may hinder the hydration of the silicate phases, which feature a much higher yield in mechanical strength [31].

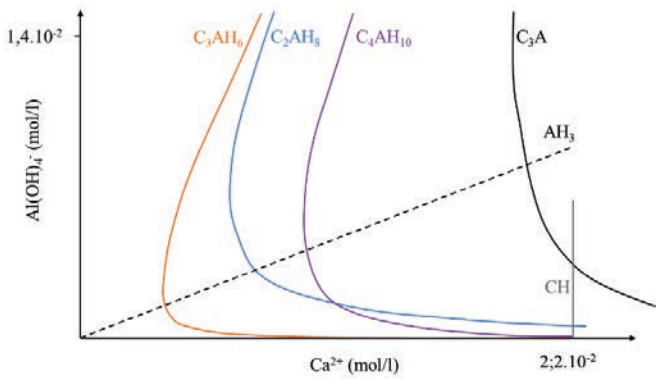


**FIG. 2.8.** – Solubility diagram of aluminate hydrates and $C_3A$ (from [32]).

The best "workaround" is to introduce a sulphate salt in the system which, by the common ion effect will impose other solubility equilibria. The natural hydration route of the aluminate phases is then re-routed towards sulfoaluminates whose cohesion and crystallization rates yield a far more workable material in the first hours after mixing. The most common sources used are gypsum $CaSO_4$, $2H_2O$ and anhydrite $CaSO_4$.

The stability domains of these new materials are represented in figure 2.9.

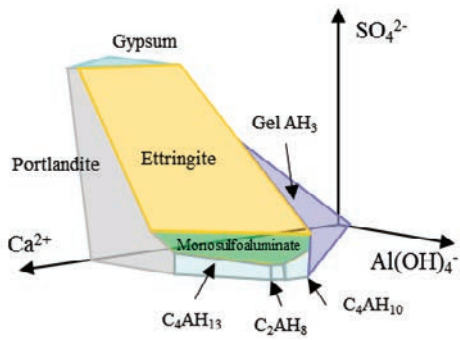


**FIG. 2.9.** – Corrected aluminate hydrate phase diagram in the presence of a sulphate source, *e.g.*, gypsum $CaSO_4.2H_2O$ (adapted from [33]).

Each calcium sulphate mineral has its own solubility equilibrium:

Gypsum: $$CaSO_4.2H_2O \rightleftarrows Ca^{2+} + SO_4^{2-} + 2H_2O \quad (2.9)$$

Anhydrite: $$CaSO_4 \rightleftarrows Ca^{2+} + SO_4^{2-} \quad (2.10)$$

Both are usually added to clinker at the grinding stage of the manufacturing process. The presence of these sulphate salts will impose the crystallisation of the trisulphoaluminate ettringite upon mixing when mixed with water [33]:

$$6Ca^{2+} + 2AlO_2^- + 3SO_4^{2-} + 4OH^- + 36H_2O \rightleftarrows Ca_6Al_2(SO_4)_3(OH)_{12}.36H_2O \quad (2.11)$$

This barely soluble salt belongs to the trigonal crystal system and forms elongated needles in the paste. This is due to a very strong anisotropy of the growth rates according to the crystal faces, so that growth may very quickly be considered as one-dimensional [34, 35]. The consumption of sulphate ions by ettringite precipitation leads to a progressive depletion of the calcium sulphate supply, which must last long enough (usually a few hours) to give way to silicate hydration reactions, described in the next paragraph.

Monosulphoaluminate phases may also appear, among them [33]:

$$4Ca^{2+} + 2AlO_2^- + SO_4^{2-} + 4OH^- + 10H_2O \rightleftarrows Ca_4Al_2(SO_4)(OH)_{12}.6H_2O \quad (2.12)$$

The above reaction is an illustrative example, since monosulphoaluminate or AFm, phases represent a wide family of minerals with various stoichiometric compositions [36-38].

Ettringite is not stable in the absence of sulphate, thus once the calcium sulphate supply is depleted, it dissolves and its constituents form monosulphoaluminate and hydroaluminates. As already mentioned, this must not happen before silicates have significantly reacted, which makes calcium sulphate addition a challenge in terms of industrial quality control.

### 2.2.4.2. Silicate phase hydration

A schematic silicate phase solubility diagram is given in figure 2.10.

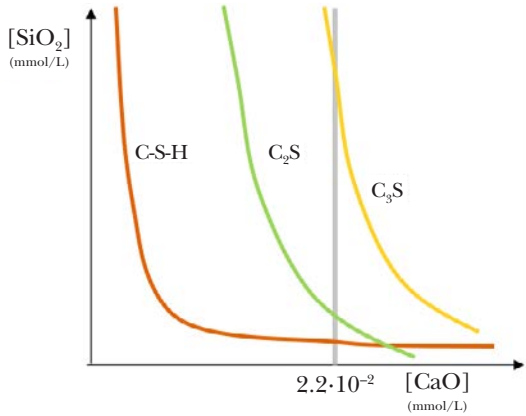


**Fig. 2.10.** – Solubility diagram of $C_3S$, $C_2S$ and C-S-H phases (inspired by [24]). The solubility equilibrium of portlandite (hydrated lime, in grey) plays a particular part (see text).

Alite $C_3S$ is the most soluble phase of the system, the yellow frontier in figure 2.10 corresponding to the equilibrium:

$$Ca_3SiO_5 + H_2O \rightleftarrows 3Ca^{2+} + SiO_4^{4-} + 2OH^- \qquad (2.13)$$

The dissolution of this phase puts then into solution calcium, silicate and hydroxide ions, the latter inducing a very quick pH rise, reaching 12.5 to 13.0 in a few seconds.

Silicate hydrates precipitation may be described by the reaction below; the stoichiometry of this reaction is not well-defined, nor even agreed upon, because it depends largely on the reaction conditions (temperature, foreign ions, *etc.*) [26, 27, 40, 41].

$$xCa^{2+} + SiO_4^{4-} + 2(x-1)OH^- + (y-x)H_2O \rightleftarrows (CaO)_x\,SiO_2\,(H_2O)_y \qquad (2.14)$$

Taking back the shorthand notation of minerals, the reaction product is named C-S-H (without stoichiometric coefficient). It is referred to as “calcium silicate hydrates”.

It is generally assumed or shown that x < 2 and y < 4 [27, 42]. Hence, C-S-H precipitation is not congruent with alite dissolution, which means that their respective stoichiometries do not match. As a result, the aqueous solution is progressively enriched in hydroxide and calcium ions, products of alite dissolution, until the system supersaturates with respect to another solid, portlandite, a hexagonal form of hydrated lime $Ca(OH)_2$. The corresponding precipitation reaction, occurring after several hours, is:

$$Ca^{2+} + 2OH^- \rightleftarrows Ca(OH)_2 \quad (2.15)$$

Belite $C_2S$ is less soluble than alite while being far more soluble than C-S-H in pure water. However, Fig. 2.10 shows that in portlandite supersaturation conditions, belite may become even less soluble than C-S-H. It ceases then to dissolve very quickly after the beginning of hydration and does not dissolve again before a much longer time [24].

It was recently shown that C-S-H nucleation kinetics is strongly coupled to alite dissolution kinetics, the latter happening through a complex process. Alite dissolution rates indeed appear to depend upon the under-saturation in alite in an uncommon fashion – the closer the IAP to the alite solubility constant, the slower the dissolution [25, 43].

After a first dissolution burst right after mixing with water, a period of a few hours during which the system does not seem to evolve rapidly, called "dormant period", is observed. The material is actually still evolving, but through very slow alite dissolution and C-S-H nucleation, until enough nuclei of the latter are formed to trigger a massive precipitation [24].

C-S-H morphology is very specific: the material does not feature a long-range ordered structure, as testified by the impossibility to obtain a clear X-ray diffractogram of this mineral [43]. It is the often referred to as amorphous, or "gel-like", but it was shown that it is composed of an assembly of platelet-shaped nanoparticles [44-46], whose crystalline structure is well described by the model units of either tobermorite or jennite [47-49]. These nano-platelets build up in the paste volume, with different scales of porosities, until they invade the whole original porosity to eventually form a continuous cohesive binder [46].

### 2.2.5. Principles of crystallisation applied to calcium aluminate cements

The diagram in figure 2.8 remains valid here, with the difference that the calcium aluminate cement anhydrous main phase (CA in most cases) controls the solution composition instead of $C_3A$.

Calcium aluminate cement hydration leads to the formation of four main hydrates: $CAH_{10}$, $C_2AH_8$, $C_3AH_6$ and $AH_3$, obeying equations (2.16) to (2.18) [12].

$$CA + 10H \rightarrow CAH_{10} \quad (2.16)$$

$$2CA + 11H \rightarrow C_2AH_8 + AH_3 \quad (2.17)$$

$$3CA + 12H \rightarrow C_3AH_6 + 2AH_3 \quad (2.18)$$

Temperature has a far greater influence than for Portland cement, especially on the hydrate composition (Table 2.1).

**Table 2.1.** – Observed hydrates forming at different temperature ranges for calcium aluminate cement.

| | $CAH_{10}$ | $C_2AH_8$ | $C_3AH_6$ |
|---|---|---|---|
| **Temperature (°C)** | 27-35 | 35-65 | > 65 |

Above 65 °C the most thermodynamically stable hydrates are $C_3AH_6$ and $AH_3$. At lower temperatures, $CAH_{10}$ and $C_2AH_8$ are observed but are thermodynamically metastable. They essentially form for kinetic reasons ($C_3AH_6$ is slower to form at such temperatures), but they gradually evolve to the thermodynamically stable $C_3AH_6$, according to equations (2.19) and (2.20).This mechanism is known as *conversion* and may take several years to complete.

$$2CAH_{10} \rightarrow C_2AH_8 + AH_3 + 9H \quad (2.19)$$

$$3C_2AH_8 \rightarrow 2C_3AH_6 + AH_3 + 9H \quad (2.20)$$

Conversion has a strong influence on the material properties. Strength development in calcium aluminate cements follows a non-monotonous trend with an increase at first, followed by a decrease and then a final, slow increasing period. This seems to be due to changes in the porosity of the hydrated material, linked to differences in the relative densities of the hydrates. $CAH_{10}$ and $C_2AH_8$ are crystals of the hexagonal group while $C_3AH_6$ is a crystal with a cubic unit, the parameters of which making this last hydrate denser than the first two.

While Portland cement hydrates are observed more often near the anhydrous grains, calcium aluminate cement hydrates seem to nucleate and grow in the interstitial pore solution (Fig. 2.11) [12]. This leads to a homogeneous hydrate localization in the interstitial volume, and a maintained dissolution of anhydrous grains, leading to a generally faster hydration.

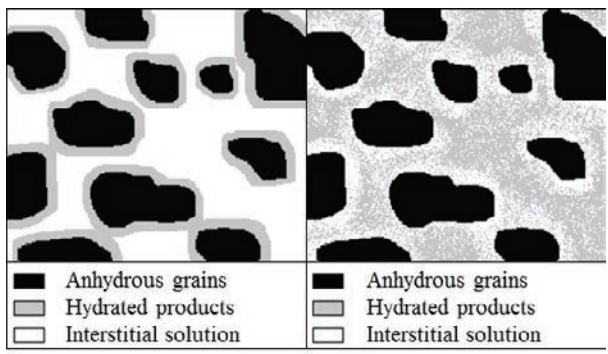


**Fig. 2.11.** – Illustrations of hydration processes of Portland cement (left) and calcium aluminate cement (right) (adapted from [12]).

## 2.3. Surface chemistry of hydrated cements

### 2.3.1. Surface charge and ζ (zeta) potential

Once dispersed in a polar liquid such as water, mineral particles may take an electrical charge on very specific sites of their surface. This is due to a range of possible phenomena:

- Ionisation: for example, acid surface groups (bearing a labile proton) lose a proton in alkaline conditions, or amino surface groups are cationised by a proton under acidic conditions.
- Adsorption of ions already present in the solution.
- Partial dissolution of the particles themselves, which is the case of cements, leading to localized charge unbalance.

If ions are present in the aqueous phase, they will be attracted by oppositely charged sites on the particle surface, condensate there and form a very dense layer. This case was described and modelled by Helmholtz in 1853, who showed that it behaves like a capacitor element.

A second population of ions, of opposite charge of the first layer – presenting the same charge as the surface itself – form a more diffuse layer, as demonstrated by Gouy and Chapman around 1910, within which the electrical potential decreases exponentially the further away you go from the surface. However, the theory fails in cases of high surface charge densities.

Around 1925, Stern combined both approaches with a so-called internal Stern layer and a Gouy-Chapman diffuse layer, under the name "double-layer model". More sophisticated models, for specific behaviours, were also developed, with an internal charge-less Helmholtz layer and a charged external layer [50]. The local electrical potential still decreases further away from the surface, but with different slopes and laws depending on the distance (Fig. 2.12).

There exists a specific plane within the diffuse ion layer where particle motion is unable to "drag" ions around, which defines a sort of a shear plane separating two domains in the solution. The electrical potential at this very location is equal to a value noted ζ (zeta) and called electro-kinetic or zeta potential (Fig. 2.12).

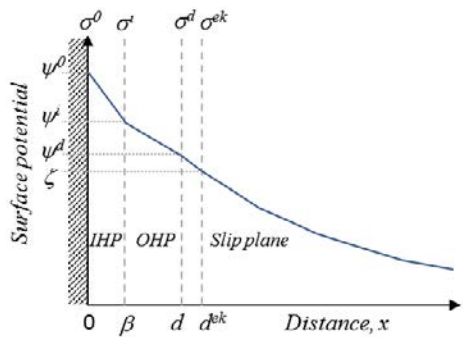


**FIG. 2.12.** – Schematic illustration of the Stern-Gouy-Chapman model (adapted from [50]).

The particle surface is supposed to bear a charge $\sigma^0$ and a potential $\psi^0$. The possibly existing ion-less Inner Helmholtz Plane (IHP) spans from the surface to a distance β into solution. At its boundary, the electrical charge is $\sigma^i$ and the potential is $\psi^i$. Beyond this point the Outer Helmholtz Plane (OHP) spans from β to a distance $d$, where the charge is $\sigma^d$ and the potential is $\psi^d$. The shear plane sits generally beyond this point, where the charge is $\sigma^{ek}$ and the potential is $\psi^{ek} = \zeta$. Its distance from the surface is $d^{ek}$, more often noted $\kappa^{-1}$, and called the Debye length.

The system electro-neutrality prescribes $\sigma^0 + \sigma^i + \sigma^d = 0$, which shows that the layers are composed of ions of alternating charge signs.

An interesting fact is that the Debye length – which defines the thickness of the ionic "shell" moving with the particle – depends upon the concentration of ions in the surrounding solution, expressed through the ionic strength $I$:

$$I = \frac{1}{2}\sum_{i=1}^{n} c_i Z_i^2 \tag{2.21}$$

In equation (2.21), $c_i$ is the concentration and $Z_i$ is the charge number of the ion $i$. A calculation example is given in table 2.6, for which a composition of cement pore solution was taken from Leemann *et al.* [51]:

**Table 2.6.** – Ionic strength calculation example (data taken from [51]).

| **Na+ (mmol L$^{-1}$)** | **K$^+$ (mmol L$^{-1}$)** | **Ca$^{2+}$ (mmol L$^{-1}$)** | **SO$_4^{2-}$ (mmol L$^{-1}$)** | **OH$^-$ (mmol L$^{-1}$)** | **I (mol L$^{-1}$)** |
|---|---|---|---|---|---|
| 47.0 | 296.0 | 29.4 | 185.0 | 160.0 | 0.7 |

Similar calculations show that ionic strength of cement pore solutions vary between 0.4 and 1.0 mol L$^{-1}$ depending on the cement and water-to-cement ratios.

The Debye length is given by equation (2.22):

$$\kappa^{-1} = \sqrt{\frac{\varepsilon\,\varepsilon_0 kT}{2N_A e^2 I}} \tag{2.22}$$

In this equation, $\varepsilon$ is the relative electrical permittivity of the medium (80.1 for water at 20 °C), $\varepsilon_0 = 8.85\ 10^{-12}$ F m$^{-1}$ the permittivity of vacuum, $k = 1.381\ 10^{-23}$ J K$^{-1}$ the Boltzmann constant, $T$ the temperature in K, $N_A \approx 6.02\ 10^{23}$ is the Avogadro number, $e = 1.6\ 10^{-19}$ C is the elementary electrical charge and still $I$ the ionic strength. A simplified version was computed at 25 °C and for an ionic strength expressed in mol L$^{-1}$:

$$\kappa^{-1} = \frac{0{,}304}{\sqrt{I}} \tag{2.23}$$

For ionic strengths between 0.4 and 1.0 mol L$^{-1}$, the Debye length lies between 0.30 and 0.48 nm, thus around 3-5 Å.

All these notions being defined, the electrostatic interaction potential between particles is given by equation (2.24) [52]:

$$U_{elec}(h) \approx 2\pi\varepsilon\varepsilon_0 a\zeta^2 e^{-\kappa(h-2\beta)} \tag{2.24}$$

This potential governs the way two approaching particles will interact — as it is always positive regardless of the sign of the ζ potential, it is always repulsive. Note however that due to the dependence of the Debye length upon the ionic strength, the repulsive range of the potential decreases when the solution ionic strength increases. This leads to the possibility of agglomerating a colloid suspension by simply adding salts.

### 2.3.2. Consequences for cementitious materials

Anhydrous cementitious materials put ions into solution through their dissolution, which increases its ionic strength, as already explained above. Moreover, most of the solid phases involved are either aluminates or silicates, amphoteric minerals able to bear different surface electrical charges depending on the pH of the solution.

It was shown that surface moieties, like silanol Si-OH, feature some Brønsted acidity — in alkaline conditions, they release a proton to become a silanolate site Si-$O^-$. This is particularly the case of C-S-H [54, 55]. Consequently, C-S-H particles can attract cations near their surface, and build up a layered ionic structure as described above. Inversions of the sign of the ζ potential of C-S-H were observed by merely increasing the concentration in lime [54, 56].

Other studies shown that the ζ potential of cement hydrate surfaces depends also on the solution composition itself. For instance, ettringite was shown to bear a positive ζ potential in the presence of dissolved lime, but a negative ζ potential in the presence of sulphate ions [57, 58].

## 2.4. Conclusion

Construction materials, beyond their apparent simplicity, feature a complex chemical and physical nature, and their manipulation and hardening rely upon very complicated notions at the border of mineral chemistry, physical chemistry and dense material physics.

In a nutshell, their fresh state behaviour may be described by stating that their mixing with water produces a consolidation through the first dissolution of mineral species, followed by the precipitation of new species that eventually invade the initial porosity and “cement” the whole volume.

The very nature of the species obtained, whether it be aluminate or silicate, induces a very specific behaviour with respect to the surrounding solution, depending on its pH, composition or ionic strength. Elements of the colloidal theory help to understand this behaviour.

## References


[1] De Larrard F. (1999) "Concrete mixture - Proportioning - A scientific approach". Modern Concrete Technology Series, 9, E & FN SPON eds, London, France, 421 p.

[2] De Larrard F., Sedran T. (1996) "Une nouvelle approche de la formulation des bétons." Ann. BTP, 6, 39-54.

[3] Fennis S., Walraven J.C., den Uijl J.A. (2009) "The use of particle packing models to design ecological concrete." HERON, 54, 185.

[4] Esping O. (2007) "Early age properties of self-compacting concrete: effects of fine aggregate and limestone filler." PhD thesis, Chalmers university of technology, Sweden.

[5] Fung W.W.S., Kwan A.K.H., Wong H.H.C. (2008) "Wet packing of crushed rock fine aggregate." Mater. Struct., 42, 631-643.

[6] Rao S.V., Rao M.V., Kumar P.R. (2010) "Effect of Size of Aggregate and Fines on Standard And High Strength Self Compacting Concrete." J. Appl. Sci. Res., 6, 433-442.

[7] Brouwers H.J.H. (2006) "Particle-size distribution and packing fraction of geometric random packings." Phys. Rev. E., 74, 031309, 1-14.

[8] Corwin E.I., Clusel M., Siemens A.O.N., Brujié J. (2010) "Model for random packing of polydisperse frictionless spheres." Soft Matter, 6, 2949-2959.

[9] Farr R.S., Groot R.D. (2009) "Close packing density of polydisperse hard spheres." J. Chem. Phys., 131, 244104, 1-8.

[10] Latham J., Munjiza A., Lu Y. (2002) "On the prediction of void porosity and packing of rock particulates." Powder Technol., 125, 0-27.

[11] Chatterjee A.K. (2011) "Chemistry and engineering of the clinkerization process - Incremental advances and lack of breakthroughs." Cem. Concr. Res., 41, 624-641.

[12] Baron J., Ollivier J., Desdevises A., Buil M., Detriche C.H., Vernet C. *et al.* (1992) "La durabilité des bétons." Collect. Assoc. Tech. Ind. Liants Hydraul., Presses de l'Ecole Nationale des Ponts et Chaussées, Paris, France, ISBN 2-85978-184-6, 453 p.

[13] Fernandez-Jimenez A., Palomo J.G., Puertas F. (1999) "Alkali-activated slag mortars. Mechanical strength behavior." Cem. Concr. Res., 29, 1313-1321.

[14] Ben Haha M., Le Saout G., Winnefeld F., Lothenbach B. (2010) "Influence of activator type on hydration kinetics, hydrate assemblage and microstructural development of alkali activated blast-furnace slags." Cem. Concr. Res., 41, 301-310.

[15] De Schutter G., Taerwe L. (1995) "General hydration model for Portland cement and blast furnace slag cement." Cem. Concr. Res., 25, 593-604.

[16] Malhotra V.M. (1989) "Fly ash, silica fume, slag, and natural pozzolans in concrete." In: Proceedings of the Third International Conference on Fly ash, silica fume, slag, and natural pozzolans in concrete, Malhotra V.M. Ed., two volumes.

[17] Bijen J., Waltje H. (1989) "Alkali-activated slag-fly ash cements." Am. Concr. Inst. SP., 114, 1565-78.
[18] Antiohos S., Tsimas S. (2004) "Activation of fly ash cementitious systems in the presence of quicklime Part I. Compressive strength and pozzolanic reaction rate." Cem. Concr. Res., 34, 769-779.
[19] Deschner F., Winnefeld F., Lothenbach B., Seufert S., Schwesig P., Dittrich S., *et al.* (2012) "Hydration of Portland cement with high replacement by siliceous fly ash." Cem. Concr. Res., 42, 1389-1400.
[20] Lilkov V., Dimitrova E., Petrov O.E. (1997) "Hydration process of cement containing fly ash and silica fume: The first 24 hours." Cem. Concr. Res., 27, 577-588.
[21] Ghrici M., Kenai S., Said-Mansour M. (2007) "Mechanical properties and durability of mortar and concrete containing natural pozzolana and limestone blended cements." Cem. Concr. Compos., 29, 542-549.
[22] Osborne G.J. (1999) "Durability of Portland blast-furnace slag cement concrete." Cem. Concr. Compos., 21, 11-21.
[23] Fernandez-Jimenez A., García-Lodeiro I., Palomo A. (2007) "Durability of alkali-activated fly ash cementitious materials." J. Mater. Sci., 42, 3055-3065.
[24] Pandey S., Singh A., Sharma R., Tiwari A. (2003) "Studies on high-performance blended/multiblended cements and their durability characteristics." Cem. Concr. Res., 33, 1433-1436.
[25] Scrivener K.L., Nonat A. (2011) "Hydration of cementitious materials, present and future." Cem. Concr. Res., 41, 651-665.
[26] Lothenbach B., Winnefeld F., Alder C., Wieland E., Lunk P. (2007) "Effect of temperature on the pore solution, microstructure and hydration products of Portland cement pastes." Cem. Concr. Res., 37, 483-491.
[27] Rothstein D., Thomas J.J., Christensen B.J., Jennings H.M. (2002) "Solubility behavior of Ca-, S-, Al-, and Si-bearing solid phases in Portland cement pore solutions as a function of hydration time." Cem. Concr. Res., 32, 1663-1671.
[28] Espitalier F. (2015) "Les Fondamentaux de la Cristallisation et de la Précipitation." La nucléation secondaire, http://nte.mines-albi.fr/CristalGemme/co/uc_NucleationScondaire.html.
[29] Espitalier F. (2015) "Les Fondamentaux de la Cristallisation et de la Précipitation." La nucléation secondaire, http://nte.mines-albi.fr/CristalGemme/co/CristalGemme_web.html.
[30] Thomas J.J., Jennings H.M., Chen J.J. (2009) "Influence of Nucleation Seeding on the Hydration Mechanisms of Tricalcium Silicate and Cement." J. Phys. Chem. C., 113, 4327-4334.
[31] Nicoleau L. (2013) "The acceleration of cement hydration by seeding: influence of the cement mineralogy." ZKG Int., 40-49.
[32] Gunay S. (2012) "Influence de la cinétique d'hydratation des phases aluminates en présence de sulfate de calcium sur celles des phases silicates: conséquences sur l'optimum de sulfatage des ciments." PhD thesis, université de Bourgogne, Dijon, France.

[33] Perez J.P. (2002) "Étude de l'hydratation des phases constitutives d'un ciment Portland et de la résistance mécanique des pâtes pures et mortiers: Influence des trialcanolamines." PhD thesis, université de Bourgogne, Dijon, France.
[34] Damidot D., Lothenbach B., Herfort D., Glasser F.P. (2011) "Thermodynamics and cement science." Cem. Concr. Res., 41, 679-695.
[35] Cody A.M., Lee H., Cody R.D., Spry P.G. (2004) "The effects of chemical environment on the nucleation, growth, and stability of ettringite $[Ca_3Al(OH)_6]$ $2(SO_{4)3}\cdot 26H_2O$." Cem. Concr. Res., 34, 869-881.
[36] Renaudin G., Segni R., Leroux F., Taviot-Gueho C. (2012) "Hexagonal or trigonal structure of ettringite revisited by Raman spectroscopy, http://renaudin.guillaume.free.fr/Publications/35_ICCC12Proceed_T2-04-2.pdf.
[37] Champenois J.B., Mesbah A., Cau Dit Coumes C., Renaudin G., Leroux F., Mercier C. *et al.* (2012) "Crystal structures of Boro-AFm and sBoro-AFt phases." Cem. Concr. Res., 42, 1362-1370.
[38] Glasser F.P., Mydala M., Balonis M. (2011) "Influence of calcium nitrate and nitrite on the constitution of AFm and AFt cement hydrates." Adv. Cem. Res., 1-15.
[39] Matschei T., Lothenbach B., Glasser F.P. (2007) "The AFm phase in Portland cement." Cem. Concr. Res., 37, 118-130.
[40] Dolado J.S., Griebel M., Hamaekers J., Dolado J.S., De Bizkaia P.T., Griebel M. *et al.* (2009) "A Molecular Dynamics Study of Cementitious Calcium Silicate Hydrate (C-S-H) Gels." J. Am. Cer. Soc., 90, 12, 3938-3942.
[41] Labbez C., Pochard I., Jönsson B., Nonat A. (2011) "C-S-H/solution interface: Experimental and Monte Carlo studies." Cem. Concr. Res., 41, 161-168.
[42] Thomas J.J., Rothstein D., Jennings H.M., Christensen B.J. (2003) "Effect of hydration temperature on the solubility behavior of Ca-, S-, Al-, and Si-bearing solid phases in Portland cement pastes." Cem. Concr. Res., 33, 2037-2047.
[43] Juilland P., Gallucci E. (2015) "Morphotopological investigation of the mechanisms and kinetic regimes of alite dissolution." Cem. Concr. Res., 76, 180-191.
[44] Grangeon S., Claret F., Linard Y., Chiaberge C. (2013) "X-ray diffraction: a powerful tool to probe and understand the structure of nanocrystalline calcium silicate hydrates." Acta Crystallogr. Sect. B Struct. Sci. Cryst. Eng. Mater., 69, 465-473.
[45] Jennings H.M. (2000) "A model for the microstructure of calcium silicate hydrate in cement paste." Cem. Concr. Res., 30, 101-116.
[46] Jennings H. (2009) "The Colloid/Nanogranular Nature of Cement Paste and Properties." Nanotechnol. Constr., 3, 27-36.
[47] Jennings H.M. (2007) "Refinements to colloid model of C-S-H in cement: CM-II." Cem. Concr. Res., 38, 275-289.
[48] Hartmann A., Buhl J.C., van Breugel K. (2007) "Structure and phase investigations on crystallization of 11 Å tobermorite in lime sand pellets." Cem. Concr. Res., 37, 21-31.

[49] Merlino S., Bonaccorsi E., Armbruster T. (2001) "The real structure of tobermorite 11A: normal and anomalous forms, OD character and polytypic modifications." Eur. J. Mineral., 13, 3, 577-590.
[50] Viehland D., Yuan L.J., Xu Z., Cong X.-D., Kirkpatrick R.J. (1997) "Structural studies of jennite and 1.4 nm tobermorite: Disordered layering along the [100] of jennite." J. Am. Cram. Soc., 80, 3021-3028.
[51] Delgado A.V., González-Caballero F., Hunter R.J., Koopal L.K., Lyklema J. (2005) "Measurement and Interpretation of Electrokinetic Phenomena (IUPAC Technical Report)." Pure Appl. Chem., 77, 1753-1805.
[52] Leemann A., Lothenbach B., Thalmann C. (2010) "Influence of superplasticizers on pore solution composition and on expansion of concrete due to alkali-silica reaction." Constr. Build. Mater., 25, 344-350.
[53] Flatt R.J., Bowen P. (2006) "Yodel: A yield stress model for suspensions." J. Am. Ceram. Soc., 89, 1244-1256.
[54] Viallis-Terrisse H., Nonat A., Petit J.C. (2001) "Zeta-Potential Study of Calcium Silicate Hydrates Interacting with Alkaline Cations." J. Colloid Interface Sci., 244, 58-65.
[55] Viallis-Terrisse H. (2000) "Interaction des Silicates de Calcium Hydratés, principaux constituants du ciment, avec les chlorures d'alcalins. Analogie avec les argiles." PhD thesis, université de Bourgogne, Dijon, France.
[56] Nägele E. (1986) "The Zeta-potential of cement." Cem. Concr. Res., 16, 853-863.
[57] Zingg A., Winnefeld F., Holzer L., Pakusch J., Becker S., Gauckler L. (2008) "Adsorption of polyelectrolytes and its influence on the rheology, zeta potential, and microstructure of various cement and hydrate phases." J. Colloid Interface Sci., 323, 301-312.
[58] Zingg A. (2008) "Cement-superplasticizer interaction: link between macroscopic phenomena and microstructural data of the early cement hydration". PhD thesis, Swiss Federal Institute of Technology Zürich, Zürich, Switzerland.

# 3 Microorganism-Concrete Interactions

**Françoise Feugeas**

## 3.1. General information

Every second in the world, 190 $m^3$ of concrete is poured, *i.e.,* 6 billion $m^3$ per year (according to different sources: infociment, UNICEM...). Concrete is now used worldwide for all types of construction such as bridges, dams in contact with fresh waters and for port infrastructures. Like all materials, concrete ages according to the environment in which it is located. An abundant literature deals with the subject of the durability of reinforced concrete structures. Many environmental factors contribute to the aging of concrete and, more recently, the biological influence on their alteration and/or deterioration has been studied. The oldest investigations taking into account these phenomena concern environments that are very rich in bacterial flora: the sewers [1]. Canalisations carrying drinking water or wastewater or purification stations are also structures in contact with microorganisms actively participating in the deterioration of colonized surfaces. The preliminary to any phenomenon of biodeterioration of a surface is its colonization. Why and how do microorganisms colonize a surface to form a biofilm? This question is simple to ask but the answer is extremely complicated to give since it implies both the understanding of microbial behaviour in an aqueous medium and that of materials, more particularly their surface and the physic chemistry of solid-liquid interfaces. Biofilms develop on all kinds of surfaces thanks to the adhesion of microorganisms. The stages of biofilm formation are the subject of much research, as illustrated in some chapters of this book.

Concrete is a word used for a very large family of composites made up of aggregates of different sizes and origins linked by cements. The complexity of the cements in terms of composition has been described in the previous chapter and makes it possible to understand what a cement surface represents. It is indeed this part of the concrete that is considered the most sensitive to colonization by microorganisms and thus susceptible to biodeterioration. Before developing this aspect, we first have to consider the parameters influencing the bioadhesion of microorganisms such as the physico-chemistry of the colonized surface, notably its roughness but also its chemistry and character more or less hydrophilic.

The problem can be expressed as follows: what are the characteristics of the surfaces of concrete that explain their colonization by microorganisms?

In order to try to provide answers to the problem, it is therefore necessary to use experimental techniques of surface science in order to characterize these and to demonstrate the influence of the parameters of this surface on its bio colonization. The aim of this chapter is not to be exhaustive regarding the methods of characterization of porous composite surfaces and only a dynamic contact angle measurement technique will be developed as an example.

## 3.2. Parameters influencing the bioreceptivity of cementitious materials

Colonization of a material by microorganisms requires aqueous environment. Water is present in a concrete at the origin since the setting and the hardening are carried out correctly only if the right amount of it is available. This value has a direct consequence on the porosity of the cements: the higher the water/cement ratio, the greater the total porosity (accessible to the water) of the cured cement is. The previous chapter also highlighted the extent to which the physical chemistry of cement grains is involved in the dissolution and precipitation processes of the different hydrates forming a cement paste. The size of the cement grains, their chemical composition and the presence of salts in the hydration water will influence the size and quality of the crystals composing the cured cement, which will have a direct effect on the geometry of the porosity inside the material [2]. The definition of the surface, as the first chapter indicates, is three-dimensional since the contact between the water molecules and the cementitious crystals is also carried out in the voids created by the heterogeneity of these as well as by the porosity of surface. The formulation made of water and cement can thus directly influence the porosity that participates in the surface roughness.

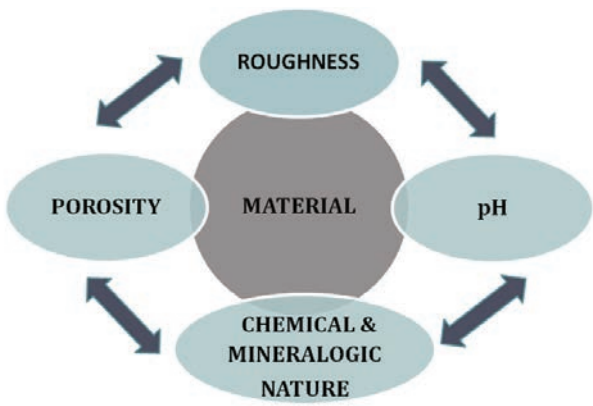


**FIG. 3.1.** – Main parameters of the material surface influencing its bioreceptivity.

The chemical nature of the surface depends on the type of hydrates formed and influences its pH value. If it is close to 13 for most "young" (recently cured) concrete, it changes more or less quickly depending on the environmental parameters, the porosity and the chemistry of the hydrates formed, thus modifying the surface energy of the material. Figure 3.1 illustrates the interactions between these parameters in aqueous environment.

### 3.2.1. Relationship between these parameters and bioreceptivity

Any cementitious surface changes with time and relative humidity through carbonation: the presence of $CO_2$ in the atmosphere causes the reaction of portlandite ($Ca(OH)_2$) of the cement matrix with the carbon dioxide of the air in the presence of moisture and leads to the formation of calcite ($CaCO_3$) according to the following reactions:

– dissolution of the concrete portlandite

$$Ca(OH)_2 \rightarrow Ca^{2+} + 2OH^- \quad (3.1)$$

– dissolution of carbon dioxide in the porosities of concrete and formation and dissolution of carbonic acid

$$H_2O + CO_2 \rightarrow HCO_3^- + H^+ \quad (3.2)$$

$$HCO_3 \rightarrow CO_3^{2-} + H^+ \quad (3.3)$$

– Neutralization of chemical reactions, final stage of carbonation

$$Ca^{2+} + 2OH^- + 2H^+ + CO_3^{2-} \rightarrow CaCO_3 + 2H_2O \quad (3.4)$$

Simplified global reaction:

$$CO_2 + Ca(OH)_2 \rightarrow CaCO_3 + H_2O \quad (3.5)$$

Carbon Dioxide + Portlandite → Calcite + Water

This phenomenon lowers the pH of the concrete surface (pH ≈ 9.5). It is thus understood that many microorganisms may then find a surface more favourable to their development than if it had remained very basic. The chemical nature of the medium generates a selection of the microorganisms present and the surface alkalinity favours the development of certain microbial species. It is important to note, however, that some species may be present in an environment that is unsuitable for their metabolism in the form of spores, in the vegetative state and, consequently, they are then likely to develop under favourable conditions of their environment.

A large number of studies have been carried out in order to show the influence of parameters such as surface roughness and the type of microorganisms

for their colonization of different surfaces. Roughness affects the attachment of microorganisms and organic materials to the substrate. It also affects the flow of water and its contact time with the surface. Rough surfaces may have a larger active surface area and protect bacteria adhered to the surface of shear forces due to flow [3]. Consequently, the colonization of the material is favoured, the roughness accentuating the trapping of nutrients.

However, the increase in roughness does not necessarily favour the colonization of a surface by microorganisms. Surface roughness appears to be not the only one parameter explaining differences in colonization on the same surface [4]. The influence of the average roughness of the surface is variable according to the bacteria [5]. In other words, the type of microorganism and its geometry, size and shape are important to consider. For example, if some filamentous algae, such as *Klebsormidium flaccidum* algae, are able to cling to roughness, other thick-walled algae prefer smooth surfaces [3]. Due to the variability of microorganism species and roughness ranges, it is difficult to conclude simply as to the effect of roughness on biocolonization. The topography of a surface is not the only parameter that evolves: surface energy is also an important parameter in the phenomena of adhesion of microorganisms [6].

### 3.2.2. Surface energy

In chapter one it has been demonstrated how a wide range of complex interactions occur when a liquid is placed in contact with a surface. If a drop of water is placed on a non-porous surface, it is possible to observe the angle of contact between this drop and the surface, which makes it possible to characterize the so-called "wettability" of the solid and, consequently, its hydrophilicity or hydrophobicity.

But when the surface is porous and therefore rough, this measurement and its interpretation become much more delicate. Indeed, one must then be interested by the dynamic wetting that describes the wetting of a drop as a function of time. Moreover, to the adsorption phenomena is added the sorption which describes the situation where the liquid molecules penetrate inside the solid surface, generating a loss of volume. This process depends on many parameters such as porosity. Finally, there is saturation when the liquid has completely penetrated the sample and appears on the opposite surface.

Liquid surface tension is an easily measurable characteristic: table 1.1 in chapter 1 sets out some examples of values. In contradistinction, the surface energy is difficult to evaluate, in particular because of the immobility of the molecules in a solid phase [7]. In recent years, different techniques have been used to obtain the surface energy of materials by measuring the contact angle with the method of drop applied, measurement of capillary rise or adsorption of steam and techniques such as reverse gas chromatography or steam sorption gravimetry.

In order to determine the surface energy values from the applied drop technique, various models establishing relationships between adhesion and surface energy can be used. The Fowkes model [8] decomposes the surface tensions

of the solid and the liquid into two parts: the dispersive and the non-dispersive one and considers that the dispersion forces are predominant at the solid-liquid interface. Using the same two-component decomposition of surface tensions, the Owens and Wendt model [9] takes account of the non-dispersive part of the hydrogen bond in the adhesion work. It is assumed that the adhesion work associated with non-dispersive forces can take the form of a geometric mean. The Van Oss *et al.* model [10] proposes another formalism to express surface free energy and its components from contact angles. The thin-layer wicking method takes into account molecular interactions *via* electron donor/acceptor processes that involve the complementary properties of the liquid and the solid. These interactions include, in particular, hydrogen bonding.

These models propose to calculate the surface energy of a solid, more precisely the solid-vapour interfacial energy, from the surface tension of a liquid (interfacial liquid-vapour energy) and the solid-liquid interfacial energy. But they are only valid for theoretical or ideal surfaces. The problem consists of connecting measurements of contact angles with these three interfacial energies in order to quantitatively evaluate the surface energy of a cementitious surface. The surface energy of a cement paste depends on a large number of physicochemical factors, in particular the size of the particles in contact with the drop of water (of the different, more or less hydrated phases), its roughness, and its porosity. The relations between the surface tension of a liquid and the interfacial energy between a liquid and a solid (adhesion work) on the one hand and those between this interfacial energy and the surface energy of the substrate (mathematical models) are very complex.

### 3.2.3. Measurement of contact angles

A liquid drop, such as water, is applied to the surface of a substrate to determine the specific properties of the material surface. The contact angle is measured by taking the inner angle between the base and the tangent to the point of contact between the liquid and the surface.

#### 3.2.3.1. Static contact angles

In this "ideal" case, Young Dupre's model determines the energy of the surface. Young Dupre's equation (equation (3.6)) defines the relation between the 3 equilibrium energies of the Liquid-Solid-Gas system and the static contact angle. The parameters influencing the shape of the drop are the characteristics of the surface, the liquid used and the external conditions.

$$\gamma_{LV} \cdot \cos\theta = \gamma_{SV} - \gamma_{SL} \tag{3.6}$$

There are other models that take into account chemical heterogeneity and surface porosity, respectively. The Wenzel model is most often applied for physically textured surfaces, the Cassie-Baxter model for chemically textured surfaces, but they are not valid when the liquid penetrates into the sample being tested [11].

### *3.2.3.2. Dynamic contact angles*

When a liquid drop is put on an absorbent surface such as a cementitious paste, there is no equilibrium phase since the contact angle will vary continuously as a function of time. It then becomes necessary to record several successive images to evaluate the dynamic interaction between the liquid and the surface. Each captured image is analysed and dynamic wetting (contact angle), liquid penetration (volume) and spreading are measured as a function of time.

If the contact angle decreases with time, the reason may be the penetration (loss of volume) but also the spreading of the drop. It is then necessary to observe whether the volume of the drop decreases (penetration) or whether the diameter of the base of the drop increases (spreading). In most cases, a combination of these two factors contributes to the change in contact angle. Moreover, the effects of the roughness of the heterogeneous substrate and the chemical interactions between the water and the latter must be taken into account for a complete analysis of the physico-chemical behaviour at the cured cement paste/aqueous phase interface.

There are a number of complex measurement techniques and models to evaluate the surface energy of compressed powders, tissues, polymer filters, *etc.* There are fewer results concerning cement pastes. Despite the difficulty of measuring the contact angle and surface energy due to the numerous techniques, the many mathematical models and the biases associated with the large number of parameters involved in phenomena of wetting coupled with sorption, authors publish their comparative results obtained with different liquid probes for a fifty year time-span.

The example given below highlights the interest of this type of measurement to evaluate the modification of the behaviour related to a drop of water put on different cement samples. If the surface energy is not calculated with respect to the difficulty of adapting a coherent model, the analyses of the evolution of the angles as a function of time allow a better understanding of the surface changes of the material.

## 3.3. Measurements of the evolution of surface properties of cementitious pastes with the technique of measurement of dynamic angles

A biosourced adjuvant was incorporated into cement pastes. This biosourced product has been the subject of various studies within the framework of the SEPOLBE project: Extra-cellular Substances for Concrete [12]. The objective of this study is to evaluate the effect of the product named bioadmixture on the evolution of contact angles of a drop of water on cement pastes. Dynamic angle measurements were performed on cement pastes containing 0 and 1.5%

bioadmixture. Evolutions of the angles and diameters of the drop were observed over time. These two information made it possible to evaluate and differentiate the phenomena of spreading and penetration of the drop.

### 3.3.1. Implementation

Cement pastes were produced according to [NF EN 196-3] standard with cement CEM I 52.5R CE CP2, the chemical composition of which is given in table 3.1:

**Table 3.1.** – Chemical composition of CEM I (% by mass).

| $SiO_2$ | $Al_2O_3$ | $Fe_2O_3$ | CaO | MgO | $SO_3$ | $K_2O$ | $Na_2O$ | $S^-$ | $Cl^-$ | $CO_2$ | $CaO_{free}$ | $Na_2O_{eq}$ active |
|---|---|---|---|---|---|---|---|---|---|---|---|---|
| 20.3 | 5.1 | 3.4 | 63.3 | 1.5 | 3.5 | 1 | 0.14 | 0 | 0.05 | 0.6 | 0.9 | 0.79 |

For the cement pastes, distilled water (pH = 5.8) was used with an E/C ratio = 0.315 determined by the Vicat consistency test [NF EN 196].

The bioadmixture (BA) is a liquid product derived from the extracellular substances of bacteria. It is incorporated into the mass during mixing as an admixture according to the standard [NF EN 934-2]. The percentages of BA are 0% and 1.5%. The cement paste is afterward poured into cylindrical moulds (Fig. 3.2). The samples obtained appear in the form of cylinders diameter 22 mm and 3 mm in thick. They are stored for 24 hours at a temperature of 20 °C and a relative humidity > 80%. Samples are then taken from moulds and stored in distilled water. After 3 days, samples are polished with three abrasive papers of successive grains (p 320, p 600 and p 1200) until obtaining of a plane and smooth surface. They undergo an ultrasonic treatment to remove polishing residues. They are finally stored in distilled and filtered water. This protocol (Fig. 3.2) guarantees a similar surface state for all samples.

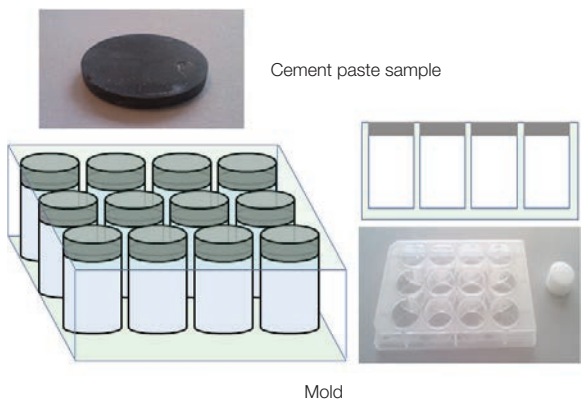


**Fig. 3.2.** – Sample preparation protocol [14].

After 58 days of wet curing and prior to measurement, the samples are re-polished using the finest grain abrasive paper (p 1200) and undergo ultra-sonic treatment to remove any surface deposits and crystallizations. The samples, whose surface pH is greater than 12, are then placed in a ventilated oven at 50 °C until their mass ($\Delta < 0.01\%$ of the initial mass of the saturated sample) is stabilized between two successive weighing spaced apart of one hour (adaptation of the standard [NF P EN 18-459] for the determination of the water content of aggregates).

Once removed from the oven, the dry samples are placed in the sample chamber to measure the contact angles.

The measurements are carried out at a temperature of 27 °C ± 1 °C and at a relative humidity of 64% ± 2%. Six samples of each assay are tested with 3 or 4 drops per sample to ensure a good repeatability of the results. A water droplet of volume V (between 2 and 4 µL) is deposited on the surface of the sample at t = 0.

Using a camera (12 frames per second), a DSA30 Kruss drop profile analyser can observe the evolution of the profile of a water droplet put on the surface of the porous sample (Fig. 3.3).

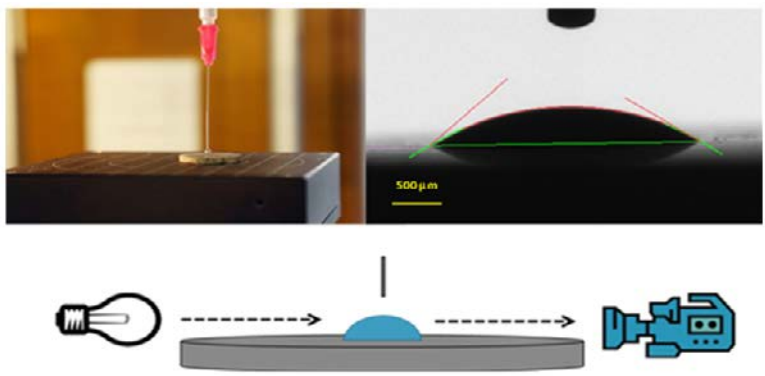


**FIG. 3.3.** – Drop put on the sample surface of cement paste and measurement set-up [14].

A video sequence is recorded and the processing of the video (DSA 4 software) makes it possible to evaluate the contact angles and the diameter of the drop.

### 3.3.2. *Evolution of contact angles as a function of time*

Figure 3.4 shows an example of the evolution of contact angles (right and left) as a function of time for a 0% sample and a 1.5% BA sample. The droplet profile is not symmetrical and there is a difference between the values of the

left angles and those of the right angles. The material studied has a rough and heterogeneous surface, which explains this dissymmetry, also observed by other researchers using this technique [15, 16].

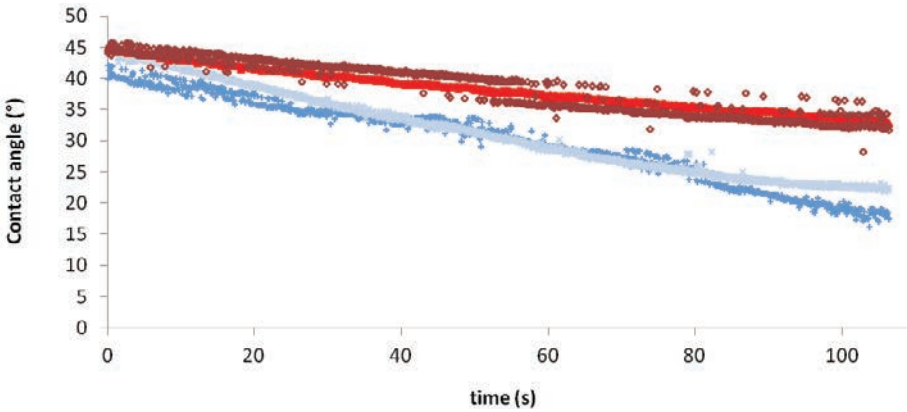


**Fig. 3.4.** – Contact angle evolution *versus* time for cement paste without BA (grey curves) and with 1.5% BA (red curves) [14].

The results show that the contact angles follow a linear evolution over time. The decrease in contact angles for the sample without the bioadmixture appears faster than that for the sample with 1.5% BA. The averages of the directing coefficients of these lines show that the presence of the BA significantly modifies the rate of decrease of the contact angles: with 1.5% BA, the angles decrease 2.5 times less rapidly than without BA.

This decrease in angles corresponds to a combination of the spreading of the droplet on the sample surface and of its penetration into the porous cementitious paste.

### 3.3.3. *Evolution of contact angles as a function of diameter*

A new technique of penetration analysis with respect to the spreading without considering the time parameter is presented here, in order to distinguish the two behaviours resulting from (1) the penetration of the drop into the sample and (2) spreading of the drop on the surface of the sample (Fig. 3.5).

Assuming that the drop penetrates (Fig. 3.5a), $\theta$, the contact angle, decreases when D, the contact diameter, decreases. On the contrary, if the drop only spreads out (Fig. 3.5b), $\theta$ decreases when D increases. In reality, it is a combination of the two phenomena that occurs when a water droplet is deposited on the surface of the cement paste samples (Fig. 3.5c).

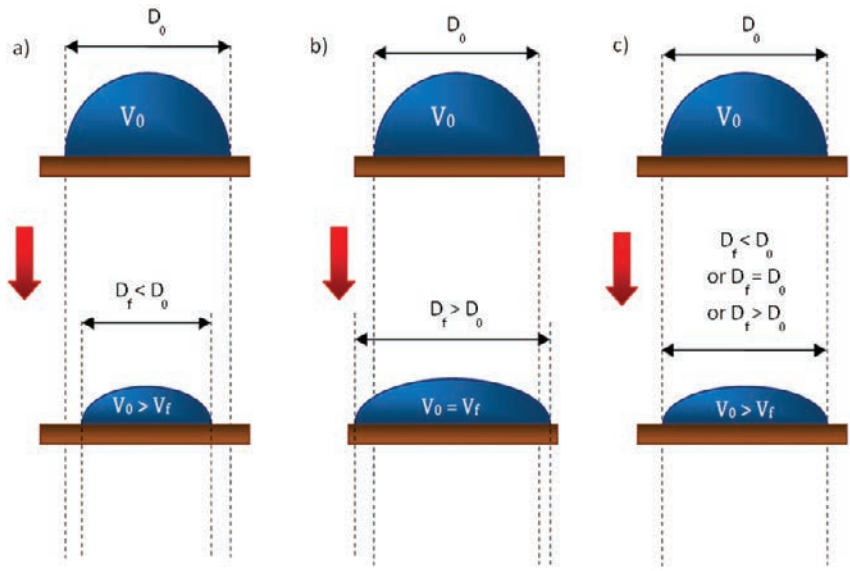


**FIG. 3.5.** – theoretical behaviour of a water droplet on the surface sample: a) penetration case, b) spreading case, c) combination of the two phenomena [14].

Several authors have already used the simplifying hypothesis of a drop represented by a spherical cap [17, 18]. The theoretical evolution of the angles as a function of the diameter can then be determined for penetration by equation (3.7) (Fig. 3.6).

$$d = D \sin \theta \qquad (3.7)$$

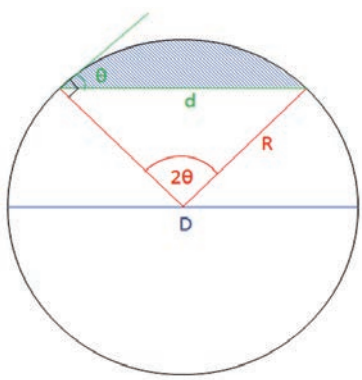


**FIG. 3.6.** – Evolution of contact angle *versus* diameter (penetration) [14].

For the spreading of the drop, it can be assimilated to the volume of a spherical cap (Fig. 3.7, Eq. (3.8)).

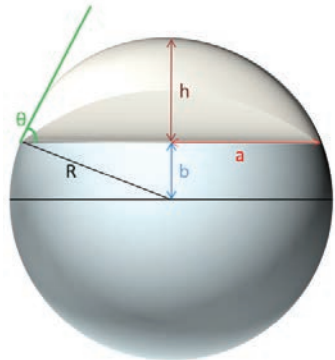


**FIG. 3.7.** – Revolution of the sphere *versus* contact angle (spreading) [14].

$$R = \sqrt[3]{\frac{6\,V_{calotte}}{\pi(1-\cos\theta)\left[3(\sin\theta)^2-(1-\cos\theta)^2\right]}} \tag{3.8}$$

By replacing D by 2*R and d by 2*a in equation (3.7), we obtain a = r*sin θ. These two curves are plotted in figure 3.8 with an arbitrarily set starting diameter of 1 mm.

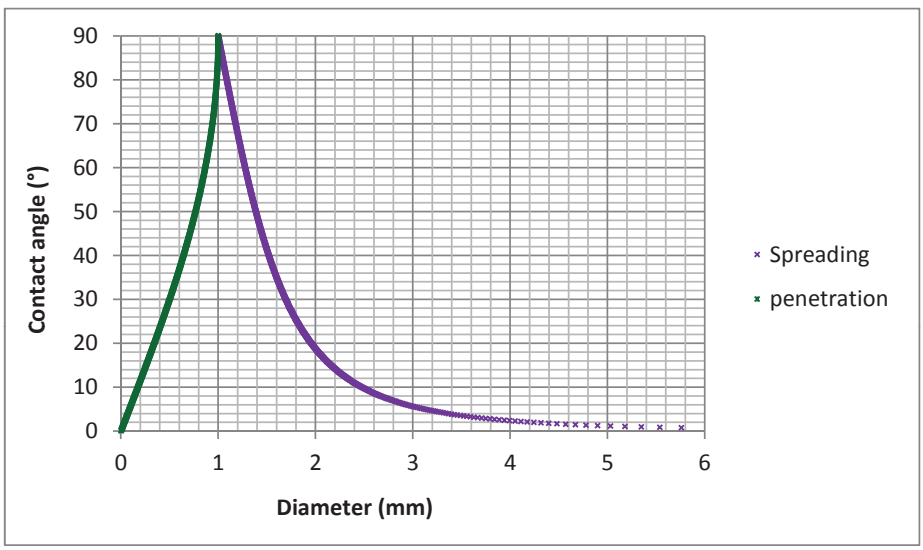


**FIG. 3.8.** – Theorical behaviour of a droplet on the sample surface [14].

The change in contact angles as a function of diameter for a 0% BA sample and a 1.5% BA sample is shown in figures 3.9 and 3.10.

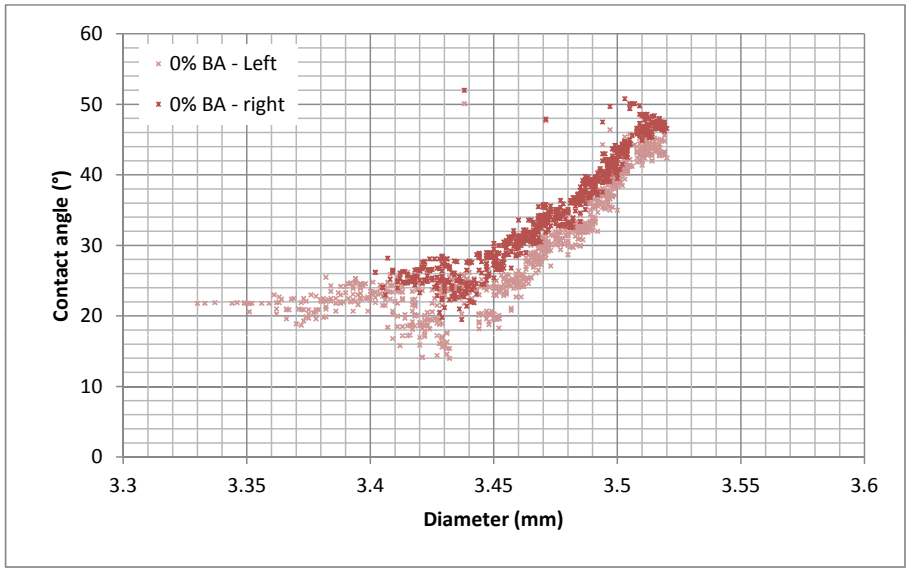


**FIG. 3.9.** – Contact angle evolution *versus* diameter for 0% BA cement paste samples [14].

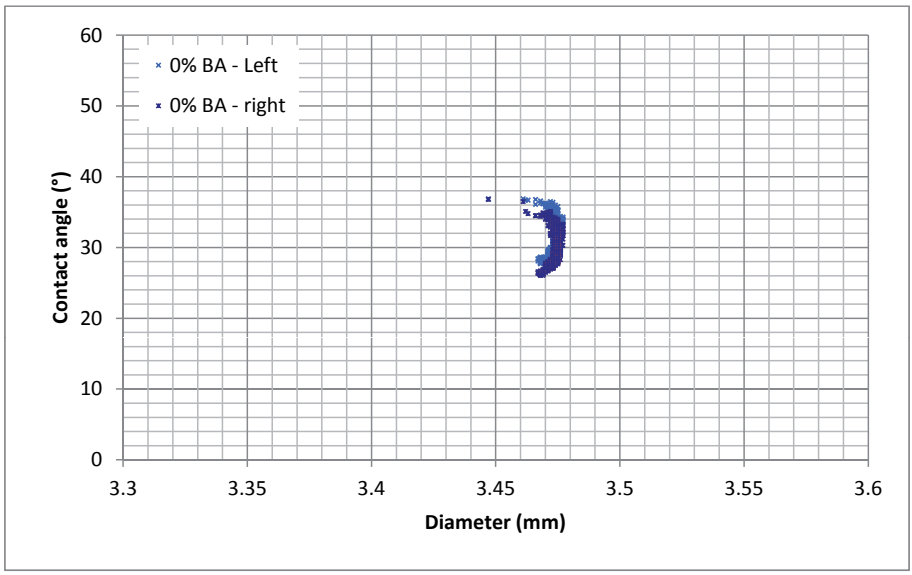


**FIG. 3.10.** – Contact angle evolution *versus* diameter for 1.5% BA cement paste samples [14].

The two tests lasted 106 seconds. For the sample without BA, the values of the contact angles are between 49 and 19°, which corresponds to a variation of 30° and a change in the diameter of 0.4 mm (Fig. 3.9). For the sample with 1.5% BA, the difference in angle values is only 10° (36° - 26°) and the diameter values vary between 3.44 and 3.48 mm, corresponds to an evolution of 0.04 mm (Fig. 3.10). The interval between the angles and the diameter of the sample with 1.5% BA is very small compared with that without BA (3 times less for angles and 10 times less for diameter) for the same number of points measured. Figures 3.9 and 3.10 are on the same scale to illustrate the great differences in angular change as a function of diameters.

On the curve of the sample without BA (Fig. 3.9), three phases can be observed: The first phase shows a decrease in the angle for a small decrease in diameter. The second phase exhibits a similar but less pronounced behaviour, *i.e.,* the decrease in angle is smaller in relation to the decrease in diameter. The third phase shows a decrease in diameter with an almost constant angle.

The curve shown in figure 3.11, on a more suitable scale, allows better observation of the angular evolution phases with 1.5% BA.

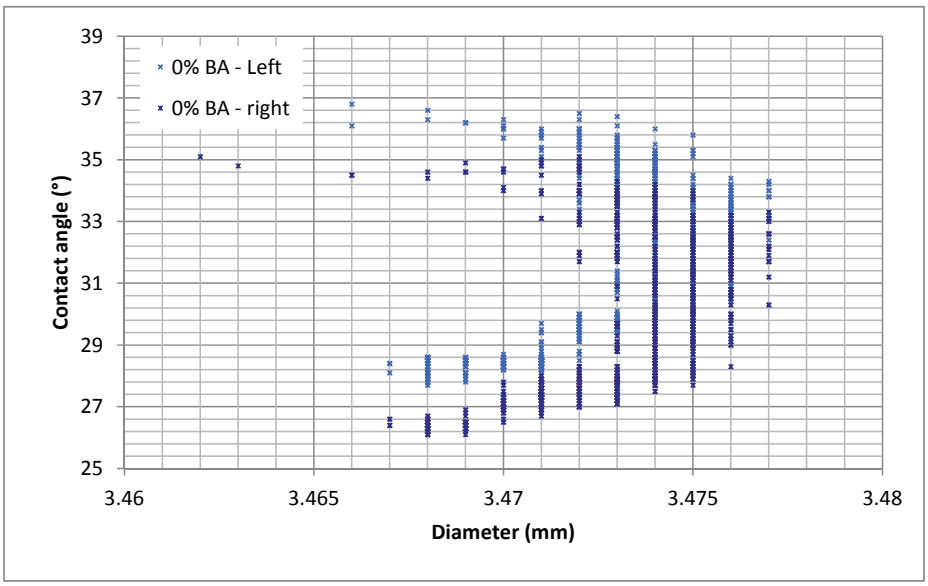


**Fig. 3.11.** – Droplet behaviour on a sample wih 1.5% de BA [14].

The diameter begins to increase with the decrease of the angle, then stabilizes while the angle continues to decrease and finally decreases very slightly with the angle. The presence of bioadmixture favours the spreading of water on the surface, this effect is particularly important in the first phase corresponding to the most important angles where the spreading, that is to say the increase in

diameter with respect to the angle, is such that the slope of the curve $\theta = f(D)$ changes sign with respect to that of the sample without BA favouring the effect of the penetration of the drop. These two types of behaviour are observed for 10 trials of each composition (0% and 1.5%). Moreover, the results concerning the speed of the contact angles decrease show a retardation of the rate of decrease in the presence of BA. The addition of BA thus induces a reduction in the penetration of the drop of water essentially due to a phenomenon of clogging porosities. The spreading of the drop shows that the surface is "wettable" and this demonstrates that the addition of BA does not render the material more hydrophobic.

## 3.4. Conclusion

Studies concerning the biodeterioration of concrete and their bioreceptivity have been intensified in recent years in the light of the new requirements for sustainable development, in the search for materials that are more eco-friendly and more resistant to different environments. The complexity of the cementitious surfaces: their physical and chemical heterogeneity, to which porosities and roughnesses that vary according to the compositions and implementations, are added, explains why many scientific and technical hurdles have yet to be crossed, in particular as regards bioreceptivity.

The scale effects between microorganisms and heterogeneous surfaces composed of particles of a few tens of microns of chemistry imply some major difficulties in demonstrating correlations between the parameters concerning the material, its surface and a potential bioreceptivity of the latter. Among all the normalized or original evaluations of the surface parameters of the materials, it appears that the measurements of the penetration behaviour of a liquid in this type of porous and multiphase material offer an interesting field of investigation in order to better understand the changes in the characteristics related to the biocolonization capacity of such materials.

## References

[1] Fritz-Feugeas F., Cornet A., Tribollet B. (2008) "Biodétérioration des matériaux. Action des microorganismes de l'échelle nanométrique à l'échelle macroscopique." Fritz-Feugeas F., Cornet A., Tribollet B. Eds, Technosup collection, Ellipses, Paris, France, ISBN 978-2-7298-3996-3, 258 p.

[2] Bur N., Roux S., Geraud Y, Feugeas F. (2011) "Porous structure of mortar: influence of cement and curing." European Journal of Environmental and Civil Engineering, EJECE, 15, 699-714.

[3] Tran T.H. (2011) "Influence des caractéristiques intrinsèques d'un mortier sur son encrassement biologique." PhD thesis, université de Saint-Étienne, Mines de Saint-Étienne et Douai, Saint-Etienne, France.

[4] Holah J.T., Thorpe R.H. (1990) "Cleanability in relation to bacterial retention on unused and abraded domestic sink materials." J. Appl. Bacteriol., 69, 599-608.
[5] Vanhaecke E., Remon J.P., Moors M., Raes F., de Rudder D., van Peteghem A. (1990) "Kinetics of *Pseudomonas aeruginosa* adhesion to 304 and 316-L stainless steel: role of cell surface hydrophobicity." Appl. Environ. Microbiol., 56, 788-795.
[6] Rouxhet P. (2008) "Interactions entre matériaux et systèmes biologiques. In: Biodétérioration des matériaux. Action des microorganismes de l'échelle nanométrique à l'échelle macroscopique." Fritz-Feugeas F., Cornet A., Tribollet B. Eds, Technosup collection, Ellipses, Paris, France, ISBN 978-2-7298-3996-3, 258 p.
[7] Tavana H., Neumann A. W. (2007) "Recent progress in the determination of solid surface tensions from contact angles." Adv. Colloid Interface Sci., 132(1), 1-32.
[8] Fowkes F. (1962) "Determination of interfacial tensions contact angles and dispersion forces in surfaces by assuming additivity of intermolecular interactions in surfaces." J. Phys. Chem., 66-382.
[9] Owens D., Wendt R. (1969) "Estimation of the surface free energy of polymers." J. of Applied Polymer Science, 13, 1741-1747.
[10] van Oss C.J., Good R.J., Chaudhury M.K. (1986) "The role of van der Waals forces and hydrogen bonds in 'hydrophobic interactions' between biopolymers and low energy surfaces." J. Colloid Interface Sci., 111, 378-390.
[11] Milne A.J.B., Amirfazli A. (2012) "The Cassie equation: How it is meant to be used." Adv. Colloid Interface Sci., 170, 1-2, 48-55.
[12] He H., Serres N., Meylheuc T., Feugeas F. (2013) "Ouvrabilité et performances mécaniques de mortiers contenant un bioadjuvant à base de substances extra-cellulaires." Mat. & Tech., 101, 1.
[13] Munzer C., He H., Serres N., Roux S., Meylheuc T., Lecomte A., Feugeas F. (2014) "Bioréceptivité des matériaux cimentaires – protocole de préparation et analyses des surfaces en fonction du temps." Rencontres Universitaires de l'Association Universitaire de Génie Civil (AUGC), Orléans, France.
[14] Munzer C., Belhaj E., Meylheuc T., Lecomte A., Feugeas F. (2015) "Effets d'un bioadjuvant sur les caractéristiques de surface de pâtes cimentaires." Mat. & Tech., DOI: 10.1051/mattech/2015024,103, 2.
[15] Wolansky G., Marmur A. (1999) "Apparent contact angles on rough surfaces: the Wenzel equation revisited." Colloids Surf. Physicochem. Eng. Asp., 156, 1, 381-388.
[16] Meiron T.S., Marmur A., Saguy I.S. (2004) "Contact angle measurement on rough surfaces." J. Colloid Interface Sci., 274, 2, 637-644.
[17] Kumar S.M., Deshpande A.P. (2006) "Dynamics of drop spreading on fibrous porous media." Colloids and Surfaces A: Physicochem. Eng. Aspects, 277, 157-163.
[18] Clarke A., Blake T.D., Carruthers K., Woodward A. (2002) "Spreading and Imbibition of Liquid Droplets on Porous Surfaces." Langmuir, 18, 8, 2980-2984.

# Theme 2
# Biofilms: actors of biodeterioration

To better understand the mechanisms of biodeterioration, improved knowledge of biofilms is indispensable; they stand at the heart of the reactions leading to the majority of biological alterations of materials. It is therefore logical that the theme of the chapters that follow is dedicated to biofilms.

Some basic knowledge of bacteria, *i.e.,* the main actors in biofilms, is provided by chapter 4.

Chapter 5 is devoted to the populations that live in the "biofilm mode", to the regulations that lead to what is often described as a "mature biofilm", illustrating perfectly the high level of organization of this type of growth. The extracellular matrix is probably the most characteristic component of biofilms; it is of major importance by its mass and its volume but also by the functions that it plays. It is dealt with in chapter 6, which describes the properties and the nature of the extracellular polymeric substances which constitute it.

Finally, chapters 7, 8 and 9 give examples where biofilms generate various health and material problems in managing the quality of water systems for human consumption or in cooling systems and in the marine environment with the corrosion of iron-based materials.

# 4 The bacterial cell: the functional unit of biofilms

**Frédéric P.A. Jorand**

## 4.1. Introduction

In response to environmental pressures such as chemical (oxidative stress), physical (UV exposition), biological (phagocytosis), and nutritional stresses (starvation in oligotrophic environments), bacteria have developed several strategies to survive or/and grow; the biofilm mode is one of these strategies. Biofilms are defined as a 3-D organized structure, made of microorganisms embedded in a self-produced extra-cellular polymeric substances (EPS) giving aggregates of bacteria in suspension or adhering to a substrate. This form of bacterial life occurs in a large diversity of environments such as on the cobbles of a riverbed, or on the vessel's hull, in the drinking water pipes, or onto the hip prostheses, and by extension, onto any surfaces in contact with water, even in humid environment such as on the leaf tree.

It was shown over the last few decades, that the cells within the biofilms can be arranged with a high level of sophistication, forgetting the very first studies on biofilms [1] suggesting a randomly arranged cell layers on the substrata (Fig. 4.1). For example, at the macroscopic scale, the architecture of thick biofilms seems to be optimised to create irrigation channels providing nutrients and electron acceptors (*e.g.,* $O_2$ from the water bulk) [2]. At a lower scale, a detailed vascularisation was recently evidenced: some bacteria are connected together by nanowires or nanotubes to exchange electrons or diverse solutes [3-4] (Fig. 4.1). Therefore, biofilms have to be considered as complex, organized structures of cells capable of communicating with each together and exchanging matter. As for multicellular organisms, organised by tissues, the cell, mainly bacterium in biofilm, is the smallest active unit that controls the biofilm growth and ageing. The cell is the motor where matter is transformed by the metabolism to provide cellular energy and new cellular material. By doing precisely this, the cells within the biofilms contribute to the biogeochemical cycles, such as the atmospheric gas composition, mobility of pollutants or stone mineralogy, and at an even lower scale, to the man-made material alterations. To better understand how biofilms might damage the integrity of man-made materials, the basic knowledge of the bacterial cell is required. Thus, the bacterial cell

structure – and especially the cell surface structures that are involved in the colonization of a solid substratum –, the basic knowledge of the cell metabolism and the diversity of the metabolic groups will be set out in this chapter. Thus, the reader will be provided with the general knowledge to understand correctly how some microorganisms, in the micrometer range, lead occasionally to severe alterations of materials in natural or industrial environments.

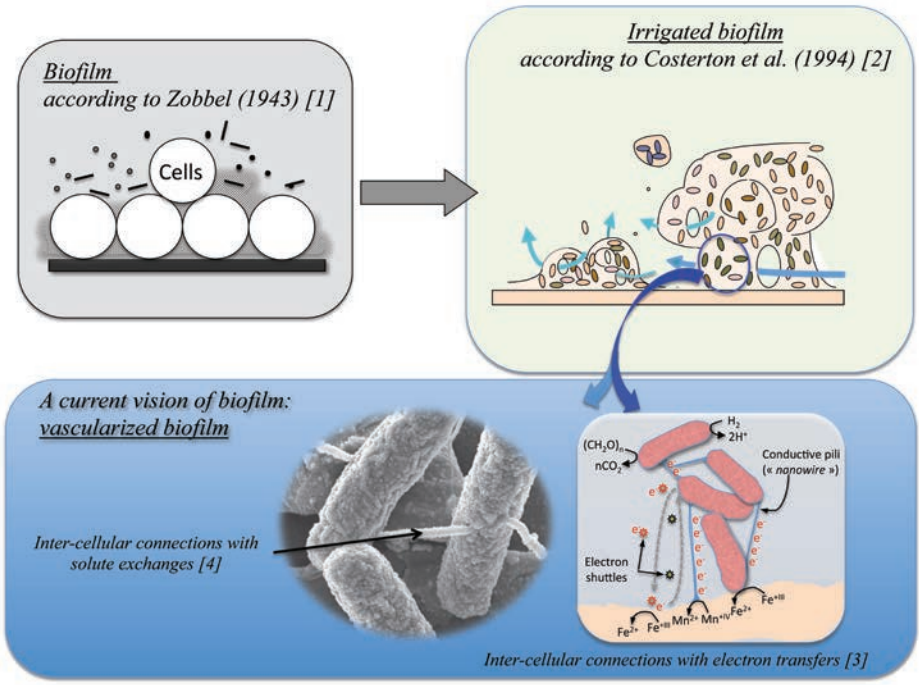


**FIG. 4.1.** – Development over time and scientific knowledge of the conceptual model of biofilm: from simple cell layers [1] to organized 3-D [2] and vascularized-like [3 & 4] structures.

## 4.2. Microorganisms

Microorganisms include all unicellular organisms invisible to the naked eye. All in all, their size ranges from ~ 0.1 µm and up to ~ 100 µm, occupying the three domains of the life, with two being exclusively prokaryotes ("unicellular microorganisms without nuclei"): *Bacteria* and *Archaea*. For convenience, we will call any of these prokaryotes "bacteria". Unicellular microorganisms that form no tissues of the *Eucarya* domain (cells containing nucleus) are generically called

"protista", again for convenience. That includes unicellular "fungus-like" (yeast and moulds), unicellular "plant-like" or algae (also called protophyta) and unicellular "animal-like" or protozoa (Fig. 4.2).

Each cell of these organisms are self-sustained, that means capable to grow as individual organism from organic or inorganic nutrients that they convert into cellular energy and cell material. In contradistinction, viruses, another group of microbes, are not able to do that: they are "obligate parasites", *i.e.,* they need to infect a cell to reproduce. Moreover, they are not cellular organisms (they are made of a proteinaceous structure, the capsid, containing the nucleic acid). Although their role in biomass regulation is evident, they are not involved, as far as we know, in biodeterioration processes. Their impact on the biofilm will be not taken into account here. However, some strategies to control surface colonization by biofilm suggest the use of bacteriophages, with the viruses infecting bacterial cells.

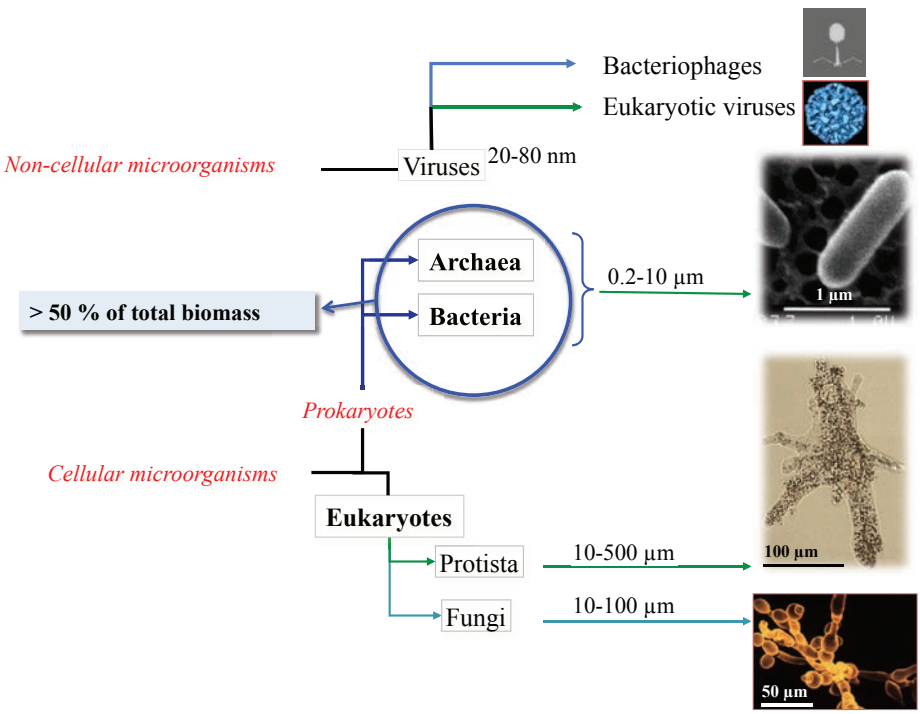


**Fig. 4.2.** – Microbe groups: eukaryotic unicellulars, prokaryotic cells with bacteria and archaea and viruses. Prokaryota account for more than 50% of the total biomass [5, 6]. They represent the most important diversity of species, although most of them are largely unknown as yet.

## 4.3. Microbial diversity and habitat diversity

Over 3.5 million years ago, the first living cells appeared on Earth. From their evolution imposed by the environmental pressure, such as strong geological and climatic events, a wide diversity of unicellular organisms has developed and continue to change nowadays. Each species acquired metabolic capabilities to be able to grow, or survive, in a specific environment, or for some of them, in diverse environments. Thus, the bacterial life has been describe to occur in the temperature range of –2 °C to +113 °C, to pressures up to 1100 atm, in saline media up to the limit of NaCl solubility, or under extreme radiations (Table 4.1). It is therefore not surprising that, *a priori* hostile environments such as the surface of firn snow in high mountain areas, or grains of sand in the Saharan desert [7], or industrial ultra-pure water networks host actively growing bacteria [8]. To give an overview of their potential habitats, the extreme values of physical and chemical parameters where bacterial activity has been recorded are reported in table 4.1.

To grow, or survive, by taking advantage of nutritional resources, bacteria have developed various specific structures and metabolisms. In order to better understand how such organisms can colonise the material surfaces and sometimes lead to severe alteration of the latter, we are going to briefly describe the bacterial cell structures with the wide range of available pertinent instruments and tools to optimise bacterial cells development or survival. After that, we will describe the main features of the bacterial metabolisms.

**TABLE 4.1.** – Some extreme values of physical and chemical parameters where bacterial activity has been recorded [7-9].

| Parameters | Extreme values | Example of bacteria |
|---|---|---|
| Hydrostatic pressure (marine or terrestrial depths) | 1-1000 atm (130 MPa):<br>–5000 m (terrestrial)<br>–10000 m (oceanic sea-bed)<br>–1600 m (oceanic underground) | *Bacillus infernus* |
| Temperature | –5 °C<br>+113 °C[a] | *Colwellia psychrerythraea*<br>*Pyrolobus fumarii* |
| Salinity | ~ 0 (ultrapure water)<br>5 M (NaCl) | *Rouxiella chamberiensis*<br>*Haloarcula marismortui*<br>*Dunaliella salina* |
| Acidity / alkalinity (pH) | ~ 0<br>12 | *Picrophilus* spp.,<br>*Cyanidium caldarium*<br>*Natronomonas pharaonis* |
| Water availability (water activity, $a_w$) | 0.75-1<br>0.60-1 | Bacteria<br>Fungi |
| Dry area | Saharan Desert | *Ramlibacter tataouinensis* |
| Radioactivity | 10000 grays (1000 × more than humans) | *Deinococcus radiodurans* |

[a] NB: under high hydrostatic pressures, such as those near the ocean floor, the water remains liquid up to 400 °C.

## 4.4. Structures and functions of the bacterial cell

Cell structures and composition can vary greatly from species to species in the bacterial world, but it also depends on the physiological state of the cell. To help understand how a cell is built, we can switch elements that constitute the cell into two parts: i) the mandatory elements, essential for cell integrity and the functionality of all species and, ii) the optional elements, not found in all bacteria, depending on their genetic make-up or on their physiological state. Figure 4.3 gives an overview of this approach.

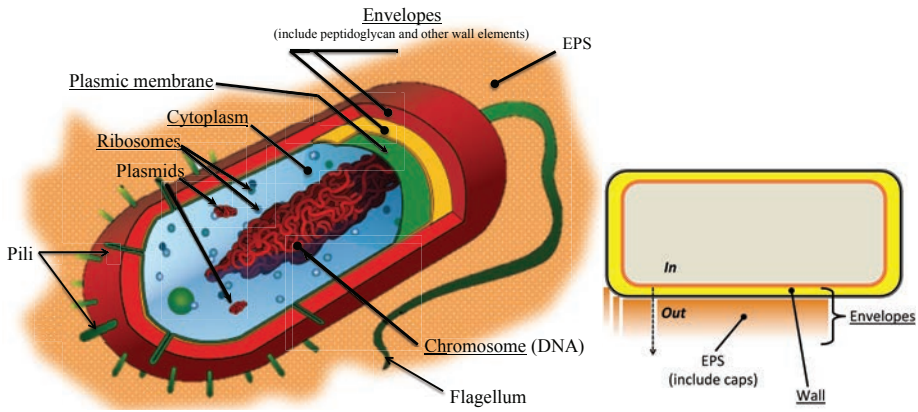


**Fig. 4.3.** – Cell structure of a bacteria. The mandatory elements are underlined. EPS means "extracellular polymeric substances".

### 4.4.1. Cytoplasm, the nucleoid, and inclusions

The cytoplasm is a slightly alkaline and hydrated gel (pH = 7.2-7.5). Roughly, it is the "compartment" containing all of the cell material: genomic DNA, other small nucleic acids, ribosomes, enzymes and metabolites; the cytoplasmic membrane delimits such compartments. Depending of the bacterial species, it includes diverse "inclusions": gaseous vacuoles, granules or diverse precipitates (polyphosphate, polycarbonate, sulphur, polyhydroxyalkanoate, glycogen, pigments, *etc.*), or protean assemblages use to store or sequester some elements such as bacterioferritine for iron[1].

[1] Iron can be stored to be used as a nutrient or captured to avoid adverse reactions with $Fe^{2+}$ such as Fenton-like reactions.

All of the material needed for the gene expression (from the gene to the protein) is included in the cytoplasm: ribosomes and small RNAs, and all enzymes involved in the transcription (synthesis of messenger RNA "mRNA", from a DNA sequencing) and translation (synthesis of a protein from the mRNA reading) processes. Ribosomes are small particles 25 nm in diam. where the protein synthesis occurs. The mRNA strings are read by the ribosomes to assemble, in a defined order, the amino acids constituting the protein encoded by the gene transcript on the mRNA. Since many proteins are essential enzymes for cell synthesis and energy conservation, the ratio of ribosomes is higher during the exponential growth phase (> 90% of the cellular RNA) than the stationary phase (< 20%) for *Escherichia coli*.

For bacteria, the nucleoid (the chromosomal DNA) is diffused into the cytoplasm; it is not included in a compartment such as the nucleus delimited by a nucleic membrane in the case of eukaryotic cells. Then, transcription and translation are two quasi-simultaneous processes; mRNAs are translated into proteins as soon as the DNA is transcribed in mRNA (mRNA doesn't need to cross a nuclear membrane or to be maturated as for eukaryotic cells). Consequently, bacteria can give a very quick response to any environmental changes (such as nutritive change) by a fast synthesis of the required proteins.

Finally, one of the specific features of bacteria is their great genetic plasticity, not only due to spontaneous mutations associated to their high growth rate. They are able to exchange genetic information horizontally (within a population from the same generation), using mobile genetic elements, extra-chromosomal DNA that can be easily duplicated and/or transferred to other cells that belong, more or less, to a close taxonomic group. There is a large diversity of tools or events involved in such genetic enrichment (*e.g.,* conjugative plasmids, transduction *via* bacteriophages, transposons) that will be not described here. This genetic plasticity can therefore explain how a survival factor (such as biocide resistance) can spread rapidly through a microbial population.

### *4.4.2. The cytoplasmic membrane*

The cytoplasmic membrane is built on the same pattern as for other cells of the living world, that is to say a double sheet of phospholipids 5 to 10 nm thick (Fig. 4.4). With its properties, it ensures the individuality of the cell compartment; generally, it is assumed the cytoplasmic membrane distinguishes the intracellular from the extracellular medium. The membrane is permeable to water, gases and small neutral molecules or any hydrophobic molecules, but is impermeable to any hydrophilic or charged solutes. The prokaryotic membrane distinguishes itself from other eukaryotes through the nature of the phospholipids and the high protein content (up to 70% of membrane dry mass). These proteins are involved in the selective transport of solutes and in major metabolic processes such as respiration or photosynthesis. To resume, the cytoplasmic membrane plays the role of a selective barrier, an essential part of the cell where central processes of the metabolism take place, mainly those linked with energy conservation.

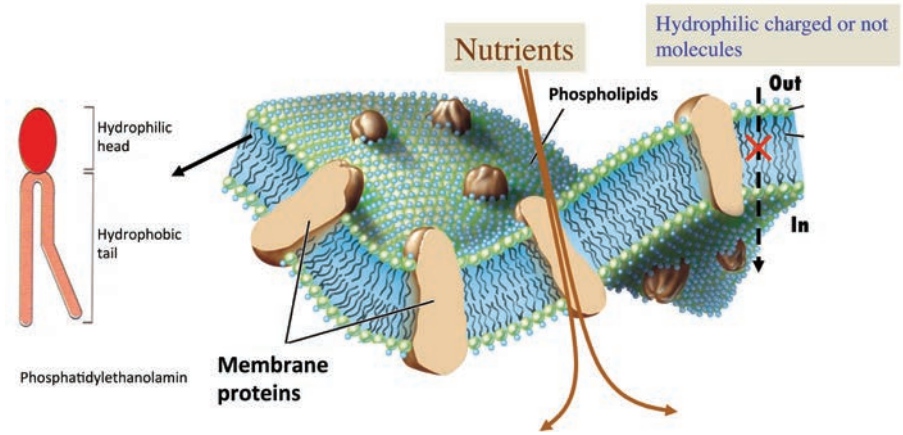


**Fig. 4.4.** – Schematic view of bacterial membrane.

Without going into details, membrane structures and composition can change drastically from one cell to another, depending on the physiological state and the taxonomic position and there is no a definite model for all types of bacteria. For *Archaea*, it can be really different, for instance, the membrane of the thermophile *Sulfolobus solfataricus* exhibits a monolayer of trans-membrane lipids [10].

### 4.4.3. Cell envelopes

At the cytoplasmic membrane periphery, there are the cellular envelopes (Fig. 4.3). Structures and composition of the envelopes can be very different from species to species, especially between *Archaea* and *Bacteria*. For *Bacteria*, the cell walls, except for some exceptions, are relatively constant structures permitting to split bacteria in two distinctive groups: the bacteria with a negative Gram's stain ($Gram^-$) or positive ($Gram^+$). They differ in both the cell wall structure (Fig. 4.5), inducing a different colour of the cell after a double-staining procedure and their phylogenetic position. For *Archæa* the great variability of the cell envelopes does not allow to categorize them in well define groups according to their cell envelopes and, even if the cells give a response to the Gram's staining, there is no evident analogy with the $Gram^+$ / $Gram^-$ cell wall structure.

The peptidoglycan is a heteropolymer found in nearly all species of the *Bacteria* kingdom (Fig. 4.6). Exception made of the nature of the carbohydrates and peptides that can change between species, its main structure is almost the same for bacteria. Several dozen polymeric layers of peptidoglycan can surround the cell; each strand can be as long as 50 nm. This polymeric structure mainly provides the cell with a mechanical protection against osmotic pressure forces. Thus, the pressure on the cells can reach 20 atm or 2-3 atm for $Gram^+$ and $Gram^-$ cells, respectively. For that reason, most of bacteria can easily withstand the high osmotic pressure induces by fresh water such as ultra-pure water (Table 4.1).

The peptidoglycan is also involved in the cellular shape. Finally, the peptidoglycan is a more or less thick layer around the cell, permeable to any solutes but strongly resistant; it has to be considered as a porous molecular mesh, like a coat of mail but not as a tin can (Fig. 4.6).

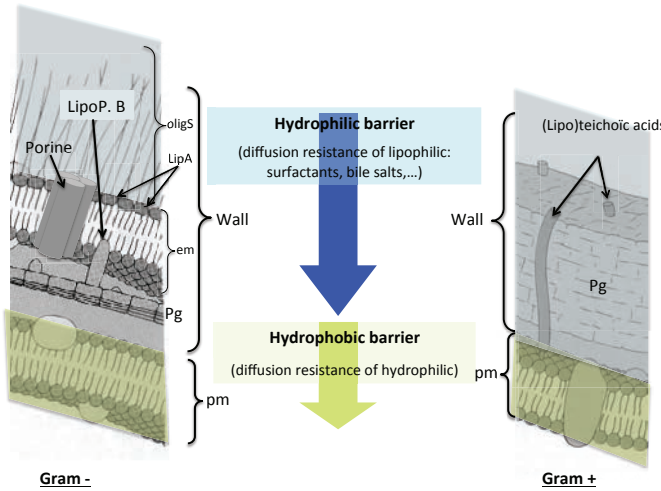


**FIG. 4.5.** – Cell walls of the negative Gram's stain (left) and positive Gram's stain (right). One analogy appears from these structure: the presence in both cases of a double barrier, one hydrophilic, constituted by polysaccharides or teichoic acids and a second, hydrophobic, constituted by plasmic membranes (pm). Both protect the cell against several chemical attacks. Pg = peptidoglycan, em = external membrane, oligS = oligosaccharides, LipA = lipid A, LPS = oligoS + LipA (lipopolysaccharide), LipoP.B = Braun's lipoprotein.

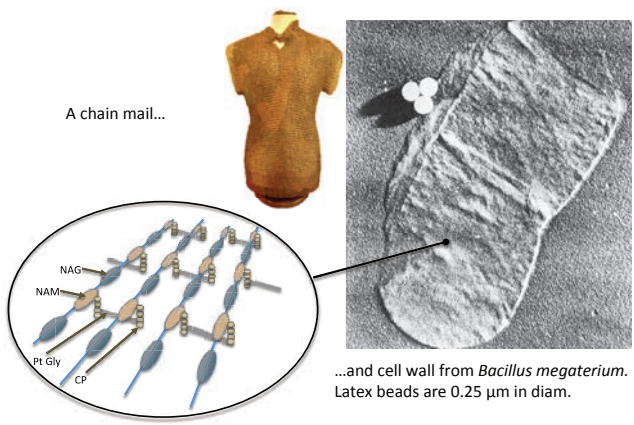


**FIG. 4.6.** – Molecular structure of the peptidoglycan (NAM = *N*-acetylmuramic acid, NAG = *N*-acetylglucosamine, CP = peptidic chain, Pt-Gly = interpeptidic bridge of pentaglycine) and scanning electronic microscopy picture of the cell wall of *B. megaterium*, isolated from the cell [11], and of a chain mail of medieval days.

Other constituents of the cell wall are firmly anchored into the cytoplasmic membrane or the external membrane for $Gram^+$ and $Gram^-$ cells, respectively. They are lipoteichoic acids or lipopolysaccharides, respectively. Such external polymers contribute to cell surface properties and can influence the adhesive properties. Based on this hydrophilic character, these external polymers can represent a barrier against lipophilic substances that could damage the cytoplasmic membrane (Fig. 4.5).

They are more external layers than the cell wall. Usually, these layers are regrouped under the generic term "extra-cellular polymeric substances" (EPS). For a long time such structures were more or less ignored by scientific community. Most probably because they were lost or not expressed during culture in rich medium but also because they are tenuous and highly hydrated, this making them difficult to evidence in electronic microscopy. Moreover, they were not resistant to aggressive treatments preceding the conventional sampling preparation for electronic observation (*e.g.,* dehydration by successive exposure to solvents). The use of sample preparation methods respecting the cellular structure integrity (*e.g.,* cryo-substitution) has help to reveal the bacterial cell surface ultrastructure and some of the EPS (Fig. 4.7). Thus, polymeric fringes of several hundred nanometers were evidenced giving a more accurate view of the thickness and diversity of bacterial cell envelopes [12]. Some of the external polymers are strongly attached to the cell and correctly define the "lookout" area of the cell. These types of polymeric materials constitute what is generally called the capsule. Others are more or less viscous and diffuse polymers, constituting slime all around the cell and where other cells can be encased. These kinds of EPS correspond to the famous polymeric matrix of the biofilm, previously called glycocalyx (Fig. 4.8). Although the EPS were assumed to be essentially polysaccharides, it is now well described that DNA, proteins and, humic-like substances contribute to the hetero-polymeric nature of the matrix.

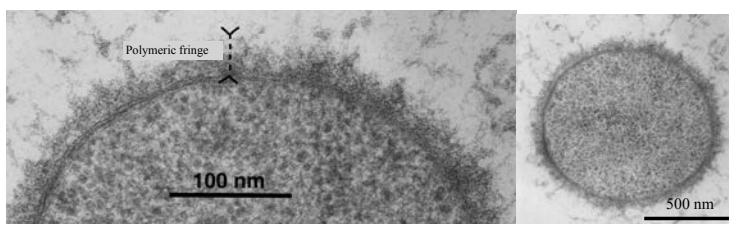


**Fig. 4.7.** – Transmission electron microscopy pictures of a cell of *Shewanella putrefaciens* CIP 80.40 illustrating ultrastructure of cell envelope where polymeric fringe is evidenced due to a sample preparation respecting the cell integrity (graciously from Dague E. and Korenevsky A.). The nature and thickness of the polymeric fringe can strongly differ from species to species and even from strain to strain [12], probably with a strong influence on the adhesive capacity of cells.

Cellular envelopes have several functions such as the mechanical protection to osmotic pressure mainly ensured by the peptidoglycan, the desiccation

resistance supported by exo-polysaccharides such as colanic acid for *E. coli*. As well, due to their chemical nature and positioning at the cell surface, envelopes are involved in the cell surface properties and contribute to the cell adhesion to various substrata. Bacteria are generally able to colonize various substrata, such as living or mineral surfaces. Physico-chemical as well as biological factors control the cell adhesion that can strongly be dependent on the cell appendages and nature of the polymers present at the cell surface.

Finally, the very structure of the bacterial cell envelope has led to consider the cells as soft particles whose thickness, elasticity, hydration and electrical charge considerably influence their properties in the aqueous phase. Taking into account these microbial specificities has completely upset the conventional approaches used until now (such as the famous DLVO theory) to model the mobility of bacteria in an electric field and predict their adhesion properties. Microbiologists and physico-chemists must now use these considerations to study the phenomena taking place at the interfaces between the bacterial cell and its external environment [13, 14].

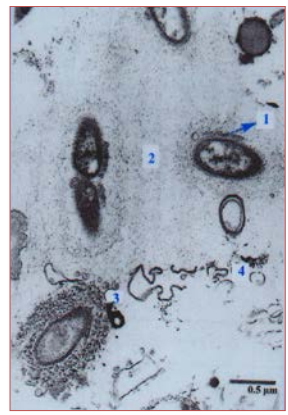


**FIG. 4.8.** – Transmission electron microscopy image of an activated sludge floc section showing bacterial cells embedded in mucoid (1, 2) or capsular (3) extracelluar polymeric substances (EPS) constituting the matrix of the aggregate. Some fragments evoke wall pieces (4) suggesting the presence of intracellular contents in the EPS matrix (from Bleich & Nehrkorn, 1989 [15]).

### 4.4.4. *Appendages, filaments and cytoplasmic extensions*

Some structures are filamentous proteins of varying thickness that are solidly anchored in the cytoplasmic membrane, which pass through the envelopes and can sometimes extend several tens of micrometers from the cell. Others are true membrane extensions and form tubes connecting to other cells or surfaces.

These structures are involved in the locomotion, adhesion and formation of the biofilm but also in the metabolism directly.

### 4.4.4.1. Pili and fimbriae

Two terms that generally refer to the same protein structures, although some authors prefer the term fimbriae to refer to the finest and most numerous pili on the surface of cells. It consists of protein fibres 3 to 10 nm in diameter that can be deployed up to several micrometers beyond the bacterial surface, and are distributed around the cell in the range ten to a thousand, depending on strains and physiological conditions. Most pili are equipped with adhesins at their extremities, which favour the specific attachment to surfaces like the "key-lock" system. They can also promote attachment to a non-specific manner surface, for example, due to the presence of hydrophobic amino acids at the extremity. In both cases, they allow the cells to come into contact with a surface while avoiding any significant electrostatic repulsion (Fig. 4.9). They are essential in the early stages of biofilm formation, namely the adhesion stage. They can function as real grapples for anchoring the cell to a surface (Fig. 4.9) [16]. Some pili, especially those of type IV, are retractable and even allow bacteria to move on the surface of their support or to form clusters together.

The curli, which are amyloid in nature, are pili and for enterobacteria are synthesized when the temperature is below 32 °C, a clear signal that the commensal bacterium is found outside its host and that it must develop survival mechanisms, such as forming a biofilm. Other types of pili, are involved in genetic transfers during conjugation. These "sexual pili" allow the donor bacterium to connect to a recipient bacterium, the DNA transfer will then occur.

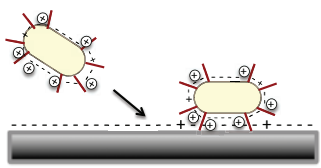

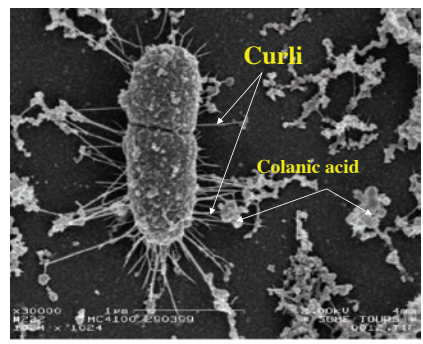


(Prigent-Combaret *et al*., 2000, *Environ. Microbiol*., **2**:450)

**Fig. 4.9.** – On the left, a diagram illustrating how the pili allow the cell to overcome the electrostatic repulsions. The energy required to pass through an electrostatic repulsion field is considerably lower for filaments or tip structures than for an entire cell. The cell makes contact *via* its pili at a distance where the repulsive fields between the surface and the cell are very small (adapted from Stafford & Wilson [17]). On the right, a scanning electron microscope image showing the curli stalking a cell (*E. coli*) (graciously from Lejeune Ph., © UMR 5122, CNRS-INSA, Lyon-Villeurbanne, FR).

### 4.4.4.2. Flagella

Flagella are other protein appendages that can equip bacterial cells. They are much larger and longer than pili, about 20 nm in diam. and several tens of micrometers long. According to the species, there is only one flagellum (*e.g.: Vibrio cholerae*, *Pseudomonas aeruginosa*, ...) or several per cell (*E. coli*, *Salmonella enterica*, ...), located at one or both extremities, even all around. In other cases, as in spirochetes, the flagellum is internal (in the periplasm in the axis of the cell) for optimal displacement in viscous medium. The main function of these flagella is therefore mobility; cells can reach speeds of the order of several tens of micrometers per second, which makes bacteria, proportionately to their size, the fastest locomotor organisms in the living world. Other bacteria can literally glide over the surface of a solid and completely invade the surface of an agar plate that makes it impossible to isolate other bacterial strains. This phenomenon is common to the *Proteus* genus.

Typically, a chemo-physical gradient, or light, directs the swimming of bacteria. For *E. coli*, the chemotaxis is said "positive" with glucose, meaning the bacterium swims from a less concentrated towards a more concentrated solution of glucose. For *Geobacter metallireducens*, it can swim in a ferrous gradient and then go to the main source: a solid made of iron oxides that the cell can colonize and use as electron acceptor (Fig. 4.10) through conductive pili [18].

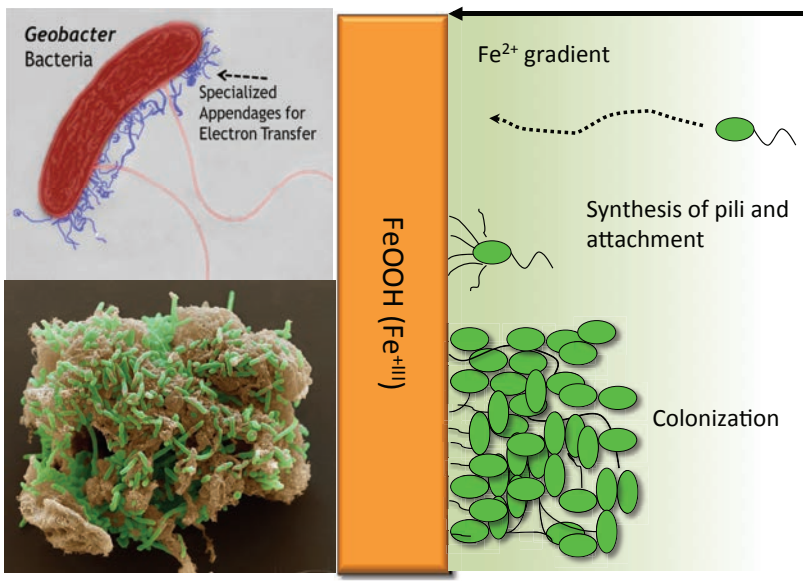


**FIG. 4.10.** – Top left: *Geobacter metallireducens* with its two flagella (pink) and its conductive pili (blue) (courtesy of Derek Lovley, Umass, Amherst, MA), bottom left: cells of *G. metallireducens* colonizing a particle of iron oxide and right schematic representation of the chemotaxis of this bacterium.

### 4.4.4.3. *Bacterium, a connected cell*

If we consider that the bacterial cells develop in the form of aggregated communities, close to each other, it comes as no surprise that they have developed several strategies to strengthen and exploit this contact by constituting a network of filaments such as: nanowires for the electron transfers [19], nanotubes as a nanopipe network [4, 20] through membrane extensions for inter-cytoplasmic exchanges of nutrients and electrons, or a real rope of flagella or pili keeping them close to each other [21, 22] (Fig. 4.11).

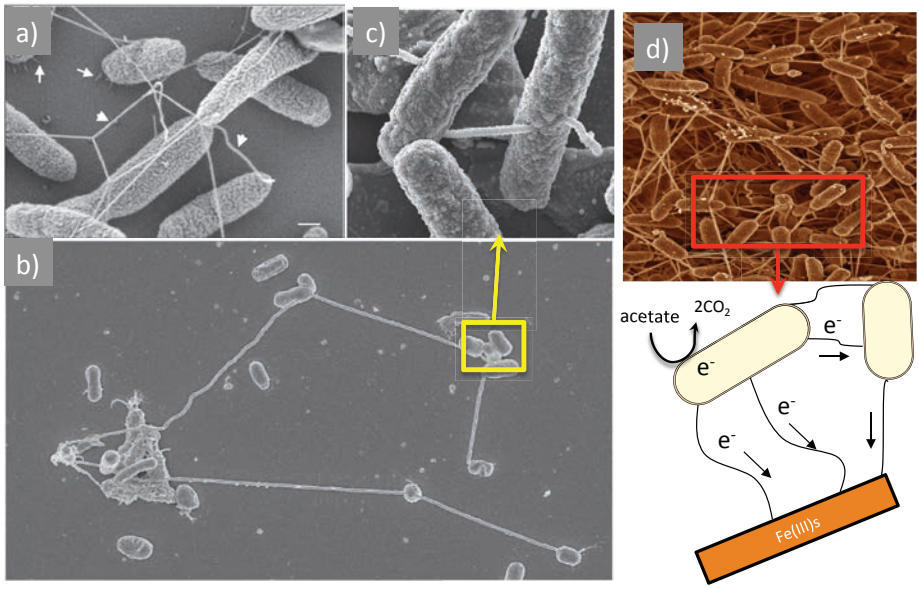


**Fig. 4.11.** – Some networks connecting bacterial cells: a) network of flagella intertwining *Stenotrophomonas maltophilia* cells on the surface of a polyvinylchloride support [22]; b) and c) projections of the cytoplasmic membranes forming channels through which various nutrients are transported between *Escherichia coli* and *Acinetobacter baylyi* [4]; and d) nanowire networks between cells of *Shewanella oneidensis* MR-1 biofilm (photo by Rizlan Bencheikh and Bruce Arey). The bottom draw illustrates the electron transfers *via* conductive nano-cables.

The mechanisms on which all these connections are based are not yet fully understood, but they indicate a level of sophistication hitherto unsuspected in the physical relations between bacterial cells. The use of inter-membrane connections (or connection to solid support) or inter-cytoplasmic connections, would allow bacterial communities of biofilm to exchange nutrients (amino acids, vitamins, ...) and electrons with a greater efficiency than if the transfers were to be extra-cellular by diffusion.

## 4.5. Metabolism in bacteria

Like any other organism, a bacterium constantly performs biosynthesis with the aim of achieving reproductive success (non-sexual and essentially by cell division in bacteria). This process intensively requires energy and a constitutive element that has to be found by the cell in its environment. Obviously, the mechanisms to obtain energy and to convert elemental nutrients into new cellular material, are very complex and involve a set of perfectly regulated reactions involving biochemical components essential for the functioning of metabolic pathways, such as enzymatic cofactors and enzymes. We will obviously not go to this level of complexity here. To summarize and make the principle of metabolism and the functions played by its different actors comprehensible, we propose a trivial metaphor where the synthesis of a new cell is similar to the construction of a house (Fig. 4.12). The chemical species providing the major constitutive elements (carbon, nitrogen, phosphorus and sulphur), the enzymatic cofactors and the enzymes involved in the cell growth correspond to the building blocks, to the working tools that allow the mason to assemble blocks, respectively.

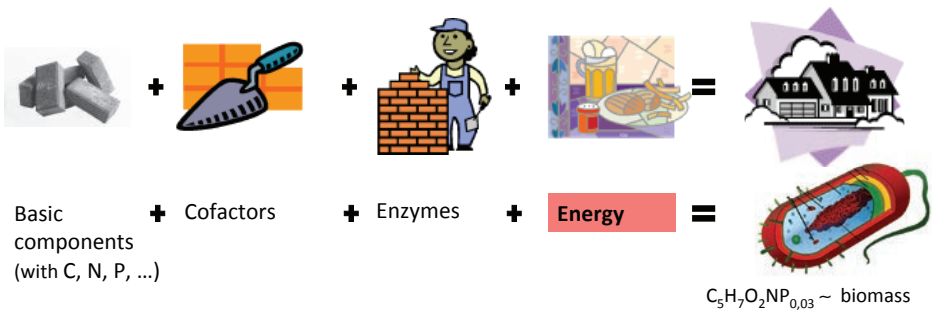


**FIG. 4.12.** – A metaphor for cell metabolism.

And what about the energy? For the mason, daily meals provide his energy. For the cell, the energy source is either chemical (chemotrophic bacteria) or light (phototrophic bacteria). For both, it is an electron flow that the cell converts into available cellular energy: mainly ATP (adenosine triphosphate). For chemotrophs this electron flux is a product of exergonic reactions catalysed by the cell (*e.g.* glucose oxidation into $CO_2$ by $O_2$). For phototrophs, this flux comes from endergonic reactions made possible due to the input in light energy (*e.g.*, the water photolysis by photosynthesis provide electron-equivalents). Finally, the metabolism consists of two parts: anabolism that includes the biosynthesis involved into the cell growth and catabolism that includes all energy conversion reactions into cellular energy (ATP equivalent) (Fig. 4.13).

The basic principle of the bacterial bioenergetics does not differ, roughly speaking, to any other cells of the world life. Depending of the species and their

environment, bacteria differ from other cells by the wide diversity of the metabolic pathways they have; they benefit from a large set of electron acceptors or donors. The nature of the "elementary bricks" (chemicals bearing nutritive element) they are able to assimilate is also very extensive (Fig. 4.13). For example, nitrogen is always included in the biomolecules in the form of ammonium that bacteria obtain mainly from amines but also from nitrate, nitrite or di-nitrogen. Some species can simply make use exclusively inorganic compounds to meet their energy and nutrient needs, even in the absence of light.

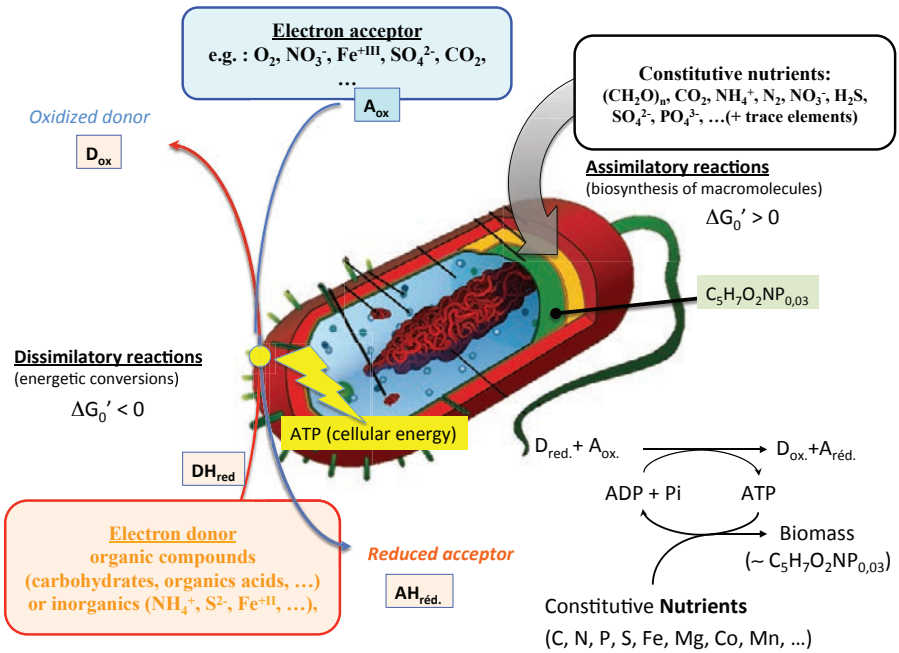


**Fig. 4.13.** – Cell metabolism with dissimilatory reactions (left) involved in energy conservation, and assimilatory reactions (top right) where nutrients are fixed in the cell to constitute the bio-molecules for the new cells. $DH_{red}$ and $D_{ox}$ = electron donor reduced and electron donor oxidised, respectively; $A_{ox}$ and $AH_{red}$ = electron acceptor oxidised and electron acceptor reduced, respectively. The energy delivered by dissimilatory reactions (exergonic redox reactions, $\Delta G^{0'} < 0$) is converted into cellular energy (ATP) that supplies the assimilatory reactions (endergonic reactions, $\Delta G^{0'} > 0$) for cell synthesis. When the electron donor is organic (*e.g.*, acetate) or inorganic (*e.g.* $NH_4^+$), the trophic group is named organotrophic and lithotrophic, respectively. As regards to the carbon source, it is named heterotrophic and autotrophic for an organic and inorganic (essentially $CO_2$) carbon source, respectively.

This flexibility and diversity of metabolisms suggests a multitude of chemical reactions to which bacteria are able to participate. We are going to review some of the noticeable metabolism groups that might be involved in biocorrosion processes.

### 4.5.1. Aerobic respiration of chemoorganotrophs

Respiration of di-oxygen coupled with the oxidation of an organic compound is a very profitable process because it involves an oxidant and a reducing agent exhibiting a great difference between the potential ($E_h°'$) [2] of the two redox couples ($E_h°'(O_2/H_2O)$ = +0.82 V and $E_h°'(CO_2/CH_2O) < \sim -0.3$ V, respectively; thus a difference ($\Delta E_h°'$) > 1.1 V), allowing a potentially high production of ATP. Single oligosaccharides are degraded in short organic acids through complex metabolic pathways (glycolysis, pentoses-phosphates and Entner-Doudoroff pathways). A low ATP can be produced through these ways by "substrate-level phosphorylation" where ATP is produced from a direct transfer of a phosphoryl group to an ADP (adenosine di-phosphate). In that case, ATP formation is not coupled to oxidation. The complete oxidation of the small organic acids with 2 or 3 C (pyruvate, acetate) then takes place through metabolic pathways such as the Krebs cycle (tricarboxylic or citric acid cycle). Two cycles are needed to oxidize completely one equivalent glucose molecule. The electrons released are carried by co-factors that can accumulate into the cytoplasmic space (*e.g.,* $NADH,H^+$ or $FADH_2$). They release their electrons when they are oxidized through a complex cascade of redox reactions between membrane proteins and quinones localized in the cytoplasmic membrane. This group of proteins with enzymes and quinones constitute the respiratory chain. At the end of the respiratory chain, the final acceptor, $O_2$ in that case, diffuse into the cytoplasm and is reduced to $H_2O$ when it received electrons from the respiratory chain. During these reactions, variable amounts of protons undergo a translocation on both sides of the membrane leading to so-called "oxidative phosphorylation" of ADP into ATP. Briefly, the accumulation of protons on the outer face of the membrane creates a so-called "proton-motive force" or electrochemical potential (from the difference in $E_h$ and pH each side of the membrane), which tends to bring the protons back into the cytoplasm. A single pass is possible for a proton to come back: through the molecular turbines named ATPases. They allow the formation of one ATP for two to three protons. The energy efficiency could be high and can reach 40% according to the free energy of the glucose when it is the electron donor.

Aerobic respiration is used by several chemo-organotrophic bacteria and occurs for the main of eukaryotic organisms. However, it is entirely dependent on organic matter as carbon and electron source. Consequently, they are dependent on the autotrophic organisms, which are the primary producers, those that convert $CO_2$ into organic matter, belonging to the litho-autotrophic group, using both an inorganic source for carbon assimilation and energy conservation.

[2] $E_h°$ is the standard electrode potential at pH 7 compared with hydrogen.

### 4.5.2. Aerobes chemolithotrophs

Without light, chemolithotrophic groups are found only in bacteria, that is to say, those using inorganics as electron donors. In the general case, and except for $H_2$, the oxidation of inorganic compounds by other than $O_2$ does not allow producing large enough energy to give ATP. Oxidized species of nitrogen (essentially nitrate and nitrite) could be used as oxidants for some lithotrophs, however the very existence of these metabolic groups remains questionable, as discussed below.

#### 4.5.2.1. Hydrogenotrophy

Dihydrogen ($H_2$) is a gas usually produced during anaerobic aqueous corrosion of iron. $H_2$ is also a frequent by-product of the fermentative metabolisms taking place in nutritionally rich anaerobic environments and is a common electron donor for many bacteria. For all that, it's a facultative source of electrons because the major part of hydrogenotrophic bacteria can use other organic or inorganic electron sources. For organotrophic bacteria, $H_2$ could save organic carbon resources; by preventing the engagement of organic carbon in dissimilatory pathways the carbon resource can be only used for assimilation. For lithotrophs, $H_2$ may represent an alternative electron donor in the absence of the "traditional" donor[3]. The electrons provided from $H_2$ pass through a respiratory chain *via* membranous hydrogenases or are used by cytoplasmic hydrogenases for $CO_2$ fixation in autotrophic bacteria.

#### 4.5.2.2. $Fe^{II}$ oxidation

Sergei Winogradsky, in the early 20$^{th}$ Century, was the first to describe the use of ferrous iron as an electron donor and $CO_2$ fixation by iron-oxidising bacteria with *Gallionella ferruginea*. Much later, it was shown that this strain has a mixotrophic growth [35]: it can switch between organotrophic and lithotrophic growth as regards to nutrient availability. Due to the instability of $Fe^{2+}$ under aerated neutral pH media, it is not surprising that bacterium such as *Acidithiobacillus ferrooxidans* (Fig. 4.14), are found under acidic environments ($pH < 4$) where $Fe^{2+}$ can be much more abundant than elsewhere. With neutral pH, other species are found that are localized at the oxic-anoxic interfaces, like *Gallionella* sp., where the $O_2$ level is too weak to react with $Fe^{2+}$, according to an abiotic reaction, and not compete with iron bacteria. The cellular energy from ferrous species oxidation coupled to $O_2$ reduction, is relatively low; the oxidation of a large amount of ferrous iron is then required to meet with the growth needs. In circumneutral pH environments, bacteria control the $Fe^{3+}$ precipitation, as *Mariprofundus ferrooxydans* or *Galionella ferruginea*, by producing fibrous polysaccharides promoting the arrangement and extrusion of ferric irons into

[3] But that may be the opposite, $H_2$ could act as the "traditional donor"

twisted stalks [23]. Then, massive precipitates of iron, relatively to the cell biomass, are found in natural or anthropized environments at the air-water interface for ferruginous groundwater. In water industry, this bacterial activity can be responsible of the massive brown-orange deposits of ferric iron that contribute to clogging filters in ground water treatments.

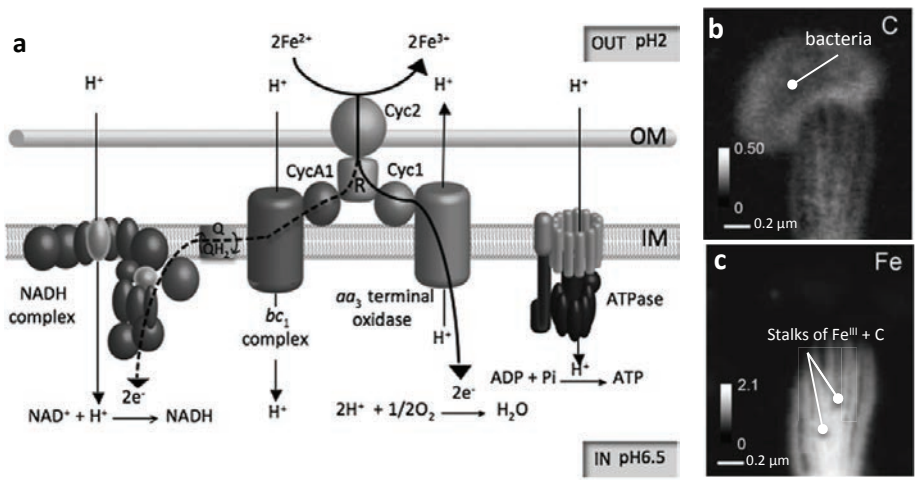


**FIG. 4.14.** – Respiratory chain for *Acidithiobacillus ferrooxidans* (a) and iron oxide stalks outside the bacterial cell (*Mariprofundus ferrooxydans*) (b and c). The $Fe^{2+}$ species are oxidized in $Fe^{3+}$ in the extracellular medium ("OUT"), while $O_2$ is reduced into the cell ("IN"). The natural habitat for *Ac. ferrooxidans* is generally acidic where $Fe^{3+}$ remains soluble. The ferrous species are oxidized in the external area of the cell; it cannot precipitate within the cytoplasm because at neutral pH $Fe^{3+}$ precipitates which would affect the cell integrity. For *M. ferrooxydans*, living in microaerobic niches at neutral pH, ferrous iron is oxidized in solid ferric compounds in the extracellular space. To avoid being encrusted by the large amount of ferric precipitates, the ferric stalks formation is induced by polysaccharides that form an iron oxide tail of several dozen of micrometers in long. The electrons from $Fe^{2+}$ are used to give NADH equivalent need for the $CO_2$ assimilation (a from [24]; b and c from [23]). IM = plasmic membrane, OM = outer membrane.

### 4.5.2.3. Oxidation of sulphur species

The reduced species of sulphur as hydrogen sulphide ($H_2S$), elemental sulphur ($S^\circ$) or thiosulphate ($S_2O_3^{2-}$) are potential electron donors for some acidophilic bacteria. Their oxidation can lead to the sulphuric acid ($H_2SO_4$) production. Among those bacteria, some are able to grow up for very low pH (pH < 1).

#### 4.5.2.4. Oxidation of nitrogen species

Ammonium ($NH_4^+$) and nitrite ($NO_2^-$) are nitrogen species serving as electron donor for a metabolic group that is of a major importance for agronomy and for biological wastewater treatment processes: the nitrifying bacteria. Actually, this group contains two distinct metabolic group of bacteria but that they usually work together: the ammonia-oxidizing bacteria and the nitrous-oxidizing bacteria that catalyse the oxidation of ammonia to nitrite and the oxidation of nitrite to nitrate, respectively. Together, these bacteria enable the nitrification process, the oxidation of ammonia to nitrate. They are microaerophilic and exhibit a relative metabolic flexibility, as *Nitrospira moscoviensis*, that become hydrogenotrophic with nitrite exhaustion [25]. Nitrifying bacteria are frequently growing close together; nitrous-oxidizing bacteria being fed by the by-product ($NO_2^-$) of ammonia-oxidizing bacteria, both benefits each other.

### 4.5.3. The anaerobic respirations

The respirations of further electron acceptors than $O_2$ are termed anaerobic respirations. Indeed, a large diversity of electron acceptors can be used by bacteria and for some of them, this ability, to take advantage of diverse electron acceptors, can be achieved by a given bacterial species or strain. One of the most documented genus with such faculty is *Shewanella* (Table 4.2).

**Table 4.2.** – Respiratory capacities of *Shewanella* spp. (modified from DiChristina, [26]).

| Electron donors | Electron acceptors |
|---|---|
| Organic acids | Oxygen [$O_2$] |
| Amino acids | Nitrogenic compounds [$NO_3^-$, $NO_2^-$, NO] |
| Carbohydrates | Manganese oxides [$Mn^{4+}$, $Mn^{3+}$] |
| Di-hydrogen | Iron oxides [$Fe^{3+}$] (ferrihydrite, lepidocrocite, goethite, magnetite, hydroxycarbonate green rust, feroxyhite,...) |
| | Sulfur compounds [$SO_3^{2-}$, $S_2O_3^{2-}$, $S^o$, DMSO] |
| | Uranyle compounds [$U^{6+}$] |
| | Technetium ions (pertechnetate) [$Tc^{7+}$] |
| | Selenium oxyanions [$Se^{6+}$, $Se^{4+}$] |
| | Trimethylamine-*N*-oxide [TMAO] |
| | Fumarate |
| | AQDS (anthraquinone disulfonate) and humic substances |
| | Other: arsenate, chromate, vanadate, neptunium (+V), deaminated histine, phenazines, ... |

Bacteria belonging to *Shewanella* adapt their respiratory chain to the most profitable electron acceptor, in regard to its redox potential $E_h^{\circ\prime}$ value. According

to the Nernst relation, the difference between the acceptor and donor $E_h°'$ couples and their relative concentration determines the energy amount expected to be released from the redox reaction between the oxidant and the reducer. Thus, at equimolar concentrations, the oxidant of the highest redox couple potential $E_h°'$ reacts with the reductant of the lowest redox couple. Any bacteria will gain significant advantage by being able to respire sequentially the electron acceptors of the highest $E_h°'$ couple. To sustain such an advantage, the genes involved in the expression of a given anaerobic respiratory chain, are generally repressed by the oxidants of the redox couple having a higher redox potential. Thus, $O_2$ ($E_h°' = +820$ mV) tends to repress the genes involved in the respiratory chain for the nitrate ($E_h°' = +713$ mV), and nitrate tends to repress genes for the $Fe^{III}$ respiration ($E_h°' < 100$ mV). This strategy allows bacteria to exhaust the most interesting oxidant before using the latter one. Consequently, chemical stratifications within biofilms or within a water column are frequently the result of bacterial activities. Finally, bacteria, including all species, are able to use oxidants from $O_2$ to $CO_2$. Carbon dioxide is the acceptor that has the lowest redox potential that can be respired by bacteria ($E_h°'$ ($CO_2/CH_4$) = –0.24 V) (Table 4.3); $CO_2$ respiration concerns only the methanogen's archaea. The three main anaerobic respirations expected to be involved in the iron biocorrosion are: nitrogen respiration, $Fe^{III}$ respiration and sulphate respiration.

### *4.5.3.1. Respiration of nitrogen species*

The chemical species in the nitrogen cycle that can be dissimilatory reduced (respiration) are: nitrate ($NO_3^-$), nitrite ($NO_2^-$), nitric oxide (NO), nitrous oxide ($N_2O$), and di-azote ($N_2$) the ultimate products from those nitrogen respirations. The term denitrification is used when nitrogen oxides results in a nitrogen gaseous phase as $N_2O$ or $N_2$. Some microorganisms can be thus considered as "false denitrifiers" because they do not carry out all reactions of denitrification. For instance, *E. coli* reduces nitrate to nitrite but does not reduce nitrite; *Wolinella succinogenes* reduces only $N_2O$ in $N_2$, while many others bacteria are fitted with the totality of the enzymes needed for the denitrification, such as *Paracoccus denitrificans* or *Pseudomonas aeruginosa* able to produce $N_2$ from nitrate (Fig. 4.15). At each stage of the denitrification process, the products resulting from the nitrogen species reduction are excreted to extracellular medium where they can in turn be used as electron acceptor (Fig. 4.15). Those full denitrifiers are intensively used in the field of biological water treatment. Among the reactive intermediates, nitrite is a very reactive and toxic chemical. For that reason, the cells have specific transport systems to rapidly excrete nitrite as soon is produced (Fig. 4.15).

The high reactivity of nitrite make them able to oxidize, without enzymatic catalysts, various reduced compounds such as $Fe^{II}$ bearing minerals.

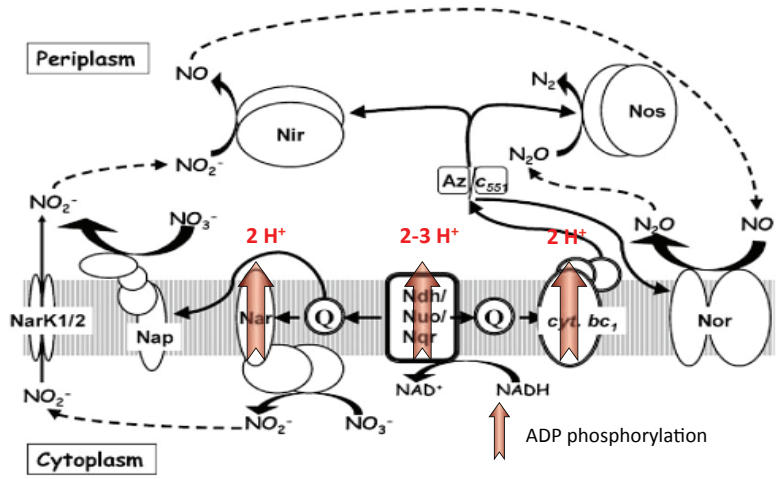


**Fig. 4.15.** – Respiratory pathways of denitrification for *Pseudomonas aeruginosa* with NADH as reductant co-factor. Nuo = NADH quinone oxydo-reductase I; Ndh = NADH quinone oxydo-reductase II; Nqr = $Na^+$ NADH quinone oxydo-reductase translocative; Q = quinone; Nar = membrane nitrate reductase; Nir = nitrite reductase; Nap = periplasmic nitrate reductase; Nir = nitrite reductase; Nos = nitrous oxide reductase; Nor = nitric oxide reductase; NarK1/2: nitrate/nitrite antiport; Az = azurine, c551 = cytochrome c551. The efficiency of the oxidative phosphorylation (ATP production) with nitrate is ~ 70% that on $O_2$ (6-7 protons/$O_2$ compared with 4-5 protons/$NO_3^-$, $NO_2^-$, NO or $N_2O$ and by NADH). Nap would have a role in aerobic denitrification (adapted from Williams *et al.* [27]).

### *4.5.3.2. Respiration of ferric species and other metallic species*

The anaerobic respiration of iron oxides by bacteria was discovered by the end of the 20th century. The resulting metabolic group actually went unnoticed before probably because the culture media used favoured some fermentative bacteria rather than anaerobic respiratory ones and because among fermentative bacteria, some are able to fortuitously reduce $Fe^{III}$. With iron respiring bacteria, the most significant novelty is the ability to respire a solid form of electron acceptor. The reduction must be carried out in the extracellular part of the cell because de the solid form cannot be internalized.

The exact mechanisms of reduction of a solid electron acceptor remain complex and have mobilized a lot and still mobilize the researchers. To resume, four mechanisms remain [28]: i) the transfer of electrons by a direct contact between surface proteins and iron oxide, ii) the electron transfer *via* conductive appendages, named nanowires, type IV pili or outer membrane extensions, iii) endogenous (*e.g.* flavine) or exogenous *(e.g.,* quinone, humic substances) electron shuttle that can diffuse from the bacterial cell to the iron oxide, and

iv) the inter-bacteria species electron transfer *via* semi-conductive iron oxides such as magnetite. In all cases, the electrons must cross the envelopes to reach the outer of cell. The most studied bacterial genus with such mechanisms are *Geobacter* and *Shewanella*, belongs to the δ-*proteobacteria* and γ-*proteobacteria*, respectively. The ability to respire iron is nevertheless well distributed in all groups of the phylogenetic tree, which is consistent with the idea that the first chemical form respired by bacteria are $Fe^{III}$ species, with $O_2$ appearing in the atmosphere after the major oxidizing event [29].

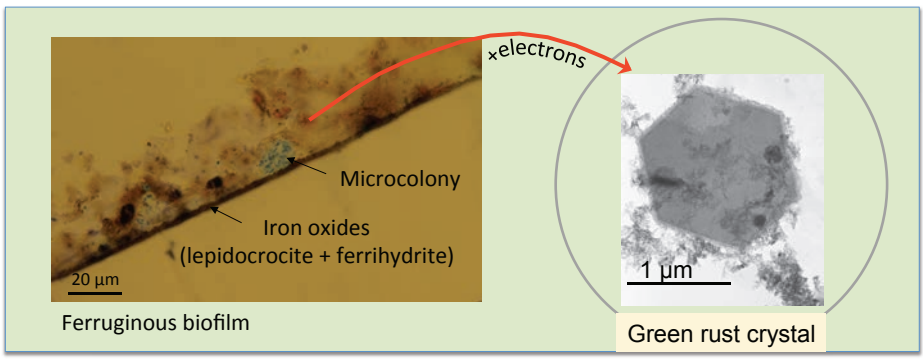


**FIG. 4.16.** – The biofilms could promote the formation of the $Fe^{II}$-bearing minerals green rust by the presence of a locally high cell density and polymeric materials stabilising the green rust crystals. The green rust crystals are produced here after incubation of ferruginous biofilm materials supplemented with organic electron donors in anaerobic conditions [31].

Once reduced, the iron is found in $Fe^{II}$ form which precipitates into different ferrous or ferrous-ferric minerals and whose properties of solubility and reactivity are variable. Ferrous carbonate as chukanovite ($Fe^{II}_2(OH)_2CO_3$) and siderite ($Fe^{II}CO_3$), mixed $Fe^{II}$-$Fe^{III}$ oxides as magnetite ($Fe^{II}Fe^{III}_2O_4$) are relatively stables while hydroxycarbonate ($Fe^{II}_4Fe^{III}_2(OH)_{12}CO_3$) or sulphate ($Fe^{II}_4Fe^{III}_2(OH)_{12}SO_4$) green rusts are metastable and exhibit a relatively high solubility. These are all secondary minerals that can be derived from microbial respirations but it is unclear to what extent bacteria direct the formation of a particular mineral. However, it has been shown that bacterial polymers influence the formation of green rust rather than magnetite [30] and that biofilms may represent favourable sites for the precipitation of these minerals [31] (Fig. 4.16), which are otherwise known as iron corrosion products [32].

Iron respiring bacteria are often able to reduce other compounds like metallic species such as $Mn^{IV}$, $U^{VI}$, or selenium oxides. Finally, the demonstration of the ability of bacteria to give up their electrons to solids has opened up a whole field of research in the field of bioelectrochemistry, where bacteria transfer, or even accept electrons, to or from electrodes [33].

### 4.5.3.3. Respiration of chemical sulphur species

Sulphate is relatively abundant in aquatic systems such as marine environment or groundwater. It can serve as electron acceptors under anaerobic conditions. The sulphate respiring bacteria are named sulphate-reducing bacteria (SRB). SRBs produce hydrogen sulphide ($H_2S$) that has the characteristic smell of rotten eggs, at low concentration, but which becomes toxic, for humans, and odourless at a higher dose. SRBs are probably, with iron bacteria, the most known bacteria to be involved in the biocorrosion of iron-based materials. Elemental sulphur ($S^0$) and thiosulphate are other sulphur species that can be respired by SRB and thiosulfate-reducer bacteria (TSRB), respectively. Thiosulfate is reduced to produce sulphate and $H_2S$ by disproportionation.

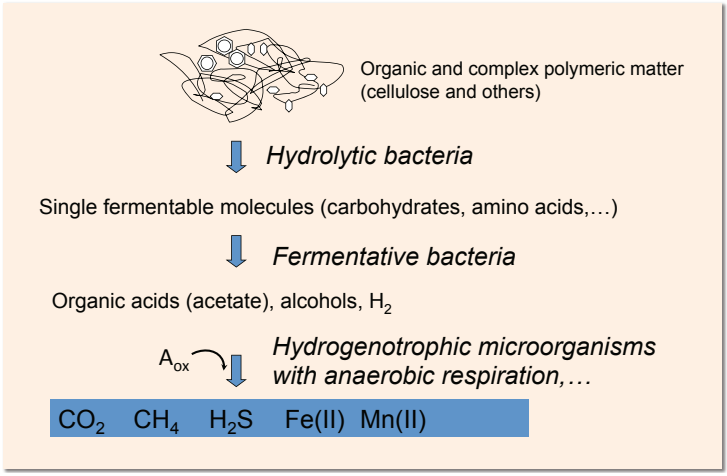


**Fig. 4.17.** – A bacterial food web.

## 4.5.4. Fermentations

Fermentations are catabolic pathways other than respiration that allow bacteria to quickly obtain some of the energy contained in organic molecules. Briefly, molecules were degraded into smaller molecules without use of external electron acceptors. Energy conservation is provided only by substrate-level phosphorylation and not from transmembrane proton transfer (proton motive force, or oxidative phosphorylation). Thus, fermentative bacteria does not need an external oxidant to conserve energy although, during the fermentations, there are oxidation and degradation steps of the substrate, but the resulting intermediates, mainly pyruvate, are re-oxidized to by-products excreted in the external environments. Many industrial applications, sometimes ancestral such

those for food conservation, are based on the nature of these by-products. They are in general short organic molecules (*e.g.,* carboxylic acids and alcohols, issued both and without $CO_2$ and $H_2$), which remain a significant source of energy for many other metabolic groups such as those with anaerobic respiration pathways. Some bacteria only have fermentative pathways to get energy; these pathways for others are optional and operate only in the absence of $O_2$.

Fermentations take place in anoxic environments rich in organic matter and, although their energy yield is low, fermentative bacteria generally dominate non-fermentative anaerobic respiring bacteria. Indeed, the simplicity of the fermentative metabolic pathways makes the cells a faster substrate metabolization. The fermentative by-products remain rich in energy, while respiratory microorganisms need complex and "time-consuming" metabolic pathways to take advantage of the energy remaining in the fermentative wastes. For that reason, some authors assume that fermentative bacteria are "selfish" because they do not give the community time to share the resource; the others (respiratory bacteria) are called "altruistic" because they gradually deplete the resource, leaving time for all the others to access and make use of it [34]. A somewhat anthropomorphic way to represent the microbial world and to see a socialization of the bacterial community. The result, however, is that metabolic groups organize themselves according to the availability of nutrients (and/or electron acceptors), and according to the waste produced by each other. A true prokaryotic trophic network can then occur, as illustrated in figure 4.17. As shown above, the bacteria can be responsible of a real physico-chemical stratification that can be seen both at the scale of a biofilm and a water column of several hundred meters in depth. It is mainly the availability in electron acceptor that will condition the installation of physicochemical gradients.

### 4.5.5. Stratification and spatiometabolic structuration, syntrophy

Substrates and electron acceptors govern the organization of microbial metabolic groups in a defined environment. As reported above, the respective $E_h°'$ values for electron donor and acceptor, controlling the amount of energy conserved from respiration, the bacterial colonization of a layer (in a water column or in a biofilm) will follow the electron acceptors the bacteria can metabolize and exhibiting the greatest $E_h°'$. Priority $O_2$, then nitrate, manganese, ferric oxides, *etc.* according to the $E_h$ of redox couples (Table 4.3). Thus, microbial activities create and sustain physicochemical gradients in several habitats. Such gradients are seen along the freshwater or marine water columns, such as Lake Pavin (France) [28] or the Black Sea, but also at much smaller scales such as sediment or within a biofilm (Fig. 4.18). Finally, biogeochemical cycles take place; a same element can be found under several speciation, as a respiratory metabolism by-product from one metabolic group or as an electron donor for another one. For example, $Fe^{III}$ is reduced by iron respiring bacteria to $Fe^{II}$ that can be used as electron donor for iron-oxidizing bacteria. Once produced

aqueous forms of $Fe^{II}$ can diffuse until aerobic or micro-aerobic environments where iron bacteria take it.

**Table 4.3.** – Some chemical reactions catalysed by bacterial metabolic groups. The redox potential are those of the oxidant couple. Acetate is given as a model for organic electron donors (data from [35] and [36]).

| Reactions | Chemical equation | $\Delta G°'$ (kJ mole$^{-1}$) or $E_h$ (*pH 7*) |
|---|---|---|
| ***Aerobic respirations*** | | $E_{h(O_2/H_2O)} = +820$ *mV* |
| Organotrophic respirations: | $CH_3COO^- + 2O_2 = H_2O + 2CO_2 + OH^-$ | –850<br>$E_{h(CO_2/acetate)} = -290$ *mV* |
| Lithotrophic respirations: | | |
| $H_2$ oxidation | $H_2 + ½O_2 = H_2O$ | –270 |
| $Fe^{II}$ oxidation | $Fe^{2+} + 2H^+ + ½O_2 = 2Fe^{3+} + H_2O$ | –32.9 |
| $H_2S$ oxidation | $H_2S + 2O_2 = SO_4^{2-} + 2H^+$ | –798 |
| $NH_4^+$ oxidation | $NH_4^+ + 3/2O_2 = NO_2^- + 2H^+ + H_2O$ | –272 |
| $NO_2^-$ oxidation | $NO_2^- + ½O_2 = NO_3^-$ | –73 |
| ***Fermentations*** *(on glucose)* | | |
| Homolactic | $C_6H_{12}O_6 = 2CH_3CHOHCOO^-$ | –198 |
| Alcoholic | $C_6H_{12}O_6 = 2CH_3CH_2OH + 2CO_2$ | –236 |
| Heterolactic (...) | $C_6H_{12}O_6 = CH_3CHOHCOO^- + CH_3CH_2OH + CO_2$ | –177 |
| ***Anaerobic respirations*** (organotrophic on acetate) | | |
| Denitrification | $CH_3COO^- + 1.6NO_3^- = 0.2H_2O + 2CO_2 + 0.8N_2 + 2.6OH^-$ | –801 *(+713 mV)* |
| $Mn^{+IV}$ respiration | $CH_3COO^- + 4MnO_2 + 3H_2O = 4Mn^{2+} + 2HCO_3^- + 7OH^-$ | –558 *(+380 mV)* |
| $Fe^{+III}$ respiration | $CH_3COO^- + 8\gamma FeOOH + 15H^+ = 8Fe^{2+} + 2HCO_3^- + 12H_2O$ | –337 *(–88 mV)*[1] |
| Sulfate respiration | $CH_3COO^- + SO_4^{2-} = HS^- + 2HCO_3^-$ | –48 *(–230 mV)* |
| Methanogenesis | $CO_2 + 4H_2 = CH_4 + 2H_2O$<br>$CH_3COO^- + H_2O = CH_4 + HCO_3^-$ | –139 *(–240 mV)*<br>–31 |

[1] The $E_h$ values can change from –314 mV (magnetite $Fe_3O_4/Fe^{2+}$) to +385 mV (ferric citrate/$Fe^{2+}$), and until +770 mV for $Fe^{3+}/Fe^{2+}$ but at circumneutral pH the trivalent forms of iron are in solid phase, $Fe^{3+}$ is very scarce and found equal to ~ $10^{-15}$ M, its consideration in $Fe^{+III}$ respiration is thus not relevant.

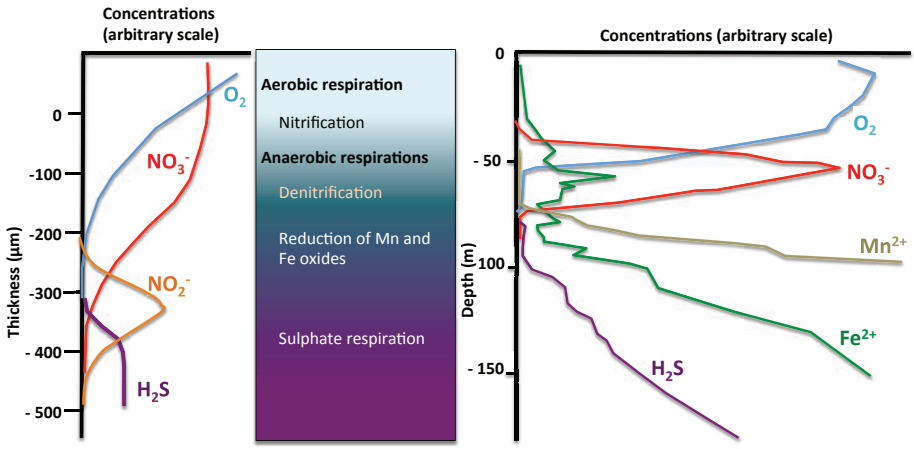


**FIG. 4.18.** – The anaerobic respiration affects the physico-chemistry of biofilms, water columns or sediments: on the left is represented a model of chemical gradients in a biofilm, oxides of iron and manganese are not represented (adapted from [37, 38]) and the Black Sea on the right (adapted from [39]).

Biosyntheses are endergonic reactions that were made possible by coupling with exergonic reactions such as ATP hydrolysis (Fig. 4.13). It is also important to point out that bacteria belonging to distinct metabolic groups can also share their metabolic activity to realize reactions, which without these so-called syntrophic associations, could never take place. Without this combination of metabolisms, these bacteria would never profit of some specific substrates. For instance, bacteria from the *Syntrophomonas* genus are known to anaerobically oxidized butyrate in acetate and $H_2$. This reaction would remain endergonic if methanogen bacteria were not consuming $H_2$. Indeed, the partial pressure of $H_2$ is kept at a low level that favours the shift of the equation (4.1) to the right (adapted from [36]).

$$\text{butyrate} + 2H_2O = 2\ \text{acetate} + H^+ + 2H_2 \qquad \Delta G^{\circ\prime} = +48.1\ \text{kJ mole}^{-1}\ (\textit{Syntrophomonas})$$
$$2H_2 + \tfrac{1}{2}CO_2 = \tfrac{1}{2}CH_4 + H_2O \qquad \Delta G^{\circ\prime} = -131\ \text{kJ mole}^{-1}\ (\text{methanogenic archaea})$$
$$\text{butyrate} + \tfrac{1}{2}CO_2 + H_2O = 2\ \text{acetate} + CH_4 + H^+ \qquad \Delta G^{\circ\prime} = -83\ \text{kJ mole}^{-1}\ (\text{balance}) \qquad (4.1)$$

Some chemical reactions catalysed by bacterial metabolic groups. The redox potential are those of the oxidant couple. Acetate is given as a model for organic electron donors (data from [35] and [36]).

Another example, widely documented, is that of anaerobic methane consumption made possible by the cooperation of hydrogenotrophic sulphate-reducing bacteria and archaea. It results from this cooperation an inverse methanogenesis [40].

So the physical proximity of bacteria within biofilms, or aggregates, allow microbial communities to achieve unexpected metabolic transformations reactions and in this way to better exploit available energy resources. The existence of nano-pipes connecting the cells by their cytoplasm (Fig. 4.11) should thus considerably favour inter-species cooperation. It is likely that new metabolic reactions will be revealed in biofilms if such "vascularization" is found to be common in biofilms. One would expect that such inter-species interactions would logically be involved in some biodeterioration processes of materials in general.

### 4.5.6. Couplings of biotic and abiotic reactions: indirect biotic reactions

The microbial activity modifies the redox state of some chemical species and thus makes entities appear in the medium that may be more chemically reactive. These can then be engaged in abiotic reactions, which are purely chemical, without any direct bacterial intervention. Thus, by providing the medium with reactive compounds, the bacteria could be responsible for physicochemical transformations; this is what is meant by "indirect biotic reactions". Such kinds of reactions were erroneously assigned to entirely biological reactions, because the "biological part" masked the abiotic one. For example, most SRBs are not able to respire $Fe^{III}$. However, in the presence of sulphate and ferric oxides, $Fe^{+III}$ is reduced to $Fe^{+II}$. In fact, sulphides issued from sulphate respiration react with $Fe^{+III}$ without direct enzymatic intervention [41].

Another example is the formation of nitrite from nitrate respiring bacteria. Nitrite is much more reactive, as an oxidant, than nitrate. Since nitrite is toxic for cells, it is quickly excreted to the extracellular medium by specific transport proteins (Fig. 4.15). In presence of $Fe^{+II}$ at the vicinity of the cell surface, nitrite reacts spontaneously with $Fe^{+II}$ to give $Fe^{II}$-$Fe^{III}$-bearing minerals such as green rusts or magnetite [42, 43]. Therefore, the oxidation of $Fe^{II}$ was made possible only due to the presence of nitrite that has been enzymatically produced. That was shown with *Klebsiella mobilis*, an enterobacteria able to reduce nitrate to nitrite (a "false denitrifier") and unable to enzymatically oxidize $Fe^{+II}$. Incubation of *K. mobilis* cells with both nitrate and $Fe^{+II}$ leads to green rust crystals formation at the cell surface (Fig. 4.19). Even in absence of exogenous organic electron donors, the endogenous reservoir of electrons (*e.g.*, [44, 45]). These results led to a serious reconsideration of the metabolic capacities of the iron oxidizing-nitrate reducing bacteria (IONRB), a metabolic group of bacteria assume to couple the $Fe^{II}$ oxidation to the nitrate reduction for energy conservation [46]. They were assumed to be lithotrophic, using $Fe^{II}$ as electron donor to respire nitrate. However, the protein involve in the $Fe^{II}$ oxidation process has yet to be identified. In addition, analytical difficulties in the determination of nitrites and $Fe^{+II}$ have led to an overestimation of the actual amounts of $Fe^{+II}$, thus accentuating the idea of an abiotic oxidation of ferrous iron [46]. It may be expected that the electrons involved in the nitrate reduction are provided by endogenic

reservoir of the cells or others, akin to what had already been observed for the organotrophic *K. mobilis* bacteria [44, 45].

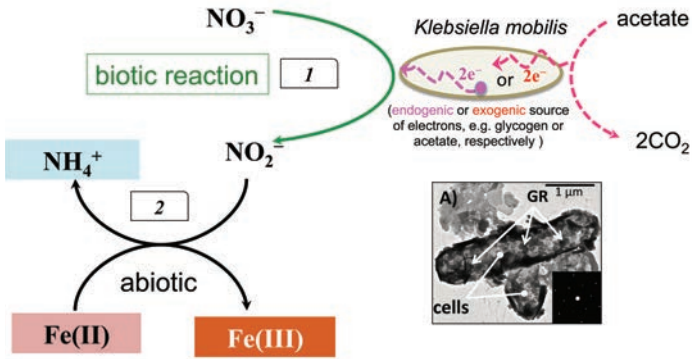


**FIG. 4.19.** – Indirect oxidation of $Fe^{+II}$ by the enterobacteria *Klebsiella mobilis* (nitrate reducing and non ferrous oxidative). There are enough endogen electron donor (or acetate traces) to enzymatically produce nitrite from nitrate (1, biotic reaction) to oxidize indirectly a subsequent amount of $Fe^{II}$ to $Fe^{II}$-$Fe^{III}$ green rust mineral (2) that fully encrust the cell (image by electronic transmission at right) (from Etique *et al.* [44)].

## 4.6. Conclusion

To colonize surfaces of diverse materials, we have seen in this chapter that bacteria have a very wide arsenal, both in relation to their envelopes and surfaces appendages, as well as *via* their metabolic capacities. They are fully able to exploit, in an optimal manner, the nutrients potentially present in their environment, thanks to various metabolic potentialities but also by cooperation with other metabolic groups. To do this, the organization in biofilms and aggregates allows them to maintain the physical proximity essential to these nutritive exchanges. The creation of a real network of pipes and cables adds a hitherto unsuspected level of organization. Thus, it would not be surprising that among these reactions, to some extent still completely unknown, some may be responsible for major changes observed on materials colonized by microbial biofilms.

## References

[1] ZoBell C.E. (1943) "The effect of solid surfaces upon bacterial activity." J. Bacteriol., 46, 39.

[2] Costerton J.W. *et al.* (1994) "Biofilms, the customized microniche." J. Bacteriol., 176, 2137.

[3] El-Naggar M.Y. *et al.* (2010) "Electrical transport along bacterial nanowires from *Shewanella oneidensis* MR-1." Proc. Natl. Acad. Sci., USA, 107, 18127.
[4] Pande S. *et al.* (2015) "Metabolic cross-feeding via intercellular nanotubes among bacteria." Nature Commun., 6, 6238.
[5] Whitman W.B. *et al.* (1998) "Prokaryotes, the unseen majority." Proc. Natl. Acad. Sci., USA, 95, 6578.
[6] Kallmeyer J. *et al.* (2012) "Global distribution of microbial abundance and biomass in subseafloor sediment." Proc. Natl. Acad. Sci., USA, 109, 16213.
[7] De Luca G. *et al.* (2011) "The Cyst-Dividing *Bacterium Ramlibacter tataouinensis* TTB310 Genome reveals a well-stocked toolbox for adaptation to a desert environment." PLoS ONE, 6(9), e23784, doi:10.1371/ journal. pone.0023784.
[8] Kulakov L.A. *et al.* (2002) "Analysis of bacteria contaminating ultrapure water in industrial systems." Appl. Environ. Microbiol., 68, 1548.
[9] Rothschild L.J., Mancinelli R.L. (2001) "Life in extreme environments." Nature, 409, 1092.
[10] Albers S.V. *et al.* (2006) "Protein secretion in the Archaea: multiple paths towards a unique cell surface." Nature Rev. Microbiol., 4, 537.
[11] Prescott L.M. *et al.* (2013) "Microbiologie." 4e édition, De Boeck Supérieur – Wesmael, Bruxelles, Belgium, SBN 9782804180393, 1070 p.
[12] Graham L.L. *et al.* (1991) "Freeze substitution of Gram-negative eubacteria: general cell morphology and envelope profiles." J. Bacteriol., 173, 1623.
[13] Dague E. *et al.* (2006) "Probing surface structures of *Shewanella* spp. by microelectrophoresis." Biophys. J., 90, 2612.
[14] Duval J.F.L., Gaboriaud F. (2010) "Progress in electrohydrodynamics of soft microbial particle interphases." Curr. Opin. Colloids, 15, 184.
[15] Bleich U., Nehrkorn A. (1989) "Elektronenmikroskopische Darstellung extrazelluIarer polymere Substanzen in Belebtschlammflocken." Zbl. Hyg., 188, 66.
[16] Prigent-Combaret C. *et al.* (2000) "Developmental pathway for biofilm formation in curli-producing *Escherichia coli* strains: role of flagella, curli and colanic acid." Environ. Microbiol., 2, 450.
[17] Stratford M., Wilson P.D.G. (1990) "Agitation effects on microbial cell-cell interactions." Let. Appl. Microbiol., 11, 1.
[18] Childers S.E. *et al.* (2002) "*Geobacter metallireducens* accesses insoluble FeIII oxide by chemotaxis." Nature, 416, 767.
[19] Reguera G. *et al.* (2005) "Extracellular electron transfer via microbial nanowires." Nature, 435, 1098.
[20] Pirbadian S. *et al.* (2014) "*Shewanella oneidensis* MR-1 nanowires are outer membrane and periplasmic extensions of the extracellular electron transport components." Proc. Natl. Acad. Sci., USA, 111, 12883.
[21] Clark M.E. *et al.* (2007) "Biofilm formation in *Desulfovibrio vulgaris* Hildenborough is dependent upon protein filaments." Environ. Microbiol., 9, 2844.

[22] de Oliveira-Garcia D. *et al.* (2002) "Characterization of flagella produced by clinical strains of *Stenotrophomonas maltophilia*." Emerg. Infect. Dis., 8, 918.
[23] Chan C.S. *et al.* (2010) "Lithotrophic iron-oxidizing bacteria produce organic stalks to control mineral growth: implications for biosignature formation." ISME J., 5, 717-727.
[24] Bonnefoy V., Holmes D.S. (2013) "Genomic insights into microbial iron oxidation and iron uptake strategies in extremely acidic environments." Environ. Microbiol., 14, 1597.
[25] Koch H. *et al.* (2014) "Growth of nitrite-oxidizing bacteria by aerobic hydrogen oxidation." Science, 345, 1052.
[26] DiChristina T.J. (2004) "New insights into the mechanism of bacterial metal respiration." Annual NABIR PI Meeting, March 15-17 2004, Warrenton, VA, USA.
[27] Williams H.D. *et al.* (2007) "Oxygen, cyanide and energy generation in the cystic fibrosis pathogen *Pseudomonas aeruginosa*." Adv. Microb. Physiol., 52, 1.
[28] Miot J., Etique M. (2016) "Formation and transformation of iron-bearing minerals by iron(II)-oxidizing and iron(III)-reducing bacteria." In: Iron oxides: from nature to materials and from formation to application, Chapter 4, Faivre D. Ed., Wiley VCH Books, 53-97, DOI: 10.1002/9783527691395.ch4.
[29] Vargas M. *et al.* (1998) "Microbiological evidence for $Fe^{III}$ reduction in early earth." Nature, 395, 65.
[30] Jorand F.P.A. *et al.* (2013) "Contribution of anionic vs neutral polymers to the formation of green rust 1 from γ-FeOOH bioreduction." Geomicrobiol. J., 30, 600.
[31] Jorand F.P.A. *et al.* (2011) "The formation of green rust induced by tropical river biofilm components." Sci. Total Environ., 409, 2586.
[32] Refait P. *et al.* Chapter 11 in this book.
[33] Bergel A. *et al.* (2013) "Des biofilms pour produire de l'électricité." Biofutur, 32/341, 45-50.
[34] Nadell C.D. *et al.* (2009) "The Sociobiology of biofilms." FEMS Microbiol., Rev., 33, 206.
[35] Konhauser K. (2007) "Introduction to geomicrobiology." Blackwell Publishing, Malden, MA, USA, 425 p.
[36] Libert M., Bonnefoy V. (2011) "Insight into the evolution of the iron oxidation pathways." Biochim. Biophys. Acta, 1827, 161.
[37] Paerl H.W., Pinckney J.L. (1996) "A mini-review of microbial consortia: their roles in aquatic production and biogeochemical cycling." Microb. Ecol., 31, 225.
[38] Okabe S. *et al.* (1999) "Analyses of spatial distributions of sulfate-reducing bacteria and their activity in aerobic wastewater biofilms." Appl. Environ. Microbiol., 65, 5107.
[39] Nealson K.H., Myers C.R. (1992) "Microbial reduction of manganese and iron: new approaches to carbon cycling." Appl. Environ. Microbiol., 58, 439.

[40] Delong E.F. (2000) "Resolving a methane mystery." Nature, 407, 577.
[41] Poulton S.W. (2003) "Sulfide oxidation and iron dissolution kinetics during the reaction of dissolved sulfide with ferrihydrite." Chem. Geol., 202, 79.
[42] Pantke C. *et al.* (2012) "Green rust formation during Fe(II) oxidation by the nitrate-reducing *Acidovorax* sp. strain BoFeN1." Environ. Sci. Technol., 46, 1439.
[43] Miot J. *et al.* (2014) "Formation of single domain magnetite by green rust oxidation promoted by microbial anaerobic nitrate-dependent iron oxidation." Geochim. Cosmochim. Acta, 139, 327.
[44] Etique M. *et al.* (2014) "Abiotic process for Fe(II) oxidation and green rust mineralization driven by a heterotrophic nitrate-reducing bacteria (*Klebsiella mobilis*)." Environ. Sci. Technol., 48, 3742.
[45] Klueglein N. *et al.* (2014) "Potential role of nitrite for abiotic Fe(II) oxidation and cell encrustation during nitrate reduction by denitrifying bacteria." Appl. Environ. Microbiol., 80, 1051.
[46] Etique M., Jorand F.P.A. (2016) "Fuzzy limit between green rust and goethite biomineralization from a nitrate-reducing bacterium (*Klebsiella mobilis*): The influence of organic electron donors." Curr. Inorg. Chem. 6(2), 119-126.
[47] Klueglein N., Kappler A. (2013) "Abiotic oxidation of Fe(II) by reactive nitrogen species in cultures of the nitrate-reducing Fe(II) oxidizer *Acidovorax* sp. BoFeN1 – questioning the existence of enzymatic Fe(II) oxidation." Geobiology, 11, 180.

# 5 Biofilm lifestyle of the microscopic inhabitants of surfaces

**Pilar Sanchez-Vizuete and Romain Briandet**

## 5.1. Biofilms, a lifestyle that concerns us

A biofilm is a community of microorganisms, associated with a surface and generally enclosed in a matrix of extracellular polymers. Biofilms, first defined by J. W. Costerton in 1978, are now considered to be the most likely lifestyle for bacteria in most environments [1] (Fig. 5.1). They are present on natural surfaces such as animal and plant tissues, soils, rivers or stromatolites [2]. The organisation of these microbial communities in biofilms allows bacteria to withstand environmental stresses such as nutrient starvation, drought or extreme pH values [3, 4]. Biofilms also play a fundamental role in the biogeochemical cycles involved in the processing of organic matter or the degradation of contaminants. The spatial association of bacteria having complementary metabolic skills (co-metabolism) allows, for example, the effective degradation of xenobiotic pollutants to take place [5, 6]. Biofilms also contribute to the protection of the rhizosphere against pathogens through the establishment of protective communities associated with plant roots [7].

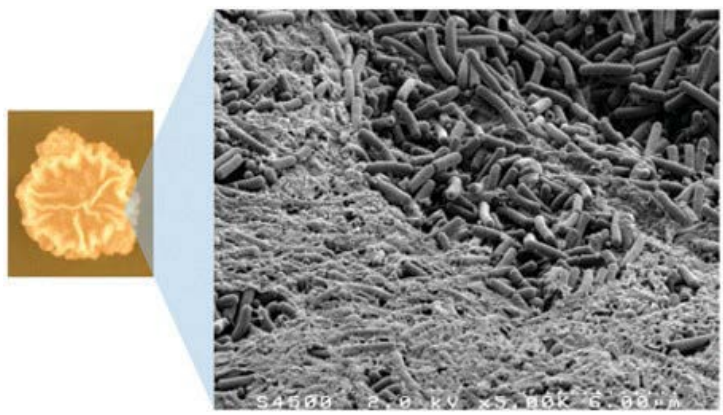

**Fig. 5.1.** – Macroscopic and microscopic view of a colony of *B. subtilis* on agar (A. Canette, MIMA2-INRA imaging platform).

Biofilms are present on a wide variety of man-made surfaces. This is the case in domestic environments such as the walls of our refrigerators, the shower heads or the bristles of our toothbrushes in our bathrooms. It is also the case of the industrial surfaces and hospital equipment that can house genuine microbial cities. Biofilms can play a useful role for humans, for example, in the treatment of wastewater or contaminated soils, the production of metabolites of interest in bioreactors, or the production of electricity using microbial cells [8-11]. In some cases, these microbial buildings can also have undesirable effects on our activities or our health. They are responsible for clogging and biocorrosion of industrial pipelines, leading to huge economic losses every year [12-14]. One of the characteristic of microbial life in these structured communities is their high resistance to environmental variations in general and to the action of antimicrobial agents in particular. The formation of biofilms on tissues of the host enhances the chronicity of infections such as certain cases of rhino-sinusitis caused by *Staphylococcus aureus*, urinary infections caused by *Escherichia coli*, otitis originated by *Haemophilus influenzae* or *Streptococcus pneumoniae* and tooth cavities and periodontitis caused by the pathogen *Streptococcus mutans* [15, 16].

*Pseudomonas aeruginosa* has been the reference species for the community of researchers working on biofilms, in particular because of the significant impact of this pathogen biofilm lifestyle on the chronicity of pulmonary infections induced in cystic fibrosis patients [17, 18]. Research on this bacterium for over 30 years has made it possible to decipher a large number of biological and physico-chemical mechanisms involved in biofilm formation processes, intercellular interactions and resistance to antimicrobials [19, 20]. Associated with tissues, these microorganisms usually produce large quantities of extracellular polymers which create a kind of organic shield that protects them against toxic compounds and the host immune system [21, 22]. The spatial organization of these communities, made possible by the presence of this organic cement, will also cause a great variability in the local cell microenvironments (nutrient, pH, oxygen...) generating a great diversification of cell types. Slow-growth subpopulations have been shown to be particularly tolerant to the action of certain antibiotics. More recently, a series of publications have shown that the presence of several "roommates" (*Burkholderia cepacia*, *Staphylococcus aureus* or *Candida albicans*) in the matrix of *Pseudomonas aeruginosa* biofilms significantly increases their resistance to biocides and their virulence [23-28].

Biofilms are likewise the cause of significant microbial persistence problems when associated to inert surfaces. The use of preventive or curative chemical treatments in industrial processing plants has a significant environmental impact due to the large amounts of disinfectants applied and released [29, 30]. Many foodborne infections and nosocomial infections are the direct result of the transfer of pathogens from inert surfaces to human tissues or food [31-33]. The surfaces encountered in agro-processing plants are favourable biotopes for these structured ecosystems. These communities are in permanent or intermittent contact with water and nutrients and may be particularly adapted to the cleaning and disinfection processes applied [34]. Foodborne infections affect more than 250,000 people every year in France. A study by the National Institute

for Public Health Surveillance (INVS) [35] estimates that nearly 60% of these infections would involve direct transfer of pathogenic microorganisms such as *E. coli, Listeria monocytogenes, Salmonella enterica, Staphylococcus* spp. *Bacillus cereus, Shigella* spp. or *Vibrio* spp. from industrial surfaces to food. In the medical sector, nosocomial infections – hospital-acquired infections – are the fourth leading cause of death in the United States with more than two million cases of infections per year and a cost of more than 5 billion $US [36]. More than 65% of these infections are associated with the development of biofilms and the persistence of pathogens on medical devices such as catheters, prostheses, valves and endoscopes [37, 38].

Today, the interest of the scientific community for biofilms continues to increase. A large number of teams are working to transfer knowledge obtained on this multicellular lifestyle to biotechnological applications: bioremediation, biomineralization, enzyme production... [8, 10]. However, most of the work still focuses on understanding the basic mechanisms of resistance to stress in order to be able to fight the sometimes undesirable presence of these microbial communities on surfaces. The increasing number of chronic biofilm infections only confirms the importance of this lifestyle in human health [35, 37, 38].

## 5.2. A continuous construction site

The construction, maintenance and renewal of these microscopic fortresses allow their residents to survive a wide spectrum of stresses and environmental upheaval [2]. In order to better control these biostructures, many laboratories strive to decipher the mechanisms involved in their life cycle. Schematically, this cycle can be described in a succession of steps, with variations in the processes observed between strains and dependent on of environmental conditions [39]. The cycle begins with the adhesion of pioneer cells to the surface, through a combination of physicochemical and biological processes. From reversible, cell adhesion becomes irreversible. The contact with the surface will trigger a real cataclysm in the physiology of the cell, a reprogramming of its genetic code. The cell changes its lifestyle: it exchanges its flagella against a matrix.

From solitary, it becomes gregarious. After consolidating its anchorage on the surface, it orchestrates with its congeners the major construction: a three-dimensional structure, a hundred times higher than a pyramid, a skyscraper, a microbial city. Once the work begins, the site never stops; it is necessary to destroy, repair, move, rebuild to adapt, survive.

It all begins with the transition from a planktonic free state to a sessile state by an association with a surface, a territory [39]. Reversible adhesion involves physicochemical interactions between the cells walls and the surface. A combination of van der Waals, electrostatic or Lewis acid-base interactions is most often invoked in these early contacts [40]. The overall bacterial cell surface envelope whether it be negative (at physiological pH) as in *Listeria monocytogenes*, or positive as some strains of *Stenotrophomonas maltophila*, has been shown to be a determining factor in the attachment of cells in weak ionic strength

environments [41-43]. The presence of extracellular appendages can also occur in this first step of adhesion and the irreversible anchoring of the cells to the substrate [44]. For *Escherichia coli*, pili are recognized as major adherence factors, whether the surface is biotic or abiotic [45]. In this species, curli (a type of pili made up of amyloid proteins) are involved in the formation and maintenance of biofilms [45-47] and in their resistance to biocides [48-50]. Some pili are also involved in cell aggregation, DNA transfer, or invasion of host cells [51]. Pili were discovered several decades ago in Gram-negative bacteria, whereas their presence and function in Gram-positive bacteria is just starting to be described [52, 53]. In *Lactococcus lactis*, pili are involved in cell aggregation and spatial organization of biofilms [53]. Flagella, in addition to their function of swimming, are also involved in the interaction with surfaces for a large number of bacterial species [54-58].

Once the contact has been established with the surface, the cell will modify its gene expression profiles, its genetic programme [59]. In several strains of *Pseudomonas*, it has been shown that after this first adhesion step, the genes involved in the production of flagella are repressed while the genes coding for the proteins necessary for the production of exopolymers are induced [60]. Under favourable conditions, these sessile cells colonize the surface forming spatially organized structures by continuing their multiplication and the production of matrix components [32, 61]. This stage of maturation is generally accompanied by the appearance of phenotypic and genetic heterogeneities of the population [62, 63]. As the biofilm ages, irrigation channels enabling the distribution of nutrients and zones of high cell lysis are frequently found [32, 64]. The three-dimensional structure of the biofilm may vary depending on the nutrients available [65], species [66-69] or the biofilm age [70, 71]. Various studies show the close link between the structure of the biofilm and its resistance to antimicrobial agents [72-74] (Fig. 5.2).

The biofilm formation cycle may be triggered in response to external or internal signals. For example, some compounds present in plant exudates such as malic acid may induce biofilm formation on the roots [75]. Some stresses, such as the presence of low doses of disinfectants or antibiotics have been demonstrated to induce the expression of the genes required for the production of matrix polymers [76-78]. Signals from neighbouring cells, whether or not from the same species, may also induce matrix production [79-84]. Under unfavourable environmental conditions, phenomena that could be assimilated to cannibalism or fratricide behaviour are also observed. They allow a small sub-population to survive by feeding on the lysed corpses of their siblings [85]. Other mechanisms allow a fluctuation between growth and decay phases which favours the dispersion of a population that will be able to explore new and more favourable territories [86]. The phases of "deconstruction" can be very finely regulated at the cellular level by systems involving, for example, nitric acid, c-di-GMP or cAMP [87-92].

Intercellular communication is an example of social behaviours that can be observed within a biofilm. Another example is the concept of "public goods", which refers to substances or functions shared within the community, such as the organic matrix of the biofilm and its nutrients and enzymes [93, 94].

This intercellular dialogue within biofilms, this coordination and this diversification of the associated cell types, is largely involved in the extraordinary adaptability of these communities to environmental stresses and variations [49, 95, 96].

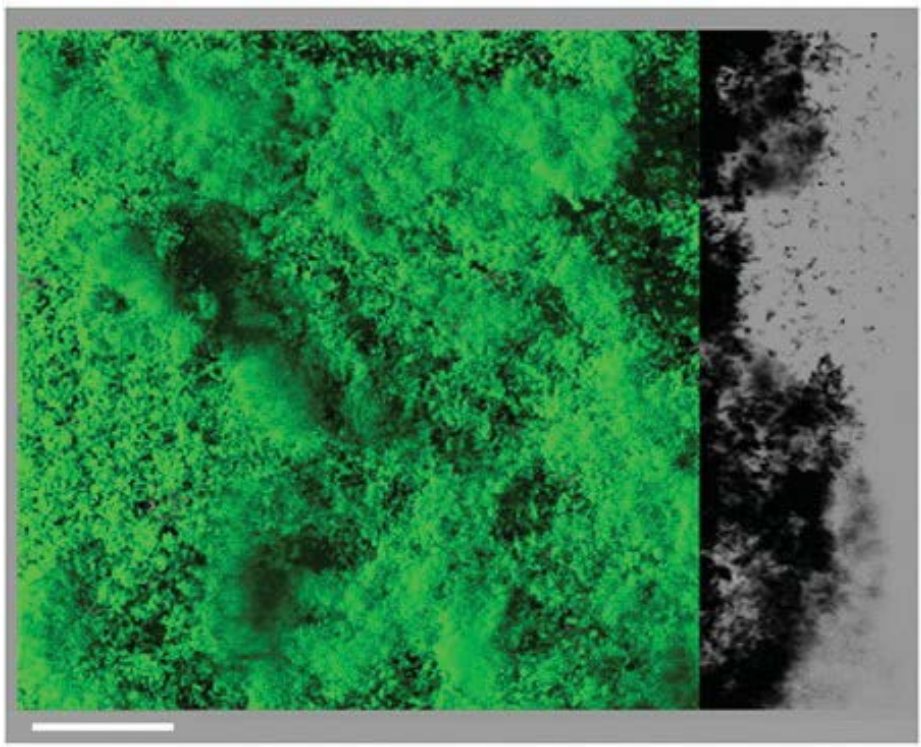

**Fig. 5.2.** – Three-dimensional structure of a *B. subtilis* biofilm. After development of the biofilm in a growth medium, a fluorescent dye capable of penetrating the cells was used to label the biofilm and analyse its architecture by confocal microscopy. The figure shows the aerial view and the thickness of the biofilm. The white scale bar corresponds to 50 micrometers.

## 5.3. A complex organic cement to maintain the edifice

The production of a gelatinous extracellular matrix is one of the most important characteristics of the biofilm lifestyle. This complex polymeric assembly is involved in various functions, including: *(i)* a structural role, the matrix allows the cohesion of the cells with each other and with the support, *(ii)* a protective role, a shield with respect to environmental stresses *(iii)* a social role, favouring spatial proximity between cells, cellular interactions and exchanges of genetic material [31, 97, 98]. This organic cement is composed of water and a mixture

of biomolecules such as proteins, polysaccharides, extracellular DNA and lipids. The biochemical composition of the matrix varies according to the age of the biofilm and the environmental conditions, the nature of the supporting material, growth medium, temperature or the species sharing the matrix [68, 97, 99, 100].

Polysaccharides are among the more abundant biological molecules of the matrix [101]. Some polysaccharides have a purely structural role in biofilms, while others induce the virulence of pathogenic species, act as control signals for their own production, or interfere with the action of antimicrobial agents [79, 102, 103]. Polysaccharides found in biofilms are generally long, linear or branched polymers such as glucans, fructans and cellulose [104, 105]. Uronic acids, alginate, xanthan or colanic acid are present in large quantities in the biofilms of *P. aeruginosa* or *E. coli* [102, 106, 107]. Other polysaccharides such as N-acetylglucosamine play an important role in the biofilms of pathogenic bacteria such as *S. aureus*, *S. epidermidis* or *E. coli* [108-110]. *P. aeruginosa* is the best example to illustrate the great variability of polysaccharides that can be found in the matrix of a biofilm formed by a single species. Depending on its environment, this species can produce, simultaneously or sequentially, alginate, levan, PsI and Pel, and cellulose. These polymers enable the formation of biofilms, their resistance to biocides and to the action of the immune system, and also the colonization of the lungs in patients with cystic fibrosis [107] (Fig. 5.3).

Proteins with structural and enzymatic functions are also major components of the matrix. Among structural proteins, certain proteins are irreversibly bound to extracellular carbohydrates (lectins) or proteins associated with the membrane. These organic structures make it possible to stabilize the matrix and constitute a bridging between the cell envelope and the extracellular polysaccharides of the matrix [111, 112]. In the biofilms of *P. aeruginosa*, the extracellular protein CdrA, that binds to the Ps1 polymer, has been shown to be necessary for the integrity of the biostructure [113]. Still in *P. aeruginosa*, type IV pili bind to extracellular DNA to form complex polymeric assemblages [114]. Similarly, aggregation of some *E. coli* fimbriae with cellulose results in stiffening of its matrix [115]. Another family of high molecular weight proteins involved in the spatial organization are the Bap proteins (Biofilm Associated Proteins). First identified in *S. aureus*, they were subsequently detected in several pathogenic species [116]. Certain proteins such as BlsA in *B. subtilis* also exhibit amphiphilic properties and form a hydrophobic layer at the interface with air [117]. Surfactine, a surfactant produced in large quantities in biofilms of *B. subtilis*, acts as a signal for neighbouring cells and triggers the expression of genes involved in the formation of biofilms [80]. Some proteins in the matrix have specific amyloid-like structures that are largely involved in surface adhesion, invasion of host cells, and induction of the immune response [118]. This is the case for curli produced by *E. coli* and *Salmonella* or the TasA protein produced by *B. subtilis* [119, 120]. The latter forms amyloid fibres anchored to the cell membranes which are necessary for the structural integrity of the pellicles [121]. Enzymes are also present in the extracellular space of biofilms. They often have functions related to the degradation of polymers, transforming the matrix into a true external digestive system. This system makes new sources of energy for

microorganisms bioavailable when environmental conditions are unfavourable [93, 97]. The degradation of structural exopolysaccharides also allows the dispersion of a population of the biofilm [86, 122, 123].

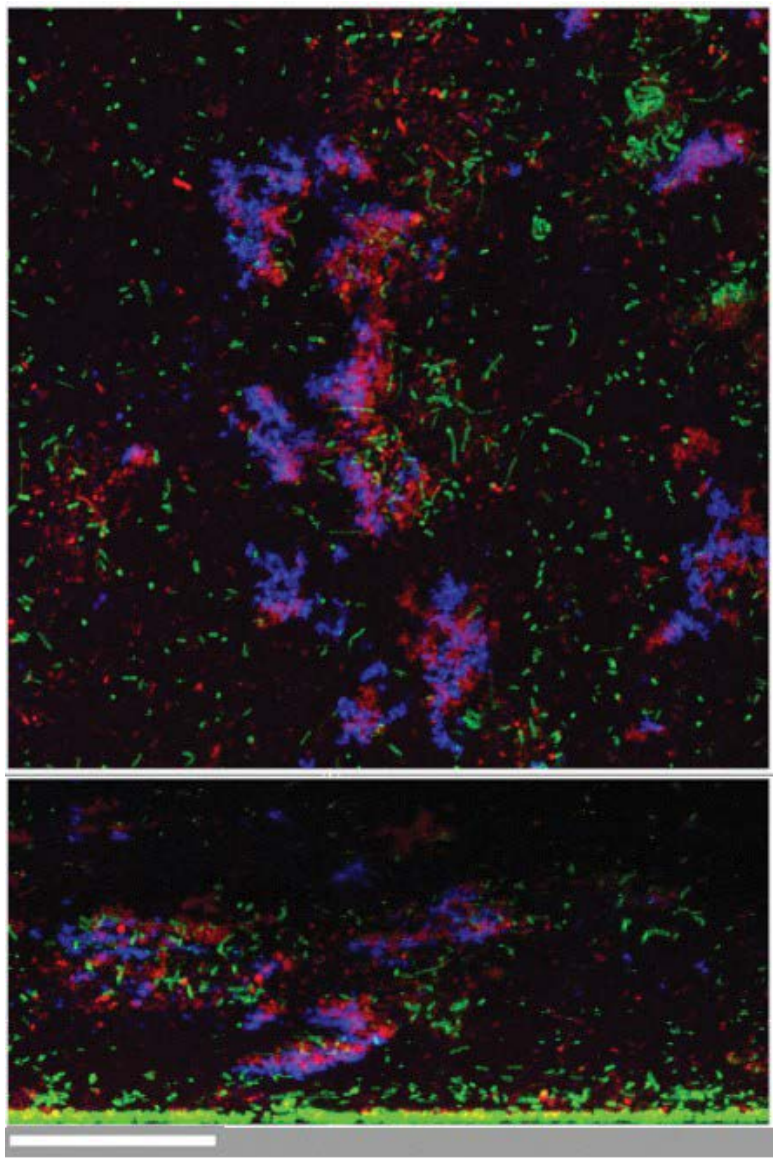

**Fig. 5.3.** – Visualization of polysaccharides in a biofilm. A *B. subtilis* biofilm (green cells) is labelled with fluorescent lectins (red and blue) allowing the identification and localization of polysaccharides in the matrix. The figure shows the aerial and lateral view of the biofilm. The white scale bar is 400 micrometers.

Extracellular DNA (DNAe), originally contemplated as a simple residue of cell lysis, is now considered to be one of the structural components of the biofilm. It is particularly important for some species such as *Pseudomonas aeruginosa, Enterococcus faecalis, S. aureus* and *S. epidermis* [122, 124-126]. The DNAe serves as intercellular connector in *P. aeruginosa* biofilms and as adhesin in *B. cereus* [127, 128]. The DNAe can also have a signalling role as postulated for the biofilms of *S. epidermis* for which this polymer, resulting from the lysis of a cell subpopulation, induces the formation of the biofilm of the neighbouring cells [129].

## 5.4. Nearly indestructible buildings

The main antimicrobials used to prevent or treat bacterial infections in patients are antibiotics and antiseptics. Disinfectants are applied to inert surfaces during cleaning and disinfection to avoid biocontamination of surfaces. While antibiotics act at low concentrations on specific cellular structures or processes to control infections of a specific bacterial type, disinfectants and antiseptics are multi-target agents that attack cell walls, cell membranes or cytoplasmic compounds, in a non-specific way [130]. The massive and uncontrolled use of certain antibiotics has led to the emergence of multi-resistant strains [131, 132]. Mechanisms of cross-resistance between antibiotics and disinfectants are also described [133-136]. It should be noted that in the context of the study of biofilms, the concept of "resistance" may be different from that usually accepted in microbiology.

Conventionally, a bacterial strain is considered to be resistant to an antimicrobial if it is not inactivated by a specific concentration, or during a precise period of time, which generally suffices to inactivate most of the other strains of the same species [130, 137]. Biofilm cells are generally considered to be resistant to a treatment compared to their planktonic counterparts [31, 138]. This resistance in biofilm can be genetically acquired or phenotypic. In the latter case, the mechanisms involved are reversible (modification of the cell membrane, the activity of the efflux pumps, phenotypes linked to the spatial organization of the biofilm, *etc.)* and the term "tolerance" should be used instead. Among the mechanisms most frequently invoked in the extraordinary resistance of these biostructures are the interference of the extracellular matrix, the heterogeneity of the cell types (physiology and genotype) associated with the spatial or the intercellular communication (Fig. 5.4).

### *5.4.1. The extracellular matrix as a protective shield*

The exo-polymer matrix produced by the cells of a biofilm can play different roles in the microbial community. As mentioned above, the matrix is the skeleton, the scaffolding necessary for the maintenance of the three-dimensional structure of the biofilm [97]. This matrix, by different mechanisms, is also directly or indirectly involved in the resistance of cells to biocides action [15, 31, 96, 98].

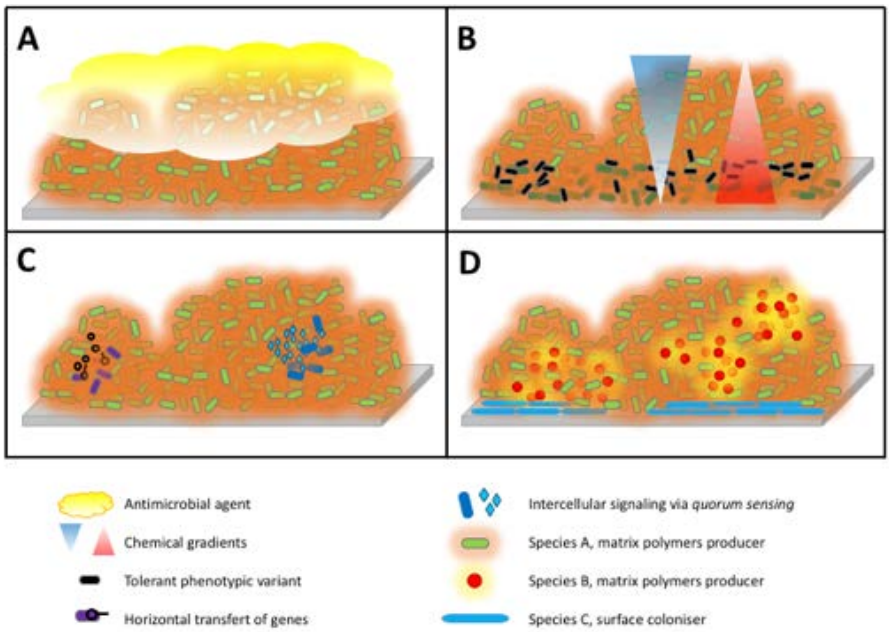


**Fig. 5.4.** – Mechanisms of resistance in biofilm cells. A. Biocides may have diffuse-reaction difficulties through the biofilm and be inactivated before reaching the cells of the deepest layers. B. The establishment of chemical gradients (nutrients, oxygen, metabolic waste) can induce the emergence of phenotypic variants tolerant to the action of antimicrobial agents. C. Some cells may become more resistant to the action of biocides by acquisition of new genetic material, *e.g.,* plasmids, or by modification of patterns of locally induced gene expression, for example, by quorum sensing signals. D. The presence of several species in a biofilm may modify resistance to biocides in the bacterial community. A species capable of colonizing the surface (blue cells) can promote the aggregation of other species (red and green cells) and these, in exchange, can produce exopolymers and thus protect them from the action of biocides [31, 33].

The polymers of the matrix can directly interfere with the diffusion-reaction of the active ingredients *via* steric or physicochemical interactions and cause a lack of bioavailability in the deepest layers of the biofilm [22, 100, 139]. The use of real-time confocal microscopy techniques has demonstrated that cell inactivation models in a *P. aeruginosa* biofilm depend on the type of disinfectant used. For example, the use of quaternary ammoniums causes non-linear inactivation of the cells, with those of the periphery being more rapidly inactivated than those of the deep layers; in contradistinction, when exposed to oxidizing agents, cellular inactivation follows linear and uniform kinetics [100]. This difference in reactivity is partly related to the size, the charge and the amphiphilic character of the molecule used which reacts differently with the matrix. Thus, it has been shown that the resistance of *P. aeruginosa* biofilms to benzalkonium chloride increased with elongation of the carbon chain of the quaternary

ammonium used [140]. It is also possible that certain matrix components, such as the BslA amphiphilic protein in *Bacillus subtilis* biofilms form a hydrophobic layer capable of blocking the penetration of liquids, including disinfectants [141]. Small molecules, which are able to diffuse well into the biofilm, can react with the organic material and be inactivated before reaching the cells of the deepest layers. Using microelectrodes, the concentration of active chlorinated derivatives found inside the biofilms formed by *P. aeruginosa* and *K. pneumoniae* was shown to be less than 20% of the concentration found in the external environment [142]. Similarly, the penetration of glutaraldehyde is delayed in an artificial biofilm model due to the interactions between the biocide and the organic components of the biofilm [143]. P. Stewart's work (CBE, USA) also shows that the time for penetration of alkaline hypochlorite is 8 times greater than for penetration of chlorosulfamate, and that these differences are related to the ability of the former to react with the components of the matrix [144]. The charge of certain active ingredients also interferes in these processes of molecular mobility [145].

These examples underline the importance of the physicochemical interactions between the biocides and the organic material of the biofilm in the resistance of cells. Nevertheless, the matrix is not always an obstacle to the spread of antimicrobials. Some antibiotics, such as rifampicin or vancomycin, freely diffuse into the biofilms of *S. epidermis* or *S. aureus* respectively and reach the cells of the deepest layers [146, 147]. However, this free diffusion capacity is not sufficient to guarantee the effectiveness of the biocide in a biofilm since other resistance mechanisms may be involved.

### 5.4.2. Differentiation and physiological adaptation

Beyond the direct involvement of the matrix in the interference with the biocidal active principles, it also interferes with the mechanisms deriving from the spatial organization of the structure.

One of the first consequences of the spatial organization of the biofilm is the appearance of chemical gradients such as gradients of nutrients, oxygen or toxic waste. To adapt to the diversity of microenvironments generated by these gradients, the cells adapt their genetic expression and reach new physiological states. For example, the lack of nutrients encountered in the deepest strata favours the entry of cells into a slow-down or dormant state. This subpopulation of cells, also called "persisters", will be less sensitive to the antimicrobial action targeting vital cellular processes (DNA replication, ribosomal protein production, synthesis of membrane components). These phenotypic variants are generally present in very small quantities in the biofilm but are highly tolerant to the action of antimicrobials and the immune system. This population can return to a "normal" state once the stress is removed in order to repopulate the residual biofilm [148-150].

Changes in gene expression patterns of biofilm cells have been demonstrated in a large number of bacterial models [151-155]. Genes important for biofilm

lifestyle such as those encoding for the synthesis of exopolymers or for the proteins necessary for adhesion of cells to surfaces are more strongly induced to adapt to this gregarious lifestyle [60, 156]. Adaptations to stress conditions, including the presence of antimicrobials, are also observed within biofilms. For example, the presence of antimicrobials at sub-lethal concentrations, a possible situation in the deepest layers of the biofilm, can induce responses leading to matrix overproduction [31, 157-159]. In *B. subtilis*, the presence of chlorine induces the expression of the genes required for matrix production [76]. This biocide also modifies the properties of *P. aeruginosa* biofilms, including the production of exopolymers and resistance to biocides [160]. Mechanisms of cross-resistance between antibiotics and disinfectants are also observed when biofilms are exposed to sub-lethal concentrations of biocides [161, 162]. In parallel with this physiological diversification of "roommates" in the matrix, cells can adapt to the constraints of the environment by modifying their genetic material.

### 5.4.3. The biofilm as a trigger of genetic plasticity in bacteria

Bacteria can integrate new genes from other cells to incorporate new functions that allow survival to stresses. The horizontal transfer of antibiotic resistance genes is one of the main causes of the spread of multi-resistant strains. This transfer is assumed to be favoured in biofilms because of the high cell density and spatial proximity between cells [163-166]. The presence of extracellular DNA in the matrix also constitutes an important "pool" of genes that can be directly incorporated by competent bacteria of the same or different species [167]. It has been shown that the competence of cells can be induced by quorum sensing signals from neighbouring cells [168, 169]. Biofilms are also very suitable environments for the transfer of plasmids between bacteria [164, 170], which can be able to increase their capacity to form biofilms and to resist the action of biocides [171, 172]. Modification of the genetic material of biofilm cells can be more that the simple horizontally incorporation of new genes. Biofilm growth can lead to the emergence of a high genetic variability within the population. High mutation rates have been observed in the biofilms of *S. aureus* and *P. aeruginosa* [173, 174]. Therefore, genetic variants emerge within a biofilm with different properties compared to the original population [175, 176]. For example, the emergence of genetic variants producing high amounts of exopolymers contributes to the increased resistance to biocides in the entire bacterial community [175, 177, 178]. This phenomenon has been studied in detail in *P. aeruginosa*, a species producing three types of variants within the biofilm classified according to the type of colonies they form on agar [175]. Among these variants, the wrinkled type is mostly implicated in the resistance of the community to hydrogen peroxide [175]. Several studies have also shown that oxidative stress increases mutation rate and thus the emergence of antimicrobial resistant variants [173, 179, 180]. Interactions between species may also induce favourable conditions for the emergence of these variants [181, 182]. Biofilm can thus

be considered an environment favouring genetic variability, which increases the probability of a variant being adapted to possible stresses.

### 5.4.4. Quorum-sensing, the social network of bacteria

When bacteria are found at high cell densities they are able to coordinate their behaviour using a regulatory process called quorum sensing [183]. Low molecular weight molecules are produced by the cells acting as signals when a certain critical threshold is reached. These signals are detected by bacteria which trigger the expression of a coordinated response. Quorum sensing molecules have been identified for communication between cells of the same species (such as N-acyl homoserine lactones) or between cells of different species [184-187].

These signals may induce responses such as genetic competence, induction of virulence factors, or biofilm formation [188]. Cell-to-cell communication can also modulate the expression of genes involved in biocide resistance, such as the efflux pumps required for the expulsion of toxic molecules [189, 190] or enzymes capable of neutralizing them [191]. It has been shown that quorum sensing signals control the expression of enzymes that modulate the resistance of *P. aeruginosa* biofilms to hydrogen peroxide (in particular catalase and superoxide dismutase) [192]. These signals also control the resistance of *P. aeruginosa* to the action of certain antibiotics such as kanamycin [193]. Quorum sensing systems can also induce a global stress response that protects cells against different types of stress [194-196]. When several species are present in the biofilm, interferences (stimulation, inhibition or inactivation) between the respective quorum sensing systems have been also described [96, 197-199].

### 5.4.5. Multispecies biofilms: a successful alliance

Until recently, biofilm antimicrobial resistance mechanisms were essentially analysed using single-species axenic models [103, 200, 201]. However, in most environments, biofilms are composed by several microbial species that can harbour bacteria, fungi, protozoa, algae and viruses [202]. The spatial proximity between species promotes cellular interactions and can induce an overall increase in biomass, specific spatial organization, polymer production or physiological response that can lead to increased resistance of the entire community or only some of its inhabitants [27, 95, 203] (Fig. 5.5). Although the risk for human health is caused by exposure to pathogenic species, they are not always the most suitable organisms to withstand the extreme aggressions encountered on surfaces, particularly during cleaning and disinfection operations. Even today, very few studies focus on resident flora that are repeatedly exposed in these extreme environments to many environmental stresses. The few studies on this type of interactions mostly describe effective protection of pathogens in these mixed biofilm contexts [48, 69, 204-206].

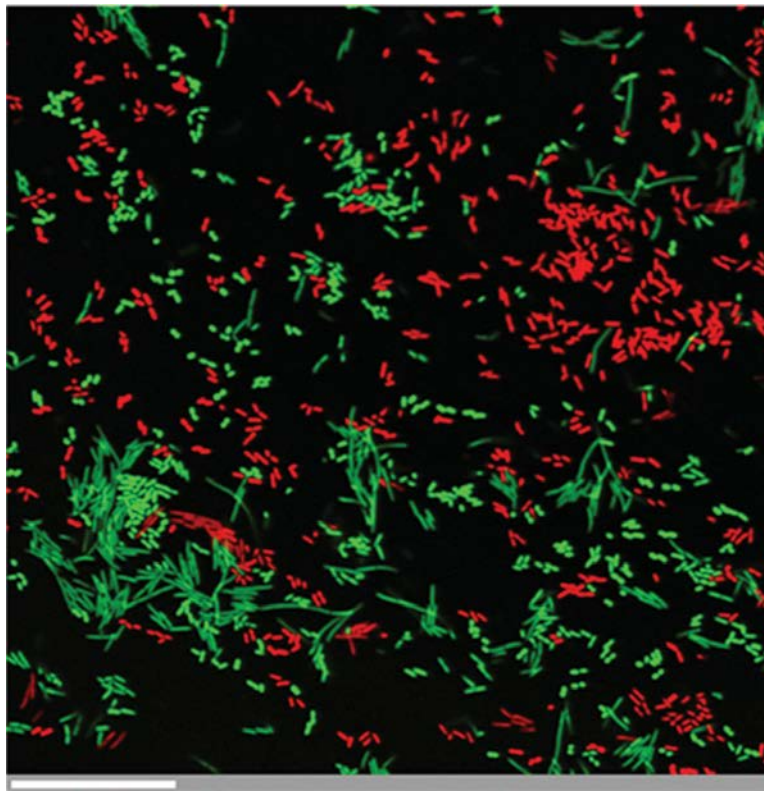

**Fig. 5.5.** – Interaction between bacterial species on surfaces. The interaction between two different species of the genus *Pseudomonas* (red or green cells) induces a morphological diversification: green cells present in the form of *Bacilli* or filaments. The white scale bar corresponds to 50 micrometers.

## 5.5. How to live with biofilms

We touch, we swallow or breathe biofilms every day. They are on our computer keyboards, shower curtains and even in our navel. Most of the time cohabitation is silent, it can even be beneficial when this flora acts as a barrier to the propagation of a pathogen, participates in the education of our immune system or contributes to a biotechnological process. But when it harbours and protects potentially harmful microorganisms such as pathogens, or when it consumes disinfectant, or when it threatens the integrity of the materials, the biofilm becomes undesirable. It must be controlled to prevent the infection from becoming chronic, the food from becoming unsuitable for consumption,

or the material from corroding irreversibly. The search for effective targeted treatments becomes a new Grail in the community of microbiologists: destructuring the biofilm, permeabilising it, eliminating it, dissolving it, perforating its protective shield (its matrix). For that purpose, scientifics use enzymes (which degrade extracellular DNA or matrix polysaccharides) [97, 207-212], disrupters of intercellular signalling (quorum sensing or c-di-GMP) [213-216], "swimmer" bacteria that infiltrate into the biofilm and sensitize it to the action of biocides [217] or the diversion of microbial antibiofilms (nitric oxide, D-amino acids, polyamines, fatty acids) [218-222]. In parallel with this search for new curative treatments, many research teams are moving towards preventive strategies for the control of unwanted biofilms. If we do not know how to eradicate a mature biofilm, we can delay its formation by limiting the initial adhesion of the cells. The adhesion of bacteria may be limited, for example by using anti-biofilm surfaces coated with polymers, nanoparticles or antimicrobial agents [206-210]. Chemical disinfectants are polluting and inefficient on biofilms. Biological approaches prevent the development of pathogens on surfaces. We talk about "biocontrol" in agriculture, "bioprotection" of industrial surfaces, "bioconservation" of food. These alternative strategies have a common feature: they draw on the specialized scientific knowledge available on the dynamics of the ecology of surface flora. A better understanding of the role of the spatial organization of these microbial buildings on their resistance and on the nature of the interspecies interactions enables us today to envisage effective and sustainable targeted approaches.

## References

[1] Costerton J.W. *et al.* (1978) "How bacteria stick." Sci. Am., 238, 86-95.
[2] Hall-Stoodley L. *et al.* (2004) "Bacterial biofilms: from the natural environment to infectious diseases." Nat. Rev. Microbiol., 2, 95-108.
[3] Davey M.E., O'Toole G.A. (2000) "Microbial Biofilms: from Ecology to Molecular Genetics." Microbiol. Mol. Biol. Rev., 64, 847-867.
[4] Costerton J.W. *et al.* (1995) "Microbial biofilms." Annu. Rev. Microbiol., 49, 711-45.
[5] Nielsen AT. *et al.* (2000) "Role of commensal relationships on the spatial structure of a surface-attached microbial consortium." Environ. Microbiol., 2, 59-68.
[6] Terada A. *et al.* (2003) "Nitrogen removal characteristics and biofilm analysis of a membrane-aerated biofilm reactor applicable to high-strength nitrogenous wastewater treatment." J. Biosci. Bioeng., 95, 170-178.
[7] Chen Y. *et al.* (2013) "Biocontrol of tomato wilt disease by *Bacillus subtilis* isolates from natural environments depends on conserved genes mediating biofilm formation." Environ. Microbiol., 15, 848-864.
[8] Halan B. *et al.* (2012) "Biofilms as living catalysts in continuous chemi- cal synthese." Trends Biotechnol., 30, 453-465.

[9] Edwards S.J., Kjellerup B.V. (2013) "Applications of biofilms in bioremediation and biotransformation of persistent organic pollutants, pharmaceuticals/personal care products, and heavy metals." Appl. Microbiol. Biotechnol., 97, 9909-9921.
[10] Singh R. *et al.* (2006) "Biofilms: implications in bioremediation." Trends Microbiol., 14, 389-397.
[11] Erable B. *et al.* (2009) "Sampling natural biofilms: a new route to build efficient microbial anodes." Environ. Sci. Technol., 43, 3194-3199.
[12] Beech I.B., Sunner, J. (2004) "Biocorrosion: towards understanding interactions between biofilms and metals." Curr. Opin. Biotechnol., 15, 181-166.
[13] Schultz M.P. *et al.* (2011) "Economic impact of biofouling on a naval surface ship." Biofouling, 27, 87-98.
[14] Flemming H.-C. *et al.* (2013) "Mini-review: microbial problems in paper production." Biofouling, 29, 683-696.
[15] Hall-Stoodley L., Stoodley, P. (2009) "Evolving concepts in biofilm infections." Cell. Microbiol., 11, 1034-1043.
[16] Marsh P.D., Bradshaw D.J. (1995) "Dental plaque as a biofilm." J. Ind. Microbiol., 15, 169-175.
[17] Mulcahy L.R. *et al.* (2014) "*Pseudomonas aeruginosa* biofilms in disease." Microb. Ecol., 68, 1-12.
[18] Rybtke M.T. *et al.* (2011) "The implication of *Pseudomonas aeruginosa* biofilms in infections." Inflamm. Allergy Drug Targets, 10, 141-157.
[19] Parsek M.R., Tolker-Nielsen T. (2008) "Pattern formation in *Pseudomonas aeruginosa* biofilms." Curr. Opin. Microbiol., 11, 560-566.
[20] Høiby N. *et al.* (2011) "The clinical impact of bacterial biofilms." Int. J. Oral Sci., 3, 55-65.
[21] Høiby N. *et al.* (2010) "Antibiotic resistance of bacterial biofilms." Int. J. Antimicrob. Agents, 35, 322-332.
[22] Jensen P.Ø. *et al.* (2010) "The immune system vs. *Pseudomonas aeruginosa* biofilms." FEMS Immunol. Med. Microbiol., 59, 292-305.
[23] Wolcott R. *et al.* (2013) "The polymicrobial nature of biofilm infection." Clin. Microbiol. Infect., 19, 107-112.
[24] Pastar I. *et al.* (2013) "Interactions of methicillin resistant *Staphylococcus aureus* USA300 and *Pseudomonas aeruginosa* in polymicrobial wound infection." PLoS One 8, e56846.
[25] Hendricks K.J. *et al.* (2001) "Synergy between *Staphylococcus aureus* and *Pseudomonas aeruginosa* in a rat model of complex orthopaedic wounds." J. Bone Joint Surg. Am., 83-A, 855-861.
[26] Peters B.M. *et al.* (2010) "Microbial interactions and differential protein expression in *Staphylococcus aureus* - *Candida albicans* dual-species biofilms." FEMS Immunol. Med. Microbiol., 59, 493-503.
[27] Elvers K.T. *et al.* (2002) "Binary and mixed population biofilms: time-lapse image analysis and disinfection with biocides." J. Ind. Microbiol. Biotechnol., 29, 331-338.

[28] Behnke S. *et al.* (2011) "Comparing the chlorine disinfection of detached biofilm clusters with those of sessile biofilms and planktonic cells in single- and dual-species cultures." Appl. Environ. Microbiol., 77, 7176-7184.
[29] Rooklidge S.J. (2004) "Environmental antimicrobial contamination from terraccumulation and diffuse pollution pathways." Sci. Total Environ., 325, 1-13.
[30] Martinez J.L. (2009) "Environmental pollution by antibiotics and by antibiotic resistance determinants." Environ. Pollut., 157, 2893-2902.
[31] Bridier A. *et al.* (2011) "Resistance of bacterial biofilms to disinfectants: a review." Biofouling, 27, 1017-1032.
[32] Donlan R.M., Costerton J.W. (2002) "Biofilms: survival mechanisms of clinically relevant microorganisms." Clin. Microbiol. Rev., 15, 167-193.
[33] Bridier A. *et al.* (2015) "Biofilm-associated persistence of food-borne pathogens." Food Microbiol., 45, 167-178.
[34] Carpentier B., Cerf O. (1993) "Biofilms and their consequences, with particular reference to hygiene in the food industry." J. Appl. Bacteriol., 75, 499-511.
[35] Anonymous (2010) "Surveillance des toxi-infections alimentaires collectives." Données de la déclaration obligatoire, 2009. Bulletin Épidémiologique Hebdomadaire, France, 2010, 1-6.
[36] Wenzel R.P. (2007) "Health care-associated infections: major issues in the early years of the 21st century." Clin. Infect. Dis., 45 Suppl 1, S85-8.
[37] Mack D. *et al.* (2006) "Biofilm formation in medical device-related infection." Int. J. Artif. Organs, 29, 343-359.
[38] Shirtliff M., Leid J. (2009) "The Role of Biofilms in Device-Related." Springer series on biofilms, Shirtliff M.E., Leid J.G. Eds, 269 p.
[39] O'Toole G. *et al.* (2000) "Biofilm Formation as Microbial development." Annu. Rev. Microbiol., 54, 49-79.
[40] Bellon-Fontaine M.N. *et al.* (1990) "A comparison of thermodynamic approaches to predict the adhesion of dairy microorganisms to solid substrata." Cell Biophysics, 17, 93-106.
[41] Briandet R. *et al.* (1999) "*Listeria monocytogenes* Scott A: cell surface charge, hydrophobicity, and electron donor and acceptor characteristics under different environmental growth conditions." Appl. Environ. Microbiol., 65, 5328-5333.
[42] Briandet R. *et al.* (1999) "Effects of the growth procedure on the surface hydrophobicity of *Listeria monocytogenes* cells and their adhesion to stainless steel." J. Food Prot., 62, 994-998.
[43] Jucker B. *et al.* (1996) "Adhesion of the positively charged bacterium *Stenotrophomonas* (*Xanthomonas*) *maltophilia* 70401 to glass and Teflon." J. Bacteriol., 178, 5472-5479.
[44] Van Houdt R., Michiels C.W. (2010) "Biofilm formation and the food industry, a focus on the bacterial outer surface." J. Appl. Microbiol., 109, 1117-1131.

[45] Cookson A.L. *et al.* (2002) "The role of type 1 and curli fimbriae of Shiga toxin-producing *Escherichia coli* in adherence to abiotic surfaces." Int. J. Med. Microbiol., 292, 195-205.
[46] Chapman M.R. *et al.* (2008) "Role of *Escherichia coli* Curli Operons in Directing Amyloid Fiber Formation." Science, 295, 851-855.
[47] Boyer R.R. *et al.* (2007) "Influence of curli expression by *Escherichia coli* 0157:H7 on the cell's overall hydrophobicity, charge, and ability to attach to lettuce." J. Food Prot., 70, 1339-1345.
[48] Wang R. *et al.* (2013) "Mixed biofilm formation by Shiga toxin-producing *Escherichia coli* and *Salmonella enterica* serovar *Typhimurium* enhanced bacterial resistance to sanitization due to extracellular polymeric substances." J. Food Prot., 76, 1513-1522.
[49] Wang R. *et al.* (2012) "Biofilm formation by Shiga toxin-producing *Escherichia coli* O157:H7 and Non-O157 strains and their tolerance to sanitizers commonly used in the food processing environment." J. Food Prot., 75, 1418-1428.
[50] Ryu J.-H., Beuchat L.R. (2005) "Biofilm formation by *Escherichia coli* O157:H7 on stainless steel: effect of exopolysaccharide and Curli production on its resistance to chlorine." Appl. Environ. Microbiol., 71, 247-254.
[51] Proft T., Baker E.N. (2009) "Pili in Gram-negative and Gram-positive bacteria - structure, assembly and their role in disease." Cell. Mol. Life Sci., 66, 613-635.
[52] Konto-Ghiorghi Y. *et al.* (2009) "Dual role for pilus in adherence to epithelial cells and biofilm formation in *Streptococcus agalactiae*." PLoS Pathog., 5, e1000422.
[53] Oxaran V. *et al.* (2012) "Pilus biogenesis in *Lactococcus lactis*: molecular characterization and role in aggregation and biofilm formation." PLoS One 7, e50989.
[54] Kim T.J. *et al.* (2008) "Effect of flagellar mutations on *Yersinia enterocolitica* biofilm formation." Appl. Environ. Microbiol., 74, 5466-5474.
[55] Pratt L.A., Kolter R. (1998) "Genetic analysis of *Escherichia coli* biofilm formation: roles of flagella, motility, chemotaxis and type I pili." Mol. Microbiol., 30, 285-293.
[56] Van Houdt R., Michiels C.W. (2005) "Role of bacterial cell surface structures in *Escherichia coli* biofilm formation." Res. Microbiol., 156, 626-633.
[57] Laverty G. *et al.* (2014) "Biomolecular Mechanisms of *Pseudomonas aeruginosa* and *Escherichia coli* Biofilm Formation." Pathogens, 3, 596-632.
[58] O'Toole G.A., Kolter R. (1998) "Flagellar and twitching motility are necessary for *Pseudomonas aeruginosa* biofilm development." Mol. Microbiol., 30, 295-304.
[59] Prigent-Combaret C. *et al.* (1999) "Abiotic surface sensing and biofilm-dependent regulation of gene expression in *Escherichia coli*." J. Bacteriol., 181, 5993-6002.
[60] Sauer K., Camper A.K. (2001) "Characterization of phenotypic changes in *Pseudomonas putida* in response to surface-associated growth." J. Bacteriol., 183, 6579-6589.

[61] Monds R.D., O'Toole G.A. (2009) "The developmental model of microbial biofilms: ten years of a paradigm up for review." Trends Microbiol., 17, 73-87.
[62] Stewart P.S., Franklin M.J. (2008) "Physiological heterogeneity in biofilms." Nat. Rev. Microbiol., 6, 199-210.
[63] Wimpenny J. *et al.* (2000) "Heterogeneity in biofilms." FEMS Microbiol. Rev., 24, 661-671.
[64] Bayles K.W. (2007) "The biological role of death and lysis in biofilm development." Nat. Rev. Microbiol., 5, 721-726.
[65] Jahid I.K. *et al.* (2013) "Influence of glucose concentrations on biofilm formation, motility, exoprotease production, and quorum sensing in *Aeromonas hydrophila*." J. Food Prot., 76, 239-247.
[66] Bridier A. *et al.* (2010) "The biofilm architecture of sixty opportunistic pathogens deciphered using a high throughput CLSM method." J. Microbiol. Methods, 82, 64-70.
[67] Stoodley P. *et al.* (2001) "Growth and Detachment of Cell Clusters from Mature Mixed-Species Biofilms." Appl. Environ. Microbiol., 67, 5608-5613.
[68] Bridier A. *et al.* (2012) "Biofilms of a *Bacillus subtilis* Hospital Isolate Protect *Staphylococcus aureus* from Biocide Action." PLoS One 7, e44506.
[69] Schwering M. *et al.* (2013) "Multi-species biofilms defined from drinking water microorganisms provide increased protection against chlorine disinfection." Biofouling, 29, 917-928.
[70] Klausen M. *et al.* (2006) "Dynamics of development and dispersal in sessile microbial communities: examples from *Pseudomonas aeruginosa* and *Pseudomonas putida* model biofilms." FEMS Microbiol. Lett., 261, 1-11.
[71] Habimana, O. *et al.* (2009) "Genetic features of resident biofilms determine attachment of *Listeria monocytogenes*." Appl. Environ. Microbiol., 75, 7814-7821.
[72] Takenaka S. *et al.* (2008) "Direct visualization of spatial and temporal patterns of antimicrobial action within model oral biofilms." Appl. Environ. Microbiol., 74, 1869-1875.
[73] Shen Y. *et al.* (2011) "Antimicrobial efficacy of chlorhexidine against bacteria in biofilms at different stages of development." J. Endod., 37, 657-661.
[74] Bridier A. *et al.* (2011) "Deciphering biofilm structure and reactivity by multiscale time-resolved fluorescence analysis." Adv. Exp. Med. Biol., 715, 333-349.
[75] Rudrappa T. *et al.* (2008) "Root-secreted malic acid recruits beneficial soil bacteria." Plant Physiol., 148, 1547-1556.
[76] Shemesh M. *et al.* (2010) "The biocide chlorine dioxide stimulates biofilm formation in *Bacillus subtilis* by activation of the histidine kinase KinC." J. Bacteriol., 192, 6352-6356.
[77] Kaplan J.B. *et al.* (2012) "Low levels of β-lactam antibiotics induce extracellular DNA release and biofilm formation in *Staphylococcus aureus*." MBio 3, e00198-12.
[78] Hoffman L.R. *et al.* (2005) "Aminoglycoside antibiotics induce bacterial biofilm formation." Nature, 436, 1171-1175.

[79] Elsholz A.K.W. *et al.* (2014) "Self-regulation of exopolysaccharide production in *Bacillus subtilis* by a tyrosine kinase." Genes Dev., 28, 1710-1720.
[80] Zeriouh H. *et al.* (2014) "Surfactin triggers biofilm formation of *Bacillus subtilis* in melon phylloplane and contributes to the biocontrol activity." Environ. Microbiol., 16, 2196-2211.
[81] Shank E.A. *et al.* (2011) "Interspecies interactions that result in *Bacillus subtilis* forming biofilms are mediated mainly by members of its own genus." Proc. Natl. Acad. Sci., USA, 108, E1236-43.
[82] Armbruster C.E. *et al.* (2010) "Indirect pathogenicity of *Haemophilus influenzae* and *Moraxella catarrhalis* in polymicrobial otitis media occurs via interspecies quorum signaling." MBio, 1(3), e00102-10.
[83] Irie, Y. *et al.* (2012) "Self-produced exopolysaccharide is a signal that stimulates biofilm formation in *Pseudomonas aeruginosa*." Proc. Natl. Acad. Sci., USA, 109, 20632-20636.
[84] López, D. *et al.* (2009) "Structurally diverse natural products that cause potassium leakage trigger multicellularity in *Bacillus subtilis*." Proc. Natl. Acad. Sci., USA, 106, 280-285.
[85] González-Pastor J.E. *et al.* (2003) "Cannibalism by sporulating bacteria." Science, 301, 510-513.
[86] Kaplan J.B. (2010) "Biofilm dispersal: mechanisms, clinical implications, and potential therapeutic uses." J. Dent. Res., 89, 205-218.
[87] Sauer, K. *et al.* (2004) "Characterization of nutrient-induced dispersion in *Pseudomonas aeruginosa* PAO1 biofilm." J. Bacteriol., 186, 7312-7326.
[88] Karatan E., Watnick P. (2009) "Signals, regulatory networks, and materials that build and break bacterial biofilms." Microbiol. Mol. Biol. Rev., 73, 310-347.
[89] Barraud N. *et al.* (2006) "Involvement of nitric oxide in biofilm dispersal of *Pseudomonas aeruginosa*." J. Bacteriol., 188, 7344-7353.
[90] McDougald D. *et al.* (2011) "Should we stay or should we go: mechanisms and ecological consequences for biofilm dispersal." Nat. Rev. Microbiol., 10, 39-50.
[91] Huynh T.T. *et al.* (2012) "Glucose starvation-induced dispersal of *Pseudomonas aeruginosa* biofilms is cAMP and energy dependent." PLoS One 7, e42874.
[92] Wood T.K. (2014) "Biofilm dispersal: deciding when it is better to travel." Mol. Microbiol., 94, 747-750.
[93] Flemming H.-C. (2011) "The perfect slime." Colloids Surf. B. Biointerfaces, 86, 251-259.
[94] Madsen, J.S. *et al.* (2012) "The interconnection between biofilm formation and horizontal gene transfer." FEMS Immunol. Med. Microbiol., 65, 183-195.
[95] Burmølle M. *et al.* (2006) "Enhanced biofilm formation and increased resistance to antimicrobial agents and bacterial invasion are caused by synergistic interactions in multispecies biofilms." Appl. Environ. Microbiol., 72, 3916-3923.

[96] Elias S., Banin E. (2012) "Multi-species biofilms: living with friendly neighbors." FEMS Microbiol. Rev., 36(5), 990-1004.
[97] Flemming H.-C., Wingender J. (2010) "The biofilm matrix." Nat. Rev. Microbiol., 8, 623-633.
[98] Branda S.S. *et al.* (2005) "Biofilms: the matrix revisited." Trends Microbiol., 13, 20-26.
[99] Dogsa I. *et al.* (2013) "Exopolymer Diversity and the Role of Levan in *Bacillus subtilis* Biofilms." PLoS One 8, e62044.
[100] Bridier A. *et al.* (2011) "Dynamics of the action of biocides in *Pseudomonas aeruginosa* biofilms." Antimicrob. Agents Chemother., 55, 2648-2654.
[101] Wingender J. *et al.* (2001) "Isolation and biochemical characterization of extracellular polymeric substances from *Pseudomonas aeruginosa*." Methods Enzymol., 336, 302-314.
[102] Høiby N. *et al.* (2010) "*Pseudomonas aeruginosa* biofilms in cystic fibrosis." Future Microbiol., 5, 1663-1674.
[103] Harmsen M. *et al.* (2010) "An update on *Pseudomonas aeruginosa* biofilm formation, tolerance, and dispersal." FEMS Immunol. Med. Microbiol., 59, 253-268.
[104] Serra D.O. *et al.* (2013) "Cellulose as an architectural element in spatially structured *Escherichia coli* biofilms." J. Bacteriol., 195, 5540-5554.
[105] Rozen R. *et al.* (2004) "*Streptococcus mutans* fructosyltransferase interactions with glucans." FEMS Microbiol. Lett., 232, 39-43.
[106] May T. *et al.* (2009) "Induction of multidrug resistance mechanism in *Escherichia coli* biofilms by interplay between tetracycline and ampicillin resistance genes." Antimicrob. Agents Chemother., 53, 4628-4639.
[107] Mann E.E., Wozniak D.J. (2012) "*Pseudomonas* biofilm matrix composition and niche biology." FEMS Microbiol. Rev., 36, 893-916.
[108] Jabbouri S., Sadovskaya I. (2010) "Characteristics of the biofilm matrix and its role as a possible target for the detection and eradication of *Staphylococcus epidermidis* associated with medical implant infections." FEMS Immunol. Med. Microbiol., 59, 280-291.
[109] O'Gara, J.P. (2007) "Ica and beyond: biofilm mechanisms and regulation in *Staphylococcus epidermidis* and *Staphylococcus aureus*." FEMS Microbiol. Lett., 270, 179-188.
[110] Barnhart M.M. *et al.* (2006) "GlcNAc-6P levels modulate the expression of Curli fibers by *Escherichia coli*." J. Bacteriol., 188, 5212-5219.
[111] Lynch D.J. *et al.* (2007) "Glucan-binding proteins are essential for shaping *Streptococcus mutans* biofilm architecture." FEMS Microbiol. Lett., 268, 158-165.
[112] Diggle S.P. *et al.* (2006) "The galactophilic lectin, LecA, contributes to biofilm development in *Pseudomonas aeruginosa*." Environ. Microbiol., 8, 1095-1104.
[113] Borlee B.R. *et al.* (2010) "*Pseudomonas aeruginosa* uses a cyclic-di-GMP-regulated adhesin to reinforce the biofilm extracellular matrix." Mol. Microbiol., 75, 827-842.

[114] van Schaik E.J. *et al.* (2005) "DNA binding: a novel function of Pseudomonas aeruginosa type IV pili." J. Bacteriol., 187, 1455-1464.
[115] Zogaj X. *et al.* (2001) "The multicellular morphotypes of *Salmonella typhimurium* and *Escherichia coli* produce cellulose as the second component of the extracellular matrix." Mol. Microbiol., 39, 1452-1463.
[116] Lasa I., Penadés J.R. (2006) "Bap: a family of surface proteins involved in biofilm formation." Res. Microbiol., 157, 99-107.
[117] Epstein A.K. *et al.* (2011) "Bacterial biofilm shows persistent resistance to liquid wetting and gas penetration." Proc. Natl. Acad. Sci., USA, 108, 995-1000.
[118] Blanco L.P. *et al.* (2012) "Diversity, biogenesis and function of microbial amyloids." Trends Microbiol., 20, 66-73.
[119] Barnhart M.M., Chapman M.R. (2006) "Curli biogenesis and function." Annu. Rev. Microbiol., 60, 131-147.
[120] Branda S.S. *et al.* (2006) "A major protein component of the *Bacillus subtilis* biofilm matrix." Mol. Microbiol., 59, 1229-1238.
[121] Romero D. *et al.* (2010) "Amyloid fibers provide structural integrity to *Bacillus subtilis* biofilms." Proc. Natl. Acad. Sci., USA, 107, 2230-2234.
[122] Mann E.E. *et al.* (2009) "Modulation of eDNA release and degradation affects *Staphylococcus aureus* biofilm maturation." PLoS One, 4, e5822.
[123] Boyd A., Chakrabarty A.M. (1994) "Role of alginate lyase in cell detachment of *Pseudomonas aeruginosa*." Appl. Environ. Microbiol., 60, 2355-2359.
[124] Whitchurch C.B. *et al.* (2002) "Extracellular DNA required for bacterial biofilm formation." Science, 295, 1487.
[125] Thomas V.C. *et al.* (2008) "Regulation of autolysis-dependent extracellular DNA release by *Enterococcus faecalis* extracellular proteases influences biofilm development." J. Bacteriol., 190, 5690-5698.
[126] Izano E.A. *et al.* (2008) "Differential roles of poly-N-acetylglucosamine surface polysaccharide and extracellular DNA in *Staphylococcus aureus* and *Staphylococcus epidermidis* biofilms." Appl. Environ. Microbiol., 74, 470-476.
[127] Nemoto K. *et al.* (2003) "Effect of Varidase (streptodornase) on biofilm formed by *Pseudomonas aeruginosa*." Chemotherapy, 49, 121-125.
[128] Vilain S. *et al.* (2009) "DNA as an adhesin: *Bacillus cereus* requires extracellular DNA to form biofilms." Appl. Environ. Microbiol., 75, 2861-2868.
[129] Molin S., Tolker-Nielsen T. (2003) "Gene transfer occurs with enhanced efficiency in biofilms and induces enhanced stabilisation of the biofilm structure." Curr. Opin. Biotechnol., 14, 255-261.
[130] McDonnell G., Russell AD. (1999) "Antiseptics and disinfectants: activity, action, and resistance." Clin. Microbiol. Rev., 12, 147-179.
[131] Ho J. *et al.* (2010) "Multiresistant Gram-negative infections: a global perspective." Curr. Opin. Infect. Dis., 23, 546-553.
[132] Moellering R.C. (2012) "MRSA: the first half century." J. Antimicrob. Chemother., 67, 4-11.

[133] Bragg R. *et al.* (2014) "Bacterial resistance to Quaternary Ammonium Compounds (QAC) disinfectants." Adv. Exp. Med. Biol., 808, 1-13.
[134] Hegstad K. *et al.* (2010) "Does the wide use of quaternary ammonium compounds enhance the selection and spread of antimicrobial resistance and thus threaten our health?." Microb. Drug Resist., 16, 91-104.
[135] Zou L. *et al.* (2014) "Presence of disinfectant resistance genes in *Escherichia coli* isolated from retail meats in the USA." J. Antimicrob. Chemother., 69(10), 2644-2649.
[136] Gilbert P. *et al.* (2002) "Biofilms in vitro and in vivo: do singular mechanisms imply cross-resistance?." J. Appl. Microbiol., 92 Suppl, 98S-110S.
[137] Russell A.D. (2003) "Similarities and differences in the responses of microorganisms to biocides." J. Antimicrob. Chemother., 52, 750-763.
[138] Russell A.D. (1999) "Bacterial resistance to disinfectants: present knowledge and future problems." J. Hosp. Infect., 43 Suppl., S57-68.
[139] Thurnheer T. *et al.* (2003) "Mass transport of macromolecules within an in vitro model of supragingival plaque." Appl. Environ. Microbiol., 69, 1702-1709.
[140] Campanac C. *et al.* (2002) "Interactions between biocide cationic agents and bacterial biofilms." Antimicrob. Agents Chemother., 46, 1469-1474.
[141] Kobayashi K., Iwano M. (2012) "BslA(YuaB) forms a hydrophobic layer on the surface of *Bacillus subtilis* biofilms." Mol. Microbiol., 85, 51-66.
[142] De Beer D. *et al.* (1994) "Direct measurement of chlorine penetration into biofilms during disinfection." Appl. Environ. Microbiol., 60, 4339-4344.
[143] Grobe K.J. *et al.* (2002) "Role of dose concentration in biocide efficacy against *Pseudomonas aeruginosa* biofilms." J. Ind. Microbiol. Biotechnol., 29, 10-15.
[144] Stewart P.S. *et al.* (2001) "Biofilm penetration and disinfection efficacy of alkaline hypochlorite and chlorosulfamates." J. Appl. Microbiol., 91, 525-532.
[145] Ganeshnarayan K. *et al.* (2009) "Poly-N-acetylglucosamine matrix polysaccharide impedes fluid convection and transport of the cationic surfactant cetylpyridinium chloride through bacterial biofilms." Appl. Environ. Microbiol., 75, 1308-1314.
[146] Zheng Z., Stewart P.S. (2002) "Penetration of rifampin through *Staphylococcus epidermidis* biofilms." Antimicrob. Agents Chemother., 46, 900-903.
[147] Daddi Oubekka S. *et al.* (2012) "Correlative time-resolved fluorescence microscopy to assess antibiotic diffusion-reaction in biofilms." Antimicrob. Agents Chemother., 56, 3349-3358.
[148] Lewis K. (2005) "Persister cells and the riddle of biofilm survival." Biochemistry, 70, 267-274.
[149] Lewis K. (2008) "Multidrug tolerance of biofilms and persister cells." Curr. Top. Microbiol. Immunol., 322, 107-131.
[150] Lewis K. (2010) "Persister cells." Annu. Rev. Microbiol., 64, 357-372.
[151] Whiteley M. *et al.* (2001) "Gene expression in *Pseudomonas aeruginosa* biofilms." Nature, 413, 860-864.

[152] Nicolas P. *et al.* (2012) "Condition-dependent transcriptome reveals high-level regulatory architecture in *Bacillus subtilis*." Science, 335, 1103-1106.
[153] Shin J.-H. *et al.* (2009) "Proteomic analysis of *Acinetobacter baumannii* in biofilm and planktonic growth mode." J. Microbiol., 47, 728-735.
[154] Resch A. *et al.* (2006) "Comparative proteome analysis of *Staphylococcus aureus* biofilm and planktonic cells and correlation with transcriptome profiling." Proteomics, 6, 1867-1877.
[155] Rani S.A. *et al.* (2007) "Spatial patterns of DNA replication, protein synthesis, and oxygen concentration within bacterial biofilms reveal diverse physiological states." J. Bacteriol., 189, 4223-4233.
[156] Prigent-Combaret C. *et al.* (2001) "Complex regulatory network controls initial adhesion and biofilm formation in *Escherichia coli* via regulation of the csgD gene." J. Bacteriol., 183, 7213-7223.
[157] Pagedar A. *et al.* (2012) "Adaptation to benzalkonium chloride and ciprofloxacin affects biofilm formation potential, efflux pump and haemolysin activity of *Escherichia coli* of dairy origin." J. Dairy Res., 79, 383-389.
[158] Coenye T. (2010) "Response of sessile cells to stress: from changes in gene expression to phenotypic adaptation." FEMS Immunol. Med. Microbiol., 59, 239-252.
[159] Bruchmann J. *et al.* (2013) "Sub-inhibitory concentrations of antibiotics and wastewater influencing biofilm formation and gene expression of multi-resistant *Pseudomonas aeruginosa* wastewater isolates." Environ. Sci. Pollut. Res. Int., 20, 3539-3549.
[160] Dynes J.J. *et al.* (2009) "Morphological and biochemical changes in *Pseudomonas fluorescens* biofilms induced by sub-inhibitory exposure to antimicrobial agents." Can. J. Microbiol., 55, 163-178.
[161] Davin-Regli A., Pagès J.M. (2012) "Cross-resistance between biocides and antimicrobials: an emerging question." Rev. Sci. Tech., 31, 89-104.
[162] Buffet-Bataillon S. *et al.* (2012) "Emergence of resistance to antibacterial agents: the role of quaternary ammonium compounds – a critical review." Int. J. Antimicrob. Agents, 39, 381-389.
[163] Christensen B.B. *et al.* (1998) "Establishment of new genetic traits in a microbial biofilm community." Appl. Environ. Microbiol., 64, 2247-2255.
[164] Hausner M., Wuertz S. (1999) "High rates of conjugation in bacterial biofilms as determined by quantitative in situ analysis." Appl. Environ. Microbiol., 65, 3710-3713.
[165] Nguyen K.T. *et al.* (2010) "Mycobacterial Biofilms Facilitate Horizontal DNA Transfer between Strains of *Mycobacterium smegmatis*." J. Bacteriol., 192, 5134-5142.
[166] Savage V.J. *et al.* (2013) "*Staphylococcus aureus* biofilms promote horizontal transfer of antibiotic resistance." Antimicrob. Agents Chemother., 57, 1968-70.
[167] Montanaro L. *et al.* (2011) "Extracellular DNA in biofilms." Int. J. Artif. Organs, 34, 824-831.

[168] Trappetti C. *et al.* (2011) "LuxS mediates iron-dependent biofilm formation, competence, and fratricide in *Streptococcus pneumoniae*." Infect. Immun., 79, 4550-4558.
[169] Antonova E.S., Hammer B.K. (2011) "Quorum-sensing autoinducer molecules produced by members of a multispecies biofilm promote horizontal gene transfer to *Vibrio cholerae*." FEMS Microbiol. Lett., 322, 68-76.
[170] Van Meervenne E. *et al.* (2014) "Biofilm models for the food industry: hot spots for plasmid transfer?." Pathog. Dis., 70, 332-338.
[171] Ghigo J.M. (2001) "Natural conjugative plasmids induce bacterial biofilm development." Nature, 412, 442-445.
[172] Teodósio J.S. *et al.* (2012) "The influence of nonconjugative *Escherichia coli* plasmids on biofilm formation and resistance." J. Appl. Microbiol., 113, 373-382.
[173] Ryder V.J. *et al.* (2012) "Increased mutability of *Staphylococci* in biofilms as a consequence of oxidative stress." PLoS One, 7, e47695.
[174] Driffield K. *et al.* (2008) "Increased mutability of *Pseudomonas aeruginosa* in biofilms." J. Antimicrob. Chemother., 61, 1053-1056.
[175] Boles B.R. *et al.* (2004) "Self-generated diversity produces 'insurance effects' in biofilm communities." Proc. Natl. Acad. Sci., USA, 101, 16630-16635.
[176] Uhlich G.A. *et al.* (2006) "Analyses of the red-dry-rough phenotype of an *Escherichia coli* O157:H7 strain and its role in biofilm formation and resistance to antibacterial agents." Appl. Environ. Microbiol., 72, 2564-2572.
[177] Morris J.G. *et al.* (1996) "*Vibrio cholerae* 01 Can Assume a Chlorine-Resistant Rugose Survival Form that Is Virulent for Humans." J. Infect. Dis., 174, 1364-1368.
[178] Starkey M. *et al.* (2009) "*Pseudomonas aeruginosa* rugose small-colony variants have adaptations that likely promote persistence in the cystic fibrosis lung." J. Bacteriol., 191, 3492-3503.
[179] Ciofu O. *et al.* (2005) "Occurrence of hypermutable *Pseudomonas aeruginosa* in cystic fibrosis patients is associated with the oxidative stress caused by chronic lung inflammation." Antimicrob. Agents Chemother., 49, 2276-2282.
[180] Silva I.N. *et al.* (2013) "Stress conditions triggering mucoid morphotype variation in *Burkholderia* species and effect on virulence in *Galleria mellonella* and biofilm formation in vitro." PLoS One, 8, e82522.
[181] Hansen S.K. *et al.* (2007) "Characterization of a *Pseudomonas putida* rough variant evolved in a mixed-species biofilm with *Acinetobacter* sp. strain C6." J. Bacteriol., 189, 4932-4943.
[182] Trejo-Hernández A. *et al.* (2014) "Interspecies competition triggers virulence and mutability in *Candida albicans* - *Pseudomonas aeruginosa* mixed biofilms." ISME J., 8, 1974-1988.
[183] Miller M.B., Bassler B.L. (2001) "Quorum Sensing in Bacteria." Annu. Rev. Genet., 55, 165-199.

[184] Fuqua C. *et al.* (2001) "Regulation of gene expression by cell-to-cell communication: acyl-homoserine lactone quorum sensing." Annu. Rev. Genet., 35, 439-468.
[185] West S.A. *et al.* (2012) "Quorum sensing and the confusion about diffusion." Trends Microbiol., 20, 586-594.
[186] Pereira C.S. *et al.* (2013) "AI-2-mediated signalling in bacteria." FEMS Microbiol. Rev., 37, 156-181.
[187] Xavier K.B., Bassler B.L. (2005) "Interference with AI-2-mediated bacterial cell-cell communication." Nature, 437, 750-753.
[188] Jayaraman A., Wood T.K. (2008) "Bacterial quorum sensing: signals, circuits, and implications for biofilms and disease." Annu. Rev. Biomed. Eng., 10, 145-167.
[189] Amaral L. *et al.* (2014) "Efflux pumps of Gram-negative bacteria: what they do, how they do it, with what and how to deal with them." Front. Pharmacol., 4, 168.
[190] Sharma M., Prasad R. (2011) "The quorum-sensing molecule farnesol is a modulator of drug efflux mediated by ABC multidrug transporters and synergizes with drugs in *Candida albicans*." Antimicrob. Agents Chemother., 55, 4834-4843.
[191] Stewart P.S. *et al.* (2000) "Effect of catalase on hydrogen peroxide penetration into *Pseudomonas aeruginosa* biofilms." Appl. Environ. Microbiol., 66, 836-838.
[192] Hassett D.J. *et al.* (1999) "Quorum sensing in *Pseudomonas aeruginosa* controls expression of catalase and superoxide dismutase genes and mediates biofilm susceptibility to hydrogen peroxide." Mol. Microbiol., 34, 1082-1093.
[193] Shih P.-C., Huang C.-T. (2002) "Effects of quorum-sensing deficiency on *Pseudomonas aeruginosa* biofilm formation and antibiotic resistance." J. Antimicrob. Chemother., 49, 309-314.
[194] Whiteley M. *et al.* (2000) "Regulation of quorum sensing by RpoS in *Pseudomonas aeruginosa*." J. Bacteriol., 182, 4356-4360.
[195] Anderson G.G., O'Toole G.A. (2008) "Innate and induced resistance mechanisms of bacterial biofilms." Curr. Top. Microbiol. Immunol., 322, 85-105.
[196] Foster P.L. (2005) "Stress responses and genetic variation in bacteria." Mutat. Res., 569, 3-11.
[197] Bauer W.D., Robinson J.B. (2002) "Disruption of bacterial quorum sensing by other organisms." Curr. Opin. Biotechnol., 13, 234-237.
[198] Zhang L.-H., Dong Y.-H. (2004) "Quorum sensing and signal interference: diverse implications." Mol. Microbiol., 53, 1563-1571.
[199] Rendueles O., Ghigo J.-M. (2012) "Multi-species biofilms: how to avoid unfriendly neighbors." FEMS Microbiol. Rev., 36, 972-989.
[200] Römling U., Balsalobre C. (2012) "Biofilm infections, their resilience to therapy and innovative treatment strategies." J. Intern. Med., 272, 541-561.

[201] Raad I. *et al.* (1998) "*Staphylococcus epidermidis*: emerging resistance and need for alternative agents." Clin. Infect. Dis., 26, 1182-7.
[202] Wingender J., Flemming H.-C. (2011) "Biofilms in drinking water and their role as reservoir for pathogens." Int. J. Hyg. Environ. Health, 214, 417-423.
[203] Leriche V. *et al.* (2003) "Ecology of mixed biofilms subjected daily to a chlorinated alkaline solution: spatial distribution of bacterial species suggests a protective effect of one species to another." Environ. Microbiol., 5, 64-71.
[204] Kara D. *et al.* (2006) "Differences between single- and dual-species biofilms of *Streptococcus mutans* and *Veillonella parvula* in growth, acidogenicity and susceptibility to chlorhexidine." Eur. J. Oral Sci., 114, 58-63.
[205] Van der Veen S., Abee T. (2011) "Mixed species biofilms of *Listeria monocytogenes* and *Lactobacillus plantarum* show enhanced resistance to benzalkonium chloride and peracetic acid." Int. J. Food Microbiol., 144, 421-431.
[206] Sanchez-Vizuete P. *et al.* (2015) "Pathogens protection against the action of disinfectants in multispecies biofilms." Front. Microbiol., 6, 705.
[207] Kaplan J.B. *et al.* (2004) "Genes involved in the synthesis and degradation of matrix polysaccharide in *Actinobacillus actinomycetemcomitans* and *Actinobacillus pleuropneumoniae* biofilms." J. Bacteriol., 186, 8213-8220.
[208] Darouiche R.O. *et al.* (2009) "Antimicrobial and antibiofilm efficacy of triclosan and DispersinB combination." J. Antimicrob. Chemother., 64, 88-93.
[209] Nguyen U.T., Burrows L.L. (2014) "DNase I and proteinase K impair Listeria monocytogenes biofilm formation and induce dispersal of pre-existing biofilms." Int. J. Food Microbiol., 187, 26-32.
[210] Banin E. *et al.* (2006) "Chelator-induced dispersal and killing of *Pseudomonas aeruginosa* cells in a biofilm." Appl. Environ. Microbiol., 72, 2064-2069.
[211] Kaplan J.B. *et al.* (2012) "Recombinant human DNase I decreases biofilm and increases antimicrobial susceptibility in *Staphylococci*." J. Antibiot. (Tokyo), 65, 73-77.
[212] Kerrigan J.E. *et al.* (2008) "Modeling and biochemical analysis of the activity of antibiofilm agent Dispersin B." Acta Biol. Hung., 59, 439-451.
[213] Rasmussen T.B. *et al.* (2005) "Screening for quorum-sensing inhibitors (QSI) by use of a novel genetic system, the QSI selector." J. Bacteriol., 187, 1799-1814.
[214] Blackledge M.S. *et al.* (2013) "Biologically inspired strategies for combating bacterial biofilms." Curr. Opin. Pharmacol., 13, 699-706.
[215] Zhu J., Kaufmann G.F. (2013) "Quo vadis quorum quenching?." Curr. Opin. Pharmacol., 13, 688-698.
[216] Sambanthamoorthy K. *et al.* (2014) "Identification of small molecules inhibiting diguanylate cyclases to control bacterial biofilm development." Biofouling, 30(1), 17-28.

[217] Houry A. *et al.* (2012) "Bacterial swimmers that infiltrate and take over the biofilm matrix." Proc. Natl. Acad. Sci., USA, 109, 13088-13093.
[218] Hochbaum A.I. *et al.* (2011) "Inhibitory effects of D-amino acids on *Staphylococcus aureus* biofilm development." J. Bacteriol., 193, 5616-5622.
[219] Sanchez Z. *et al.* (2013) "Extensive reduction of cell viability and enhanced matrix production in *Pseudomonas aeruginosa* PAO1 flow biofilms treated with a D-amino acid mixture." Appl. Environ. Microbiol., 79, 1396-1399.
[220] Kolodkin-Gal I. *et al.* (2010) "D-amino acids trigger biofilm disassembly." Science, 328, 627-629.
[221] Kolodkin-Gal I. *et al.* (2012) "A self-produced trigger for biofilm disassembly that targets exopolysaccharide." Cell, 149, 684-692.
[222] Davies D.G., Marques C.N.H. (2009) "A fatty acid messenger is responsible for inducing dispersion in microbial biofilms." J. Bacteriol., 191, 1393-1403.

# 6 Journey to the centre of biofilms: nature, cohesiveness and functions of the exopolymer matrix

**Jean-Claude Block and Grégory Francius**

Biofilms could be defined as "more or less cohesive deposits made up of cells and organic polymers, which adhere to surfaces (soft or hard, mineral or organic surfaces)". Such a definition highlights the role of the organic polymers, which bind the cells together and to the surface of the colonized material. These extra- or exocellular polymers[1] (acronym EPS) are synthesized by the microorganisms themselves. They represent a large mass fraction and determine the volume of the intercellular space of biofilms. Some of their characteristics and functions are reported in this chapter. Our literature review is mainly based on publications on multispecies biofilms grown in the environment (not on laboratory-grown pure species biofilms) and subjected to environmental stresses such as those found in rivers, drinking water distribution systems and sewer systems.

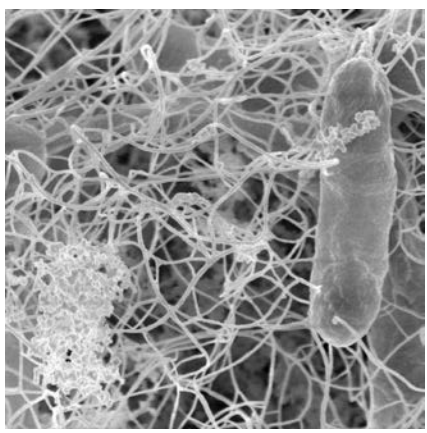

**Fig. 6.1.** – Exopolymeric network and bacterial cells in an acidophilic biofilm sampled from a drilling site - Confocal microscopy image of 5 µm by 5 µm. Courtesy Professor Steven K. Lower (Ohio State University, Colombus, USA). See also [1].

[1] The two prefix exo- (Greek root) and extra- (Latin root) both mean "a relation to something which is external", and are used equally for exopolymers or extracellular polymers.

The EPS can be compared to a flexible, intertwined network of cables, which controls the 3D architecture of the whole biofilm (Fig. 6.1). They contribute to the building of soft, hydrated, viscoelastic structures of a few hundred micrometers in thickness (sometimes several millimetres!), bearing negative charges associated with carboxylates, phosphates and, more rarely, sulphates [2]. As a result, they are able to swell or shrink, depending on the pH and ionic concentration in the liquid, as it has been shown for polymers on the surface of planktonic bacterial cells [3].

This EPS matrix delimits a very particular reactive domain, which is functionalized by some hydrolytic exo-enzymes. The diffusion of many chemical species is generally slowed down by reaction or consumption in/with the matrix (protons, di-oxygen, nitrates, chlorine, nutritive molecules, quorum sensing molecules). It generates a chemical gradient from the bulk to the bottom of the biofilm, and many minerals can precipitate inside the matrix (calcium carbonate, iron oxides) [4, 5].

It is important to recognize that the EPS network generates a functional environment, the organization of which is governed by the microorganisms [6], constantly re-organized as soon as environmental conditions change [7]. *De facto*, many functions are associated to EPS (Table 6.1). This very particular situation undoubtedly explains the advantages of life in biofilms over planktonic existence. These advantages are shared by the different partners of the sessile community which together handle the "common good" and associated resources. Even though the formation and growth of the EPS network can be assessed with some mathematical laws of chaos, one has to bear in mind that such organization is oriented and bacteria dependent as the biological activity of live bacteria is its main driver.

**TABLE 6.1.** – Functions associated with biofilm EPS.

| Functions/Properties | EPS |
|---|---|
| Construction – cohesion – mechanical resistance | All EPS, with particular prominence of amyloid fibres, and eDNA |
| Signalling – information | Lectins, eDNA, nanowires (electron transport) |
| Enzymatic activities and redox | Exo- and ecto-enzymes |
| Nutrition | All biodegradable EPS + exogenous biodegradable macromolecules |
| Protection against grazing, desiccation, toxic molecules, *etc.* | All EPS (overproduction of EPS reinforces protection) |

This chapter is organized into three major sections: the chemistry of EPS, their contribution to the cohesiveness of the biofilm and their reactivity (reservoir of ions and hydrophobic matter, associated enzymatic activity).

## 6.1. Chemistry of EPS in environmental biofilms

Depending on the state of knowledge and the analytical techniques used, biofilm EPS have been called by different names from a very general name (extracellular polymeric substances) to a more specific one (*i.e.*, exo-polysaccharides). Indeed, the latter was used at a time (1970-80) when biofilm exopolymers were thought to be formed exclusively by sugars (see the short review by [8]), which is now known to be false (especially for multi-species biofilms found in aquatic environments). Several reviews of interest show this shift and our progress toward a better description of the very complex EPS matrix named xPS by some authors [8-16]. In general terms, one may recognize that polymers excreted by microorganisms and forming the biofilm matrix are a mixture of molecules with different signatures such as polysaccharides, proteins, lipids, nucleic acids, as well as cellular material after the lysis of some cells. It means they are both homo- and hetero-polymers still difficult to analyse in such complex mixtures (Table 6.2).

**Table 6.2.** – Homo- and hetero-polymers identified in the EPS matrix of biofilms (see the reviews [8, 13]).

| Nature of EPS | Characteristics |
|---|---|
| Linear or ramified polysaccharides | Alginates, cellulose, poly-N-acetyl-glucosamine, glycogen, teichoic acids, colanic acid /0.5 to 2 $10^6$ daltons (some are insoluble and hygroscopic and constitute viscoelastic gels) |
| Glycoconjugates | Glycoproteins, poly-N-acetylglucosamine, polysaccharide intercellular adhesins (PIA), glycolipids including lipopolysaccharides (LPS), lipoteichoic acids |
| Enzymatic and non enzymatic proteins | Flagella residues, fimbriae, pili<br>amyloid fibres from 0.1 to 10 µm; curli (*Escherichia coli, Salmonella*); TasA (*Bacillus subtilis*); FaB (*Pseudomonas*); nanowires; lectins; proteases, glucosidases, esterases, oxidoreductases, *etc.* |
| Extracellular DNA (eDNA) | Identified since 2000, eDNA differs from cellular DNA (its excretion could be controlled by a release programme) |
| Lipids | Sometimes as vesicles |

Extraction methods of EPS – in particular those highly aggressive using hot alkali, phenols, EDTA or ultrasounds, which have been used for a long time as a preliminary step before analysis – are no longer used where possible. Indeed, since the extraction yields are unknown, these methods lyse some cells, spoil the extracts and the chemicals used generate interferences with the analytical methods [17]. Useful developments have been made in the field of EPS analysis with the use of non-destructive techniques combining for example fluorochrome staining, labelling with lectins or hydrophobic probes with confocal microscopy and spectroscopy techniques such as IR, Raman, fluorescence correlation spectroscopy, atomic force microscopy (AFM) and NMR.

Some examples are given here to illustrate the type of information gained from these different methods. Then, Wagner *et al.* [18] using Raman spectroscopy showed that glycoproteins varied and accumulated during biofilm ageing. Similar observations were reported by Jiao *et al.* [19] with biofilms analysed by two techniques: $^{13}C$ NMR and infrared Fourier transform infrared spectroscopy (FTIR). By combining labelling with lectins linked to fluorochromes and confocal microscopy, Zippel and Neu [5] drew a map of the glycoconjugate distribution and calcite precipitates in biofilms grown on tuff rocks. Quilès *et al.* [20] and Fahs *et al.* [21] using vibration spectroscopies (infrared and Raman) and force microscopy of single molecules proved the presence of extracellular glycogen and glycoproteins in the matrix of *Pseudomonas fluorescens* biofilms. Finally, in addition to these examples, pH assessment of the liquid phase in the intercellular space of biofilms is made possible in a non-destructive way (*i.e.,* without using microelectrodes) by measuring the fluorescence emitted by specific fluorochromes, which diffuse only in the intercellular space [22].

EPS distribution in biofilms appears non-homogeneous but with specific zonations, which show spatiotemporal variations. For example, there is some sort of stratification of polysaccharides in biofilms, the highest concentration being found in the deeper layers [23], and in aerated biofilms [24]. Additionally, Lawrence *et al.* [25] showed domains in bacterial colonies with EPS organized into three zones with differentiated enzymatic activities. Slight chemical modifications of EPS significantly affect their properties as shown with the O-acetylation of mannuronic residues of *Pseudomonas* alginate which as a result becomes much more viscous [26]. Finally, another example was provided by Taglialegna *et al.* [27]. The authors reported that bacteria build a biofilm matrix scaffold from exopolysaccharides or proteins, and DNA. They showed that pathogenic *Staphylococcus aureus* produces a protein scaffold based on amyloid assembly of fragments from the biofilm-associated protein. Amyloidogenesis occurred in response to environmental signals (as pH and $Ca^{2+}$ concentration) [28].

## 6.2. Contribution of EPS to the cohesiveness of biofilms

The mechanical resistance of the biofilm to its dispersion in water and under hydraulic shear stresses generated by water circulation can only be explained by the fact that biopolymers that constitute the extracellular matrix are tightly and properly bonded to one another (Fig. 6.2).

Three groups of bonds or interactions are involved in this assembly: strong bonds such as coordination bonds (by the bridging of divalent cations); moderate bonds such as interactions between molecules (van der Waals interactions generated in a polar solvent such as water by dipole-dipole interactions, induced dipole-induced dipole and π-stacking) and weak bonds such as hydrogen bonds. All these forces are additive and proportional to the number of biopolymers in interaction and therefore can be extremely high.

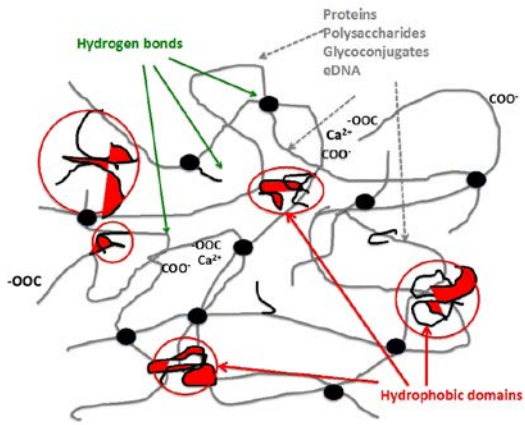


**Fig. 6.2.** – Examples of weak physicochemical interactions and exopolymer entanglement within a biofilm (adapted from [29]).

As the cohesion of the whole biofilm is tightly locked by the EPS, the forces required to detach the aggregates forming the biofilm are inversely proportional to their respective volumes. As a result, the hydrodynamic shear stress that can be applied on the biofilm by circulating water (in a 20 cm diameter pipe at a speed of 5 m $s^{-1}$) does not exceed 10 Pa and does not allow the removal of biofilm aggregates smaller than 200 $\mu m^3$ as shown in figure 6.3.

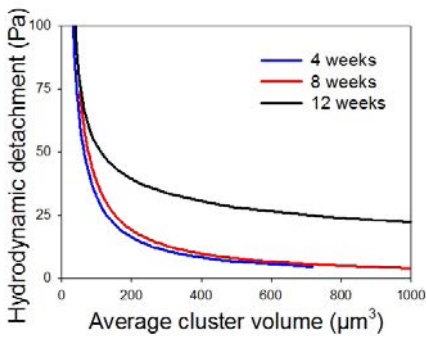


**Fig. 6.3.** – Relation between the volume of the biofilm aggregates and the hydrodynamic forces required for their removal (adapted from [30]).

To explain this mechanical resistance, Abe *et al.* [31] described a dual-scale mechanical model to predict the biofilm's mechanical detachment. This model is based on two assumptions. The first assumption is that the biofilm is composed of finite and interconnected elastic and viscous components. The second assumption is that the mechanical resistance of the biofilm is related to the

binding force that holds biofilm components together, on one hand and to the pulling force required to remove it from the substrate, on the other. In this approach, the authors sought to establish a relationship between the volume of biofilm aggregates and their elastic cohesion that comes from the thermal activation energy. Thus, assuming that a biofilm aggregate consists of a network of interconnections between the exopolymers on one hand, and the bacteria and the substrate on the other, it is possible to define a parameter denoted by $\xi$ that reflects the cohesion factor of this bacterial aggregate. This means that $\xi$ is a physical parameter proportional to the entanglement or cross-linking rate within the biofilm aggregate. This last hypothesis makes it possible to determine the relation existing between the elastic energy, the volume of the aggregate and its cohesion factor with the following equation:

$$E_{elas} \approx G L^3 \approx G(\xi d)^3 \approx G \xi^3 V_{cluster} \tag{6.1}$$

where $G$ is the elastic shear modulus, $L^3$ the volume of the considered bacterial aggregate, $\xi$ the cohesion factor or entanglement ratio and d the mesh size.

The total energy of the aggregate corresponds to the difference between its mechanical energy and the activation energy or thermal agitation:

$$E_{total} = E_{elas} - k_B T \tag{6.2}$$

with $T$ the absolute temperature and $k_B$ the Boltzmann constant.

At equilibrium, it may be considered that the elastic energy is of the same order of magnitude as the thermal agitation energy, thus allowing equations (6.1) and (6.2) to be combined as follows:

$$G \xi^3 V_{cluster} = k_B T \tag{6.3}$$

Consequently, the volume of the biofilm aggregate is inversely proportional to the elastic shear modulus according to equation (6.4):

$$V_{cluster} = \frac{k_B T}{\xi^3 G} \tag{6.4}$$

Excluding the cohesion factor $\xi$, equation (6.4) derives from the classical mechanic equations that are generally found for suspended particle systems. The authors referred to this last equation in order to measure by AFM the mechanical shear stresses exerted on bacterial aggregates constituting drinking water biofilms of 4, 8 and 12 weeks of age. They were finally able to deduce and predict the corresponding hydrodynamic shear stresses required for the total detachment of biofilm aggregates as shown in figure 6.3.

The predictive model of hydrodynamic detachment shear stress has already been described for mechanical systems such as suspension of non-spherical particles [32, 33]. This approach was taken up by Abe *et al.* [30] and adapted for the bacterial aggregates that form the biofilm. The authors described the hydrodynamic detachment stress $\sigma$ as the sum of a viscous term $\sigma_{ij}^{f}$ and an elastic

term $\sigma^b$ which are exerted respectively on a surface denoted $A_1$ and a surface $A_1$-$A_0$, where $A_0$ and $A_1$ correspond to the area occupied by the aggregate before and after the action of the mechanical shear stress:

$$\sigma_{ij} = \frac{1}{V}\sum_{1}^{n}\left(\int_{A_0-A_1}\sigma_{ik}\,x_j\,n_k\,dA + \int_{A_1}\sigma_{ik}^{b}\,x_j\,n_k\,dA\right) \tag{6.5}$$

with $V$ the volume of the considered bacterial aggregate, $\sigma_{ij}$ and $\sigma_{ik}$ the shear stress tensors, $i$, $j$ and $k$ the floating directions of space, and $x_j$ and $n_k$ are vectors.

This equation (Eq. (6.5)) can be simplified by introducing the physical parameters $C$ and $\xi$, which correspond to the average bacterial concentration within the aggregate and the cohesion ratio of the aggregate, respectively.

$$\sigma_{ij} = \sigma_{ij}^{f} C(1-\xi) + \sigma_{ij}^{b} C\,\xi \tag{6.6}$$

where the viscous and the elastic strains are derived respectively from the shear rate $\gamma$ (corresponding to the viscosity of the shearing fluid) and $\mu$ the mechanical deformation of the aggregate.

This makes it possible to simplify the above equation as follows:

$$\sigma_{ij}^{f} = \mu\frac{d\varepsilon}{dt} = \mu\,\gamma \text{ and } \sigma_{ij}^{b} = G\,\varepsilon \tag{6.7}$$

Moreover, it can be underlined that equation (6.6) is equivalent to the common expression of the average mechanical shear stress applied to a viscoelastic element denoted by Kelvin-Voigt element. As a result, the sum of $\sigma^f$ and $\sigma^b$ terms can be rewritten as follows:

$$\tau = \mu\,C(1-\xi)\frac{d\varepsilon}{dt} + G\,C\,\xi\,\varepsilon \tag{6.8}$$

If the shear flow describes a step function (Heaviside step function), then the solution of equation (6.8) is proportional to the modulus $f(t)$ of the bacterial aggregate, which depends on the deformation or strain $\varepsilon$.

$$f(t) = \frac{1}{G\,\xi}\left(1 - e^{\frac{-t}{\theta}}\right) \quad \text{and} \quad \theta = \frac{\mu(1-\xi)}{G\,\xi} \tag{6.9}$$

where $\theta$ corresponds to the viscoelastic relaxation time.

From equation (6.9), it is now possible to calculate the time required for the deformation stress to be distributed to the whole of the biofilm aggregate when it is subjected to a mechanical shear stress. The elastic deformation of the aggregate is then instantaneous if the cohesion factor $\xi$ is close to 1. This behaviour is generally observed for materials behaving as an elastic solid. If the cohesion factor $\xi$ is low, *i.e.* close to 0, then the material creeps or flows like a viscous liquid. In the case of intermediate values, *i.e.* $0 < \xi < 1$, the behaviour of the biofilm aggregates is equivalent to that of a viscoelastic solid.

The equations described above allow estimation of the threshold hydrodynamic shear stress values for detachment of a biofilm aggregate characterized by a volume $V_{cluster}$ and an elastic modulus $G$. In equation (6.8), the total shear stress exerted on the aggregate may fall to zero when the aggregate collapses. In this case, the hydrodynamic shear stress is equal to the mechanical shear stress (the deformation is maximum during the detachment of the aggregate, *i.e.*, $\varepsilon \sim 1$).

$$\mu \frac{d\varepsilon}{dt} C(1-\xi) = \mu \gamma C(1-\xi) = G C \xi \varepsilon_{max} \tag{6.10}$$

If $\varepsilon_{max} \sim 1$, equation (6.10) can be rewritten as follows:

$$\tau_{hyd} = \mu\gamma = \frac{G\xi}{1-\xi} \tag{6.11}$$

Equation (6.11) expresses the evolution of the hydrodynamic detachment stress $\tau_{hyd}$ as a function of the volume of the aggregate and of its cohesion factor $\xi$. The expression of the cohesion factor can then be deduced from equation (6.4):

$$\xi = \sqrt[3]{\frac{k_B T}{G\, V_{cluster}}} \tag{6.12}$$

This physical parameter is proportional to the correlation length $\lambda$ (elementary mesh size) defined below:

$$\lambda = \sqrt[3]{\frac{k_B T}{G}} \tag{6.13}$$

This expression is well known for mechanical description of colloidal suspensions of particles and polymers. However, there is not a lot of literature on estimated values of $\lambda$ for biofilms. Using this definition of the elementary mesh for each aggregate, one can estimate the number of contact points between the biopolymers that provide the structural cohesion of the biofilm.

For an elementary polymer chain of length $L$ and a mesh length $\lambda$ in the structure, the number of contact points $N$ can be described according to the following equation:

$$N = (L/\lambda)^3 \tag{6.14}$$

For an aggregate of volume $V_{cluster}$ containing $n$ elementary volumes $L^3$ ($nL^3 \sim V_{cluster}$), the expression of the total number of contact points $N$ can be written from equations (6.13) and (6.14) as follows:

$$N = \frac{G \cdot V_{cluster}}{k_B T} \tag{6.15}$$

where $T$ is the absolute temperature, $G$ the mechanical shear stress modulus and $k_B$ the Boltzmann coefficient.

Equation (6.15) shows that the number of contact points increases linearly with the volume of the aggregate. Besides, it is also related to the ratio of the cohesive energy of the aggregate denoted by $GV_{cluster}$ and the thermal agitation energy $k_BT$. It can be noted that the cohesion of the biofilm and its elastic modulus are intrinsically related to the number of contact points per unit volume of the biofilm. The last parameter is highly dependent on the nature and the number of biopolymers that forming the extracellular matrix of the biofilm.

Abe *et al.* [30] and Mathieu *et al.* [34] have shown that in some cases, biofilm cohesion can be enhanced by hydrodynamic stress. The authors proposed an explanation for such a mechanical behaviour based on two assumptions. The first relates to the fact that the aggregates of the biofilm can be considered as a stratified, or layered structure in which each layer is increasingly stiff as one goes deeper into the aggregate. Indeed, the stratification of environmental biofilms has already been described and the presence of a soft top layer and a more cohesive basal layer has already been reported by several authors [35, 36]. Furthermore, Abe *et al.* [30] have confirmed this layered structure using a layer-by-layer mechanical scraping method. In such experiments, the authors assumed all layers of the biofilm are composed of similar cohesive elements. The difference in cohesion between each successive layer could be explained by differences in the composition of the aggregates (nature and quantity of biopolymers and their entanglement rate, bacterial diversity, cations, *etc.*) as well as by the cohesion interactions between all these components with the substrate [30, 37, 38].

The second hypothesis that has been expressed by the authors is that the hydrodynamic shear stress can reinforce the cohesion of the biofilm structure by deforming the aggregate so as to densify the network of biopolymers. This hypothesis was verified by Stoodley *et al.* [39] who observed that biofilms formed under significant hydrodynamic shear conditions ($\tau_{hyd} = 10$ Pa) were more resistant and cohesive than those formed under less intense hydrodynamic conditions ($\tau_{hyd} = 0$ or 5 Pa). These authors also pointed out that the lateral deformation and stiffness of the biofilm had also been increased with hydrodynamic shear stress. Consequently, the porosity and interstitial channels of the aggregates were reduced and some flattening of the biofilm structure could be observed [30].

Therefore, it can be hypothesized that, under increasing conditions of hydrodynamic shear stress, the extracellular matrix of EPS is subjected to dehydration processes [40], which could lead to the matrix shrinking [41-43]. In addition, the variations in biofilm cohesion may reflect a change in the spatial distribution of the biopolymers and consequently in their entanglement rate [44, 45]. This rearrangement can in turn reduce the mesh size (correlation length) of the biopolymer network and, accordingly, change the number of contact points ($N$) within the biofilm extracellular matrix.

The evolution of $N$ as a function of the aggregates volume described in equation (6.15) has been evidenced for drinking water biofilms subjected to a hydrodynamic shear stress treatment [34]. The authors have demonstrated that the

number of contact points per unit volume increases from 1.6 $10^6$ µm$^{-3}$ to more than 3 $10^6$ µm$^{-3}$ after applying a hydrodynamic shear stress of 10 Pa. The reduction in mesh size of the primary structure of the biofilm is a consolidation phenomenon developed by Laspidou and Rittman [46, 47] and leading to biofilm compression as described by Paul *et al.* [43] and Péchaud *et al.* [48].

Moreover, the sudden increase in the hydrodynamic shear stress induces a normal mechanical shear stress, which is responsible for increased compactness of the biopolymers constituting the biofilm extracellular matrix. This increase in compactness is largely due to the high flexibility of the biopolymers. Besides, several authors [49, 50] have estimated radii of gyration $r_g$ (natural size of the biopolymers in their folded conformation) ranging from 10 to 100 nm for polysaccharides extracted in biofilms.

These values are lower than those reported by Abe e*t al.* [30] and Camesano and Abu-Lail [51] who measured the length of unfolded polysaccharides present in biofilms in the range 1-10 µm. This proves that the biopolymers forming the biofilm may be folded into ball-like structures, thus leading to entanglement and a high number of contact points. The entanglement rate $N^*$ resulting from the ball-like conformation of the biopolymers can be estimated from the ratio between the contour length $L_c$ and the radius of gyration $r_g$:

$$N^* \propto \frac{L_c}{r_g} \tag{6.16}$$

where $L_c$ corresponds to the maximum size attainable with a completely unfolded biopolymer. In the present case, the authors [30, 34] have estimated values in the range of 10-1,000 for the parameter $N^*$, *i.e.,* each polymer can generate between 10 and 1,000 contact points. Estimating the maximum number of polymers per µm$^3$ inside a biofilm ($N_{mol}$) is a good indicator of the number of contact points within the extracellular matrix. Considering the following equation:

$$N_{mol} = \frac{1}{r_g^3} \tag{6.17}$$

It can be deduced that 1 µm$^3$ of biofilm could contain up to $10^3$ to $10^4$ polymers. In this case, the maximum number of contact points originating from the entanglement of all the biopolymers $N_{max}$ can be estimated according to the following equation:

$$N_{max} \propto N_{mol} \times N^* \tag{6.18}$$

In this case, the biofilm would be characterized by $N_{max}$ values of between $10^4$ and $10^7$ contact points per µm$^3$. These values were experimentally verified by Mathieu *et al.* [34] who measured values of about $10^6$ contact points per µm$^3$ for drinking water biofilms.

## 6.3. Reactivity of EPS in biofilms

### 6.3.1. Trapping ions and organics by EPS

The accumulation of metallic ions and low soluble organic molecules is possible thanks to negative sites and hydrophobic domains found in the EPS matrix, respectively. The negative charges associated with EPS determine the cation exchange capacity [19, 52]. This observation is in good agreement with the properties of activated sludge EPS [53]. It also explains that positively charged antiseptics such as quaternary ammonium compounds (benzalkonium chloride and cetylpyridinium) diffuse very slowly in biofilms. The hydrophobic domains distributed in the matrix play another key role (more effectively than cells) in trapping poorly soluble or amphiphilic molecules such as benzene, toluene, pyrene [52], or detergents and steroid molecules [54]. These hydrophobic domains were identified in activated sludge flocs [55], and found in large numbers within the biofilm EPS matrix using labelled nanoparticles [56, 57] (Fig. 6.4).

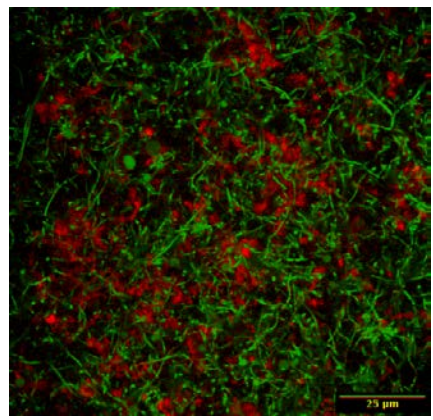


**Fig. 6.4.** – Distribution of nanoparticles as quantum dots (QDs) functionalized with hydrophobic ligands in *Shewanella oneidensis* biofilms. The bacterial cells stained with fluorochrome Syto9 appear green, while the hydrophobic zones of the intercellular space accumulating QDs appear red.

The same can be shown with hydrophobic viral particles (average diameter = 23 nm), which accumulate in biofilms more rapidly than hydrophilic particles [58]. Such observations are in good agreement with previous works: (i) van Loosdreecht *et al.* [59] showed greater adhesion of hydrophobic cells on polystyrene than hydrophilic cells; (ii) Zita and Hermansson [60] showed significant accumulation of hydrophobic *E. coli* in activated sludge aggregates; and (iii) Tatchou-Nyamsi-König *et al.* [61] by comparing the behaviour of two bacterial adsorption events on PET (polyethylene terephthalate) showed that

*Mycobacterium* (that is both very hydrophobic and negatively charged) was adhering in higher number than the smaller and very hydrophilic *Campylobacter*.

Thanks to their EPS, biofilms can trap (and later hydrolyse – section 6.3.2) exogenous biodegradable polymers and particles that unicellular bacteria cannot assimilate directly. Indeed, Guellil *et al.* [62] showed that a large fraction of colloidal organic matter from wastewater was sorbed on activated sludge flocs, and rapidly hydrolysed in low molecular weight units easy to assimilate. It represents a major advantage for the aggregated community.

### 6.3.2. Hydrolytic enzymes associated with EPS

Many enzymatic functions are associated with the EPS matrix (Table 6.3). These enzymes excreted in the intercellular space of biofilms are produced by all the organisms found in mixed environmental biofilms [63]. The substratum of these enzymes is made up of water-soluble compounds (polysaccharides, proteins and nucleic acids), water-insoluble compounds (chitin and lipids) or organic particles. Immobilized in the EPS matrix, these enzymes are both stabilized by their interactions with EPS and confined close to the bacterial cells, limiting their loss or dilution. It confers to the matrix the role of an "extracellular digestive tract" allowing the hydrolysis of macromolecules. Their regulation is complex and, for example, Sack *et al.* [64] showed that drinking water biofilms were able to grow on amylopectin used as primary substratum *via* extracellular enzymes induced in the presence of maltose.

**TABLE 6.3.** – Exo- and ecto-cellular enzymatic activities associated with EPS and bacterial cells in biofilms (adapted from [63, 65]).

| Algae | Bacteria | Protozoa | Fungi |
|---|---|---|---|
| Phosphatases | Peptidases; Glucosidases<br>ß-xylosidases<br>ß- glucose aminidases<br>Lipases<br>Phosphatases<br>DNAses | Chitinases | Phenol oxidase<br>Cellobiohydrolase<br>ß-glucosidases<br>ß-xylosidases<br>ß- glucose-aminidases<br>Phosphatases |

### 6.3.3. Protection of biofilms against disinfectants

The resistance of biofilms to disinfectants (*e.g.,* chlorinated products used in water disinfection such as chlorine (bleach) and chloramines) has been documented since the 1990s by De Beer *et al.* [66] and Huang *et al.* [67]. The diffusion of chlorine in the biofilm is limited by its intense and rapid reaction with the biomass and EPS have been recognized as very reactive (especially if they contain nitrogen) [68, 69]. Approximately 80% of the oxidant is consumed in the first micrometers of the biofilm and its complete consumption is achieved

in the next ten or twenty micrometers (Fig. 6.5). The reactivity of the oxidants (governed by their standard redox potential) is a key parameter. As a result, the penetration in biofilms of two neighbouring compounds (chlorine and chloramines) is slightly different, and the less reactive chloramines diffuse more deeply in the biofilm than chlorine HClO/$ClO^-$ [70].

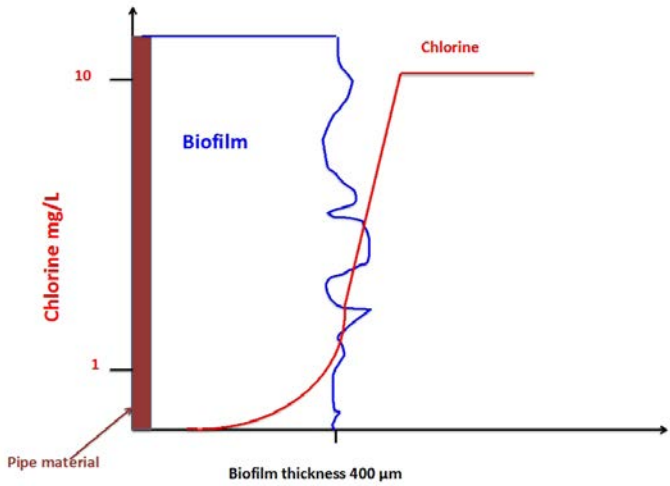


**Fig. 6.5.** – Diffusion profile of oxidants (chlorine or chloramine) in a thick biofilm measured with redox microprobe (adapted from [66, 68, 70]).

Such diffusion limited by the reaction of oxidants is also reported for other disinfectants such as quaternary ammonium compounds, whose positive charges favour their interactions with negatively charged EPS. They do diffuse slowly in the deeper layers as the first negative sites are gradually occupied by the quaternary ammonium compounds [71, 72].

## 6.4. Conclusion

There is not only one type of EPS matrix, just as there is not only one type of biofilm, but a great diversity of EPS in terms of quality and quantity, which are generated according to scenarios not yet fully understood. Their expression is multi-parametric depending on bacterial species, their interactions in a multi-species community and their responses to multiple environmental stresses.

In biofilms, the EPS matrix composed of many heteropolymers such as glycoconjugates (glycoproteins, glycolipids, *etc.)* is a relatively flexible, reticulated, very cohesive structure, which is essential for organizing such a hydrated edifice. Modelling estimated to $10^{15}$ $mm^{-3}$ the number of entanglement points in the EPS network. The nature and the density of the EPS produced by the bacteria

in turn control the areas surrounding of the bacteria as well as the flux of nutrients to the cells. Indeed, functions associated with EPS provide significant advantages to the cells of the community: gene transfer, reservoir of exogenous nutrients trapped in the matrix and biodegradable EPS, reservoir of hydrolytic enzymes able to digest the intercellular material, water retention, and protection against toxicants and grazing.

In one of his reviews: "*The perfect slime*", H.-C. Flemming enthusiastically and extensively illustrated the advantages of living together in biofilms and the key functions associated to EPS [73]. The word "*perfect*" in this case could be seen as misnomer as it suggests the perfection of the biofilm organization. If so, biofilm would be an ultimate system with no chance or need for evolution or progress. The word *"perfectibility*" could be more appropriate since it means that microorganisms are able to improve – still today, gradually, in next to no time and infinitely – their strategies (and their EPS) in order to colonize Earth. Indeed, as pointed out by Dobzhansky [74], nothing in biology makes sense except in the light of evolution.

## References

[1] Taylor E.S., Lower S.K. (2008) "Thickness and surface density of extracellular polymers on *Acidithiobacillus ferrooxidans*." Appl. Environ. Microbiol., 74(1), 309-311.

[2] Braissant O., Decho A.W., Dupraz C., Glunk C., Prezkop K.M., Visscher P.T. (2007) "Exopolymeric substances of sulfate-reducing bacteria: Interactions with calcium at alkaline pH and implication for formation of carbonate minerals." Geobiology, 5(4), 401-411.

[3] Gaboriaud F., Gee M.L., Strugnell R., Duval J.F.L. (2008) "Coupled electrostatic, hydrodynamic, and mechanical properties of bacterial interfaces in aqueous media." Langmuir, 24(19), 10988-10995.

[4] Jorand F., Zegeye A., Ghanbaja J., Abdelmoula M. (2011) "The formation of green rust induced by tropical river biofilm components." Sci. Total Environ., 409, 2586-2596.

[5] Zippel B., Neu T.R. (2011) "Characterization of glycoconjugates of extracellular polymeric substances in tufa-associated biofilms by using fluorescence lectin-binding analysis." Appl. Environ. Microbiol., 77(2), 505-516.

[6] Albertsen M., Stensballe A., Nielsen K.L., Nielsen P.H. (2013) "Digging into the extracellular matrix of a complex microbial community using a combined metagenomic and metaproteomic approach." Wat. Sci. Technol., 67(7), 1650-1656.

[7] Ras M., Lefebvre D., Derlon N., Paul E., Girbal-Neuhauser E. (2011) "Extracellular polymeric substances diversity of biofilms grown under contrasted environmental conditions." Water Research, 45, 1529-1538.

[8] Neu T.R., Lawrence J.R. (2009) "Extracellular polymeric substances in microbial biofilms", In: Microbial glycobiology: Structures, relevance and

applications. Moran A., Brennan P., Holst O., von Itzstein M. Eds, Elsevier, San Diego, USA, 735-758.
[9] Characklis W.G. and Marshall K.C. (eds) (1990) "Biofilms." Wiley, NY, USA, 796 p.
[10] Wingender J., Neu T.R., Flemming H.C. (1999) "Microbial extracellular polymeric substances. Characterization, structure and function." Wingender J., Neu T.R., Flemming H.C. Eds, Springer, 258 p.
[11] Sutherland I.W. (2001) "The biofilm matrix – an immobilized but dynamic microbial environment." TRENDS in Microbiology, 9(5), 222-227.
[12] Branda S.S., Vik A., Friedman L., Kolter R. (2005) "Biofilms: the matrix revisited." TRENDS in Microbiology, 13(1), 20-26.
[13] Pamp S.J., Gjermansen M., Tolker-Nielsen T. (2007) "The biofilm matrix: a sticky framework." In: The biofilm mode of life: mechanisms and adaptation, Kjelleberg S., Givskov M.C. Eds, Horizon BioScience, Wymondham, UK, 37-68.
[14] Flemming H.C., Wingender J. (2010) "The biofilm matrix." Nature Reviews Microbiology, 8, 623-633.
[15] Giraud C., Bernard C., Ruer S., de Bentzmann S. (2010) "Biological 'glue' and 'Velcro': molecular tools for adhesion and biofilm formation in the hairy and gluey bug *Pseudomonas aeruginosa*." Environmental Microbiology Reports, 2(3), 343-358.
[16] Lembre P., Lorentz C., Di Martino P.D. (2012) "Exopolysaccharides of the biofilm matrix: a complex biophysical world." In: The complex world of polysaccharides, Karunaratne D.N. Ed., INTECH, Chapter 13, 371-392.
[17] Comte S., Guibaud G., Baudu M. (2006) "Relations between extraction protocols for activated sludge extracellular polymeric substances (EPS) and EPS complexation properties: Part I. Comparison of the efficiency of eight EPS extraction methods." Enzyme Microb. Technol., 38 (1-2), 237–245.
[18] Wagner M., Ivleva N.P., Haisch C., Niessner R., Horn H. (2009) "Combined use of confocal laser scanning microscopy (CLSM) and Raman microscopy (RM): Investigations on EPS-matrix." Water Research, 43(1), 63-76.
[19] Jiao Y., D'Haeseleer P., Dill B.D., Shah M., Nathan C., VerBerkmoes N.C., Hettich R.C., Banfield J.F., Thelen M.P. (2010) "Identification of biofilm matrix-associated proteins from an acid mine drainage microbial community." Appl. Environ. Microbiol., 77(15), 5230-5237.
[20] Quilès F., Polyakov P., Humbert F., Francius G. (2012) "Production of extracellular glycogen by *Pseudomonas fluorescens*: spectroscopic evidence and conformational analysis by biomolecular recognition." Biomacromolecules, 13, 2118-2127.
[21] Fahs A., Quilès F., Jamal D., Humbert F., Francius G. (2014) "*In situ* analysis of bacterial extracellular polymeric substances from a *Pseudomonas fluorescens* biofilm by combined vibrational and single molecules force spectroscopies." J. Phys. Chem. B, 118, 6702-6713.
[22] Schlafer S., Garcia J.E., Greve M., Raarup M.K., Nyvad B., Dige I. (2015) "Ratiometric imaging of extracellular pH in bacterial biofilms with C-SNARF-4." Appl. Environ. Microbiol., 81, 1267-1273.

[23] Ahimou F., Semmens M.J., Haugstad G., Novak P.J. (2007) "Effect of protein, polysaccharide, and oxygen concentration profiles on biofilm cohesiveness." Appl. Environ. Microbiol., 73(9), 2905-2910.
[24] Applegate D.H., Bryers J.D. (1991) "Effects of carbon and oxygen limitations and calcium concentrations on biofilm removal processes." Biotechnol. Bioeng., 37(1), 17-25.
[25] Lawrence J.R., Swerhone G.D.W., Kuliche U., Neu T.R. (2007) "*In situ* evidence for microdomains in the polymer matrix of bacterial microcolonies." Can. J. Microbiol., 53, 450-458.
[26] Nivens D.E., Ohman D.E., Williams J., Franklin M.J. (2001) "Role of alginate and its o-acetylation in formation of *Pseudomonas aeruginosa* microcolonies and biofilm." J. Bacteriol., 183, 1047-1057.
[27] Taglialegna A., Navarro S., Ventura S., Garnett J.A., Matthews S., Penades J.R., Lasa I., Valle J. (2016) "Staphylococcal Bap proteins build amyloid scaffold biofilm matrices in response to environmental signals." PLOS Pathogens, DOI:10.1371/journal.ppat.1005711.
[28] Di Martino P. (2016) "Bap: A new type of functional amyloid." Trends in Microbiology, 24(9), 682-684.
[29] Miquelard-Garnier G., Creton C., Hourdet D. (2007) "Synthesis and viscoelastic properties of hydrophobically modified hydrogels." Macromolecular Symposia, 256(1), 189-194.
[30] Abe Y., Skali-Lami S., Block J.-C., Francius G. (2012) "Cohesiveness and hydrodynamic properties of young drinking water biofilms." Water Research, 46, 1155-1166.
[31] Abe Y., Polyakov P., Skali-Lami S., Francius G. (2011) "Elasticity and physico-chemical properties during drinking water biofilm formation." Biofouling, 27(7), 739-750.
[32] Batchelor G.K. (1970) "Slender-body theory for particles arbitrary cross-section in Stokes flow." Journal of Fluid Mechanics, 44(3), 419-440.
[33] Batchelor G.K. (1971) "The stress generated in a non-dilute suspension of elongated particles by pure straining motion." Journal of Fluid Mechanics, 46(4), 813-829.
[34] Mathieu L., Bertrand I., Abe Y., Angel E., Block J.C., Skali-Lami S., Francius G. (2014) "Drinking water biofilm cohesiveness changes under chlorination or hydrodynamic stress." Water Research, 55, 175-184.
[35] Möhle R.B., Langemann T., Haesner M., Augustin W., Scholl S., Neu T.R., Hempel D.C., Horn H. (2007) "Structure and shear strength of microbial biofilms as determined with confocal laser scanning microscopy and fluid dynamic gauging using a novel rotating disc biofilm reactor." Biotechnol. Bioeng., 98, 747-755.
[36] Derlon N., Masse A., Escudie R., Bernet N., Paul E. (2008) "Stratification in the cohesion of biofilms grown under various environmental conditions." Water Research, 42, 2102-2110.
[37] Chen X., Stewart P.S. (2002) "Role of electrostatic interactions in cohesion of bacterial biofilms." Appl. Environ. Microbiol., 59, 718-720.

[38] Simoes M., Cleto S., Pereira M.O., Vieira M.J. (2007) "Influence of biofilm composition on the resistance to detachment." Wat. Sci. Technol. 55, 473-480.
[39] Stoodley P., Cargo R., Rupp C.J., Wilson S., Klapper I. (2002) "Biofilm material properties as related to shear-induced deformation and detachment phenomena." J. Industr. Microbiol. Biotechnol., 29(6), 361–367.
[40] Stoodley P., Lewandowski Z., Boyle J.D., Lappin-Scott H.M. (1999) "Structural deformation of bacterial biofilms caused by short term fluctuations in flow velocity: an *in situ* demonstration of biofilm viscoelasticity." Biotechnol. Bioeng., 65, 83–92.
[41] Schmitt J., Fringeli U.P., Flemming H.C. (1998) "Structural and temporal behavior of biofilms investigated by FTIR-ATR spectroscopy." In: Proceedings of Fourier Transform Spectroscopy International Conference, Athens, GA, 430, 312-315.
[42] Mayer C., Moritz R., Kirschner C., Borchard W., Maibaum R., Wingender J., Flemming H.-C. (1999) "The role of intermolecular interactions studies on model systems for bacterial biofilms." Int. J. Biol. Macromol., 26, 3–16.
[43] Paul E., Ochoa J.C., Péchaud Y., Liu Y., Line A. (2012) "Effect of shear stress and growth conditions on detachment and physical properties of biofilms." Water Research, 46, 5499–5508.
[44] Vincent J. (2012) "Structural biomaterials" Vincent J. Ed., 3rd edition. Princeton Univ. Press, Princeton, New Jersey, USA, 228 p.
[45] Klapper I., Rupp C.J., Cargo R., Purvedorj B., Stoodley P. (2002) "A viscoelastic fluid description of bacterial biofilm material properties." Biotechnol. Bioeng., 80, 289–296.
[46] Laspidou C.S., Rittmann B.E. (2004a) "Modeling the development of biofilm density including active bacteria, inert biomass and extracellular polymeric substances." Water Research 38, 3349-3361.
[47] Laspidou C.S., Rittmann B.E. (2004b) "Evaluating trends in biofilm density using the UMCCA model." Water Research, 38, 3362-3372.
[48] Péchaud Y., Marcato-Romain C.E., Girbal-Neuhauser E., Queinnec I., Bessière Y., Paul E. (2012) "Combining hydrodynamic and enzymatic treatments to improve multi-species thick biofilm removal." Chemical Engineering Science, 80, 109-118.
[49] McFadden D.C., De Jesus M., Casadevall A. (2006) "The physical properties of the capsular polysaccharides from *Cryptococcus neoformans* suggest features for capsule construction." J. Biol. Chem., 281, 1868-1875.
[50] Ganesan M., Stewart E.J., Szafranski, J., Satorius A.E., Younger J.G., Solomon M. J. (2013) "Molar mass, entanglement, and associations of the biofilm polysaccharide of *Staphylococcus epidermidis*." Biomacromolecules, 14, 1474–1481.
[51] Camesano T.A., Abu-Lail N.I. (2002) "Heterogeneity in bacterial surface polysaccharides, probed on a single-molecule basis." Biomacromolecules, 3(4), 661–667.

[52] Späth R., Flemming H.C., Wuertz S. (1998) "Sorption properties of biofilms." Wat. Sci. Technol., 37, 207-210.
[53] Guibaud G., van Hellebusch E., Bordas F. (2006) "Lead and cadmium biosorption by extracellular polymeric substances (EPS) extracted from activated sludges: pH-sorption edge tests and mathematical equilibrium modelling." Chemosphere, 64, 1955-1962.
[54] Writer J.H., Ryan J.N., Barber L.B. (2011) "Role of biofilms in sorptive removal of steroidal hormones and 4-nonylphenol compounds from streams." Environ. Sci. Technol., 45(17), 7275-7283.
[55] Jorand F., Boué-Bigne F., Block J.C. and Urbain V. (1998) "Hydrophobic/hydrophilic properties of activated sludge exopolymeric substances." Wat. Sci. Technol., 37(4-5), 307-315.
[56] Morrow J.B, Catalina Arango P., Holbrook R. D. (2010) "Association of quantum dot nanoparticles with biofilm." Journal of Environmental Quality, 39(6), 1934-1941.
[57] Aldeek F., Schneider R., Fontaine-Aupart M.-P., Mustin C., Lécart S., Merlin C., Block J.C. (2013) "Patterned hydrophobic domains in the exopolymeric matrix of *Shewanella oneidensis* MR-1 biofilms." Appl. Environ. Microbiol., 79(4), 1400-1402.
[58] Hébrant M., Pelleïeux S., Mathieu L., Skali-Lami S., Gantzer C., Bertrand I., Block J.-C. (2014) "Distinct adsorption kinetics of Qβ and GA bacteriophages on drinking water biofilms." Adsorption, 20(5-6), 823-828.
[59] Van Loosdrecht M.V., Lyklema J., Norde W., Schraa G., Zehnder A.J.B. (1987) "Electrophoretic mobility and hydrophobicity as a measure to predict the initial steps of bacterial adhesion." Appl. Environ. Microbiol., 53(8), 1898-1901.
[60] Zita A., Hermansson M. (1997) "Effects of bacterial cell surface structures and hydrophobicity on attachment to activated sludge flocs." Appl. Environ. Microbiol., 63(3), 1168-1170.
[61] Tatchou-Nyamsi-König J.-A., Dague E., Mullet M., Duval J.F.L., Gaboriaud F., Block J.-C. (2008) "Adhesion of *Campylobacter jejuni* and *Mycobacterium avium* onto polyethylene terephtalate (PET) used for bottled waters." Water Research, 42, 4751-4760.
[62] Guellil A., Thomas F., Block J.C., Bersillon J.L. and Ginestet Ph. (2001) "Transfer of organic matter between wastewater and activated sludge flocs." Water Research, 35(1), 143-150.
[63] Romani A.M., Artigas J., Ylla I. (2012) "Extracellular enzymes in aquatic biofilms: microbial interactions *versus* water quality effects in the use of organic matter." In: Microbial biofilms. Current research and applications, Lear G. and Lewis G. Eds. Caister Academic Press, New Zealand, Chapter 9, 153-174.
[64] Sack E.L.W., van der Wielen P.W.J.J., van der Kooij D. (2014) "Polysaccharides and proteins added to flowing drinking water at microgram-per-liter levels promote the formation of biofilms predominated by *Bacteroidetes* and *Proteobacteria*." Appl. Environ. Microbiol., 80(8), 2360-2371.

[65] Cadoret A., Conrad A., Block J.C. (2002) "Availability of low and high molecular weight substrates to extracellular enzymes in whole and dispersed activated sludges." Enzyme Microb. Technol., 31(1), 179-186.
[66] De Beer D., Srinivasan R., Stewart P.S. (1994) "Direct measurement of chlorine penetration into biofilms during disinfection." Appl. Environ. Microbiol., 60(12), 4339-4344.
[67] Huang C.T., Yu F.P., McFeters G.A., Stewart P.S. (1995) "Nonuniform spatial patterns of respiratory activity within biofilms during disinfection." Appl. Environ. Microbiol., 61(6), 2252-2256.
[68] Szabo J.G., Rice E., Bishop P.L. (2006) "Persistence of *Klebsiella pneumoniae* on simulated biofilm in a model drinking water system." Environ. Sci. Technol., 40, 4996-5002.
[69] Xue Z., Lee W.H., Coburn K.M., Seo Y. (2014) "Selective reactivity of monochloramine with extracellular matrix components affects the disinfection of biofilm and detached clusters." Environ. Sci. Technol., 48, 3832–3839.
[70] Lee W.H., Wahman D.G., Bishop P.L., Pressman J.G. (2011) "Free chlorine and monochloramine application to nitrifying biofilm: comparison of biofilm penetration, activity, and viability." Environ. Sci. Technol., 45, 1412–1419.
[71] Bridier A., Dubois-Brissonnet F., Greub G., Thomas V., Briandet R. (2011) "Dynamics of the action of biocides in *Pseudomonas aeruginosa* biofilms." Antimicrob. Agents Chemother., 55(6), 2648–2654.
[72] Ganeshnarayan K., Shah S.M., Libera M.R., Santostefano A., Kaplan J.B. (2009) "Poly-N-acetylglucosamine matrix polysaccharide impedes fluid convection and transport of the cationic surfactant cetylpyridinium chloride through bacterial biofilms." Appl. Environ. Microbiol., 75(5), 1308-1314.
[73] Flemming H.-C. (2011) "The perfect slime." Colloids and Surfaces B: Biointerfaces, 86, 251-259.
[74] Dobzhansky T. (1973) "Nothing in biology makes sense except in the light of evolution." The American Biology Teacher., 35, 125-129.

# 7 Biofilms in a marine environment: example of intertidal mud flats and metallic port structures

**Sophie Sablé, Philippe Refait, René Sabot, Marc Jeannin, Ibtissem Doghri, Mickaël Langumier, Isabelle Lanneluc**

## 7.1. Biofilm life of marine bacteria

Seawater covers more than 70% of the earth's surface. Oceans are the most important source of biodiversity on the planet. They are organized in complex ecosystems comprising all kinds of microorganisms, such as viruses, prokaryotes (bacteria and archaea), protozoa, microalgae, yeasts, mould and a lot of other multicellular organisms. Paradoxically, microorganisms in the marine environment are still largely unknown. This is partly due to the great diversity of aquatic ecosystems (water and sediment, surface or deep water, polar waters, lagoons, estuaries, hot springs...) and, for the most part, the difficulty of sampling them correctly (difficult access, dispersive media, ...) [1]. There is also another difficulty, which constitutes a major obstacle to the study of microorganisms: it is not yet known how to cultivate more than 99% of them [2]. For the last fifteen years, however, environmental molecular analyses based on the ribosomal DNA sequence libraries have been used to describe a large number of microbial species, some of which have been shown to be still unknown [1].

Within these microorganisms, bacteria represent an important part. Under natural conditions, they develop in two forms: a free form, particularly in water (planktonic), and a sessile form (attached *via* biofilm). A planktonic lifestyle allows microorganisms to proliferate and colonize new environmental niches. Then, by attaching to a surface irreversibly, the bacteria can adopt a sessile life form, which would be their preferred way of life [3, 4]. Once attached, bacteria grow and produce extracellular polymers, forming a matrix with high water content, proteins, polysaccharides and lipids [5]. The proximity between bacteria within the matrix allows them to exchange signals and nutrients. This complex set, which forms a biofilm, is perceived as essential for the survival of marine bacteria. This way of life indeed improves access to nutrients and protects microorganisms from environmental stress such as chemical (oxidizing) or biological (predators) disturbances [3, 6]. Within biofilms, bacteria can associate with other organisms, especially microalgae (diatoms), which can be abundant in biofilms of photic zones of the marine environment [7].

Biofilms are very heterogeneous and constantly remodelled according to endogenous and exogenous factors. The differences may be at the structural level (mono- or multi-species biofilms, different thicknesses and architectures) as on colonized surfaces. The diversity of biofilms could be one of the key elements of their robustness to external aggressions [8]. In the marine environment, biofilms can form on very different biotic and abiotic surfaces. Marine animals such as turtles or whales can be colonized by biofilms, thus creating very specific relationships between the host and the colonizing organisms [9]. Substrates such as mud at low tide or submerged rocks are also covered with biofilms. They can also develop on artificial surfaces such as ship hulls, harbour pontoons, offshore platforms, aquaculture facilities, oceanographic equipment immersed for days to months or even years, positively or negatively impacting most human activities in the marine environment.

## 7.2. Consequences of the establishment of biofilms on human activity in the marine environment

By immersing glass slides in sea water, Zobell and Allen [10], as early as 1935, showed that bacteria, and to a lesser extent diatoms and actinomycetes, generally precede the fixation of barnacles and other organisms. Indeed, biofilms create anchor points for other microorganisms, then for larvae and then for macroorganisms. This phenomenon will have different consequences on human activity, depending on the structure on which the biofilms will form.

The process of colonization of a submerged substrate is called biofouling. It is broken down into four main sequences according to the model proposed by Wahl [9] (Fig. 7.1): 1) chemical conditioning of the surface by near-instantaneous adsorption of organic and inorganic molecules, 2) colonization by bacteria, then 3) by unicellular eukaryotic organisms, and finally 4) by multicellular eukaryotic organisms. "*Microfouling*" corresponds to the formation of biofilms with fixation of bacteria, followed by microalgae (diatoms), yeasts and protozoa. During "*macrofouling*", the microbial biofilms evolves into a more complex system including grazers, primary multicellular producers, until the final stage of colonization involving the establishment and growth of marine invertebrates (barnacles, mussels, tunicates, ...) as well as macroalgae. Macrofouling is therefore colonization by multicellular eukaryotic organisms.

The nature of the involved phenomena evolves gradually from a physical to a biological process. Thus, term "*biofouling*" refers to all living organisms that develop on supports. By extension, it also includes the deterioration that will result from these colonizations.

The negative effects of biofilms on materials and equipment are numerous and pose a major problem for the industry and the activities of the sea in general.

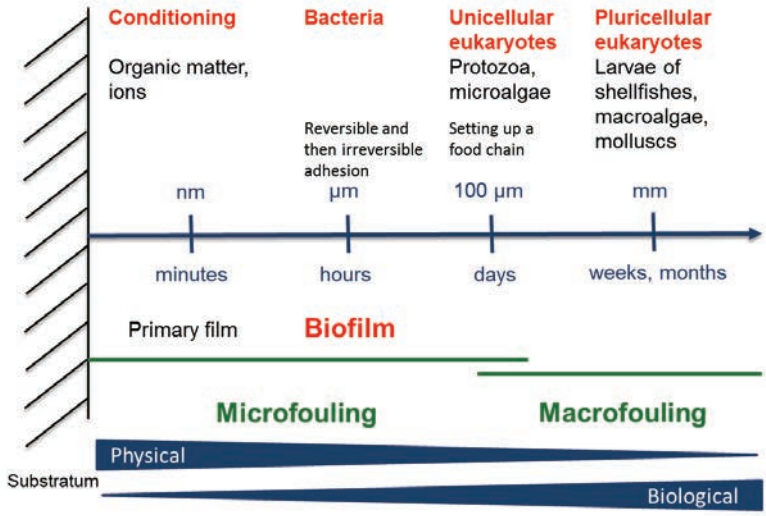


**Fig. 7.1.** – Schematic representation of the phases of marine fouling establishment on a surface.

In the case of ships, fouling causes an increase in the roughness of the hull and therefore frictional forces when advancing, manoeuvring in water, thus creating a hydrodynamic shield. For example, a biofilm 100 µm thick results in a 5-15% increase in friction resistance [11]. A 1 mm thick biofilms results in a 15% reduction in vessel speed [12]. The biomass that adheres to the hulls of ships also induces an overweight, albeit to a lesser extent. This biofouling processes lead to fuel over-consumption, increasing the costs of shipping and the emission of greenhouse gases (GHGs). For example, the overall cost associated with biofouling is estimated at US $ 56 million per year for all US vessels from the DDG-51 class [13].

Biofouling also affects other marine structures, particularly pontoons, buoys and all floating equipment, which are thus subject to considerable overweight. At the level of cooling circuits, problems of marine fouling reduce the efficiency of heat transfer and increase energy consumption, thus influencing the performance of the installations and their durability. It was shown in the late 1980s that the cost of fouling from heat exchangers for industrialized countries such as the United States and the United Kingdom was 0.25% of gross national product (GNP) [14].

Moreover, the presence of biofilms induces a drift of the measurements made by submerged oceanographic sensors, such as optical detectors, underwater cameras, pH, temperature or toxicity sensors.

As in other environments, marine biofilms can also alter the properties of colonized materials through the phenomenon of biocorrosion or biodeterioration,

due in particular to an intense metabolic activity of certain types of bacteria having a dissimilative metabolism of iron or sulphur [15]. The influence of microorganisms can lead to very severe localized corrosion phenomena associated with corrosion rates of up to 1 cm per year. The cost of biocorrosion is estimated to be 20% of the total costs of corrosion control of materials, including corrosion in the marine environment.

The presence of biofouling on human installations also has a strong ecological impact. Indeed, in addition to the economic disadvantages associated with the presence of fouling on the ship hulls, these surfaces can be vectors for the dissemination of different organisms on a large scale. More than 3000 species of marine organisms travel daily around the world in the ballast water of ships [16] and can be introduced into ecosystems where they can weaken the balance. Biofouling therefore contributes to global change in biotopes and ecosystems through the introduction of invasive species. For example, the introduction in France of *Crepidula fornicata*, a mollusc originating from North America, which took advantage of the Allied landing during the Second World War to invade the Normandy coasts. Similarly, *Elminius modestus*, a barnacle native of New Zealand and Australia, was introduced to the English coasts during the Second World War before spreading rapidly in France during the landing in 1944.

Overall, marine biofilms are now recognized as a major problem for a wide range of artificial structures. Therefore, antifouling coatings are essential, but their renewal results in a drastic increase in the costs of maintaining the submerged infrastructures and their toxicity poses significant problems for the environment.

While the impact of biofilms on human activity is generally considered as negative, this is not always the case. The growth of a biofilm can be very important in establishing the food chain. For example, biofilms that form on the surface of rocks and sediments (Section 7.3.1) are a major source of food for many marine macroorganisms (oysters, mussels, fish, *etc.*) [17]. In addition to this nutritional aspect, biofilms also have a positive impact in shellfish aquaculture, as they form substrates favouring the fixation of oysters. Thus, biofilm development is sought on the surface of shellfish aquaculture facilities.

## 7.3. Bacterial communities of two examples of marine biofilms that may have different impacts

The formation mechanisms and the structural organization of biofilms result mainly from interactions between the environment, the microbial flora and the material (Fig. 7.2). Biofilms are therefore dependent on the parameters specific to each of the three actors, in particular oxygenation, pH, temperature, access to light, hydrodynamics, quantity of organic matter with regard to the environment, microstructure and surface condition for the material, and metabolism,

secreted polymers, cellular interactions, migration/emigration capabilities for microorganisms.

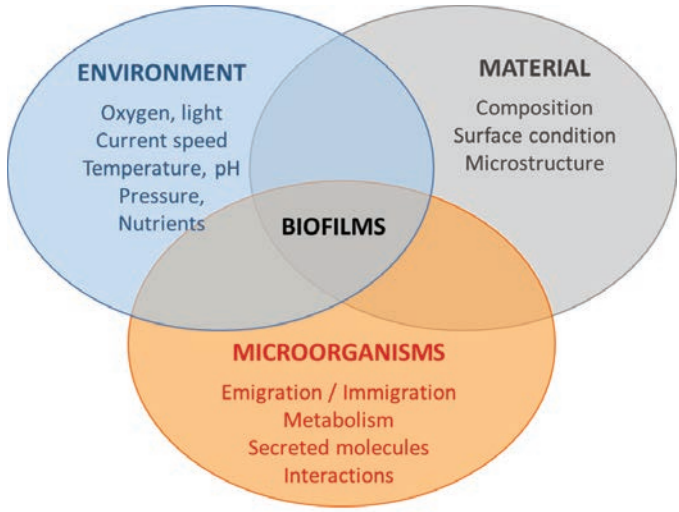


**Fig. 7.2.** – Factors influencing the formation and structuring of marine biofilms.

For example, in the marine environment, temperature [18], nutrients [19], light, pH and dissolved oxygen [20] have been shown to affect the structure of biofilm microbial communities more than do different salinities tested (20, 27, 34‰) [18]. Hydrodynamics can have a strong influence on the destructuring of biofilms, as in the case of biofilms that form on intertidal mudflats [21]. The structure of diatom communities in biofilms also shows significant differences depending on the surface and the seasons. These differences were attributed to the physicochemical and biological changes of both the water column and the surfaces [22]. Surfaces with different degrees of hydrophobicity or hydrophilicity will show differences in the pioneer bacteria that colonize them [6, 23]. However, after 155 days of immersion of different materials in the high seas (up to 4500 m deep), Bellou *et al.* [24] found that microbial diversity within biofilms appears to be less affected by surface type than by depth, and that diversity increases with the depth.

In this chapter the bacterial communities of two models of marine biofilms will be presented, as follows:

– a transient biofilm that can enter the trophic network, developing at the solid/air interface on a natural surface, an intertidal mudflat, a nutrient-rich porous support,
– a permanent biofilm, formed at the solid/water interface, on an artificial steel support, potentially involved in biocorrosion.

### 7.3.1. The biofilms of the intertidal mudflats

The intertidal mudflats are mudflats of the littoral localized between the extreme limits of the tide. They therefore constitute a key interface between the ocean, the atmosphere and the terrestrial environment. These mudflats play the role of "pantry" for many animal species and nursery for juvenile fish by providing shelter and food for several species of commercial interest [25]. These areas of high biological productivity are conducive to the establishment of aquaculture activities, especially for shellfish aquaculture, giving an important socio-economic dimension to these mudflats.

Intertidal mudflats are characterized by frequent fluctuations in temperature, salt concentrations, desiccation, UV irradiation, currents and waves, which are challenging for the microorganisms that inhabit this environment. These mudflats have the particularity and originality that, in order to access the light necessary for their photosynthesis, the microalgae of the sediment migrate during the low tide to the surface of these mudflats [26] where they form transient biofilms with bacteria that may originate from the sediment. Then, when the sea rises or overnight, microalgae re-bury in the sediment [27] and the biofilm breaks down. These biofilms are therefore subject both to the nictemeral rhythm and to the rhythm of the tides, sometimes with saturating irradiances and long periods of darkness during periods of immersion or at night. During fluxes and refluxes, the transitions between the different light, salinity and temperature conditions are abrupt [28]. When the tide rises, parts of the biofilms are resuspended and can then enter the food chain of the organisms present in the sea water. This is an original example of biofilms which differ from those conventionally described (Fig. 7.1), notably because of their formation speed and limited lifetime.

These biofilms are essentially composed of microalgae (diatoms), bacteria and extracellular polymeric substances (EPS) [29-31]. EPS are secreted by both microalgae and bacteria [31, 32], they can limit desiccation of the sediment, stabilize it and protect microalgae from bacterial hydrolases [33]. EPS can also chelate toxic metals and other contaminants that may enter the food web. In the European intertidal mudflats, epipelic (mobile) diatoms can constitute up to 97% of the microalgae of this biofilms [29, 30]. The most frequently isolated species in France (Atlantic coast) are: *Navicula phyllepta*, *Navicula digitoradiata*, *Navicula gregaria*, *Staurophora wislouchii*, *Gyrosigma fasciola* and *Nitzschia dissipata* [34]. Concerning bacteria, there are usually $10^9$ per $cm^3$ of sediment [17]. Although planktonic bacteria (suspended in water) represent one of the most studied environmental communities, benthic bacteria (from sediment and biofilms) remain little characterized, even though they are 1000 times more abundant [35]. Several studies on different oceans show that in marine sediments, *Gammaproteobacteria* are dominant, as well as sometimes *Deltaproteobacteria* [36-38]. In fact, bacterial communities differ according to the depth of the sediment studied, and *Gammaproteobacteria* account for almost 90% in samples close to the surface (0-2 cm) [39], as well as in the biofilms (personal data).

The biofilms of intertidal mudflats are the site of numerous chemical reactions involving microorganisms and have a major role in marine geochemistry. The physicochemical conditions and the bacterial communities involved are particularly those of the sulphur cycle, which are also found in corrosion deposits on metal surfaces.

### 7.3.2. The biofilms of metallic port structures

As soon as a metallic structure is immersed in seawater, the process of electrochemical corrosion of the iron takes place and the metal quickly covers up with a layer of corrosion products. At the same time, different microbial communities, both planktonic and benthic, are deposited on the surface of the metal, adhere and develop to form a biofilm. This biomass is intimately associated with the corrosion products. We will thus speak about a composite "microorganisms/corrosion product" biofilm. As described in section 7.2, bacteria are pioneers in adhesion phenomena on metallic surfaces in marine environments and are the main subject of study of the biocorrosion phenomena of these surfaces. Thus, the microorganisms most frequently invoked are sulphato-reducing bacteria (SRB) [40-42]. Nevertheless, SRB do not necessarily lead to severe localized corrosion, and bacterial consortia could be involved (Chapter 11). Indeed, composite biofilm creates an ecosystem in which different microbial communities can interact, forming synergies that can affect electrochemical processes through a cooperative metabolism and thus can influence corrosion phenomena. The bacterial communities within this biofilm are very diverse but have so far been little studied. The precise identification of the species involved in these various phenomena is a prerequisite for the implementation of strategies to combat these biofilms, which are most often the cause of the material accidents due to corrosion.

In this context, composite biofilms were sampled directly from metallic port structures or from steel coupons immersed for different times in different harbours, and characterization of the microbial flora associated with the corrosion products was carried out [40, 43-47]. Moreover, in order to better understand the phenomena of corrosion in the natural environment, it seems essential to link the evolution of the microbial flora to that of the properties of the rust layer and in particular to the nature of the present phases. This is why bacterial flora and corrosion products have been analysed in parallel on the same samples in several studies [43, 46, 47]. In this chapter we will focus on the study of the bacterial flora on carbon steels immersed in seawater while the layer of corrosion products will be described in chapter 11 of this book.

The bacterial abundance was evaluated in biofilms formed on steel test coupons immersed for 1 to 8 weeks in a harbour of La Rochelle (France) [43], and for 6 or 12 months in the ports of Le Havre, Nantes-St-Nazaire and Marseille (France) [46]. Regardless of site and time of immersion, a relatively large bacterial density was observed ($10^7$ to $10^9$ bacteria/g of biofilm). When metallic test coupons were immersed for 11 years in the port of La Rochelle (France),

a thick (7-8 mm) composite "microorganisms/corrosion product" biofilm developed over time [47, 48]. The highest bacterial density was observed in the outer and middle layers of this biofilm (respectively 2 $10^{10}$ and 1 $10^{10}$ bacteria/g of biofilm). In contrast, bacterial abundance of the inner layer in contact with the metal was too low (<$10^7$ bacteria/g of biofilm) to be reliably determined. The more extreme environmental conditions of this area (anoxic conditions, altered pH, higher concentrations of metal and trace elements...) probably have severely limited the growth of bacteria. Moreover, nutrient supply from the outside environment must be extremely low because nutrients are probably consumed within the outer and middle layers. As already described [2, 49], a bacterial count of the same samples after culture on a rich solid medium under aerobic or anaerobic conditions shows that only a very small fraction of the total number of bacteria (estimated by direct count of bacteria by nucleic acid staining) is culturable (between 0.01 and 1.8%) [43, 46, 47]. This low capacity to cultivate marine bacteria in laboratory limits the study of these bacterial communities. This probably results from a non-suitability of the proposed culture medium with the nutrient requirements of bacterial species, but may also be related to a physiological state limiting the ability to grow microorganisms. This is why two approaches have been followed for microbiological analysis. The first comprises a step of culturing the bacteria. It makes it possible to obtain culturable bacteria which can be more easily studied and which are expected to be representative of biocorrosion phenomena. The second approach gives an overall analysis of the bacterial communities by using molecular biology tools that allows to eliminate the culture stage. It is probably more faithful to the reality but limits the fields of study when the bacteria are not cultivated. It nevertheless allows us to have an idea of the relative abundance of different bacterial species in the community and to check that the species isolated with culture methods are representative of this community or not.

After culturing various samples of composite "microorganisms/corrosion product" biofilms and isolation of the bacteria, different bacterial classes have been identified. The diversity of culturable bacteria appears to increase with immersion time (Fig. 7.3). From 1 to 8 weeks, there are mainly *Bacilli* (genus *Bacillus*) and *Alphaproteobacteria* (genus *Erythrobacter* and *Roseobacter*) and in smaller proportions, *Gammaproteobacteria* and *Flavobacteriia*, as well as some *Actinobacteria* [43]. The same classes are detected for immersion times of 6 or 12 months [46], but in different proportions, and an additional minority class, *Epsilonproteobacteria*, appears. On the coupon immerged for 11 years, the same classes as for short times, as well as *Deltaproteobacteria*, *Fusobacteriia* and *Clostridia*, were detected [48].

Although molecular biology techniques do not allow all bacteria to be detected *sensu stricto*, the flora analysed in this way will be referred to as *"total bacterial flora"* in this chapter. Variations in diversity studied with these techniques are observed as a function of time and of the immersion site (Fig. 7.4). Indeed, on the coupons immersed at La Rochelle (France), the analysis of the total flora shows an increase in the number of bacterial classes with the immersion time (as for the culturable flora). Moreover, a higher diversity is

observed in Cherbourg (France), for coupons immersed the same time in both ports (1 month). However, whatever the harbour, dominance of *Proteobacteria* is clear, as has already been demonstrated in marine sediments (Section 7.3.1). *Gammaproteobacteria* appear or form an important class on the test coupon immersed 1 month and then decrease. *Deltaproteobacteria* appear early (2 weeks of immersion) and increase overall over time, unlike *Epsilonproteobacteria*.

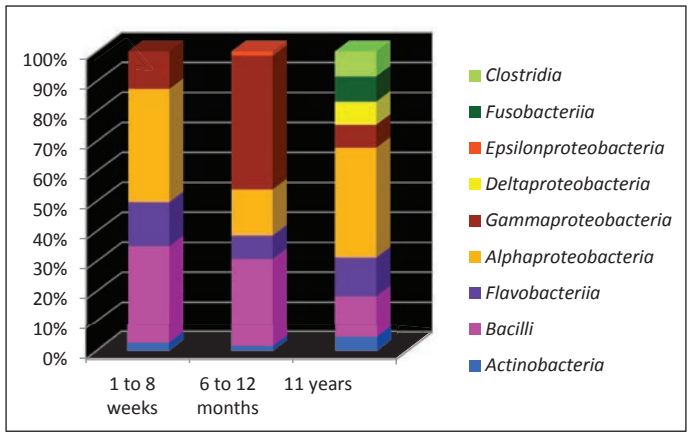


**Fig. 7.3.** – Average diversity of culturable bacteria from metallic test coupons immersed for 1 to 8 weeks in the harbour of La Rochelle (France) [43], 6 and 12 months in the harbours of Le Havre (France), St-Nazaire and Marseille (France) [46], and 11 years in the harbour of La Rochelle (France) [48].

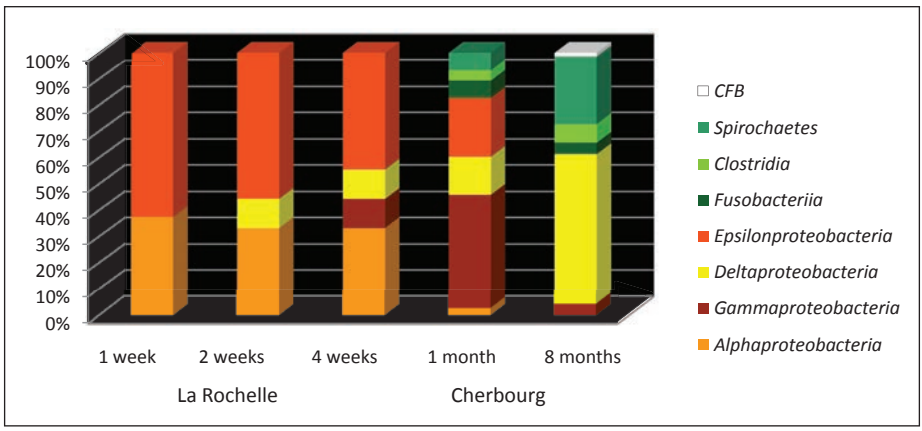


**Fig. 7.4.** – Evolution over time of the diversity of "total bacterial flora" in the ports of La Rochelle (France) [43] and Cherbourg (France) [40]. CFB: *Cytophaga-Flexibacter-Bacteroides*.

The analysis of all these different research investigations shows that in composite biofilms, the diversity of the culturable flora is clearly different from that of the total flora (Fig. 7.3 and Fig. 7.4). Moreover, the bacteria identified (at the level of the class and the genus) are common in marine environment. Indeed, the *Alpha-* and *Gamma- Proteobacteria,* for example, would represent more than 75% of the bacteria of this biotope [50]. Bacteria of the *Roseobacter* genus (belonging to the *Alphaproteobacteria* class), which have been detected both in culturable bacteria and in the total flora of steel coupons [43, 40], account for more than 25% of marine bacterioplankton [51]. They belong to a taxonomic group cited as dominant and easy to grow from coastal waters [51]. These bacteria could play an important role in the sulphur cycle within composite biofilms, due to their ability to oxidize inorganic forms of sulphur. Another sulpho-oxidizing *Alphaproteobacteria* involved in the sulphur cycle, *Sulfitobacter mediterraneus*, was detected in the total flora of the metallic coupons immersed a short time (1-8 weeks) [43]. *Gammaproteobacteria*, meanwhile, are observed in many marine biotopes, both in water and in sediments [36-38]. Among the *Gammaproteobacteria* detected [40, 43], *Marinobacter* is able to oxidize Fe (II) to Fe (III) and could therefore be indirectly involved in the oxidation of sulphides in marine sediments *via* production of $Fe^{3+}$. The *Flavobacteriia* class, detected after culture, is also very common in estuary areas where it may be dominant among culturable bacteria [52], as bacteria of the *Bacillus* genus [53]. Thus, many *Bacilli* have been obtained after culture, but no bacteria of this class have been detected in the total flora where *Proteobacteria* appear to be the majority (Fig. 7.4). Conversely, whereas *Epsilonproteobacteria* alone can constitute up to 62% of the total flora in young composite biofilms (1 to 4 weeks), none of these bacteria was detected after culture of the same samples (Fig. 7.3 and Fig. 7.4). Among these *Epsilonproteobacteria*, *Sulfurospirillum arcachonense*, a sulphurogenic bacterium able to reduce sulphur to sulphide, and *Sulfurimonas autotrophica*, a sulphur-oxidizing bacterium, have been identified and could play an important role in the sulphur cycle. No bacteria of the *Deltaproteobacteria* class, which includes most sulphidogenic bacteria (mainly SRB), were observed after culture of samples from coupons immersed from 1 week to 12 months (Fig. 7.3). Only the coupon immersed for 11 years allowed this class of bacteria to be detected after culture (Fig. 7.3). However, SRB of the *Deltaproteobacteria* class are detected early in the total flora (Fig. 7.4). This is consistent with the detection of iron sulphide at some points of the coupon immersed for 1 month [43]. However, it is clear that these SRB are a minority in these corrosion stages. This is in agreement with the work of Bermont-Bouis *et al.* [40], which showed that bacteria of the *Desulfovibrio* genus dominate in the total flora only after eight months of immersion (Fig. 7.4). Early detection of SRB could be explained by the occurrence of environmental conditions suitable for SRB growth (such as anaerobic conditions) in highly localized areas of the corrosion layer. By using molecular biology techniques, Pineau *et al.* [42, 46] specifically looked for SRB present in various harbours and principally detected *Desulfobulbus*, *Desulfovibrio* and *Desulfomicrobium* genera, in particular in low-water zones, after 6 and 12 months of immersion and essentially in the inner part of the

composite layer. Other studies have shown an even greater diversity of SRB in the middle and inner layers of natural deposits of corrosion on port structures of several decades [44].

Future research will therefore seek to determine in laboratory, among all these detected bacteria, which ones are responsible for the phenomena of biocorrosion, isolated or in consortia.

### 7.3.3. Interactions within marine biofilms

Interactions between marine biofilm bacteria have been mainly studied through cell-to-cell communication within single-species or bi-species biofilms through quorum sensing [54, 55]. Indeed, molecules of intra- and inter-specific communication are known to play a role in the regulation of the processes of adhesion and formation of biofilms. This cellular communication system, originally discovered on marine bacteria, depends on the cell density. The increase in the number of cells of a given species can therefore induce a metabolic or physiological modification of this population, such as motility (displacement of the cells towards a zone more suitable for their development), virulence (production of toxins for example), or sporulation (survival process while awaiting more favourable conditions). These molecules of communication could also influence the colonization and/or multiplication of certain other microbial species.

Other data, mainly concerning molecules with anti-biofilm activity, are also available. It has been shown that various strains of *Pseudoalteromonas* were able to inhibit the formation of different marine biofilms [56] and that actinomycetes could inhibit the formation of a *Vibrio* biofilm or even destroy it [57]. Moreover, EPS are known to play a crucial role in the adhesion and development of bacterial biofilms. Recent studies have shown, however, that EPS produced by marine bacteria (in particular *Vibrio* or *Bacillus* genera) could inhibit the formation of biofilms and even destroy an established biofilms [58, 59].

The works on diatom/bacterial interactions within microbial biofilms are rather rare, even though these microorganisms are recognized as essential to the biogeochemistry of marine ecosystems [60]. For planktonic diatoms, there are several examples of specific associations with some bacterial groups. These examples are much more rare for sediment diatoms [61, 62], particularly in the marine environment. However, in mudflats, there is a strong correlation between diatom biomass and bacterial abundance within biofilms [63, 64]. Bacterial growth is favoured by the consumption of organic matter excreted by diatoms and synthesized by photosynthesis or released during the decomposition of these dead microalgae. Conversely, it is known that bacteria are involved in the growth of diatoms, as has been observed in laboratory, without us really knowing or understanding fully the mechanisms. Thus, the bacteria of the *Proteobacteria* and *Bacteroidetes* groups appear to be particularly well-adapted to the microenvironment of biofilms and their presence is essential for the optimal growth of certain diatom strains [60-62]. The different types of beneficial interactions between bacteria and diatoms are complex and numerous [60].

Regarding mudflat biofilms, EPS are a major element of the interactions between bacteria and diatoms. In the light, modification of diatom metabolism by bacteria results in stimulation of excretion by diatoms of EPS from which bacteria feed [61, 65, 66]. Several stimulating bacterial substances (including vitamins and amino acids) are suspected [60, 62]. For a given diatom strain, the amount and composition of EPS may vary, depending on the bacterial groups with which it is in contact [62]. The amount and composition of EPS would govern aggregation of planktonic diatom cells [66] and biofilms stabilization [67]. On the other hand, the EPS secreted by the diatoms may stimulate or, on the contrary, inhibit the formation of bacterial biofilms, depending on the bacterial species [68]. Thus, biofilms would be dependent on the one hand on diatoms and bacteria that constitute the biofilms, and on the other hand on the EPS produced by the interactions between these microbial groups.

## 7.4. Conclusion

The immersion in sea water of a biotic or an abiotic surface generally leads, within the following hours, to the formation of a biofilm containing bacteria, microalgae and EPS, to which macroorganisms, algae and invertebrates, will attach themselves; it is the phenomenon of biofouling. In marine environment, *Proteobacteria* are among the first bacteria to colonize a virgin substrate and dominate in the different types of biofilms. The succession of populations within these biofilms is controlled by biological interactions. These interactions become more and more predominant with the maturation of biofilms. Thus, young biofilms are characterized by numerous interactions with oxygenated water, numerous free spaces and a nutrient supply by water, while the more mature biofilms, thickening over time, are characterized by a limited diffusion of oxygen and the appearance of microgradients over their thickness. This leads to a significant diversity of physical microhabitats, and therefore of ecological niches, allowing the development of a large number of different metabolic groups. The presence of microniches in aerobic biofilms thus allows the survival of anaerobic microorganisms, such as SRB, which will multiply until they become the majority when the conditions become more favourable to their development: thickening of the biofilms and creation of genuine anoxic zones in the deep layers of the biofilms. At the extreme points of mature biofilms with a thickness of several millimetres, the conditions are radically different. For example, for biofilms on metallic port structures, the deep layer directly in contact with the support could have a bactericidal or bacteriostatic effect, induced by higher concentrations of elements such as Cu, Ni, Zn or Cr. Conversely, the upper layer, directly in contact with the seawater, is extremely biodiverse and rich in microorganisms coming from seawater. This layer is highly influenced by the colonization by diatoms, algae, shellfish and other invertebrates, to form a “macrobiofilm”.

Microbial biofilms can thus participate in the phenomena of alteration of surfaces and can impair the integrity of artificial structures and thus their

durability. Research into microbial composition of biofilms and in their evolution over time should therefore lead to a better understanding and thereby to a better control of their role in the biodeterioration processes of materials.

## References

[1] Not F., Debroas D., Jebbar M., Jaillon O. (2011) "Ces acteurs invisibles qui contrôlent les milieux aquatiques." Biofutur, 319, 34-38.
[2] Amann R.I., Ludwig W., Schleifer K.H. (1995) "Phylogenetic identification and in situ detection of individual microbial cells without cultivation." Microbiol. Rev., 59, 143-169.
[3] Costerton J.W., Stewart P.S., Greenberg E.P. (1999) "Bacterial biofilms: a common cause of persistent infections." Science, 284, 1318-1322.
[4] Karatan E., Watnick P. (2009) "Signals regulatory network and materials that build and break bacterial biofilms." Microbiol. Mol. Biol. Rev., 73, 310-347.
[5] Sutherland I.W. (2001) "The biofilms matrix - an immobilized but dynamic microbial environment." Trends Microbiol., 9, 222-227.
[6] Dang H., Lovell C.R. (2000) "Bacterial primary colonization and early succession on surfaces in marine waters as determined by amplified rRNA gene restriction analysis and sequence analysis of 16S rRNA genes." Applied and Environmental Microbiology, 66, 467-475.
[7] Salta M., Wharton J.A., Blache Y., Stokes K.R., Briand J.F. (2013) "Marine bio-films on artificial surfaces: structure and dynamics." Environ. Microbiol., 15, 2879-2893.
[8] Singh P.K., Parsek M.R., Greenberg E.T., Welsh M.J. (2002) "A component of innate immunity prevents bacterial biofilms development." Nature, 417, 552-555.
[9] Wahl M. (1989) "Marine epibiosis. I. Fouling and antifouling: some basic aspects." Marine ecology progress series, 58, 175-189.
[10] Zobell C.E., Allen E.C. (1935) "The Significance of Marine Bacteria in the Fouling of Submerged Surfaces." J. Bacteriol., 29, 239-251.
[11] Characklis W.G. (1990) "Microbial fouling, Biofilms." Characklis W.G. and Marshall K.C. Eds, Wiley, New York, USA, 523-584.
[12] Callow M. (1986) "A world-wide survey of slime formation on antifouling paints, algal biofouling, studies environmental science." Evans L. and Hoagland K. Eds, Elsevier, New York, USA, 1-20.
[13] Schultz M.P., Bendick J.A., Holm E.R., Hertel W.M. (2011) "Economic impact of biofouling on a naval surface ship." Biofouling, 27, 87-98.
[14] Pritchard A.M. (1987) "The economics of fouling, Fouling science and technology." NATO ASI Series E, Melo L.F., Bott T.R., Bernardo C.A. Eds, Kluwer Academic Publishers, 31-45.
[15] Lee W., Lewandowski Z., Nielsen P.H., Hamilton W.A. (1995) "Role of sulfate-reducing bacteria in corrosion of mild steel: a review." Biofouling, 8, 165-194.

[16] Piola R.F., Dafforn K.A., Johnston E.L. (2009) "Mini-review: the influence of antifouling practices on marine invasions." Biofouling, 25, 633-644.
[17] Pascal P.Y., Dupuy C., Richard P., Mallet C., Armynot du Châtelet E., Niquil N. (2009) "Seasonal variation in consumption of benthic bacteria by meio- and macrofauna in an intertidal mudflat." Limnology and Oceanography, 54, 1048-1059.
[18] Lau S., Thiyagarajan V., Cheung S., Qian P. (2005) "Roles of bacterial community composition in biofilms as a mediator for larval settlement of three marine invertebrates." Aquatic Microbial Ecology, 38, 41-51.
[19] Chiu J., Zhang R., Wang H., Thiyagarajan V., Qian P. (2008) "Nutrient effects on intertidal community: from bacteria to invertebrates." Marine Ecology Progress Series, 358, 41-50.
[20] Nayar S., Goh B., Chou L. (2005) "Settlement of marine periphytic algae in a tropical estuary." Estuarine, Coastal and Shelf Science, 64, 241-248.
[21] Blanchard G.F., Simon-Bouhet B., Guarini, J.-M. (2002) "Properties of the dynamics of in-tertidal microphytobentic biomass." Journal of the Marine Biological Association of the UK, 82, 1027-1028.
[22] Patil J., Anil A. (2005) "Biofilm diatom community structure: influence of temporal and substratum variability." Biofouling, 21, 189-206.
[23] Lee J.W., Nam J.H., Kim Y.H., Lee K.H., Lee D.H. (2008) "Bacterial communities in the initial stage of marine biofilms formation on artificial surfaces." J. Microbiol., 46, 174-182.
[24] Bellou N., Papathanassiou E., Dobretsov S., Lykousis V., Colijn F. (2012) "The effect of substratum type, orientation and depth on the development of bacterial deep-sea biofilm communities grown on artificial substrata deployed in the Eastern Mediterranean." Biofouling, 28, 199-213.
[25] Beck M.W., Heck K.L., Able K.W., Childers D.L., Eggleston D.B., Gillanders B.M., Halpern B., Hays C.G., Hoshino K., Minello T.J., Orth R.J., Sheridan P.F., Weinstein M.P. (2001) "The identification, conservation and management of estuarine and marine nurseries for fish and invertebrates." Bioscience, 51, 633-641.
[26] Blanchard G.F., Guarini J.-M., Orvain F., Sauriau P.-G. (2001) "Dynamic behaviour of benthic microalgal biomass in intertidal mudflats." Journal of Experimental Marine Biology and Ecology, 264, 85-100.
[27] Serôdio J., Vieira S., Barroso F. (2007) "Relationship of variable chlorophyll fluorescence indices to photosynthetic rates in microphytobenthos." Aquatic Microbial Ecology, 49, 71-85.
[28] Serôdio J., Vieira S., Cruz S. (2008) "Photosynthetic activity, photoprotection and photoinhibition in intertidal microphytobenthos as studied in situ using variable chlorophyll fluorescence." Continental Shelf Research, 28, 1363-1375.
[29] Admiraal W., Peletier H., Brouwer T. (1984) "The seasonal succession patterns of diatom species on an intertidal mudflat – an experimental analysis." Oikos, 42, 30-40.

[30] Underwood G., Kronkamp R. (1999) "Primary production by phytoplankton and microphytobenthos in estuaries." Advances in Ecological Research, 29, 93-153.
[31] van Duyl F.C., Winder B.D., Kop A.J., Wollenzien U. (2000) "Consequences of diatom mat erosion for carbohydrate concentrations and heterotrophic bacterial activities in intertidal sediments of the Ems-Dollard estuary." Continental Shelf Research, 20, 1335-1349.
[32] Decho A.W. (2000) "Microbial biofilms in intertidal systems: an overview." Continental Shelf Research, 20, 1257-1273.
[33] Orvain F., De Crignis M., Guizien K., Lefebvre S., Mallet C., Takahashi E., Dupuy C. (2014) "Tidal and seasonal effects on the short-term temporal patterns of bacteria, microphytobenthos and exopolymers in natural intertidal bio-filmss (Brouage, France)." Journal of Sea Research, 92, 6-18.
[34] Haubois A.G., Sylvestre F., Guarini J.M., Richard P., Blanchard G.F. (2005) "Spatio-temporal structure of the epipelic diatom assemblage from an intertidal mudflat in Marennes-Oléron Bay, France." Estuarine, Coastal and Shelf Science, 64, 385-394.
[35] Schmidt J.L., Deming J.W., Jumars P.A., Keil R.G. (1998) "Constancy of bacterial abundance in surficial marine sediments." Limnology and Oceanography, 43, 976-982.
[36] Ravenschlag K., Sahm K., Amann R. (2001) "Quantitative Molecular Analysis of the Microbial Community in Marine Arctic Sediments (Svalbard)." Appl. Environ. Microbiol., 67, 387-395.
[37] Zinger L., Amaral-Zettler L.A., Fuhrman J.A., Horner-Devine M.C., Huse S.M., Welch D.B.M., Martiny J.B.H., Sogin M., Boetius A., Ramette A. (2011) "Global patterns of bacterial beta-diversity in seafloor and seawater ecosystems." PLoS ONE, 6, e24570.
[38] Lavergne C. (2014) "Rôle (structure et fonction) des communautés procaryotes (bactéries et archées) dans le cycle de l'azote d'une vasière littorale du Pertuis Charentais: Influence des facteurs biotiques et abiotiques par une approche multi-échelle." PhD thesis, université de La Rochelle, La Rochelle, France.
[39] Urakawa H., Yoshida T., Nishimura M., Ohwada K. (2000) "Characterization of depth-related population variation in microbial communities of a coastal marine sediment using 16S rDNA-based approaches and quinone profiling." Environ. Microbiol., 2, 542-554.
[40] Bermont-Bouis D., Janvier M., Grimont P.A.D., Dupont I., Vallaeys T. (2007) "Both sulfate-reducing bacteria and Enterobacteriaceae take part in marine biocorrosion of carbon steel." J. Appl. Microbiol., 102, 161-168.
[41] Langumier M., Sabot R., Obame-Ndong R., Jeannin M., Sablé S., Refait P. (2009) "Formation of Fe(III)-containing mackinawite from hydroxysulphate green rust by sulphate reducing bacteria." Corrosion Science, 51, 2694-2702.
[42] Pineau S., Sabot R., Quillet L., Jeannin M., Caplat C., Dupont-Morral I., Refait P. (2008) "Formation of the Fe(II-III) hydroxysulphate green rust

during marine corrosion of steel associated to molecular detection of dissimilatory sulphite-reductase." Corrosion Science, 50, 1099-1111.
[43] Lanneluc I., Langumier M., Sabot R., Jeannin M., Refait P., Sablé S. (2015) "On the bacterial communities associated with the corrosion product layer during the early stages of marine corrosion of carbon steel." International Biodeterioration & Biodegradation, 99, 55-65.
[44] Païssé S., Ghiglione J.-F., Marty F., Abbas B., Gueuné H., Sanchez Amaya J.M., Muyzer G., Quillet L. (2013) "Sulfate-reducing bacteria inhabiting natural corrosion deposits from marine steel structures." Applied Microbiology and Biotechnology, 97, 7493-7504.
[45] Boudaud N., Coton M., Coton E., Pineau S., Travert J., Amiel C. (2010) "Biodiversity analysis by polyphasic study of marine bacteria associated with biocorrosion phenomena." J. Appl. Microbiol., 109, 166-179.
[46] Pineau S. (2006) "Interactions entre les communautés bactériennes et les processus de corrosion accélérée des structures métalliques en environnement marin." PhD thesis, université de Technologie de Compiègne, France.
[47] Langumier M., Lanneluc I., Sabot R., Jeannin M., Refait P., Sablé S. (2011) "Quelles sont les bactéries présentes dans les biofilms formés sur acier en milieu marin?." Mat. & Tech., 99, 591-603.
[48] Langumier M. (2011) "Biodétérioration des structures portuaires en acier: synergie entre la physico-chimie du fer en milieu marin et les microorganismes sulfurogènes." PhD thesis, université de La Rochelle, La Rochelle, France.
[49] Lebaron P., Servais, P, Troussellier M., Courties C., Muyzer G., Bernard L., Scheafer H., Pukall R., Stackebrandt E., Guindulain T., Vives-Rego J. (2001) "Microbial community dynamics in Mediterranean nutrient-enriched seawater mesocosms: changes in abundances, activity and composition." FEMS Microbiology Ecology, 34, 255-266.
[50] Hugenholtz P., Goebel B.M., Pace N.R. (1998) "Impact of culture-independent studies on the emerging phylogenetic view of bacterial diversity." J. Bacteriol., 180, 4765-4774.
[51] González J.M., Moran M.A. (1997) "Numerical dominance of a group of marine bacteria in the alpha-subclass of the class *Proteobacteria* in coastal seawater." Applied and Environmental Microbiology, 63, 4237-4242.
[52] Kisand V., Cuadros R., Wikner J. (2002) "Phylogeny of culturable estuarine bacteria catabolizing riverine organic matter in the northern Baltic sea." Applied and Environmental Microbiology, 68, 379-388.
[53] Frette L., Johnsen K., Jørgensen N.O.G., Nybroe O., Kroer N. (2004) "Functional characteristics of culturable bacterioplankton from marine and estuarine environments." International Microbiology, 7, 219-227.
[54] Pasmore M., Costerton J.W. (2003) "Biofilms, bacterial signaling, and their ties to marine biology." Journal of Industrial Microbiology & Biotechnology, 30, 407-413.
[55] Antonova E.S., Hammer B.K. (2011) "Quorum-sensing autoinducer molecules produced by members of a multispecies biofilms promote

horizontal gene transfer to *Vibrio cholerae*." FEMS Microbiology Letters, 322, 68-76.
[56] Klein G., Soum-Soutéra E., Guede Z., Bazire A., Compère C., Dufour A. (2011) "The anti-biofilms activity secreted by a marine *Pseudoalteromonas* strain." Biofouling, 27, 931-940.
[57] You J., Xue X., Cao L., Lu X., Wang J., Zhang L., Zhou S. (2007) "Inhibition of *Vibrio* biofilms formation by a marine actinomycete strain A66." Appl. Microbiol. Biotechnol., 76, 1137-1144.
[58] Jiang P., Li J., Han F., Duan G., Lu X., Gu Y., Yu W. (2011) "Anti-biofilms activity of an exopolysaccharide from marine bacterium *Vibrio* sp. QY101." PLoS One, 7, e18514.
[59] Sayem S.M., Manzo E., Ciavatta L., Tramice A., Cordone A., Zanfardino A., De Felice M., Varcamonti M. (2011) "Anti-biofilms activity of an exopolysaccharide from a sponge-associated strain of *Bacillus licheniformis*." Microbial Cell Factories, 10, 74.
[60] Amin S.A., Parker M.S., Armbrust E.V. (2012) "Interactions between diatoms and bacteria." Microbiol. Mol. Biol. Rev., 76, 667-684.
[61] Bruckner C.G., Bahulikar R., Rahalkar M., Schink B., Kroth P.G. (2008) "Bacteria associated with benthic diatoms from Lake Constance: phylogeny and influences on diatom growth and secretion of extracellular polymeric substances." Appl. Environ. Microbiol., 74, 7740-7749.
[62] Bruckner C.G., Rehm C., Grossart H.P., Kroth P.G. (2011) "Growth and release of extracellular organic compounds by benthic diatoms depend on interactions with bacteria." Environmental Microbiology, 13, 1052-1063.
[63] Goto N., Mitamura O., Terai H. (2001) "Biodegradation of photosynthetically produced extracellular organic carbon from intertidal benthic algae." Journal of Experimental Marine Biology and Ecology, 20, 73-86.
[64] Bellinger B., Underwood G., Ziegler S., Gretz M. (2009) "Significance of diatom-derived polymers in carbon flowdynamics within estuarine biofilms determined through isotopic enrichment." Aquatic Microbial Ecology, 55, 169-187.
[65] Orvain F., Galois R., Barnard C., Sylvestre A., Blanchard G., Sauriau P.G. (2003) "Carbohydrate production in relation to microphytobenthic biofilms development: an integrated approach in a tidal mesocosm." Microbial Ecology, 45, 237-251.
[66] Gärdes A., Iversen M.H., Grossart H.-P., Passow U., Ullrich M.S. (2011) "Diatom-associated bacteria are required for aggregation of *Thalassiosira weissflogii*." The ISME Journal, 5, 436-445.
[67] Lubarsky H.V., Hubas C., Chocholek M., Larson F., Manz W., Paterson D.M., Gerbersdorf S.U. (2010) "The Stabilisation Potential of Individual and Mixed Assemblages of Natural Bacteria and Microalgae." PLoS ONE, 5, e13794.
[68] Doghri I., Lavaud J., Dufour A., Bazire A., Lanneluc I., Sablé S. (2017) "Cell-bound exopolysaccharides from an axenic culture of the intertidal mudflat *Navicula phyllepta* diatom affect biofilms formation by benthic bacteria." Journal of Applied Phycology, 29, 165-177.

# 8 Biofilms and management of microbial quality in drinking water supply systems

**Yves Levi**

Uninterrupted city production and distribution of tap water for human consumption represents a major technological challenge. The goal is to guarantee the distribution of appropriate volumes 24 hours a day, 365 days a year. These tons of products are transported to each point of use, at a price acceptable to all, while certifying compliance according to those quality standards requested by health regulations, whatever:

- the qualitative variations of raw waters contents;
- the characteristics of the distribution system (topography, age, flow rates, materials...);
- consumer sensitivity towards health risks (pregnancy, immunocompromised or dialyzed persons, children...);
- the requirements of the professionals involved (agro-food, precision industries, healthcare organizations, *etc.*).

The natural development of bacterial biomasses within the distribution systems is now obvious, thanks to numerous research investigations carried out and published over the last thirty years on the subject.

It would be too ambitious to describe, in just a few pages, all the elements developed or known about biofilms in drinking water distribution systems (DWDS). The subject is huge, and the expertise is numerous and sometimes competitive, as in the case of the best management practices of water quality in DWDS using residual chlorine or by reducing the dissolved or particulate nutrient content for biomass.

This chapter therefore describes important points that have helped guide operators of drinking water treatment plants (DWTPs) and distribution systems in order to better manage the quality of the final delivered product. It refers to review articles or collective books in which the reader will find out all details and comparisons about study methods and results. It is important to keep in mind that, given the importance of the topic, management actions aimed specifically at limiting biofilms in public drinking water distribution networks are very few and more documented in economically developed countries. This topic has recently appeared in the specifications for the renovation or construction of

DWTPs, particularly when parameters such as dissolved organic matter and chlorine demand are involved. There are still major challenges to be faced, not only in large DWDSs but also particularly in building plumbing networks.

## 8.1. From treatment plant to the tap: a vast, and complex to manage, chemical and biological reactor

DWTPs with DWDSs are large physico-chemical and biological reactors. Originating in a production unit in which the product is continuously manufactured, they then continue through public networks made of pipes of very different quality, age and materials and water towers and tanks with important interfaces with air. They are completed by plumbing networks inside buildings and houses which represent in themselves reactors of particular characteristics.

The notion of reactor is justified by the simultaneous presence of biodegradable matters and reactive compounds (oxidizing agents in particular) in water, active circulating or fixed biomasses on internal surfaces of pipes and structures and chemical exchanges with air and materials.

Thus, the quality of water produced and distributed evolves necessarily and must be optimized and all the components of the networks/reactors that can lead to possible degradation must be managed and considered carefully. The question involves both health issues (contaminations) but also risks of structural degradations (corrosions, materials release...). This requires that the management policies be perfectly designed, integrated and followed by a global and integrated vision from raw water to the points of use.

The resource water quality, even before its passage into the DWTP, is able to influence and drive microbiological stability in the network. The important parameters are particularly temperature, biodegradable organic matter (BOM) content, precursors of disinfection by-products, reducing compounds that can neutralize chlorine and, of course, circulating microorganisms. All the parameters which can affect the integrity of the network materials (corrosion, calco-carbonic equilibrium, pH, hardness, particles, *etc.*) are also very important.

DWTPs technologies and management strategies must be selected and controlled to adapt to the nature and qualitative variability of the raw water contents in order to ensure permanent health security for consumers and water uses. The reduction of the microbial load is achieved by the so-called "multi-barrier" concept (filtration, ozonation, ultraviolet radiations, chlorination) and the implementation of Water Safety Plans [1] based on the principles of hazard analysis and critical control points (HACCP) [2].

The final disinfection step must, however, absolutely be carried out inside the plant, before distribution. The goal is to guarantee the distribution of drinking water without pathogenic microorganisms but, under no circumstances, the production of "sterile" water. If, in the 1980s, there has often been a mistaken

reference to "sterilization" of drinking water in DWTPs and a "sterile" water supply, these terms are obviously to be banned as there is no sterility in the drinking water supply chain.

When the water leaves the production unit, it passes through large diameter pipes with a low surface to volume ratio. The temperature is that existing at the exit of the production and the water velocity is fast. Gradually in the network, the diameters decrease with the residence time, materials can be very old, distances can be larger and speeds slower and slower. In water towers and tanks in which water is interfacing with air, good management leads to evacuating every day the largest volume in order to limit stagnation. In the absence of booster chlorination stations during distribution and depending on the quality of water, the residual disinfectant gradually decreases and becomes undetectable in the internal plumbing networks.

The design or modification of distribution network structure and management goals should therefore be carried out on the basis of the best hydraulic simulations, in order to limit any water stagnation zones. If this is the case for new networks, especially thanks to modern models with simulation modules for chlorine residuals, the situation is much more complex when it comes to old, urbanized areas.

Distribution takes place in more or less extensive and diffuse networks. These are open systems in which work is constantly carried out for renovation, extension, cleaning and disinfection purposes and are subject to corrosion phenomena, particulate matters and sediments, leaks and pipe breaks. This vast reactor is therefore constantly evolving as a function of the residence time.

DWTPs must minimize spreading of particles that, not only promote the transport of microorganisms, but also constitute deposits in stagnant areas which are ecological niches. Indeed, accumulations of particles in water towers and tanks, in low-flow pipelines and hot water storage tanks are protective zones for microbial development. The shear forces are especially low, the slow diffusion of water reduces oxygen content and prevents chlorine from penetrating and the particulate developed surface allows for the production of an important biomass [3]. Water must not be corrosive to reduce the risk of colouring and accumulation of rust particles and the consumption of residual chlorine. The calco-carbonic equilibrium is also adjusted to prevent scale deposits. The possible diffusion of iron and manganese can induce the formation of particles and sediments and decrease residual chlorine.

Some of the particulate and dissolved organic materials are used as nutrients for microorganisms and may also interact with chlorine to generate by-products, some of which (trihalomethanes) are subject to regulatory limits in tap water. The general principle of attempting to manage microbiological quality in the networks by using a residual of an oxidizing disinfectant agent requires the production of a water containing as little as possible reactive substances capable of neutralizing the biocidal activity. The materials themselves must not be able to promote the formation of "ecological niches" because of the nature of their components or their surface state. It is unquestionably necessary, parallel to

the management of residual chlorine, to reduce the concentration of BOM to limit the nutrients. These two objectives can only be achieved through a DWTP that combines various complementary and reliable steps adapted to this specific purpose.

Thus, the key rule for ensuring the distribution of stable drinking water quality at every point of use in a network, especially in large and megacities, is to design and refine treatment technologies and accuracy at the DWTPs, considering the parameters which determine the stability in the network. The network itself must, of course, be structured, controlled and maintained to be as closed and inert as possible.

## 8.2. The water-material interfaces in drinking water distribution systems

Given the problems of non-compliance with microbiological parameters in water samples taken from networks, questions have surged which researchers have tried to answer since the 1980s. Does the microbiological quality of distributed water inevitably deteriorate? If so, is it a function of the residence time? Are there health and/or degradation risks? How can we avoid these problems? What are the parameters to deal with to limit circulating biomasses and their disadvantages?

Distribution networks are organized according to a hydraulic scheme which can be either linear, with water shifted from production to the point of service end, or meshed in large urban networks. In this case, water follows a diversified path and may even come back to the very same point after a complex flow, which makes it more difficult to calculate the residence time. We are referring here to several thousands of kilometres of buried pipelines coupled with storage facilities (reservoirs, water towers) in which daily technical interventions take place [4]. The interfaces with the external environment are particularly numerous and create a source of potential retro-contamination.

In almost all European countries, all materials in contact with drinking water must have been evaluated to obtain a certificate of sanitary compliance [5].

Unfortunately, despite numerous international studies, the European protocols for validating conformity of materials do not yet require, in all countries, an evaluation of their influence on the growth of biofilms. Several methods do however exist, thanks to studies carried out in Germany, Great Britain and the Netherlands but which do not contain a validation of harmonized criteria of acceptability. Basically, the Dutch proposal is based on ATP (Adenosine Tri Phosphate, an energy source reflecting cell metabolic activity) by decoupling the biomass from three 50 $cm^2$ material surface samples and the free biomass, after several incubation periods of 56 to 112 days. Biomass recoveries are done by extraction in an ultrasonic bath. Germany suggests measuring a volume of scraped-off biomass with a surface area of 800 $cm^2$ after 4 to 12 weeks of incubation under a test water stream. The United Kingdom proposes the measurement

of dissolved oxygen depletion in water incubated with biomass from river water and material test coupons at 30 °C for 7 weeks with renewals. This led to the drafting of the European standard (EN 16421 [6]) which describes the three methods and lets the national legislators/authorities choose one with no regulatory obligation.

The pipe materials in public networks are sometimes very old and diverse in nature (steel, ductile iron, grey cast iron, cement, PVC, polyethylene, epoxy coatings...). In plumbing systems, the situation is also very diverse with a wide variety of materials, small pipe diameters, cold water lines heated by nearby hot water pipes, mix of cold and hot waters inside taps, very long residence times, periods and zones of stagnation, variable flows and hydraulic disturbances. And yet, every consumer has the right to obtain perfectly potable water at all times at his tap.

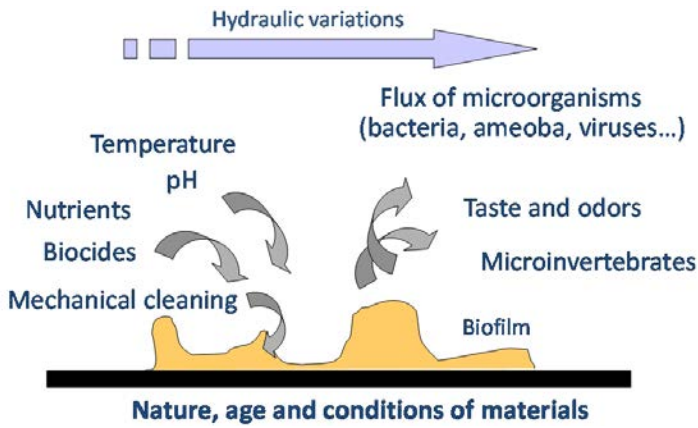


**Fig. 8.1.** – Parameters influencing the behaviour of biofilms in drinking water distribution systems and impacts on biological quality of distributed waters.

## 8.3. Evolution of understanding of the causes for bacterial growth in drinking water distribution systems

In the 1990s, despite the progress made in improving the efficiency of drinking water supply systems, it has been demonstrated that heterotrophic plate counts (HPC) for bacterial flora increase in relationship with water residence time and distance in many distribution systems [7, 8]. Others note that summer is more prone to exceed quality limit values, especially for “coliforms” during distribution [9].

### 8.3.1. Biodegradable organic matters

In many cases, water plant supply managers are convinced that their DWTP cannot be the cause of these degradations and assign responsibility to the network, suggesting contamination and poor maintenance. This is, of course, disputed by those in charge of network management. The question has therefore been raised to identify the causes of microbial proliferation in the networks in order to be able to control them. If the water leaving the plants showed an absence of HPC and coliforms, it was not the same at the network point of service. The hypotheses mentioned were that the circulating biomasses could be:

- due to poorly maintained and damaged networks contaminating water by introducing bacteria and organic matters;
- partially made of bacteria insufficiently disinfected at the exit of the treatment process and susceptible to revivification;
- linked to the biomasses fixed throughout the structures and capable of releasing bacterial cells in the water flow.

The first hypothesis was, of course, valid in networks that were poorly maintained. While there is no doubt that all networks are leaky and intrusions still exist, there were no notable differences between those in large European cities with the same leakage rate. This, while developing policies to reduce leakage, to renew oldest pipelines and improve monitoring, led to focus on assumptions related to water and material quality (Fig. 8.2).

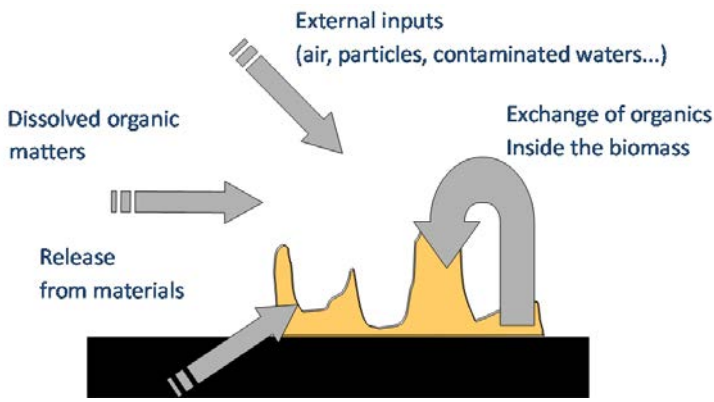


**FIG. 8.2.** – Flow of nutrient elements for biofilms in drinking water distribution systems.

The influence of *in situ* biofilms quickly became obvious as the main cause of these phenomena in well-maintained networks supplied by well-disinfected water. Analytical methods have been developed to measure or predict the potential of biodegradable organic dissolved matters. The objective was to predict, on one hand and based on the analysis of a water sample taken at the plant, the risk

of developing biomass relative to the water residence time and, on the other, to help optimize drinking water treatments technologies and streams to reduce this risk. Several methods have been developed in Europe and the United States and have resulted in numerous comparative or complementary studies.

The assimilable organic carbon (AOC) assay developed at KIWA in the Netherlands by van der Kooij and his team [10] is included in the Standard Methods for Water and Wastewater [11]. It is based on measuring the maximum number of specific strains of bacteria which can grow in the sample. The maximum count is obtained at the plateau of the growth curve for strains of bacteria inoculated in water previously decontaminated by moderate heating. The result is expressed in µg Carbon·$L^{-1}$ of acetate equivalent referring to a calibration curve of sodium acetate.

The determination of the bioeliminable dissolved organic carbon (BDOC) is standardized by the French standards agency (AFNOR), using bacterial biofilms on sand according to the method developed by Joret and Levi [12, 13, 14] or using suspended heterotrophic bacteria according to the method developed by Servais *et al.* [15, 16]. The term "bioeliminable" is preferred to the term "biodegradable" since the assay is carried out using a total organic carbon analyser. The latter makes it possible to distinguish just the organic carbon mass removed from the sample and not the biodegradation and metabolization leading to the same overall mass of carbon. The BDOC value is the difference between the initial dissolved organic carbon value of a sample and the one measured after a contact period with a mixed biomass population until its stabilization. The result is expressed in mg·$L^{-1}$ of carbon (Fig. 8.3).

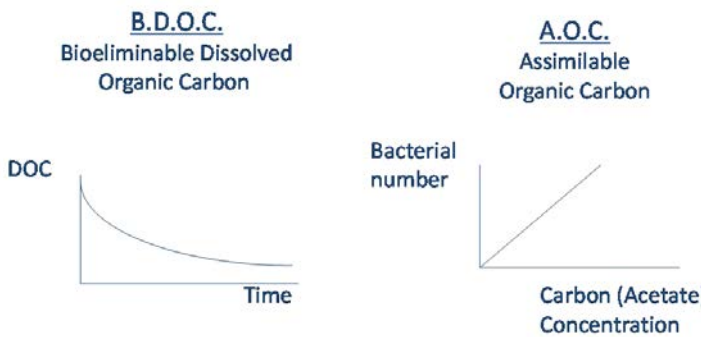


**Fig. 8.3.** – Basics of the two major analytical methods for biodegradable dissolved organic matters measurement inducing biofilm growth and behaviour in drinking water distribution systems. BDOC corresponds to the measurement of the decrease of dissolved organic carbon along incubation time with heterotrophic biofilms attached to sand. AOC correspond to the measurement of the maximum number of free bacteria at the plateau of the growth curve for a sample incubated with pure bacteria strains (mainly *Pseudomonas*) with reference to a calibration curve obtained with different controlled concentrations of sodium acetate).

It would take too long to detail all the comparative and inter-calibration studies between AOC and BDOC carried out during the years 1990-2000 but elements of synthesis exist [17, 18]. Many authors have compared the links between the two types of results obtained [19, 20].

Depending on periods and countries, these methods are used to help reduce the load of biodegradable elements to limit biomass getting into the networks. The inventors of these methods published guideline values or limit values for controlling network bacterial counts in circulating water (Table 8.1). Despite all the work published since the development of these parameters, they have not really frequently been taken into account in the management of DWTPs. The AOC or BDOC parameters sometimes appear in the specifications for renewal or building of DWTPs, but practically never as part of the routine monitoring parameters.

**TABLE 8.1.** – References values to be attained at the plant outlet for different methods allowing for measurement of biodegradable dissolved organic matters in order to limit global heterotrophic circulating bacteria or coliforms in drinking water distribution systems.

| Target bacteria | Parameters | Concentrations ($\mu g\ L^{-1}$) | References |
|---|---|---|---|
| Heterotrophic bacteria | AOC | < 10 | Van der Kooij *et al.* [21] |
| Heterotrophic bacteria | BDOC Biofilm on sand | < 200 | Levi and Joret [22] |
| Heterotrophic bacteria | BDOC Bacteria in suspension | < 150 | Servais *et al.* [23] |
| Coliforms | AOC | < 50 | Le Chevallier *et al.* [24] |
| Coliforms | BDOC Biofilm on sand | < 150 | Volk and Joret [25] |

### 8.3.2. Knowledge on biofilms

Simultaneously, numerous studies have been carried out to measure the different characteristic of biofilms in drinking water networks. These biomasses are the source of health risks and significant financial losses for water producers and industries. In addition to their influence on quality decrease in the distribution systems, they play an important role in fouling and clogging of filtration membranes, degradation of material surfaces in the DWDS and induced corrosion. They particularly generate risks of nosocomial infections in healthcare facilities, lead to losses of thermal and mechanical energies and induce measurement errors on in-line sensors or analysers.

In the field of drinking water supply, the incubation or observation devices developed for the measurement of biofilms have been very diverse. In order to obtain a simulation as close as possible to reality, it is necessary to create – in a laboratory or other conditions – the control of the most important parameters like hydraulic conditions, temperature and inlet water quality with no or a minimum bias. All observation scales have been approached from the circulation of water between two microscope slides to installations connected to the real network through semi-industrial pilots using real pipes extracted from a real water network [26]. Considering that the nature, structure and dynamics of biofilms are related to pipes materials, their surface condition, hydraulic forces and their variations, residence time, water dissolved content (including the residual of disinfectant) and temperature, the studies pilots or devices must allow the control of all these variables. Most pilot devices induce bias, so the type of installation must be adapted to the desired objectives while aiming at reducing variables and minimizing bias. The main devices used have been: rototorques with forced circular velocity between two cylinders [27], Propella ™ whose laminar velocity is forced by a propeller [28], new or old pipe cascading loops [29], on-line incubators incorporating glass beads and fed directly to the network by a waste water stream [30]. This diversity of devices and experiments has helped to dramatically improve the knowledge on biofilms structure and behaviour in DWDSs [31].

In order to evaluate the nature of bacteria likely to contaminate water, it is necessary to identify the biomass populations and to ensure an efficient, reproducible biomass extraction/scraping without disturbing the metabolic activity of the cells. Extraction techniques are as yet not standardized despite numerous attempts to harmonize protocols: ultra-sonication (probe or bath), mechanically scraping of the surface, agitation more or less strong using micro-glass beads... The international laboratory tests we were able to conduct under the most rigorous conditions on the same colonized glass beads shared between laboratories, showed a great variability of the biofilm measurements after ultrasonic extraction [32].

Each device and observation method for biofilms (thickness, metabolic activity, ATP content, density, enumeration, species identification, measurement of extracellular polymeric substances (EPS), confocal imaging, electron microscopy, *etc.*) provide interesting and complementary information but sometimes with great variability between studies and, nevertheless, with some common conclusions. The results show that colonization is fast and a pseudo-equilibrium of growth is reached after about one month of incubation.

Due to their three-dimensional architecture, to the large presence of exopolymeric substances (EPS) and to their microbiological diversity, biofilms ensure protection and promotion of bacterial ecologies because oxidative disinfectants – at the concentration levels observed in the distributed waters – penetrate weakly into the biomass. The structure adapts to the various stressors, especially in front of hydraulic movements, heat and drying.

In DWDS, numerous studies have shown the presence of about $10^6$ bacteria per $cm^2$ (total number of cells) on colonized surfaces in a semi-equilibrium

state. This is only about 2% of the surface, not including EPS. It is therefore not a real film but colonization structures which can evolve, disappearing and recreating colonies or swarming according to the variations of water quality.

## 8.4. Controlling biofilms in drinking water distribution systems

After two decades of international studies, the knowledge gained on biofilms in DWDS has not really led to the emergence of new pipes or coating materials limiting biomass or new orientations changing the design, management, maintenance and monitoring of networks. Of course, further attention has been paid to quality assurance and good disinfection practices, but biofilm measurement is still not a routine control parameter to ensure good quality during water distribution. Knowledge synthesis elements are summarized in the references [26, 33, 34].

Controlling circulating and attached microbial biomass first requires the reduction of BOMs. As a result, the drinking water treatment concepts had to evolve. First of all, it is necessary in Europe to comply with the limits defined by the European directive 98/83/EC and each Member State's implementation. Above all, water disinfection must be perfectly carried out inside the DWTP before any distribution of the produced water. In addition, it is essential to reduce turbidity, BOM concentration, and particularly BDOC at a concentration of less than 0.2 mg $L^{-1}$ carbon equivalent, chlorine demand and corrosion potential as much as possible.

The distributed water will thus be of quite optimal quality to limit the growth potential of biomass. This is of the most importance if the water temperature exceeds 16-17 °C, which represents a threshold beyond which growth is enhanced in the distribution network [35].

The reduction of BOMs in the DWTPs is carried out by biodegradation thanks to the biomasses present inside the sand and activated carbon filters or even in the pulsed sludge blanket clarifiers in which the water is in good contact with a suspended biomass. The removal is also carried out by retention, adsorption on activated carbon or resins, but also by nanofiltration and reverse osmosis. Flocculation at acidic pH using ferric chloride also has a good capacity to trap part of the BOM on the floc. Conversely, ozonation generates BOMs by degrading total organic carbon, which is why ozonation in the final stage of drinking water supply plants has been stopped [18].

It is also necessary to ensure the presence of a residual of biocide at the optimal place and during the necessary periods. Global practices generally favour free chlorine or monochloramine mainly in the Anglo-Saxon countries [36]. WHO recommends a chlorine residual of less than 5 mg $L^{-1}$, but for many reasons, and in particular organoleptic impacts, residuals levels vary in Europe between 0 and 1 mg $L^{-1}$. Low doses of biocides cannot compensate for insufficiently treated and poorly disinfected water leaving the treatment plant. Active

chlorine only penetrates to a small extent into the biofilms and is neutralized by reducing mineral and organic matters in the water, the deposits and the pipe walls [37, 38]. Thus, the management of residual chlorine is a real challenge. In Europe, many medium-sized and large cities distribute water without a chlorine residual either because of the excellent natural quality of the raw water or because of the development of an optimized treatment chain optimized to reduce, as much as possible, the content of BOM. The associated networks are well maintained without adapting however a particular strategy because of this lack of chlorine residual.

Since the biofilms vary in structure and behaviour depending on the seasons and the water residence time, the chlorine residual undergoes significant changes at the same location according to the time of day and the general conditions of distribution. Therefore, it is not a continuous and homogeneous biostatic efficiency.

Models have been developed to predict chlorine residuals as a function of hydraulic conditions [39, 40]. They enable strategies to define and optimize possible network booster chlorination stations. Predictive models of HPC flora were constructed based on temperature, BOM, chlorine residual, hydraulic data, and calculates free and fixed bacterial biomass. These are the Sancho model [41] and the Piccobio model [42, 43] which provide a mapping of areas and periods risking biomass proliferation.

## 8.5. Conclusion

The presence of biofilms in drinking water distribution systems has been widely recognized for 20 years. This has been achieved thanks to research data, and the levels of knowledge on structures, colonization kinetics and impacts have considerably increased. The effects are important on the microbial ecology of the networks (trophic chain that can lead to the appearance of macro-invertebrates) and health risks (legionellosis, nosocomial infections, free amoeba...) as well as degradation of structures (biocorrosion, leaks...) clogging of filtration membranes, taste and odours and non-compliance with bacterial quality limits and quality references of potable water regulations.

And yet, the means of action are limited. Efforts should focus on the quality of water that will be introduced into a network that is to be maintained and whose integrity is constantly verified and corrected.

The reduction of BOMs is a priority objective and the DWTPs having been renewed or designed with this objective in mind have seen the microbiological quality of the water distributed greatly improved, especially during hot periods. If water quality conditions are acceptable, the networks supplied with perfectly disinfected water but without residual chlorine distribute a product of very good quality.

The results of the knowledge on biofilms in the DWDSs are thus both encouraging and disappointing.

They are encouraging inasmuch as management objectives have been established and recognized at international level, observation tools are available and microbial ecology is better understood. All questions cannot be resolved, particularly in megacity networks, or conversely, in small distribution units without sufficient budgets.

They are disappointing, in that the criteria for the prevention of risks related to microbial ecology are still not sufficiently applied and many networks are still managed in curative mode or by using excessive doses of disinfectant residuals to try to limit the risks.

The case of building plumbing networks in which there is no disinfectant residuals, hydraulic conditions, materials and temperature are unfavourable, is a field of study and action still to be developed. These are other chemical and microbiological reactors of great diversity with a complex management. Beyond the biofilms which are a target of choice, the goal is, using preventive actions, to limit particular ecologies such as those of *Pseudomonas aeruginosa*, *Legionella* and amoeba as their hosts.

Many areas remain to be explored, including interrelationships between auto- and hetero-trophic populations, ecology of free *amoebae*, behaviour of antibiotic-resistant bacteria in health care facilities, innovative materials limiting the growth of biofilms.

## References

[1] WHO (2005) Water Safety Plans: Managing drinking-water quality from catchment to consumer. WHO/SDE/WSH/*05.06*www.who.int/water_ sanitation_health/dwq/wsp170805.pdf.

[2] WHO, IWA (2010) Plans de gestion de la sécurité sanitaire de l'eau : Manuel de gestion des risques par étapes à l'intention des distributeurs d'eau de boisson. www.who.int/water_sanitation_health/publication_ 9789241562638/fr.

[3] Liu G., Bakker G.L., Li S., Vreeburg J.H.G., Verbeck J.Q.J.C., *et al.* (2014) "Pyrosequencing reveals bacterial communities in unchlorinated drinking water distribution system: an integral study of bulk water, suspended solids, loose deposits and pipe wall biofilm." Environ. Sci. Technol., 48, 5467-5476.

[4] ONEMA, ASTEE, AITF (2013) Gestion patrimoniale des réseaux d'eau potable, www.onema.fr/IMG/pdf/Guide_Gestion_Patrimoniale-HD_DEF.pdf.

[5] Ministère des affaires sociales et de la santé (2015) http://social-sante.gouv.fr/sante-et-environnement/eaux/article/materiaux-entrant-en-contact-avec-l-eau-destinee-a-la-consommation-humaine.

[6] AFNOR (2015) Norme NF EN 16421, Influence des matériaux sur l'eau destinée à la consommation humaine – Stimulation de la croissance microbienne (SCM).

[7] van der Kooij D., van Lieverloo J.H. M., Schellart J., Hiemstra P. (1999) "Managing quality without a disinfectant residual." Journal of American Water Works Association, 91, 1, 55-64.
[8] Kerneïs A., Nakache F., Deguin A. (1995) "The effects of water residence time on the biological quality in a distribution network." Water Research, 29, 7, 1719-1727.
[9] Le Chevallier M.W. (2003) "Conditions favouring coliform and HPC bacterial growth in drinking water and on water contact surfaces." In: WHO, Heterotrophic plate counts and drinking-water safety, Bartram J., Cotruvo J., Exner M., Fricker C., Glasmacher A. Eds, IWA Publishing, London, UK.
[10] van der Kooij, D. (1992) "Assimilable organic carbon as an indicator of bacterial regrowth." Journal of American Water Works Association, 84, 57-65.
[11] APHA, AWWA, WEF (2012) "Standard Methods for Examination of Water and Wastewater." 22nd ed.
[12] Joret J.C., Levi Y. (1986) "Méthode rapide d'évaluation du carbone éliminable des eaux par voie biologique." Trib. Cebedeau, 510, 39, 3-9.
[13] Joret J.C., Levi Y., Volk C. (1991) "Biodegradable dissolved organic carbon (BDOC) content of drinking water and potential regrowth of bacteria." Water Science & Technology, 24, 2, 95-101.
[14] XP T90-319 (1995) "Essais des eaux – Évaluation en milieu aqueux du carbone organique dissous biodégradable. Méthode par bactéries fixées." AFNOR.
[15] Servais P., Anzil A., Ventresque C. (1989) "Simple method for determination of biodegradable dissolved organic carbon in water." Appl. Environ. Microbiol., 55, 10, 2732-2734.
[16] XP T90-318 (1995) "Essais des eaux – Évaluation en milieu aqueux du carbone organique dissous biodégradable – Méthode par bactéries en suspension." AFNOR.
[17] Numéro spécial de la revue des sciences de l'eau (1992) "Matière organique biodégradable." Revue des Sciences de l'Eau, 5, 243 p.
[18] Prest E.I., Hammes F., van Loosdrecht M.C.M., Vrouwenvelder J.S. (2016) "Biological stability of drinking water: Controlling factors, methods, and challenges." Front. Microbiol., 1, 7-45.
[19] Volk C.J., LeChevallier M.W. (2002) "Effects of conventional treatment on AOC and DBOC levels." Journal American Water Works Association, 94, 6, 112-123.
[20] Escobar I.C., Randall A.A. (2001) "Assimilable organic carbon (AOC) and biodegradable dissolved organic carbon (BDOC): complementary measurements." Water Research, 35, 18, 4444-4454.
[21] van der Kooij D., Hijnen W.A.M., Kruithof J.C. (1989) "The effect of ozonation, biological filtration and distribution on concentration of assimilable organic carbon." Ozone Science and Engineering, 11, 297-311.
[22] Levi Y., Joret J.C. (1990) "Importance of bioeliminable dissolved organic carbon (BDOC) control in strategies for maintaining the quality of

drinking water in distribution systems." Proc. AWWA WQTC, San Diego, USA, 1267-1279.
[23] Servais P., Billen G., Laurent P., Levi Y., Randon G. (1992) "Studies of BDOC and bacterial dynamics in the drinking water distribution system of the northern parisian suburbs." Revue des Sciences de l'Eau, 5, 69-89.
[24] Le Chevallier M.W., Schulz W., Lee R.G. (1991) "Bacterial nutriments in drinking water." Appl. Environ. Microbiol., 57, 857-862.
[25] Volk C., Joret J. C. (1994) "Paramètres prédictifs de l'apparition des coliformes dans les réseaux de distribution d'eau d'alimentation." Revue des sciences de l'Eau, 7, 2, 131-152.
[26] Keevil C.W., Godfree A., Holt D., Dow C. (1999) "Biofilms in the aquatic environment." Keevil C.W., Godfree A., Holt D., Dow C. Eds, Royal Society of Chemistry, London, UK, ISBN 0-85404-758-1, 242 p.
[27] van Der Wende E., Charaklis W.G. (1990) "Biofilms in potable water distribution systems, In: Drinking Water Microbiology: Progress and Recent Developments." McFeters G.A. Ed, New York, USA, Springer Verlag, 249-268.
[28] Appenzeller B.M., Batté M., Mathieu L., Block J.C., Lahoussine V., Cavard J., Gatel. D. (2001) "Effect of adding phosphate to drinking water on bacterial growth in slightly and highly corroded pipes." Water Research, 35, 1100-1105.
[29] Paquin, J.L., Block, J.C., Haudidier, K., Hartemann, P., Colin, F., Levi, Y. (1992) "Effect of chlorine on the bacterial colonisation of a model distribution system." Revue des Sciences de l'Eau, 5, 399-414.
[30] Delahaye E., Welte B., Levi Y., Leblon G., Montiel A. (2003) "An ATP-based method for monitoring the microbiological drinking water quality in a distribution network." Water Research, 37, 3689-3696.
[31] Gomes I.B., Simões, M., Simões L.C. (2014) "An overview on the reactors to study drinking water biofilms." Water Research, 62, 63-87.
[32] AGHTM Biofilm European working group (1999) "Standard method to evaluate aquatic biofilm." In: Biofilms in the aquatic environment. Keevil C.W., Godfree A., Holt D., Dow C. Eds, Royal Society of Chemistry, London, UK, ISBN 0-85404-758-1, 210-219.
[33] van der Kooij D., van der Wielen P.W.J.J. (2013) "Microbial growth in drinking water supplies: Problems, causes, control and research needs." IWA Publishing, 500 p.
[34] Batté M., Appenzeller B.M.R., Grandjean D., Fass S., Gauthier V., Jorand F., Mathieu L., Boualam M., Saby S., Block J.C. (2003) "Biofilms in drinking water distribution systems." Rev. Environ. Sci. Bio/Technol., 2, 147-168.
[35] Pinto A.J., Schroeder J., Lunn M., Sloan W., Raskin L. (2014) "Spatial-temporal survey and occupancy-abundance modeling to predict bacterial community dynamics in the drinking water microbiome." mBio, 5, 3:e01135-14, doi:10.1128/mBio.01135-14.
[36] Zhang W., DiGiano F. A. (2002) "Comparison of bacterial regrowth in distribution systems using free chlorine and chloramine: a statistical study of causative factors." Water Research, 36, 1469-1482.

[37] Lu W., Kiéné L., Levi Y., (1999) "Chlorine demand of biofilms in water distribution systems." Water Research, 33, 3, 827-835.
[38] Hallam N.B, West J.R., Forster C.F., Powell J.C, Spencer I. (2002) "The decay of chlorine associated with the pipe wall in water distribution systems." Water Research, 36, 14, 3479-3488.
[39] EPANET "Software That Models the Hydraulic and Water Quality Behavior of Water Distribution Piping Systems." http://www.epa.gov/water-research/epanet.
[40] Heraud J., Kiene L., Detay M., Levi Y. (1997) "Optimised modelling of chlorine residual in a drinking water distribution system with a combination of on-line sensors." Aqua, 46, 2, 59-70.
[41] Laurent P., Servais P., Prévost M., Gatel D., Clément B. (1997) "Testing the Sancho model on distribution systems." Journal of American Waterworks Association, 89, 7, 92-103.
[42] Piriou P., Dukan S., Levi Y., Jarrige P.A. (1997) "Prevention of bacterial growth in drinking water distribution systems." Water Science and Technology, 35, 283-287.
[43] Piriou P., Dukan S., Levi Y., Guyon F., Villon P. (1996) "Dynamic modeling of bacterial growth in drinking water networks." Water Research, 30, 9, 1991-2002.

# 9 Biofilms in industrial cooling circuits

**Michèle Merchat, Christophe Forêt**

## 9.1. Introduction

Biofilms are a source of industrial problems fraught with consequences. They reduce heat transfers in heat exchangers through their insulating nature and/or generate other risks due to the presence of microorganisms (health hazards, risk of corrosion). The nature of microbial species that proliferate in them depends on the ambient conditions, which can encourage organisms detrimental to infrastructures or pose a health hazard. For instance, the first layers of the biofilm generate aerobic bacteria like *Legionella*, some of which are pathogenic and can be transmitted to humans if the installations allow the water to be aerosolized [3, 28, 29, 30]. Conversely, under the deposit, at the interface of the biofilm and the base material, where the release of oxygen is reduced, anaerobic and optional aerobic bacteria develop [12]. The process corrosion of piping materials in water circuits can be aggraved by the metabolism of the bacteria living in the biofilm.

It is impossible to eradicate the biofilm to make the installations safer or more sustainable.

Consequently, the operator's responsibility consists of putting in place specific means of prevention to reduce the appearance of the identified risk (health hazard or risk of corrosion for instance).

The first step in this task begins with identifying all the factors in the installation that favour the appearance of the risk induced by the biofilm: those intrinsically related to the installation (design, water quality, surface state, hydraulics, *etc.*), and those related to risk management practices already implemented by the operator (shortcomings in the maintenance plan, the monitoring plan, *etc.*).

The second step consists of establishing risk control means for each of the previously identified factors, when they cannot be eliminated by curative actions.

Such means, once defined and implemented, constitute the installation's maintenance plan; in the form of preventive and remedial actions.

These actions draw on tools, such as chemical and/or physical processes, water management and maintenance procedures... which fit into a strategy formulated according to the type of risk, type of circuit and its operating conditions.

Reliable measurements of relevant indicators, taken from samples that are representative of the installation in question, can be used to evaluate and to ascertain the performance of these implemented actions. Both are needed for effective risk management [30].

Once this exercise has been carried out, one still needs to define the means implemented by personnel trained to recognize risks and mindful of maintenance procedures and of variations in indicators. Organizational barriers like training and maintenance are the support functions required for the efficiency of a good microbial risk management system, be it the risk of *Legionella* or that of corrosion induced by microorganisms.

Ultimately the efficiency of such a system is just as important for health or for the operational life expectancy of the installations as for the environment: it is a matter of maintaining the performance and integrity of the installations while mitigating both the health and the environmental impacts.

The strategy and the resources used to effectively fight biofilm microorganisms, which induce a health hazard when highly concentrated in water (risk of *Legionella*), differ from the strategy and resources used against those under the deposits involved in corrosion processes.

Through the example of two specific biofilm-related risks, the *Legionella* risk, on one hand and the risk of corrosion induced by microorganisms, on the other, this chapter attempts to describe the role of biofilm and how biological and technical approaches can be adopted to select and guide the choice of preventive and remedial measures to guarantee their effectiveness, and reduce the environmental impact and operating costs.

## 9.2. Biofilm and evaporative cooling circuits: health hazard

### *9.2.1. Evaporative cooling circuits*

Evaporative cooling systems through dispersal of water in an air flow are used to remove the heat lost in industrial processes, or the calories in the condensers of refrigerating units in industrial or commercial refrigeration processes (cold rooms, office air-conditioning, hotels, museums, *etc.*). The heat in the water is removed through cooling towers associated with a circuit in the form of steam. Water droplets can be directly drawn into the circuit by the rising air flow, despite the presence of antispray guards or droplet separators above the water supply ducts. This aerosolized water, also known as "vesicular entrainment", has the same composition as the water in the circuit.

There are several types of cooling tower design, which differ in their ventilation method (natural or mechanical), the water flows (counter-current or cross-current), their shape (round or rectilinear) or the type of associated circuit (open circuit, closed circuit, cooling by direct contact or not), but they all operate on the same principle (Fig. 9.1).

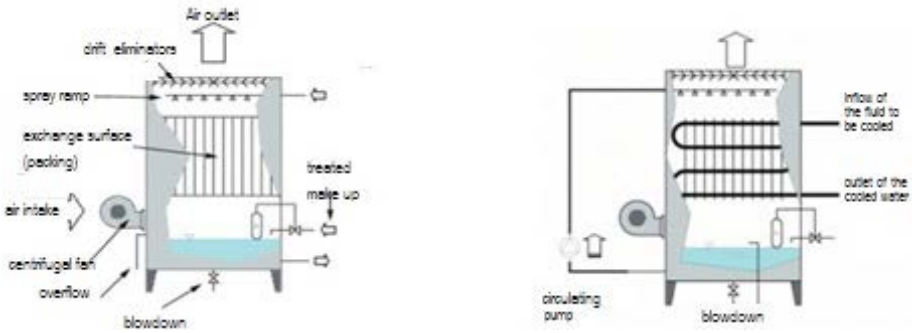


Open circuit Closed circuit

**FIG. 9.1.** – Diagram of forced draught and counter-current cooling towers, with open circuit (on the left) or closed circuit (on the right), the water not being in direct contact with the product (according to http://www.reunion.drire.gouv.fr).

The losses of pure water through evaporation cause an increase in the mineral salt concentration in the water of the circuit associated with one or more cooling towers. Blowdowns prevent excessive salinity in the circuit's water and control a stable concentration factor.

To offset the losses (from a few litres to several hundred $m^3$ per hour depending on the installation), the quality of make-up water differs according to the type of installation (softened or hard mains water, surface water, drill water, industrial water, *etc.*).

To sum up, the evaporative type of cooling circuits are mainly characterized by:

- the presence of a cooling towers that remove the heat through evaporation and that produce aerosols;
- direct contact between the water in the circuit and the air (comparable to a phenomenon of air being washed by water);
- temperatures very often ranging from 35 to 45 °C, but they can also be much lower;
- excessive concentration of mineral, organic and dissolved gas elements (especially $O_2$) in the circuit water;
- a variety of metals (galvanized steel, carbon steel, stainless steel, copper, *etc.*) and polymers (polyvinyl chloride, polythene, polypropylene, *etc.*);
- water quality that varies from one circuit to another, according to the source of the make-up water (surface water, drinking water, industrial water, *etc.*) and the cooling process;
- variable hydraulic conditions: laminar state in exchangers, turbulent state in pipes, state variations in normal operation when certain parts of the installation are idle for technical reasons or when starting and stopping...

Evaporative cooling circuits combine special conditions that give biofilm particular characteristics that must be factored in when choosing preventive measures.

### 9.2.2. Characteristics of biofilms in the circuits

The distinctive features of an evaporative cooling circuit, described in the previous paragraph, induce conditions that favour the appearance of certain "pathologies" in the water network, like the formation of incrusting deposits (precipitation, scaling, sludge) or deterioration (corrosion). The nature of the biofilm that forms on all the internal surfaces depends on the characteristics of these circuits and on those of the cooling water with which it is in contact. This is illustrated by the diversity of deposits that can be found in this type of installation. Figure 9.2 shows examples of extreme cases of deposits containing biofilm that, if present in large quantities, has a viscous appearance to the touch. But we should point out that in the vast majority of cases biofilm is not visible to the naked eye.

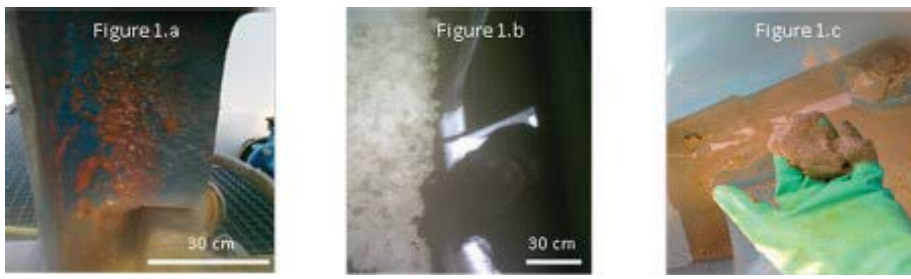


**FIG. 9.2.** – Diversity of the deposits observed in cooling circuits. 1.a: reddish deposit on the internal surface of the tower's immersed plastic elements. 1.b: blackish deposit in the bottom of a cooling tower basin. 1.c: deposit recovered at the lowest point of a cooling tower basin after a chemical cleaning operation.

"Biofilm" is described as an organized assembly of microbial cells irreversibly associated with a surface [5, 10, 13, 21] and coated with a matrix of extracellular polymeric substances (EPS) made up of an organic component (polysaccharides, proteins, nucleic acids... (Chapter 6)) but also a significant mineral component due to the nature of the base material and captured from the aquatic environment in question. This mineral phase can contain clay, silica, calcite in natural water systems, but can also be enriched in metallic oxides and oxyhydroxides (corrosion by-products) and other specific precipitates of artificial water circuits.

In evaporative cooling circuits, where conditions are conducive to corrosion phenomena (concentration of $O_2$ dissolved to saturation) and scale formation (concentration and excess saturation of mineral salts), the mineral matter can represent a substantial proportion of the biofilm.

Analyses of biofilms formed in an evaporative fed by surface water, analysed with confocal electron microscopy or inductively coupled plasma mass spectrometry, show the presence of a variety of elements such as calcium (in the form of calcite), iron (in the form of oxides making up to 30% of the dry mass of the biofilms), silicon (in the form of silicates and silica) and magnesium.

These elements, sometimes only present in circulating water in traces (less than 0.2 µg $L^{-1}$ for Fe for instance) [13, 21], are concentrated in the biofilm, the mineral proportion of which can represent up to 50% of the dry mass) [23] (Fig. 9.3).

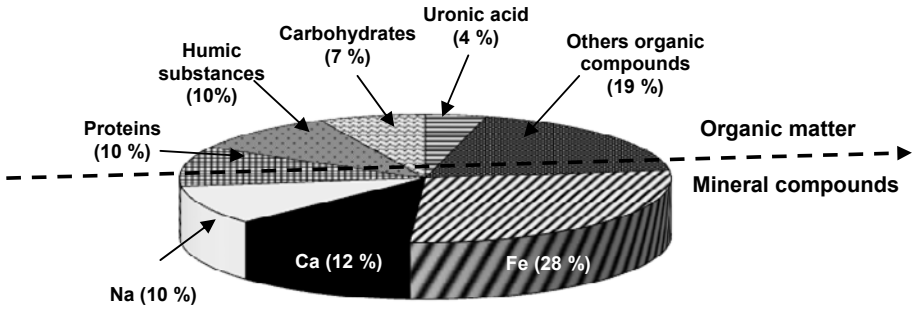


**Fig. 9.3.** – Chemical composition (%) of the dry mass of a biofilm in an evaporative circuit (adapted from [12]).

A far-infrared spectrometry analysis of a biofilm sampled in the basin of an industrial evaporative shows a very particular profile [24] (Fig. 9.4).

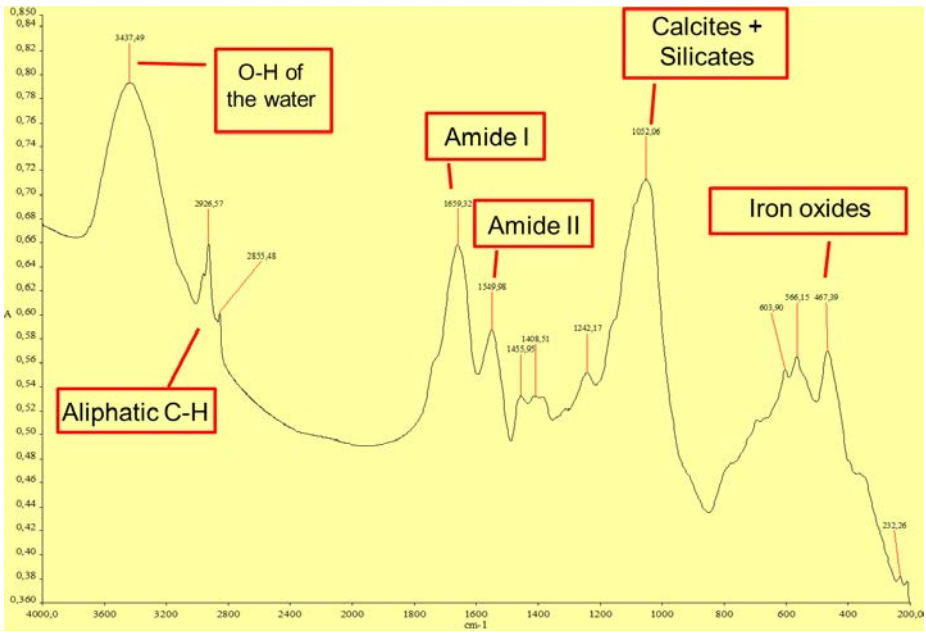


**Fig. 9.4.** – Far-infrared spectrum (before calcination) of a biofilm sampled in the basin of an industrial water circuit [24].

The high proportion of bacterial matter is confirmed by the simultaneous detection of aliphatic C-H bands (in the region of 2926 $cm^{-1}$), amide bands (1652, 1545 $cm^{-1}$) corresponding to the proteins making up the cell membranes of the bacterial biofilms [23] and the characteristic peak of silicates (1000 and 1100 $cm^{-1}$), a characteristic and structural element of the mineral matrix of bacterial biofilms [13, 21, 24]. In this example, the latter is mainly made up of iron oxyhydroxides (FeOOH), the origin of which is accounted for by the presence of carbon steel corrosion products in the cooling tower pool (as confirmed by visual observation). The iron corrosion products in this biofilm among others include lepidocrocite γ-FeOOH and maghemite γ-$Fe_2O_3$.

This mineral matrix plays a role in the structural properties of the biofilm. Surface water with high total hardness (TH = 27°F) with slight to moderate scaling potential leads to the formation or a more mineralized biofilm than softer water (TH = 3.5°F) and with slight aggressive potential [13, 21].

This difference in composition has a significant impact on the intrinsic properties of the biofilm, more particularly on its porosity and elasticity [13].

The latter characteristic is of paramount importance for the management of risk due to the presence of biofilm in a cooling circuit. This is because elasticity influences the behaviour of the biofilm and its capacity to erode under the effects of variable hydraulic forces (shearing forces), or become compacted under the mechanical effects of the water.

Consequently, it influences the transfer of *Legionella* from the biofilm to the circulating water. In other respects, the elasticity of the biofilm can guide the choice of a treatment strategy, or even explain why the efficiency of the implemented processes is poor or even non-existent in certain cases.

### 9.2.3. Detection and measurement of the biofilm

Several research programmes have been conducted over the past ten years to develop biofilm sensors. The basic principle consists in measuring a signal differential between a surface colonized by a biofilm (after a period of immersion in the circuit in question) and a non-colonized and clean surface.

The deposit formed by the biofilm induces resistance to the measured signal. For instance, if we take sensors that measure a heat transfer coefficient and those that take electrochemical measurements to determine a diffusion coefficient.

One method based on an electrochemical principle [13] uses a cell with three electrodes: one work rotating disc electrode, one calomel reference electrode and one counter-electrode (Fig. 9.5). This method takes amperometric measurements of the flow of matter in one electroactive specie (electrochemical tracer) on the surface of the electrode (*i.e.,* at the metal/biofilm interface) for different applied rotation speeds. The measured diffusion current enables one to estimate indirectly the thickness of the biofilm.

Platinum electrodes are used for this application. Immersed in the water circuit, their surfaces become covered with biofilm; they are used to measure the thickness.

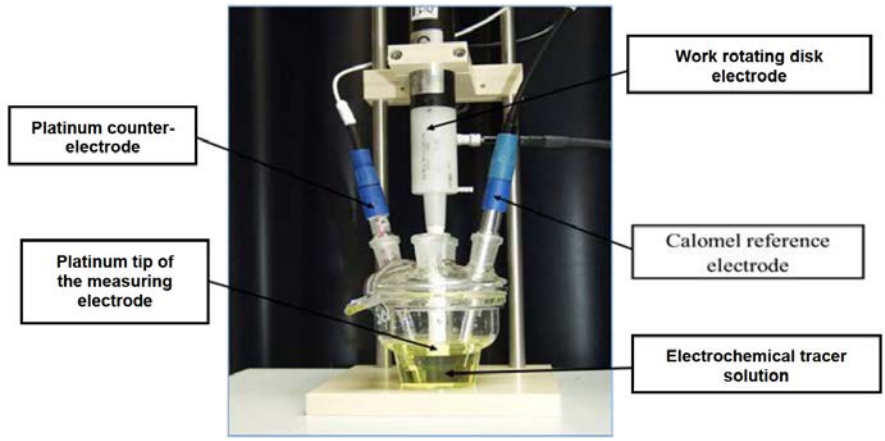


**Fig. 9.5.** – Analytical cell used for electrochemical measurements.

The measuring electrodes can be immersed directly in the water of the basin or tank in the cooling circuit or in manifold-type "reactors" installed on pipe bypasses (Fig. 9.6) with a constant flow rate.

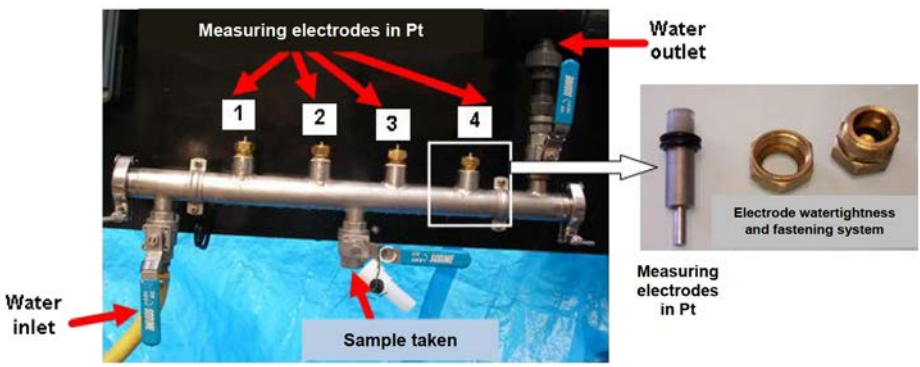


**Fig. 9.6.** – Manifold used as a support for the platinum electrodes.

By monitoring the growth of biofilms in the water circuit over time with this type of sensor, various different aspects can be evaluated, such as:

- the influence of the quality of the water circuit on the speed of growth of the biofilm;
- the elasticity of the biofilm and thus its capacity to withstand or yield to hydraulic variations;
- the efficiency of conditions of chemical treatment programs applied.

Biofilm measurements on four electrodes immersed for two weeks in the water of two different installations show relatively small and homogeneous thicknesses of 4 to 6 µm (Fig. 9.7). These two biofilms however present different growth kinetics: in one case (biofilm A) the maximum thickness (5 to 6 µm) is attained in eight days, whereas in the second case (biofilm B) maximum thickness (5 to 6 µm) is reached as early as the second day of immersion then remains virtually stable until the end of the colonization phase.

It is interesting to note that the thickness measurements taken in parallel with several electrodes over identical immersion times on the same circuit show no significant difference.

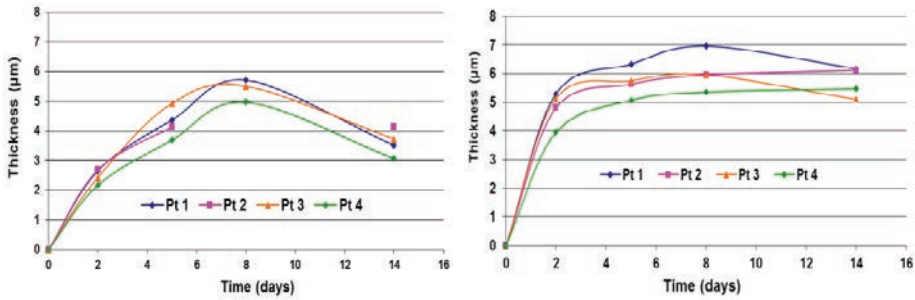


**FIG. 9.7.** – Thickness at 300 rpm of biofilms in two distinct industrial cooling circuits fed by surface water (river) after 14 days of colonization: biofilm A (on the left) and biofilm B (on the right). The measurements were taken with four platinum electrodes (Pt 1 to Pt 4) [13, 14].

### 9.2.4. "Risk of Legionella" and the role of biofilm

Evaporative cooling circuits can present conditions particularly conducive to the multiplication of *Legionella*, a pathogenic opportunistic bacterial species found in small concentrations in the natural environment. Inhalation of *Legionella*-contaminated water aerosols by a sensitive individual can cause a serious pneumopathy: legionellosis.

In water circuits, these strictly aerobic bacteria find some conditions favourable to their growth: hot water at the ideal temperature, nutrients in the biofilms on surfaces in contact with the water and protective and amplifying host organisms like free amoeba, or ciliates such as *Tetrahymena*, which have the capacity to store hundreds of *Legionella* cells in "granules" smaller than 5 µm, before excreting and releasing them into the water at a rate of one to five granules per hour [2, 3, 17]. The bacteria contained in these granules are protected and could be inhaled by persons exposed to the aerosols dispersed by cooling tower.

So-called "mature" biofilm can result from a balance between factors tending to increase its thickness and factors tending to reduce it, going as far as causing its detachment owing to natural regulation during growth, to the

erosion induced by the circulating water, to a mechanical shock or to the action of a chemical treatment process. The microorganisms in biofilm, including *Legionella*, are then transferred randomly into the circulating water [2, 34, 35].

In evaporative-type cooling circuits, the presence of *Legionella pneumophila* in circulating water at concentrations of $1\ 10^5$ CFU $L^{-1}$ represents a hazard liable to lead to cases of legionellosis, and requires immediate shutdown of the ventilation, implementation of remedial measures (generally biocide injection program), a search for the cause of the problem and notification to the inspection services [19].

Regulatory requirements oblige the operator to keep the concentration of *Legionella pneumophila* below $1\ 10^3$ CFU $L^{-1}$. To that end, he is responsible for implementing a maintenance and monitoring plan based on a methodical risk assessment.

As the biofilm and the *Legionella* host organisms favour high concentrations of *Legionella* in the circulating water, preventive measures aim to limit its development and/or limit the transfer of *Legionella* to the circulating water.

The choice between these two distinct modes of action depends mainly on the type of circuit and the operating conditions induced by technical requirements. The characteristics inherent in the composition of the biofilm (mineral/organic fraction) are some of the criteria that influence the choice of the treatment program and the strategy to apply.

### 9.2.5. Major health hazard factors

A water temperature of between 25 and 45 °C in an evaporative circuit is particularly favourable to the proliferation of *Legionella*. However, this parameter cannot be modified. So it is a matter of identifying other risk factors that can be modified to reduce the likelihood of the hazard appearing (a physical count of high concentrations of *Legionella* in the water), those concerning the installation itself (water quality, surface state, hydraulics) but also those relating to the preventive measures are in place (methodical risk assessments, preventive and remedial maintenance plans including the conditions under which water treatment strategies are implemented, monitoring plans, maintenance plans, training).

#### 9.2.5.1. The inner surface states of the circuit

Generally speaking, biofilm colonizes rough surfaces more easily. Surface state depends on the materials used but also on their deterioration through scale formation or corrosion. Treatment processes for these pathologies must be implemented on the make-up water and/or the water in the circuit.

- *Scale formation*

Deposits of carbonated and/or silicated and/or sulphated scale found in a cooling tower due to a scale formation phenomenon are an ideal colonization medium for biofilm to attach to and develop. The operating principle of the

evaporative circuit favours the formation of such deposits. This is because the evaporation of water in cooling towers entails a loss of $CO_2$ through degassing and accordingly the alkalizing of the water. For instance, in an evaporative circuit supplied with softened or hard drinking water (pH ~ 7.5), this alkalinisation naturally leads to pH values in the region of 8.5 or 9.

In view of the high temperature conditions in these circuits, the simultaneous increase in pH and concentration in mineral salts (excess saturation conditions due to evaporation) favours scale formation, more particularly the formation of calcium carbonate (mainly in the form of calcite), as its solubility is lower than that of other bodies likely to precipitate (Fig. 9.8).

**FIG. 9.8.** – Scale deposits on the surfaces of pipework (on the left), tubular exchanger (in the centre) and at the bottom of the cooling tower's pool (on the right).

- *Corrosion*

The water in the evaporate cooling circuits, which naturally contains chloride ions and sulphate, saturated in oxygen as they are continually aerated in the cooling tower, is corrosive to the installation's metallic materials: carbon steel (pipework), galvanized steel (cooling tower basin, heat exchanger), stainless steel (heat exchanger, pipework), copper (heat exchanger)... This corrosiveness can be aggravated by poor practice (misuse of oxidizing halogenated biocide [4, 26], wrong choice of materials and/or poor passivating of the latter, in the case of galvanized steel for example [25] (Fig. 9.9).

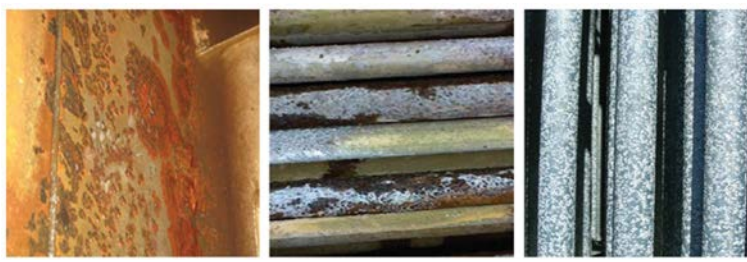

**FIG. 9.9.** – Corroded internal surfaces of cooling tower pool (on the left), a galvanized steel tubular exchanger (in the centre and on the right).

### 9.2.5.2. Water quality

The input of nutrients (organic and/or minerals), microorganisms, suspended matter, *etc.*, into evaporative cooling circuits mainly stems from three sources:

- the quality of the make-up water;
- the quality of the air in contact with the cooling water (dust, pollen, plant debris, insects or any other dirt relating to the industrial process of the circuit in question);
- and can originate from the product being cooled if it is in direct contact with the cooling water, either because that is part of the industrial process, or due to accidental leaks (pollution).

Proper risk management involves supplying make-up water of a relatively stable quality. To that end, chemical and/or physical processes should be implemented directly on the make-up water and the cooling circuit (oxidizing biocides, filtration, *etc.*).

### 9.2.5.3. Hydraulics

In the water circuit, as well as water quality, the hydraulic characteristics defined by the geometry of the circuits and by operating conditions (flow rate, velocity of flow) influence biofilm thickness.

As mentioned previously, the composition and more particularly the mineral/biological fraction influences its elasticity and thus its sensitivity to the mechanical action of the water and its capacity to become compacted or erode [29].

The influence of hydraulics can be illustrated by electrochemical measurement of the thickness of biofilm [13] deposited on measuring electrodes subjected to increasing rotation speeds. The thickness of a biofilm, primarily of an organic nature, is highly dependent on hydraulic conditions. As shown by the results in figure 9.10, its thickness decreases as the speed of rotation applied to the electrode increases.

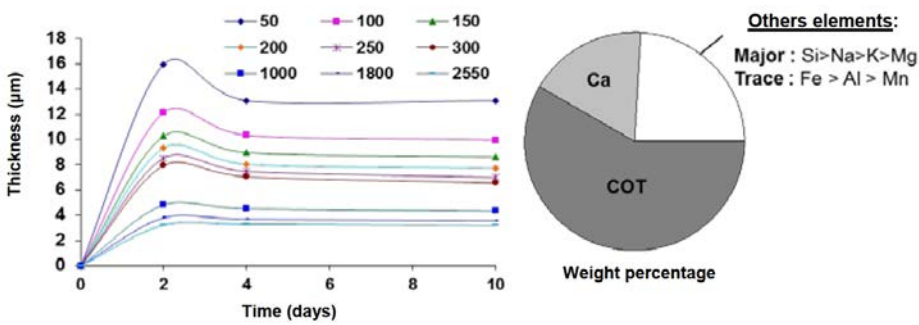


**Fig. 9.10.** – Influence of speed of rotation of an electrode (rotating disc electrode), colonized by a biofilm, on the latter's thickness (on the left) and connection with the physico-chemical composition of the biofilm [13].

The thickness of a biofilm with mineral components (calcite in this study) is characterized by low elasticity, which reflects its low dependence on hydraulic conditions (Fig. 9.10).

## 9.2.6. "Legionella risk" management strategy

Among the tools available, besides scale inhibitors, corrosion inhibitors, dispersing agents and filtration systems, management of the *Legionella* risk in evaporative cooling circuits generally involves implementing three "types" of chemical processes whose functions are distinct: oxidizing biocides, non-oxidizing biocides and surface-active agents.

It is worth noting that the chemical action could be supplemented or replaced with physical action if it has the same desired effect and if its effectiveness has been proven to be comparable. But given the current state of the art and in the absence of feedback on physical treatments, chemical treatments still remain the primary option operators have to date.

### 9.2.6.1. Biocide processes

Biocides work directly through contact with the target microorganism and have a bactericidal or bacteriostatic effect [20, 31]. Their effectiveness depends on a number of parameters, including length of contact between the molecule and the bacterium, not forgetting the type of product used. There are two types of biocides, oxidizing and non-oxidizing.

Oxidizing biocides are bactericides with a broad action spectrum that oxidize all the organic matter in the circuit's water. Once a portion of the oxidant has reacted with the most reactive reducing chemical compounds, the residual concentration will be active towards cells, and through dispersion could reach the interior of the bacterial cell and oxidize its main compounds. This approach to treatment, which acts directly on the organic matter and on the microbial concentration of the circulating water, is essentially used as a preventive treatment, by continuous injection that maintains an excess residual concentration available to perform its biocidal function. It is sometimes used as a curative treatment, but in that case the risk of corrosion is significantly augmented towards the installation's metallic materials.

Non-oxidizing biocides are synthetic organic molecules. Their action spectrum is narrower than that of oxidizing biocides, because their specific mode of action leads to bactericidal and bacteriostatic action through inhibition of certain metabolic mechanisms of the target microorganisms [30, 31] which include *Legionella pneumophila*. They are generally adapted and applied for curative actions and sometimes used in discontinuous injection, provided a major risk factor has been identified for an installation and as long as the risk has not been brought fully under control.

Whatever biocide is used, only planktonic and/or sessile yet accessible *Legionella* is affected. Those found in biofilms and protected by extracellular

polymers, by the mineral matrix or even by host organisms or their structure (*e.g.*, granules of *Tetrahymena*), are hardly (or not at all) affected. Consequently, direct action on the biofilm is needed to limit or even control its development or to limit the transfer of bacteria into the circulating water.

#### 9.2.6.2. Surface-active processes

Surfactants and tensio-active agents, commonly called "biodispersants" or "biodetergents", have properties relating to their amphiphilic structure that give them an affinity with the water-biofilm interface. They lower the free energy of these interfaces, leading to a gradual detachment of the miscible constituent elements of the biofilm with the hydrophobic part of the molecule [19, 20].

Implementing surface-active agents consists of reducing the thickness of the biofilm. To that end the implementation conditions are strict and necessarily combined with the mechanical action of the water. The presence or absence of surface-active agents in an installation determines water management; in particular, the method used for managing volumes of water after prolonged stagnation.

#### 9.2.6.3. Hydraulic conditions control

Apart from the fact that water circulation ensures distributed treatment, hydraulic conditions control is one of the key factors in *Legionella* risk management. It determines the effectiveness of both action strategies against biofilm, depending on the presence or absence of surface-active agents.

For installations for which a surface-active agent cannot or should not be used, appropriate water management reduces transfers of *Legionella* from the biofilm.

The hydraulic conditions control is different if a surface-active agent is present. Whether by erosion or by disintegration, the thickness of the biofilm is not immediately reduced when the process is used for the first time, but can continue for several weeks until a residual thickness is achieved, this depending on the maximum speed of the circulating water [19]. In an evaporative cooling circuit, this phase presents a risk, as the biofilm's bacteria, including *Legionella*, circulates in the water. This stage however is essential and varies on length, from a few days to a few months, depending on the size of the installation, its management method, the quality of the water, the composition of the biofilm (mineral/organic ratio), the length of time during which the water stays in the installation, the mechanical action of the water and probably many other factors.

During this phase of contamination of the circulating water, it is advisable to manage the risk by curative disinfection [19].

Results obtained on a series of electrodes immersed in the water of an evaporative circuit show that each injection of biodispersant significantly reduces the thickness of the biofilm [13, 14]. Between two shock injections, the residual concentration of the surface-active agent is too small to prevent it growing again (Fig. 9.11). On each injection, the newly formed biofilm becomes suspended

again quickly, which prolongs the risk of detecting high concentrations of *Legionella* in the water. Such a strategy increases the risk rather than reducing it and results in excessive injections of biocides. This observation confirms the dangerousness of carrying out repeated shock treatments with this biodispersant process [19].

The implementing conditions for this type of process intended to reduce and to remove biofilm are strict and require a stable permanent concentration combined with the mechanical action of the water. If these conditions are met, after a prolonged period during which the water becomes laden with elements coming from the biofilm, the latter attains a minimum thickness, thereby reducing the transfer of bacteria in the water. The minimum thickness of the biofilm depends on the hydraulics of the installation, in particular the boundary layer confined to the water/material interface, where water velocity is nil but rises gradually the further you go from the surface of the material until it reaches the velocity of the water. This micro-space, in which the water has no effect, depends on the average velocity of the water in the pipework [19]. That is why the hydraulic conditions control procedure is a key strategy on certain installations, in particular those where the circulation rate varies for technical reasons.

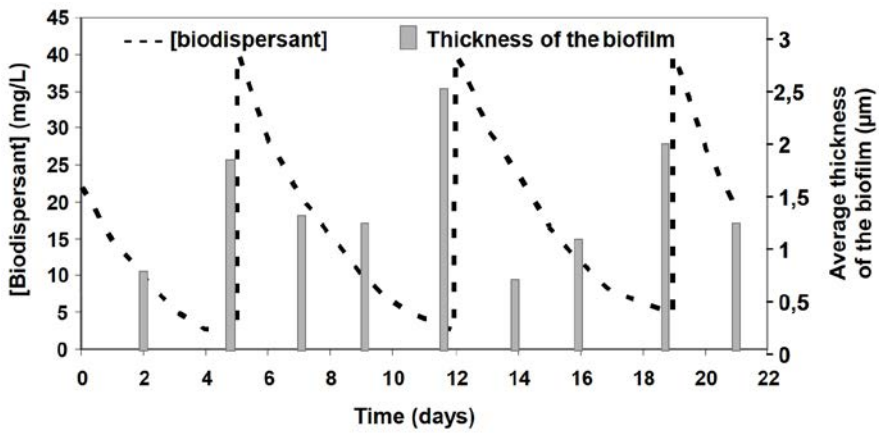


**FIG. 9.11.** – Influence of treatment with shock-injected biodispersant on the average thickness of a biofilm measured on 5 electrodes immersed in an industrial circuit [14].

Managing the "*Legionella* risk" in an evaporative cooling circuit necessarily consists of defining the measures suited to different installations that are capable of effectively combatting biofilm, but also against all the risk factors identified as favourable to its formation and or the transfer of bacteria in the circulating water.

Water treatment strategies are based on the implementation of specific processes inevitably combined with appropriate hydraulic conditions control. While the choice of processes depends on conventionally adopted parameters,

such as water quality and the type of materials, the choice of strategy depends on the type of installation and its method of use.

## 9.3. Biofilm in a refrigerated system: the risk of corrosion

The corrosion induced by microorganisms that develop under the deposits at the biofilm/base material interface affects all types of circuits. This phenomenon is illustrated in this chapter by the lessons learned on an iced-water system (or cold water piping system).

### *9.3.1. Cold water piping system*

An urban cold water piping system – also known as a cooling energy system – comprises collective equipment that distributes iced-water produced by central refrigerating plants and conveyed by distribution piping systems that deliver some of the cooling energy to the installations of the supplied buildings.

This is a closed circuit that therefore always comprises at least two separate piping systems: one that conveys the iced-water to the users, the other that returns the warm water to the plants. The water temperatures in this closed circuit range from 1 to 4 °C in the outgoing pipes, and 10 to 14 °C in the return pipes.

The cold water piping system thus involves three fundamental elements: the refrigerating plants, the distribution system and the points of supply (POS). The size of the distribution system can be limited to a single building, a district or extend to a whole town.

One characteristic of this closed circuit compared with other types of industrial facilities concerns the design of the systems and their management method. The piping system of a cold water system is a technical and economic element of such importance that the functional and operating savings depend to a great extent on its reliability, regardless of whether it is installed in a new sector or an existing urban area [8].

The technical constraints inherent in the location show that there is no universal solution. For each new installation, everything must be designed as a function of the number of future customers, the space available for pipework, the layout of the distribution piping (area, service gallery, shallow concrete or underground gutter). Cold water piping systems is characterized the virtual impossibility to control the hydraulics because of the technical design and operating choices:

- variable flow rate distribution (with constant return temperature);
- the coverage of the system which, contrary to branch systems where each customer is served by a single plant, can supply a given customer through several different routes. When part of the system is undergoing maintenance work, the customer is still supplied by another piping system;

– continual adaptation of pumps to the system's variable parameters;
– the variability of a consumer's needs according to season and changes in the connected premises;
– the variable waiting time between water priming and entry into service.

### 9.3.2. Characteristics of biofilms in cold water piping systems

Corrosion influenced by microorganisms aggregates all the corrosion phenomena where bacteria act directly, or through their metabolism, creating conditions conducive to its formation [6]. The phenomenon can be very fast and affect all the structures, in particular their durability. Several bacterial species play a part in corrosion mechanisms. This complex subject still comprises many unknown factors [33, 36].

Three major groups of bacteria are often cited and incriminated in steel corrosion phenomena. Sulphurogenic bacteria: sulphato-reducers and thiosulphato-reducers, which are anaerobic. Ferro-oxidizing bacteria and acidogenic bacteria, which are aerobic and part of a complex biological process in aerobic or aero-anaerobic environments. Study results show that the biofilm inhibits widespread corrosion of carbon steel and induces incipient localized corrosion (pitting). The microorganisms under deposits modify the physical chemistry at the material-water interface (pH, oxygen concentration, concentrations of chemical elements, *etc.*) either indirectly, through formed layers presenting considerable physical and biological differences, or directly through metabolites of bacterial heaps released transiently, in mainly anaerobic "niches", which locally induces a significant decrease in the medium's pH [16]. These conditions favour local acceleration of corrosion and induce the formation of "holes" covered by an accumulation of corrosion products forming characteristic tubercles, hardened crusts [7, 18, 32].

The speed with which this phenomenon occurs depends mainly on ambient conditions. Sulphurogenic bacteria cannot develop in the biofilm as long as the latter is thin and well-ventilated. The duration of mainly aerobic phases can be very long in sites laden with few settleable particles, and by contrast very short in zones highly polluted by deposits [7].

### 9.3.3. Danger due to corrosion induced by microorganisms

As the kinetics of most physico-chemical and biological reactions (like bacterial growth) are limited by cold temperatures, little attention has been paid hitherto to the possible corrosion processes induced by microorganisms in a cold water piping system. The scientific approach has led to a simplified schematization of the mechanisms at play on a microscopic scale, providing an understanding of the complexity of the process resulting from an interaction between

the living world and materials. This interaction is always summarized as being an unfavourable conjunction of three factors: microorganisms, water and the material [11, 29].

- Phase 0: colonization of the surface by the biofilm and a complex mixture of materials dependent on the medium. Bacterial metabolites can already influence the spread of corrosion if the stock of nutrients is large enough to allow them to grow rapidly.
- Phase 1: oxidation of the metal, controlled by the concentration of oxygen in the metallic surface.
- Phase 2: increase in the corroded layer, which delays the spread of oxygen to the metal. The concentration of oxygen at the metal/corrosion product interface is greatly reduced, leading to a slowdown in corrosion kinetics. These new interface conditions become conducive to the development of anaerobic bacteria such as sulphurogens.
- Phase 3: corrosion favoured of the sulphurogenic bacteria find conditions conducive to their development. The activity of the bacteria depends on the concentration of nutrients in their immediate vicinity. At the metal/corrosion layer interface, a balance is reached between the bacterial activity and the input of nutrients through corrosion products.

Microorganisms develop under the incrusted deposit, forming "tubercles" of corrosion. These protuberances present large contact surfaces with the water phase and thus trap more circulating organic matter while, at the same time, offering protection against disinfectants by limiting their dispersal or through the reaction of corrosion products with oxidizing biocides [15]. In the absence of water circulation, if the development of this tubercle seems slower, the bacteria in the niche still establish themselves just as much. When the water circulates again, either the mechanical action will suffice to "tear off" the tubercle (which contaminates the downstream system), or it will have no effect on this protuberance, under which bacterial activity will continue or even accelerate.

### 9.3.4. Major risk factors

Any material in contact with a biologically active medium is prone to corrosion influenced by microorganisms. Through their metabolism, microorganisms drastically modify the physico-chemical conditions at the material-environment interface (pH, concentration of $O_2$, concentration of chemical compounds, *etc.*), creating conditions at the root of corrosion. Microorganisms can thus be considered as catalysts of electrochemical phenomena, corresponding to precise typologies of corrosion. During their metabolism, certain bacteria like sulphato-reducers can influence and destabilize the passive layer of protection of pipes [1].

For these corrodible metals, the presence of corrosion products in the metallic materials accentuates the activity and the production of biomass. Bacterial production can thus be up to ten times greater on a corrodible material.

While the choice of materials meets technical and environmental criteria, the operating mode of the cold water piping system influences all the risk factors, which therefore can no longer be considered individually.

### *9.3.4.1. Water quality*

Water has a complex influence, firstly because of many interacting phenomena, and secondly because it is influenced by numerous environments defined locally, in particular by the hydraulic conditions and the depositing of particles borne by the water. Depending on local conditions in the pipe, the physicochemical nature of the medium (oxygen content, pH, availability of metallic ions used by the bacteria on which their metabolism is dependent, *etc.*), accentuates or slows down the corrosion process.

The "water quality" factor cannot be dissociated from the development of grid-like cold water piping systems. On an existing system, a new section on standby will be filled with water from the system itself. The quality of this "filling" water does not always meet the quality criteria of make-up water. In particular, it may contain a large amount of settleable matter, bringing with it bacteria probably in variable concentrations. In the absence of appropriate management and conditioning, this new section will be filled with all the ingredients conducive to the corrosion processes induced by microorganisms (deposits, nutrients, bacteria involved) that play a part in the formation of protective tubercles.

### *9.3.4.2. Settleable matter content*

The particles in the cold water piping system's water originate either from the quality of the make-up water, or from unsuitable conditions initiated at design time (storage of steel tubes without protection), on priming (filling with poor quality water, lack of passivating leaching, prolonged shutdown without conditioning the water) and after the section concerned is brought into operation (unsuitable water treatment, repeated curative actions).

Depending on their densities, grain size and water velocity, the particles in the water can settle or be transported. The accumulation of various deposits (sediments, biofilm) in certain parts of the system contributes locally to the disappearance of the dissolved oxygen and can produce differential aeration couples. For particles exceeeding 1 µm in diameter, the formation of deposits in the pipes is put down to sedimentation. For smaller particles (< 1 µm), electric charges are responsible for keeping them suspended and the depositing of these particles is put down to captures by the wall during shocks [22, 27].

Parts that are lightly oxygenated under the deposits act as anodes and corrode, whereas zones that are more oxygenated act as cathodes and are thus protected [18].

When negative pressure occurs further to excess pressure caused by a water hammer, gases are released ($O_2$ and $CO_2$) and build up at the high points, thereby intensifying corrosion through the formation of piles of differential aeration [37].

### 9.3.4.3. Hydraulics

Most recommendations stress the importance of appropriate dimensioning of systems to guarantee turbulent states and thereby avert the build-up of deposits. An understanding of the method of operation of the cold water piping system and its technical constraints shows that the water regime is never established, that it is variable and can include periods of inevitable stagnation. Pipes are laid before they are connected to buildings and they are primed before they are brought into operation, which determines their energy consumption and in consequence the water circulation. Therefore a cold water piping system offers hydraulic conditions conducive to the settling of matter borne by the water, which is displaced as and when production needs evolve, thereby defining the different hydraulic configurations. Settling depends on the speed and density of the particles. One study has observed the influence of the water regime on the type of deposits formed and on the speed of corrosion in different pipes of an iced-water system [9]. We should point out that only the process is reproducible in the results presented. The identified critical speeds depend on the type of system and the type of particle.

For constantly low speeds or even nil speeds, the silting up rate is high. If no fresh water (and thus nutrients) is added, the speed of corrosion is slow (Fig. 9.12). These conditions can, for instance, be observed at the end of branches of the water system or on pipes awaiting connection to future customers. Renewal of the water subsequently accelerates corrosion.

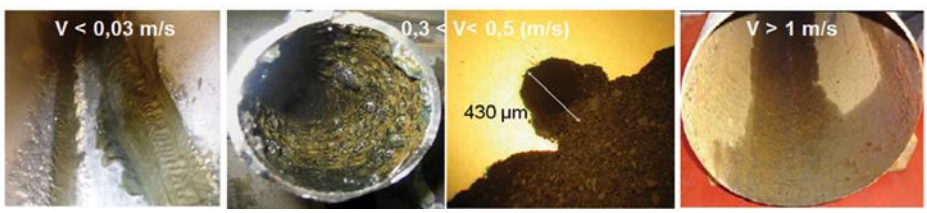


**Fig. 9.12.** – Influence of velocities on the type of deposits found in cold water piping systems.

In pipes where low velocity of flow is applied, there is less silt, and large tubercles that penetrate further are observed (Fig. 9.12). An examination of the general condition of the surfaces shows the presence of oxides and tubercles (with bases several cm in diameter) occupying 10 to 70% of the surface, depending on the sample taken. Under the pustules, through scanning electron microscopy, one observes wide cavities; numerous dimples line these cavities. The penetration observed is fairly deep (500 to 800 µm). These hydraulic configurations are observed for instance in the winter, when less cold water is used, or in zones on confluence in the cold water piping system, *i.e.,* in the zone between the inlet of cold water supplied by two different production sites.

A pipe whose flow velocity is greater than 1 m $s^{-1}$ does not present any pustules (Fig. 9.12). It is worth noting that low velocity of flow alone is not a sufficient risk factor increasing the likelihood of a process of corrosion being initiated by the microorganisms. The vast majority of pipes see periods of low speeds in winter, without the input of particles, certainly settling in the more sensitive zones. Similarly, water velocity alone is not a sufficient condition to identify sections of pipes presenting a high likelihood of corrosion induced by the microorganisms. Conditions conducive to incipient corrosion induced by microorganisms may be related to hydraulic configurations pre-dating the period of observation.

### 9.3.5. Corrosion risk management strategy

An understanding of the processes of corrosion induced by microorganisms immediately suggests the major risk factors are the hydraulics and the presence of settleable matter. However, it is virtually impossible to eliminate the hydraulics risk factor on this type of system, given the technical constraints.

The strategy, which is all the more complex as the system is extensive and grid-like, is thus underpinned by actions that limit the formation of deposits. Such actions implement different processes, depending on whether one is dealing with a new section or an existing system.

On an existing system, apart from anticorrosion and mineral dispersant processes, there are no effective chemical processes that prevent the formation of zones confined under deposits conducive to the development of the microorganisms involved in corrosion processes. The actions taken essentially concern the fight against moving deposits, whether or not they suspended. While processes that filter or capture these deposits are effective, most efforts concerns operating practices.

#### 9.3.5.1. Biocides

When bacteria are trapped in tubercles of corrosion under the metal, they are less accessible to biocides, be they oxidizing biocides consumed by organic matter and corrosion products [15], or non-oxidizing biocides.

Consequently, the use of biocides is only relevant when filling a pipe with poor quality water, long before tubercles begin to form. This therefore only concerns new sections of pipe when they are filled with water. Disinfection, generally done by injecting a non-oxidizing biocide, must be maintained for the necessary length of time.

Furthermore, we should point out that the pipes awaiting laying are plugged at their ends to limit as much as possible the length of chemical leaching and passivating procedures. These specific operations consist in eliminating the by-products of oxidation formed during the waiting period, which are liable to be released again when the pipes are conditioned. In addition, the internal surfaces of the pipes undergo a passivating stage following the deoxidation stage. The length of these operations is defined by on-site performance indicators.

The conditioning of the water in the section will then depend on the length of stagnation between priming and entry into service.

On an existing system affected by the development of bacteria involved in the corrosion process, generally the actions are mainly curative, involving pipe replacements.

#### *9.3.5.2. Surface-active agents*

As the danger factor behind the target risk is located at the interface between the material and the biofilm, the presence of a biodispersant combined with disinfection is only effective when filling a new section with poor quality water, or when restarting a circuit after a technical shutdown of the installation before it is fully drained, before reconditioning, to eliminate the suspended matter of the deposits.

The management of risk factors, leading to the danger of corrosion induced by microorganisms, therefore varies greatly depending on whether one is dealing with an existing cold water piping system or an extension to the system. Chemical processes are only effective before the bacteria irreversibly "takes root" under the deposits. When the system is contaminated, only appropriate operating practices can reduce piercing phenomena.

## 9.4. Conclusion

Biofilm is at the root of different problems in water systems, either because it generates a health hazard by releasing potentially pathogenic bacteria into circulating water, or because it offers zones conducive to the development of microorganisms that induce or aggravate a process of corrosion through pitting under the deposit at the interface with the material.

Normal conditions of use of a circuit sometimes favour the appearance of a biofilm-related hazard. That is why the approach to managing this risk must absolutely factor in technical requirements in order for preventive action to be effective and limit the implementation of curative action.

While the fight against the *Legionella pneumophila* risk amounts to fighting biofilm, the fight against bacteria involved in corrosion processes relies on preventive actions at the system design stage.

Beyond application of regulatory requirements alone (*Legionella pneumophila* risk), the search for a maximum reduction of a biofilm-induced risk often presupposes serious questioning of operating practices or habits and a proper understanding of the mechanisms leading to the appearance of the hazard at the root of the risk, as well as sound knowledge of the tools available (including treatment processes). Poor process implementing conditions, or the misuse of curative treatments, increase the risk in most cases.

That is why the management of an industrial water system is not only a matter for specialists. It must concern and involve all site operators and managers.

## References

[1] Angell P., Urbanic K. (2000) "Sulphate reducing bacterial activity as a parameter to predict localized corrosion of stainless alloys." Corrosion Science, 42, 897-912.

[2] Barbarry J.M., Fields B.S., Feeley J.C., Gorman W.G., Martini W.T. (1986) "Isolation of protozoa from water associated with a legionellosis outbreak and demonstration of intracellular multiplication of *Legionella pneumophila*." Appl. Environ. Microbiol., 51, 422-424.

[3] Berk S.G., Ting R.S., Turner G.W., Ashburn R.J. (1998) "Production of respirable vesicles containing live *Legionella pneumophila* cells by two *Acanthamoeba* spp." Appl. Environ. Microbiol., 64(1), 279-286.

[4] Blériot P., Bour Beucler V. (2014) "Retour d'expérience sur le traitement inhibiteur de corrosion des circuits de refroidissement : influence des modifications de la rubrique 2921 sur les vitesses de corrosion." Journées Scientifiques et Techniques du Centre Français de l'Anticorrosion (CEFRACOR), Paris, France.

[5] Brehm U., Gorbushina A., Mottershead D. (2005) "The role of microorganisms and biofilms in the breakdown and dissolution of quartz and glass." Palaeogeography, Palaeoclimatology, Palaeoecology, 219, 117-129.

[6] Chantereau J., Bouffard A.-M. (1980) "Corrosion bactérienne : Bactéries de la corrosion." Technique et Documentation Lavoisier, ISBN 978-2-85206-044-9, Paris, France, 262 p.

[7] Dagbert C. (2009) "Biocorrosion – Techniques d'études et d'évaluation, Techniques Ingénieur." Techniques de l'ingénieur, Matériaux, Corrosion Vieillissement, vol. COR1, COR130, http://www.techniques-ingenieur.fr.

[8] Delbes J., Vadrot A. (2000) "Réseaux de froid urbain – Production et stockage du froid." Techniques de l'Ingénieur, BE9321, 16 p., http://www.techniques-ingenieur.fr.

[9] Deumier A., Merchat M. (2006) "Recherche des facteurs de risque de biocorrosion dans un dans un réseau d'eau glacée." Climespace, internal report.

[10] Donlan R.M. (2002) "Biofilms: Microbial Life on Surfaces." Emerg. Infect. Dis., 8(9), 881-890.

[11] Féron D., Compère C., Dupont I., Magot M. (2002) "Biodéterioration des matériaux métalliques ou biocorrosion." In: Corrosion des métaux et alliages, Béranger G. and Bazille H. Eds, Lavoisier-Hermès Sciences, Paris, France, ISBN 2-7462-0466-5, 385-405.

[12] Flemming H.C., Wingender J., Griebe T., Mayer C. (2000) "Physicochemical properties of biofilms." In: Recent advances in their study and control, Evans L.V. Ed, Harwood Academic Publishers, Amsterdam, The Netherlands, 19-34.

[13] Forêt C. (2006) "Maintien de la qualité des eaux dans les réseaux par des procédés innovants de traitement et de détection des biofilms." PhD thesis, université de Poitiers, Poitiers, France.

[14] Forêt C., Merlet N., Tribollet B., Chaussec G., Cauvin F., Legube B. (2006) "Détermination électrochimique de l'épaisseur des biofilms dans les circuits d'eau." Mat. & Tech., 94, 467-476.
[15] Frateur I. (1997) "Incidence de la corrosion des matériaux ferreux sur la demande en chlore libre en réseaux de distribution d'eau potable." PhD thesis, université de Paris VI, Paris, France, 204 p.
[16] Fritz Feugeas F. (1998) "Caractérisation des biofilms formés sur différents aciers plongés dans la nappe phréatique. Étude de leur influence sur la corrosion des aciers." PhD thesis, université Louis Pasteur, Strasbourg, France, 179 p.
[17] Garduno E., Faulkner G., Ortiz-Jimenez M.A., Berk S., Garduno R.A. (2005) "Interaction with ciliate *Tetrahymena* sp. may predispose *Legionella pneumophila* to infect human cells." In: 6th International Conference on *Legionella*, Chicago, Illinois, USA, October 16-20 2005.
[18] Gueuné H. (2013) "Influence des microorganismes acidogènes sur la corrosion d'une infrastructure en acier au carbone en milieu marin à faible marnage." Mat. & Tech., 101, 5-6.
[19] MEDDE (2006) "Guide Traitements pour la gestion du risque de prolifération des légionelles dans les installations de refroidissement." https://www.researchgate.net/publication/282185138_Guide_traitement_des_circuits_tour_aerorefrigerantes.
[20] Guide Syprodeau des professionnels de l'eau (2011) "Traitement des eaux et gestion du risque de prolifération des légionelles dans les installations de refroidissement avec tour aéroréfrigérante." http://www.syprodeau.org/Evenements-et-Publications/Images/Guide-Syprodeau-des-professionnels-de-l-eau.
[21] Hiernaux P. (2005) "Contribution de la fraction minérale des eaux au développement et à la structure des biofilms : apport des méthodes microscopiques et spectroscopiques." PhD thesis, université de Poitiers, Poitiers France.
[22] Hull M., Kitchener J.A. (1969) "Interaction of Spherical Colloidal Particles with Planar Surfaces." Transactions of the Faraday Society, 65, 3093-3104.
[23] Jorand F., Zegeye A., Ghanbaja J., Abdelmoula M. (2011) "The formation of green rust induced by tropical river biofilm components." Sci. Total Environ., 409, 2586-2596.
[24] Lédion J., Forêt C. (2012) "Maîtrise du développement de biofilm dans des cuves de stockage d'eau alimentaire des générateurs de vapeur, Matériaux, Corrosion, Qualité des eaux, Pérennité des réseaux." Colloque de l'Association Scientifique Européenne pour L'Eau et la Santé (ASEES) et le Centre Français de l'Anticorrosion (CEFRACOR), Paris, France.
[25] Lédion J., Néel L. (2014) "L'acier galvanisé dans les circuits d'eaux : règles pour assurer la pérennité des installations." Journées Information Eaux, Poitiers, France.
[26] Leroy P. (1993) "Influence des traitements de désinfection sur l'évolution de la corrosion des réseaux en acier galvanisé, Le zinc et l'Anticorrosion :

Essais et performances." Centre Français de l'Anticorrosion (CEFRACOR) et le Centre du zinc, CEREC – St-Ouen, Ed. de Physique, chapter 4, 234 p.
[27] Marshall J.K., Kitchener J.A. (1966) "The deposition of colloidal particles on smooth solids." Journal of Colloid and Interface Science, 22, 342-351.
[28] Mathieu L. *et al.* (2009) "Reversible shift in the α-, β- and γ-proteobacteria populations of drinking water biofilms during discontinuous chlorination." Water Research, 43, 3375-3386.
[29] Melchers R.E., Wells T. (2006) "Models for the anaerobic phases of marine immersion corrosion." Corrosion Science, 48, 1791-1811.
[30] Merchat M., Ricordel F. (2011) "La gestion du risque légionelle dans les systèmes de refroidissement, Risques toxique et sanitaire." Print Industrie, la revue du syndicat national des ingénieurs de l'industrie et des mines, France, 48, 131-141.
[31] Moran F. (2002) "Traitement des eaux : chauffage – climatisation – installation sanitaires." ISBN: 2-86-243-059-5, 134 p.
[32] Pineau S. (2006) "Interactions entre les communautés bactériennes et les processus de corrosion accélérée des structures métalliques en environnement marin." PhD thesis, université de technologie de Compiègne, Compiègne, France.
[33] Refait P. *et al.* (2013) "Electrochemical formation and transformation of corrosion products on carbon steel under cathodic protection in seawater." Corrosion Sciences, 71, 32-36.
[34] Squinazi F. (2006) "Biofilm et matériaux des réseaux intérieurs de distribution d'eau, de la maîtrise des réseaux à la qualité de l'eau." Laboratoire d'hygiène de la ville de Paris, France, 52-63.
[35] Surman S.B., Morton L.H.G., Skinner A., Fitzgeorge R.B., Keevil C.W. (1999) "Growth of *Legionella pneumophila* is not dependent on intracellular replication." Royal Society of Chemistry, 242, 160-170.
[36] Videla H.A., Herera L.K. (2009) "Understanding microbial inhibition of corrosion. A comprehensive overview." International Biodeterioration & Biodegradation, 63(7), 896-900.
[37] Vrignaud E. (1998) "Le monde enterré des canalisations publiques." Mémoire Diplôme Universitaire "Eau et Environnement", Direction Études permanentes, université de Picardie Jules Verne, Saint-Quentin, France, 53 p. + annexes.

# Theme 3
# Biocorrosion of metallic materials

Chapter 10 is devoted to the electrochemical methods for biocorrosion studies. Two examples are presented; both concern the effect of adsorbed biomolecules on the electrochemical behaviour of metallic materials in sea water.

The iron-sulphur interactions and the role played by iron sulphides on the corrosion processes are considered in the chapter 11. Likewise, the reader will find two examples developed, one in sea water and the other one in soil. Some similarities in the proposed mechanisms are to be noted, in spite of the large difference between the media under investigation.

The reader must refer to chapter 16: "Choice of metallic materials and biocorrosion" which also deals with corrosion induced by microorganisms.

Some general remarks on electrochemical methods or on surface analysis are developed in the book corresponding to the previous summer school on the biodeterioration of materials: Fritz-Feugeas F., Cornet A. and Tribollet B., *Biodétérioration des matériaux. Action des microorganismes, de l'échelle nanométrique à l'échelle macroscopique*, Technosup collection, Ellipses, Paris, France (2008).

# 10 Electrochemical methods applied to biocorrosion

**Isabelle Frateur**

## 10.1. Introduction

Microorganisms existing in all non-sterile environments, as sea water, attach themselves to solid surfaces and form biofilm leading to biofouling of these surfaces. The first step in the formation of biofilms in aqueous solution is the adsorption of biomolecules, especially proteins, present in the environment. In the case of metal materials, a possible harmful effect of biofilms is corrosion induced by microorganisms (MIC) or biocorrosion. Instead, some biofilms can slow down corrosion and, in this case, one speaks of microorganism induced corrosion inhibition (MICI).

Microorganisms are known to produce a large number of macromolecules (polysaccharides, proteins, lipids, DNA, humic substances and others), referred as extracellular polymeric substances (EPS), with various chemical and functional properties [1]. These exopolymers play a fundamental role in the different stages of biofilm formation, maturation and maintenance [2]. The EPS are organised around the cell in a particular way. The capsular EPS, mainly of polysaccharide nature, form capsules or sheaths associated closely with cell surfaces, sometimes by covalent bonds and are clearly delineated around the cell [3-5]. Subsequently, these well-differentiated capsules will be named TB EPS (for Tightly Bound EPS). Moreover, secretion of viscous polymers, weakly associated with the cell or free in the medium is called "slime" and is the matrix of the biofilm. Subsequently, these EPS non (or little) differentiated will be named LB EPS (for Loosely Bound EPS). Some authors also use planktonic or free EPS to name this layer spread of polymers [4, 5].

The overall objective of this work was to study the influence of biomolecules adsorbed (EPS from two marine bacterial strains: *Pseudomonas* sp. NCIMB 2021 and *Desulfovibrio alaskensis* AL1) on the electrochemical behaviour of metallic materials (70Cu-30Ni and mild steel alloy) in a sea water environment [6, 7]. To do this, electrochemical measurements (monitoring of the corrosion potential $E_{corr}$ in function of the immersion time, curves of polarisation, electrochemical impedance spectroscopy) were performed in the early stages of formation of the metal oxide layers (1 to 2 hours immersion). In particular, the objective was to analyse the electrochemical impedance data obtained at $E_{corr}$.

The results presented below are part of the European project BIOCOR ITN (FP7-PEOPLE-ITN-2008).

## 10.2. Influence of EPS obtained from *Pseudomonas* sp. NCIMB 2021 on the corrosion behaviour of 70Cu-30Ni alloy in sea water

Power plants require cooling circuits with seawater or fresh water as the cooling agent. In sea water, copper and copper alloys are commonly used in condensers and heat exchangers due to their high thermal and electrical conductivity, both excellent mechanical workability and resistance to corrosion. However, these copper alloys are vulnerable to biocorrosion.

*Pseudomonas* are known to produce EPS which play a mediator role in cell adhesion on solid surfaces and which contribute to the mechanical stability of biofilms, forming a three-dimensional polymeric network [3]. These bacterial species have been identified in condensers [8] and it has been shown that they accelerated the corrosion of copper and copper alloys [9].

In cooling circuits, the water is usually circulating but, frequently, plant outages cause provisional stagnant condition that can persist for hours or, at worst, for days. Static conditions are of particular concern for corrosion risk, especially at the beginning of plant operation.

### *10.2.1. Experimental methods*

#### *10.2.1.1. Metallic material, electrolyte*

The material under study was 70Cu-30Ni alloy (Cu 68.5, Ni 30, Mn 0.8, Fe 0.7 wt.%). Its electrochemical behaviour was studied in aerated artificial seawater (ASW; composition (g $L^{-1}$): NaCl (24.615), KCl (0.783), $Na_2SO_4$ (4.105), $MgCl_2(H_2O)_6$ (11.060), $CaCl_2$ (1.160), $NaHCO_3$ (0.201); pH = 8.0).

The samples provided by RSE S.p.A. were disks cut from real new condenser tubes and then flattened. The geometrical surface area exposed to the solution was 0.45 $cm^2$. Before electrochemical measurements, samples were mechanically polished with SiC papers down to grade 1200, then degreased in an ultrasonic bath three times in acetone for 5 minutes, once in ethanol for 10 minutes, and once again in ultra-pure water for 10 minutes, dried under an argon flow and finally exposed to UV for 15 minutes (sample sterilization).

#### *10.2.1.2. Biomolecules*

In this work, the effect of tightly bound (TB) and loosely bound (LB) extracellular polymeric substances (EPS) secreted by *Pseudomonas* sp. NCIMB 2021 marine

strain on the corrosion behaviour of 70Cu-30Ni alloy in artificial sea water was studied.

The EPS extraction procedure, which was developed at the Biofilm Centre, University of Duisburg-Essen, Germany, is illustrated in figure 10.1 [7, 10].

The bulk composition of EPS from *Pseudomonas* sp. NCIMB 2021, deduced from colorimetric analyses, is shown in table 10.1 [6, 10].

**Table 10.1.** – Composition of EPS extracted from *Pseudomonas* sp. NCIMB 2021 marine strain and of the negative control (sterile growth medium).

| Composition (mg $L^{-1}$) | Proteins | Sugars | DNA | Uronic acids |
|---|---|---|---|---|
| Negative control | 9.3 | 89.7 | 0.4 | 3.7 |
| Tightly bound EPS | 4187.6 | 640.1 | 1.0 | 25.0 |
| Loosely bound EPS | 20.6 | 50.0 | 0.3 | 4.0 |

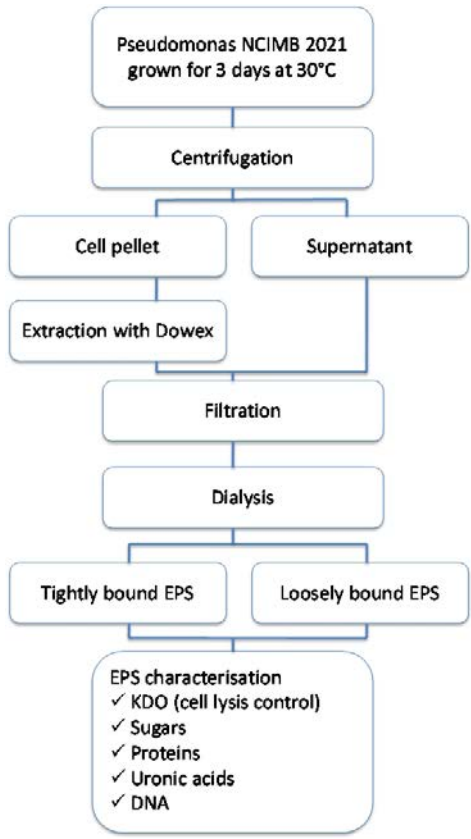


**Fig. 10.1.** – Schematic drawing of the EPS extraction procedure (from [7, 10]).

The KDO (2-keto-3-deoxyoctanate) concentration indicates that cell lysis level in extracted EPS is less than 1%. The composition of the negative control (sterile growth medium) is also given for comparison (Marine Broth 2216; 37.4 g $L^{-1}$). In this table, proteins appear to be the main components of TB EPS, whereas sugars seem to be dominant in "slime" (LB EPS) and in the negative control. Furthermore, it was shown that the molecular weight of proteins in the TB and LB EPS are between 25 and 100 kDa (kg $mol^{-1}$).

As comparison, the effect of bovine serum albumin (BSA) on the corrosion behaviour of 70Cu-30Ni alloy in seawater was evaluated. BSA is a model protein, with a molecular weight of ~ 66 kDa (*i.e.* 66 kg $mol^{-1}$), which is often used to study protein-surface interactions. The concentration of BSA (~99% purity (Fraction V); Sigma Aldrich) in solution was 20 mg $L^{-1}$.

For electrochemical measurements and surface analysis, ASW solutions were prepared with the secreted TB and LB EPS, keeping the same protein concentration as for the BSA-containing solution (20 mg $L^{-1}$), in order to compare the results with those obtained in the presence of the model protein. Thus, LB EPS aliquots were used as isolated *i.e.,* were not diluted (protein concentration after isolation: 20.6 mg $L^{-1}$), whereas TB EPS aliquots were diluted about 200 times in ASW (protein concentration after extraction: ~ 4190 mg $L^{-1}$).

#### *10.2.1.3. Electrochemical measurements*

The electrochemical measurements were performed with a three-electrode cell and an EC6Lab SP-200 from BioLogic. The working electrode was the 70Cu-30Ni alloy (disk samples), the counter-electrode was a platinum wire and the reference electrode was a saturated calomel electrode (SCE; 0.245 V *vs.* SHE), the solution volume was about 0.1 L. Experiments were carried out at room temperature and in stagnant conditions (static working electrode and solution). Electrochemical impedance diagrams were plotted at $E_{corr}$ after 1 h of immersion, with a frequency domain ranging from $10^5$ Hz to $10^{-3}$ Hz, 7 points per decade, and an amplitude of 10 mV peak-to-peak.

### *10.2.2. Results: electrochemical measurements*

The different $E_{corr}$ steady-state values after 1 h of immersion without (and with) biomolecules are shown in table 10.2. The corrosion potential is similar for the three biomolecules and is more cathodic in the absence of biomolecules (difference of ~30 mV).

The cathodic polarisation curves of 70Cu-30Ni alloy recorded in the different solutions are presented in figure 10.2a. In all cases, except with LB EPS, two plateaus can be observed: a short plateau close to $E_{corr}$ that illustrates the first step of dissolved oxygen reduction (transfer of 2 electrons) and a wide plateau for potentials ranging from –0.40 to –1.00 V *vs.* SCE corresponding to the second step of $O_2$ reduction (transfer of 4 electrons). It is well-known that this reaction is limited by mass transport. Only the second plateau is clearly visible in the presence of LB EPS. Effect of biomolecules on the cathodic behaviour of the alloy can be observed. Indeed, the presence of biomolecules induced current

densities more weak in the field of potential range corresponding to the second plateau (current plateau up to 3.3 times lower).

**Table 10.2.** – Corrosion potential values for 70Cu-30Ni alloy after 1 h of immersion in static aerated ASW without and with biomolecules (protein concentration: 20 mg $L^{-1}$).

| | $E_{corr}$ (V *vs* SCE) |
|---|---|
| **ASW** | –0.230 ± 0.009 |
| **ASW + BSA** | –0.203 ± 0.005 |
| **ASW + TB EPS** | –0.199 ± 0.005 |
| **ASW + LB EPS** | –0.203 ± 0.007 |

The anodic polarisation curves of 70Cu-30Ni alloy in the same solutions are presented in figure 10.2b. In absence of biomolecules, the curve can be described by four parts: 1) the current density increase up to ~ 0.25 V *vs* SCE, 2) fall of the current density, 3) pseudo-plateau corresponding to a very high current density (~ 2.5 mA $cm^{-2}$ at ~ 0.4 V *vs* SCE), 4) further increase of the current density beyond 0.5 V *vs* SCE. The presence of biomolecules induced current densities lower for potential lower than 0.05 V *vs* SCE. Beyond 0.05 V *vs* SCE, all curves have the same shape and current densities are similar except in the presence of LB EPS (current densities lower by up to 0.25 V *vs* SCE and observable peaks between 0.25 and 0.5 V *vs* SCE).

An effect of the rotation speed on the anodic polarisation curves plotted with a rotating ring electrode was evidenced below 0.3 V *vs* SCE (results not shown here) [6]. However, the curves exhibit no anodic plateau, unlike pure copper in acidic and neutral chloride solution for which a limiting-current region can be observed around 0 V *vs* SCE [11, 12]. These results show partial mass transport limitation *i.e.,* mixed kinetics for the anodic reaction(s) at not too high anodic potential (*viz.,* below 0.3 V *vs* SCE).

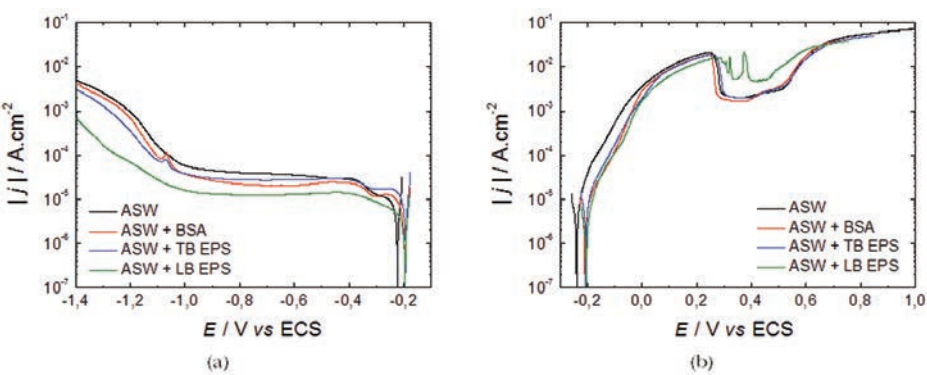


**Fig. 10.2.** – (a) Cathodic and (b) anodic polarisation curves of 70Cu-30Ni after 1 h immersion at $E_{corr}$ in static aerated ASW, in the absence and in the presence of biomolecules (BSA, TB EPS, LB EPS) with a protein concentration of 20 mg $L^{-1}$. Scan rate: 0.5 mV $s^{-1}$.

The impedance diagrams plotted after 1 hour immersion at $E_{corr}$ in static ASW without (and with) biomolecules are shown in figure 10.3. The shape is the same in all cases and two loops can be observed: one depressed high frequency (HF) loop and one ill-defined low frequency (LF) loop. The size of the HF loop in the presence of TB EPS is the same as that without biomolecules. However, it is slightly higher in the presence of BSA, and much higher in the presence of LB EPS.

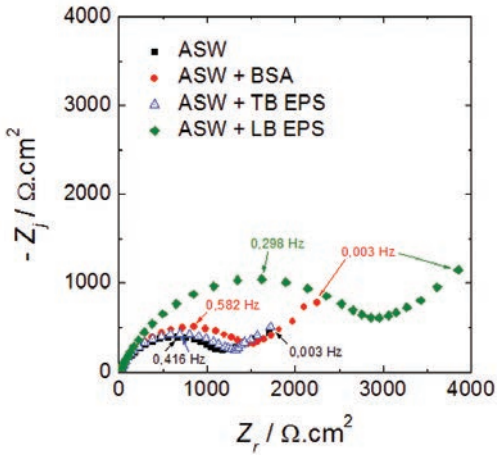


**FIG. 10.3.** – Experimental impedance diagrams in the complex plane (Nyquist diagrams) of 70Cu-30Ni after 1 h immersion at $E_{corr}$ in static aerated ASW, in the absence and in the presence of biomolecules (BSA, TB EPS, LB EPS) with a protein concentration of 20 mg $L^{-1}$.

### 10.2.3. Corrosion mechanism

The anodic dissolution of pure copper in acidic and neutral chloride media has been extensively studied in the literature. The final model in agreement with all published experimental data is [11-16]:

$$Cu + Cl^- \Leftrightarrow CuCl + e^- \quad (10.1)$$

$$CuCl + Cl^- \Leftrightarrow CuCl_2^- \quad (10.2)$$

In this mechanism, the soluble cuprous complex $CuCl_2^-$ is the diffusing species and the insoluble adsorbed intermediate CuCl is the blocking species (surface coverage: $\gamma$), which is electrochemically formed in a first step (Eq. (10.1)) and chemically dissolved in a second step (Eq. (10.2)).

From that mechanism shown for pure copper dissolution in chloride media at low anodic potential and in order to take into account the presence of an oxide layer as shown by surface analysis [17, 18, 10], a modified mechanism

can be drawn for the anodic partial reaction of 70Cu-30Ni alloy at $E_{corr}$ in ASW without and with biomolecules:

$$Cu \rightarrow Cu^{+} + e^{-} \quad \text{oxidation at the alloy/oxide interface} \quad (10.3)$$

$$Cu^{+}_{alloy/oxide} \rightarrow Cu^{+}_{oxide/solution} \quad \text{solid-state mass transport} \quad (10.4)$$

$$Cu^{+} + Cl^{-} \Leftrightarrow Cl_{ads} - Cu_{Cu_2O} \quad \text{adsorption at the oxide/solution interface} \quad (10.5)$$

$$Cl_{ads} - Cu_{Cu_2O} + Cl^{-} \Leftrightarrow CuCl_2^{-} \quad \text{dissolution at the oxide/solution interface} \quad (10.6)$$

This mechanism involves four steps:

1) oxidation of Cu as $Cu^{+}$ at the alloy/oxide interface;
2) mass transport of $Cu^{+}$ by diffusion and migration in the solid phase from the alloy/oxide interface to the oxide/solution interface;
3) adsorption of chloride on a $Cu^{+}$ surface site of the $Cu_2O$ oxide at the oxide/solution interface;
4) dissolution of copper as $CuCl_2^{-}$ at the oxide/solution interface, followed by mass transport of $CuCl_2^{-}$ by diffusion in the liquid phase from the oxide/solution interface to the bulk solution.

In aerated solution, the cathodic partial reaction is the reduction of dissolved oxygen that takes place at the oxide/solution interface. Then, both anodic and cathodic reactions are mass transport limited.

### 10.2.4. Impedance model

At $E_{corr}$, the anodic and cathodic currents have the same magnitude and the net current is equal to zero. By principles of summation of currents, the Faradaic anodic impedance $Z_F^a$ and the cathodic impedance $Z_F^c$ must be in parallel and the usual electric equivalent circuit at $E_{corr}$ is given in figure 10.4 with $C_{dc}$ the double layer capacitance.

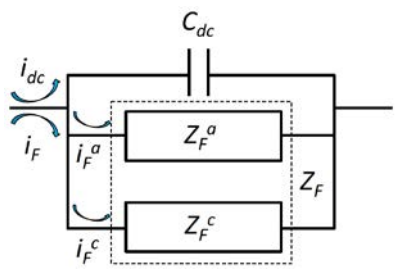


**Fig. 10.4.** – Equivalent electrical circuit at $E_{corr}$.

For the 70Cu-30Ni alloy, the polarization curves show that both the anodic and the cathodic reactions are affected by mass transport. Therefore, the anodic

Faradaic impedance can be depicted by a charge transfer resistance ($R_t^a$) in series with an impedance that illustrates $Cu^+$ and/or $CuCl_2^-$ mass transport and partial blocking effect by adsorbed species, such as CuCl ($Z_{\theta,D}{}^a$); whereas the cathodic impedance can be depicted by a charge transfer resistance ($R_t^c$) in series with an impedance that illustrates $O_2$ mass transport ($Z_D{}^c$). As the impedance response for electrochemical systems often reflects a distribution of reactivity that is commonly represented in equivalent electrical circuits as a constant-phase element (CPE), $C_{dl}$ is replaced here by $CPE_{dl}$ which is a constant phase element related to the double layer. The CPE impedance is expressed in terms of model parameters α and $Q$ as:

$$Z_{CPE}(\omega) = \frac{1}{Q(j\omega)^{\alpha}} \tag{10.7}$$

The two parameters $Q$ and α are independent of the frequency. When α = 1, the parameter $Q$ has units of capacitance (F $cm^{-2}$); otherwise, $Q$ has units of $\Omega^{-1}$ $cm^{-2}$ $s^{\alpha}$ or F $cm^{-2}$ $s^{(\alpha-1)}$ and α is dimensionless. Thus, the general impedance model for 70Cu-30Ni alloy in seawater, without and with biomolecules, is illustrated in figure 10.5a, where $R_e$ is the electrolyte resistance [18].

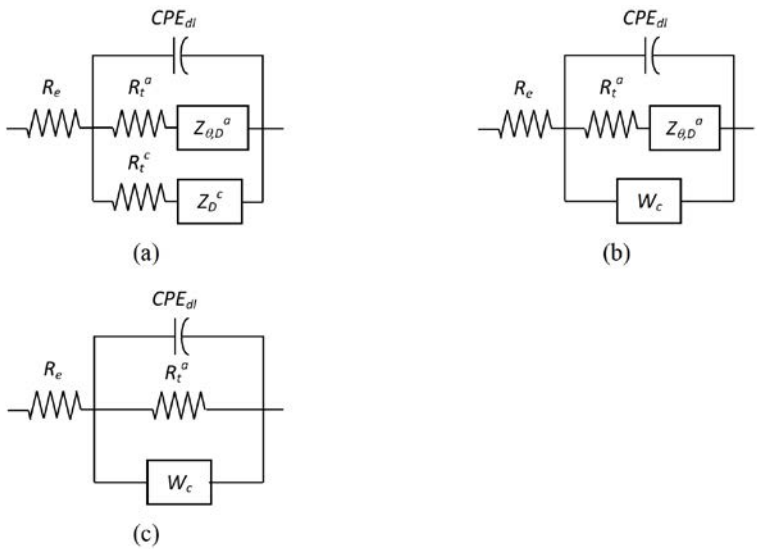


**FIG. 10.5.** – Equivalent electrical circuits to model the 70Cu-30Ni/ASW system, without (and with) biomolecules (BSA, TB EPS, LB EPS): (a) general circuit, (b) simplified circuit taking into account experimental cathodic polarization curves, and (c) circuit used to analyse the HF loop of experimental impedance diagrams.

The cathodic polarization curves show a first current plateau for the reduction of dissolved oxygen (transfer of 2 electrons) close to $E_{corr}$. If it is assumed that this plateau can be extrapolated down to $E_{corr}$ *i.e.* pure mass transport

limitation for the cathodic partial reaction at $E_{corr}$, then $R_t^c$ can be neglected and the cathodic mass transport impedance is a Warburg impedance ($W_c$) given by:

$$Z_{W_c} = 1/\left(k_c\sqrt{j\omega}\right) \tag{10.8}$$

with $k_c$ expressed in $s^{0.5}\ \Omega^{-1}\ cm^{-2}$. Taking into account experimental cathodic polarization curves, the 70Cu-30Ni/ASW system without and with biomolecules can be modelled by the simplified circuit presented in figure 10.5b [18].

In conclusion, the HF loop of the experimental impedance diagrams corresponds to the $CPE_{dl}//R_t^a//W_c$ equivalent circuit (Fig. 10.5c) and illustrates mainly the anodic charge transfer (diameter equal to $R_t^a$), and its depressed shape is partly due to the CPE and partly due to the cathodic Warburg impedance in parallel. Whereas the LF loop ($Z_{0,D}{}^a$) is related to the anodic mass transport and partial blocking effect by adsorbed species as CuCl.

The circuits of figures 10.5a and 10.5b take into account the presence of an oxide layer, as shown by surface analysis, through $Z_{0,D}{}^a$ that partly illustrates $Cu^+$ mass transport within that layer.

As the LF loop of impedance diagrams is not well defined (described only by a few points in figure 10.6), the single HF loop was analysed by regression of the equivalent circuit presented in figure 10.5c, using Simad® software developed at LISE. As shown in figure 10.6, the fit is good in all cases. The regression results are presented in table 10.3. The experimental frequency ranges taken into account for the regression are also indicated in table 10.3, but the fitted curves in figure 10.6 are shown in the whole frequency range (0.003 Hz – 100 kHz), with parameters values corresponding to those given in table 10.3.

If the CPE behaviour is assumed to be associated with surface distributed time constants for charge-transfer reactions (time-constant distribution along the electrode surface), then it is possible to apply the equation derived by Brug *et al.* to calculate the effective capacitance associated with the CPE [19, 20]:

$$C_{eff} = Q^{1/\alpha}\left(R_e{}^{-1} + R_t^{a\,-1}\right)^{(\alpha-1)/\alpha} \tag{10.9}$$

**Table 10.3.** – Experimental frequency range taken into account for the regression, parameters values (electrolyte resistance $R_e$, anodic charge transfer resistance $R_t^a$, constant of the cathodic Warburg impedance $k_c$, and CPE parameters α and $Q$) obtained from the regression of the equivalent circuit presented in figure 10.5c to the HF experimental impedance data shown in figure 10.3, and effective capacitance $C_{eff}$ associated with the CPE calculated from equation (10.9).

| | Frequency range (Hz) | $R_e$ ($\Omega\ cm^2$) | $R_t^a$ ($\Omega\ cm^2$) | $k_c$ ($s^{0.5}\ \Omega^{-1}\ cm^{-2}$) | α | $Q$ ($F\ cm^{-2}\ s^{(\alpha-1)}$) | $C_{eff}$ ($\mu F\ cm^{-2}$) |
|---|---|---|---|---|---|---|---|
| **ASW** | $10^5$-5.6 $10^{-2}$ | 12 | 1390 | 2.5 $10^{-4}$ | 0.78 | 1.99 $10^{-4}$ | 37 |
| **ASW + BSA** | $10^5$-1.08 $10^{-1}$ | 12 | 1690 | 1.2 $10^{-4}$ | 0.76 | 2.03 $10^{-4}$ | 30 |
| **ASW + TB EPS** | $10^5$-1.08 $10^{-1}$ | 12 | 1480 | 2.1 $10^{-4}$ | 0.84 | 1.33 $10^{-4}$ | 39 |
| **ASW + LB EPS** | $10^5$-7.8 $10^{-2}$ | 14 | 3530 | 1.1 $10^{-4}$ | 0.82 | 1.13 $10^{-4}$ | 27 |

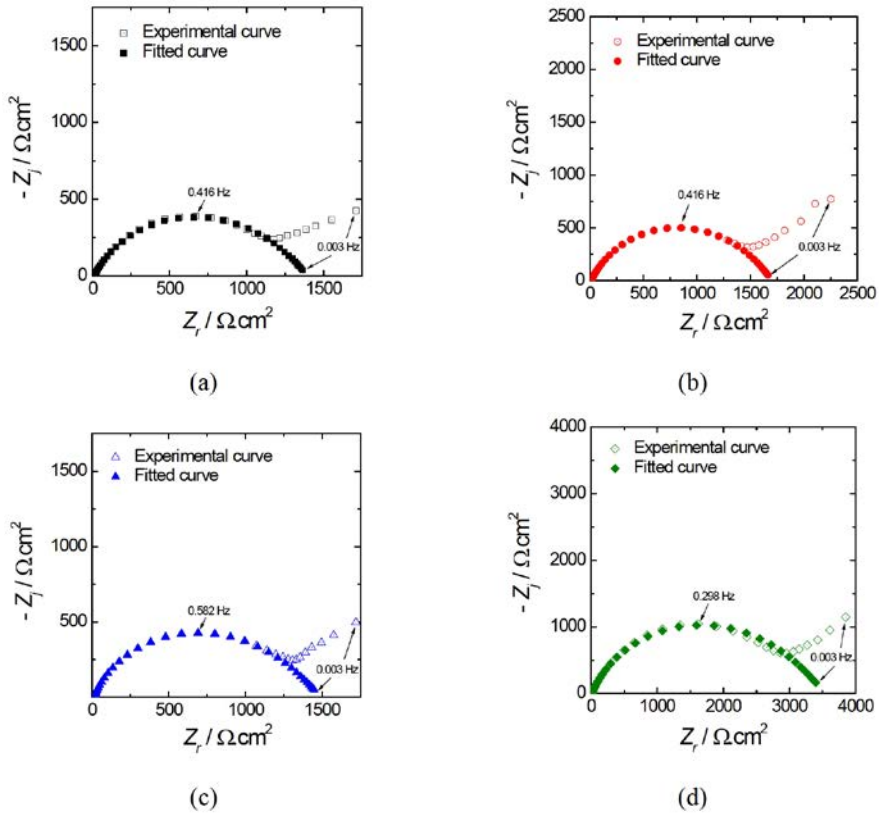


**FIG. 10.6.** – High frequency loops of Nyquist diagrams obtained for 70Cu-30Ni at $E_{corr}$ after 1 hour immersion in static aerated ASW (a) without biomolecules, (b) with BSA (20 mg $L^{-1}$), (c) with TB EPS (protein concentration: 20 mg $L^{-1}$) and (d) with LB EPS (protein concentration: 20 mg $L^{-1}$). Experimental curves and fit of the impedance model presented in figure 10.5c to the HF data. Same data as in figure 10.3.

The capacitance values calculated from the impedance diagrams shown in figure 10.3, taking for $R_e$ and $R_t^a$ the values extracted from the regression procedure (Table 10.3), are also given in table 10.3. These capacitance values, of the order of several tens of μF $cm^{-2}$, are typical of those for a double layer capacitance, which validates the equivalent circuits proposed in figure 10.5. Therefore, the HF loop illustrates mainly the anodic charge transfer and its diameter is equal to $R_t^a$.

Compared to the value obtained in static ASW without biomolecules, $R_t^a$ is ~ 22% higher in the presence of BSA, 6.5% higher in the presence of TB EPS, and ~ 150% higher in the presence of LB EPS.

### 10.2.5. Results: corrosion current

Under assumption of Tafel kinetics (pure kinetic control) for the anodic partial reaction, the corrosion current density $j_{corr}$ is related to $R_t^a$ by [21]:

$$j_{corr} = \frac{1}{B \times R_t^a} = \frac{b_a}{2.303} \times \frac{1}{R_t^a} \tag{10.10}$$

with

$$B = \frac{\alpha nF}{RT} \geq 0 \tag{10.11}$$

Where $n$ is the number of transferred electrons ($n = 1$ in equation (10.3)), $\alpha$ the symmetry factor or coefficient of charge transfer and $b_a$ the anodic Tafel constant (in V/decade). A corrosion rate (in µm per year, for example) can be determined from $j_{corr}$ and the proportionality coefficient given by the Faraday law.

In table 10.4, the $j_{corr}$ values were calculated by application of equation (10.10), with $n = 1$ and $\alpha = 0.5$, which correspond to a $b_a$ value of about 120 mV/dec ($b_a = 2.303/B$ with T = 293 K).

The corrosion current density of 70Cu-30Ni alloy after 1 h of immersion in static ASW is slightly lower with BSA and similar with TB EPS compared to that estimated in the absence of biomolecules. A significant decrease of $j_{corr}$ value is observed in the presence of LB EPS. Therefore, these results show a clear corrosion inhibition effect for LB EPS, a small beneficial effect for BSA and no detrimental effect for TB EPS.

**Table 10.4.** – Corrosion current density values obtained from $R_t^a$, by application of equation (10.10) with $n = 1$ and $\alpha = 0.5$ ($b_a \approx 120$ mV/dec).

| | $R_t^a$ (Ω cm²) | $j_{corr}$ (µA cm$^{-2}$) |
|---|---|---|
| **ASW** | 1390 | 36 |
| **ASW + BSA** | 1690 | 30 |
| **ASW + TB EPS** | 1480 | 34 |
| **ASW + LB EPS** | 3530 | 14 |

## 10.3. Influence of EPS extracted from *Desulfovibrio alaskensis* on the corrosion behaviour of carbon steel St37-2 in sea water

Recent work were conducted to assess the role of EPS extracted from *Desulfovibrio alaskensis*, marine sulphate-reducing bacteria (SRB) in oil and gas anaerobic middle, in induction or inhibition of the biocorrosion of mild steels in a marine environment [7, 22]. Indeed, sea water is an environment inherent in oil rigs

and mild steels are widely used as materials of construction of facilities of transportation and storage of oil. The aim is to study the electrochemical response of mild steel St37-2 in artificial seawater in the presence of EPS extracted from *Desulfovibrio alaskensis* AL1.

## 10.3.1. Experimental results

### 10.3.1.1. Metal, electrolyte

The electrochemical measurements were performed with disk electrodes in mild steel St37-2 (Fe: matrix; C: max. 0.2%; Mn: max. 1.4%; N: max. 0.009; S: max. 0.045%; P: max. 0.045%; wt. %) immersed in artificial sea water (ASW), with an area in contact with the solution of 0.454 $cm^2$. Before each experiment, the samples were mechanically polished with SiC papers down to grade 600, then degreased three times in acetone ultrasonic bath for 5 min, then dried under a flow of argon and finally exposed to UV for 20 min.

### 10.3.1.2. Biomolecules

In this work, the marine strain of *Desulfovibrio alaskensis* AL1, isolated from an oil well in the Bay of Purdu, Alaska [23], was used and grown in anaerobic conditions. This bacterial species is able to reduce the sulphates, sulphites, thiosulfate and nitrates by using acetate, fumarate, lactate, propionate, pyruvate, alanine and ethanol as electron donors. In this work, the source of carbon for *D. alaskensis* is lactate-added in the culture medium in the form of lactate of sodium with a concentration of 53.6 or 5.36 mM $L^{-1}$, corresponding to 0.6 or 0.06% (m/v). In the following, the notations 0.6 and 0.06 refer to these concentrations of lactate in the culture medium. Extracellular polymeric substances (TB EPS and LB EPS) secreted by *Desulfovibrio alaskensis* AL1 were extracted according to the same procedure as described on figure 10.1.

For electrochemical measurements and as well as for the system 70Cu-30Ni/ASW, the EPS were diluted in artificial seawater with a same protein concentration equal to 20 mg $L^{-1}$.

### 10.3.1.3. Electrochemical measurements

The electrochemical measurements were performed with a three-electrode cell and an EC6Lab SP-200 from BioLogic. The working electrode was a disk of mild steel St37-2, the counter-electrode was a graphite sheet, the reference electrode was a saturated calomel electrode and the solution volume was about 0.1 L. The experiments were performed at room temperature, in static and anaerobic conditions (bubbling of argon in the solution for at least 1 hour before the beginning of each experiment and maintaining an atmosphere of argon above the solution during the impedance measurements). Electrochemical impedance diagrams have been plotted at $E_{corr}$, with a frequency range from $10^5$ to $10^{-3}$ Hz, 7 points per decade and with an amplitude of 10 mV peak-to-peak.

## 10.3.2. Results

### 10.3.2.1. Electrochemical measurements

After 2 hours immersion in artificial seawater without biomolecules, the corrosion potential of mild steel reached a stationary value of 0.777 ± 0.011 V *vs* SCE. The presence of EPS induced no significant variation in the value of $E_{corr}$.

EIS measurements were performed at $E_{corr}$ after 2 hours immersion in deaerated ASW, without (and with) EPS. The impedance data were presented in figure 10.7. One single capacitive loop, looking like a depressed semi–circle, could be observed for all solutions. The diameter of this loop is higher in the presence of EPS compared to without, showing a protective effect of EPS. The highest effect was obtained for LB EPS.

It is shown that the capacitive loop mainly illustrates the anodic charge transfer and its diameter is equal to the resistance of anodic charge transfer $R_{ta}$ [7]. In this work – and unlike the 70Cu-30Ni/ASW system – $R_{ta}$ is not obtained from a fitting procedure but is estimated graphically using Nyquist diagrams as follows: $R_{ta} = 2 \times Z_{rmax}$, with $Z_{rmax}$ the real part of impedance corresponding to the maximum of the imaginary part – $Z_j$ (top of the flattened semi-circle). Estimated values for $R_{ta}$ in different solutions are presented in table 10.5. $R_{ta}$ is always higher in presence of EPS compared to ASW without biomolecules; the ratio $R_{ta}$ (ASW+EPS) / $R_{ta}$ (ASW) varies between 1.2 for ASW + 0.6 TB EPS up to 3.9 for ASW + 0.6 LB EPS.

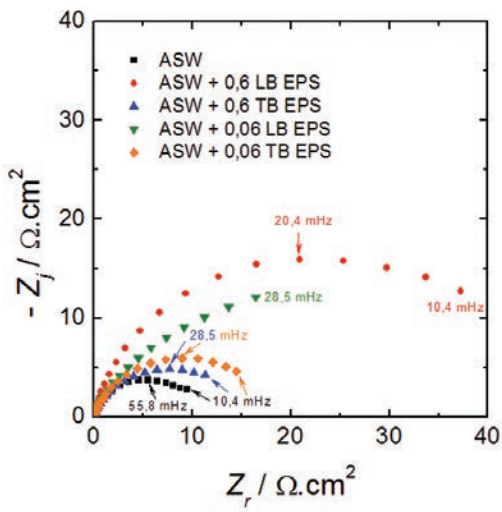


**Fig. 10.7.** – Experimental impedance diagrams in the complex plane (Nyquist diagrams) of mild steel St37-2 after 2 hours immersion in static artificial sea water at $E_{corr}$, without (and with) EPS (protein concentration: 20 mg $L^{-1}$). 0.06 and 0.6 correspond to the lactate concentration (0.6% and 0.06% (m/v), respectively) in the culture medium of *D. alaskensis* AL1 before extraction of the EPS.

**TABLE 10.5.** – Corrosion current density obtained from $R_{ta}$ and the anodic Tafel constant $b_a$ by application of equation (10.10) averaged from two independent measurements values.

| | $R_t^a$ (Ω cm²) | $b_a$ (mV decade⁻¹) | $j_{corr}$ (μA cm⁻²) |
|---|---|---|---|
| **ASW** | 11500 | 0.08 | 3.0 |
| **ASW + 0.6 LB EPS** | 45000 | 0.06 | 0.6 |
| **ASW + 0.6 TB EPS** | 14500 | 0.09 | 2.7 |
| **ASW + 0.06 LB EPS** | 37300 | 0.06 | 0.8 |
| **ASW + 0.06 TB EPS** | 18400 | 0.09 | 2.0 |

### *10.3.2.2. Corrosion current*

For the system 70Cu-30Ni/ASW, the corrosion current density $j_{corr}$ was calculated from $R_{ta}$ by applying of equation (10.10), and by using impedance data and polarization curves (not shown here). $R_{ta}$ is the diameter of the capacitive loop and the Tafel anodic constant $b_a$ is equal to the reciprocal of the slope of the anodic polarization curve, in the representation $\log |j|$ *vs* E, in the domain of linear variation near $E_{corr}$ (Tafel domain; anodic reaction entirely limited by the kinetic). Estimated values for $b_a$ and $j_{corr}$ are also given in table 10.5.

For the 70Cu-30Ni/ASW system, these results show an important inhibition effect on corrosion for 0.6 and 0.06 LB EPS, with a ratio of current densities $j_{corr}$(ASW)/$j_{corr}$(ASW+EPS) between about 4 and 5. While a negligible or weak inhibiting effect can be observed for 0.6 and 0.06 TB EPS ($j_{corr}$(ASW)/$j_{corr}$(ASW+EPS) equal to 1.1 and 1.5, respectively).

## 10.4. Conclusion

This work presents an evaluation of the influence of EPS extracted from two marine bacterial species (*Pseudomonas* sp. *NCIMB 2021* and *Desulfovibrio alaskensis* AL1) on marine corrosion behaviour of two metallic materials (70Cu-30Ni alloy and mild steel St37-2) in sea water. The results were compared to those obtained with a protein model, the BSA. For both systems, 70Cu-30Ni / ASW + EPS from *Pseudomonas* and mild steel St37-2 / ASW + EPS from *D. alaskensis*, the conclusions are similar and are summarized in table 10.6.

These observed electrochemical behaviour differences – depending on the kind of biomolecules present in solution – must be related with the chemical composition and thickness of surface layers, oxide layer and adsorbed organic layer, estimated from the XPS results (X-ray-induced photoelectron spectroscopy). Thus, in the case of the alloy 70Cu-30Ni, the stronger effect for the corrosion inhibition observed in the presence of LB EPS is in agreement with the lower content $Cu^+$ in the oxide layer and with the lower thickness of the oxide

layer (~ 1.6 nm) [6, 8]. Moreover, XPS data show that the adsorbed organic layer covering the oxide layer is mainly made up of protein. Unlike the volume composition EPS extracted from *Pseudomonas* sp. *NCIMB 2021* (Table 10.1), proteins are more concentrated on the surface in the presence of LB EPS than in the presence of TB EPS, with a mass percentage similar to that obtained for the adsorbed BSA [6]. For the BSA and the LB EPS, the inhibitor effect on corrosion induced by biomolecules cannot be explained only by the amount of protein adsorbed on the metal surface but also by the nature of the adsorbed biomolecules.

**Table 10.6.** – Effect on corrosion behaviour of two metallic materials (alloy 70Cu-30Ni and mild steel St37-2) of BSA and of the EPS extracted from two marine bacterial species (*Desulfovibrio alaskensis* AL1 and *Pseudomonas* sp. *NCIMB 2021*).

| | **70Cu-30 Ni / ASW**<br>**Mild steel / ASW** |
|---|---|
| **Current / corrosion rate TB EPS** | No negative effect<br>or weak inhibitor effect |
| **LB EPS** | Important inhibitor effect |

## Acknowledgments

Research leading to the present results received funding of the seventh framework programme of the European Union (FP7-2007-2013, grant No. 238579 agreement). The project web site: www.biocor.eu/ip8 (RSP3).

## References

[1] Rehm B.H.A. (2010) "Bacterial polymers: biosynthesis, modifications and applications." Nat. Rev. Microbiol., 8, 578-592.

[2] Karatan E., Watnick P. (2009) "Signals, regulatory networks, and materials that build and break bacterial biofilms." Microbiol. Mol. Biol. Rev., 73, 310-347.

[3] Flemming H.-C., Wingender J. (2010) "The biofilm matrix." Nat. Rev. Microbiol., 8, 623-633.

[4] Beech I., Hanjagsit L., Kalaji M., Neal A.L., Zinkevich V. (1999) "Chemical and structural characterization of exopolymers produced by *Pseudomonas* sp. NCIMB 2021 in continuous culture." Microbiology, 145, 1491-1497.

[5] Beech I.B., Gubner R., Zinkevich V., Hanjangsit L., Avci R. (2000) "Characterisation of conditioning layers formed by exopolymeric substances of *Pseudomonas* NCIMB 2021 on surfaces of AISI 316 stainless steel." Biofouling, 16(2-4), 93-104.

[6] Torres-Bautista B.E. (2014) "Effect of biomolecules adsorption on oxide layers developed on metallic materials used in cooling water systems." PhD thesis, université Paris VI, France.
[7] Wikieł A.J. (2013) "Role of extracellular polymeric substances on biocorrosion initiation or inhibition." PhD thesis, universität Duisburg-Essen, Germany.
[8] Carvalho M. (2014) "Corrosion of copper alloys in natural seawater – Effects of hydrodynamics and pH." PhD thesis, université Paris VI, Paris, France.
[9] Schiffrin D.J., De Sanchez S.R. (1985) "The effect of pollutants and bacterial microfouling on the corrosion of copper base alloys in seawater." Corrosion, 41, 31-38.
[10] Torres Bautista B.E., Wikieł A.J., Datsenko I., Vera M., Sand W., Seyeux A., Zanna S., Frateur I., Marcus P. (2015) "Influence of extracellular polymeric substances (EPS) from *Pseudomonas* NCIMB 2021 on the corrosion behaviour of 70Cu-30Ni alloy in seawater." J. Electroanal. Chem., 737, 184-197.
[11] Barcia O.E., Mattos O.R., Pébère N., Tribollet B. (1993) "Study for the electrodissolution of copper in 1M hydrochloric acid solution by impedance." J. Electrochem. Soc., 140(10), 2825-2832.
[12] D'Elia E., Barcia O.E., Mattos O.R., Pébère N., Tribollet B. (1996) "High-Rate Copper Dissolution in Hydrochloric Acid Solution." J. Electrochem. Soc., 143(3), 961-967.
[13] Deslouis C., Tribollet B., Mengoli G., Musiani M.M. (1988) "Electrochemical behaviour of copper in neutral aerated chloride solution. I. Steady-state investigation." J. Appl. Electrochem., 18, 374-383.
[14] Deslouis C., Tribollet B., Mengoli G., Musiani M.M. (1988) "Electrochemical behaviour of copper in neutral aerated chloride solution. II. Impedance investigation." J. Appl. Electrochem., 18, 384-393.
[15] Diard J.-P., Le Canut J.-M., Le Gorrec B., Montella C. (1998) "Copper electrodissolution in 1 M HCl at low current densities. I. General steady-state study." Electrochim. Acta, 43, 2469-2483.
[16] Diard J.-P., Le Canut J.-M., Le Gorrec B., Montella C. (1998) "Copper electrodissolution in 1 M HCl at low current densities. II. Electrochemical impedance spectroscopy study." Electrochim. Acta, 43, 2485-2501.
[17] Torres B., Seyeux A., Zanna S., Tribollet B., Marcus P., Frateur I. (2013) "Effet de l'adsorption de biomolécules sur les couches d'oxydes développées sur l'alliage Cu70-Ni30 en eau de mer artificielle statique." Mat. & Tech., 101(1), 106.
[18] Torres B., Bautista B.E., Carvalho M.L., Seyeux A., Zanna S., Cristiani P., Tribollet B., Marcus P., Frateur I. (2014) "Effect of protein adsorption on the corrosion behaviour of 70Cu-30Ni alloy in artificial seawater." Bioelectrochemistry, 97, 34-42.
[19] Brug G.J., van den Eeden A.L.G., Sluyters-Rehbach M., Sluyters J.H. (1984) "The analysis of electrode impedances complicated by the presence of a constant phase element." J. Electroanal. Chem., 176, 275-295.

[20] Hirschorn B., Orazem M.E., Tribollet B., Vivier V., Frateur I., Musiani M. (2010) "Determination of effective capacitance and film thickness from constant-phase-element parameters." Electrochim. Acta, 55, 6218-6227.
[21] Epelboin I., Gabrielli C., Keddam M., Takenouti H. (1981) "Electrochemical Corrosion Testing, ASTM STP 727." F. Mansfeld and U. Bertocci Eds, American Society for Testing and Materials, 150.
[22] Wikieł A.J., Datsenko I., Vera M., Sand W. (2014) "Impact of *Desulfovibrio alaskensis* biofilms on corrosion behaviour of carbon steel in marine environment." Bioelectrochemistry, 97, 52-60.
[23] Feio M.J., Zinkevich V., Beech I.B., Llobet–Brossa E., Eaton P., Schmitt J., Guezennec J. (2004) "*Desulfovibrio alaskensis* sp. nov., a sulphate-reducing bacterium from a soured oil reservoir." Int. J. Syst. Evol. Microbiol., 54, 1747-1752.

# 11 On the iron-sulphur interactions involved in biocorrosion phenomena

**Ph. Refait, M. Jeannin, R. Sabot, S. Sablé, I. Lanneluc, A. Romaine, S. Necib, S. Pineau**

## 11.1. Introduction

Microbiologically induced corrosion (MIC) phenomena can be classified into two main categories [1]. The first phenomenon involves an increase of the potential of the metal in aerobic conditions and can induce pitting corrosion processes. It mainly concerns passive metals and alloys such as stainless steels. The second phenomenon takes place in anaerobic conditions and involves sulphide-producing microorganisms. It concerns non-passivating materials such as copper and carbon steel. In the last case, the sulphide species produced by microorganisms induce the precipitation of iron sulphide near the steel surface. The bacteria then lead to the formation of solid phases that do not form in abiotic conditions. If these solid phases are only obtained locally, the corrosion product layer covering the metal surface becomes heterogeneous, which can lead to galvanic coupling between the areas of the surface covered by different compounds. Actually, most of the corrosion products (*e.g.,* Fe (III) oxyhydroxides, Fe (II-III) hydroxysalt green rusts, ...) are insulating, except for magnetite that is an electronic conductor. Conversely, the iron sulphides produced by bacteria, *e.g.,* mackinawite FeS, are mostly electronic conductors. In their study devoted to the role of electroactive sulphate-reducing bacteria (SRB), Enning *et al.* [2] have shown that the adherent layer biogenerated by these SRB was indeed conductive (measured conductivity of 50 S $m^{-1}$ while that of a semiconductor like silicon is equal to 1.6 $10^{-3}$ S $m^{-1}$). Iron sulphides may then act as cathode in the same way as magnetite while the rest of the metal surface covered by a porous layer of insulating compounds behaves as anode (Figure 11.1).

The formation of iron sulphides takes place instead of that of the corrosion products that characterise the abiotic conditions. Consequently, in the presence of sulphide-producing bacteria at least two processes compete, the predominance of one or the other being linked to the intensity of bacterial activity.

One of the crucial points when dealing with carbon steel biocorrosion is then associated with iron-sulphur interactions and the changes to the corrosion product layer they may induce. This is the topic of the current chapter that is developed in two different contexts. First, we will deal with marine corrosion of

carbon steel. In seawater, sulphur is present only as sulphate species so that the formation of iron sulphides can in most cases be attributed unambiguously to bacterial activity. In the second part, the particular case of the corrosion of carbon steel in claystone is described. This topic is tightly linked to nuclear waste management. In France, it is envisaged to store high-level radioactive waste at a depth of ~500 m in a deep geological disposal, drilled in very stiff (indurated) clay (Callovo-Oxfordian COx claystone so-called "argillite") formation. The waste will be trapped in a glass-matrix set inside a stainless steel container, itself set in a carbon steel "overpack". Numerous studies were then conducted by the French national radioactive waste management agency (ANDRA) to understand, model and predict the behaviour of carbon steel in argillite, a rock that contains various clays, quartz and carbonates (*e.g.,* calcite) [3, 4]. Sulphide minerals are also present, the main one being pyrite $FeS_2$, so that sulphide-producing bacteria, likely to grow in this peculiar medium, are not the only possible source of dissolved sulphide species. In this case, the role of Fe-S interactions goes beyond the scope of biocorrosion.

## 11.2. Marine corrosion of carbon steel

Numerous investigations have been carried out over the last decades to understand the mechanisms associated with the influence of sulphide-producing bacteria (in particular SRB) and various models were proposed. Most of the recent articles only complete, precise or confirm/invalidate previous conclusions. For instance, E. Malard *et al.* [5] compared the corrosion behaviour of two alloys, a carbon steel and a low alloy steel containing 2 wt. % Cr, in sterilized natural seawater and in untreated natural seawater. The results obtained with the two materials proved similar. At the beginning of the experiment, the corrosion rates measured in both media were identical. After 5-6 months of immersion, the corrosion rate of the alloys in untreated seawater increased and became significantly higher than that measured in sterilized seawater. The analysis of the corrosion products formed after 300 days of immersion demonstrated that iron sulphides were present all over the surface of the alloys left in untreated natural seawater. These results are perfectly consistent with the phenomenological model proposed by R. Melchers [6, 7] to describe marine corrosion of carbon steel. In this model, the transition between the aerated conditions that prevail at the beginning of the process, and the anoxic conditions associated with the growth and increasing activity of SRB, is characterized by an increase of corrosion rate (Section 11.2.1). According to [5] this transition occurred before 6 months of immersion, in agreement with another study performed with carbon steel test coupons set in various French seaports [8]. It is also important to note that the authors of [5] did not observe severe localized corrosion processes. This shows once again that the presence and activity of SRB do not necessarily lead to an especially severe localized degradation of the metal. The various reported cases of severe localized MIC processes result consequently from the combination of

several factors, the production of sulphide species by bacterial activity being only one of these factors. One of the assumptions made 15-20 years ago was that peculiar bacterial consortia may be required to damage strongly the metal. Actually, the key role of the association of SRB with sulphur-oxidizing bacteria (SOB) has been evidenced [9]. Acid-producing bacteria may also be involved [10]. The combination of microorganisms associated with the redox cycle of sulphur (SRB/SOB) with microorganisms associated with the redox cycle of iron has also been considered. Duan *et al.* [11] studied the behaviour of carbon steel coupons in media containing only SRB or a mixture of SRB and iron-reducing bacteria (IRB). They however observed that the combination SRB/IRB led to lower corrosion rates. As a matter of fact, the mechanisms leading to severe localized corrosion phenomena of carbon steel in seawater are not completely understood yet.

The most recent important findings relate to electro-active SRB, *i.e.*, bacteria that can exchange electrons with the metal surface. In 2012, the existence of a peculiar corrosion process, associated with the electro-activity of the bacteria and thus referred to as "EMIC" (Electrical Microbiologically Influenced Corrosion), was demonstrated [2]. It was confirmed later by further research work [12, 13].

### 11.2.1. Role of the corrosion product layer

It is generally admitted that the layer of corrosion products that gradually covers the steel surface acts as a physical barrier between the metal surface and the aggressive environment. The transport of matter between the medium and the metal is then controlled by this layer and depends on its physical properties, *e.g.,* thickness, porosity, *etc.* This is clearly illustrated by the phenomenological model proposed by R. Melchers [6, 7] to describe the uniform corrosion process of carbon steel in seawater.

According to this model, five stages must be distinguished. For each stage, the kinetics of the corrosion process is controlled by a particular mechanism. The evolution of the degradation over time is then different for each stage. The five stages also define two main periods, the aerated period (stages 0-2) when dissolved oxygen plays a major role, and the anoxic period (stages 3-4) when the kinetics of the corrosion process is controlled by the activity of sulphide-producing bacteria.

During stage 0, the bare steel surface is directly in contact with aerated seawater while the oxygen concentration is maximal and the corrosion rate is consequently very high. This situation does not persist for a long time and stage 0 consequently has no practical interest. The oxygen concentration at the steel surface decreases rapidly and the process is then controlled by the diffusion of oxygen in the electrolyte. This corresponds to stage 1. The corrosion product layer is growing, however, and finally it plays a major role on the kinetic of the process. During stage 2, the corrosion rate is then controlled by the diffusion of oxygen through the corrosion product layer. It decreases with time because the layer becomes thicker and hinders more strongly the transport of oxygen.

Besides, the corrosion product layer is colonized by aerobic microorganisms that consume oxygen. Consequently, at a time called $t_a$, oxygen cannot reach the steel surface anymore. The surface of the metal and the inner part of the corrosion product layer are then in anoxic conditions. Time $t_a$ varies mainly with the average temperature of seawater. For instance, $t_a \approx 6$ months at 30 °C and $t_a \approx 4$ years at 5 °C [7].

During stage 3, *i.e.*, at the beginning of the anoxic period, the corrosion rate increases rapidly. The progressive transition from aerated to anoxic conditions made it possible for anaerobe sulphide-producing bacteria to grow. The previous development and activity of aerobe bacteria has led, moreover, to the accumulation of dead cells and associated organics species. This reservoir of nutrients favours the rapid growth of anaerobe microorganisms. Stage 3 corresponds to a maximum of bacterial activity and consequently to rather high corrosion rates. The previously accumulated nutrients are finally consumed and during stage 4 bacterial activity is controlled by the transport of nutrients from seawater to the metal surface through the corrosion product layer. Once again, this layer plays a major role on the kinetic of the corrosion process. Stage 4 is also the part of the overall process that mostly influences the long-term behaviour of the metal, *i.e.*, the lifetime of a carbon steel structure in seawater depends mainly on the processes occurring during stage 4. The thickness loss, for long immersion times, can then be expressed in first approximation by a linear law:

$$c = c_s + r_s.t$$

Parameters $c_s$ and $r_s$ were quantified using numerous data collected from various corrosion studies performed in different natural exposure sites [6]. It appears that $c_s$ mainly depends on the amount of nutrients present in seawater whereas $r_s$ mainly depends on temperature. Both temperature and amount of nutrients stimulate the metabolic activity of microorganisms and their increase induces that of $c_s$ and $r_s$ and consequently that of the corrosion rate.

This phenomenological model provides a basic plausible description of the phenomena associated with uniform corrosion of carbon/low alloy steel permanently immersed in a marine environment. It allows us to propose various assumptions about the possible localization of the corrosion process. Actually, the transport of matter, and especially that of dissolved oxygen that influences strongly the corrosion rate is, in any case, controlled by the corrosion product layer. This implies that the corrosion can only be uniform if this layer is homogeneous, or more precisely, if the properties of this layer that govern the transport of matter are uniform.

### 11.2.2. Description of the corrosion product layer

Although the important role of the corrosion product layer is generally admitted, few studies were devoted to a detailed thorough description of this layer, including the identification of the solid phases it contains. The research program build in France around the PhD thesis of Samuel Pineau [14] brought

the first accurate information. This joint program involved various French seaports (Marseille, Le Havre and Nantes-Saint Nazaire (France)), various industrial partners (Arcelor-Mittal and BAC Corrosion Control) and various research labs. So as to accumulate information, hundreds of carbon steel coupons were immersed in various areas of three seaports in both low water zone and tidal zone. After 6-12 months, the corrosion product layers covering the coupons were characterized by X-ray diffraction, μ-Raman spectroscopy and scanning electron microscopy. Meanwhile, the bacteria present inside the pores of the corrosion product layer were studied by a combination of classical microbiological methods and molecular biology techniques. The obtained results proved similar whatever the seaport and the exposure site [8].

The corrosion product layer was in any case constituted of an outer orange-brown stratum mainly composed of Fe(III) oxyhydroxides (goethite α-FeOOH and lepidocrocite γ-FeOOH) covering an inner dark stratum. This inner stratum, in contact with the steel surface, is mainly composed of green rust $GR(SO_4^{2-})$, a Fe(II,III) hydroxysulphate with formula $Fe^{II}_4Fe^{III}_2(OH)_{12}SO_4, 8H_2O$, iron sulphide FeS (mackinawite), and magnetite $Fe_3O_4$. This result indicates that $GR(SO_4^{2-})$ is the solid phase that precipitates from the iron dissolved species produced by the purely electrochemical, *i.e.*, abiotic, corrosion process of iron and carbon steel in a marine environment. Fe(III) oxyhydroxides (and more likely magnetite) then result from the oxidation of $GR(SO_4^{2-})$ by dissolved $O_2$. This result is interesting because the growth of a $GR(SO_4^{2-})$ layer on the steel surface may favour the subsequent growth and activity of SRB. Various studies demonstrated that $GR(SO_4^{2-})$ could constitute a reservoir of sulphate species for SRB [15, 16].

After 12 months of immersion, FeS and $GR(SO_4^{2-})$ are distributed more or less homogeneously in the inner stratum of the corrosion product layer. This shows that anoxic conditions were already established at the vicinity of the steel surface and inside the inner stratum. FeS can only result from the activity of sulphide-producing bacteria and the microbiological analysis confirmed that SRB were present in the inner dark stratum of the corrosion product layer together with FeS and $GR(SO_4^{2-})$. This indicates that the aerated/anoxic transition had already taken place. According to the phenomenological model proposed by R. Melchers this transition would rather take place after two years for an average temperature of 15 °C and after three years for an average temperature of 10 °C [7]. The results given by [5] and [8] indicate that this transition more likely occurs earlier.

Additional information was obtained *via* the analysis of carbon steel coupons permanently immersed for 11 years in the low water zone of the French seaport "Les Minimes" at La Rochelle (Atlantic Ocean, France) [17]. Inside the thick (7-8 mm) layers covering the steel surface at that time, anoxic conditions prevail almost everywhere, except in a thin outer stratum. The main corrosion products were FeS, $Fe_3O_4$ and $GR(SO_4^{2-})$. Laboratory experiments demonstrated that $GR(SO_4^{2-})$ was the main compound resulting from the purely electrochemical abiotic corrosion process, even in anoxic conditions [17]. Conversely, the formation of FeS results from the metabolic activity of SRB, while $Fe_3O_4$ can be obtained whether directly from the corrosion of the metal or indirectly as the result of the transformation of $GR(SO_4^{2-})$.

Short immersion times were also considered. The corrosion product layers obtained after 1 week to 2 months immersion (French seaport "Les Minimes") were recently characterized, combining once again physico-chemical analysis and microbiological study [18]. The evolution over time and the possible implications are summarized in figure 11.1. During the first 15 days of immersion, the metal is rapidly covered by a two-stratum layer of corrosion products (Fig. 11.1a). The inner stratum is only composed of GR($SO_4^{2-}$) whereas the outer stratum is mainly composed of lepidocrocite γ-FeOOH. During this first stage, aerated conditions prevail and SRB do not influence the corrosion process, in agreement with the phenomenological model of R. Melchers [6, 7]. The purely electrochemical abiotic process prevails here and leads to GR($SO_4^{2-}$). The outer stratum of γ-FeOOH results from the oxidation of GR($SO_4^{2-}$) by dissolved oxygen.

After 1-2 months immersion, the corrosion product becomes sufficiently thick to hinder the transport of dissolved oxygen from seawater towards the steel surface. This phenomenon may not be uniform so that, at the beginning, only a few de-aerated or weakly aerated areas are created here and there on the steel surface and inside the corrosion product layer. The first consequence is that various oxidation products of GR($SO_4^{2-}$) can be obtained. Together with lepidocrocite that forms in strongly aerated conditions [19], goethite α-FeOOH, usually obtained for a moderate aeration [19], and magnetite, only obtained by oxidation of green rusts in very weakly aerated conditions [20], are now present (Fig. 11.1b). As a second consequence, FeS could be identified locally and only for a few test coupons, in the inner dark stratum as soon as 1 month immersion. This shows that SRB have already grown and are already active in the first de-aerated zones created inside the corrosion product layer. The identification of SRB by DNA sequencing in the corresponding corrosion product layers validated this assumption [18]. In figure 11.1b, it is then assumed that FeS and $Fe_3O_4$ are obtained together in the same area because the formation of these two compounds requires de-aerated conditions.

Moreover, when the corrosion product layer is sufficiently thick to hinder the transport of dissolved $O_2$, oxygen diffuses mainly inside the pores of the layer (Figs. 11.1b and 11.1c). In the most weakly aerated areas, the metabolic activity of SRB increases, the formation of FeS is promoted and the oxidation of GR($SO_4^{2-}$) leads mainly to magnetite. FeS and $Fe_3O_4$ are both electronic conductors. In the areas where their formation is favoured, the metal could then be electrically connected to the bottom of some pores (Fig. 11.1c). The bottom of such pores would then act as a cathodic zone, where oxygen is reduced preferentially, while the surface of the metal underneath would become an anodic zone suffering accelerated corrosion. This kind of corrosion cell would reinforce the effects induced by bacterial activity (*i.e.,* production of sulphide species) thus explaining, at least partially, some of the severe localized corrosion phenomena associated with SRB. This phenomenon could persist even if anoxic conditions prevail on the metal surface and inside the inner part of the corrosion product layer and even if the influence of SRB tends to be uniform. The required condition for this phenomenon to remain active is the persistence of

an electronic bridge, formed by FeS and $Fe_3O_4$ particles, connecting the metal surface to pores accessible by aerated seawater. It must also be recalled that a corrosion cell, like the one represented in figure 11.1c, implies an acidification of the medium close to the anodic zone and an increase of pH at the cathodic zone. This effect could lead to an aggravation of the local degradation of the metal in the anodic zones.

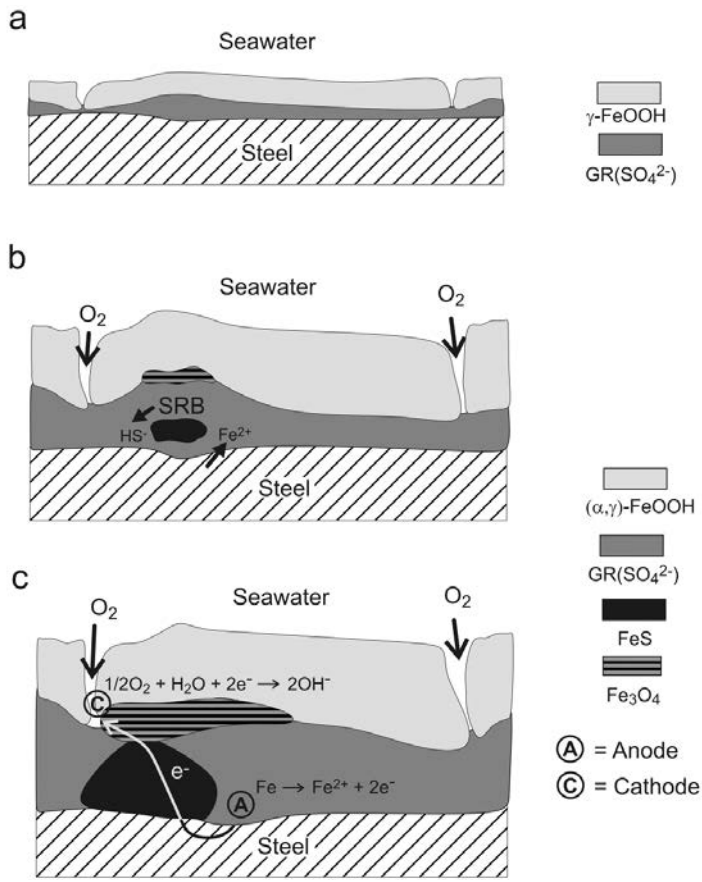


**Fig. 11.1.** – Corrosion process of carbon steel permanently immersed in seawater: schematic representation of the first stages and mechanism leading to a localized degradation. The proposed mechanism is based on the formation of corrosion cells induced by the heterogeneity of the corrosion product layer.

In conclusion, the thorough detailed description of the corrosion product layer and its evolution over time confirms that the corrosion of carbon steel in a natural marine milieu is in any case influenced by sulphide-producing bacteria. In the phenomenological model proposed by R. Melchers *et al.* [6, 7], it is

even assumed that the corrosion rate, for long immersion times (> 1-3 years), is controlled by bacterial activity and consequently by the transport of nutrients through the corrosion product layer. The mechanism associated with uniform corrosion is then rather well understood but the localized corrosion processes associated with bacterial activity are not completely elucidated. They cannot be simply attributed to sulphide-producing bacteria because these microorganisms finally colonize the overall steel surface thus leading to a uniform MIC process. Severe local degradations require specific local conditions, maybe involving peculiar bacterial consortia, peculiar microorganisms (*e.g.,* electro-active SRB), or corrosion cells associated with "electronic bridges" constituted by FeS and $Fe_3O_4$ particles, as described above.

## 11.3. Corrosion of carbon steel in argillite and corrosion cells associated with heterogeneous corrosion product layers

The PhD work of Alexandre Romaine [21] pointed out that galvanic cells could result from the heterogeneity of the corrosion product layer. This thesis, financially supported by ANDRA (French national radioactive waste management agency), dealt with the corrosion mechanisms of carbon steel electrodes covered by a 5 mm thick argillite layer and immersed in $NaHCO_3$ + NaCl solutions at 80 °C. Such a temperature will be reached at the surface of the carbon steel overpack because of the radioactivity of the waste. The argillite used in this study originated from the site envisioned for the deep (~500 m) geological disposal. It was ground to powder so that a layer of argillite could be easily deposited and compacted onto the surface of the steel electrodes.

The corrosion process addressed here relates to an unusual time period, *i.e.,* hundreds or even thousands of years, required to ensure that the radioactive species remain confined in the disposal repository. It involves, like marine corrosion, a transition from initially aerated conditions to anoxic conditions. The tunnels containing the nuclear waste will be sealed and the amount of oxygen trapped in these tunnels will be consumed by the corrosion process, inevitably leading to anoxic conditions. In view of the expected lifetime of the system, the anoxic conditions will prevail most of the time and anaerobe microorganisms such as SRB may be involved.

### *11.3.1. Heterogeneity of the corrosion product layer*

Corrosion product layers, assumed to be representative to those that will form in the real waste disposal system, were prepared using solutions with various NaCl and $NaHCO_3$ concentrations, *via* various methods and in particular galvanostatic anodic polarization [22]. They were often heterogeneous. These layers being constituted of various strata more or less parallel to the steel surface, the

term "heterogeneous" is used when the composition of a given stratum varies along the steel surface.

The results described here relate to a steel electrode covered with an argillite layer and immersed 15 days at the open circuit potential (OCP) in a 0.01 M $NaHCO_3$ + 0.01 M NaCl solution at 80 °C. The pH of the electrolyte was adjusted at 7.0 at the beginning of the experiment. Figure 11.2 shows a picture of the electrode at the end of the experiment and a graph that summarizes the results of the μ-Raman spectroscopy analysis of the corrosion product layer. The photograph was taken after removal of the argillite layer by a gentle rinsing with de-ionized water. It is observed that the center of the electrode is darker than the periphery, which could result from a change of the corrosion product layer composition.

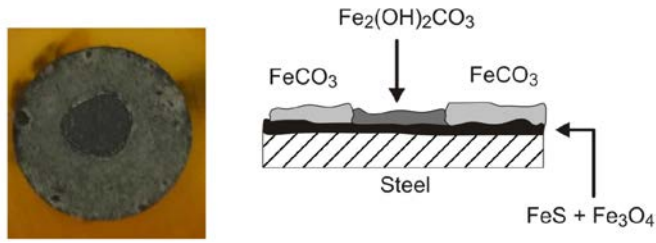


**Fig. 11.2.** – Photograph (top view) of a carbon steel electrode covered with an argillite layer and immersed 15 days at 80 °C in a 0.01 M $NaHCO_3$ + 0.01 M NaCl solution, and schematic representation (cross section) of the resulting corrosion product layer. The argillite layer was removed by rinsing carefully the electrode before the photograph was taken.

Raman spectroscopy confirmed visual observations. The outer stratum of the corrosion product layer proved composed of chukanovite $Fe_2(OH)_2CO_3$ in the central part of the electrode (dark area) while it is composed of siderite, $FeCO_3$, in the periphery. The siderite stratum incorporates components of the argillite layer and there is actually an intermediate region, between the corrosion product layer (only made of Fe compounds) and the argillite layer where Fe compounds resulting from the corrosion of steel are mixed with mineral phases coming from the argillite. This intermediate region was systematically observed around iron archaeological artefacts excavated from soils and was called "transformed medium" [23]. Under the outer stratum made up of carbonate-containing corrosion products, an inner layer in contact with the metal is present. It is made of a mixture of mackinawite FeS and $Fe_3O_4$ but its composition is homogeneous, *i.e.,* is the same whatever the composition of the outer stratum lying above.

The formation of the heterogeneous outer stratum results from two competitive processes, one leading to siderite, the other leading to chukanovite. These processes are governed by the $Fe^{2+}$, $OH^-$ and $HCO_3^-/CO_3^{2-}$ concentrations [24]. Siderite is for instance favoured by low $[OH^-]/[Fe^{2+}]$ ratios while chukanovite is favoured by larger $[OH^-]/[Fe^{2+}]$ ratios, in particular that corresponding to its composition, *i.e.,* $[OH^-]/[Fe^{2+}] = 1$. The heterogeneity of the corrosion product

layer is then more likely due to variations of carbonate concentration and/or pH. These variations could be linked to the transport of matter through the intrinsically heterogeneous argillite layer.

The presence of mackinawite in the corrosion product layer was unexpected. It implies that sulphide species are present in the argillite layer. These species may come from pyrite $FeS_2$, a mineral present in argillite (~1 wt %) or from a previous bacterial sulphide-producing activity. The resulting sulphide concentration is however low so that the formation of FeS is accompanied by that of $Fe_3O_4$.

In conclusion, it proved possible to obtain heterogeneous corrosion product layers involving electronic conductors (FeS and $Fe_3O_4$) and thus to demonstrate that corrosion cells, *i.e.*, galvanic effects, could be induced by this heterogeneity.

### 11.3.2. Galvanic cells and heterogeneity of the corrosion product layer

A carbon steel electrode was previously covered with a heterogeneous corrosion product layer prepared in experimental conditions similar to those described above. After removal of the argillite layer by a gentle rinsing, the obtained corrosion product layer was characterized by μ-Raman spectroscopy. Figure 11.3 displays a photograph of the electrode and three typical Raman spectra.

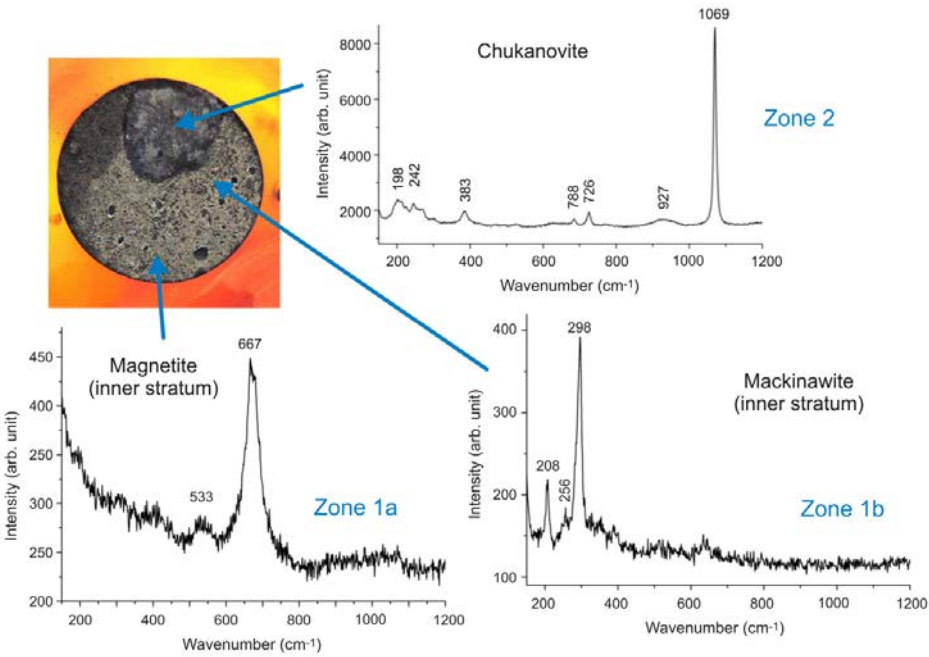


**FIG. 11.3.** – Photograph of a carbon steel electrode covered with a heterogeneous corrosion product layer and typical μ-Raman spectra obtained during the analysis of the various zones of the surface.

Two zones can be visually distinguished. The main part of the surface is covered with a light coloured, outer stratum composed mainly of siderite (Raman spectrum not shown). This part of the electrode surface can be called zone 1. The rest of the surface, *i.e.,* the smaller zone 2, is covered with a darker and thinner layer, only composed of chukanovite. In zone 1, an inner dark layer is present under the outer siderite layer. This inner layer proved heterogeneous too. Far from zone 2, it is composed mainly of magnetite. Let us call zone 1a this part of the electrode surface. Around zone 2, the main component of the inner dark stratum is mackinawite. This zone is called 1b. Finally, the chukanovite layer in zone 2 is in contact with the metal, *i.e.,* the corrosion product layer is in this particular case constituted of a single stratum (a complete interpretation of the phenomena that led to this peculiar heterogeneous corrosion product layer can be found in [25]).

Once the corrosion product layer was characterized, the electrochemical activity of the electrode was studied with the scanning vibrating electrode technique (SVET). For that purpose, the electrode was immersed in an aerated 0.01 M $NaHCO_3$ + 0.01 M NaCl solution at room temperature. The main cathodic process was then $O_2$ reduction.

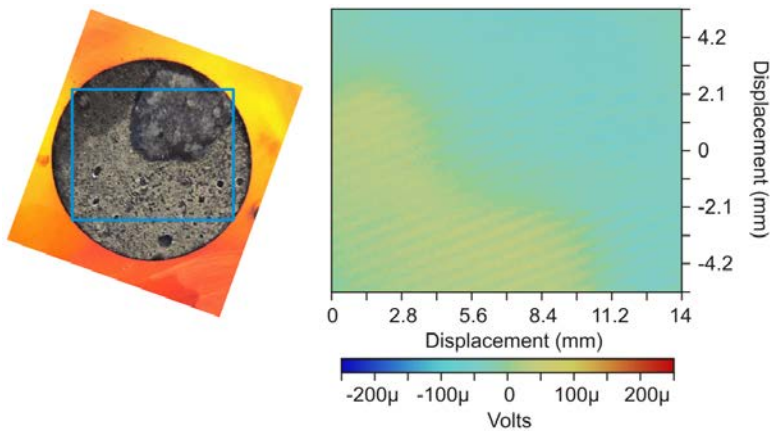


**Fig. 11.4.** – Zone scanned by SVET and corresponding electrochemical activity map [25].

An electrochemical activity map was first obtained with the electrode left at OCP (Fig. 11.4). It clearly reveals the presence of a cathodic zone (in blue) and an anodic zone (in yellow). The blue rectangle drawn on the photograph of the electrode corresponds to the mapped zone. This shows that the cathodic zone corresponds to the areas covered with chukanovite (zone 2) and with a mackinawite/siderite bilayer (zone 1b). The rest of the electrode surface is anodic and corresponds to the area covered with a magnetite/siderite bilayer (zone 1a). The argillite layer initially present on the electrode surface was heterogeneous

which, as discussed above, explains at least partially the formation of a heterogeneous corrosion product layer. However, the electrode is now immersed in a homogeneous medium, *i.e.* the 0.01 M $NaHCO_3$ + 0.01 M NaCl solution, and the galvanic effect revealed by the electrochemical activity map is necessarily due to the heterogeneity of the corrosion product layer.

The electrode was finally subjected to anodic polarization at a constant current density of 25 µA $cm^{-2}$. The obtained results are displayed in figure 11.5. It is first observed that the new map is similar to the previous one obtained at OCP. The electrochemical activity has however increased in the anodic zone, an expected result due to the anodic polarization. However, the cathodic zone remains, which illustrates the importance of the galvanic effect induced by the heterogeneous corrosion product layer. The photograph of the electrode at the end of the experiment illustrates very clearly the phenomenon. Orange corrosion products, *i.e.,* Fe(III) oxyhydroxides, have accumulated on the anodic zone. They result from the oxidation by dissolved oxygen of the Fe(II) compounds produced by the corrosion of the metal. In contrast, the corrosion products covering the cathodic zone do not seem to have been oxidized though they are Fe(II) compounds too. Raman spectroscopy confirmed it (spectra not shown). In other words, chukanovite, siderite and mackinawite that were present in the cathodic zone of the surface were not (or only slightly) oxidized when anodic polarization was applied. This confirms that oxygen reduction in the cathodic zone consumes mainly the electrons produced by the oxidation of iron occurring in the anodic zones.

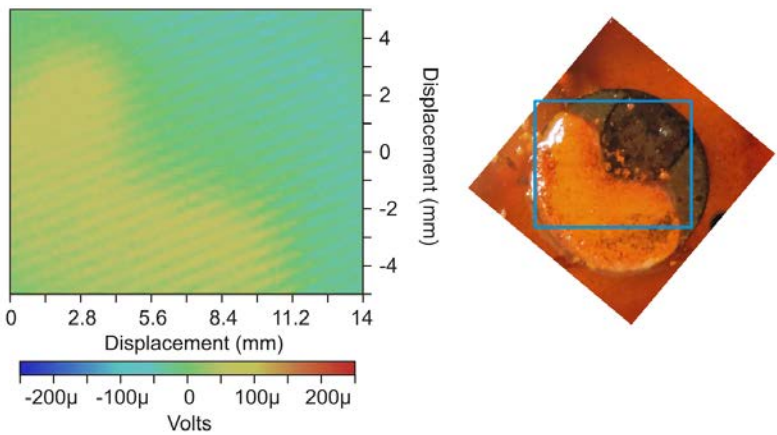


**FIG. 11.5.** – Electrochemical activity map (SVET) of the electrode under galvanostatic anodic polarization (25 µA $cm^{-2}$) and photograph of the electrode at the end of the experiment [25].

In conclusion, the heterogeneity of a corrosion product layer, whatever its origin, can induce galvanic effects leading to a locally (anodic zone) accelerated

corrosion process. In the example described above, the inner layer of mackinawite present in zone 1b acts as cathode because FeS is an electronic conductor, and thus favours the creation of corrosion cells. This confirms the possible important role of iron sulphides.

It must finally be noted that zone 2, covered by chukanovite, was also observed to be cathodic. The electrical properties of chukanovite are not known and the interpretation of this result is difficult. It must however be recalled that the chukanovite layer of zone 2 was much thinner that the bilayer covering the rest of the surface. If this thin layer was moreover porous, its influence on the transport of matter would have been negligible and oxygen would have then easily reached the steel surface underneath. More generally, it must be considered that any heterogeneity of the corrosion product layer that affects the transport of matter (electronic conduction, $O_2$ diffusion, migration of ionic species) may induce galvanic effects.

## 11.4. Conclusion

Biocorrosion of carbon/low alloy steel in natural environments is in most cases associated with sulphide-producing bacteria. When anoxic conditions are established at the steel/environment interface, the growth of these anaerobic microorganisms becomes possible which finally leads to the formation of iron sulphide. This process due to bacterial activity then competes with the abiotic processes that lead to other corrosion products. Figure 11.6 displays two diagrams that list the various processes expected in anoxic conditions. One relates to marine environments, the other relates to soils. Various similarities are observed.

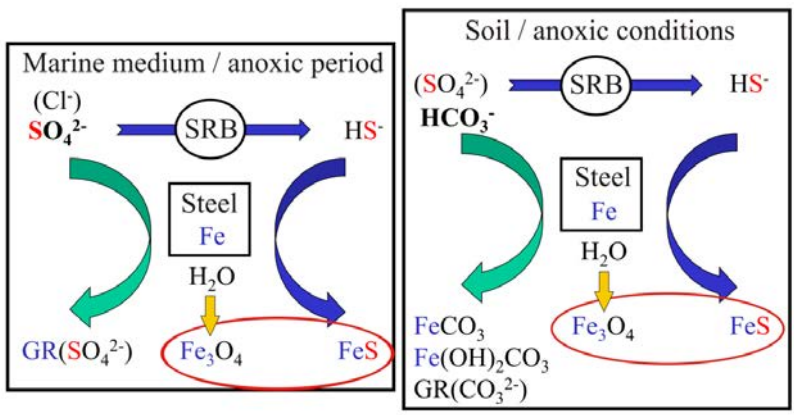


**Fig. 11.6.** – Diagrams showing the different processes involved in the formation of corrosion product layers in anoxic conditions and in the presence of sulphide-producing bacteria. The red ellipses surround the electronic conductors.

The first common feature is the presence in both media of dissolved and bioavailable sulphate species. Sulphate ions fuel the energy metabolism of bacteria *via* their reduction into sulphide species. In seawater, sulphate ions are also involved in the formation of one of the main corrosion products, *i.e.* the sulphated green rust $GR(SO_4^{2-})$ (with chemical formula $Fe^{II}_4Fe^{III}_2(OH)_{12}SO_4 \cdot 8H_2O$). In soils, the carbonate to sulphate concentration ratio is higher and carbonate-containing corrosion products, *i.e.* siderite $FeCO_3$, chukanovite $Fe_2(OH)_2CO_3$ or carbonated green rust $GR(CO_3^{2-}) = Fe^{II}_4Fe^{III}_2(OH)_{12}CO_3 \cdot 2H_2O$, are obtained. In this last case, the processes leading to the various carbonated compounds can themselves lead to a heterogeneous corrosion product layer, as described in section 11.3.1.

The second common feature is magnetite that can be obtained in both media. This Fe(II,III) oxide is in fact the compound able to form in any anoxic aqueous environment because its formation requires only water and is not dependent on the presence and availability of any specific anionic species (*e.g.*, sulphate, carbonate or sulphide). It can result, moreover, from the oxidation of Fe(II)-based compounds. In theory, its formation should be favoured by an increase of pH or a decrease of sulphate concentration (marine medium) or carbonate concentration (soils) at the steel/environment interface. Consequently, heterogeneous corrosion products can be obtained even in abiotic conditions because in any case various processes compete and each of these processes can be favoured locally as the result of local changes in the environment. To be exhaustive, it must also be noted that the Fe(II) hydroxychloride $\beta$-$Fe_2(OH)_3Cl$ is another corrosion product likely to form in anoxic conditions for very high chloride concentrations [26]. It was observed inside corrosion product layers covering iron archaeological artefacts coming from marine media [27] or soils [28, 29].

Finally, the metabolic activity of sulphide-producing bacteria induces the formation of FeS and this process necessarily competes with abiotic processes. This increases the probability of forming a heterogeneous corrosion product layer. Because FeS is an electronic conductor, this also increases the probability of forming corrosion cells between areas of the metal surface covered by different corrosion products. A mechanism based on electronic bridges connecting the metal and the aerated medium *via* FeS and $Fe_3O_4$ particles can then be proposed (Fig. 11.1, section 11.2.2). The persistence of differential aeration cells due to the heterogeneity of the corrosion product layer was recently confirmed for carbon steel in natural seawater [30].

## References

[1] Little B.J., Lee J.S., Ray R.I. (2008) "The influence of marine biofilms on corrosion: A concise review." Electrochimica Acta, 54, 2-7.

[2] Enning D., Venzlaff H., Garrelfs J., Dinh H.T., Meyer V., Mayrhofer K., Hassel A.W., Stratmann M., Widdel F. (2012) "Marine sulfate-reducing

bacteria cause serious corrosion of iron under electroconductive biogenic mineral crust." Environmental Microbiology, 14, 1772–1787.

[3] Gaucher. E, Robelin C., Matray J. M., Negrel G., Gros Y., Heitz J. F., Vinsot A., Rebours H., Cassabagnere A., Bouchet A. (2004) "ANDRA underground research laboratory: Interpre-tation of the mineralogical and geochemical data acquired in the Callovo-Oxfordian Formation by investigative drilling." Physics and Chemistry of the Earth, 29, 55-77.

[4] Yven B., Sammartino S., Geraud Y., Homand F., Villieras F. (2007) "Mineralogy, texture and porosity of Callovo-Oxfordian argillites of the Meuse/Haute-Marne region (eastern Paris Basin)." Mém. Soc. géol. France, 178, 73-90.

[5] Malard E., Kervadec D., Gil O., Lefevre Y., Malard S. (2008) "Interactions between steels and sulphide-producing bacteria-Corrosion of carbon steels and low-alloy steels in natural seawater." Electrochimica Acta, 54, 8-13.

[6] Melchers R.E., Wells T. (2006) "Models for the anaerobic phases of marine immersion corrosion." Corrosion Science, 48, 1791-1811.

[7] Melchers R.E., Jeffrey R. (2005) "Early corrosion of mild steel in seawater." Corrosion Science, 47, 1678-1693.

[8] Pineau S., Sabot R., Quillet L., Jeannin M., Caplat Ch., Dupont-Morral I., Refait Ph. (2008) "Formation of the Fe(II-III) hydroxysulphate green rust during marine corrosion of steel associated to molecular detection of dissimilatory sulphite-reductase." Corrosion Science, 50, 1099-1111.

[9] Beech I.B., Campbell S.A. (2008) "Accelerated low water corrosion of carbon steel in the presence of a biofilm harbouring sulphate-reducing and sulphur-oxidizing bacteria recovered from a marine sediment." Electrochimica Acta, 54, 14-21.

[10] Gueuné H., Refait Ph., Jeannin M., Sabot R., Paugam L., Memet J.B., Malard E. (2013) "Influence of acid-producing microorganisms on corrosion of carbon steel structures in marine environment with low tidal variations [Influence des microorganismes acidogènes sur la corrosion d'une infrastructure en acier au carbone en milieu marin à faible marnage]." Matériaux & Techniques, 101 (5-6) 502.

[11] Duan J., Wu S., Zhang X., Huang G., Du M., Hou, B. (2008) "Corrosion of carbon steel influenced by anaerobic biofilm in natural seawater" Electrochimica Acta, 54, 22-28.

[12] Venzlaff H., Enning D., Srinivasan J., Mayrhofer K.J.J., Hassel A.W., Widdel F., Stratmann M. (2013) "Accelerated cathodic reaction in microbial corrosion of iron due to direct electron uptake by sulfate-reducing bacteria." Corrosion Science, 66, 88-96.

[13] Yu L., Duan J., Du X., Huang Y., Hou B. (2013) "Accelerated anaerobic corrosion of electroactive sulfate-reducing bacteria by electrochemical impedance spectroscopy and chronoamperometry." Electrochemistry Communications, 26, 101-104.

[14] Pineau S. (2006) “Interactions entre les communautés bactériennes et les processus de corrosion accélérée des structures métalliques en environnement marin.” PhD thesis, université de Technologie de Compiègne, Compiègne, France.
[15] Zegeye A., Huguet L., Abdelmoula M., Carteret C., Mullet M., Jorand F. (2007) “Biogenic hydroxysulfate green rust, a potential electron acceptor for SRB activity.” Geochim. Cosmochim. Acta 71, 5450-5462.
[16] Langumier M., Sabot R., Obame-Ndong R., Jeannin M., Sablé S., Refait Ph. (2009) “Formation of Fe(III)-containing mackinawite from hydroxysulphate green rust by sulphate reducing bacteria.” Corrosion Science, 51, 2694-2702.
[17] Refait Ph., Nguyen D.D., Jeannin M., Sablé S., Langumier M., Sabot R. (2011) “Electro-chemical formation of green rusts in deaerated seawater-like solutions.” Electrochimica Acta, 56, 6481-6488.
[18] I. Lanneluc, M. Langumier, R. Sabot, M. Jeannin, Ph. Refait, S. Sablé (2015) “On the bacterial communities associated with the corrosion product layer during the early stages of marine corrosion of carbon steel.” International Biodeterioration & Biodegradation, 99, 55-65.
[19] Gilbert F., Refait Ph., Lévêque F., Remazeilles C., Conforto E. (2008) “Synthesis of goe-thite from $Fe(OH)_2$ precipitates: influence of Fe(II) concentration and stirring speed, Journal of Physics and Chemistry of Solids.” 69, 2124-2130.
[20] Ruby C., Abdelmoula M., Naille S., Renard A., Khare V., Ona-Nguema G., Morin G., Génin J-M.R. (2010) “Oxidation modes and thermodynamics of Fe(II-III) oxyhydroxycar-bonate green rust: Dissolution-precipitation versus in situ deprotonation.” Geochim. Cosmo-chim. Acta, 74, 953-966.
[21] Romaine A. (2014) “Rôle des espèces sulphures dans la corrosion des aciers non alliés : Hétérogénéités de la couche de produits de corrosion et couplages galvaniques.” PhD thesis, université de la Rochelle, La Rochelle, France.
[22] Romaine A., Sabot R., Jeannin M., Necib S., Refait Ph. (2013) “Electrochemical synthesis and characterization of corrosion products on carbon steel under argillite layers in carbonated media at 80 °C.” Electrochimica Acta, 114, 152-158.
[23] Neff D., Dillmann P., Bellot-Gurlet L., Béranger G. (2005) “Corrosion of iron archaeo-logical artefacts in soil: Characterisation of the corrosion system.” Corrosion Science, 47, 515-535.
[24] Refait Ph., Bourdoiseau J.A., Jeannin M., Nguyen D.D., Romaine A., Sabot R. (2012) “Electrochemical formation of carbonated corrosion products on carbon steel in deaerated solutions.” Electrochimica Acta, 79, 210-217.
[25] Romaine A., Jeannin M., Sabot R., Necib S., Refait Ph. (2015) “Corrosion processes of carbon steel in argillite: Galvanic effects associated with the heterogeneity of the corrosion product layer.” Electrochimica Acta, 182, 1019-1028.

[26] Rémazeilles C., Refait Ph. (2008) "Formation, fast oxidation and thermodynamic data of Fe(II) hydroxychlorides." Corrosion Science, 50, 856-864.
[27] Rémazeilles C., Neff D., Kergourlay F., Foy E., Conforto E., Guilminot E., Reguer S., Refait Ph., Dillmann Ph. (2009) "Mechanisms of long-term anaerobic corrosion of iron archaeological artefacts in seawater." Corrosion Science, 51, 2932-2941.
[28] Reguer S., Dillmann P., Mirambet F., Bellot-Gurlet L. (2005) "Local and structural char-acterisation of chlorinated phases formed on ferrous archaeological artefacts by μXRD and μXANES." Nuclear Instruments and Methods in Physics Research B, 240, 500–504.
[29] Réguer S., Dillmann P., Mirambet F. (2007) "Buried iron archaeological artefacts: Corrosion mechanisms related to the presence of Cl-containing phases." Corrosion Science, 49, 2726–2744.
[30] Refait Ph., Grolleau A.-M., Jeannin M., François E., Sabot R. (2016) "Localized corrosion of carbon steel in marine media: galvanic coupling and heterogeneity of the corrosion product layer." Corrosion Science, 111, 583-595.

# Theme 4
# Biodeterioration of non-metallic materials

Biodeterioration affects many non-metallic materials, including cementitious materials (concrete, mortar, plaster...) as well as stones, used to build structures and homes. As the economic issues are very important for this land heritage, pathologies induced by biodeterioration that can reduce the lifetime of structures are being studied in order to understand the mechanisms involved and find means of prevention.

Biodeterioration results from interactions between the environment, microorganisms, and the material. A global approach to these interactions applied to cementitious materials is developed in chapter 12. In particular, this approach targets the main criteria that can lead to the different types of biodeterioration with aesthetic, physical, or chemical consequences. The development of laboratory tests capable of reproducing biodeterioration of cementitious materials stands out as one of the key points in this chapter.

Chapter 13 provides a detailed description of concrete physical chemistry as well as the processes of chemical biodeterioration. The chapter also describes the main formulation parameters leading to improved concrete resistance to chemical biodeterioration.

These different aspects are set out in chapter 14, which specifically deals with the biodeterioration of cementitious materials in sewage works. This case of biodeterioration involves major socio-economic stakes since it can sometimes ruin sewage networks in less than ten years.

Chapter 15 broadens the range of materials likely to be bioaltered by considering the conservation of cultural heritage. Indeed, the biodeterioration of historical monuments is not limited to stone but also affects wood and stained-glass windows and remedies must be found for them. Mural decorations, paint and tapestries can also undergo biodeterioration caused by various microorganisms depending on the environmental conditions.

# 12 Biodeterioration of cementitious materials: interactions environment - microorganisms - materials

**Christine Lors**

## 12.1. Introduction

Cementitious materials, widely used in the construction of buildings, monuments, civil-engineering structures and industrial plants (*e.g.,* oil refineries and harbour facilities), are subject to ageing depending on their service environments. Thus, the French standard NF EN 206/CN [1] and its supplement FD P 18-011 [2] define the exposure classes that determine the proportions of a cementitious material's main components and some of its required service properties. The proliferation of microorganisms also depends on their host environment. When the ageing of a cementitious material creates a bioreceptive surface and the environment is conducive to their development, microorganisms can colonize the surface of the cementitious materials and sometimes penetrate to a given depth. The microorganisms involved are bacteria, cyanobacteria, fungi, and algae. How colonization affects the cementitious materials depends primarily on the metabolites generated by the microorganisms. The cementitious material could be aesthetically damaged or undergo more marked deteriorated through mechanical or chemical processes, thereby causing a reduction in some of its properties [3]. Generally, biodeterioration is defined as any undesirable modification in the material's properties due to the activity of living organisms [4]. In the case of cementitious materials, bideterioration could cause complications for the structure, even leading to its destruction.

This chapter addresses the principal interactions leading to biodeterioration (Fig. 12.1):

1. Interactions between the environment and microorganisms, which describe the conditions under which microbial growth can appear with a possible accumulation of metabolites in the environment.
2. Interactions between the environment and cementitious materials that lead to the ageing of the cementitious materials and, under some conditions, to surface bioreceptivity.
3. Interactions between microorganisms and cementitious materials that could lead to aesthetic, mechanical, or chemical biodeterioration of the

cementitious materials. In some cases, microorganisms can negatively affect these materials. In others, which are not dealt with in this chapter, microorganisms can have a beneficial effect on cementitious materials, such as in repairing microcracks through calcite bioprecipitation, a process referred to as biohealing [5, 6].

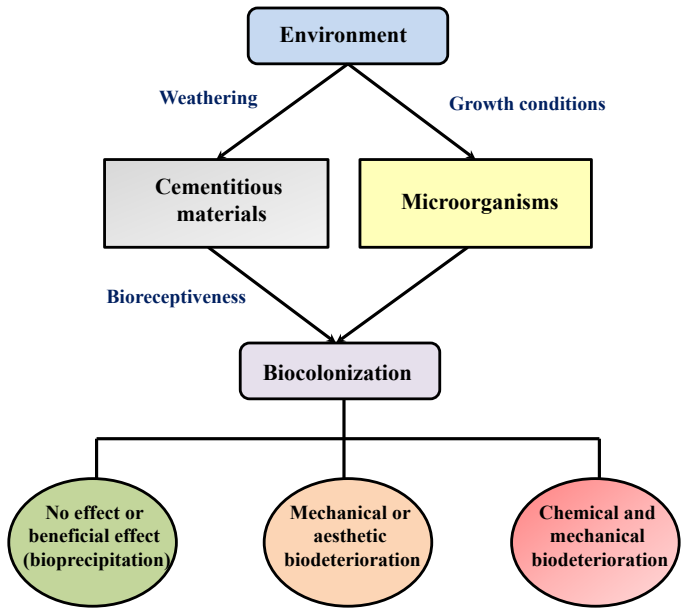


**FIG. 12.1.** – Interactions between the environment, microorganisms and cementitious materials.

## 12.2. Interactions between the environment and microorganisms

The environment determines microorganism growth and selects microorganisms that could develop on the surface of bioreceptive cementitious materials (Fig. 12.1). The different types of microorganisms are presented below with emphasis on their growth conditions and metabolism.

### *12.2.1. Algae and cyanobacteria*

Algae are eukaryotes (complex cells with many organelles and a nucleus) and unicellular or multicellular organisms generally ranging between 0.5 µm and 1 mm in size. They are photoautotrophic, because they can synthesize organic

matter from atmospheric carbon dioxide in reaction with water in the presence of light. The overall reaction of photosynthesis can be represented as:

$$H_2O + CO_2 \rightarrow CH_2O + O_2 \quad (12.1)$$

During the day, light absorbed by photosynthetic pigments oxidizes the water:

$$2H_2O \rightarrow O_2 + 4H^+ + 4e^- \quad (12.2)$$

Light energy is converted and stored as adenosine triphosphate (ATP) and in reduced nicotinamide dinucleotide phosphate (NADPH). The reduction of the carbon dioxide into carbohydrate occurs during the night according to the following reaction:

$$CO_2 + 4H^+ + 4e^- \rightarrow CH_2O + H_2O \quad (12.3)$$

Algae contain two types of photosynthetic pigments: chlorophyll and carotenoids. Green algae contain high concentrations of chlorophyll, while the dominant constitutive pigments in red algae are carotenoids. Algae are autotrophic organisms, which do not need organic carbon sources for synthesis. These microorganisms can be found on mineral supports, such as cementitious materials. They also need other elements, such as vitamins and elements (N, S, P, K, $M_g$, and Fe) that are present in their environment. The main parameters influencing algal development are humidity, heat, light, and inorganic nutrients. Algal development is favourable under conditions of high and prolonged humidity [7].

Cyanobacteria are prokaryotic organisms characterized by a relatively simple structure without organelles and with a nuclear system (DNA) not delimited by a membrane. Since they are autotrophic, they can use inorganic carbon sources, such as carbon dioxide in the atmosphere or dissolved in water. In contrast to algae, cyanobacteria are much more resistant to adverse conditions, such as high temperatures, UV exposure, and periods of drying. They also contain chlorophyll and other pigments that yield a blue colour. Like algae, their energy source comes from photosynthesis.

### 12.2.2. Fungi

Fungi are chemotrophic eukaryotic organisms unable to photosynthesize, producing their energy from oxidation/reduction reactions. The vegetative apparatus (called the thallus), which allows fungal growth, is composed of elongated vegetative cells, called hyphae. The set of these hyphae establishes a network called the mycelium. Hyphae grow from the tip or apex, which is where the synthesis and degradation reactions of primary metabolism occur and which are essential for the construction of fungal cells. Hyphal tips are characterized by the presence of many cytoplasmic vesicles containing enzymes and synthetic precursors of new polymers. The most common secondary metabolites stored

in the subapical region are pigments and mycotoxins. Substrate colonization occurs through hyphal extension and branching. Hyphae develop from a spore (sexual or asexual) by the emergence of one or more germ tubes and by the growth of a single terminal cell, which is surrounded by a thick protective wall that isolates it from the ambient environment. Spores are produced in large numbers and can survive for several months to several years. Fungi spread as spores settling on new supports. Under favourable conditions, they germinate and produce mycelia.

Fungi are heterotrophic for carbon, because they can only synthetize their cellular components from an organic source of carbon. Fungi are found on organic supports (such as paints) as well as on dead and living organisms. A fungal colonization on cementitious materials requires an accumulation of organic matter on its surface. Fungi have a very high need of moisture, which explains their presence on walls with condensation or capillary action. Increasing moisture leads to the successive appearance of fungal genera, called first (*Aspergillus, Penicillium*), second (*Cladosporium, Ulocladium*), and third colonization (*Stachybotys*). Nevertheless, some fungal strains, such as *Alternaria alternata*, are resistant to extreme conditions, such as very low temperatures and very dry conditions.

*Aspergillus*, *Penicillium*, and *Trichoderma* produce a wide variety of organic acids (acetic, formic, oxalic, and tartaric acids). Some fungal strains, such as *Alternaria*, *Uloclodium*, and *Clodosporium*, produce a dark pigment called melanin. This pigment, present inside the cells, protects them from irradiation, extreme temperatures, and possible desiccation [8].

### 12.2.3. Bacteria

Bacteria are unicellular prokaryotic organisms of medium size varying between 0.1 to 4 μm in width and 0.2 to 50 μm in length. They can be autotrophic or heterotrophic, because they are able to use a mineral or organic carbon source and develop on any type of support, generally inside a biofilm containing a high quantity of water. Most bacteria are chemotropic and use the energy to develop from redox reactions mainly involving reduced sulphur ($H_2S$, $S^0$, $S_2O_3^{2-}$) or nitrogen compounds ($NH_4^+$, $NO_2^-$). The bacteria involved are, respectively, sulphate-reducing/sulphur-oxidizing bacteria and nitrifying bacteria.

Nitrifying bacteria transform ammonium ions into nitrate ions by nitrification, which consists of two reactions: the first is performed by bacteria such as *Nitrosomonas* to form nitrite ions (Eq. (12.4)); the second, by bacteria such as *Nitrobacter* to form nitrate ions (Eq. (12.5)). Both kinds are aerobic and autotrophic bacteria, which draw their carbon source from inorganic sources (gaseous $CO_2$ or dissolved aqueous species such as $CO_3^{2-}$ / $HCO_3^-$). Nitrification consumes $HCO_3^-$ and releases $H^+$; the latter combine with $NO_3^-$ to form nitric acid ($HNO_3$).

$$NH_4^+ + 3/2\,O_2 \rightarrow NO_2^- + 2H^+ + H_2O \tag{12.4}$$

$$NO_2^- + 1/2\,O_2 \rightarrow NO_3^- \tag{12.5}$$

Sulphate-reducing bacteria, which are strictly anaerobic, can use sulphur compounds (mainly sulphate ions) as a final acceptor of electrons in the cellular respiration process. Organic matter, used as an electron donor, is oxidized to carbon dioxide, while the sulphate ions are reduced to hydrogen sulphide (Eq. (12.6)). *Desulfovibrio* and *Desulfobulbus* are the bacteria most commonly involved in this reaction.

$$SO_4^{2-} + \text{organic matter} \rightarrow H_2S + H_2O + CO_2 \quad (12.6)$$

Under aerobic conditions, sulphur-oxidizing bacteria are able to oxidize the sulphur-containing compounds generated ($S^0$, $S_2O_3^{2-}$) into sulphate ions and sulphuric acid (Eq. (12.7) and Eq. (12.8)).

$$S_2O_3^{2-} + 2O_2 + H_2O \rightarrow 2SO_4^{2-} + 2H^+ \quad (12.7)$$

$$S^0 + {}^3\!/_2 O_2 + H_2O \rightarrow SO_4^{2-} + 2H^+ \quad (12.8)$$

Sulphur-oxidizing bacteria can be divided into two groups, according to their pH growth range [9, 10, 11, 12] (Table 12.1):

- Sulphur-oxidizing neutrophilic bacteria, such as *Thiobacillus thioparus, Starkeya novella, Halothiobacillus neapolitanus* and *Thiomonas intermedia.*
- Sulphur-oxidizing acidophilic bacteria, such as *Acidithiobacillus thiooxidans.*

**Table 12.1.** – Growth characteristics of sulphur-oxidizing bacteria responsible for the biodeterioration of cementitious materials.

| | Growth pH | Optimum growth temperature (°C) | Sulphur source | Final products |
|---|---|---|---|---|
| ***T. thioparus*** | 4.5 – 10 | 30 | $H_2S$, $S^0$, $S_2O_3^{2-}$ | $SO_4^{2-}$, $H^+$ |
| ***S. novella*** | 5.0 – 9 | 25 – 30 | $S_2O_3^{2-}$ | $SO_4^{2-}$, $H^+$ |
| ***T. intermedia*** | 1.7 – 9 | 30 | $S_2O_3^{2-}$ | $SO_4^{2-}$, $H^+$ |
| ***H. neapolitanus*** | 3.0 – 8 | 28 – 30 | $H_2S$, $S^0$, $S_4O_6^{2-}$, $S_2O_3^{2-}$ | $SO_4^{2-}$, $H^+$ |
| ***A. thiooxidans*** | 0.5 – 5 | 28 – 30 | $S^0$, $H_2S$, $S_4O_6^{2-}$, $S_2O_3^{2-}$ | $SO_4^{2-}$, $H^+$ |

## 12.3. Interactions between the environment and cementitious materials

### *12.3.1. Ageing of cementitious materials according to the environment*

A cementitious material is made from cement, water, and sand; aggregates can be added to produce concrete. The addition of steel reinforcement yields reinforced concrete.

There are several types of cement, including Portland cements, which are the most widespread with an annual production of around three billion tons. The base component of Portland cement is clinker, which is formed at 1450 °C from a mixture of limestone and clay and contains calcium silicates and calcium aluminates. The French standard NF EN 197-1 [13] defines the proportion of clinker and other constituents of Portland cements. Portland cement CEM I, containing at least 95% clinker, is used as an example in this chapter.

Portland cement reacts with the water supplied during mixing, resulting in many complex chemical reactions grouped under the generic term "hydration". These chemical reactions can vary from one type of Portland cement to another [14]. A paste made with Portland cement CEM I, when fully hydrated, contains as a percentage by weight:

- 15 – 20% portlandite ($Ca(OH)_2$);
- 65 – 70% of hydrated calcium silicate, noted as C-S-H ($1.75\ CaO{\cdot}SiO_2{\cdot}4H_2O$);
- 10 – 20% hydrated calcium aluminates: hydrated calcium monosulphoaluminate ($3CaO{\cdot}Al_2O_3{\cdot}CaSO_4{\cdot}14H_2O$) and ettringite ($3CaO{\cdot}Al_2O_3{\cdot}3CaSO_4{\cdot}32H_2O$).

The main consequence of these chemical reactions is to change the mixture from a fluid state to a solid state by increasing the volume of solids. This volume variation is due to a lower density of the solids formed during hydration compared to the initial solids contained in the cement. This decreased density results from the presence of water molecules in the structure of the solids formed, hence the term "hydration". Nevertheless, the volume of solids at the end of the hydration reaction remains lower than the initial volume of cement and water required for the hydration reaction. This leads to a network of pores in the cement paste. The observed porosity is generally much higher than the theoretical porosity considering solely the stoichiometry of the chemical reactions, since an excess of water improves the workability of cementitious materials. Thus, the total porosity and pore distribution are important parameters affecting the ageing of cement paste because the exchange of matter with the environment occurs primarily through connected porosity.

Material exchanges between cement paste and the environment are fostered as the physico-chemical parameters of a Portland cement paste are generally very different from those of the service environment of the cementitious material. The first major difference is relative humidity. In fact, the porosity of the cement paste, initially filled with water, will progressively contain a gaseous phase as water is consumed by hydration reactions. In addition, depending on the relative humidity of the cementitious material's surrounding environment, part of the pore water can be lost to evaporation. Laplace's law can be used to define the critical pore diameter: smaller pores will be filled with an aqueous phase, while larger pores will be filled with water vapour. The pH of the pore aqueous phase is another difference between cement paste and its environment. Indeed, the pores are not filled with pure water but with an aqueous phase high in NaOH and KOH in equilibrium with the solids formed by hydration reactions. Thus, the pH of a cement paste is higher than 13.

Matter exchanges with the external environment are governed by different mechanisms:

- *Diffusion*, which corresponds to the movements of chemicals in a liquid or gaseous phase, outwards or outside the cement paste according to a concentration gradient.
- *Permeability*, which corresponds to a movement of fluid (including any contained elements) into the cement paste under the effect of a pressure gradient, such as hydraulic pressure.

Matter exchanges modify the chemical equilibrium within the cement paste and induce modifications in mineralogy, which affect the porosity of the cement paste. Relatively complex chemical reactions involve dissolution reactions and mineral precipitations [15]. These modifications, which affect mineralogy and porosity, can lead to a reduction in the mechanical performance of the cement paste and cementitious material. The end point of these mechanisms is sometimes the destruction of the structure. Generally, the ageing state of the cementitious material is higher at the surface, since the transport mechanisms of elements start at the surface and propagate deeper into the material.

Depending on the exposure conditions, water (pure or containing aggressive ions) as well as atmospheric carbon dioxide and oxygen can penetrate into a cement paste and cause ageing. Thus, the environmental conditions depend on the cementitious material's position in the structure. For example, foundations might be in contact with interstitial groundwater, while an interior wall would only be in contact with the air. The standard NF EN 206/CN [1] defines suitable concrete formulations based on concrete exposure classes. The moisture state of the cementitious material is one of the most important parameters. Indeed, a dry environment, as for a cementitious material inside a building, would not be conducive to material transport in a liquid phase involving diffusion or permeability. Such an environment would be efficient in transporting material in a gaseous phase. Dissolution and precipitation reactions have very slow kinetics in cementitious materials at low water contents. In contrast, the surface of an exterior cementitious material, subjected to wetting-drying cycles following periods of rain, would rapidly evolve primarily due to two mechanisms: leaching of the cement paste by the water supplied by the external medium, and carbonation of the minerals in the cement paste due to atmospheric carbon dioxide.

Leaching reduces NaOH and KOH concentrations, thereby decreasing the pH of the aqueous phase in the cement-paste pores. This process gradually dissolves the minerals in the cement paste with which the aqueous phase is in equilibrium. Thus, the most soluble minerals will dissolve faster, leading to the creation of porosity and sometimes to the precipitation of less soluble minerals. Portlandite, one of the main minerals in Portland-cement paste, is the most soluble with a solubility close to 20 mmol $L^{-1}$ in pure water at 20 °C. Other hydrates, such as calcium silicate hydrate, have a solubility of the order of a few µmol $L^{-1}$. This lower solubility confers good resistance to leaching.

Ions penetrating cement-paste pores can induce new chemical reactions by reacting with the ions in the pore aqueous phase. Thus, carbon dioxide penetrates the pores of the cementitious matrix in a gaseous phase, before dissolving and hydrating as carbonic acid ($H_2CO_3$) in the pore aqueous phase. Calcium ions in the aqueous phase – in particular to achieve equilibrium with portlandite – can react to form calcium carbonate, usually calcite. Thus, the carbonation of cement paste initially transforms portlandite into calcite. When all the portlandite has been carbonated, greater carbonation can affect all the other hydrates, in particular, calcium silicate hydrate (C-S-H) [16].

Carbonation and leaching reactions lead to a decrease in the interstitial solution pH in equilibrium with the new minerals formed, in particular, calcite. Thus, the pH gradually decreases from 13 to 9 between the unaltered core and the altered surface of the cementitious material [17]. In general, if diffusion alone is considered as a material transport mechanism, the altered thickness varies as a square-root function of time (initial approximation). Thus, the surface of a cementitious material subjected to wetting-drying cycles is rapidly leached and carbonized from 1 to 3 mm in depth, depending on the cement-paste characteristics and, in particular, its total porosity. In addition, large altered thicknesses can be observed over longer periods of time, which can lead to the most frequent pathology affecting reinforced concrete: reinforcement corrosion. Indeed, steel reinforcement in contact with an undamaged cement paste with a pH higher than 13 is protected by the passivating alkaline environment. When the pH drops below 10 due to carbonation and leaching, the steel becomes exposed to more acidic conditions, resulting in generalized corrosion.

Leaching is more severe when produced by acidic pH levels. The mechanisms involved are chemical and/or acidic attack of the cementitious material. All acids dissolve cement-paste solids with an intensity that increases with the solubility of the calcium salt formed with the acid's anion. For instance, hydrochloric acid (HCl) attacks more aggressively than sulphuric acid ($H_2SO_4$), since $CaCl_2 \cdot xH_2O$ is far more soluble than calcium sulphates, especially gypsum ($CaSO_4 \cdot 2H_2O$). Organic acids are also known to be very aggressive towards cement paste.

Generally speaking, increased temperature in the environment accelerates the different chemical reaction kinetics involved in altering cementitious materials. Increased temperature also tends to accelerate material transport rates, in particular, by increasing the diffusion coefficient value.

### *12.3.2. Biocolonization of cementitious materials*

Biocolonization is known to occur much slower on freshly-built surfaces, such as concrete and cementitious materials, when the surface pH is initially higher than 11. With time, the combined action of water and atmospheric carbonation leads to a progressive decrease in pH on the building surface. At about 9, it is low enough to allow microbial growth because the surface of cementitious

materials represents a good substrate for microorganisms. Biocolonization mainly depends on the environmental conditions conducive to the development of microorganisms. Temperature and water are the main parameters related to climate and seasons for cementitious materials in external environments.

The optimal temperature for most microorganisms ranges from 15 °C to 35 °C. Too low a temperature reduces the kinetics of the enzymatic reaction, which governs microbial metabolism and growth. Too high a temperature damages microbial cells by distorting enzymes and proteins in their transport systems. Some microorganisms, however, are able to withstand temperatures close to 0 °C (psychrophilic organisms) and equal or higher than 70 °C (thermophilic organisms). Sulphur-oxidizing bacteria in sewage systems are mesophilic and have optimal growth temperatures of around 30 °C [18]. Thus, countries with warm climates experience higher biodeterioration in sewer pipes. The thermal properties of the cementitious material can impact the temperature of the surface on which microorganisms develop. A cementitious material exposed to solar radiation can have a surface temperature higher than that of ambient air, leading to different levels of colonization on northern and southern faces.

Humidity is very important in the biocolonization process, because water is an essential component in microorganism development. In addition to being essential to the functioning of microorganisms, water is involved in transporting gases and nutrients. The water available depends, in turn, on the environment. The cementitious material can have an impact on water retention and on its availability to microorganisms under drier conditions. Nevertheless, phototrophic microorganisms may develop mechanisms of dehydration resistance. Algae may secrete mucilaginous substances to prevent water loss [19] or produce intracellular polyols as desiccation protectants [7].

Material porosity and, more specifically, pore size, are parameters that govern matter exchange, on one hand, and, on the other hand, the quantity of water absorption and retention. High porosity associated with small-diameter pores, such as in concrete paste, allows humidity to penetrate deeply in the material while limiting evaporation when the relative humidity of the external environment decreases. Thus, materials with small pores facilitate microorganism development on their surface [20]. A facade that is often wet is conducive the growth of microorganisms, such as algae and cyanobacteria [21]. Thus, only water, light, and an acceptable temperature are needed to allow these microorganisms to grow on the carbonated and/or leached surface of a cementitious material.

Algae and cyanobacteria do not require the presence of organic or inorganic compounds, such as carbon and energy sources. These microorganisms derive their energy from photosynthesis. Accordingly, the total absence of light is an inhibiting factor, but this, of course, is never the case outdoors. Excessive or extended sunlight, however, has an inhibiting effect as the result of excessive light intensity and the material drying out more quickly. Sun and shadow conditions determine which species will grow. Non-photosynthetic microorganisms

require an accumulation of carbon and energy sources on the surface of the cementitious material, which can be facilitated by increased surface roughness. The air pollution linked to urbanization produces organic and inorganic particles that are deposited on materials (like facade coverings) and serve as nutrient sources for microorganisms. Wind plays a role in transporting and dispersing these particles and microorganisms, facilitating the biocolonization of different supports. Facades become soiled more rapidly when facing north and exposed to prevailing winds. Rain and wind can really accelerate this process. Conversely, wind can dry out walls and facades in dry, warm climates. In some confined environments, such as sewer pipes, fluctuations in wastewater flows directly influence the development of sulphate-reducing and sulphur-oxidizing bacteria. Indeed, these fluctuations change wastewater composition, more or less rapidly renewing nutrients, dissolving oxygen, and releasing hydrogen sulphide from the wastewater to the exposed portions of pipes with surface condensation. Some components of cementitious materials can also serve a source of nutrients for microorganisms. For example, some plant fibres – such as hemp, which is used increasingly in cementitious materials – can be a source of organic carbon. Some aggregates and limestone fines can also contribute mineral carbon as carbonate ions. Moreover, *Pseudomonas* can use chemical elements in glass phases, such as the blast-furnace slag added to some Portland cements.

The roughness of the cementitious material's surface is also an important parameter for microorganism attachment. Indeed, surface asperities serve as anchor points, facilitating water and nutrient retention, and improve the conditions for microorganism development. The roughest materials are the most colonized by microorganisms [22]. Tran *et al.* [23] have observed that *Klebsormidium flaccidum* algal cells grow better on rough mortars than on smooth ones. Other parameters related to bioreceptiveness need to be considered: the zeta potential or the tension of the cementitious material's surface can influence the adhesion of microorganisms and biofilm.

Microorganism colonization of materials is nevertheless complex because it involves a succession of microorganisms that are naturally selected according to the environmental conditions and the cementitious material's properties. The development of the first colonizers changes the physicochemical parameters of the surface, paving the way for colonization by new microorganisms. Wall colonization is a prime example of microbial succession [24]. Among the strains isolated, the green algae *Klebsormidium* is the main strain detected on the facades in Europe [25, 26]. Other algal strains have been isolated: *Trentepohlia* [27], *Stichoccus*, *Trebouxia* [25, 26], and *Chlorella* [26, 28]. Samplings at European sites reveal that algae and cyanobacteria are often found together, with a predominance of algae. *Phormidium* and *Microcoleus* (filamentous form) and *Gleocapsa* and *Chroococcus* (unicellular form) are the cyanobacteria most commonly encountered [22, 26]. Sewer pipes also host a succession of microorganisms, depending on the surface pH of the cementitious material covering the pipe [12].

## 12.4. Interactions between the environment and cementitious materials: biodeterioration

The biodeterioration of cementitious materials most often occurs due to the combined effects of several microorganisms (bacteria, cyanobacteria, fungi, algae) that colonize the material's surface, generally resulting from the development of a biofilm when environmental conditions are conducive. This can lead to various kinds of biodeterioration (aesthetic, mechanical, or chemical) that can change the properties of a material, such as its mechanical characteristics, and entail a structural risk to the building.

### *12.4.1. Aesthetic biodeterioration*

The development of microorganisms on the surface of cementitious materials can have aesthetic impacts without any loss of material performance. This can take the form of stains, which appear mainly on facades, walls, and slabs. The colours observed are primarily green, red, yellow-orange, grey, and black, depending on the biogenic pigment secreted by the species (Urzi *et al.,* 1992, 1993) [29, 30]. The stains appear in various colours caused by the development of several microorganisms in the biofilm.

This biological fouling is due to climatic cycles, especially differences in temperature and brightness between seasons, and humidity variations between rainy and dry periods, which allow the development of microorganisms, such as fungi, algae, and cyanobacteria.

Fungi are involved in this process because they produce pigments, such as melanin and melanoidins, which produce a brownish-black discoloration of material surfaces, such as is the case with *Alternaria alternata* and strains of the genera *Dematiceous* and *Exopholia* [31]. Fungi generally form blackish visible dirt with circular shapes. Algae and cyanobacteria produce photosynthetic pigments, such as chlorophyll, responsible for the green stains observed on facades under wet and humid conditions [29, 31]. Large trails of dirt are formed, along water lines when the edges of facades are poorly protected. Other algae, belonging to the *Trentepohliales* order, produce large quantity of carotenoids, in particular β-carotene, which give them their typical red, orange, or yellow pigmentation [32].

Biological fouling represents a significant economic loss due to maintenance and repair costs.

### *12.4.2. Mechanical biodeterioration*

Physical biodeterioration results from the pressure exerted by growing microorganisms on the inorganic materials. In fact, fungal colonization can lead to cracks of the cementitious materials. Like tree roots, which can produce cracks in houses and roads, fungal hyphae can penetrate the material's open porosity. Their development can generate some mechanical pressure within the

cementitious material, which can lead to microcrack formation once the material's elastic limit has been exceeded, and ultimately to superficial scaling of the cementitious material as multiple microcracks coalesce [24]. Dematiaceous fungi, like *Phoma*, *Conosporium*, and *Alternaria*, are responsible for the physical attack of cementitious materials, such as marble and limestone [33]. *Alternaria alternata* is frequently found on sampling sites [34]. In addition to its role in the aesthetic deterioration of a material, *Alternaria alternata* could cause physical deterioration by the deep hyphal anchoring.

The polymeric extracellular substances of the biofilm, containing polysaccharides, (glycol)proteins, and (glycol)lipids, are also involved in the biodeterioration of cementitious materials. Indeed, during dry and wet cycles, they undergo shrinkage and swelling. While the cementitious material is also subject to some volumetric variations during these cycles, such variations differ between the biofilm and cementitious material. After repeated cycles, these volumetric variations could lead to pressure at the interface between the biofilm and cementitious material. If this mechanical pressure exceeds the material's elastic limit, microcracks are generated. Even though they do not destroy the cementitious material, these microcracks constitute key areas of opportunity for new pathologies, such as the corrosion of steel reinforcement.

### 12.4.3. Chemical / mechanical biodeterioration

Chemical deterioration results from the action of chemicals metabolized by microorganisms on the components of cementitious materials. Generally, all acids produced by microorganisms can dissolve the cementitious matrix and sometimes lead to the precipitation of reaction products, such as poorly soluble calcium salts formed with the anion of the acid. The precipitation of minerals in the cement paste's porosity can induce high crystallization pressures, which initially lead to microcracking and then followed, at more advanced stages, to an expansion of the cementitious material with an almost total loss of mechanical strength. Dissolution of the minerals in the cement paste is also responsible for a decrease in the cementitious material's mechanical strength; due, in this case, to increased porosity, as dissolved solids are not replaced.

Microorganisms can metabolize acetic, carbonic, gluconic, nitric, sulphuric acids, and other types of acid. Fungal strains, such as *Aspergillus*, *Penicillium*, and *Trichoderma*, are acidogenic, since they produce organic acids, such as oxalic, citric and propionic acids. *Aspergillus niger* is the species often identified during sampling on altered buildings [35]. Subsequent to mycelial growth on the surface of materials, the organic acids produced solubilize calcite and secondary minerals, which precipitate along the hyphae and on the top of mycelia [36], leading to crust formation.

Bacteria are also involved in chemical biodeterioration subsequent to the metabolizing of sulphuric acid by sulphur-oxidizing bacteria or nitric acid by nitrifying bacteria, such as *Nitrosomonas* and *Nitrobacter*.

Nitrifying bacteria are responsible for altering cementitious materials in water-treatment ponds, which contain wastewater with both carbon and nitrogen

pollution [37]. More precisely, this alteration occurs in nitrification tanks. The organic nitrogen contained in wastewater is initially oxidized to ammonium ions with or without bacteria. Ammonium ions are then biotransformed into nitrate ions by nitrification (Eq. (12.4) and Eq. (12.5)). The $H^+$ released during this reaction associate with the nitrate ions to form nitric acid (Eq. (12.9)).

$$NH_4^+ + 2O_2 \rightarrow NO_3^- + 2H^+ + H_2O \quad (12.9)$$

Portlandite, which is the most soluble phase, is the least resistant to acid attack. Biogenic nitric acid reacts first with portlandite ($Ca(OH)_2$) in the cementitious material to form calcium nitrate, which is very soluble and does not precipitate in the cementitious matrix (Eq. (12.10)).

$$HNO_3 + Ca(OH)_2 \rightarrow Ca(NO_3)_2 + H_2O \quad (12.10)$$

Cementitious materials are generally not completely destroyed by this acid attack in water-treatment plants [37]. The loss of mechanical performance, however, leads to integrity problems in certain technical areas, such as floors containing injection nozzles.

Sewage networks are not favourable environments for the durability of cementitious materials in pipes, manholes and wastewater collectors. Alteration of cementitious materials in sewers is due to sulphuric acid generated by sulphur-oxidizing bacteria. The water flowing into the sewer pipes is necessary for the implementation of the biodeterioration process because the water fosters oxidation of the hydrogen sulphide on pipe surfaces and allows sulphur-oxidizing bacteria to develop optimally. Water accelerates reaction kinetics by acting on the reaction substrate ($S^0$, $S_2O_3^{2-}$) and by allowing the transport of aggressive molecules ($H^+$, $SO_4^{2-}$) from the surface to the core of the cementitious material. In the case of sewer systems, wastewater pH affects the microbial species that colonize the immersed part of the pipe and the nature of the chemicals. As wastewater is slightly acidic (pH of about 6), the hydrogen sulphide produced by the sulphate-reducing bacteria is essentially $H_2S$ (aqueous phase). The pH of the surface of the sewer pipes influences colonization and biodeterioration rates. Indeed, different species of sulphur-oxidizing bacteria will develop: initially, depending on the material's surface pH: neutrophilic bacteria and, then, acidophilic bacteria, when the pH reaches about 5 [11, 12]. biodeterioration will therefore be the combined effect of a chemical attack due to the presence of $H^+$ and a sulphate attack linked to the occurrence of sulphate. The acid attack initially begins to dissolve primarily portlandite, which is the most soluble hydrate in cement paste. Thus, significant quantities of calcium ions can be in contact with sulphate ions, which might lead to gypsum precipitation (Eq. (12.11)):

$$Ca(OH)_2 + H_2SO_4 \rightarrow CaSO_4 \cdot 2H_2O \quad (12.11)$$

The gypsum formed reacts with hydrated calcium monosulphoaluminate to form ettringite (Eq. (12.12)):

$$2CaSO_4 \cdot 2H_2O + 3CaO \cdot Al_2O_3 \cdot CaSO_4 \cdot 12H_2O + 18H_2O \rightarrow 3CaO \cdot Al_2O_3 \cdot 3CaSO_4 \cdot 32H_2O \quad (12.12)$$

Gypsum and ettringite precipitation can damage the cementitious material by generating microcracks if the volume precipitated of these solids is greater than the material's porosity, especially if the pore size is less than 1 μm. Continued acid attack keeps decreasing the pH of the cement paste. Hydrated calcium monosulphoaluminate and ettringite dissolve in turn. This leads to the precipitation of aluminium hydroxide (often poorly crystallized), but generally no gypsum, since the sulphate concentration is not high enough (Eq. (12.13) and Eq. (12.14)):

$$3CaO{\cdot}Al_2O_3{\cdot}CaSO_4{\cdot}12H_2O + 3H_2SO_4 \rightarrow 4(Ca^{2+}, SO_4^{2-}) + 12H_2O + 2Al(OH)_3 \quad (12.13)$$

$$3CaO{\cdot}Al_2O_3{\cdot}3CaSO_4{\cdot}32H_2O + 3H_2SO_4 \rightarrow 6(Ca^{2+}, SO_4^{2-}) + 32H_2O + 2Al(OH)_3 \quad (12.14)$$

Concomitantly, the calcium silicate hydrate (C-S-H) gradually loses part of its calcium: the $CaO$ / $SiO_2$ molar ratio increases from 1.75 to 1. Then, C-S-H dissolves when the pH falls below 4. This leads to the formation of a silica gel (Eq. (12.15)):

$$CaO{\cdot}SiO_2{\cdot}3H_2O + H_2SO_4 \rightarrow (Ca^{2+}, SO_4^{2-}) + 2H_2O + Si(OH)_4 \quad (12.15)$$

When the pH of the deteriorated zone drops below 3, aluminium hydroxide dissolves (Eq. (12.16)):

$$2Al(OH)_3 + 3H_2SO_4 \rightarrow 3(2Al^{3+}, 3SO_4^{2-}) + 6H_2O \quad (12.16)$$

The final product resulting from the complete dissolution of the Portland-cement-based cementitious material is silica gel, which is very difficult to dissolve, even at very low pH levels. Nevertheless, the chemical reactions described above take place successively. This fact leads to a succession of zones within the cementitious material that are increasingly less deteriorated from its surface to its core (Fig. 12.2). The highly deteriorated zones close to the surface lose all their mechanical performance. The dissolution of portlandite decreases the elastic modulus of the cement paste by 50%. It is not uncommon for a sewer pipe to collapse due to the loss of mechanical performance, since it can no longer support the weight of the soil covering it.

| | | | | | |
|---|---|---|---|---|---|
| C-S-H<br>Ettringite<br>Calcium monosulphoaluminate<br>Portlandite | C-S-H d<br>Ettringite<br>Calcium monosulphoaluminate<br>Gypsum | C-S-H d<br>Ettringite<br>$Al(OH)_3$ | C-S-H d<br>$Al(OH)_3$ | $Si(OH)_4$<br>$Al(OH)_3$ | $Si(OH)_4$ |

C-S-H d: decalcified C-S-H

**FIG. 12.2.** – Zonation of a Portland-cement paste resulting from attack by biogenerated sulphuric acid.

## 12.5. Scientific approach to study the biodeterioration of cementitious materials

Taking biodeterioration of building materials into account is a recent consideration; only the most severe or costly cases are studied with a scientific approach aimed at developing more resistant cementitious materials. The various stages of this procedure, shown in figure 12.3, requires many years of investigation. It starts with the discovery of a pathology induced by microorganisms. Once the conditions underlying the appearance of the biodeterioration are known, it is advisable to try to reproduce the "pathology" in laboratory with tests conducted under controlled (and often simplified) conditions, such as the use of only a single microorganism instead of multiple microorganisms. These laboratory tests must yield an understanding of bio-physico-chemical mechanisms and their impact on the cementitious material's properties. Performance tests, sometimes standardized, are used to develop optimized materials. Nevertheless, these tests must be supplemented by numerical simulations, because longer durations, which are difficult to obtain even with accelerated conditions, should be taken into account.

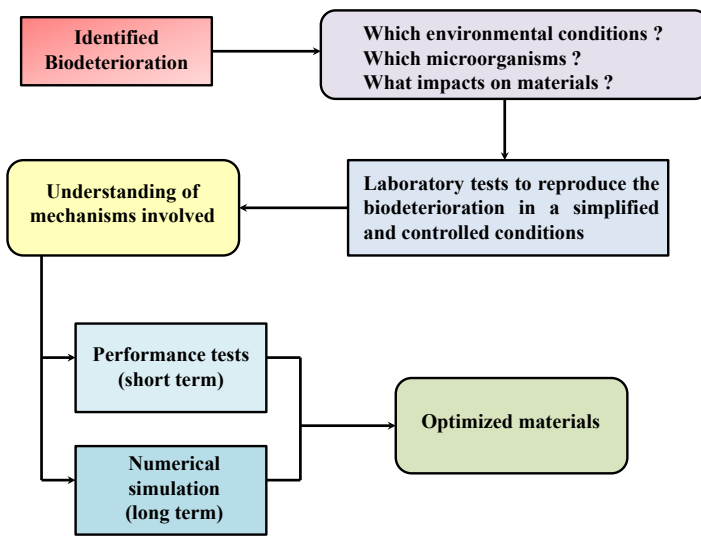


**Fig. 12.3.** – Scientific approach to the biodeterioration of cementitious materials.

Laboratory tests have been developed in the last 20 years to study accelerated biodeterioration and to simulate *in situ* conditions in laboratory that increasingly reflect field conditions. These tests are complex to implement because they must take into account:

- The optimal conditions for microbial growth and the influence of chemicals from the bacteria on the material;

- The evolution in microbial activity and the biological metabolites produced during the biodeterioration process;
- The chemical evolution of the reaction medium in which the biodeterioration occurs and the impact of the chemicals released by microbial activity;
- Microscopic and macroscopic evolutions of materials.

At this point in time, there are no effective tests on which consensus has been reached in Europe. Only laboratory tests aimed at studying the aesthetic biodeterioration of facades and chemical biodeterioration in sewage networks have been developed.

### 12.5.1. Laboratory tests for aesthetic biodeterioration

Several tests have been developed recently to assess the bioreceptivity of cementitious materials. They are generally based on the same concept: the generation of a flow of microbial suspension on the surface of a material inclined at 45° [23, 25, 38]. The test devices are equipped with neon lamps to reproduce a 12-hour photoperiod for the development of phototrophic microorganisms. These tests differ according to substrate type and the microorganisms tested, which may be algae or cyanobacteria, studied individually or as a mixture (Table 12.2).

**TABLE 12.2.** – Aesthetic biodeterioration tests in laboratory.

| Materials | Microorganisms | Methods for biomass quantification | References |
|---|---|---|---|
| Small calcareous granite<br>Siliceous stone<br>White cellular concrete<br>Portland mortar<br>Brick | Mixture of algae (*Chlorella* sp., *Stichococcus bacillaris, Klebsormidium flaccidum*), cyanobacteria (*Lyngbya diguetii*), and mosses (*T. muralis*) | Visual observations | [39] |
| Portland mortars CEM I | *Chroococcidiopsis, Lyngbya, Nostoc Chlorella, Chlorhormidium, Stichococcus, Haematococcus, Trentepohlia* | Image analysis<br>Reflectance<br>Chl *a* and Pheo *a* | [22, 40] |
| Paintings<br>Portland CEM I mortars | Native algae: *Klebsormidium flaccidum, Chlorella mirabilis*, and *Stichococcus bacillaris*<br>Native cyanobacteria: *Chroococcidiopsis fissurarum* | Image analysis | [41] |
| Portland CEM I mortars, carbonated or not | *Klebsormidium flaccidum* | Image analysis<br>Colorimetry<br>Fluorescence<br>Dry mass<br>Optical density | [42] |

| Materials | Microorganisms | Methods for biomass quantification | References |
|---|---|---|---|
| Portland CEM I mortars treated with biocides and water repellents | *Chlorella vulgaris* | Image analysis<br>Colorimetry | [43] |
| Portland mortars CEM I MPC* mortars | *Chlorella vulgaris* | Image analysis<br>Colorimetry<br>Chl *a*<br>Fluorescence<br>Dry mass | [38] |
| Portland mortars treated with $TiO_2$ in emulsion | Mixture of *Chorella, Volvox, Aphanothece, Mallomonas* | Image analysis<br>Colorimetry | [44] |
| Portland mortars<br>Aluminous mortars | *Klebsormidium flaccidum* | Image analysis<br>Colorimetry<br>Fluorescence<br>Dry mass<br>Optical density | [45] |

*: MPC mortars: mortars based on magnesium phosphate cement

These laboratory tests have revealed the influence of the intrinsic characteristics of these materials. The influence of roughness has been clearly demonstrated by the tests presented in table 12.2, whereas the effect of the porosity remains controversial, since these tests are most often conducted under conditions with water-vapour saturation [23]. Surface pH also appears to be one of the main parameters influencing colonization rate [23, 38]. These devices have also provided for determining the influence of the material's chemical composition by testing different types of cements (Portland cements, calcium aluminate cements, *etc.*) [45]. The surface application of biocides (silver nanoparticles), of substances destroying organic matter in the presence of a light source ($TiO_2$) [44], and of water repellents (aluminium stearate, alkyl alkoxy silane) [43] made it possible to assess their effectiveness in limiting microbial colonization.

### 12.5.2. Laboratory tests for the chemical/mechanical biodeterioration

Many experimental devices have been introduced to study the mechanisms involved in attacks by acid biodeterioration in sewage systems. The laboratory tests vary, depending on the experimental protocol used (nutrient source, bacterial strains, kinds of test), temperature, humidity, the materials used, and the means implemented to study the microstructure and mineralogy of the cementitious material (Table 12.3).

**Table 12.3.** – Laboratory tests of biodeterioration by an acid biological attack.

| Tests | Materials | Bacteria | Nutrients | Conditions | Measured parameters | References |
|---|---|---|---|---|---|---|
| Periodic spraying with a concentrated bacterial culture of concrete samples placed vertically<br>Periodic spraying of the sulphide source | OPC concretes<br>60 × 11 × 7 cm | Mixture of NSOB (*T. int.*, *S. nov.*, *H. neapo.*), and ASOB (*A. thio.*) | $H_2S$, $CH_3SH$, or $S_2O_3^{2-}$ | 30°C<br>270 days | pH surface<br>Sample weight<br>Bacterial density | [50] |
| Mortar samples half immersed individually in wastewater in a specific environment or distilled water.<br>Inoculation every two weeks with a mature bacterial culture | OPC mortars<br>4 × 4 × 16 cm | *A. thio.* | $H_2S$ | 180 days | Damaged thickness<br>Bacterial density | [53] |
| Fermentor connected to a bioreactor containing mortar samples immersed 5 min every hour in a mature bacterial culture | OPC and CAC mortars<br>6 × 1 × 1 cm | *A. thio.* | $S^0$ | 28°C –30°C<br>150 days | Sample weight<br>Bacterial density on mortar surface | [54] |
| Fermentor connected to a Soxhlet extractor containing samples of cement paste immersed every 7 hours for 1 month in a mature bacterial culture | Cylindrical cement paste OPC<br>1.5 × 2 cm | *A. thio.* | $S_4O_6^{2-}$ | 40 days | pH of leachate<br>$[SO_4^{2-}]$, [Ca]<br>Damaged thickness<br>Microstructure (SEM) | [55] |
| Concrete samples immersed in the environment with a bacterial suspension for 17 days, then incubated in a chamber containing a high concentration of $H_2S$<br>4 cycles performed | Cylindric concrete<br>OPC (CEM I or III)<br>Siliceous or calcareous aggregates<br>8 × 1.5 cm | Mixture of SOB | $H_2S$ | 20°C<br>17 days | Damaged thickness<br>Loss of weight<br>Roughness<br>State of surface (SEM) | [49] |

| Tests | Materials | Bacteria | Nutrients | Conditions | Measured parameters | References |
|---|---|---|---|---|---|---|
| Concrete samples suspended individually in an Erlenmeyer flask (1 L) containing 600 mL of wastewater in contact with $H_2S$ | OPC concrete<br>5 × 2 × 2 cm | Mixture of *Acid. cryp, H. neapo.*, T thiop., *A. thio.* | $H_2S$ | 25°C<br>240 days | Damaged thickness<br>Loss of weight<br>Bacterial density<br>pH of the reaction solution<br>$[SO_4^{2-}]$, [Ca], $[H_2S]$<br>Surface microstructure (XRD) | [46] |
| Mortar samples placed in a test room (1 $m^3$) equipped with a spray system to vaporize the bacterial suspension in an atmosphere containing $H_2S$ | Cubic mortars<br>OPC (CEM I and CEM III)<br>CAC<br>2 cm cubes | Mixture of *S. nov.*, *H. neapo.*, *A. thio.* | $H_2S$ | 30°C<br>100% RH<br>1080 days | Loss of weight<br>pH surface<br>Bacterial density | [51] |
| Mortar samples immersed individually in 600 mL of a mature bacterial culture | Cylindrical mortars<br>OPC and CAC<br>2.2 × 7 cm | *A. thio.* | $S_2O_3^{2-}$ | 30°C<br>150 days | Bacterial density<br>pH of the reaction solution<br>Damaged thickness<br>[Al], [Si], [Ca]<br>Microstructure (SEM)<br>Attack index | [47] |
| Mortar samples immersed individually in 600 mL of a bacterial culture at the beginning of the exponential phase<br>4 cycles lasting 21 days | Cylindrical mortars<br>OPC and CAC<br>2.9 × 6.3 cm | *H. neapo.*<br>*A. thio.*<br>*H. neapo. / A. thio.* | $S_2O_3^{2-}$ | 30°C<br>84 days | Bacterial density<br>pH of reaction medium<br>Damaged thickness<br>[Al], [Si], [Ca], [Fe]<br>Microstructure (SEM)<br>Volumetric attack index | [48] |

*Acid. cryp.*: *Acidiphilium cryptum*; *H. neapo.*: *H. neapolitanus*; T. *thiop.*: *T. thioparus.*; *A. thio.*: *A. thiooxidans*; SOB : sulphur-oxidizing bacteria; NSOB : neutrophilic sulphur-oxidizing bacteria; ASOB: acidophilic sulphur-oxidizing bacteria

Studying biodeterioration in laboratory requires a sterile environment to avoid any external contamination. In order to achieve a mass balance at the end of the test between the cementitious material and the chemicals released into the reactive medium, it is necessary to study the biodeterioration of the samples of the cementitious material individually [12, 46, 47, 48].

In the case of an attack by sulphuric acid generated by sulphur-oxidizing bacteria, different sources of sulphide can be used, such as $S^0$, $S_2O_3^{2-}$, $S_4O_6^{2-}$, and $H_2S$. Most devices use *A. thiooxidans* [46, 47, 49, 50], which is an acidophilic sulphur-oxidizing bacterium and few devices are based on neutrophilic sulphur-oxidizing bacteria, such as *Halothiobacillus neapolitanus* [51]. It only represents the last step of the biodeterioration process and does not reflect the actual process of bacterial succession from neutrophilic to acidophilic bacteria. While tests using a mixture of neutrophilic and acidophilic sulphur-oxidizing bacteria are more representative of *in situ* conditions, they are very slow, taking up to a year of experimentation [48, 52].

Biodeterioration can be quantified with an attack index calculated from the proportion of major chemical elements (Ca, Si, Al, Fe) leached for a given amount of biogenerated acid [51]. This attack index has been related to the attacked volume relative to the initial volume of the material sample in order to differentiate an intensive surface attack from a moderate attack affecting a larger volume due to deeper penetration [48]. The volumetric attack index also allows for differentiating the intensity of the attack by neutrophilic or acidophilic sulphur-oxidizing bacteria. Indeed, the volumetric attack index induced by the acidophilic bacteria is higher, which is a sign of more extensive biodeterioration.

## 12.6. Conclusion

The biodeterioration of cementitious materials is the result of complex interactions between materials, environment and microorganisms. The multitude of factors occurring in this process makes it difficult to understand the mechanisms involved and the factors that have a dominant impact on microorganisms. The biodeterioration of cementitious materials has only been studied recently due to some cases of alteration of structures, such as sewer systems, which stand out as major economic and societal challenges. In addition to the scientific aspects aimed at better understanding the phenomena involved, consideration should be given to the potential of biodeterioration being linked to a given environment when designing structures that require durability guarantees. This approach can be found in the French standard NF EN 206/CN [1], associated with supplement FD P 18-011 [2]. The latter could be extended to take into account the potentialities of biodeterioration according to service environment.

It is also important to remember that steel corrosion is the main “pathology” affecting reinforced concrete and that microorganisms can also participate in corrosion mechanisms. Thus, under given severe environmental conditions, the

combined effect of chemical attacks and biodeterioration can lead to the destruction of the best concretes currently made, the ultra-high-performance fibre concretes, in only a few years [56]. This example demonstrates that knowledge about service environment based on conventional physico-chemical aspects is not always sufficient enough. Therefore, consideration also needs to be given to the biodiversity of the service environment, the impact of which, on the material, could be initially estimated with a simplified approach. It might be worth considering environmental conditions in order to determine the potential of a microorganism to develop on a cementitious material (Fig. 12.4).

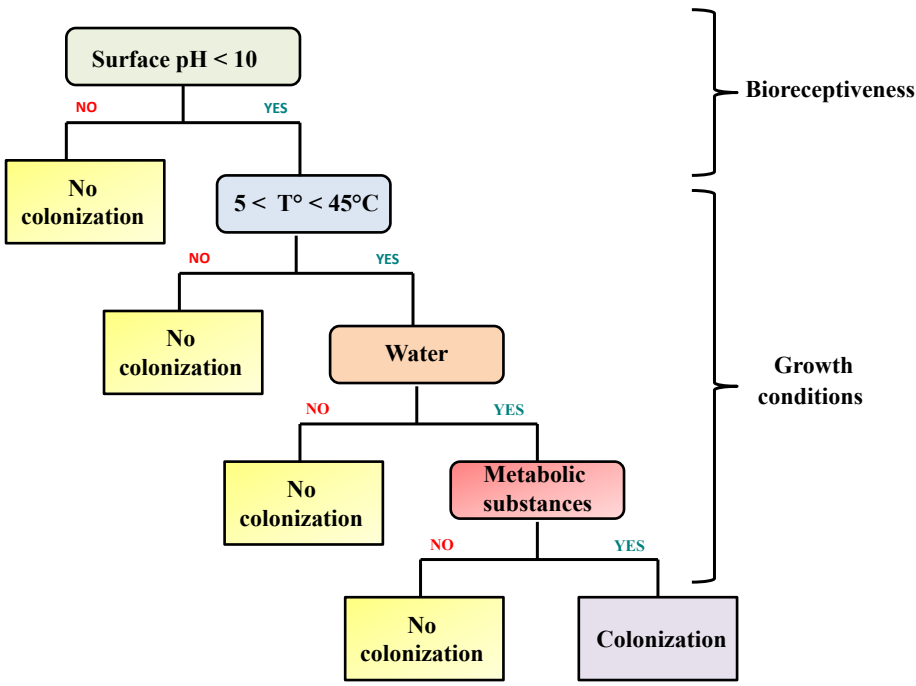


**Fig. 12.4.** – Decision tree for estimating the potentiality of microbial colonization of a cementitious material. T°: temperature.

If environmental conditions allow microbial development, improved knowledge about metabolic substances in the service environment might define the main types of interaction between microorganisms and cementitious materials (Fig. 12.5). The decision tree (Fig. 12.5) provides for a distinction between various types of biodeterioration: aesthetic, mechanical, and chemical (attack by organic or mineral acids) biodeteriorations. This tree also considers the beneficial interactions between microorganisms and cementitious materials, such as during the bioprecipitation of calcite, which can heal microcracks [57, 58].

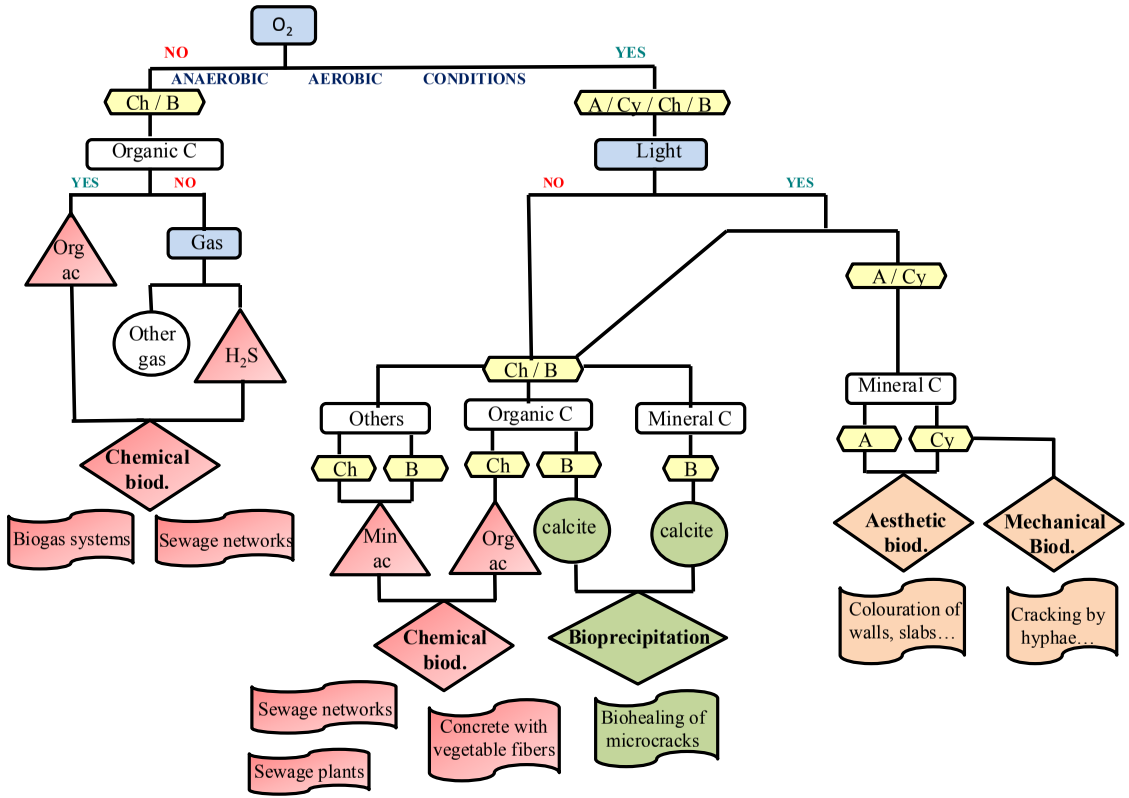


**FIG. 12.5.** – Decision tree for estimating the types of interaction between microorganisms and cementitious materials according to the metabolic substances in the service environment.

*A:* algae; Cy: cyanobacteria; Ch: fungi; B: bacteria; Orga ac: organic acid; Min acid: mineral acid; Organic C: organic carbon source; C mineral: mineral carbon source; Biod: biodeterioration

## References

[1] NF EN 206/CN (2014) Béton - Spécification, performance, production et conformité. Complément national à la norme NF EN 206. AFNOR.
[2] FD P18-011 (2009) Béton - Définition et classification des environnements chimiquement agressifs - Recommandations pour la formulation des béton. AFNOR.
[3] Eggins H.O.W., Oxley T.A. (1980) Biodeterioration and biodegradation. International Biodeterioration Bulletin, 16, 53-56.
[4] Hueck H.J. (1965) The biodeterioration of materials as part of hylobiology. Material und Organismen, 1(1), 5-34.
[5] Van Tittelboom K., De Belie N., De Muynck W., Verstraete W. (2010) Use of bacteria to repair cracks in concrete. Cement Concrete Research, 40, 157-166.
[6] Ducasse Lapeyrusse J. (2014) Autocicatrisation et biocicatrisation des matériaux cimentaires fissurés. PhD thesis, université de Sherbrooke, université de Lille 1, Mines Douai, Sherbrooke et Lille, Canada et France.
[7] Gaylarde P., Gaylarde C. (2004) Deterioration of siliceous stone monuments in Latin America: micro-organism and mechanisms. Corrosion Reviews, 22, 95-415.
[8] Zhdanova N.N., Pokhodenko V.D. (1973) The possible participation of melanin pigment in the protection of the fungus cell from desiccation. Microbiology, 42, 753-757.
[9] Hondjuila Miokono E., Lors C., Lamberet S., Damidot D. (2011) Mise au point d'un test accéléré de mortiers mettant en jeu une succession de bactéries sulfo-oxydantes. Matériaux & Techniques, 99, 555-563.
[10] Lors C., Hajj Chehade M., Damidot D. (2009) pH variations during growth of *Acidithiobacillus thiooxidans* in buffered media designed for an assay to evaluate concrete biodeterioration. International Biodeterioration & Biodegradation, 63(7), 880-883.
[11] Parker C.D., Prisk J. (1953) The oxidation of inorganic compounds of sulphur by various sulphur bacteria. Journal of General Microbiology, 8, 344-364.
[12] Roberts D.J., Nica D., Zuo G., Davis, J. L. (2002) Quantifying microbially induced deterioration of concrete: Initial studies. International Biodeterioration & Biodegradation, 49(4), 221-234.
[13] NF EN 197-1 (2012) Ciment - Partie 1 : composition, spécifications et critères de conformité des ciments courants. AFNOR.
[14] Gartner E., Young J.F., Damidot D., Jawed I. (2002) Hydration of Portland Cement. Bensted J., Barnes P. Eds, Structure and Performance of Cements, Spon Spress, London, UK, 57-113.
[15] Ollivier J.P., Vichot A. (2008) La durabilité des bétons : bases scientifiques pour la formulation de bétons durables dans leur environnement. Ollivier J.P., Vichot A. Eds, Presses Ponts et Chaussées, Paris, France, ISBN 978-2-8578-434-8, 853 p.

[16] Thiery M. (2005) Modélisation de la carbonatation atmosphérique des matériaux cimentaires : Prise en compte des effets cinétiques et des modifications microstructurales et hydriques. PhD thesis, Ecole Nationale des Ponts et Chaussées, Paris, France.
[17] Pu Q., Jiang L., Xu J., Chu H., Xu Y., Zhang Y. (2012) Evolution of pH and chemical composition of pore solution in carbonated concrete. Construction and Building Materials, 28, 519-524.
[18] Parker C. (1945) The Corrosion of Concrete. Aust. J. Exp. Biol. Med., 23, 81-90.
[19] Rindi F. (2011) Terrestrial green algae: Systematics, biogeography and expected responses to climate change. Hodkinson T., Jones S., Waldren S., Parnell J. Eds., Climate change, ecology and systematics, Cambridge University Press, Cambridge, UK, 201-227.
[20] Warscheid T., Becker Th., Braams J., Bruggerhoff S., Gehrmann C., Krumbein W.E., Petersen K. (1993) Studies on the temporal development of microbial infection of different types of sedimentary rocks and its effect on the alteration of the physico-chemical properties in building materials. Thiel M.-J. Ed., Conservation of Stone and Other Materials, E & FN Spon, London, UK, 1, 303-310.
[21] Ortega-Calvo J.J., Arino X., Mernandez-Marine M., Saiz-Jimenez C. (1996) Factors affecting the weathering and colonization of monuments by phototrophic micro-organism. Sciences of the Total Environment, 167, 329-341.
[22] Dubosc A. (2000) Etude du développement de salissures biologiques sur les parements en béton : Mise au point d'essais accélérés de vieillissement. PhD thesis, Institut National des Sciences Appliquées de Toulouse, Toulouse, France.
[23] Tran T.H., Govin A., Guyonnet R., Grosseau P., Lors C., Garcia-Diaz E., Damidot D., Devès O., Ruot B. (2012) Influence of the intrinsic characteristics of mortars on biofouling by *Klebsormidium flaccidum*. International Biodeterioration & Biodegradation, 70, 31-39.
[24] Gaylarde C.C., Gaylarde, P.M. (2005) A comparative study of the major microbial biomass of biofilms on exteriors of buildings in Europe and Latin America. International Biodeterioration & Biodegradation, 55, 131-139.
[25] Barberousse H. (2006) Etude de la diversité des algues et cyanobactéries colonisant les revêtements de façade en France et recherche des facteurs favorisant leur implantation. PhD thesis, Muséum National d'Histoire Naturelle, Paris, France.
[26] Rindi F., Guiry M.D. (2004) Composition and spatial variability of terrestrial algal assemblages occuring at the bases of urban walls in Europe. Phycologia, 43, 225-235.
[27] Crispim C.A., Gaylarde P.M., Gaylarde C.C. (2003) Algal and cyanobacterial biofilms on calcareous historic buildings. Current Microbiology, 46, 79-82.
[28] Tomaselli L., Lamenti G., Bosco M., Tiano P. (2000) Biodiversity of photosynthetic micro-organisms dwelling on stone monuments. International Biodeterioration & Biodegradation, 46, 251-258.

[29] Urzi C.E., Krumbein W.E., Warscheid Th. (1992) On the question of biogenic colour changes of mediterranean monuments (coating-crustmicrostromatoloite-patina-scialbatura-skin-rock varnish). In: Proceedings of the Second International Symposium on The Conservation of Monuments in the Mediterranean Basins. Decrouez, D., Chamay, J., Zezza, F. Eds., Geneva, 397-420.

[30] Urzi C.E., Criseo G., Krumbein W.E., Wollenzien U., Gorbushina A.A. (1993) Are colour changes of rocks caused by climate, pollution, biological growth, or by interactions of the three? Thiel M.-J. Ed, Conservation of Stone and Other Materials, E & FN Spon, London, UK, 1, 279-286.

[31] Warscheid Th., Braams J. (2000) Biodeterioration of stone: a review. International Biodeterioration & Biodegradation, 46, 343-368.

[32] López-Bautista J.M., Waters D.A., Chapman R.L. (2002) The Trentepohliales revisited. Constancea, 83.

[33] Diakumaku E., Gorbushina A.A., Krumbein W.E., Panina L., Soukharjevski S. (1995) Black fungi in marble and limestones – an aesthetical, chemical and physical problem for the conservation of monuments. The Science of the Total Environment, 167, 295-304.

[34] Simonovicova A., Godyova M., Sevc J. (2004) Airborne and soil microfungi as contaminants of stone in a hypogean cemetery. International Biodeterioration & Biodegradation, 54, 7-11.

[35] Urzi C., Realini M. (1998) Colour changes of Notos calcareous sandstone as related to its colonisation by micro-organism. International Biodeterioration & Biodegradation, 42, 45-54.

[36] Fomina M., Podgorsky V.S., Olishevska S.V., KadoshnikovV.M., Pisanska I.R., Hillier S., Gadd G.M. (2007) Fungal deterioration of barrier concrete used in nuclear waste disposal. Geomicrobiology Journal, 24, 643-653.

[37] Leemann A., Lothenbach B., Hoffmann C. (2010) Biologically induced concrete deterioration in a wastewater treatment plant assessed by combining microstructural analysis with thermodynamic modeling. Cement and Concrete Research, 40, 1157-1164.

[38] Manso S., Muynck W.D., Segura I., Aguado A., Steppe K., Boon N., De Belie N. (2014) Bioreceptivity evaluation of cementitious materials designed to stimulate biological growth. Science of The Total Environment, 481, 232-241.

[39] Guillitte O., Dreesen R. (1995) Laboratory chamber studies and petrographical analysis as bioreceptivity assessment tools of buildings materials. Science of The Total Environnement, 167, 365-374.

[40] Escadeillas G., Bertron A., Ringot E., Blanc P., Dubosc A. (2009) Accelerated testing of biological stain growth on external concrete walls. Materials and structures, 42, 937-945.

[41] Barberousse H., Ruot B., Yéprémian C., Boulon G. (2007) An assessment of facade coatings against colonisation by aerial algae and cyanobacteria. Building and Environment, 42, 2555-2561.

[42] Tran T.H. (2011) Influence des caractéristiques intrinsèques d'un mortier sur son encrassement biologique. PhD thesis, université de Saint-Etienne, Mines Saint-Etienne et Mines Douai, Saint-Etienne, France.
[43] De Muynck W., Ramirez A.M., De Belie N., Verstraete W. (2009) Evaluation of strategies to prevent algal fouling on white architectural and cellular concrete. International Biodeterioration & Biodegradation, 63, 679-689.
[44] Radulovic J., MacMullen J., Zhang Z., Dhakal H.N., Hannant S., Daniels L., Elford J., Herodotou C., Totomis M., Bennett N. (2013) Biofouling resistance and practical constraints of titanium dioxide nanoparticulate silane/siloxane exterior facade treatments. Building and Environment, 68, 150-158.
[45] Dalod E. (2015) Influence de la composition chimique de mortiers sur leur biodétérioration par les algues. PhD thesis, université de Saint-Etienne, Mines Saint-Etienne et Mines Douai, Saint-Etienne, France.
[46] Gutiérrez-Padilla M.G.D., Bielefeldt A., Ovtchinnikov S., Hernandez M., Silverstein J. (2010) Biogenic sulfuric acid attack on different types of commercially produced concrete sewer pipes. Cement and Concrete Research, 40, 293-301.
[47] Hajj Chehade M. (2010) Biodétérioration du béton armé par *Acidithiobacillus thiooxidans*. PhD thesis, université de Lille 1, Mines de Douai, Lille, France.
[48] Hondjuila Miokono E. (2013) Essai de biodétérioration de mortiers par une succession de bactéries sulfo-oxydantes neutrophiles/acidophiles. PhD thesis, université de Lille 1, Mines Douai, Lille, France.
[49] De Belie N., Monteny J., Beeldens A., Vincke E., Van Gemert D., Verstraete W. (2004) Experimental research and prediction of the effect of chemical and biogenic sulfuric acid on different types of commercially produced concrete sewer pipes. Cement and Concrete Research, 34, 2223-2236.
[50] Sand W. (1987) Importance of hydrogen sulfide, thiosulfate, and methylmercaptan for growth of Thiobacilli during simulation of concrete corrosion. Applied and Environmental Microbiology, 53, 1645-1648.
[51] Lors C., Hondjuila Miokono E.D., Damidot D. (2017) Interactions between *Halothiobacillus neapolitanus* and mortars: Comparison of the biodeterioration between Portland cement and calcium aluminate cement. International Biodeterioration & Biodegradation, 121, 19-25.
[52] Herisson J. (2012) Biodétérioration des matériaux cimentaires dans les ouvrages d'assainissement : étude comparative du ciment d'aluminate de calcium et du ciment Portland. PhD thesis, université Paris-Est, Paris, France.
[53] Mori T., Nonaka T., Tazaki K., Koga M., Hikosaka Y., Noda S. (1992) Interactions of nutrients, moisture, and pH on microbial corrosion of concrete sewer pipes. Water Research, 26, 29-37.
[54] Hormann K., Hofmann F.-J., Schmidt M. (1997) Concrete with grater resistance to acid and to biogenic sulphuric acid corrosion. Betonwerk + Fertigteil-Technik, 4, 1-8.

[55] Rogers R.D., Knight J.J., Cheeseman C.R., Wolfram J.H., Idachaba M., Nyavor K., Egiebor N.O. (2003) Development of test methods for assessing microbial influenced degradation of cement-solidified radioactive and industrial waste. Cement and Concrete Research, 33(12), 2069-2076.
[56] Hagelia P. (2011) Deterioration mechanisms and durability of sprayed concrete for rock support in Tunnels. PhD thesis, Delft university of technology, Delft, The Netherlands.
[57] Ducasse-Lapeyrusse J., Lors C., Gagné R., Damidot D. (2015) Biocicatrisation : application à la réparation de mortiers âgés. Matériaux & Techniques, 103, 207.
[58] Lors C., Ducasse-Lapeyrusse J., Gagné R., Damidot D. (2017) Microbiologically induced calcium carbonate precipitation to repair microcracks remaining after autogenous healing of mortars. Construction and Building Materials, 141, 461-469.

# 13 Concrete biodeterioration

**Sébastien Roux**

## 13.1. Introduction

Concrete is a material widely used in many fields such as civil engineering, building construction or industrial equipment. With about 4.42 billion tons produced worldwide in 2014, cement-based materials (including concrete) are the most widely used family of materials. As happens to all materials, concrete suffers from aging and that is why cement industry has invested in many studies since the 19th century to increase the resistance of concrete to the environments to which they are subjected [1, 2, 3] and to design and develop more sustainable materials [4].

Cement-based materials alteration is caused by many factors: physical and mechanical – overload (EN 1990 - Eurocode 0, EN 1991 - Eurocode 1, EN 1992 - Eurocode 2 standards), exposure to fire, *etc.* [5] – chemical (carbonation [6, 7], acidic attacks [10, 11, 12]) – rebar corrosion [8, 9] – biological [13]. The deterioration of concrete is generally due to interactions among many of these factors. Concretes are artificial rocks mainly made from cement, aggregates and water. Admixtures used to optimize some properties of the fresh or hardened material also influence its properties for longer or shorter terms. The behaviour of the concrete is influenced by its composition and its implementation which determine its properties of use but also of its microstructure. Microorganisms (bacteria, fungi, algae, lichens, *etc.*) are generally neglected during studies about durability of cement-based materials although they may induce bioalteration (staining and biofilm formation) or biodegradation (mechanical erosion, expansive or soluble product formation, *etc.*) [13].

## 13.2. Material biodeterioration, specificities of concrete

The consideration of the biological factor in aging and evaluation of the durability of cement-based materials is limited by the variability of the parameters, intrinsic and extrinsic and linked especially to the materials themselves. This variability is both induced by their constituents and implementation.

### 13.2.1. Chemical specificity

The specificity and variability of the chemistry of a cement-based material are mainly due to the different constituent elements: cement, aggregates, admixtures and water. Each of these elements influences the physical-chemistry of the hardened material and thus its resistance to bioinduced attacks.

#### 13.2.1.1. Basic ingredients

There are today ten standardized ingredients that can be used in the composition of cements. These are produced specifically for the manufacture of cements (clinker, limestone) or are sub/co-products or residues of industrial processes (high-furnace slag, silica fume, fly ashes). European standard (NF EN 197-1, 2001) defines, according to the proportions of these constituents, so-called main components (> 5% total cement mass), 27 classes of cement for each of which it is possible to add up to 5% of so-called secondary constituents. Hydration of cement, which makes it possible to obtain the concrete mechanical strengths, leads to the crystallization of various hydrates: hydrated calcium silicates, Porlandite, ettringite and hydrated calcium monosulphoaluminate in various rates according to the relative proportions of the basic constituents and of the conditions of hardening (temperature, hygrometry, *etc.*). Each of these standardized ingredients has a compositional variability linked to:

- the raw materials used: natural deposit, treated waste composition, *etc.*
- production sites: manufacturing process, energy sources, *etc.*

Aggregates are the main constituent of concrete with about 70% of their volume. Methods of concrete formulation (Dreux-Gorisse [14], De Larrard [15], *etc.*) are based on the optimization of a granular skeleton maintained in position by a "glue", the cement paste. The aggregates currently used come from two types of deposit:

- massive crushed rocks, usually limestone;
- loose rocks, alluvial, generally siliceous.

The prevalence of transport in the overall cost of aggregates induces the manufacturing of concretes using locally produced aggregates.

#### 13.2.1.2. Admixtures

In order to adapt the materials to the environment or to the conditions of implementation, the use of an admixture originating from the chemical industry is used almost systematically. These admixtures are chemical products of an organic, mineral or organo-mineral nature (poly-carboxylates, lignosulphonates, *etc.*). They are intended to modify the properties of fresh and/or hardened concrete: workability, setting time, reduction of the pore volume, fragmentation of the porosity, rheology, *etc.* Because of the important economic issue of admixture and of the frequency of industrial innovations in this sector, it is particularly difficult to obtain information on the actual composition of

admixtures. The influence of these products on colonization and resistance of cement-based materials to bioinduced attacks has not been studied to date.

### 13.2.2. Physics specificities

The properties of the basic constituents of concrete and their process of implementation also influence the physic properties of the hardened materials and thus the possibilities of contact between the material and the microorganisms.

#### 13.2.2.1. Porous structure

The porous structure of cement-based materials is complex and extends on a large range from nanometre (inter-crystalline porosity of hydrated calcium silicate) up to centimetre (occluded air bubbles). The properties of the porous network depend on:

- the formulation (granular skeleton, porosity and morphology of the aggregates, water content);
- the implementation (temperature, mixing, vibration setting);
- the curing conditions – conditions of materials hardening (temperature, relative humidity).

Two concretes with exactly the same composition can have very different porosity ratio and surface roughness. A large number of standards and articles deal with this phenomenon [16]. The different porosities of the cement paste are connected by a network of capillaries which, due to their shape, their connectivity and their tortuosity, are responsible for the properties of hydric and gaseous transfer through the material.

Different phenomena can locally modify the properties of transfers through the porous network of the material (Fig. 13.1):

- the skin. It is the part of the material in contact with the outside and of which porosity (structuring, texture) is different from the bulk of the material, fluids transfers in it are therefore specific [17];
- micro-cracking of the material. Hydration/hardening reactions of cement result in shrinkage phenomena which, in turn, can generate local cracking. These cracks constitute vectors of rapid penetration of the external agents, whether they be aggressive or not, into the material [18].

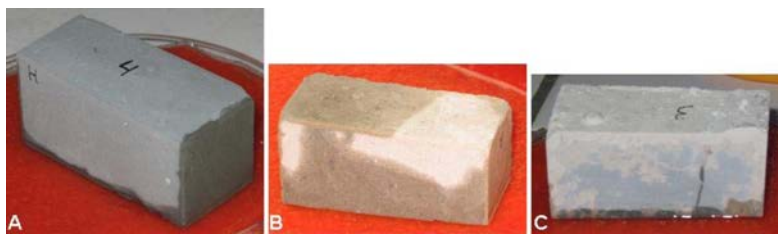


**Fig. 13.1.** – Capillary imbibition tests - skin effect and influence of cracking [18].

### *13.2.2.2. Surface condition: roughness and cracking*

The surface roughness of a cement-based material relates in particular to the quality of the formworks used during pouring and the conditions of compacting of the concrete at fresh state. The surface roughness constitutes anchoring sites for microorganisms and specific sites for deposits of nutrients. The relationship between roughness and biological fouling of material surfaces is thus often mentioned but no direct correlation has been clearly determined. Tests carried out on similar samples but with different surface roughness factors highlight this phenomenon: the density of colonization of these materials according to their roughness seems to present an optimum. [18].

The cracks of very variable openings allow the penetration of microorganisms [19] and thus the secretion of aggressive metabolites at depth in the material (Fig. 13.2).

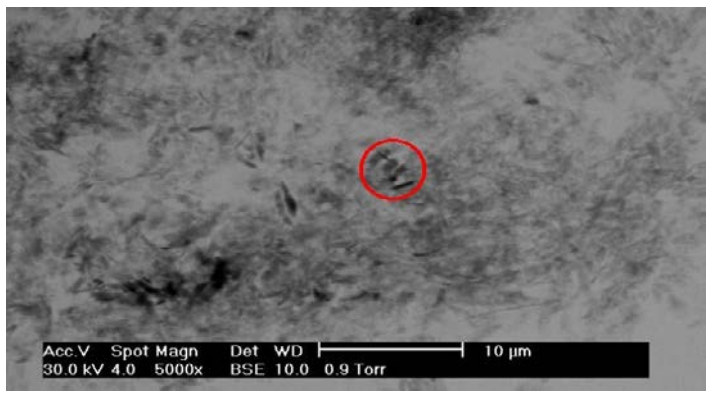


**FIG. 13.2.** – Penetration of bacteria into the cracks of a cement paste: bacteria observed on the walls of the crack (STEM observation) [20].

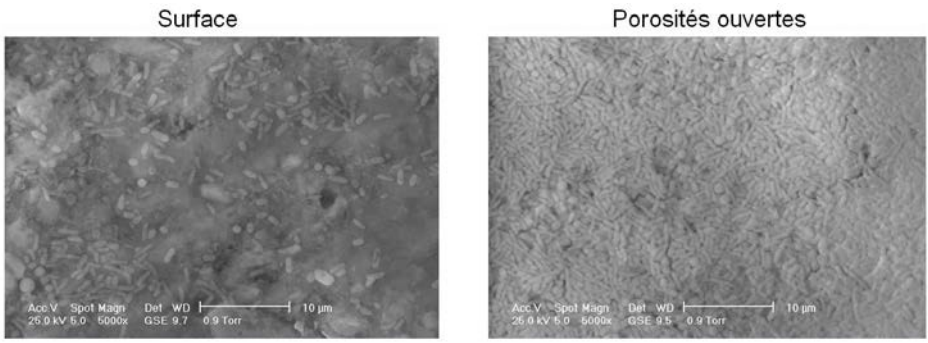


**FIG. 13.3.** – CEM V cement paste in general laboratory environment: comparative colonization of the surface and opened porosities [20].

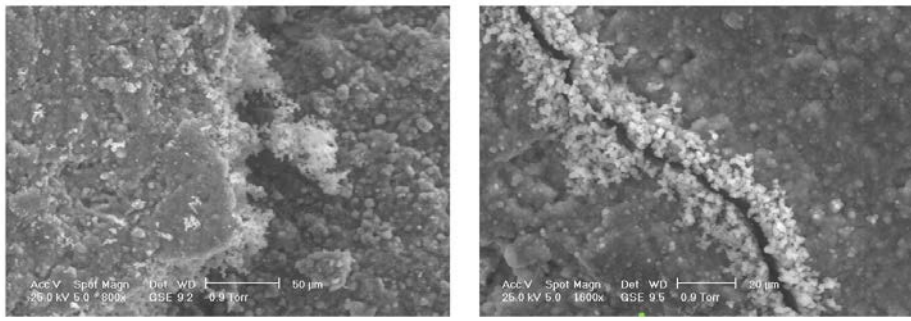


**Fig. 13.4.** – Cement pastes: specific colonization of a splint and a crack fissure [20].

The surface of the material and the cracks are also more conducive to microbial colonization because the surface pH of cement-based materials is generally reduced, down to about 9 due to the carbonation of its hydrates. The surface asperity (cracks and roughness) are zones in which the ratio of surface to volume of material allows a more pronounced carbonation and thus accelerates the local "colonizability" (Figs 13.3 and 13.4).

### *13.2.3. Specificity of the study of the actual biodeterioration of concrete*

The wide variability in the physical and chemical properties of concretes and exposure environments does not allow the development of universal models for predicting the biodeterioration of cement-based materials. Many studies have been carried out to build a database on the chemical composition of cements, the properties of aggregates, the water content or the implementation parameters. However, the influence of admixtures remains less explored and it is extremely complicated to understand precisely the evolutions and properties of natural environments on a time scale consistent with the lifetime of a structure.

## 13.3. Generic biodeterioration process

Any biodeterioration of cement-based materials is necessarily due to the colonization of its surface by one or more types of microorganisms. The sensitivity of the materials to biological fouling depends on many factors, internal and external to the material. The formation and development of microbial consortium on the concrete surface has been the main purpose of many studies [21, 22], among which Guilitte [23] defined the bioreceptivity of a material as its *"ability to be colonized by one or more groups of living microorganisms without necessarily undergoing biodegradation"*. Bioreceptivity can only be defined by considering the

environment to which the material is exposed. In fact, the material bioreceptivity factor evolves due to the aging of the material considered (surface physicchemistry, topography, *etc.*) and environmental conditions (humidity, illumination, pollution, *etc.*).

It is thus possible to distinguish:

- intrinsic bioreceptivity only related to the properties specific to the material;
- extrinsic bioreceptivity linked to the environment (temperature, humidity, salinity, oxygen content, *etc.*), to the different microorganisms it hosts, and to the formation of exogenous deposits allowing their development. Intrinsic bioreceptivity is managed by the physicochemical properties of the concrete surface such as porosity and surface condition (roughness) as well as the chemical composition of the concrete.

The aging states of the material have also a major influence on the microbial colonization of its surface. The pH of healthy concretes is about 13 and inhibits all the bacterial colonization. The development of a biofilm on their surface therefore depends on their conditioning, that is to say, in the case of cement-based materials, their carbonation state. The carbonation of the different hydrates of the cement matrix, normal step of aging of the concrete, results from their reaction with the carbon dioxide coming from the environment. This leads to the formation of calcite and a significant acidification of the surface, down to a surface pH close to 9. Portlandite is the hydrated compound of the cement-based materials that is the most involved in the carbonation process of the concretes.

In wet environments, portlandite dissolves in the interstitial solution:

$$Ca(OH)_{2(s)} \rightarrow Ca^{2+}_{(aq)} + 2OH^{-}_{(aq)} \tag{13.1}$$

The carbon dioxide of the air dissolves in the water contained in the pores of the concrete:

$$H_2O + CO_{2(g)} \rightarrow HCO^{-}_{3(aq)} + H^{+}_{(aq)} \tag{13.2}$$

$$HCO^{-}_{3(aq)} \rightarrow CO^{2-}_{3(aq)} + H^{+}_{(aq)} \tag{13.3}$$

These two dissolutions lead to the neutralization of chemical reactions and thus the carbonation of portlandite:

$$Ca^{2+}_{(aq)} + 2OH^{-}_{(aq)} + 2H^{+}_{(aq)} + CO^{2-}_{3(aq)} \rightarrow CaCO_{3(s)} + 2H_2O \tag{13.4}$$

All of these reactions result in the simplified reaction below:

$$CO_2 + Ca(OH)_2 \rightarrow CaCO_3 + H_2O \tag{13.5}$$

The other cement phases (hydrated calcium silicate CSH, ettringite and hydrated calcium monosulphoaluminate) might also be carbonating and

contribute to the decrease of the pH of the surface due to the formation of calcite associated with other phases more or less soluble:

- CSH carbonation:

$$C_xS_yH_z + xH_2CO_3 \rightarrow xCaCO_3 + ySiO_2{\cdot}tH_2O + (x\text{-}t+z)H_2O \quad (13.6)$$

- Ettringite carbonation:

$$3CaO{\cdot}Al_2O_3{\cdot}3CaSO_4{\cdot}32H_2O + 3CO_2 \rightarrow 3CaCO_3 + 3(CaSO_4{\cdot}2H_2O) + Al_2O_3{\cdot}xH_2O + (26\text{-}x)H_2O \quad (13.7)$$

All these phenomena are the first step of a drop in the pH of the concretes surface down to about 9.5. This low alkalinity then allows the development of neutrophilic microorganisms and then the development of a biofilm, a prior stage to any biodeterioration [24, 25].

The biodeterioration of aesthetic facades and facings is a very current problem. Indeed, there is now very little documented knowledge about biological colonization of modern building materials whose aesthetics is one of the major properties: pigmented concrete, white concrete, *etc.* The durability of the use of these materials allowing a new architectural approach is mainly linked to the persistence of their appearance. Whatever the concrete used, many structures and buildings are affected by this "pathology". Various specific solutions have been developed against biofouling and bioalteration of concrete, by treatment of the surface or in the mass of the material.

The surface treatments, applied after the construction of the structure, can be decomposed into two families:

- *Biocide coatings*. These coatings contain biocide agents whose aim is to destroy the living biological elements and thus to reduce biofilm development. These solutions, although they may be justified in the case of local treatment, generally have different disadvantages, such as a high cost due to the area to be treated, a moderate effectiveness over time, limited compatibility with other coatings and difficulty in repairing degraded areas.
- *Surface effect coatings*. These treatments, initially designed for boats, do not reduce the bacterial colonization but are intended to facilitate natural cleaning (runoff, flow) or man-made (human action) surfaces.

The development of these two families of solutions is now limited by taking account of environmental requirements and the potential release/leaching of active compounds into the environment. Moreover, these coating makes the surface air and waterproof, thus creating problems of resistance to freeze-thaw cycles and limiting the "breathability" of the work that influence the indoor air quality.

There are few treatments in the bulk of the material used against surface biocontamination. The only solution commercialized at present consists in the incorporation of titanium oxides (*aka* anatase) in a cement which degrades the organic compounds using photo-catalysis. Under ultraviolet radiation, titanium oxides catalyse the formation of reactive compounds (free radicals) allowing the

degradation of organic compounds. These materials, known as self-cleaning, not only degrade living cells (viruses, bacteria, mosses, fungal, algae) but also some pollutants (NOx, VOC) and allergens (pollen, acarida). This solution requires UV radiation and its efficiency is thus dependent on the conditions of exposure of the surface because of the small range of wavelengths of radiation allowing the initiation of the reaction. Moreover, due to its high cost, titanium oxide materials are currently reserved for exceptional works, such as the Jubilee Church, Rome.

In addition to the biogenic chemical degradation resulting from sulphuric acid or nitric acid secreted by bacteria (case of sewage systems and wastewater treatment plants as addressed in chapters 14 and 16), the literature contains many examples of microorganisms that have led to severe alteration of concrete although no real case has necessarily been isolated. Microorganisms such as *Aspergillus Niger* (fungus) or *Chaetomorpha antenia* (algae) are able to colonize concrete surface and secrete various organic acids. The reaction of these acids (AH) with the cement matrix leads to the formation of calcium salts ($CaA_2$) [26] according to equations 9 and 10.

The dissolution of the concrete then depends on the solubility of the calcium salt formed in the surrounding environment.

$$Ca(OH)_2 + 2AH \rightarrow CaA_2 + 2H_2O \tag{13.9}$$

$$x\text{CaO}\cdot y\text{SiO}_2\cdot z\text{H}_2\text{O} + 2x\text{AH} \rightarrow y\text{Si(OH)}_4 + (x\text{–}2y\text{+}z)\text{H}_2\text{O} \tag{13.10}$$

*Chaetomorpha antenia* algae are implicated in the degradation of concretes by dissolving the cement matrix due to their production of organic acids such as saturated fatty acids ($C_{20}H_{40}O_2$), fatty acids ($C_{14}H_{26}O_2$) or acids ($C_{19}H_{34}O_2$) [ 22]. Their metabolism includes consumption of calcium, aluminium, silica, iron. *Chaetomorpha antenia* solubilise these elements from concrete because of their reactions with the secreted organic acids. Tests carried out on M20 concretes show that yeelimite ($Ca_3Al_6CaSO_4$), gismondine ($CaAl_2Si_2O_8\cdot 4H_2O$) and portlandite ($Ca(OH)_2$) of the concrete were consumed by *Chaetomorpha antenia* under laboratory but also in natural conditions [27].

*Aspergillus Niger* fungi is an omnipresent microbial species commonly found in soil and used in several studies [28, 29]. This fungus produces organic acids such as butyric acid ($C_4H_8O_2$), lactic acid ($C_3H_6O_3$), oxalic acid ($C_2H_2O_4$) or acetic acid ($C_2H_4O_2$), which induce a pH decrease of its surrounding environment and of the surface it colonizes [30]. This production of acids can lead to serious deterioration of the concretes by reaction with portlandite and C-S-H. The main deterioration of concretes due to *Aspergillus Niger* is caused by the production of organic acids rather than the production of carbonic acid or the penetration of hyphae inside the porous network of concrete [31].

As the nitric acid, acetic acid produced by *Aspergillus Niger* [29, 30, 31] may induce dissolution of the cement matrix. Its reaction with portlandite leads to the formation of soluble calcium acetate and can cause the disintegration of material [32].

$$Ca(OH)_2 + 2(CH_3COOH) \rightarrow Ca(CH_3COO)_2 + 2H_2O \tag{13.11}$$

Calcium leaching is caused by the complexation of calcium which affects the mechanical properties and the deformation modulus of the material [26]. The decomposition of the cement matrix starts with the leaching of portlandite ($Ca(OH)_2$) and C-S-H. At the end of their reaction with organic acids, calcium salts of variable solubility and dependent on the physic chemistry of the medium are formed. *Aspergillus Niger* can induce the formation of calcite and calcium oxalate (weddellite $CaC_2O_4 \cdot 2H_2O$ and whewellite $CaC_2O_4 \cdot H_2O$) [26]. Since the oxalates are insoluble in water, their formation leads to the obstruction of the surface porosity, limiting the leaching of calcium and therefore the degradation. After a 15-month exposure, *Aspergillus niger* induced bioleaching study conducted on a CEM I cement paste showed that the depth of alteration was about 8.7 mm. A mineral evolution of the altered zone is also observed across different zones, as shown in figure 13.5 [26].

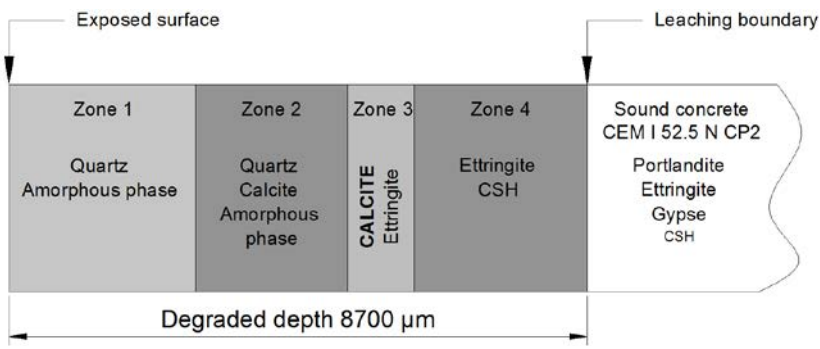


**Fig. 13.5.** – Leaching biodeterioration of cement paste exposed 15 months to *Aspergillus niger* [26].

## 13.4. Measurement of concrete biodeterioration

The biodeterioration of concrete influences its physicochemical properties. These modifications can then be used for measuring the biodeterioration of a concrete.

### *13.4.1. Physical Properties*

The reduction of the mechanical characteristics of concrete is the cause of the loss of its structural properties. Therefore, the measurement of the mechanical resistance makes it possible to estimate the level of deterioration of a concrete [33]. Indeed, the biodeterioration of concretes leads, depending on the case, to a reduction of the amount of hydrates in the cement paste and the formation of degradation products. These modifications of the microstructure

can lead to an increase in the porosity but also to the cracking of the material. All these phenomena result in an overall degradation of the mechanical properties of the material.

Some authors [34, 35, 36] use the loss of mass as measurement parameters. However, this parameter does not defer a surface attack from a more in-depth attack of the material [37].

### 13.4.2. Chemical properties

Colonization of the concrete by microorganisms necessarily leads to a decrease in the pH of the surface of the material [34, 35, 38].

The attack of the concretes by acids resulting from the metabolic activity of the microorganisms is accompanied by the release into the surrounding environment of chemical species resulting from the concrete: calcium, silicon and aluminium ions in variable amount depending on the cement base used. Thus the presence of calcium ions in the medium and the evolution of its concentration is a sign of alteration of the cement matrix [49]. The biodeterioration of cement-based materials can also be quantified by an index of attack calculated from the proportion of the major chemical elements (Ca, Si, Al, Fe) released for a given quantity of biogenic acid [37, 39].

## 13.5. Improvement of concrete strength

### 13.5.1. Concrete composition

#### 13.5.1.1. Cement and water

The influence of the chemistry of concrete on its biodeterioration depends on its bioreceptivity and the reactivity of its components with the microbial metabolites produced in the biofilm covering it.

Consideration of the risks of biodeterioration of concretes can be made by selecting the composition of the cement, limiting the proportion of compounds reacting with acids of biological origin. Portlandite is the first concrete compound that reacts with these acids. A cement paste with a small proportion of portlandite thus has a better resistance [40]. The addition of, for example, blast furnace slag or silica fumes to the cement constitutive of a concrete, makes it possible to reduce its proportion of portlandite, in particular to form a large amount of C-S-H. This evolution of the mineralogy thus improves the resistance of the material [34].

A study by Hofmann [36] highlighted the excellent behaviour of calcium aluminates cements to the acid attack of biological origin. Hydration of these cements results in the formation of hydrated calcium aluminates and aluminium hydroxide. The attack of calcium aluminates in an acid medium leads to the formation of aluminium hydroxide which can buffer the pH but also form protective layers on the surface (Chapter 14).

Although Portland cement (CEM I) is only composed of mineral phases, the mixing water and admixtures used to compose of the material can contain organic materials that can provide nutrients to the microorganisms. admixtures, such as plasticizers, contain surface-active surfactants composed of lignosulfonates, organic acid salts, sulfonates, melamine, naphthalene sulfonates, naphthalene or melamine derivatives. The curing products are formulated on the basis of resin, wax or paraffin in aqueous emulsion, natural or synthetic resin, wax or paraffin dissolved in a solvent. The organic compounds of these products can also constitute a source of nutrients with regard to the carbonaceous metabolism of the microorganisms. Nevertheless, no study on their influence on the bioreceptivity of concrete appears to have been carried out to date.

To prevent corrosion of steel rebars, it is common practice to apply spray corrosion inhibitors of very variable nature (sulphoxides, thiazoles, chromates, *etc.*). These inhibitors are intended to migrate through the porous concrete network up to steel reinforcements to protect them from corrosion. These chemicals may also be conducive to the growth of bacteria implied in sulphur cycle, which may ultimately lead to impairment of the corrosion inhibiting properties of these compounds [41].

#### *13.5.1.2. Aggregates*

Depending on local availability, aggregates generally selected for the manufacture of concrete are siliceous and therefore usually considered to be chemically inert with respect to substances secreted by microorganisms. However, mineralogical and chemical compositions of aggregates influence the resistance of concrete submitted to bioinduced attacks [36]. For example, a concrete made with limestone aggregates has a lower depth of deterioration and less loss of thickness. However, the loss of mass is slightly greater than the one of a concrete made with inert aggregates. In fact, the calcareous aggregates may also be degraded, which leads to a global attack on the concrete instead of a localized attack on the cement matrix of the concrete.

### *13.5.2. Implementation*

Although the porosity, the geometry, the distribution and the surface roughness of the concrete are factors that are difficult to control, they have a great influence on its durability. Indeed, they depend not only on the composition of the material (cement type, aggregates, mixing water, admixture), but also on its implementation (water/cement mass ratio, type of formwork, setting of fresh paste, curing and hardening condition, *etc.*).

Nevertheless, various techniques can be used to limit the porosity of the material and its influence on resistance to biodeterioration.

- *Limitation of the ratio of water mass to cement mass used (W/C).* This ratio is one of the most important parameters of the implementation of concretes. It is determined in order to obtain the desired workability of the fresh

paste and to ensure the hydration of the cement grains. However, the water in excess according to the stoichiometry of the hydration reaction of the cement is not fixed during the crystallization of the hydrates but fills a volume in the fresh paste which then constitutes a capillary porosity that strongly influences the strength and durability of the hardened material. The use of a high W/C ratio makes it possible to obtain a fresh concrete that is easy to work and to use but which becomes a more porous material once the hardening has been attained. Thus, a decrease in W/C can significantly reduce the permeability [45] and the porosity of the concrete: concrete prepared with an W/C of 0.65 has porosity four times higher than that of a prepared concrete with an W/C of 0.40 [16]. A study by Gutiérrez-Padilla *et al.* [42] showed that an W/C concrete equal to 0.33, after immersion in artificial waste water, had a degradation rate of 0.08 mm/year compared with 0.208 mm/year for a concrete of W/C of 0.42. The W/C parameter must therefore be carefully considered, or even limited (W/C < 0.45 [36]). In addition, there is a strong correlation between the W/C ratio and the biological fouling intensity [43]: an increase in W/C leads to an increase in biological fouling due to the greater porosity that induces a larger surface available for its conditioning (carbonation, nutrient deposition, moisture concentration).

- *The curing conditions* (temperature, humidity) influence the porous structure of the concrete and especially the state of the surface called "skin effect" [17, 44]. Good curing conditions allow the formation of a less porous skin and the development of a less permeable microstructure [45], limiting transfers from the outside to the inside of the porous network.
- *The addition of fine particles such as silica fume* [33, 39, 46] leads to a reduction in the porosity of the concrete. The concretes containing these particles have good resistance to bioinduced and/or chemical attack. These additions also reduce the permeability of concrete, which limits the penetration of aggressive chemicals and microorganisms deep into healthy areas. Similarly, the use of fly ash makes it possible to improve the characteristics of concrete in the same way as the addition of silica fumes, but to a lesser extent [34].
- *Use of some polymers.* Different studies have shown the influence of the use of some polymers in concretes [46, 48, 49, 50]. The presence of polymers mainly makes it possible to seal the porosities and to fill the microcracks inside the matrix. These polymers (styrene, acrylic, acrylic ester-styrene, *etc.*) do not protect against the biological acid attack of concrete, but they improve material cohesion and can delay its erosion. The clogging of the porous network may also delay the penetration of aggressive compounds into the porous concrete network [46, 47].
- *Covering the concrete surface*, for example by using polyurethane, allows the concrete to exhibit very good behaviour when subjected to chemical or biological attacks. When the covering layer and the concrete have good cohesion and the product used is suitable, this layer acts as a barrier for clogging the porosity to the concrete surface. This layer limits the contact

between aggressive chemical compounds and concrete. Nevertheless, the durability of this layer is sometimes lower than the durability required for the structure.

## 13.6. Differences between chemical attack and biological attack

The bioinduced chemical degradation of concretes results from the reaction of the components of the cementitious matrix with the aggressive chemicals metabolized inside the biofilm. From this it may seem simpler to consider the study of the biodeterioration of concrete as that of the interactions between the cement matrix and the chemical substances secreted in the biofilm. Nevertheless, although the substances considered are the same, the authors [34] differentiate in their approach as in their analysis the purely chemical attacks of those induced by the metabolic activity of microorganisms. The main difference between these two types of attack is the way in which the reactants (*e.g.*, acids) are in contact. By analogy with the corrosion of steels, it is possible to compare conventional acid attack (acid effluents, *etc.)* with generalized corrosion whereas bioinduced attack can be compared to a localized attack limited to the zone covered by the biofilm (on the surface or in porosities). Consequently, the severity and the consequences of these attacks may be different depending on the conditions [47]. Different comparative studies have highlighted the more aggressive nature of bioinduced attacks compared to purely chemical attacks [34]. This difference is explained by the speed and depth of diffusion of the aggressive substances through the porous network of the concrete. Nevertheless, these results are still to be taken with caution since the bacterial activity is not generally known during the tests of biodeterioration and thus it is not certain that the amounts of acid between the bioinduced attacks and the attacks purely chemical are identical.

The case of attack by sulphuric acid made it possible to highlight the main differences between these two attacks [50]:

- alteration products resulting the reaction of concrete with biogenic or purely chemical sulphuric acid are identical: gypsum and ettringite. In the case of a purely chemical attack, the acid/cement matrix reaction causes the formation of a superficial layer of alteration products acting as a diffusion barrier for the aggressive agents thus providing protection for the healthy part of the concrete. On the other hand, in the case of bioinduced attack, the layer of products formed by the reaction then constitutes a preferred development zone for the biofilm in which the bacteria responsible for the formation of sulphuric acid can continue their metabolic activity. This new zone of biofilm development is located in contact with the healthy part of the concrete and thus constitutes a new reaction surface allowing the displacement of the weathering front. However, precipitation of gypsum in the case of attack by sulphuric acid of chemical

origin may be reduced and thus not lead to a protective effect depending on the experimental protocol and in particular on the ratio between the volume of solution relative to the surface of the sample. Thus, the observed differences are more attributable in these tests to differences in attack conditions than a difference in attack mechanisms.

- During these two types of acidic attack, the samples are submitted to different amounts of sulphuric acid as indicated by the change in pH which is different. When the concrete is in contact with a purely chemical acid solution, the pH of the solution and therefore of the surrounding medium is strongly acid (pH≈1). Conversely, when an acidic attack of biological origin is considered, the acid is produced in small quantities within the biofilm and the quantity produced changes with the evolution of the biofilm. The pH of the surface evolves slowly and gradually to reach the same level of acidity as during a chemical attack. This slow evolution and the continuous production of acids allow an equally continuous displacement of the degradation front. Nevertheless, this trend would be found with an acid attack of chemical origin using lower concentrations.

This example illustrates the complexity of the mechanisms involved and the difficulty of comparing results obtained with different experimental protocols. The adoption of standardized tests for the biodegradation of cement based materials is therefore an important issue.

## 13.7. Conclusion

The relationships between microorganisms and concretes are not necessarily harmful for concrete because the biomineralisation [51, 52, 53] can lead to an improvement of the microstructure and in the major part of cases the biocolonisation of the surface of concrete do not induced any structural disorder.

The complexity of concrete biodeterioration phenomena is due to the multitude of factors involved in (bio)deterioration processes that operate over a large time scale (from a few hours to several decades). The problems of bacterial development and its control constitute many issues concerning the sustainability of the structure, its aesthetic quality but are also a public health issue [49]. In fact, the biofilm covering the surface of the concrete may contain pathogenic microorganisms, such as *Pseudomonas aeruginosa*, *Aeromonas, Pleisiomonas*, *Lycobacterium, Flavobacterium* or *Serratia*, in drinking water networks, for example.

The diversity of the microorganisms involved and the potential evolutions of their metabolisms during the development and life of the biofilm depending, among other things, on the environment, explain the difficulty in developing laboratory protocols representative of real cases. The comparison of these laboratory tests with *in situ* degradation is therefore difficult due to differences in the composition of the concretes, environmental characteristics (*e.g.,* chemical composition of wastewater), aeration conditions (aerobic or anaerobic), flow conditions, etc. [42].

## References

[1] Malier Y. (2007) "De Marcus Vitrivius aux nanomatériaux ou l'apport de la singulière histoire du béton à une réflexion prospective sur la recherche universitaire en génie civil." Bordeaux (France) 23-25 may 2007, 25ème rencontres universitaires du génie civil. AUGC, 1-13

[2] Bertron *et al.* (2005) "Accelerated tests of hardened cement pastes alteration by organic acids: analysis of the pH effect." Cem. Concr. Res., 35, 155-166.

[3] Neville A. (2004) "The confused world of sulfate attack on concrete." Cem. Concr. Res., 34, 1275-1296.

[4] Ollivier J.P. and Vichot A. (2008) "La durabilité des bétons - Bases scientifiques pour la formulation de bétons durables dans leur environnement." Ollivier J.-P. and Vichot A. Eds, Presses de l'Ecole Nationale des Ponts et Chaussées, Paris, France, IBSN 978-2-85978-434-8, 1-868.

[5] Fletcher I.A. *et al.* (2007) "Behaviour of concrete structures in fire." Therm. Sci., 11, 37-52.

[6] Damidot D. and Le Bescop P. (2008) "La stabilité chimique des hydrates et le transport réactif dans les bétons." In: "La durabilité des bétons - Bases scientifiques pour la formulation de bétons durables dans leur environnement". Ollivier J.P., Vichot A. Eds, Presses de l'école nationale des Ponts et Chaussées, Paris, France, IBSN 978-2-85978-434-8, 135-166.

[7] Isgor O.B. and Razaqpur A.G. (2004) "Finite element modeling of coupled heat transfer, moisture transport and carbonation processes in concrete structures." Cem. Concr. Comp., 26, 57-73.

[8] Ahmad S. (2003) "Reinforcement corrosion in concrete structures, its monitoring and service life prediction-a review." Cem. Concr. Comp., 25, 459-471.

[9] Baroghel-Bouny V. *et al.* (2008) "La durabilité des armatures et du béton d'enrobage." In: La durabilité des bétons - Bases scientifiques pour la formulation de bétons durables dans leur environnement. Ollivier J.P., Vichot A. Eds, Presses de l'Ecole Nationale des Ponts et Chaussées, Paris, France, IBSN 978-2-85978-434-8, 135-166

[10] Bertron A. *et al.* (2005) "Attack of cement pastes exposed to organic acids in manure." Cem. Concr. Comp., 27, 898-909.

[11] Escadeillas G. and Hornain H. (2008) "La durabilité des bétons vis-à-vis des environnements chimiquement agressifs." In: La durabilité des bétons - Bases scientifiques pour la formulation de bétons durables dans leur environnement. Ollivier J.P., Vichot A. Eds, Presses de l'Ecole Nationale des Ponts et Chaussées, Paris, France, IBSN 978-2-85978-434-8, 613-705.

[12] Zivica V. and Bajza A. (2001) "Acidic attack of cement based materials — a review. Part 1 Principle of acidic attack." Construction and Building Materials, 15, 331-340.

[13] De Belie N. (2010) "Microorganisms versus stony materials: a love–hate relationship." Materials and Structures, 43, 1-12.

[14] Dreux G. (1990) "Nouveau guide du béton." Eyrolles Edition, Paris, France, 1-416.
[15] De Larrard F. (2000) "Structures granulaires et formulation des bétons." ENPC, Nantes, 1-441.
[16] Sahu S. *et al.* (2004), "Determination of water–cement ratio of hardened concrete by scanning electron microscopy." Cem. Concr. Comp., 26, 987-992.
[17] Delmas L. (2006) "La porosité des bétons : Influence de la formulation et de la cure sur la porosité de peau des bétons." End of studies' project, Institut National des Sciences Appliquées, Strasbourg, France, 1-62.
[18] Roux S. (2008) "Evaluation des risques de biodégradation des bétons en contact avec une eau douce naturelle." PhD thesis, université Louis Pasteur, INSA de Strasbourg, Strasbourg, France.
[19] Roux S. *et al.* (2006) "Study of mortars and cement paste biodeterioration by ESEM, STEM and EDS." Microscopy and Analysis, 104, 15-17.
[20] Roux S. *et al.* (2006) "Altération des pâtes de ciment par colonisation bactérienne." Mat. & Tech., 94, 295-506.
[21] Dubosc A. (2000) "Etude du développement de salissures biologiques sur les parements en béton : mise au point d'essais accélérés de vieillissement." PhD thesis, Institut National des Sciences Appliquées de Toulouse, Toulouse, France.
[22] Gaylarde C.C. and Gaylarde P.M. (2005) "A comparative study of the major microbial biomass of biofilms on exteriors of buildings in Europe and Latin America." International Biodeterioration & Biodegradation, 55, 131-139.
[23] Guillitte O. (1995) "Bioreceptivity: A new concept for building ecology studies." Science of the Total Environment, 167, 215-220.
[24] Vincke E. *et al.* (2001) "Analysis of the microbial communities on corroded concrete sewer pipes – a case study." Applied Microbiology and Biotechnology, 57, 776-785.
[25] Yamanaka T. *et al.* (2002). "Corrosion by bacteria of concrete in sewerage systems and inhibitory effects of formates on their growth." Water Research, 36, 2636-2642.
[26] Lajili H. *et al.* (2008) "Alteration of a cement matrix subjected to biolixiviation test." Materials and Structures, 41, 1633-1645.
[27] Jayakumar S. and Saravanane R. (2009) "Biodeterioration of coastal concrete structures by Macroalgae - *Chaetomorpha antennina*." Materials Research, 12, 465-472.
[28] De Windt L. and Devillers P. (2009) "Coupled modelling of cement paste by degradation by microbial activity, Concrete in aggressive aqueous environments." RILEM Publication, 63, 196-203.
[29] Wiktor V. (2008) "Biodétérioration d'une matrice cimentaire par des champignons : Mise au point d'un test accéléré de laboratoire.", PhD thesis, université de Saint-Etienne, Mines Saint-Etienne et Mines Douai, Saint-Etienne, France.

[30] Perfettini J.V. *et al.* (1991) "Evaluation of cement degradation induced by the metabolic products of two fungal strains." Cellular and Molecular Life Sciences, 47, 527-533.
[31] De Windt L. and Devillers P. (2010) "Modeling the degradation of Portland cement pastes by biogenic organic acids." Cem. Concr. Res., 40, 1165-1174.
[32] Beddoe R.E. (2005) "Modelling acid attack on concrete: Part I. The essential mechanisms." Cem. Concr. Res., 35, 2333-2339.
[33] Berndt M.L. (2001) "Protection of concrete in cooling towers from microbiologically influenced corrosion." Geothermal Resources Council Transactions, 25, 1-8.
[34] De Belie N. (2004) "Experimental research and prediction of the effect of chemical and biogenic sulfuric acid on different types of commercially produced concrete sewer pipes." Cem. Concr. Res., 34, 2223-2236.
[35] Gu J.-D. *et al.* (1998) "Biodeterioration of concrete by the fungus *Fusarium*." International Biodeterioration & Biodegradation, 41, 101-109.
[36] Hofmann F.-J. *et al.* (1997) "Concrete with grater resistance to acid and to biogenic sulfuric acid corrosion." Offprint from Betonwerk Fertigteil Technik, 4, 1-8.
[37] Hondjuila Miokono E. (2013) "Essai de biodétérioration de mortiers par une succession de bactéries sulfo-oxydantes neutrophiles/acidophiles." PhD thesis, université de Lille 1, Mines Douai, Lille, France.
[38] Tulliani J.-M. *et al.* (2002) "Sulfate attack of concrete building foundations induced by sewage waters." Cem. Concr. Res., 32, 843-849.
[39] Hajj Chehade M. (2010) "Biodétérioration du béton armé par *Acidithiobacillus thiooxidans*." PhD thesis, université de Lille 1, Mines de Douai, Lille, France.
[40] Taché G. (1998) "Corrosion bactérienne des bétons." In: Biodétérioration des matériaux, Lemaître C., Pebere N., Festy D. Eds, EDP Sciences, Paris (France), ISBN 2-86883-329-2, 115-126.
[41] Bach M. *et al.* (2004) "Evaluation de la corrosion organique dans le cadre de la préservation des monuments historiques, influence bactérienne." Mat. & Tech., 7-8-9, 3-8.
[42] Gutiérrez-Padilla M.G.D. *et al.* (2010) "Biogenic sulfuric acid attack on different types of commercially produced concrete sewer pipes." Cem. Concr. Res., 40, 293-301.
[43] Giannantonio D.J. *et al.* (2009) "Molecular characterizations of microbial communities fouling painted and unpainted concrete structures." International Biodeterioration & Biodegradation, 63, 30-40.
[44] Bur N. *et al.* (2011) "Pore structure of mortar." European Journal of Environmental and Civil Engineering, 15, 699-714.
[45] Leemann A. *et al.* (2010) "Influence of water hardness on concrete surface deterioration caused by nitrifying biofilms in wastewater treatment plants." International Biodeterioration & Biodegradation, 64, 489-498.

[46] Vincke E. *et al.* (1999) "A new test procedure for biogenic sulfuric acid corrosion of concrete." Biodegradation, 10, 421-428.
[47] Beeldens A. *et al.* (2001) "Resistance to biogenic sulphuric acid corrosion of polymer-modified mortars." Cem. Concr. Comp., 23, 47-56.
[48] Monteny J. *et al.* (2001) "Chemical and microbiological tests to simulate sulfuric acid corrosion of polymer-modified concrete." Cem. Concr. Res., 31, 1359-1365.
[49] Huang B. *et al.* (2010) "Laboratory evaluation of permeability and strength of polymer-modified pervious concrete." Construction and Building Materials, 24, 818-823.
[50] Vincke E. *et al.* (2002) "Influence of polymer addition on biogenic sulfuric acid attack of concrete." International Biodeterioration & Biodegradation, 49, 283-292.
[51] Van Tittelboom K. *et al.* (2010) "Use of bacteria to repair cracks in concrete." Cem. Concr. Res., 40, 157-166.
[52] Anne S. *et al.* (2010) "Evidence of a bacterial carbonate coating on plaster samples subjected to the Calcite Bioconcept biomineralization technique." Construction and Building Materials, 24, 1036-1042.
[53] Ducasse-Lapeyrusse J. *et al.* (2017) "Microbiologically induced calcium carbonate precipitation to repair microcracks remaining after autogenous healing of mortars." Construction and Building Materials, 141, 461-469.

# 14 Biodeterioration of cementitious materials in sewage structures

**Jean Herisson**

## 14.1. Introduction

Sewage structures are used for the drainage and treatment of wastewater. Drainage refers to all the procedures implemented to collect and remove waste quickly, whereas treatment covers all the processes waste passes through before it is discharged into the natural environment.

In 1998, the International Office for Water [1] estimated the length of wastewater pipes in mainland France as being 250000 km. The progression in the length of piping for the period between 1962 and 1998 is given in figure 14.1. The urban wastewater and sewage systems are mainly between 40 and 50 years old and require significant repairs. According to Satin and Selmi [2], 10% of the pipes are over 60 years old and were initially built for a lifetime of between 60 and 80 years. These figures show that the French sewage and wastewater systems are aging. This statement also applies to all industrialized countries.

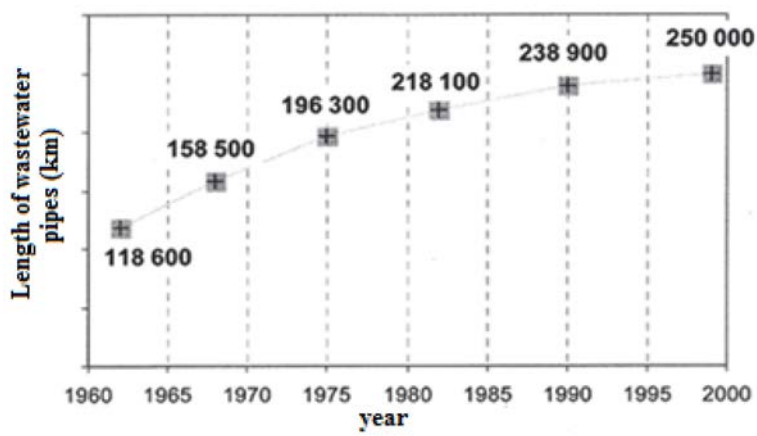


**Fig. 14.1.** – Estimate of the progression of the length of wastewater and sewage pipes throughout mainland France between 1962 and 1998 [1].

To address local constraints (topography, rainfall, type of habitat, hard landscaping, flood protection, *etc.*), budget restrictions and future developments, choices are made with regard to the types of structure used to construct the sewage and wastewater system. The pipes will therefore have a wide range of sizes and shapes and will be made of very different materials.

The materials encountered in sewage and wastewater systems are mainly concrete and stone. Brick, plastics and cast iron are also found to a lesser extent. Table 14.1 gives the example of the distribution of each material in the German systems in 1999.

**TABLE 14.1.** – Materials encountered in the German sewage and wastewater systems (according to Kaempfer and Berndt [3]).

| Proportions (%) | Concrete | Stone | Brick | Iron | Plastic |
|---|---|---|---|---|---|
| | 46 | 38 | 6 | 5 | 5 |

This proportion tends to develop with an increasingly large fraction occupied by plastic, especially for small diameters (less than 300 mm), but cement materials remain the most common for larger diameters.

All these materials are generally prefabricated elements assembled on-site to blend with the local topographical features and restrictions as far as possible. Once in place, the materials can be exposed to attack from various sources. Most of the damage encountered is generated by cracks, faulty joints between the pipes, joints that have moved and corrosion (Table 14.2).

**TABLE 14.2.** – Distribution of faults in pipes in Germany (according to Kaempfer and Berndt [3]).

| Faults | Proportions (%) |
|---|---|
| Connection fault | 24 |
| Cracks | 22.1 |
| Displaced joint | 22.1 |
| Biodeterioration / Gas attack | 8.7 |
| Surface erosion | 5.8 |
| Holes | 5.8 |
| Deformation | 3.8 |
| Incrustation | 3.8 |
| Plant roots | 3.8 |

This damage is mainly due to poor design, poor construction or too high a flow rate and is sometimes the cause of pollution of underground water. According to an estimate by Kaempfer and Berndt [3], 500 million cubic meters

of wastewater per year pollutes the ground soils and underground water in Germany. According to this same study, 9% of damage is due to biological, physical and chemical attack, 6% is due to surface erosion and 22% to cracking. All of this damage can be caused to a greater or lesser extent by the action of microorganisms. It is therefore of major importance to understand the chemical and biological mechanisms of deterioration in order to construct, repair and rehabilitate the sewage and wastewater systems.

## 14.2. How does biodeterioration manifest itself in sewage and wastewater structures?

Biodeterioration is a dangerous phenomenon because it involves the presence of hydrogen sulphide ($H_2S$) which is toxic to humans and damaging for cement materials in the sewage and wastewater structures. It was studied for the first time in 1900 by Olmstead and Hamlin [4], who described the deterioration of mortar in the joints between the bricks of a spillway in the Los Angeles system in the United States. Since then, other studies were conducted, showing that the loss of material can be as much as several millimeters per year (Table 14.3).

**Table 14.3.** – Values for the rates of deterioration of cement materials in the sewage and wastewater systems.

| References | Rates of deterioration (mm year$^{-1}$) | Types of materials |
|---|---|---|
| US EPA, 1991 [5] | 2.5-10 | Concrete |
| Morton *et al.*, 1991 [6] | 2.7 | Concrete |
| Mori *et al.*, 1992 [7] | 4.3-4.7 | Concrete |
| Ismail *et al.*, 1993 [8] | 2-4 | Mortar |
| Davis, 1998 [9] | 3.1 | Concrete |
| Monteny *et al.*, 2001 [10] | 1.0-1.3 | Mortar |
| Vincke *et al.*, 2002 [11] | 1.1-1.8 | Concrete |
| Wells and Melchers, 2014 [12] | 0.6-12.7 | Concrete |

The biodeterioration of cementitious materials in sewage and wastewater structures is characterized by a gradual deterioration of the structure in the above-water part of the system (Fig. 14.2) without damage to the immersed part. Initially, the above-water part of the pipe will become covered in a whitish deposit, mainly composed of gypsum that may or may not be accompanied by a viscous film generated by microorganisms, the biofilm. Subsequently, fragmentation will appear at the surface of the material. It will crumble away in successive layers. In the long term, the cement material will completely dissolve.

The separation of the material will lead to the loss of all its physical and mechanical properties and if regular inspections are not made, a hole may form in the structure of the pipe. In the worst case scenario, there is a possible risk of collapse. Repairing this damage entails significant cost (repair work, diverting the water flow, diverting around the collapsed area, *etc.*). All of this process occurs in the atmosphere in the pipe containing hydrogen sulphide ($H_2S$), a poisonous gas with a characteristic smell of rotten eggs.

**FIG. 14.2.** – Image of a sewage pipe subject to different stages of biodeterioration.

The deterioration caused by microorganisms is a process that occurs in several stages (Fig. 14.3), with first of all, the sedimentation of sludge and sediments present in suspension in the wastewater. These will form anoxic areas (deprived of oxygen) in which sulphate-reducing bacteria (*Desulfovibrio* sp., *Desulfobulbus* sp.) will be able to develop, reducing organic molecules and sulphates to sulphides [13]. The hydrogen sulphide thus formed can then degas further downstream when the effluent encounters turbulence. Once released into the atmosphere of the pipe, $H_2S$ will serve as the energy source for other types of bacteria, sulphur-oxidizing bacteria. These bacteria will oxide it to form sulphuric acid on the walls of the pipe, leading to the deterioration of the latter, and the formation of expansive and/or non-cohesive products such as gypsum ($CaSO_4 \cdot 2H_2O$) and ettringite ($3CaO \cdot Al_2O_3 \cdot 3CaSO_4 \cdot 32H_2O$).

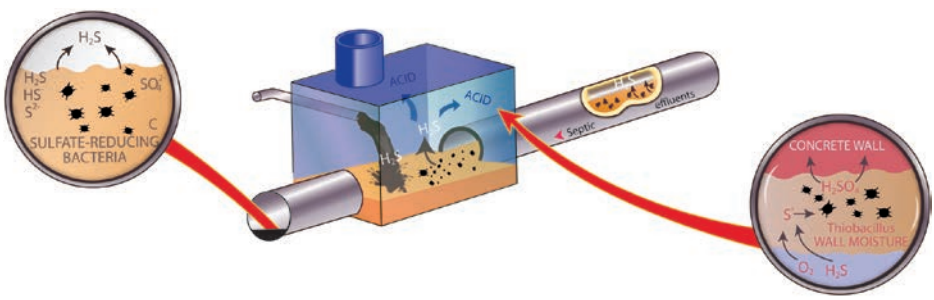


**FIG. 14.3.** – Mechanism of the biodeterioration of cement materials in a sewage system [14].

Deterioration of the cementitious material in the air above the waterline, caused by microorganisms, is gradual and occurs in three successive stages (Fig. 14.4). For Portland cement-based concrete, the first stage is characterized by a moderate drop in pH from 13 to 9 due to the mainly abiotic neutralization of the portlandite ($Ca(OH)_2$) by $CO_2$ and $H_2S$. The second step is marked by a further drop in pH due to the appearance of a succession of neutrophilic microbial colonizations oxidizing the sulphides or elemental sulphur into sulphuric acid without the loss in mass of the concrete being significant. The main microorganisms present on the concrete develop, introducing the following genera, among others [14]: *Acidithiobacillus*, *Thiobacillus*, *Thiomonas* and *Halothiobacillus*. These species are very probably responsible for the production of sulphuric acid leading to the drop in pH. It can be noted that these microorganisms have pH-dependent growth ranges which intersect, allowing this continuous fall in pH [15]. The last stage is marked by the emergence of an acidophilic bacterial colonization oxidizing the sulphides (or elemental sulphur) and by severe deterioration of the concrete. It was observed [16, 17] that the considerable loss of mass of the concrete coincides with the appearance of *Acidithiobacillus thiooxidans,* which has an optimum growth pH of 2-3 [18]. Nevertheless, depending on the strains studied and the growth conditions, the growth optimum may differ. Miokono *et al.* [15] demonstrated that this strain cultivated from thiosulphate had a maximum growth rate at a pH of approximately 4. It was therefore already in a stationary phase at a pH of 2.

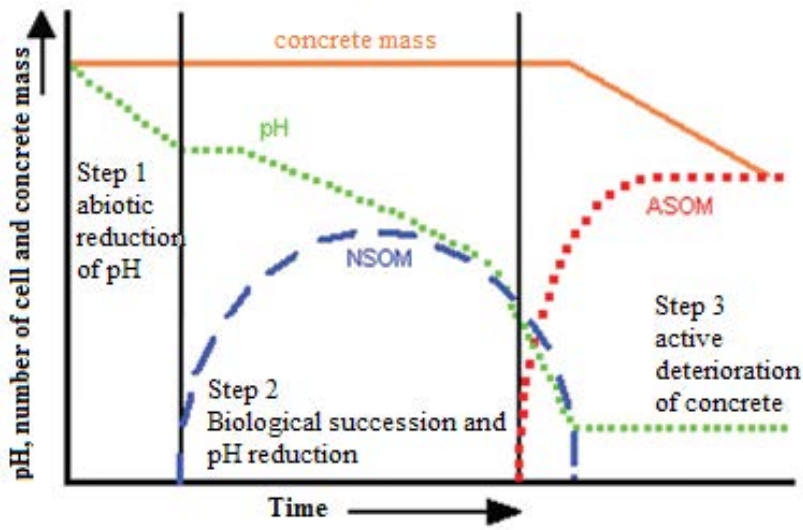


**Fig. 14.4.** – Theoretical changes in the biological and physical properties of Portland cement-based concrete over time during the deterioration process. NSOM: neutrophilic sulphur-oxidizing microorganisms, ASOM: acidophilic sulphur-oxidizing microorganisms [19].

## 14.3. Hydrogen sulphide: the main vector of biodeterioration phenomenon in sewage structures

The mechanism by which cementitious materials biodeteriorate in sewage structures is closely linked to the sulphur cycle. Hydrogen sulphide is the main vector.

Hydrogen sulphide is a poisonous, corrosive, fatal gas that worries sewage system managers for four main reasons:

*The first reason*, and the most important, is the risk of complaints from residents, as sewage system managers are rarely the owners and they are assessed based on, among other things, the number of complaints received from residents.

*The second reason* is linked to the health risks to the operating personnel. The personnel who have to work in the systems must not be exposed to this potentially fatal gas. Safety procedures are set up before any work to avoid exposure. Hydrogen sulphide can be detected by humans from a level of $2.8\ 10^{-2}$ to $1.4\ 10^{-1}$ mg $m^{-3}$ depending on the sensitivity of the person. It can cause irreversible and/or lethal effects depending on its concentration and the exposure time (Table 14.4). From approximately 140 mg $m^{-3}$, the olfactory nerve is inhibited and therefore the person loses the ability to detect it. For this reason, personnel working in the system are always equipped with a mobile detector. Moreover, above $5.6\ 10^{4}$ mg $m^{-3}$, there is a risk of explosion.

**TABLE 14.4.** – Thresholds of effects caused by $H_2S$ as a function of time [20].

| Time (minutes) | 10 | 20 | 30 | 60 | 120 |
|---|---|---|---|---|---|
| **Lethal effect thresholds (mg $m^{-3}$)** | 963 | 759 | 661 | 521 | 448 |
| **Irreversible effect thresholds (mg $m^{-3}$)** | 504 | 462 | 420 | - | - |

The regulatory exposure values are 7 mg $m^{-3}$ for the TWA (Time-Weighted Average exposure) and 14 mg $m^{-3}$ for the STEL (Short-Term Exposure Limit). As the TWA is the average authorized concentration which, according to current scientific knowledge, does not endanger the health of almost all healthy workers exposed to it, for a period of 42 hours weekly, 8 hours a day, for long periods. The STEL reflects the maximum concentration to which a person can be exposed over a period of 15 minutes. This value is intended to protect people against the short-term or immediate toxic effects.

*The third reason* concerning managers relates to the deterioration of assets.

*The final reason* is the impact hydrogen sulphide can have on the treatment of wastewater in sewage plants. At high levels, the dissolved $H_2S$ (dissolution in water = 5 g $L^{-1}$; $pKa_1 = 7.04$; $pKa_2 = 11.96$) can disrupt the biological treatment set up to purify the water before it is discharged into the natural environment.

Different parameters affect the production of hydrogen sulphide in sewage systems:

- *The oxygen content*

Hydrogen sulphide is produced in sludge and sediment that builds up in the bottom of pipes. If the oxygen concentration in the water is greater than 1 mg $L^{-1}$ [13], the sulphides produced are oxidized by the dissolved oxygen before they can be emitted into the atmosphere in the pipe. Conversely, if the oxygen concentration falls below 0.1 mg $L^{-1}$, the sulphides produced can be emitted into the space above the water.

- *The sulphate concentration*

Sulphates, like sulphites and some organic molecules containing sulphur, are reduced to sulphide by the action of sulphate-reducing bacteria. The more sulphates there are, the greater the production potential.

- *The concentration in nutrients (BOD)*

According to Pomeroy [13], the concentration in organic material and nutrients is correlated in most sewage systems to the *biochemical oxygen demand* (BOD). This parameter represents the amount of oxygen consumed by the biochemical oxidation phenomena in the aerobic phase. If there is an excess of sulphates, *i.e.,* for concentrations of 20 to 100 mg $L^{-1}$ the production of sulphides is linked to the BOD. According to Thistlethwayte [21], the sulphide production rate evolves with the BOD, according to the ratio $(BOD)^{0.8}$.

- *Temperature*

The temperature has a significant effect on bacterial activity. In general, an increase of 10 °C results in a two-fold increase in bacterial activity [22]. Beyond the maximum growth temperature for microorganisms, which depends on each strain, an increase in temperature will lead to a fall in activity. The temperatures reached in sewage systems are generally within the temperature range for the growth of sulphate-reducing microorganisms. Consequently, the higher the temperature, the greater the sulphate reduction and the higher the production of $H_2S$. In the same way, the temperature also has an effect on the solubility of hydrogen sulphide. A high temperature facilitates degassing of the sulphides into the atmosphere above the water. Overall, it appears that an increase of one degree Celsius leads to a 7% increase in $H_2S$ production [13].

- *Design*

The design of the sewage system itself also has an impact on the production of hydrogen sulphide. The more wastewater stagnates in the pipes without a supply of fresh air, the higher the risk of anaerobic conditions being created at the bottom of the pipe. Stagnating wastewater and slow flow rates therefore represent the most favourable conditions for $H_2S$ production. After this long anaerobic phase, $H_2S$ will be emitted in areas of turbulence (waterfalls, strong eddies, *etc.*).

In this context, the policy to reduce water consumption adopted over the past few years has led to the appearance of problems in systems, as with half the

water volume, effluent flow rates are limited and they contain more material thereby facilitating sedimentation of the elements in suspension.

Moreover, the current design of the systems takes into account future urban development to cater for urban densification or towns expanding. Systems are therefore oversized and extend over increasingly long distances.

Finally, areas with busy tourist seasons, such as seaside resorts, represent a particular design problem, as the wastewater flows are not constant throughout the year. Consequently, a "perfect" design is not possible and the production of $H_2S$ must be planned for during the design phase.

Different authors have worked on the development of equations to predict the kinetics of $H_2S$ production. Among them, Thistlethwayte [21] developed the following empirical relationship between the production of sulphides and the concentration in sulphate ions.

$$\frac{dS}{dt} = 0.5\,10^{-3} \times Vs \times (\mathrm{BOD}_5)^{0.8} \times (\mathrm{SO}_4^{2-})^{0.4} \times 1.139^{T-20^\circ\mathrm{C}} \times r^{-1}$$

With:

| | | |
|---|---|---|
| $\frac{dS}{dt}$ | $H_2S$ production kinetics | mg $L^{-1}$ $h^{-1}$ |
| $Vs$ | Average speed of the effluent | m $s^{-1}$ |
| $BOD_5$ | Biochemical oxygen demand at 5 days | mg $L^{-1}$ |
| $SO_4^{2-}$ | $SO_4^{2-}$ concentration | mg $L^{-1}$ |
| $T$ | Temperature of the effluent | °C |
| $r$ | Hydraulic radius | m |

This model predicts that sulphide production increases in line with the concentration of sulphate ions. It was demonstrated by Pomeroy and Bowlus [23] that this equation was not reliable if sulphates are in excess.

Pomeroy also proposed his model [13] based on the study of forty discharge pipes.

$$\frac{dS}{dt} = 1.0\,10^{-3} \times (\mathrm{BOD}_5) \times 1.07^{T-20^\circ\mathrm{C}} \times r^{-1} \times (1 + 0.37 \times \varnothing)$$

With:

| | | |
|---|---|---|
| $\frac{dS}{dt}$ | $H_2S$ production kinetics | mg $L^{-1}$ $h^{-1}$ |
| $BOD_5$ | Biochemical oxygen demand at 5 days | mg $L^{-1}$ |
| $T$ | Temperature of the effluent | °C |
| $r$ | Hydraulic radius | M |
| $\varnothing$ | Diameter of the pipe | m |

However, for this model to be valid, several conditions must be respected. Firstly, the sulphides must only be produced by bacteria. There must not be any

external supply. Secondly, the sulphides must not escape from the effluent to the part above the water or precipitate in the effluent. Finally, this model was adjusted for cases of high hydrogen sulphide production, *i.e.*, with a high sulphate concentration with no inhibition of bacteria and in the complete absence of oxygen. This model gives a pessimistic vision of the presence of $H_2S$ in sewage systems.

## 14.4. Impact of biodeterioration on cement materials

The phenomena of biodegradation in cementitious materials in the air in sewage systems can be seen as a mechanism with four successive stages. Firstly, the $H_2S$ in the atmosphere of the pipe will oxidize at the surface of the material as elemental sulphur. This can then be used by sulphur-oxidizing microorganisms. These microorganisms will oxidize all the reduced sulphur molecules to sulphuric acid. In a third step, the latter can permeate into a possible layer of deterioration and attack the underlying sound material.

However, not all cement materials react in the same way to biodeterioration (Fig. 14.5). Materials based on standard Portland cement (CEM I) are severely affected and will suffer a drop in their pH down to values as low as 1 or even less and will be severely damaged. The pH of materials based on calcium aluminate cement (CAC) will fall gradually and stabilize around 4. Their physical and mechanical integrity is preserved for a much longer period of time, as is their protective role. They therefore perform well on-site.

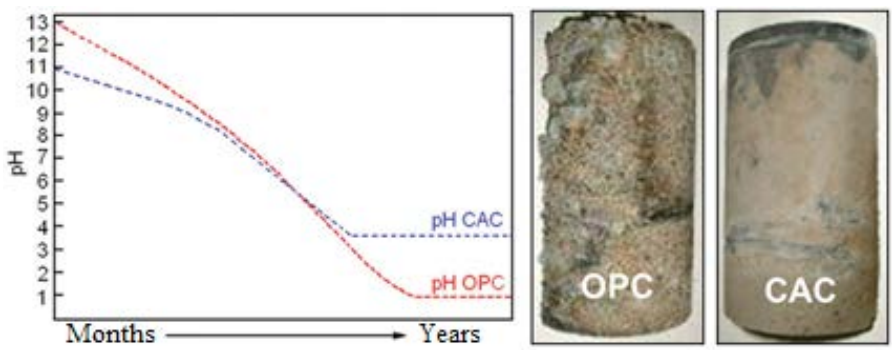


**Fig. 14.5.** – Evolution of the surface pH of cement materials based on ordinary Portland cement (OPC) and calcium aluminate cement (CAC). Pictures of two samples of concrete exposed during a period of 17 months in the Virginia Experimental Sewer [24].

The AFNOR standard FD P18-011 (2009) [25] defines aggressive chemical environments and proposes a list of suitable materials. Hydrogen sulphide in a

damp environment was added in the latest edition. Three levels of chemical aggressiveness defined according to the standard NF EN 206-1 [26] were proposed:

- XA1 < 0.1 mg $m^{-3}$;
- XA2 ≥ 0.1 and ≤ 10 mg $m^{-3}$;
- XA3 > 10 and ≤ 200 mg $m^{-3}$;

If the level of aggressiveness exceeds the threshold XA3, the standard FD P18-011 [25] recommends external protection (rendering, coating) or internal protection (impregnation). In general, managers opt to apply an epoxy resin type polymer coating which is inert to acid.

In an acid environment with an exposure class XA3, this publication recommends the use of five types of cement:

- CEM III/A, B and C;
- CEM IV/B;
- CEM V/A and B,
- Oversulphated cements;
- Calcium Aluminate Cement (CAC).

### *14.4.1. Influence of the chemical composition of the cement material on its durability in sewage systems*

The durability of sewage systems in areas subjected to biodeterioration depends, among other things, on the type of material used to build the structure. Each element in the formulation of the material (cement, sand, additives) will lead to a level of resistance to these aggressive environments.

Standard FD P18-011 (2009) [25] recommends incorporating a hydraulic or pozzolanic additive (blast kiln slag, fly ash, silica fume used as a partial substitute for ordinary Portland cement or incorporated into the concrete without being substituted for cement) to reduce the portlandite content ($Ca(OH)_2$) and thus ensure the cement performs well in contact with acidic solutions. This is the case of CEM III, CEM IV and CEM V. The portlandite content can also be reduced by using an oversulphated cement. This cement is prepared from blast kiln slag (≥ 80%), calcium sulphate (≤ 20%) and an activation system. The hydration process for this cement enables it to consume all the portlandite, leading to good resistance to chemical attack. As the hydration kinetics of this cement lead to very slow hardening, this type of cement has been largely abandoned. It is therefore rarely used in sewage systems.

By replacing the siliceous aggregates used traditionally to make cement materials with aggregates that are reactive to acid, such as calcareous or calcium aluminate aggregates, it is possible to significantly increase resistance to biodeterioration. The increase corresponds to a factor of 3 in the case of calcareous aggregates and a factor of 10 for calcium aluminate aggregates [27].

The durability of sewage systems can also be affected by modifying the chemistry of the cement phase, as proposed by CEM III and CEM V cements or by

calcium aluminate cements (CAC). The French standard NF P 15-315 describes alumina cement as a hydraulic binder resulting from the fine grinding to the point of fusion of a clinker mixture composed mainly of alumina, lime, iron oxides and silica in proportions such that at least 30% of the mass of the cement obtained is composed of alumina. Its chemical composition, particularly rich in aluminum in relation to silicon (unlike Portland cement) and which leads to the absence of formation of calcium hydroxide when hydrated, enables it to withstand many aggressive agents (pure water, sulphates, seawater, organic and mineral acids, *etc.*).

In sewage systems, calcium aluminate cement displays interesting properties by acting at several levels. Globally, its surface chemistry is not favourable to the oxidation of $H_2S$ and a three-fold protection gradually develops during exposure to aggressive conditions. This protection is the result of a better acid-neutralizing capacity than ordinary Portland cement, the formation of alumina gel that limits surface exchanges and a slowing effect, or even inhibiting effect in some cases, on microbial activity.

Herisson *et al.* [28] placed Portland CEM I and CAC mortars made with silica sand in contact for a period of three months in a controlled environment (30 °C and 100% relative humidity) in presence of a constant flow of hydrogen sulphide at 20 ppm (28 mg $m^{-3}$) and without adding any particular microorganisms. The materials were exposed to the air in the laboratory to allow natural carbonation of the surfaces. Analyses by scanning electron microscope performed at the end of this experiment revealed that only CEM I becomes covered with sulphur crystals formed by the oxidation of $H_2S$ (Fig. 14.6). The same experiment was performed in the same conditions but with a flow of 50 ppm (70 mg $m^{-3}$) of $H_2S$. In this case, sulphur crystals were observed on both materials but the quantity deposited was 3.5 times greater on the CEM I than on the CAC. Moreover, whereas the crystals on CEM I had the orthorhombic shape characteristic of elemental sulphur, those observed on the CAC were imperfect and displayed holes. It would therefore appear that the surface chemistry of calcium aluminate cements is less favourable to abiotic oxidation of hydrogen sulphide than that of CEM I.

During the biodeterioration process, calcium aluminate cement-based materials implement three protection mechanisms closely linked to the chemistry of the binder. The first is caused by a greater acid neutralization capacity than that of CEM I. This test, defined by standard XP CEN TS 15364 [29], consists in introducing a defined amount of finely ground material into different concentrations of nitric acid and monitoring the pH of the solution after 48 hours of immersion. The work presented in figure 14.7 was obtained from solutions of sulphuric acid in which 15 g of mortar were immersed. The acid neutralization capacity of CEM I is initially high, but it falls rapidly, reaching a very low value which lasts when a silica gel is formed. Conversely, calcium aluminate cement has an acid neutralization capacity that is initially lower, falls rapidly and reaches a plateau with pH values lying between 4 and 3. When the pH falls below 3, the material dissolves. Globally, this experiment shows that calcium aluminate cement has a higher capacity to buffer the pH between 3 and 4. Thus, reducing the surface pH of a CAC-based mortar to less than 3 would require a greater production of sulfuric acid by the sulphur-oxidizing microorganisms.

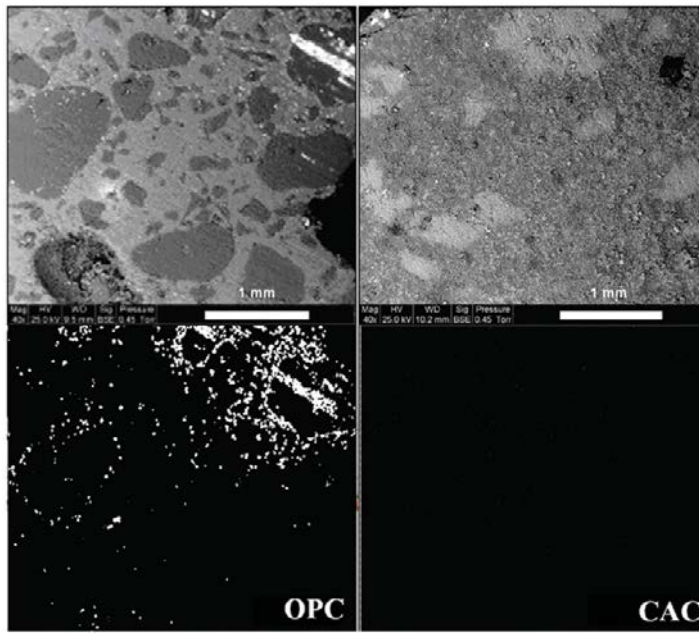


**FIG. 14.6.** – Top, SEM images in backscattered electron mode of two samples of mortars exposed for 3 months to 20 ppm (28 mg $m^{-3}$) of $H_2S$, 30 °C and 100% RH. Bottom, mapping of the sulphur associated with these images (same scale). Left, Portland cement-based mortar, right CAC-based mortar (image reproduced from [28] with the permission of IHS BRE Press).

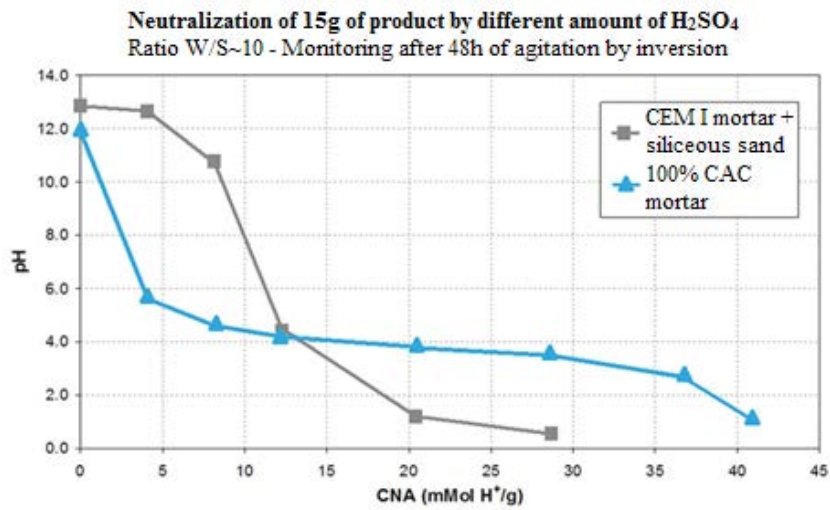


**FIG. 14.7.** – Estimated sulphuric acid neutralizing capacity for a CEM I Portland mortar with silica sand and a 100% alumina mortar (CAC cement and CAC-based sand).

The alkalinity of the calcium aluminate cement-based materials is provided by the main hydrated aluminates ($CAH_{10}$, $C_2AH_8$, $C_3AH_6$ and $AH_3$) [30]. The reaction of the calcium aluminate hydrates with acid leads to the precipitation of alumina trihydrate ($AH_3$ or $Al(OH)_3$) at the surface of the materials or in the close porosity, which can thus restrict access to the underlying sound material [31]. Moreover, $AH_3$ is a compound with a low solubility over a wide pH range from 3-4 to 10. Thus $AH_3$ will only dissolve in large quantities if the pH falls below 3-4. As acid attacks on calcium aluminate cement-based mortars lead to the transformation of the hydrates ($CAH_{10}$, $C_2AH_8$ and $C_3AH_6$) into $AH_3$, these materials have a high potential to withstand acid environments. Moreover, the literature indicates that the most detrimental microbial species in the biodeterioration process is *Acidithiobacillus thiooxidans*, which develops at a pH of between 0.5 and 5 [15]. By keeping the surface pH around 3-4 for a long period, CAC slows down the growth of this strain of bacteria [32].

The alumina trihydrate formed during the acid attack will also participate in setting up a second protection mechanism. By precipitating in the form of a gel in the porosity and on the surface of the material under attack, $AH_3$ will limit the kinetics of the exchanges between the acid and the material, thus slowing the aggressive action of the biogenic acid. The formation of this gel at the surface will also reduce the roughness of the surface of the material. This will make it more difficult for microorganisms to attach and form the biofilm. In comparison, CEM I remains rough, thus facilitating the development of the biofilm.

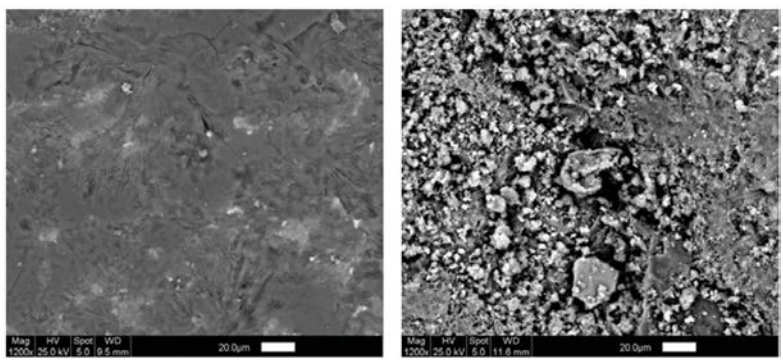


**Fig. 14.8.** – Observations by scanning electron microscope of mortars subjected to biodeterioration. Left: surface of a 100% alumina mortar smoothed by the formation of $AH_3$ gel. Right: surface of a Portland cement mortar displaying typical surface roughness.

Finally, this alumina gel is also the source of the last protective effect. During an acid attack, the alumina dissolves gradually releasing aluminum ions very locally. These ions display a bacteriostatic effect on the microorganisms associated with the biodeterioration process. Ehrich [33] showed that the $Al^{3+}$ ion reduces the activity of bacteria of the *Thiobacillus* genus with a threshold concentration that differs depending on the species. For *Halothiobacillus neapolitanus*, this

threshold is 250 mg $L^{-1}$, for *Starkella novella* 75 mg $L^{-1}$, for *Thiomonas intermedia* 50 mg $L^{-1}$ and for *Acidithiobacillus thiooxidans* 750 mg $L^{-1}$. A site study conducted by Herisson *et al.* [34] revealed that from 350 mg $L^{-1}$, the aluminum level is sufficient to inhibit microbial activity. This activity was quantified in samples of condensed water in contact with different cement matrices regulating the concentration of adenosine triphosphate (nucleotide present in all living beings and used to store and transport energy). In reality, microorganisms are always present and alive on the surface of the material but their functions are affected. Thus CAC will generate a highly localized defence mechanism that will protect it by reducing the production of biogenic acid.

All these mechanisms combine to achieve the response observed on-site (Fig. 14.5), a good performance of calcium aluminate cements in relation to the biodeterioration of cement materials.

### 14.4.2. Polymer coatings as protection for cement materials in sewage and wastewater systems

Polymer coatings are known to be inert in presence of acid. They should therefore be strong candidates for application in sewage systems for areas where the aggressiveness exceeds the XA3 threshold defined by standard FD P18-011 [25], for repairs or refurbishment. However, this solution is not necessarily adapted to damp environments due to the likelihood of generating poor reticulation of the polymer which in the long term may lead to defects (pitting, bubbles, cracks, *etc.*) or even to the coating becoming detached from the substrate. Even the smallest entry to the underlying material will be the starting point for an even more harmful deterioration process, as in this case the pure acid produced at the surface of the inert polymers will run over the coating and directly impact the underlying material without taking into account its bioreceptivity. There is therefore a risk of the cementitious material being exposed to a larger amount of sulphuric acid than if it had not been protected. The reaction of the pure biogenic sulfuric acid with the cement materials or metal materials will lead to the formation of expansive products capable of bursting the coating (Fig. 14.9).

**FIG. 14.9.** – Observations of a manhole protected with a polymer coating that was not effective in protecting the concrete structure on the left and the steel cover on the right.

Applying polymers in confined spaces such as sewage systems must also take into account an important health and safety aspect, as these repair solutions often contain solvents and/or components that are potentially dangerous to humans.

## 14.5. Tests *in situ* for the study of the biodeterioration phenomenon in sewage and wastewater systems

As the phenomenon of biodeterioration of cement materials in sewage systems consists in the production of sulphuric acid by microorganisms and as the surface pH of most materials is measured at values of 1 in damaged areas, it would seem logical to carry out sulphuric acid resistance tests at this same pH. However, purely chemical tests are not representative of the reality and can even lead to abnormal results for materials with a different bioreceptivity such as calcium aluminate cement. Laboratory tests aiming to be representative of biodeterioration phenomena must therefore involve microorganisms that will modulate their acid production according to the surface with which they are in contact. Reproduction in the laboratory of all the stages involved in biodeterioration is therefore difficult. This leads to tests also being carried out *in situ* despite the duration being generally longer and the conditions less controlled than a laboratory test.

### *14.5.1. Exposure in South Africa, the Virginia Experimental Sewer*

This type of work was set up in Virginia in South Africa [27] by the prefabricated pipe manufacturing industry in 1989 and is still being studied today. In an area with a reputation for its high levels of hydrogen sulphide, a system 65 meters long and 900 mm in diameter was built using new pipes with different compositions. This section was equipped with a diversion channel allowing the effluent to be diverted during inspections, which took place after 5, 12 and 14 years of service. Complete sections of some of the pipes made of ordinary Portland cement had deteriorated so badly during the last inspection that they had to be dug up to prevent collapse. New sections of pipe were installed in their place to study new cement formulations.

Based on all the results collected at the Virginia Sewer Network, Goyns *et al.* [35] put forward an improved version of the LFM (*Life Factor Method*), initially developed by Pomeroy and Pakhurst [36]. Whereas the initial LFM only considered the alkalinity of the cement materials, the study conducted in Virginia provided a new parameter closely linked to the material, the *Material Factor*, which includes the response of the material to the environment. This *Material Factor*

was set at 1 for the reference of the study (Table 14.5), a concrete composed of siliceous aggregates and an ordinary Portland cement binder. The *Material Factors* of the other materials were calculated according to their difference in relation to the reference, based on the average rates of deterioration.

**TABLE 14.5.** – Measurement of loss of thickness, calculation of rates of deterioration and the *Material Factor* (according to Goyns [27]).

| Cement/Aggregate | Estimate after 14 years | | *Material Factor* |
|---|---|---|---|
| | Total (mm) | Average (mm year$^{-1}$) | |
| CEM I/Silica | > 105 | > 7.5 | 1.000 |
| CEM I/Dolomite | 43 | 3.1 | 0.410 |
| CAC/Silica | 26 | 1.9 | 0.250 |
| CAC/Dolomite | 8.4 | 0.6 | 0.085 |
| 100% CAC | | | 0.025 |

The *Material Factor* proposed for concrete based on CAC and silica aggregates is 0.250 in relation to the reference. This indicates that the rates of deterioration proposed by Pomeroy and Pakhurst [36] must be divided by four to come close to reality. In the same way, the *Material Factor* calculated for a material made of 100% CAC is estimated at 0.025 in relation to the reference. This indicates that the resistance of this material is forty times higher than that of the reference sample and ten times higher than that of CAC/Silica.

The value of the *Material Factor* on this material was estimated not calculated because the material losses were too low to be quantifiable.

### 14.5.2. Exposure in Japan, Hokkaido university

Another Japanese research team also placed samples of ordinary Portland cement-based mortar in a sewage system in 2007 [37]. The aim of this research team was to better understand the bacterial succession behind the deterioration by monitoring the biodiversity during the exposure time. A large number of readings were made during the first six months, then work prevented access to the exposure zone. The last samples were recovered one year after they were set up.

The samples that were left in the sewage network for less than six months did not show any deterioration, just colonization by microorganisms. Conversely, those recovered after one year of exposure were severely deteriorated. A one centimeter layer of gypsum had developed on the surface of the material, which had lost half its thickness.

Analyses of the biodiversity revealed that there was indeed a bacterial succession on the surface of the exposed test specimens involving bacteria of the *Thiotrix*, *Thiomonas*, *Thiobacillus*, *Halothiobacillus*, *Acidiphilium* and *Acidithiobacillus* genus. During the first 70 days of exposure, no sulphur-oxidizing bacteria were

detected on the surface of the materials. From day 83, a filamentous bacterium of the genus *Thiotrix* spp. was revealed. It was replaced by *Thiomonas intermedia* from 102 days of exposure, then by *Halothiobacillus neapolitanus* after 130 days. After one year of exposure, *Acidithiobacillus thiooxidans* was the dominant strain. The maximum activity of this acidophilic bacterium is observed at the surface of the layer of deterioration on the material, coinciding with high concentrations of $O_2$ and $H_2S$. This study validates the three-stage mechanism described by Islander *et al.* [16].

### 14.5.3. Exposure in France, Ifsttar

Exposure on-site was also carried out by Herisson [38] in a French sewage system. Exposure consisted in introducing different mortar formulations into a crate suspended in the air above the water in the pipe and monitoring the evolution of these test specimens over a four-month period. As for most studies of this type, CEM I is used as a positive control for deterioration. If this reference sample deteriorates, conditions for biodeterioration are deemed present.

This study ran for almost three years and is still ongoing. All the samples placed in this system have shown an increase in mass, associated with the saturation of the porous network by the high level of humidity in the system (Fig. 14.10). After one year on-site, the reference started to significantly deteriorate (Fig. 14.11) whereas the test specimens made of calcium aluminate cement showed no significant loss of mass.

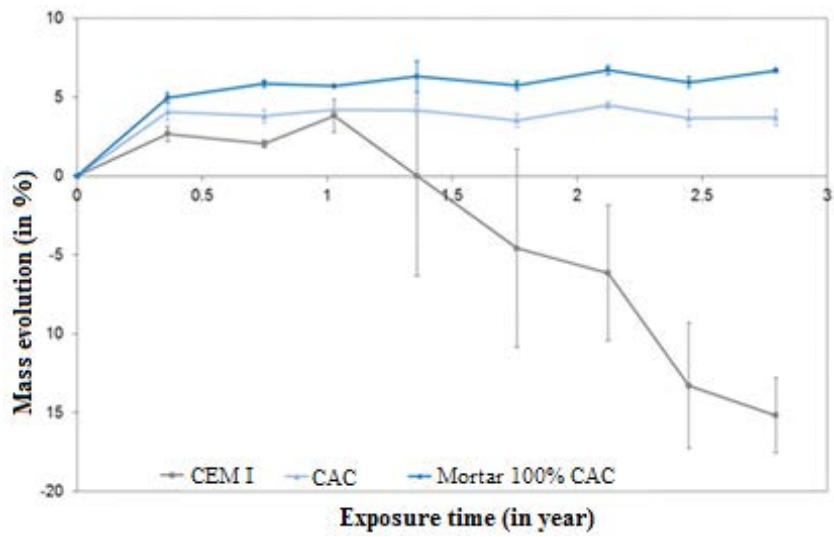


**Fig. 14.10.** – Change in mass during the exposure time of three mortars (CEM I + Silica sand, CAC + Silica sand and 100% CAC) exposed in a French sewage system for 3 years [38].


**FIG. 14.11.** – Typical evolution of the positive control for deterioration (CEM I + Silica sand) during 3 years of exposure on-site [38].

The evolution seen on this site is similar to that found in other studies carried out around the world. There is therefore a certain degree of universality in the mechanisms at stake due to the involvement of the ubiquitous sulphur-oxidizing microorganisms, which as they develop, produce sulphuric acid that is harmful to the materials.

## 14.6. Conclusion

Biodeterioration of cementitious materials in sewage and wastewater systems is due to the presence of hydrogen sulphide which is metabolized into sulphuric acid by sulphur-oxidizing microorganisms. This gas is formed by sulphur-reducing microorganisms in the sludge and sediments that build up at the bottom of the pipes. These systems, mainly constructed using cement-based materials, are severely affected by this production of biogenic sulphuric acid which dissolves the cement matrix and leads to the formation of gypsum and/or ettringite, which are expansive, non-cohesive products. In the long-term, if nothing is done to combat this detrimental phenomenon, there is a risk of the structure collapsing, incurring high costs to repair it.

Not all cement materials in these areas behave in the same way. Standard FD P18-011 [25] recommends different types of material according to the aggressiveness of the environment, represented by its level of hydrogen sulphide. Among the five cements recommended for the formulation of cement materials subject to exposure class XA3, calcium aluminate cement has been the most studied and its effectiveness is explained by a triple protection mechanism. For the harshest condition areas, above XA3, the standard recommends the application of a coating to preserve the cement material. If this coating is of polymer origin, it does not always provide a satisfactory protection. Based solely on the

good resistance displayed by calcium aluminate cement-based materials used to coat cast-iron pipes, managers can be considered to have a suitable cement material at their disposal to produce coatings to protect sewage systems.

Nevertheless, the formulation of cement materials used in sewage and wastewater systems can still be optimized. This involves conducting biodeterioration tests on-site or in the laboratory. Tests *in situ* offer the advantage of being representative of real phenomena, but they are not controlled and can be very long. Conversely, laboratory tests using microorganisms are generally shorter and better controlled, but are not always totally representative. Purely chemical tests are not suitable as they do not take into account the bioreceptivity of the materials. Work is currently in progress to finalise the development of a standardized test that will allow the performance of cement materials to be quantified in identical conditions in order to better compare their performances.

## References

[1] Le Gauffre P., Joannis C., Breysse D., Gibello C., Desmulliez J.J. (2005) "Gestion patrimoniale des réseaux d'assainissement urbains: Guide méthodologique." Editors: Tec & Doc Lavoisier Ed, Paris, France, ISBN 978-2743007485, 416 p.

[2] Satin M., Selmi B. (1999) "Guide technique de l'assainissement : Moniteur référence technique." Éditions du Moniteur, Paris, France, ISBN 978-2281111842, 660 p.

[3] Kaempfer W., Berndt M. (1999) "Estimation of service life of concrete pipes in sewer networks." Durability of Building Materials and Components, 8, 36-45.

[4] Olmstead W.M., Hamlin H. (1900) "Converting portions of the Los Angeles outfall sewer into a septic tank." Engineering News, 44, 317-338.

[5] United States Environmental Protection Agency (1991) "Hydrogen sulphide corrosion in wastewater collection and treatment systems." Technical Report, 430/09-91-010.

[6] Morton R.L., Yanko W.A., Grahom D.W., Arnold R.G. (1991) "Relationship between metal concentrations and crown corrosion in Los Angeles County sewers." Research Journal of Water Pollution Control Federation, 63, 789-798.

[7] Mori T., Nonaka T., Tazaki K., Koga M., Hikosaka Y., Noda S. (1992) "Interactions of nutrients, moisture, and pH on microbial corrosion of concrete sewer pipes." Water Research, 26, 29-37.

[8] Ismail, N., Nonaka, T., Noda S., Mori T. (1993) "Effect of carbonation on microbial corrosion of concrete." Journal of Construction Management and Engineering, 20, 133-138.

[9] Davis J.L. (1998) "Characterization and modeling of microbially induced corrosion of concrete sewer pipes." Ph.D. thesis, University of Houston, Houston, TX, USA.

[10] Monteny J., De Belie N., Vincke E., Verstraete W., Taerwe L. (2001) "Chemical and microbiological tests to simulate sulfuric acid corrosion of polymer-modified concrete." Cem. Concr. Res., 31, 1359-1365.
[11] Vincke E., Van Wanseel, E., Monteny J., Beeldens A., De Belie N., Taerwe L., Van Gemert D., Verstraete W. (2002) "Influence of polymer addition on biogenic sulfuric acid attack." International Biodeterioration & Biodegradation, 49, 283-292.
[12] Wells P.A., Melchers R.E. (2014) "Findings of a 4 years study of concrete sewer pipe corrosion." Corrosion & Prevention, 22, 1-12.
[13] United States Environmental Protection Agency (1974) "Process Design Manual for Sulphide Control in Sanitary Sewerage systems.", 136 p.
[14] Saucier F. and Herisson J. (2015) "Use of Calcium Aluminate Cements in H2S Biogenic Environment." Institute of Concrete Technology, Yearbook, 2015-2016.
[15] Hondjuila Miokono E., Lors C., Lamberet S., Damidot D. (2011) "Mise au point d'un test accéléré de biodétérioration de mortiers mettant en jeu une succession de bactéries sulfo-oxydantes." Mat. & Tech., 99, 555-563.
[16] Islander R.L., Devinny J.S., Mansfeld F., Postyn A., Shih H. (1991) "Microbial ecology of crown corrosion in sewers." Journal of Environmental Engineering, 117, 751-770.
[17] Okabe S., Itoh T., Satoh H., Watanabe Y. (1999) "Analyses of spatial distributions of sulphate-reducing bacteria and their activity in aerobic wastewater biofilms." Applied Environmental Microbiology, 65, 5107-5116.
[18] Kelly D., Wood A. (2000) "Reclassification of some species of *Thiobacillus* to the newly designated genera *Acidithiobacillus* gen. nov., *Halothiobacillus* gen. nov. and *Thermithiobacillus* gen. nov." International Journal of Systematic and Evolutionary Microbiology, 50, 511-516.
[19] Roberts D.J., Nica D., Zuo G., Davis J.L. (2002) "Quantifying microbially induced deterioration of concrete: initial studies." International Biodeterioration & Biodegradation, 49, 227-234.
[20] Tissot S., Pichard A. (2010) "Seuils de toxicité aiguë, hydrogène sulfuré ($H_2S$)." Rapport final de l'INERIS (France), Ministère de l'Écologie et du Développement durable, Ministère de la Santé, de la Famille et des Personnes handicapées, 37 p. https://substances.ineris.fr/fr/substance/getDocument/2667
[21] Thistlethwayte D.K.B. (1972) "The control of sulphides in sewerage systems." Ann Arbor Science, Ann Arbor, MI.
[22] Prescott L.M., Harley J.P., Klein D.A. (2003) "Microbiologie." De Boek Ed, ISBN 2-8041-1591-7, 1137 p.
[23] Pomeroy R.D., Bowlus F.D. (1946) "Progress Report on Sulphide Control Research." Sewage Works Journal, 18, 597-640.
[24] Alexander M.G., Goyns A., Fourie C. (2008) "Experiences with a full-scale experimental sewer made with CAC and other cementitious binders in Virginia, South Africa – Calcium Aluminate Cement." In: Proceedings of the Centenary Conference, Avignon, June 30-July 2 2008, Fentiman C.H., Mangabhai R.J. and Scrivener K.L. Eds. IHS BRE Press, 2008, EP94.

[25] FD P18-011 (2010) Béton – Définition et classification des environnements chimiquement agressifs – Recommandations pour la formulation des bétons. AFNOR.
[26] NF EN 206/CN (2014) Béton – Spécification, performance, production et conformité – Complément national à la norme NF EN 206. AFNOR.
[27] Goyns A. (2008) "Sewer Design Manual." Pipe and Infrastructural Product Division, CMA, Midrand, South-Africa.
[28] Herisson J., van Hullebusch E.D., Guéguen-Minerbe M., Chaussadent T. (2014) "Biogenic corrosion mechanism: study of parameters explaining calcium aluminate cement durability - Calcium aluminate". In: Proceedings of the International Conference, Avignon (France), May 18-21 2014, Fentiman C.H., Mangabhai R.J. and Scrivener K.L. Eds, IHS BRE Press, 2014, EP104, 633-644.
[29] XP CEN TS 15364 (2006) Caractérisation des déchets – Essais de comportement à la lixiviation – Essai de capacité de neutralisation acide et basique. AFNOR.
[30] Scrivener K.L., Capmas A. (1988) Chapter 13: "Calcium Aluminate Cement." In: Lea's chemistry of cement and concrete, Fourth edition, Hewlett P.C. Ed, Elsevier Science & Technology Books (2004), 713-782.
[31] Lamberet S., Guinot D., Lempereur E., Talley J., Alt C. (2008) "Field investigations of high performance calcium aluminate mortar for wastewater applications – Calcium aluminate Cements." In: Proceedings of the centenary Conference, Avignon (France), 30 June-July 2 2008, Fentiman C.H., Mangabhai R.J. and Scrivener K.L. Eds, IHS BRE Press, 2008, EP94, 269-277.
[32] Geoffroy V.A., Bachelet M., Crovisier J-L., Aouad G., Damidot D. (2008) "Evaluation of aluminium sensitivity on a biodegrading bacteria *Acidithiobacillus thiooxidans*: definition of a specific growth medium– Calcium aluminate Cements". In: Proceedings of the centenary Conference, Avignon (France), June 30-July 2 2008, Fentiman C.H., Mangabhai R.J. and Scrivener K.L. Eds, IHS BRE Press, 2008, EP94, 309-319.
[33] Ehrich S. (1998) "Untersuchungen zur biogenen Schwefelsäurekorrosion von zementgebundenen Baustoffen." PhD thesis, Hamburg university, Germany.
[34] Herisson J., Guéguen-Minerbe M., van Hullebusch E.D., Chaussadent T. (2014) "Behaviour of Different Cementitious Material Formulations in Sewer Networks." Water Science & Technology, 69, 1502-1508.
[35] Goyns A., Alexander M.G., Fourie C. (2008) "Applying experimental data to concrete sewer design and rehabilitation – Calcium Aluminate Cement." In: Proceedings of the Centenary Conference, Avignon (France), June 30-July 2 2008, Fentiman C.H., Mangabhai R.J. and Scrivener K.L. Eds, IHS BRE Press, 2008, EP94, 293-308.
[36] Pomeroy R.D., Parkhurst J.D. (1976) "The Forecasting of Sulphide Build-up Rates in Sewers." Conference of International Association of Water Pollution Research, Sydney, Australia.

[37] Okabe S., Odagiri M., Ito T., Satoh H. (2007) "Succession of sulfur-oxidizing bacteria in the microbial community on corroding concrete in sewer systems." Applied and Environmental Microbiology, 73, 971-980.
[38] Herisson J. (2012) "Biodétérioration des matériaux cimentaires dans les réseaux d'assainissement – Étude comparative du ciment d'aluminate de calcium et du ciment Portland". PhD thesis, université Paris-Est, Paris, France, 233 p.

# 15 Biodeterioration of cultural properties

**Faisl Bousta**

## 15.1. Introduction

Cultural property is submitted to numerous alteration factors, including those related to biodeterioration which should not be neglected. This type of damage corresponds to any physical or chemical change that a material may sustain under the effect of living organisms such as microorganisms, but also by insects and/or rodents.

All of the materials encountered in cultural heritage, whether they be traditional such as stone, stained glass, paintings, paper, textile, or more modern materials, such as concrete, synthetic fibres, resins and plastics, *etc.*, may be potential targets of microbial contamination.

A general principle could thus be formulated: it is necessary to be acquainted with microorganisms and their mechanisms of action to better understand them and to better understand them to protect oneself against them [1].

Numerous research is undertaken by teams worldwide to characterise biodeterioration phenomena and one only needs to refer to the existing bibliography on this subject to assess its full extent [2]. However, certain aspects of bio-deterioration mechanisms are yet to be discovered or further studied. The microbiology department of the LRMH[1] participates, at its own level, to an improvement of our knowledge in this area and has worked more particularly on highlighting bacterial participation in the oxidisation phenomena of the manganese present in medieval stained glass windows [3, 4].

When microbiological developments are confirmed, the control and the management of biodeterioration turn out to be very important. Curative treatments are then often inevitable. In many cases, chemical treatments are implemented, but alternative solutions are being optimised, such as the use of artificial lighting to block the photosynthesis of chlorophyllous microorganisms [5].

[1] LRMH – Laboratoire de Recherche des Monuments Historiques, Champs-sur-Marne, just East of Paris (France).

Then, the best way to fight biological deterioration remains preventive conservation.

All the illustrations presented in this chapter are from the LRMH collection.

## 15.2. Microorganisms involved in the biodeterioration of cultural property

The microorganisms that are involved in the biological alteration phenomena of the materials that make up the cultural heritage can be divided into three groups:

- microscopic fungi (moulds) and macroscopic fungi (*basidiomycota*);
- bacteria, a vast group of microorganisms, well known to be part of various alteration mechanisms;
- chlorophyllous organisms (algae, lichens).

In this chapter, the majority of microorganisms encountered on heritage properties will be summarized.

### *15.2.1. Microscopic fungi*

Other microbiological activity can sometimes be first detected in an olfactory manner. The "musty" smell perceived when entering into a church or a confined and humid space is the first sign of the presence of mould. A more careful visual inspection will reveal the little white or green down spots that punctuate the artworks.

The colonisation of a substrate is undertaken through an extension and a ramification of the hyphae. The growth of the mycelium takes place at its terminal parts where the major parts of syntheses occur.

Globally, fungus will damage the support it colonises through an emission of acids or enzymes. It will then extract the substances it needs, assimilate them inside the cell and dispose of the waste outside. The active (and therefore younger) cells are on the periphery of the growth area of the fungus, which corresponds to a zone of intense metabolic activity.

Fungi play a major role in the degradation of cultural heritage. It can colonise paintings, textiles, paper and parchment, leather, and many more materials [6] (Fig. 15.1).

Besides chemical alterations, fungus can provoke physical damage, through the pressure exerted on the substrate during the penetration of the mycelium in the microcracks. (Fig. 15.2 and Fig. 15.3).

Additionally, some fungi produce pigments such as black melanin which result in very harmful stains on the contaminated substrate.

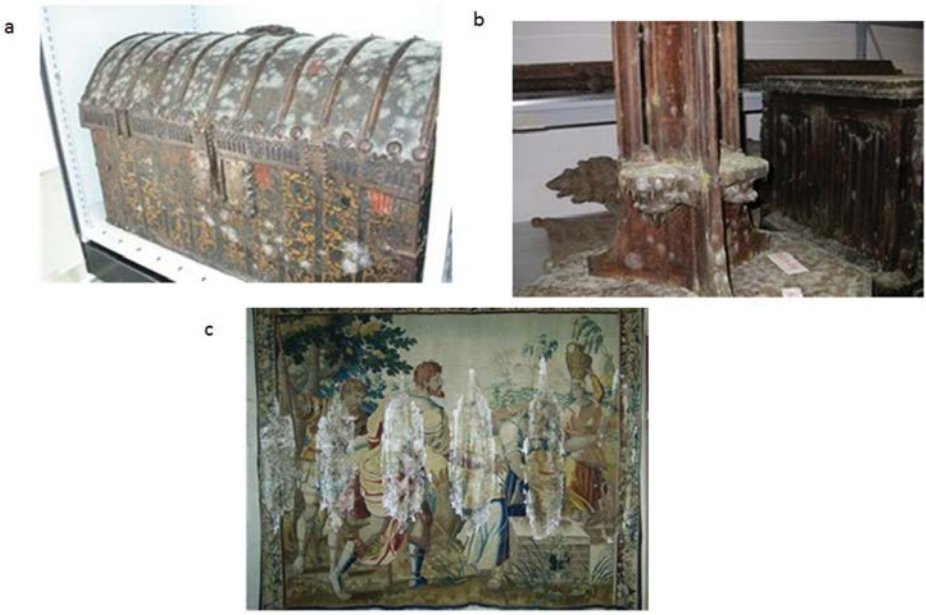


**Fig. 15.1.** – Examples of colonization by microscopic fungi on: a) a wooden coffer, b) wood pillar and c) a tapestry.

**Fig. 15.2.** – The lining of a tapestry completely altered by fungi.

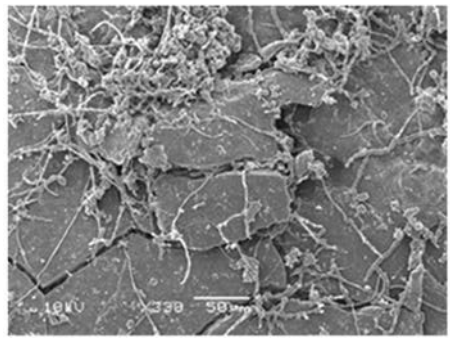


**FIG. 15.3.** – SEM view of the penetration of hyphae under scales of mural painting.

### *15.2.2. Basidiomycetes*

Wood is a material that is contemporary with man. Along with stone, it was one of the first building materials ever used. This presentation will focus on describing the main wood-destroying fungi encountered in historic monuments. Biological attacks that damage the condition of timber are primarily caused by microorganisms (fungi), xylophagous insects (which feed on wood) or insects nesting in wood.

The severity of attacks depends on characteristics linked to the wood species – particularly its chemical composition – as well external factors, such as climate and the wood service conditions, which facilitate or inhibit degradation.

The chemical composition of the various components of the lignocellulosic wall has an influence on the preference of white and soft rot agents for hardwoods and of brown rot agents for softwoods [7, 8].

The degradation mechanisms of the various components of wood have been extensively described in the literature and will not be covered in this chapter.

The basidiomycetes regularly found in historical monuments are cubic or brown rot agents, which primarily grow on softwoods. The second group concerns fibrous or white rot agents, which degrade the lignins of hardwood species. These fungi are capable of partially or totally destroying the wood. These are classified according to the damage they cause and the type of polymer they are capable of degrading (lignins, hemicelluloses or cellulose).

The consistency of material makes it possible to differentiate between the various types of rot:

- Fibrous or white rot – the wood is transformed into fibre with a white colour.
- Cubic or brown rot – the wood breaks down into cubes with a brown colour.
- Soft rot – the wood is soft and yields when pressed with the finger. This type of decay is generally encountered on exterior wood.

We will describe below the first two groups.

### 15.2.2.1. Brown rot agents

The wood attacked by these fungi becomes friable and its colour darkens following preferential degradation of cellulose and hemicelluloses. After drying out, wide longitudinal and transverse cracks appear, marking out volumes that are more or less cuboid in shape (Fig. 15.4), hence the alternative name *"cubic rot"*. The fungi regularly encountered in historic monuments belonging to this group are *Serpula lacrymans* (dry rot).

This fungus is not found in the natural environment. It appears to occur in homes only. Its specific physiology may at least partially explain this growth in a well-defined environment and only in temperate regions of Europe.

The sporophore varies in size. Initially it is greyish in colour, before turning rusty brown with the production of spores. This fungus grows very quickly in the wood and causes 5 cm deep cracks, accompanied by marked browning of the wood. The wood's compounds are then turned into a dark brown powder. The dry rot very quickly develops a high mass of mycelium on the surface of the materials it attacks.

This strain has the specific characteristic of developing rhizomorphs (also known as mycelial cords), *i.e.,* hyphae capable of carrying water. These may have diameters of up to 5 to 8 mm, and are capable of penetrating masonry joints or even brick if it is porous (Fig. 15.5).

**Fig. 15.4.** – Appearance of wood panelling damaged by dry rot.

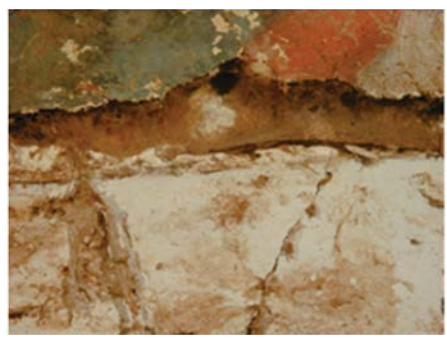

**Fig. 15.5.** – Dry rot filaments on a wall painting.

Other fungi found in historic monuments also cause brown rot, such as *Coniophora puteana* (Fig. 15.6) and *Poria placenta* (Fig. 15.7).

**FIG. 15.6.** – Ryzhomorphs of *Coniophora puteana* emerging from a wall.

**FIG. 15.7.** – Development of *Poria placenta* on a beam.

### *15.2.2.2. White rot agents*

The most frequently encountered fungus causing damage to historic monuments is *Phellinus megaloporus* (*Donkioporia expansa*).

This fungus is very widespread in France. A number of castles, including Versailles and Ancy-Le-Franc (France), have been victims of this fungus. It is found in the old beams of cellars or very damp roof timbers. It thrives particularly in the built-in joints of masonry structures. It is much slower acting than dry rot.

The fruiting body is typical, taking the form of a large patch ranging from a camel colour to brown (Fig. 15.8) and growing in upright forms depending on its initial position. Its maximum size is around 15 to 20 cm. The presence of several layers, in the form of tubes, can also be observed.

The colour of the timber lightens and becomes white, following preferential use of lignins, leaving the cellulose intact. At the end of the attack, the wood has the appearance of fibre bundles, which separate from one another (Fig. 15.9), hence the name fibrous rot.

This is undoubtedly the fungus most capable of damaging oak wood, subject to persistent re-humidification, used in buildings. However, it is very sensitive to the absence of large quantities of water.

Like dry rot, *Phellinus megaloporus* promotes death-watch beetle attacks, as encountered at several locations, including the castle of Ancy-Le-Franc (France), for example.

**Fig. 15.8.** – *Phellinus megaloporus* sporophore.

**Fig. 15.9.** – Damage caused by *Phellinus megaloporus.*

### *15.2.3. Non-photosynthetic bacteria*

There is another type of biodeterioration of materials, related to the anarchic activity of certain bacteria, which cannot however be brought to light by a plain visual examination. In fact, bacteria hardly ever generate visible coats on works of art. The major studies of bacterial attack concern building materials.

Chemoorganotrophic bacteria as well as fungi, use organic compounds as energy source. Dust and other particles carried by the wind and rain, as well as organic biomass (*e.g.,* photosynthetic organisms) contribute to the supply of organic matter. These bacteria are involved in biofilm formation on the surface

of the stone, causing changes in the physico-chemical properties of the mineral structure [9]. They can release complex organic acids that may induce phenomena of material dissolution.

Other material colonisation by chemoorganotrophic bacteria (oxidizing sulphur, nitrogen) has been highlighted.

A mention must be made for *Thiobacillus* which can oxidise sulphur to sulphates, salts that are harmful to stone conservation. This type of biodeterioration was first described in the 1960s [10], on monuments in France and Cambodia. The colonisation of marble by oxidising sulphur was also later widely documented by Italian researchers [11, 12]. Of course, the growth of these bacteria is dependent on the presence of sulphur in the material (in the shape of $SO_3^{2-}$, $H_2S$) provided by air pollution and/or *via* capillary action.

Similarly, nitrifying bacteria (*Nitrosomonas, Nitrobacter*) can cause the formation of nitrates (saltpetre) depending on the presence of ammonia compounds [9].

More generally, the phenomenon of bacterial alteration is more insidious than that caused by photosynthetic microorganisms or fungi because the bacteria are not visible to the naked eye. Their presence and participation in an alteration can only really be confirmed by laboratory analyses.

### 15.2.4. Photosynthetic microorganisms

Some biological colonisations can be seen with the naked eye. Large green or black stripes, or orange or greyish crusts on the facades of monument or on statues in parks and gardens, caused by the development of algae or lichen.

The factors that play a role in the installation of algae and cyanobacteria and their development are essentially humidity and light for photosynthesis, as algae require very few nutrients as such. Algae are very often the first colonisers that form a visible biofilm on the surface of the material [13, 16]. The nature of the substrate does not seem very significant since algae can be found on limestone, granite as well as coatings, concrete or even wall paintings (Fig. 15.10 and Fig. 15.11).

**FIG. 15.10.** – Head of a sculpture from the park of Courances castle (France), colonised by algae).

**Fig. 15.11.** – Interior of the Salles Lavauguyon church (France), the walls and pillars of which are highly colonised by algae.

The colonisation leads to aesthetic damage for the materials, but also represents a hazard for their preservation [9, 17]. In fact, certain algae have the capacity to mobilise calcium, either through precipitation around their mucilaginous cell wall, or through a solubilisation effect. They also lead to mechanical stress, through cell volume variation, during alternating dry and wet periods.

Besides aesthetic, chemical and physical impacts, algae also act as a substrate for other microorganisms such as bacteria.

On the other hand, alkali pH coatings as well as hydrophilic surfaces have turned out to be efficient against the development of algae [13, 18].

In addition to algae, the walls and facades of monuments often show a biodiversity rich in different species of lichens, which is a symbiotic association between an alga (*photobionte*) and a fungus (*mycobionte*) (Fig. 15.2).

**Fig. 15.12.** – Colonization of a roof by orange lichens.

The conditions that will initiate the growth of such or such other lichen are pH, humidity, luminosity and nitrogen input [19].

Lichen contributes to the deterioration of materials through physical, chemical and mechanical processes. Mechanical damage is due to the penetration of the hyphae in the substrate. The depth to which the thallus can penetrate depends on the species of lichen and the nature of the substrate (Fig. 15.13). A loss of cohesion may also occur due to the expansion and the contraction of the thallus during alternating dry and humid periods.

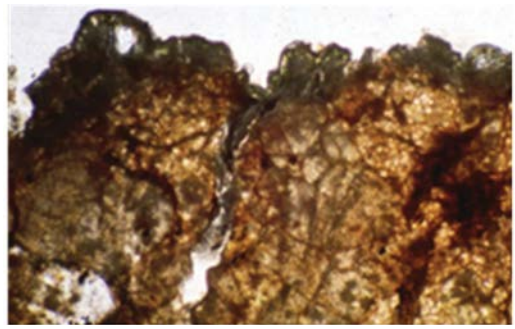

**FIG. 15.13.** – Optical microscopic view of a thin-section which shows the penetration of lichen roots inside the substrate.

Lichen may also chemically damage a substrate through the carbon dioxide produced by the respiration of the thallus and/or the secretion of lichenic and oxalic acids. These acid elements may, in the presence of humidity, lead to dissolution phenomena, especially when in the presence of limestone [19].

The real impact of lichen coverage on the conservation of materials is often very difficult to assess.

Cazzano [20] recently suggested an index of the biodeterioration potential of lichens (Lichen Potential Biodeteriogenic Activity (LPBA) should be established. He suggested a calculation of this index, by lithotype and in relationship to various parameters:

- the species in question;
- the surface of the covering;
- its reproduction capacity;
- the penetration depth of the hyphae;
- physical and chemical actions.

A first calculation attempt, undertaken for six different colonised substrates shows that taking into account these various factors involved into biodeterioration, provides a different and more exhaustive assessment of the impact of lichens [20].

The calculation of the LPBA index now needs to be optimised to evolve into a practical tool to evaluate the biodeterioration due to lichens, which could help scientists involved in the conservation of the cultural heritage.

## 15.3. Fungi detection methods

Visual inspection is the first step required to determine the presence of fungi (mould or basidiomycetes) in the buildings. This involves looking for any signs suggestive of fungal contamination: patches of dampness, signs of water damage (skirting boards detached, paint blistered), suspect odour, visible fungal growth.

To support this initial diagnosis, the investigation methods used nowadays are destructive methods, which consist in conducting probe tests, uncovering wooden elements or making holes in plaster or walls (Fig. 15.14). The person carrying out the diagnosis will determine the areas to be probed.

**Fig. 15.14.** – Drilling to check the health status of the woods.

Other methods also exist to diagnose the presence of basidiomycetes in buildings, such as: endoscopes [21], resistographs, micro-drilling, ultrasound or infrared thermography [22].

One of the methods currently being developed in the laboratory, in collaboration with the CSTB (French centre for scientific and technical building research), is the detection of microbial Volatile Organic Compounds (VOCm) released by fungi.

Whenever they start to grow, fungi give off volatile substances (Volatile Organic Compounds – VOC) *via* metabolic processes or the degradation of the material by the enzymes or acids they produce. Unlike spores, these compounds are dispersed in the environment, without being trapped by media. Consequently, detection of some of these compounds specific to one or more fungal species would enable, firstly, an identification of contamination from the onset of fungal growth and, secondly, detection of "hidden" contamination, for which spores are not released into the environment.

This non-invasive method consists in taking air samples in the room being investigated and analysing them by GC/MS to detect the presence or absence of growth of these fungi [23].

In all the environments investigated (castles, museums, libraries, *etc.*), contamination by fungi and basidiomycetes was detected by identification of these

targets coupled with a fungal contamination index based on the presence of specific VOCm [24, 25, 26, 27].

A microsystem for continuous air analysis is in the process of being developed in collaboration with the CSTB. This promising tool is designed to continuously analyse air in enclosed spaces and detect fungal contamination from the onset of growth.

## 15.4. Manganese oxidation of medieval stained glass windows

In recent decades, the corrosion of ancient stained glass has been the subject of numerous studies. The damage, mainly due to water and air pollution, appears either in the form of uniform crusts rich in alteration products or as corrosion craters. "Browning" is one of the figures of alteration that is commonly encountered. It is described as a dense surface layer which significantly reduces the transparency of the window (Fig. 15.15). Chemical investigations mainly attributed this phenomenon to the oxidation of manganese ions in the surface layer of the material, along with a decrease in the concentration of the same ions in the matrix. This browning was observed on various materials rich in manganese and iron, which is the case of stained glass from the Middle Ages, However, the origin of the browning process is not clearly identified: is it just chemical or would there be a microbial intervention?

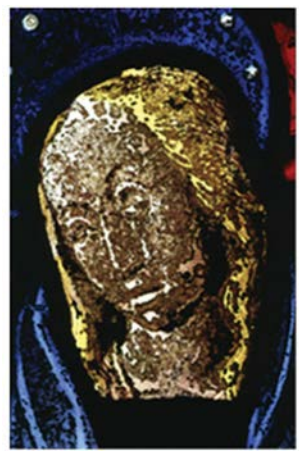

**FIG. 15.15.** – Browning on the surface of a fifteenth century stained glass window (Les Noës-Près-Troyes church, France).

The first objective of this research concerned the knowledge of the microbial community present on the stained glass surface. Specimens, whether brown or

not, from different French historical monuments, deposited pieces in archives or pieces still on-site were carefully selected as a basis for the study.

The count of the microflora present on the surface of the glass specimens followed two approaches: agar plate inoculation either by direct contact of the sample on the agar, or with a solution after thorough rinsing of the sample.

Several synthetic culture media were thus inoculated to highlight manganese-oxidizing bacteria.

After culture, the identification of the isolated bacterial strain provided interesting information: 11 strains potentially capable of oxidising manganese were discriminated in the whole visible colonies. Taxonomic differentiation indicated that 10 of them belong to the *Burkolderia cepacia* species and the last one was identified as *Chryseomonas luteola*. The study was then continued with the simulation of the phenomenon, first of all on a specific culture medium, with an identical chemical composition to that of ancient stained glass, and on model glass, with the bacteria isolated during the first step. The simulation of a synthetic culture medium was undertaken with culture media rich in manganese. After inoculation with the previously isolated bacteria and six weeks of incubation, the proof of the biooxidation of manganese was found in the form of black spots on the surface of the agar (Figs. 15.16a and 15.16b).

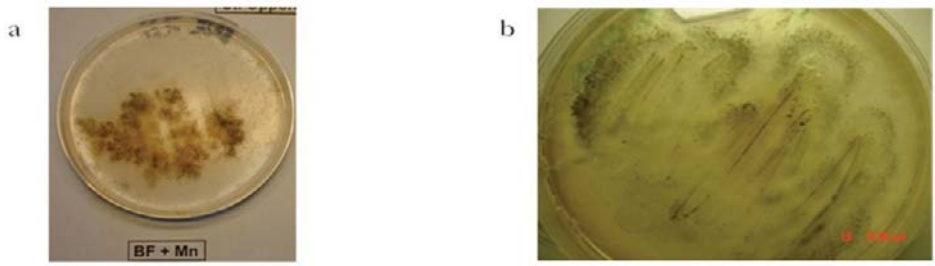


**Fig. 15.16.** – Specific culture medium manganese enriched: a) Aspect of the bacteria culture b) The black deposit is the result of a manganese biooxidation.

After the proof of the ability of bacteria to oxidize manganese in synthetic media, it was necessary to directly recreate the process on model glass. These samples were thus seeded with *Burkolderia cepacia* strains. After three weeks of incubation, the brown colouring phenomenon appeared, symptomatic of an early glass alteration [3].

In this study, it was shown that, even from stained glass deposited and conserved in archives for several years, it was possible to reactivate a specific bacterial flora involved in the oxidation of manganese. The simulations, first on synthetic media, then on model glass, were used to verify that, in the presence of manganese ions and after three weeks of culture, these bacteria were able to form black deposits resulting from a change in the chemical environment of the manganese (Fig. 15.17).

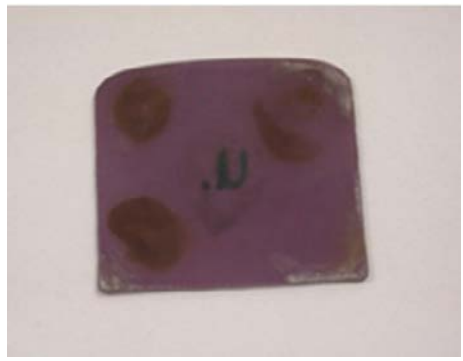

**FIG. 15.17.** – Simulation of the oxidation of the manganese on the model glass with two bacterial strains of *Burkolderia cepacia.*

The improved understanding of this browning phenomenon and the ability to recreate it, represent a breakthrough in our comprehension of the deterioration problems of ancient stained glass and will further help the development of new conservation tools (biocide treatments, enzymatic reduction, process inhibition...).

## 15.5. Treatments methods: the use of UV-C radiation

Currently, the only solution to eradicate biological coatings remains chemical treatment. The fight against these developments is a difficult problem to the extent that, if the products used must be efficient, they must also show durability over time and safety for the treated support. The algaecides used in biocide treatments are essentially alkyl quaternary ammonium. Experience shows that these products – although they belong to the same chemical family – do not give identical results in terms of efficiency, depending on the situation of contamination encountered. In addition, the leaching of biocides through water infiltration and the risk of groundwater contamination is a problem for the environment. In addition, biocidal products were targeted in February 1998 by a European Directive on the placing on the market of biocides (Directive 98/8/EC of 16 February 1998), in order to regulate their use and presence on the market [28, 14].

Other strategies to prevent microorganisms from colonizing materials were evaluated in 2009 by De Muynck *et al.* [15]. The use of light, more particularly of UV-C radiation, is being optimized to eradicate the growth of microorganisms.

Ultraviolet radiation is an electromagnetic radiation with a wavelength between that of the visible light and of X-rays. There are three types of ultraviolet: UV-A (400-315 nm), UV-B (315-280 nm) and UV-C (280-250 nm).

The effects of algae exposure to UV-C were analysed. The objectives were to seek an optimal exposure to UV-C in terms of radiation duration and frequency on algae grown on a solid support and also to highlight the impact of UV-C. For this, several additional parameters of macroscopic order (recovery rate in % and surface occupancy in $mm^2$) and physiological (survival rate, colorimetric viability test, amount of chlorophyll pigments and DNA extraction) were analysed.

The first experiment consisted in exposing an algal culture on a liquid medium, twice 15 hours, to UV-C. Between the two phases of treatment, the algae were placed one week at rest in a culture chamber. The measurements were carried out at T0, 1 day and 2 days for the macroscopic parameters and directly after exposure for the physiological parameters (chlorophyll assay, viability test and DNA extraction). The second experiment consisted in exposing in the laboratory (65 hours of UV-C) blocks of stone, on which a fixed surface had been inoculated with an algal suspension. Measurements of colonized surfaces and colour measurements were made after exposure.

The results obtained showed that exposure UV-C eradicated the algae in liquid medium with a lightening of the culture medium. The survival and the amount of chlorophyll measured after exposure were drastically reduced. On the stone blocks, the results showed a significant decrease in the colonized surface, which meant that the ability of the algae to expand and colonize the substrate was halted. This decrease was observed regardless of the exposure time and independently of the amount of algae seeded on the blocks.

Similarly, the recovery rate of algae deposited on the specimen decreased after exposure to UV-C. It should be emphasized that the observed decrease in the recovery rate corresponds to a bleaching of certain algal colonies, linked to the degradation of chlorophyll. This effect is all the more marked that the number of cells deposited is low. The results show that the effectiveness of UV-C treatment depends on the thickness of the algae layer, on the exposure time and the power of the lamps used [5]. After the laboratory experiments, a first treatment of stone blocks recovered *in situ*, with an algal overlap, was carried out (Fig. 15.18a and Fig. 15.18b) and (Fig 15.19a and Fig.15.19b).

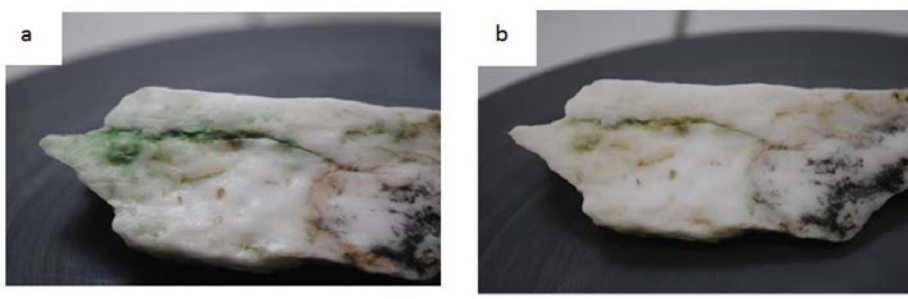


**Fig. 15.18.** – Sample of colonized limestone: a) treated surface and b) untreated surface.

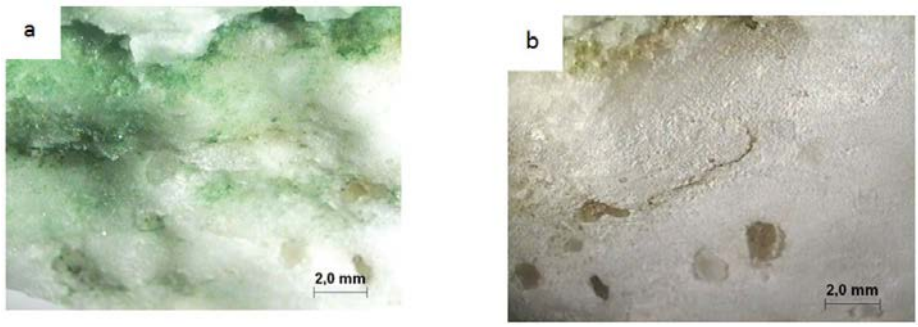


**FIG. 15.19.** – Area detail: a) treated surface and b) untreated surface.

Colorimetric measurements and photographs were taken before and after exposure. The results obtained show an elimination of the chlorophylls which results in a thinning of the treated surface. Experiments made it possible to optimize the irradiation times as a function of the lamp power and the thickness of the algae covering [5]. Finally, a combined approach between laboratory experiments and experiments in natural conditions is essential to advancing research in this area. Some initial field trials have already shown encouraging results (Figs 15.20a and 15.20b). In conclusion, a combined approach between laboratory experiments and experiments under natural conditions is essential to advance research in this field.


**FIG. 15.20.** – *In situ* test, colonized stone pillar: a) before treatment and b) after treatment.

## 15.6. Conclusion

Cultural heritage property is not immune to colonization by microorganisms. The latter are ubiquitous in indoor environments and numerous studies have demonstrated their role in the deterioration of the materials they invade (wood, textile, paper, pigment, varnish, *etc.*) until the partial or total destruction of the substrates. At present, the various heritage conservation services are deprived of the uncontrolled development of microorganisms and carry out corrective actions to treat altered materials. Probably due to the economic impact of biodeterioration, in recent decades this problem has taken its place in the field of scientific research, with many advances in knowledge of deterioration mechanisms, methods of treatment, methods of prevention and control of contamination before significant damage is noticed.

Even if we still have a long way to go, we need to persevere to understand better, identify, assess risks and solve (or try to solve) biodeterioration problems.

Only an integrated approach and a sharing of learning and experiences among scientists, managers of works of art and restoration professionals will lead to finding the most suitable strategies for the conservation of cultural property.

## References

[1] Roquebert M.F. (2002) "Les contaminants biologiques des biens culturels." Collection patrimoine, Elsevier Masson Ed., Paris, France, ISBN 2-84299-322-5, 419 p.

[2] Koestler R.J., Vedral J. (1991) "Biodeterioration of cultural property: A bibliography." International Biodeterioration & Biodegradation, 28, 229-340.

[3] Orial G. *et al.* (2007) "Incidence bactérienne dans les phénomènes de brunissement des vitraux anciens." L'actualité chimique, 312-317, 34-39.

[4] Ferrand J. *et al.* (2015) "Browning phenomenon of medieval stained glass windows." Anal. Chem., 87(7), 3662-3669.

[5] Borderie F. (2014) "Utilisation du rayonnement UV-C comme méthode alternative aux produits chimiques dans la lutte et le contrôle de la prolifération des microorganismes sur les matériaux du patrimoine." PhD thesis, université Franche-Comté, Besançon, France.

[6] Sterflinger K. (2012) "Fungi: Their role in deterioration of cultural heritage." Fungal Biology Reviews, 24, 47-55.

[7] Highely T.L. (1976) "Hemicellulases of white and brown-rot fungi in relation to host preferences." Mat. U. Org., 11(1), 25-36.

[8] Nilson T., Daniel G. (1987) "Influence of variable lignin content on brown-rot decay wood." Doc. IRG/WP/1320.

[9] Warscheid Th., Braams J. (2000) "Biodeterioration of stone: A review." International Biodeterioration & Biodegradation, 46, 343-68.

[10] Pochon J. *et al.* (1960) "Dégradation des temples d'Angkor et processus biologiques." Annales de l'Institut Pasteur, Paris, France, 98, 457-461.
[11] Lepidi A.A., Schippa G. (1972) "Growth of a sulphide oxidizing bacterium estimated by various methods and a new method of sulphide determination." In: Proceedings of 1st International symposium on the deterioration of building stones, La Rochelle, France, 139-141.
[12] Barcellona-Vero L., Mont-Sila M. (1975) "Isolation of various sulphur-oxidizing bacteria from stone monuments." In: Proceedings of the International Symposium - The Conservation of Stone I, Rossi-Manaresi R. Ed., Bologna, Italy, 233-234.
[13] Barberousse H. (2006) "Étude de la diversité des algues et des cyanobactéries colonisant les revêtements de façade en France et recherche des facteurs favorisant leur implantation." PhD thesis, Museum National d'Histoire Naturelle, Paris, France.
[14] Caneva G. *et al.* (2008) "Plant biology for cultural heritage: biodeterioration and conservation." Getty Conservation Institute, Getty publications, 408.
[15] De Muynck W. *et al.* (2009) "Evaluation of strategies to prevent algal fouling on white architectural and cellular concrete." International Biodeterioration & Biodegradation, 63, 679-689.
[16] Nugari M.P. *et al.* (2009) "Biodeterioration of mural paintings in a rocky habitat: The crypt of the Original Sin (Matera, Italy)." International Biodeterioration & Biodegradation, 63, 705-711.
[17] Crispim C.A., Gaylarde C.C. (2005) "*Cyanobacteria* and biodeterioration of cultural heritage: A review." Microbial Ecology, 49, 1-9.
[18] Dubosc A. (2000) "Étude du développement de salissures biologiques sur les parements en béton: mise au point d'essais accélérés de vieillissement." PhD thesis, Institut National des Sciences Appliquées de Toulouse, Toulouse, France.
[19] Lisci M.M. *et al.* (2003) "Lichens and higher plants on stone: A review." International Biodeterioration & Biodegradation, 51, 1-17.
[20] Gazzano C. *et al.* (2009) "Index of Lichen Potential Biodeteriogenic Activity (LPBA): A tentative tool to evaluate the lichen impact on stonework." International Biodeterioration and Biodegradation, 63, 836-843.
[21] Singh J. (1991) "Non-destructive inspection of the building fabric." In: Proceedings of Building Pathology, Bahns T. Ed, 90, UK, 215.
[22] Demaus R. (2001) "Non-destructive location and assessment of structural. English heritage research transaction." Timber 4, 100-109.
[23] Moularat S. *et al.* (2011) "Airborne fungal volatile organic compounds in rural and urban dwellings: Detection of mould contamination in 94 homes determined by visual inspection and airborne fungal volatile organic compounds method." Science of The Total Environment, 409, 2005-2009.
[24] Moularat S., Metri N. (2007) "Application d'un indice chimique de contamination fongique aux données de la campagne nationale logement de

l'observatoire de la qualité de l'air intérieur." Colloque La qualité de l'air intérieur, lieux de vie et santé, CSTB – DGS, Champs-sur-Marne, France.
[25] Moularat S. *et al.* (2008) "Detection of fungal development in a closed environment through the identification of specific VOC: Demonstration of a specific VOC fingerprint for fungal development." Science of the Total Environment, 407, 139-146.
[26] Moularat S. *et al.* (2008) "Detection of fungal development in closed spaces through the determination of specific chemical targets." Chemosphere, 72(2), 224-232.
[27] Joblin Y. *et al.* (2010) "Detection of moulds by volatile organic compounds: Application to heritage conservation." International Biodeterioration & Biodegradation, 64(3), 210-217.
[28] Caneva G.A. *et al.* (1989) "Correlation analysis in the biodeterioration of stone." International Biodeterioration & Biodegradation, 25, 161-167.

# Theme 5
# Design and modification of materials

Chapter 16 deals first with the choice of metallic material to resist corrosion and biocorrosion as a function of the environment.

Different strategies are presented in chapter 17 to prepare antimicrobial surfaces on various types of materials, such as polymers and metals. The surfaces can be modified, to make them antibacterial or more “cleanable”.

Finally, it is possible to modify the material structure, such as cementitious materials, in order to make them more resistant to environmental aggressions and to the colonization of their surfaces. The development of biosourced products, especially made from microbial extracellular substances, should make it possible to offer a genuinely environmentally satisfactory alternative, as described in chapter 18.

# 16 Choosing metallic materials with respect to microbial induced corrosion

**Damien Féron**

## 16.1. Introduction

The choice of a material is based essentially on the application for which it is intended. This choice will be based on the functional analysis of the final component and on the properties of the chosen materials. These are usually physical properties (mechanical, thermal, electrical, aesthetic or magnetic), but other criteria can also be important, such as price and/or availability, ease of forming, compliance with regulatory standards, *etc.* and sometimes corrosion resistance.

Metals, in the periodic table, are electropositive elements, thus electron donors in the language of microbiologists. It is generally the presence of a cloud of delocalised electrons which makes them electrical and thermal conductors. Their toughness and ductility are important properties for their forming. The excellent mechanical properties of metal alloys are generally associated with specific thermomechanical treatments. The most commonly used metals and alloys are various types of steel, copper and nickel alloys, aluminium and titanium with their alloys.

- Steels (iron-carbon alloys) are characterised by good mechanical properties (high elastic limit). Their low prices, the ease of forming and the weldability make them indispensable in numerous applications. Stainless steels contain a minimum of 12% chromium. It is this chromium which makes them passive (formation of a protective layer of chromium oxide a few nanometres thick).
- However, nickel alloys are generally used at high temperatures where their mechanical properties are partly maintained. In aqueous environments, they are passive, also due to the presence of chromium in the alloy, as with stainless steels.
- Aluminium and titanium and their alloys are characterised, in particular, by their low density and good mechanical properties and are often considered to have good corrosion resistance in aqueous environments. These materials are also passivable, with the formation of a protective layer of aluminium or titanium oxide respectively.

- Copper alloys are considered to be good electrical and thermal conductors and fairly resistant to aqueous corrosion, in particular in seawater. These alloys are also considered to have varying bactericidal properties. They behave differently from other metals and alloys in natural environments and in the presence of bacteria. This point will not, however, be covered here.

Metals and metal alloys have varying degrees of sensitivity to corrosion phenomena [1-9]. This sensitivity will depend on the environment (atmospheric corrosion, corrosion by gases or dry corrosion, presence of bacteria, *etc.*) and on the corrosion phenomenon concerned (general corrosion, localised corrosion, stress corrosion, hydrogen embrittlement, *etc.*). An assessment of risks must be carried out for each environment and corrosion phenomenon considered, for each alloy (Fig. 16.1). In this chapter, only corrosion phenomena in the presence of microorganisms, referred to as "MIC" (microbial induced corrosion) from now on, will be taken into consideration for choosing a metal material in the presence of microorganisms.

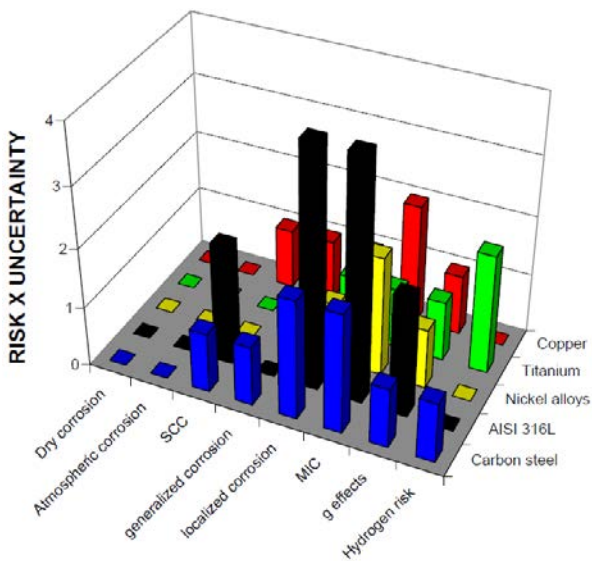


**FIG. 16.1.** – Assessment of the corrosion risk before choosing the most appropriate material for containers designed to storing nuclear waste. The risk is rated from 0 (improbable) to 4 (certainty of occurrence) [10].

Fundamentally, the industrial metals and alloys used are not thermodynamically stable in the aqueous environments to which they are exposed. It is therefore thermodynamically completely normal that they degrade. The rate of this degradation is the important factor. This rate must be compatible with the planned operating life of the industrial facility. If it is accelerated by the

presence of bacteria or microorganisms, there will also be a MIC phenomenon to be faced. The basic mechanisms of corrosion and MIC phenomena are described at the beginning of this document. The phenomena involved are complex, multi-phase and multi-physical: metal, oxides and hydroxides, aqueous solutions and bacteria. They also change in space and time with numerous metal/oxide, oxide/biofilm and biofilm/solution interfaces.

Two extreme cases of sensitivity to microorganisms, that of titanium and its alloys, and that of aluminium and its alloys, will be examined. This will be followed by discussion of the choice of steels based on the estimation of the corrosion rates (pits or general corrosion) and then stainless steels, with criteria associated with their passive nature.

## 16.2. Titanium and its alloys

Titanium and its alloys are considered to be insensitive to the presence of bacteria [11]. This behaviour is attributed to the stability of the protective oxide layer: at temperatures below 100 °C and in aqueous environments, titanium oxide is thermodynamically stable across virtually the whole of the stability region of water in the Pourbaix diagram [12].

In aerated natural environments (seawater or river water), the corrosion potential of titanium or its alloys increases at the start of exposure, like that of stainless steel, but at slower kinetics (Fig. 16.2), to reach values of approximately 300 mV/SCE (Standard Calomel Electrode) in natural seawater after two months' exposure. The presence of a biofilm in aerated conditions affects the electrochemical behaviour of titanium and its alloys. However, since these materials remain in their passive region even at these high potentials, this increase in corrosion potential has no effect on their behaviour in these environments.

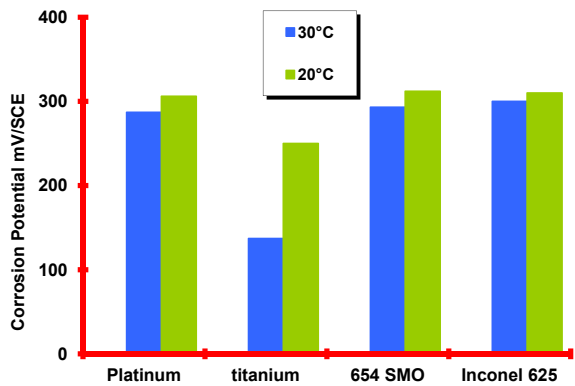


**Fig. 16.2.** – Free corrosion potential observed with platinum, titanium (grade 2), stainless steel (654 SMO®) and a nickel alloy (alloy 625), after 30 days in aerated, flowing seawater at 20 °C and 30 °C.

In deaerated conditions, to the best of our knowledge there is only one study describing pitting of titanium (grade 2) in the presence of sulphate-reducing bacteria, which attributes this degradation to the passive titanium oxide layer being attacked by sulphides to form $TiS_2$ [13]. However, other tests in the presence of high sulphide contents have never resulted in the formation of $TiS_2$ and demonstrate excellent resistance of the passive titanium oxide layer even at very reducing potentials [14].

In the risk assessment study (Fig. 16.1), the risk of MIC of titanium and its alloys is rated at 1 (out of 4): in fact, although the behaviour of titanium in the presence of bacteria is considered to be excellent (feedback), it is relatively poorly documented.

## 16.3. Aluminium and its alloys

The corrosion resistance of aluminium is associated with the formation of an aluminium oxide based passive film. This oxide is only thermodynamically stable in aqueous environments in a small pH range, between approximately 4 and 8 in the Pourbaix diagram [12]. Aluminium and its alloys are particularly sensitive to localised corrosion phenomena, which makes them vulnerable in the presence of microorganisms.

Unexpected severe degradation was obtained on aluminium and its alloys and attributed to the presence of microorganisms: around 1950 the US air force observed corrosion on the fuel tanks of aircraft associated with the presence of microorganisms [15]. Numerous other cases have been reported since then [16, 17]. Corrosion occurs in tanks when an aqueous phase is present at the interface between the fuel and the aluminium. The anaerobic zone that is created is favourable to the development of microorganisms and in particular fungi such as *Cladosporium* [16] or *Hormoconis* [18].

It should be noted that, in some cases there is no bacterial corrosion of the aluminium in natural environments [19], while for others aluminium and its alloys are particularly sensitive to the presence of bacteria, with in particular preferential attack of zinc or magnesium inclusions [17], or Al-Fe-Si or Al-Ti-Si precipitates [20].

The mechanisms involved include the production of metabolites that are corrosive for aluminium such as organic acids or sulphides (destruction of the passive layer), the role of enzymes, the creation of differential aeration cells, the degradation of corrosion inhibitors by bacteria such as the transformation of nitrates (inhibitor) into nitrites in closed circuits.

In practical terms, when aluminium alloys are chosen to be used when microorganisms may be present or in natural environments, protection against the microorganisms is added:

– Use of bactericides and rigorous constraints to limit the aqueous phase (always applied in the case of aircraft fuel tanks) [21].

– Use of corrosion inhibitors and bactericides in closed circuits, usually coupled with a special surface preparation (anodization).
– Cathodic protection in particular when aluminium or its alloys are used for structural elements.

It should also be noted that some laboratory tests demonstrate protection of aluminium by bacteria. In the case of *Aspergillus niger,* results obtained show either an acceleration or slowing down of the corrosion kinetics according to the conditions of exposure [22]. In industrial or natural environments, inhibiting effects of the presence of specific bacteria or the increases of corrosion by other bacteria are in fact not really under control.

## 16.4. Non-alloy steels

A great many terms are used to identify steels. According to standard BS EN 10020 (2000) which defines the term steel and establishes a steel classification, steel is a *"material containing in mass more iron by mass than any other element, of which the carbon content is generally less than 2% and which contains other elements... "*. This standard distinguishes between (i) non-alloy steels with low contents of alloying elements (maximum contents specified for numerous elements, for example maximum chromium content 0.3% or less), (ii) stainless steels which contain at least 10.5% chromium and less than 1.2% carbon, and (iii) alloy steels which cover all other steels. Although this is not the most commonly-used terminology, it will be used in this chapter. Non-alloy steels therefore include the terms "mild steels", "black steels", "carbon steels" and even "ordinary steels" which are still widely used.

Non-alloy steels are used extensively, in particular in natural environments and therefore in contact with seawater, river water, groundwater or in soil. Under these conditions, their general corrosion rates are usually significant (in particular in aerated conditions) and they are often used with added protection (for example, paint and/or cathodic protection) or with an additional "corrosion" thickness (as in the case of the steel sheet piles of quays in harbours). In closed circuits, it is normal practice to deaerate the aqueous environment and to use corrosion inhibitors, which results in lower general corrosion rates. Bacteria often produce the effect, in both aerobic and anaerobic conditions, of initiating localised corrosion (pits) and sometimes speeding up the general corrosion rate [1-9]. Although steel is rarely chosen based on considerations associated with corrosion (mechanical aspects, use, price, etc. are often the main criteria), it should be sized correctly. For the correct sizing of non-alloy steels, even when bacteria are present, two complementary methods based on semi-empirical models are proposed here: the pitting factor method and modelling the general corrosion.

### 16.4.1. Pitting factor

The pitting factor F is defined as being the ratio of the maximum pit depth to the average general corrosion depth:

$$F(t) = P/X \quad (16.1)$$

Where
P: maximum depth of the localised corrosion at time t
X: average loss of thickness of the metal due to general corrosion at time t

These values are determined schematically on cross-sections (Fig. 16.3). The uncertainties on the determination of pitting factor F concern both P (knowing whether the measured pit is the deepest) and X (in particular on old objects and the determination of the initial thickness of the object).

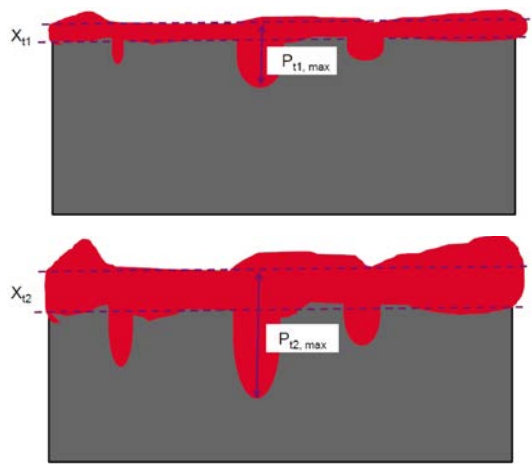


**FIG. 16.3.** – Determination of pitting factor (F) and how it changes (the layer of corrosion products is shown in red and the inner material in grey – X represents the observed general corrosion and P the depth of the pits, $P_{max}$ being the deepest pit observed): at time $t_1$, $F_{t1} = P_{t1,max}/X_{t1}$ (first diagram) and at time $t_2$, $F_{t2} = P_{t2,max}/X_{t2}$ (second diagram).

The changes to this pitting factor F show a decrease in its value with the loss of thickness associated with general corrosion (Fig. 16.4) which brings together data deduced from examinations carried out on non-alloy steels and cast iron, under various conditions, including:

- Temperatures between ambient temperature and 90 °C.
- Water which is almost neutral, slightly alkaline or cement water (pH 12).
- Clay or slightly, moderately or highly aerated soils.
- Environments that are (or are not) kept aerated.

– Extremely variable natural waters (clayed water, granitic water or seawater).
– Damage due to pits or caused by crevice corrosion
– The confirmed (or unconfirmed) presence of bacteria.

The latest compilation carried out by the Japanese is shown in figure 16.4 [24]. It includes laboratory data on localised corrosion at welds. These compilations are consistent with the initial results presented in 2000 which essentially included observations obtained on objects exposed in natural conditions [23].

Thus, the pitting factor values are systematically located below an envelope line described by a power law. This law expresses a decrease in the pitting factor with the depth of general corrosion. The law proposed for sizing gives slightly higher results than those given in figure 16.4. It is expressed by:

$$F = 4.64\ X^{-0.67} \tag{16.2}$$

*i.e.*

$$P = 4.64\ X^{0.33} \tag{16.3}$$

Where P and X are expressed in mm.

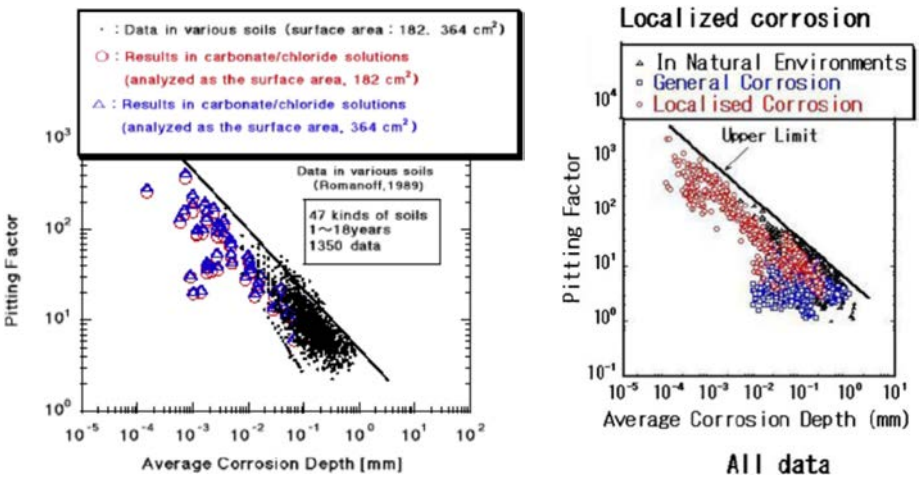


2000 compilation 2011 compilation

**Fig. 16.4.** – Changing pitting factor F as a function of the depth of the general corrosion (X in µm), first compilation in 2000 [23] and latest compilation [24].

Localised corrosion is therefore associated one-to-one with general corrosion which, ultimately, controls the degradation kinetics of steel, according to equation (16.1). The morphological variation in the corrosion front that can be inferred does not however tend towards a decrease in the surface roughness. In fact the maximum depth of the localised corrosion *P* continues to increase

with the depth of the general corrosion $X$, in accordance with the above law. However, a decrease in the importance of the localised corrosion in relation to that of the general corrosion is clearly seen over time (Fig. 16.5), in the case of a constant general corrosion rate of 10 μm year$^{-1}$. It can therefore be confirmed that the depth of localised corrosion becomes less than that of the general corrosion when the general corrosion exceeds 10 mm, *i.e.*, after a period of 1000 years in the example shown. The semi-empirical law on the variation in the pitting factor as a function of the general corrosion depth shows a greater slowing-down in the pit propagation kinetics than that of general corrosion.

The shape of the curve illustrating the variation in the pitting factor has been justified theoretically using electrochemical models in which it seems that the ohmic drop inside the pit leads to a maximum depth, resulting in a decrease in the pitting factor when this maximum depth is reached and the general corrosion continues. Other models, based on stochastic mechanisms (cellular automatons) also show a decrease in the pitting factor with the general corrosion. However this approach leads to relatively large additional "corrosion" thicknesses, and therefore to solid, heavy objects, which is often not a practical possibility, both in terms of cost and feasibility.

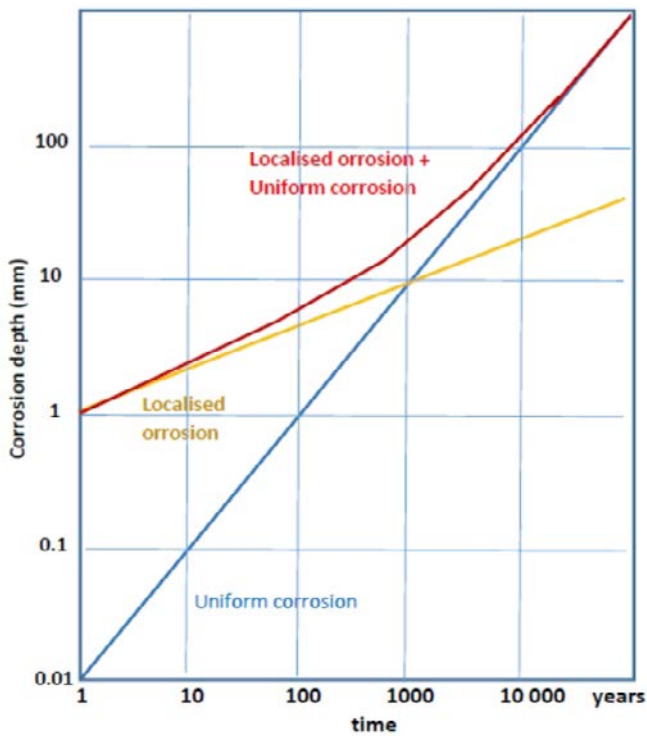


**FIG. 16.5.** – Variation of the depths of general and localised corrosion over time.

### 16.4.2. Quantification of general corrosion in natural water

In the context of the behaviour of steel bridges and infrastructures exposed to natural water (in rivers, estuaries or the sea) in Australia, R.E. Melchers [25-30] has developed modelling of the degradation of the steels used for these structures. This semi-empirical modelling is based on feedback and statistical use of the data gathered. The loss of sound metal is a probabilistic function expressed as follows:

$$\mathbf{c}(t, E) = \mathbf{b}(t, E).\mathbf{f}(t, E) + \varepsilon(t, E) \quad (16.4)$$

$\mathbf{c}(t, E)$ represents the loss of sound metal or the depth of corrosion (usually expressed in mm) which is dependent on time t (expressed in years) and factors grouped together in vector E which includes the environmental conditions, and the parameters of the material and its surface.
$\mathbf{f}(t, E)$ represents the expected average values or the observed average corrosion degradation.
$\mathbf{b}(t, E)$ is a bias function equal to one when $\mathbf{f}(t, E)$ represents the exact observed or expected metal losses.
$\varepsilon(t, E)$ is an uncertainty function which groups together the influence of all the parameters not included in $\mathbf{f}(t, E)$, such as the differences between similar samples (same material, same surface preparation, *etc.*) exposed to the same environmental conditions or the uncertainties in the determination of the feedback data.

Functions $\mathbf{b}(t, E)$ and $\varepsilon(t, E)$ must be known for operational application of this modelling. However, only data relating to $\mathbf{f}(t, E)$ are provided in the literature. It is therefore the average of the degradation associated with corrosion (loss of mass or depth), with no bias or uncertainty.

The variation in the function $\mathbf{f}(t, E)$ consists of a succession of four main phases (Fig. 16.6). For greater clarity, the term "corrosion kinetics" given below corresponds to the instantaneous corrosion rates.

The initial phase, "phase 0", is very short and is a matter of days, during which the kinetics are governed by local electrochemical reactions. It is during this phase that the surface is colonised by microorganisms.

Phase 1 is the period during which the diffusion of oxygen in the aqueous environment in contact with the surface of the metal limits the corrosion kinetics. These kinetics are linear, represented by the linear function $r_1$. It is also during this phase that the corrosion products form to reach a sufficient thickness and a consistency to limit the corrosion kinetics, leading to phase 2.

During phase 2, the corrosion kinetics are controlled by the diffusion of oxygen in the layer of corrosion products, and they therefore decrease as a function of the exposure time, but they can be described theoretically fairly simply [25]. As the layer of corrosion products is increasing, the kinetics of the oxygen diffusion and therefore the corrosion kinetics, decrease. With the development of the biofilm and the corrosion products, the oxygen concentration at

the metal interface decreases until anaerobic conditions are reached. Phase 3 then starts. The duration of phases 1 and 2 (labelled $t_a$) is an important parameter in the model as it indicates the time before which the corrosion is speeded up by bacteria.

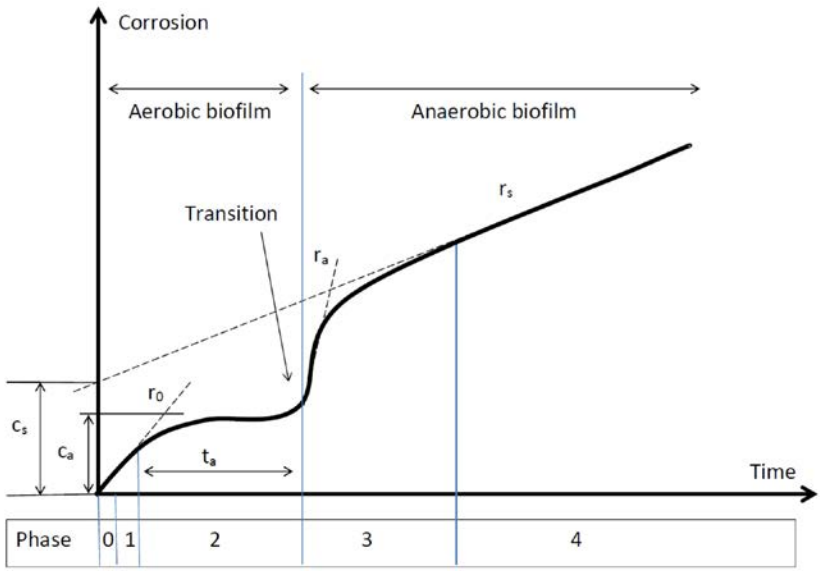


**FIG. 16.6.** – Variation in corrosion (loss of mass or thickness) as a function of time with indication of the parameters of function **f**(t, E) [25].

Phase 3 corresponds to the corrosion kinetics controlled by the presence of anaerobic bacteria and therefore corresponds to anaerobic conditions, although these conditions can be very heterogeneous. It is characterised by a more or less significant increase in the corrosion kinetics (labelled $r_a$), which will vary depending on the concentrations of nutrients in the aqueous environment.

In phase 4 of the model the corrosion kinetics are constant (labelled $r_s$), observed in numerous natural environments over long periods.

It must be emphasised that it is not assumed that a metal surface changes uniformly: function **f**(t, E) can differ according to the metal surface. It can thus describe the depth of a pit.

The environmental vector E includes the temperature, the dissolved oxygen and the nutrients (usually represented by the concentration of ammonium, and sometimes that of nitrates, phosphates or sulphates in the environment), and the pH of the water, but factors such as salinity or turbidity are not included. In addition, if parameters such as the season when the metal is immersed or the flow rate of the water are high at the start of exposure, these factors seem to play a lesser role over the long term and are not included.

The values of these parameters of **f**(t, E) have been calculated and presented in numerous publications for different steels and different natural environments:

- Non-alloy and alloy steels (mild and low-alloy steels) in seawater [25, 29, 30].
- Structural steels in fresh and brackish water [26, 27].
- Steels in ships' ballast tanks [28].

Graphs can be used to summarise the variation in these parameters, according to the environmental data grouped together in vector E. This variation is sometimes simple, such as the relationship associating parameters $c_s$ and $c_{sa}$ ($c_{sa} = c_s - c_a$) with the ammonium content ($NH_4^+$) in the natural environment (Fig. 16.7). However it is often a great deal more complex, as for the values of parameter $t_a$ according to the average temperature of the water in the aqueous environment and its pH (Fig. 16.8).

Over the long term (several years' exposure), only the value of $r_s$ becomes important and the extrapolation can be summarised by equation (16.5), assuming there is no bias or uncertainty:

$$\mathbf{c}(t, E) = \mathbf{f}(t, E) = c_s + r_s t \tag{16.5}$$

in which the damage **c**(t, E) is expressed in mm and t in years, and $c_s$ (mm) and $r_s$ (mm year$^{-1}$) depend principally, in natural seawater, on the temperature and nutrients in the dissolved mineral nitrogen content (inorganic) and expressed in mg of nitrogen per litre (mg N L$^{-1}$).

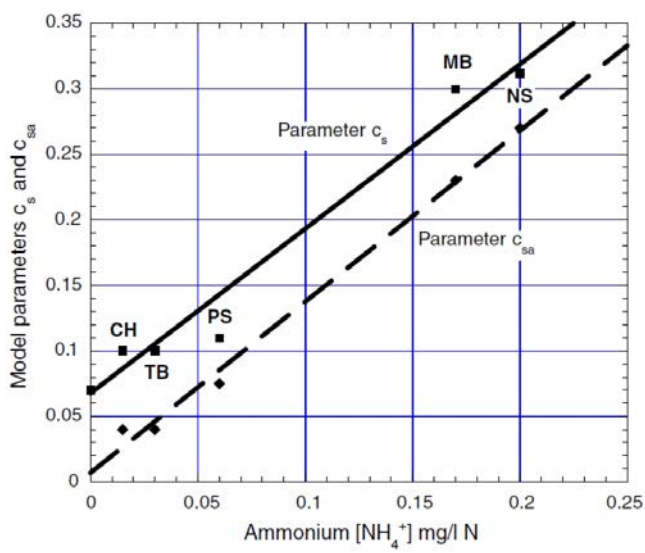


**Fig. 16.7.** – Variation in the parameters in model $c_s$ and $c_{sa}$ ($c_{sa} = c_s - c_a$) according to the ammonium content ($NH_4^+$) in the aqueous environment [27].

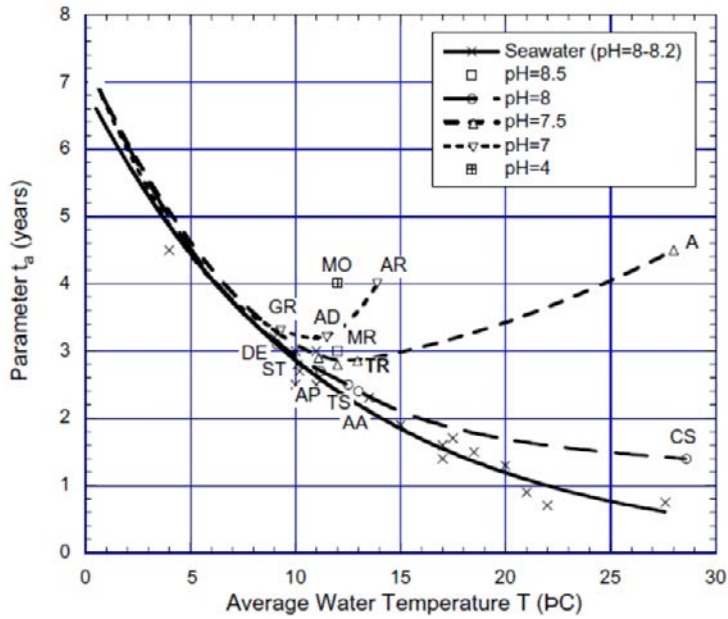


**FIG. 16.8.** – Variation in parameter $t_a$ in the model in figure 16.6 according to the mean temperature of the aqueous environment and its pH [26].

The values in Table 16.1 indicate a significant acceleration of corrosion in the presence of bacteria which, for example in the North Sea (average temperature 10 °C) result in doubling of the damage after 20 years' exposure in comparison with the values with (0.4 mg N $L^{-1}$) and without (0 mg N $L^{-1}$) bacteria.

**TABLE 16.1.** – Values of parameters $c_s$ (mm) and $r_s$ (mm $an^{-1}$) in natural seawater according to the temperature and the dissolved mineral nitrogen content [29].

| **Dissolved mineral nitrogen** | **Temperature: 10 °C** | | **Temperature: 25 °C** | |
|---|---|---|---|---|
| | **$c_s$ (mm)** | **$r_s$ (mm $year^{-1}$)** | **$c_s$** | **$r_s$ (mm $year^{-1}$)** |
| 0 mg N $L^{-1}$ | 0.15 | 0.050 | 0.10 | 0.068 |
| 0.2 mg N $L^{-1}$ | 0.39 | 0.054 | 0.30 | 0.075 |
| 0.4 mg N $L^{-1}$ | 0.61 | 0.057 | 0.50 | 0.092 |

## 16.5. Stainless steels

Although standard NF EN 10020 (2000) considers that a steel is stainless if it contains at least 10.5% chromium and less than 1.2% carbon, it is common practice to consider a steel to be stainless if it contains *at least* 12% chromium [9]. The good performance of these alloys is attributed to the presence of a film of chromium oxide (hydroxide) a few nanometres thick which protects the material from any additional oxidation, thus giving it its passive behaviour. These alloys are used increasingly in natural environments (seawater, river water, groundwater, *etc.*). Although their behaviour is generally very satisfactory in these environments, crevice corrosion in seawater or pits on welds or thermally affected areas in freshwater are observed and attributed to the presence of biofilms. It is therefore advisable to revise the criteria for choosing stainless steels with regard to their behaviour in these environments, taking the presence of these natural biofilms into consideration.

Several criteria can be used to classify stainless steels with regard to corrosion phenomena: the pitting index, the critical pitting temperature, the depassivation pH, the depassivation potential, *etc.*

In environments containing chlorides, the pitting index (PI) is certainly the first criterion used to classify stainless steels. It is usually determined based on the percentage of chromium, molybdenum and nitrogen in the alloy.

$$PI = \%Cr + 3.3x\%Mo + 16x\%N \quad (16.6)$$

In seawater, an index of more than 25-30 (depending on the authors) is required to avoid pitting at ambient temperature and an index greater than 40-45 is recommended to avoid crevice corrosion.

A stainless steel will generally behave satisfactorily if at least its corrosion potential $E_{cor}$ remains below the depassivation potential, $E_{dep}$. The following considerations are based on this criterion. It will be noted that purists believe that the corrosion potential should remain below the repassivation potential $E_{rep}$.

The usual chemical compositions of the stainless steels mentioned in this chapter are given in table 16.2, for information purposes.

**Table 16.2.** – Average chemical composition of some stainless steels (Bal. = balance).

| Common name | Ni (%) | Cr (%) | Mo (%) | Si (%) | C (%) | Fe (%) |
|---|---|---|---|---|---|---|
| 304L | 8.8 | 18 | 0 | 0.5 | < 0.03 | Bal. |
| 316L | 12 | 18 | 2.5 | 0.4 | < 0.03 | Bal. |
| 904L | 25 | 20 | 4 | <1.0 | < 0.03 | Bal. |
| 254 SMO | 18 | 20 | 6 | 0.4 | < 0.02 | Bal. |

### 16.5.1. Aerated environments

When exposed to natural environments, a biofilm develops on stainless steels which has the effect of increasing the free corrosion potential of these steels (Figs 16.9 and 16.10) [31-33]. This increase in the free corrosion potential (sometimes called "ennoblement") can occur not only in seawater to reach about 300 mV/SCE (Fig. 16.9) but also in fresh water such as in rivers where values exceeding 300 mV/SCE are sometimes recorded (Fig. 16.10). The increase in these corrosion potentials results in an increased risk of localised corrosion for these steels, particularly in the welds, heat-affected areas and confined areas (crevice corrosion). For the low alloyed steel grades (particularly those containing little molybdenum), there is a considerable risk of corrosion by pitting and crevices in the presence of chlorides.

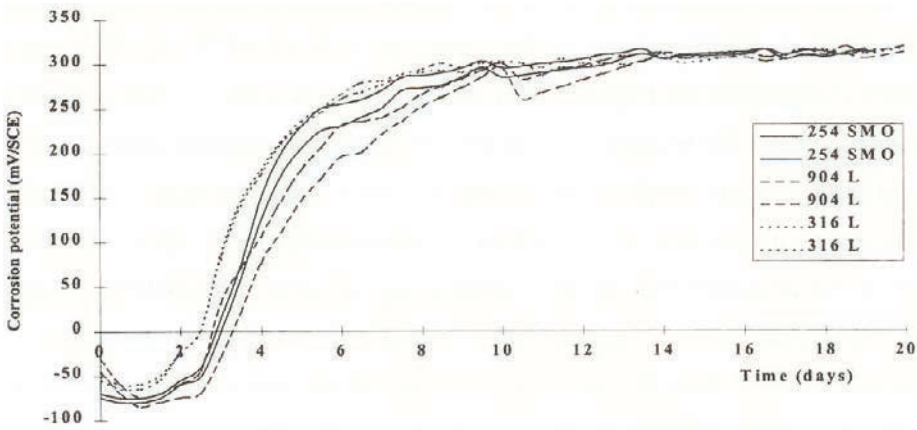


**FIG. 16.9.** – Variation in the free corrosion potential of stainless steels in natural seawater.

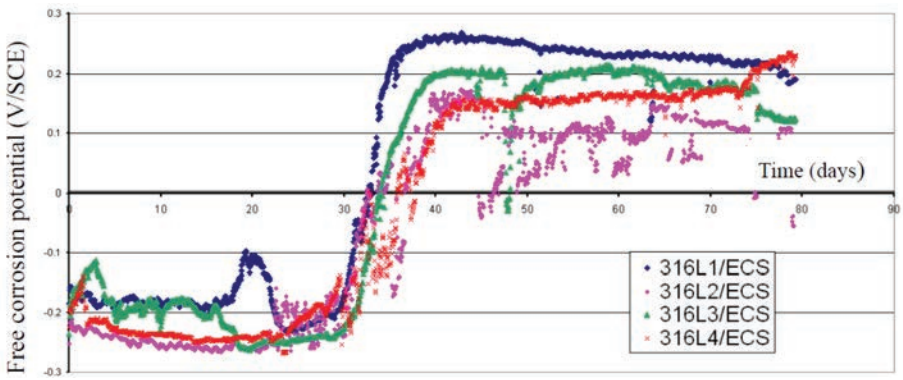


**FIG. 16.10.** – Variation in the free corrosion potential of an austenitic stainless steel in river water (Seine River, France).

The impact of the chemistry of natural waters (such as river waters) on the resistance of stainless steels also needs to be borne in mind. The increased corrosion potentials increase the risk of localised corrosion (pitting, crevice corrosion) in waters that contain high levels of chlorides. These waters can also naturally contain inhibitors of localised corrosion, such as sulphates and nitrates in particular, which thereby reduce the risk of localised corrosion. Consequently, semi-empirical laws have been established where the pitting potential and the repassivation potential are a linear function of the chloride concentration logarithm [34]. The following values were obtained:

For 304L stainless steel:

$$E_{dep(304L)} = -118 \log[Cl^-] + 526 \quad (16.7)$$

$$E_{dep(304L)} = -215 \log[Cl^-] + 475 \quad (16.8)$$

Whereas for 316L steel:

$$E_{dep(304L)} = -225 \log[Cl^-] + 1016 \quad (16.9)$$

$$E_{dep(304L)} = -215 \log[Cl^-] + 545 \quad (16.10)$$

Where the potentials are expressed in mV/SCE and the chloride concentrations in mg $L^{-1}$.

It should be pointed out that the beneficial effect of nitrates that inhibit pitting as soon as the ratio of the $[NO_3^-]/[Cl^-]$ concentrations reaches 1/10, whereas the $[SO_4^{2-}]/[Cl^-]$ ratio must reach the unit for sulphates so pitting inhibition can be observed.

It should also be pointed out that passivable alloys (titanium and alloys, nickel-based alloys) tend to behave in a similar manner electrochemically to stainless steels in natural waters: their free corrosion potential increases at the start of exposure as far as reaching values of around +250 to +400 mV/SCE.

### 16.5.2. Deaerated environments

Stainless steels are not only used in natural waters. Their utilisation in deaerated environments is also widespread: the deaeration of seawater is one of the most common treatments used in closed circuits to avoid localised corrosion, especially crevice corrosion.

Corrosion potential monitoring has shown that the electrochemical behaviour of stainless steels tested (austenitic and ferritic) is mainly determined by the sulphide content and the pH rather than the presence of sulphate-reducing bacterial (SRB). For instance, there is no difference between the free corrosion potentials of stainless steels in the presence or absence of *Desulfovibrio vulgaris* or *Desulfovibrio gigas* when the chemical composition – particularly the pH and sulphide content – are identical in environments with or without bacteria [35].

Identical results were obtained for depassivation potentials (pitting and crevice corrosion when there were crevices), as shown in figure 16.11 for 316L austenitic steel. There is no difference in the depassivation potential (initiation of crevice corrosion) when the pH, sulphide and chloride levels are identical, *i.e.* the same value and same uniform results are obtained. The potential values are very low in the presence of sulphides (400 ppm in the case of figure 16.11) or in pure cultures of sulphate-reducing bacteria, once again with identical levels in terms of the pH, sulphide concentration and chloride concentration. These conditions are the same as those sometimes found in marine sedimentation and marine mud. Nevertheless, sulphite contents generally are not as high, particularly in the case of biofilms which develop on the walls of circuits, even in an anaerobic environment.

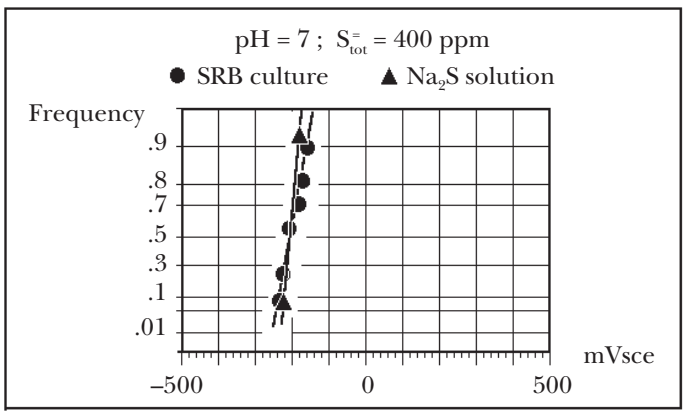


**FIG. 16.11.** – Crevice corrosion initiation potential (depassivation potential in the case of a crevice) of a stainless steel in 400 ppm of sulphide contained in seawater (sulphide content obtained either by using sulphate-reducing bacteria or by adding $Na_2S$). A frequency of 0.9 on the y-axis indicates that 90% of the samples have an initiation potential below the value given on the x-axis.

The effect of sulphate-reducing bacteria on the behaviour of stainless steels in a chlorinated anaerobic environment can therefore be simulated by using a sterile environment whose chemical conditions (the pH and sulphide content in particular) are equivalent to those obtained in the presence of these bacteria. The effect of sulphate-reducing bacteria on stainless steels therefore mainly relates to the chemical changes (pH and sulphide levels) that these bacteria impose on the surrounding environment. This in turn makes it possible to perform tests to determine the depassivation potentials under representative abiotic conditions. Before choosing a stainless steel, we must make sure that its free corrosion potential in the expected environment is below the depassivation potential, with or without crevices.

### 16.5.3. Mixed environments (with aerated and deaerated zones)

The electrochemical behaviour of stainless steels under mixed conditions, *i.e.,* with aerated zones and anaerobic zones, is illustrated in figure 16.12, which explains the deterioration observed based on the example of a 316L stainless steel in seawater [35]. With other stainless steels or with waters containing lower chloride contents, the initiation potentials of localised corrosion have different values but the reasoning remains the same:

- In a bacteria-free environment (sterile environment, synthetic water, *etc.*), the corrosion potential of the stainless steel used in our example is calculated at about 0 mV/SCE, whereas its crevice corrosion initiation potential is about +200 mV/SCE: the stainless steel will resist under this conditions of exposure (Fig. 16.12a).
- In an aerated natural environment, the material's corrosion potential rises to +300 mV/SCE. These high potentials are related to the formation of a biofilm, as mentioned earlier in the document. The material therefore displays potentials higher than or equal to the initiation potential of localised corrosion. The risk of localised corrosion due to crevice corrosion is real under these conditions (Fig. 16.12b).
- In mixed conditions, the potential of stainless steel reaches relatively high values due to the aerobic biofilm whereas the presence of sulphides makes the initiation potential of localised corrosion drop in the anaerobic zones: the material has no chance of resisting under these mixed conditions. The higher the sulphide content, the easier this corrosion will develop (Fig. 16.12c).

Mixed conditions therefore prove to be the most dangerous for these passivable materials: their corrosion potential is enhanced by the action of aerobic bacteria in the biofilm, while the presence of sulphate-reducing bacteria in anaerobic zones of the biofilm significantly decreases the passivable alloy's resistance to localised corrosion. In other words, the cathodic reaction is enhanced by the aerobic biofilm while the anodic reaction is impacted by the presence of sulphate-reducing bacteria. The increased rate of the cathodic reaction leads to an increase in the corrosion potential, while the presence of sulphides leads to a decrease in the depassivation potential in zones where the sulphate-reducing bacteria are present.

It is therefore necessary to avoid such mixed exposure conditions, or to choose an alloy the depassivation potential of which is higher than the corrosion potential, even in the presence of anaerobic zones containing sulphates. In reality, a compromise between these two solutions is often reached. Zones with high sulphide contents are avoided by making sure the biofilm is cleaned more or less regularly to prevent it from becoming too thick, and a more alloyed steel (*e.g.,* super-austenitic) with relatively high depassivation potentials is chosen.

The behaviour of nickel-based alloys is considered to be identical to that of stainless steel in aqueous environments. The same reasoning as that developed in this paragraph therefore applies, with different corrosion potential and depassivation values but with similar variations.

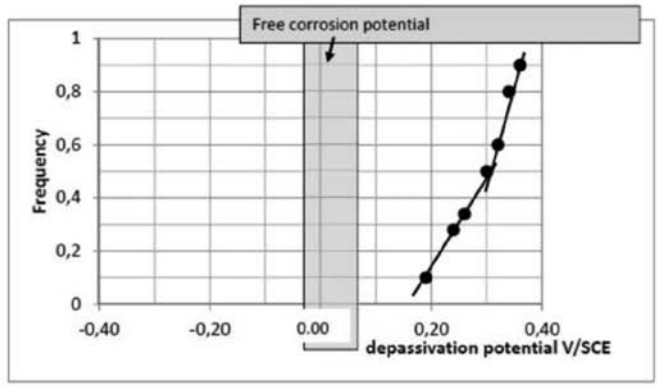


(a)

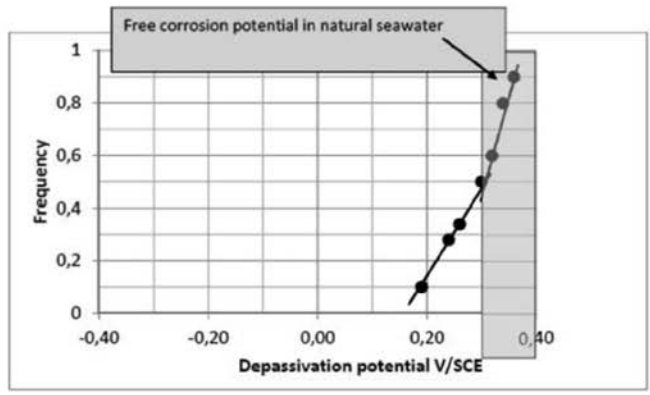


(b)

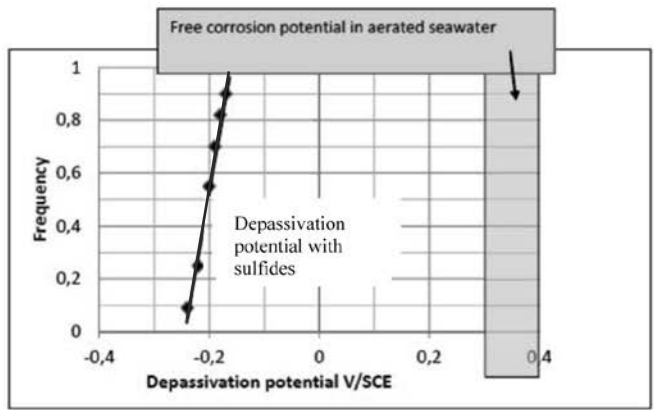


(c)

**FIG. 16.12.** – Illustration of the localised corrosion behaviour of stainless steels in sterile and natural environments (a) Sterile environment (*e.g.*, synthetic seawater) (b) Natural environment (natural seawater) (c) Natural environment with an old biofilm (natural seawater with an old biofilm on the steel).

## 16.6. Conclusion

Most metals and alloys are therefore sensitive to the presence of microorganisms: the behaviour of steels (including stainless steels), nickel-based alloys, aluminium and aluminium alloys can be impacted by the presence of microorganisms. Only titanium, tantalum and zirconium (including their alloys) appear to be unaffected by accelerated deterioration in the presence of microorganisms, even if their electrochemical behaviour can be marked by the same microorganisms. The reasons seems to be the thermodynamic stability of their passive layer in the domain in which these microorganisms exist.

To be able to choose alloys capable of resisting such bacteria, the behaviour of the alloy must be understood correctly, since each alloy behaves differently:

- Concerning titanium and its alloys, the presence of bacteria – whether aerobic or anaerobic – does not seem to pose any problems even if they do have a certain electrochemical effect.
- Conversely, aluminium alloys are very sensitive to the presence of microorganisms; using bactericides or cathodic-type protection currently seem to be the best solution to prevent their degradation.
- Non-alloy steels are also sensitive to microorganisms, but tools are available and they should be used, *e.g.*, the pitting factor to assess the depth of pitting caused by bacteria, or general corrosion models to determine the increase in the corrosion rate due to the presence of bacteria.
- Concerning stainless steels, their depassivation potentials must be reassessed to take into account the effect of anaerobic bacteria, and the free corrosion potentials must be estimated taking into account the increased cathodic reaction due to aerobic biofilms. Stainless steels thus chosen will have a greater probability of behaving correctly, even in the presence of microorganisms.

It must also be pointed out that the usual means of fighting corrosion (not discussed in this chapter) are effective to minimize MIC (coatings, paint, cathodic protection, inhibitors, *etc.*). Cathodic protection is commonly used to limit the corrosion of structures and equipment. This solution is particularly efficient for steels (non-alloys and stainless steels).

In addition to choosing alloys based on the existence of microorganisms, several other precautions can also help significantly limit the risks of MIC:

- The quality of the water used is also a key point. It is important to reduce the water's turbidity and suspended particles to avoid deposits and the development of anaerobic bacteria under such deposits. Limiting the concentration of organic molecules – particularly biodegradable organic carbon – helps reduce the development of microbes.
- The existence of confinement or stagnation zones can be penalising during operation, while monitoring the protective measures (like potentials or applied currents for cathodic protection, injection of inhibitors or biocides) is beneficial.
- Where possible, the periodic cleaning of volumes and pipes limits the development of thick biofilms and thus electrochemical cell phenomena.

Mixed conditions certainly represent the most risk in terms of microorganism-related deterioration as they correspond to the simultaneous presence of aerobic and anaerobic zones.

In fundamental terms, microorganisms only accelerate or modify one of the electrochemical reactions occurring during aqueous phenomena. One of the main problems is that it is still difficult to assess the real risk of MIC for new facilities. Though an increased risk of corrosion due to the presence of bacteria is often related to the increased kinetics of the cathodic reaction, the existence of protective biofilms must nevertheless be underlined as they have a reverse impact than corrosive biofilms: they do not facilitate the cathodic reaction (removal of electrons produced by corrosion), but instead inject electrons into the material. This is known as cathodic "bioprotection". These biofilms are developed within the scope of microbial fuel cells. Though it is currently true that we do not have any control over biofilms which accelerate the cathodic reaction, any more than we do over anodic biofilms, this will probably not be the case in the future.

## References

[1] Chantereau J. (1980) "Corrosion bactérienne – Bactéries de la corrosion." Technique et documentation, Paris, France, ISBN 2-85206-044-2.

[2] Tiller A.K., Sequeira C.A.C. (1995) "Microbial corrosion." The Institute of Materials, European Federation of Corrosion Publications, 15, London, UK, ISBN 0-901716-62-6.

[3] Lemaître C. *et al.* (1998) "Biodétérioration des matériaux." Lemaître C., Pebere N., Festy D. Eds, EDP Sciences, Paris, France, ISBN 2-86883-329-2.

[4] Bergel A., Féron D. (2001) "Actes du IV Forum Biodetérioration des Matériaux". IOM communications, London, UK, ISBN 2-9516844-0-1, CEFRACOR, Paris, France.

[5] Matériaux & Techniques (2005) "Numéro hors série du VII Forum Biodétérioration des Matériaux", EDP Sciences, Paris, France, 93.

[6] Fritz-Feugeas F. *et al.* (2008) "Biodeterioration des matériaux. Action des micro-organismes de l'échelle nanométrique à l'échelle macroscopique." Fritz-Feugeas F., Cornet A., Tribollet B. Eds, Technosup collection, Ellipses, Paris, France, ISBN 978-2-7298-3996-3, 258 p.

[7] Bergel A., Féron D., Flemming H.-C. (2014) "Bioelectrochemistry" Special issue Biocorrosion 2012 – From advanced technics towards scientific perspectives, 97(1).

[8] Liegen T. *et al.* (2014) "Understanding Biocorrosion: fundamentals and applications." EFC publication, Woodhead publishing Limited, Cambridge, UK, 66.

[9] Lacombe P. *et al.* (1990) "Les aciers inoxydables." Les Éditions de Physique, EDP Sciences, Paris, France, ISBN 2-86883-142-7, 1016 p.

[10] Le Calvar M. (2006) "Corrosion in geological disposal of high nuclear waste." In: ICG EAC Meeting, May 14-19 2006, Charleston, USA.
[11] Schutz R.W. (1991) "A case for titanium's resistance to microbiologically influenced corrosion." Material Performance, 30, 58-61.
[12] Pourbaix M. (1963) "Atlas d'équilibres électrochimiques à 25 °C." Gauthier-Villars Cie, Paris, France, 644 p.
[13] Rao T.S. *et al.* (2005) "Pitting corrosion of titanium by a freshwater strain of sulphate reducing bacteria (*Desulfovibrio vulgaris*)." Corrosion Science, 47, 1071-1084.
[14] Rauscher A. *et al.* (1990) "Effects of hydrogen sulphide and temperature on passive behavior of titanium." Corrosion Science, 3I, 255-260.
[15] Hedrick H.G. (1970) "Microbiological corrosion of aluminium." In: Proceedings of 25th conference NACE, 609-619.
[16] Churchill A.V. (1963) "Microbial fuel tank corrosion." Material Protection, 6, 19-23.
[17] Hedrick H.G. (1970) "Microbiological corrosion of aluminum." Material Protection, 1, 27-31.
[18] Rosales B.M., Iannuzzi M. (2008) "Aluminium AA2024 T351 aeronauocal alloy Part 1. Microbial influenced corrosion analysis." Materials Science and Engineering, A472, 15-25.
[19] Vargel C. (1999) "Corrosion de l'aluminium." Dunod, Paris, France, ISBN 978-2-100-06569-1.
[20] Forte Giacobone A.F. *et al.* (2011) "Microbiological induced corrosion of AA6061 nuclear alloy in highly diluted media by *Bacillus cereus* RE 10." International Biodeterioration & Biodegradation, 65, 1161-1168.
[21] Passman F.J. (2013) "Microbial contamination and its control in fuels and fuel system since 1980: a review." International Biodeterioration & Biodegradation, 81, 88-104.
[22] Juzeliunas E. *et al.* (2007) Microbially influenced corrosion of zinc and aluminium - two year subjecvtion to influence of *Aspergillus niger*. Corrosion science, 49, 4098-4112.
[23] JNC (2000) "H12: Project to establish the scientific and technical basis for HLW disposal in Japan." Second Progress Report, Japan Nuclear Cycle Development Institute.
[24] Tanigushi N. *et al.* (2011) "Propagation behaviour of general and localised corrosion of carbon steel in alkaline media." Corrosion Engineering, Science and Technology, 46, 2, 117-123.
[25] Melchers R.E. (2003) "Mathematical modelling of the diffusion controlled phase in marine immersion corrosion of mild steel." Corrosion Science, 45, 923-940.
[26] Melchers R.E. (2006) "Modelling immersion corrosion of structural steels in natural fresh and brackish waters." Corrosion Science, 48, 4174-4201.
[27] Melchers R.E. (2007) "The effects of water pollution on the immersion corrosion of mild and low alloy steels." Corrosion Science, 49, 3149-3167.

[28] Melchers R.E. (2008) "Operational based corrosion analysis in naval ships." Corrosion Science, 50, 3296-3307.
[29] Melchers R.E. (2014) "Long-term immersion corrosion of steels in seawaters with elevated nutrient concentration." Corrosion Science, 81, 110-116.
[30] Melchers R.E. (2014) "Microbiological and abiotic processes in modelling longer-term marine corrosion of steel." Bioelectrochemistry, 97, 89-96.
[31] Mollica A., Trévis A. (1976) Influence of the microbiological film on stainless steel s in natural seawater." In: Proceedings of Fourth Congress on Marine Corrosion and Fouling, Antibes, France, 351-36.
[32] Féron D. *et al.* (2001) "Marine Corrosion of Stainless Steels: testing, selection, experience, protection and monitoring." European Federation of Corrosion Publications, IOM communications, London, UK, 33.
[33] Féron D. (2004) "Contribution à l'étude des phénomènes de biocorrosion des matériaux métalliques", CEA-R-6064 report, (ISSN 0429-3460).
[34] Féron D., Roy M. (2000) "Corrosion behaviour of stainless steels in natural waters: focus on microbiological and chemical aspects." Eurocorr 2000, London, UK.
[35] Libert M. *et al.* (2014) "Impact of microbial activity on the radioactive waste disposal: long term prediction of biocorrosion processes." Bioelectrochemistry, 97, 162-168.
[36] Bergel A. *et al.* (2010) "From fundamentals to microbial power plants: Electrochemically Active Biofilms." Special issue, Bioelectrochemistry, 78, 1-96.

# 17 Antimicrobial surfaces: A tool to combat biofilm development

**Catherine Debiemme-Chouvy**

## 17.1. Introduction

By avoiding or minimizing surface colonization by bacteria, antimicrobial coatings allow, *inter alia*, to prevent nosocomial infections or development of biofilms on the material surface. The latter can promote surface deterioration notably through corrosion phenomena in the case of materials containing metals. Biofilms present on material surfaces make a number of impacts that intervene in very various domains, some examples being given in figure 17.1, with effects such as public health as well as economical point of view. To fight against biofilm development on materials, various strategies can be implemented to treat their surfaces in order to confer anti adhesive properties for proteins and bacteria (initial step of biofilm formation). These surface modifications can be structural, topographical and/or chemical ones [1-3].

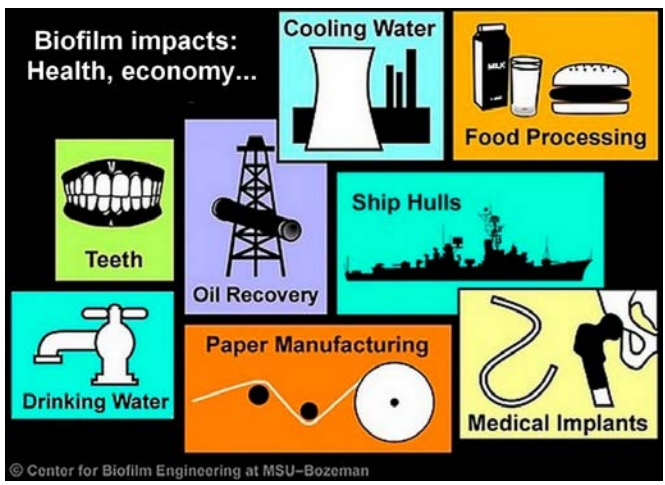


**Fig. 17.1.** – Illustration of fields impacted by biofilms. Image adapted from that published by the Center for Biofilm Engineering, Montana State University.

In the first part of this chapter, the main surface modifications to be considered for hampering biofilm formation will be presented. As depicted in figure 17.2, this result will be due to an effect which can be either bacteriostatic (protein or bacterial anti-adhesion) or bactericidal (death of bacteria before or after cell contact with the material), or even a mix of the two [4]. Surface nanostructuration (bioinspired approach), antibacterial peptides (mainly natural, from animal or vegetal source), anti-adhesive polymers, metal or metal oxide nanoparticles and polymers with biocidal properties (synthetic or natural cationic polymers) will be reviewed [5].The second part will be devoted to *N*-halamine coatings. These coatings are characterized by the presence of haloamine functions (> N-Cl or > N-Br) giving the surface biocidal (oxidizing) properties due to the +I oxidation state of halogens [6]. Polymers prepared from proteins will be particularly described.

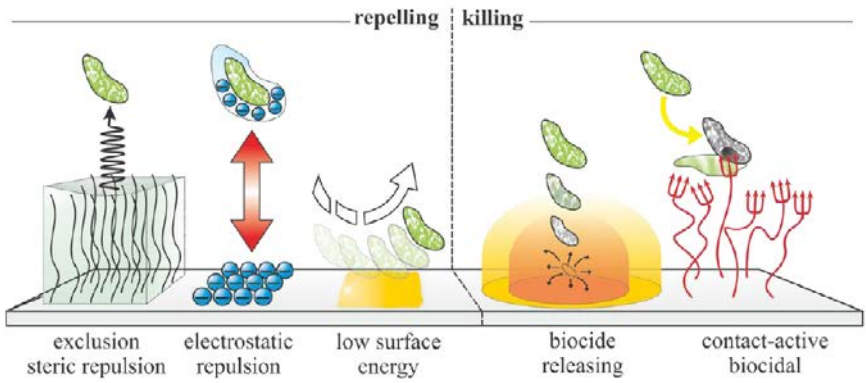


**FIG. 17.2.** – General principles of actions of antimicrobial surfaces [4].

## 17.2. Different types of antimicrobial surfaces or coatings

### *17.2.1. Nanostructured surfaces*

The surface of the wings of dragonflies or cicada is nanostructured. It is composed with a network of nanopillars which gives the wings a bactericidal power. Indeed, as shown in figure 17.3, the nanopillars are going through the bacteria present on the surface of a cicada wing.

Starting from this result and *via* a bioinspired approach, some researchers developed topographical modifications of materials leading to the building of nanopillar nets. This is the case of black silicon, discovered in 1999. The latter is produced by damaging the surface of a silicon wafer with a high power laser beam yielding to an arrangement of wells and protuberances (Fig. 17.4I). On such surface, bacteria appear to be impaled onto the pillars (Fig. 17.4II).

Therefore the bactericidal effect is due to a mechanical action as depicted in figure 17.5a. When the surface of contact between the bacteria membrane and a nanopillar (A zone) increases, there is a stretching of the part of the membrane which is not in contact, possibly leading to its breaking.

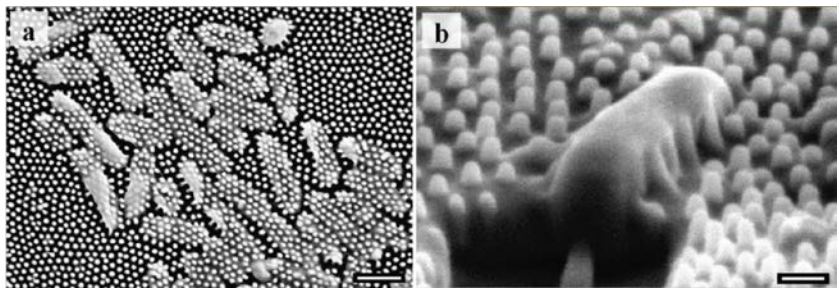


**Fig. 17.3. –** Bactericidal effect of cicada wing surface upon *Pseudomonas aeruginosa*. SEM images of a) *Pseudomonas aeruginosa* cells on the surface of a cicada wing (top view), b) a *Pseudomonas aeruginosa* cell sinking between the nanopillars on the cicada wing surface (side view, $\theta = 53°$). A section at the front has been excavated using focused ion beam SEM (FIB-SEM) to enable visualization of a cross section of the cell. Scale bar: a) 1 µm, b) 200 nm (adapted from [10]).

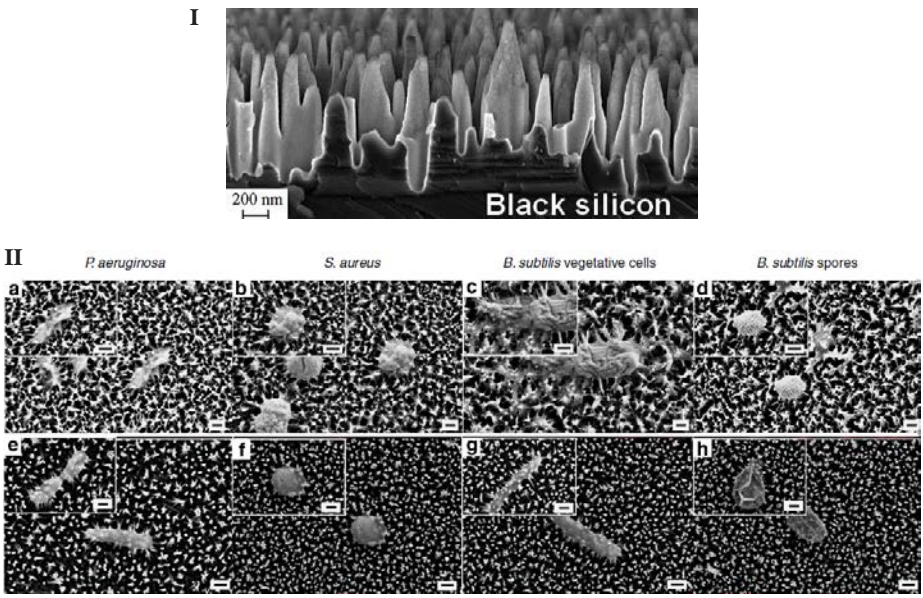


**Fig. 17.4. – I)** SEM micrography of a black silicon sample. Scale bar: 200 nm. **II)** SEM micrographies of *P. aeruginosa*, *S. aureus*, *B. subtilis* vegetative cells and *B. subtilis* spores on cicada wing (a-d) and on black silicon (e-h). *P. aeruginosa (a, e), S. aureus (b, f), B. subtilis (c, g)* and spores *of B. subtilis (d, h)*. Scale bar: 200 nm (adapted from [7]).

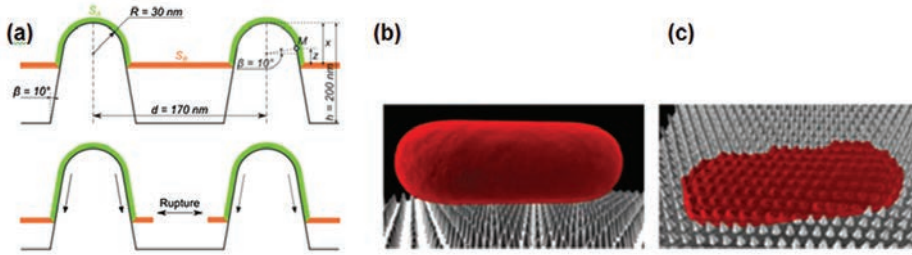


**FIG. 17.5.** – Biophysical model of the interactions between cicada (*P. claripennis*) wing nanopillars and bacterial cells. (a) Scheme of a bacterial outer layer adsorbing onto cicada wing nanopillars. The adsorbed layer can be divided into two regions: region A (in contact with the pillars, in green) and region B (suspended between the pillars, in orange). Because region A adsorbs and the surface area of the region increases, region B is stretched and eventually ruptures. (b–c) Three-dimensional representation of the modeled interactions between a rod-shaped cell and the wing surface. As the cell comes into contact (b) and collapses onto the surface (c). Images (b) and (c) are screen shots from an animation of the mechanism available at https://www.youtube.com/watch?v=KSdMYX4gqp8 (adapted from [11]).

Recently, Ivanova *et al.* [8] have studied the bactericidal effect of cicada wings on seven types of bacteria, combining the bacteria shape (bacillus or coccus) and the structure of the bacteria membrane (Gram-positive or Gram-negative bacteria). It was shown that, whatever their morphology, the Gram-negative bacteria had no chance of survival when in contact with a cicada wing. On the contrary, Gram-positive bacteria were more robust. The relation between the structure of the surface of plants and insects at the micro or nanometric scale and their superhydrophilic or self-cleaning property has been described in a recent review paper [9].

### *17.2.2. Antimicrobial peptides*

At the present time, the data base for antimicrobial peptides (AMPs) (http://aps.unmc.edu/AP/) contains 2987 peptides among which 2508 which are identified as having antibacterial properties. These are generally small peptides, composed with 10 to 50 amino acids (AAs), being mainly characterized by a cationic overall charge and a hydrophobic character (Fig. 17.6). Most of AMPs originates from nature, two thirds of them coming from animal kingdom (Fig. 17.6).

There is a large number of classes of antimicrobial peptides, which have been classified according to different criteria. Currently, the AMPs classification, reached by consensus, is based on their global ionic charge and their structural diversity (secondary and ternary structure, with or not the presence of disulphide bridges) [12]. Cationic peptides can be divided into several subclasses: linear peptides with α-helix (Fig. 17.7A), linear peptides containing a large amount of less common amino acids and peptides containing a lot of cysteine residues forming one or several disulphide bridges.

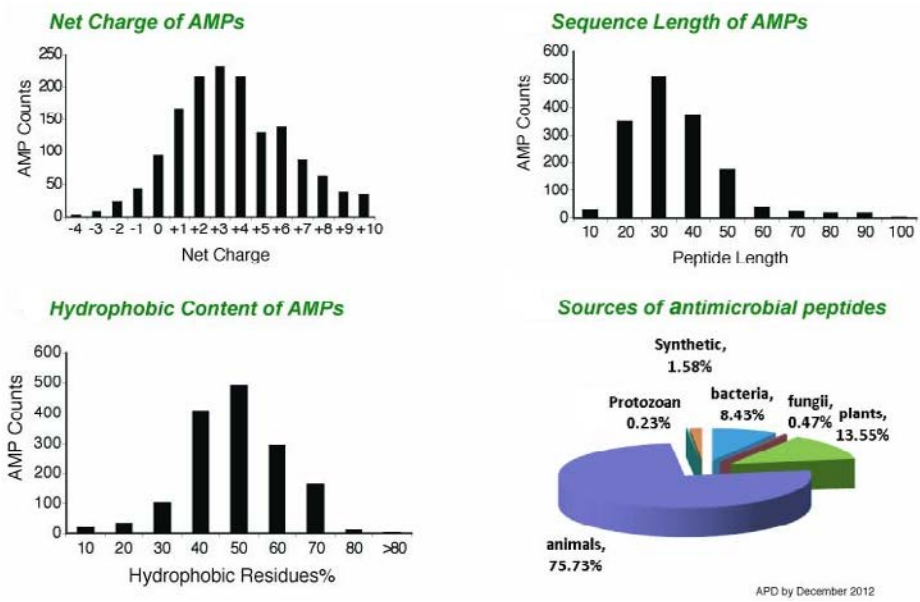


**Fig. 17.6.** – Antimicrobial peptides (AMPs). Distribution of AMPs as a function of their ionic net charge, of their length, of their hydrophobic residue percentage, and of their origin (adapted from http://aps.unmc.edu/AP/facts.php).

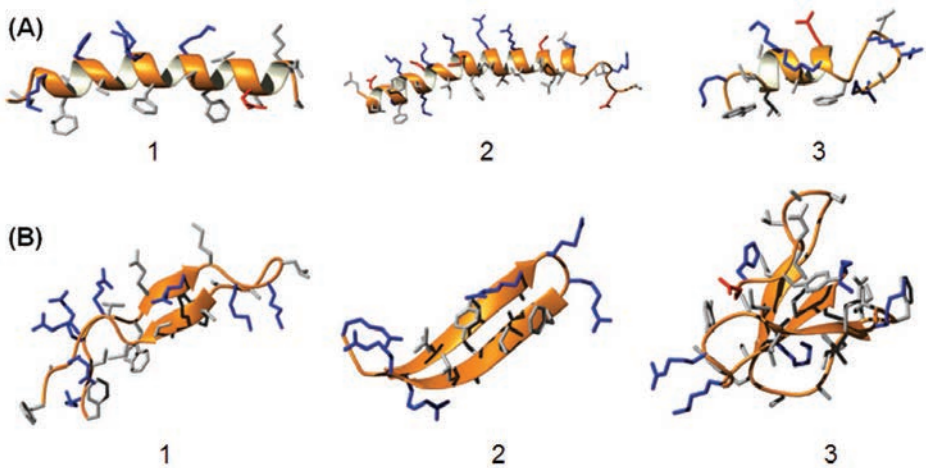


**Fig. 17.7.** – Examples of structural classes of antimicrobial peptides (AMPs). (A) α-helical peptides, (B) β-sheet peptides. The positively charged side chains are represented in blue, those negatively charged in red, and the neutral side chains are in grey (adapted from [16]).

Some antimicrobial peptides present mixed structure combining α-helix and β-sheet, other being peptides containing a large amount of particular amino acids, such as glycine, proline, or arginine, which are not able to form α-helix. Among the natural peptides, those with α-helix and β-sheet are the most numerous (Fig. 17.7). Let us note that only one class of linear peptides with α-helix is described among mammals, namely the cathelicidins, the most studied being the human one LL-37.

An example of AMP used to design antimicrobial surfaces is magainin that is composed of 23 AAs (peptide A-1 shown in figure 17.7). The first magainins were discovered in 1987 in *Xenopus laevis* (amphibian).

The main target of these peptides is the bacterial cell membrane (Fig. 17.8). It is well recognised that the AMPs interact with the membrane through electrostatic interactions between the cationic residues of the peptides and the anionic groups of the membrane. The different processes that could take place in the case of a linear peptide with α-helix are summarized in figure 17.8. The mechanisms of action of these molecules on bacteria are based on pore formation inducing the osmotic lysis of the cell [13, 14, 15]. These mechanisms have been recently described in a review article [16].

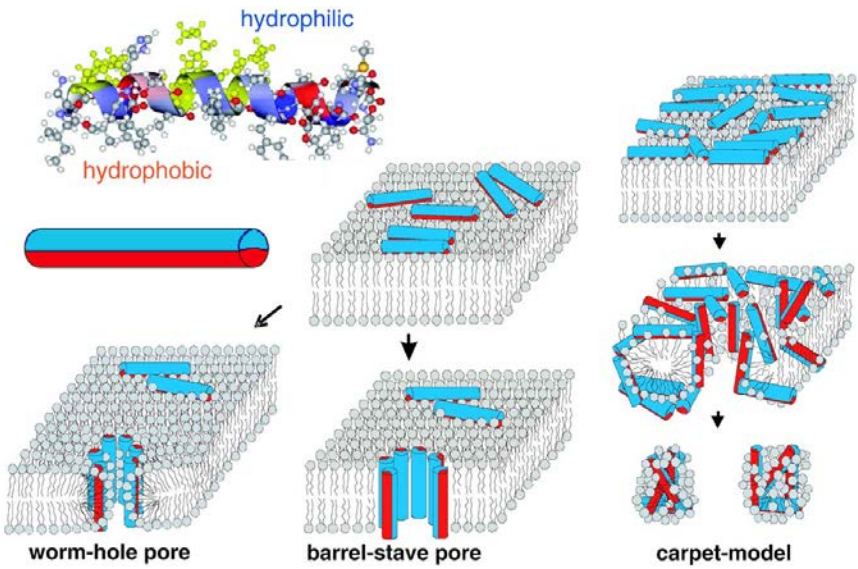


**FIG. 17.8.** – Sketch of different models describing the functional mechanisms and underlying structure of antimicrobial peptides interacting with lipid bilayers. (top, left): α-helical conformation of magainin with its hydrophilic (blue) and hydrophobic (red) sides of the helix, as quantified by helical wheel analysis, along with the representation as a amphiphilic cylinder. (bottom, left): worm-hole pore model as proposed for magainin. (top, center and right): surface (S) state of antimicrobial peptides with the hydrophobic side groups anchored in the hydrophobic core of the bilayer. (bottom, center): barrel-stave pore model, as proposed for alamethicin. (bottom, right): Carpet model antimicrobial peptides crowding in the S state, and leading subsequently to micellation (adapted from [22]).

In order to use AMPs to create antifouling surfaces, these species have to be immobilized on the surface of the material to be protected against biofilm development. For instance, magainine I has been immobilized on stainless steel and on $TiO_2$ [17-19]. Other AMPs have been fixed on the surface of medical prosthesis [20]. In a review paper, Onaizi and Leong give a description of the different methods for immobilizing AMPs at a material surface [21]. It can be notably done by a chemical route either by building a covalent bond between the peptides and the surface or by using an intermediary compound (a spacer) to attach the peptides onto the surface [17]. The antimicrobial activity of the peptides is strongly depending on their orientation with respect of the material surface.

### 17.2.3. Polymer with anti-adhesive property: polyethylene glycol

Polyethylene glycol (PEG) is a neutral and hydrophilic organic polymer (H-(O-$CH_2$-$CH_2$-)$_n$-OH). Surfaces coated with PEG acquire bacteriostatic properties. Indeed, proteins and bacteria adsorption is hampered, minimizing the interaction between microorganisms and the material surface. The use of this polymer is often associated with another agent such as an antibacterial peptide [19].

The reason why bacteria are not able to adhere to a surface covered with PEG is not yet well understood. It is tentatively thought to be due to hydrophilicity and to the large flexibility of the polymer, both associated with a steric hindrance [23]. Gour *et al.* have just published a review paper showing all the results obtained with such a polymer [24].

### 17.2.4. Coating containing nanoparticles (Ag, Cu, $TiO_2$, ZnO, CuO)

Various coatings or films containing metal or metal oxide nanoparticles (NPs) have been developed during the last years in order to fight against bacterial colonization of material surfaces [25, 26]. Globally there are two ways for nanoparticles to develop antibacterial properties, either the release of cations or, in the case of semiconducting oxides ($TiO_2$, CuO, ZnO [27]), the process of photoactivation with formation of electron-hole pairs within the nanoparticles (Eq. (17.1)). Photogenerated holes in the valence band ($h_{BV}^+$) give rise to hydroxyl radicals (reaction (17.2)), which have a strong oxidizing power (Fig. 17.9), whereas photogenerated electrons in the conduction band ($e_{BC}^-$) give rise to the production of superoxide ions (Eq. (17.3)); $OH^\bullet$ and $O_2^{\bullet -}$, as well as $^1O_2$ and $H_2O_2$ are reactive oxygen species (ROS) [28-30].

$$h\nu \rightarrow h_{BV}^+ + e_{BC}^- \quad (17.1)$$

$$h_{BV}^+ + H_2O \rightarrow OH^\bullet + H^+ \quad (17.2)$$

$$e_{BC}^- + O_2 \rightarrow O_2^{\bullet -} \quad (17.3)$$

To ensure that the reaction (17.1) takes place, the energy of incident photons has to be larger than the forbidden gap energy (see the energy diagram in figure 17.9), for instance in the case of $TiO_2$ light with wavelength lower than 388 nm has to be used.

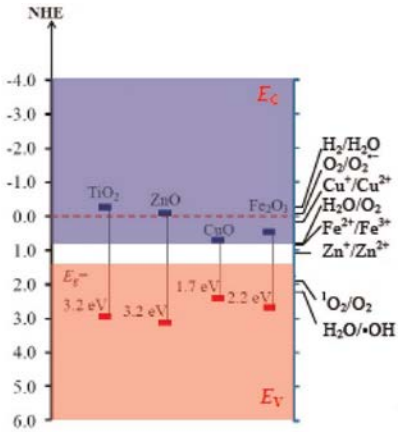


**Average Concentrations of ROS Generated by Different Metal Oxides under UV Irradiation**

| particles | | $^{\bullet}OH$ ($\mu M$) | $^1O_2$ ($\mu M$) | $O_2^{\bullet-}$ ($\mu M$) | total ($\mu M$) |
|---|---|---|---|---|---|
| $TiO_2$ | NPs | 19.3 ± 0.8 | 417.3 ± 18.8 | 8.0 ± 0.4 | 442.9 ± 20.0 |
| | bulk | 4.9 ± 0.2 | N.D.*a* | N.D. | 4.9 ± 0.2 |
| ZnO | NPs | 9.5 ± 0.6 | 100.8 ± 6.4 | 167 ± 8.6 | 277.3 ± 15.6 |
| | bulk | 1.9 ± 0.1 | N.D. | 81.8 ± 0.3 | 83.7 ± 0.4 |
| CuO | NPs | N.D. | N.D. | N.D. | 0 |
| | bulk | N.D. | N.D. | N.D. | 0 |
| $Fe_2O_3$ | NPs | 2.3 ± 0.1 | N.D. | 18.1 ± 1.1 | 20.4 ± 1.2 |
| | bulk | N.D. | N.D. | N.D. | 0 |

[a] N.D. indicates that ROS were not detected or were not statistically significant.

**FIG. 17.9.** – Left: Energy diagram. Band edge positions of four metal oxides in contact with aqueous solution at pH 5.6. The lower edge of conduction band ($E_c$) and upper edge of valence band ($E_v$) are presented along with the band gap ($E_g$) in eV. The energy scale is drawn with respect to the normal hydrogen electrode (NHE). On the right side the redox potentials of several redox couples are presented. Right: Average concentrations of reactive oxygen species generated by metal oxides under UV irradiation (adapted from [30]).

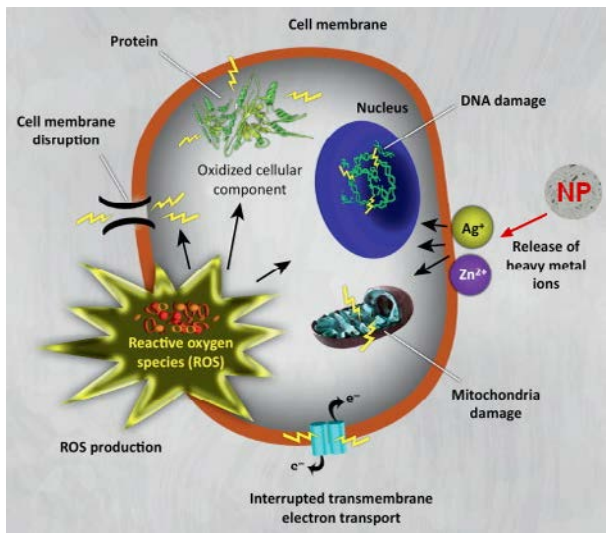


**FIG. 17.10.** – Schematic representation of toxicological effect of nanoparticles (NPs) upon a bacterial cell (adapted from [36]).

Among the metallic NPs, the most employed and studied are silver NPs [31-33]. Copper NPs are also of interest though less commonly used [34, 35]. The toxicity of metallic NPs is due to the release of metal ions. The mechanisms involved in the toxicity of NPs against bacteria are summarized in the scheme depicted in figure 17.10 [36]. Metallic cations enter the cell and disturb its metabolism [37]. Finally the immobilization of NPs on material surfaces is well documented in literature. For instance, one can cite the holding back of silver NPs inside polymeric matrix [38].

### 17.2.5. Biocidal polymers (hydrophobic cationic polymers, N-halamines)

Globally speaking, bacterial shell is negatively charged. Thus, cationic polymers can adsorb easily on the cell surface. Furthermore, if these polymers have an amphiphilic character, they are able to penetrate the bacteria membrane, to create openings allowing cytoplasm components to run away, yielding finally to the bacteria death.

Most cationic polymers contain phosphonium, sulphonium, guadinium or quaternary ammonium groups [24, 39, 40]. Very often these polymers have a hydrophobic character due to the presence of alkyl chains supported by the main chain of the polymer, such as the polyethyleneimine (PEI). An example of a *N*-alkyl-PEI polymer is presented in figure 17.11B.

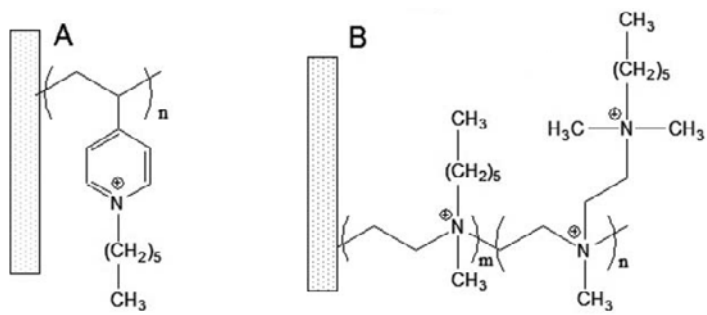


**Fig. 17.11.** – Schematic structural depiction of covalently immobilized (A) poly(4-vinyl-*N*-hexylpyridinium) and (B) branched *N*-hexyl,*N*-methyl-polyethyleneimine used as microbiocidal coatings (adapted from [46]).

Some cationic polymers are of natural origin. This is the case of some polysaccharides like chitosan coming from deacetylation of chitin (the most abundant polysaccharide after cellulose), a biopolymer notably extracted from the shells of crustaceans (Fig. 17.12). Amine functions of chitosan have a pKa about 6.5. As a consequence, contrary to chitin, it is soluble in acidic medium in which it is in the ionized state. Moreover, it is biodegradable and non-toxic [41, 42].

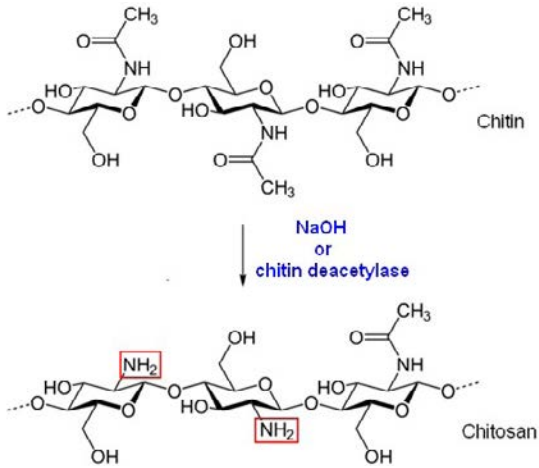


**FIG. 17.12.** – Reaction scheme for chitosan synthesis from chitin. The amount of deacetylation can vary from 60 to 100%.

The bactericidal property of this polymer is due to its ionic charge [43]. The former is evidently pH dependent. Some chemical modifications of chitosan have been studied in order to remedy to such a dependence [44].

It has been demonstrated that a surface covered with chitosan avoids a biofilm of bacteria or yeasts being formed. After an incubation period of 54 hours of a chitosan film, with respect to a reference specimen, it was observed a reduction of the number of living cells by an amount of 95 to 99.9% in the case of *Staphylococcus epidermidis, Staphylococcus aureus, Klebsiella pneumoniae, Pseudomonas aeruginosa* and *Candida albicans* [45].

## 17.3. Focus on *N*-halamine coatings (regenerable)

At the beginning of their use, during the 1980's, the *N*-halamine compounds added to water for disinfection purpose, were small organic molecules. An *N*-halamine compound can be defined as a molecule containing at least one covalent nitrogen-halogen bond, the halogen atom (*X*) being at the oxidation state +I. Such a bond is formed by halogenation of an imide, amide or amine group (reaction with NaO*X*, substitution of one H bound to nitrogen by one *X*). This bond is called haloamine by biologists and *N*-halamine by physicochemists. The basic compound is hydantoin ($C_3H_4N_2O_2$, see insert in figure 17.13).

To avoid bacteria proliferation in water, one can add compounds containing halogen atoms at the oxidation state + I *i.e.* oxidizing agents, such as sodium hypochlorite, NaOCl ("Javel water"). As previously indicated, small organic molecules have been tested for water disinfectant, with the emerging problem of the presence of organic residues. Therefore, immobilization of haloamine

functions on polymers has been and is always developed to overcome this problem. Examples are shown in figure 17.13, which concerns polystyrene-based polymers containing hydantoin-like groups.

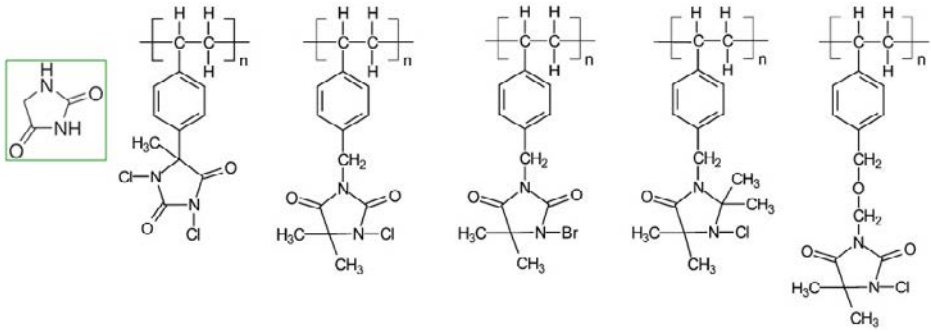

**Fig. 17.13.** – Hydantoin molecule (green insert) and *N*-halamine polystyrene-based polymers (adapted from [47]).

Generation of haloamine functions can be performed in particular by using an electrochemical treatment. Actually, this process is based on the oxidation of halide anions leading to hypochloride/hypobromide which is able to react with amine functions (primary or secondary amines, amides, imines) leading to haloamine functions. Indeed oxidation of halide ions ($X^-$) gives rise to HO*X* or O$X^-$ production depending on the solution pH at the electrode-solution interface (Fig. 17.14). The electrode to be used has to present an overpotential for water oxidation, which is the case for an antimony-doped $SnO_2$ electrode. As depicted in figure 17.15, in the presence of chloride ions (curve b), bromide ions (curve c), or in natural seawater (curve d) containing chloride ions (at 0.5 M) and bromide ions (at $10^{-3}$ M), the anodic current starts at a lower potential than in the absence of halide ions ($Na_2SO_4$, curve a).

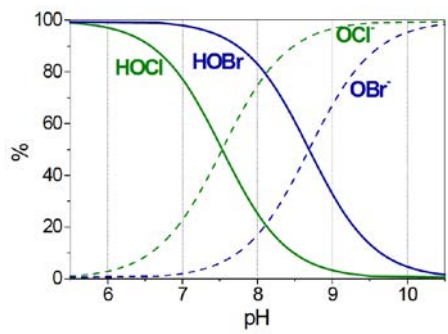


**Fig. 17.14.** – Distribution of HOCl/$OCl^-$ (pKa = 7.5) and HOBr/$OBr^-$ (pKa = 8.7) in water at different pH values.

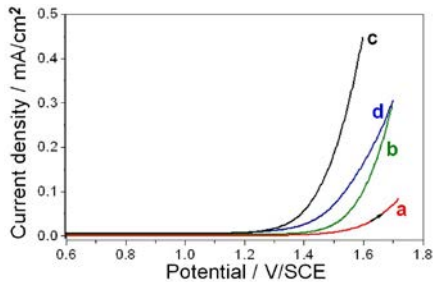


**FIG. 17.15.** – Current density *vs.* applied potential at a $SnO_2$:Sb electrode in contact with various electrolytes. (**a**) 0.5 M $Na_2SO_4$, (**b**) 0.5 M NaCl, (**c**) 0.5 M NaBr, (**d**) natural seawater. Potential scan rate: 5 mV $s^{-1}$.

In the presence of organic matter and, in particular, proteins such as bovine serum albumin (BSA), halide oxidation leads to the formation of a halogenated polymer on the electrode surface. BSA (molecular weight: 66 kDa) is composed of 610 amino acids (AAs) and it is rich in AAs containing amine functions such as lysine (59) and thiol functions indeed this protein contains 35 cysteine residues which form 17 cystine (disulphide bridge).

The anodic current due to the oxidation of the chloride ions is not modified in the presence of BSA, but a deposit is formed onto the electrode surface. The electrode mass increases as soon as the anodic current is starting around 1.5 V/SCE (Figs. 17.15 and 17.16). If the electrode is maintained under anodic polarization for several hours, the deposit becomes very thick and visible to the naked eye (Fig. 17.17). At shorter polarization times, existence and growth of the deposit were confirmed by SEM observations. As shown by micrography C in figure 17.18, aggregates are present at the sample surface, after polarization at +1.5 V/SCE in a solution containing chloride ions and BSA. Therefore these aggregates are definitively due to chloride oxidation in the presence of BSA, because no deposit is formed in the absence of chloride ions (Fig. 17.18B). As shown in figure 17.19, the composition of the aggregates has been determined by EDS analyses. They are composed of organic matter (C, O, N and S) and also of Cl atoms which are bound to the organic matter since no signal for sodium is detected (1 keV). In the same way, in sodium bromide solution or in natural seawater when BSA is present, oxidation of bromide and/or chloride ions leads to the formation of a deposit (Sn signals due to the electrode substrate are less high), which contains Br and Cl atoms (Fig. 17.20).

Analyses by X-ray photoelectron spectroscopy (XPS) have been performed. The elementary composition of the electrochemically deposited film has been confirmed (see the survey spectrum, figure 17.21), but XPS was especially valuable to obtain information about the chemical state of S, Br and Cl. From the analysis of the high resolution spectra, it was found that sulphur is under two forms: a reduced one (-SH, -SS-) and an oxidized form ($-SO_2^-$). There are also two forms of halogens in the anodically deposited film, the first one is haloamine bonds, the second one corresponds to *sulphonyle halide* functions.

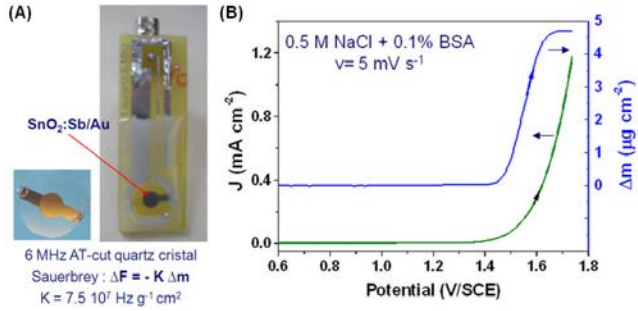


**FIG. 17.16.** – A) Optical images of a quartz before and after assembly for electrochemical and gravimetric measurement. B) Current density (J) and mass variation of the electrode ($SnO_2$:Sb) with the applied potential. Electrolyte: 0.5 mol $L^{-1}$ NaCl + 1 mg $mL^{-1}$ BSA in water solution.

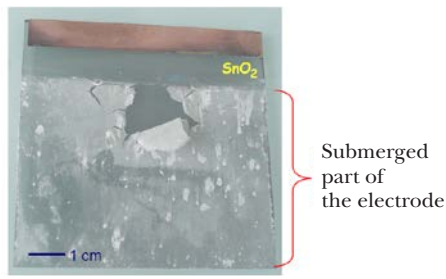


**FIG. 17.17.** – Optical image of a $SnO_2$:Sb anode after polarization at 1.5 V/SCE for 8 hours in a 0.5 mol $L^{-1}$ NaCl solution containing 3 mg $mL^{-1}$ of BSA.

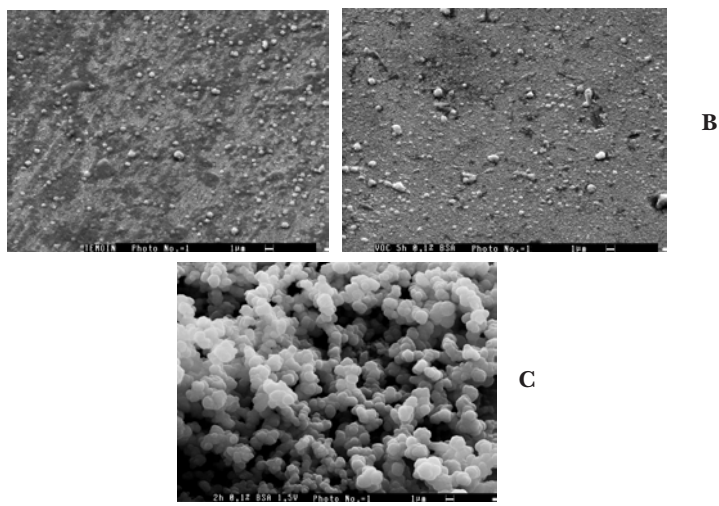


**FIG. 17.18.** – SEM images obtained from a $SnO_2$ sample (A) pristine, (B-C) after contact with a 0.5 M NaCl + 1 mg $mL^{-1}$ BSA solution, (B) at open circuit potential for 54 hours, and (C) under polarization at 1.5 V/SCE for 2 hours (adapted from [48]).

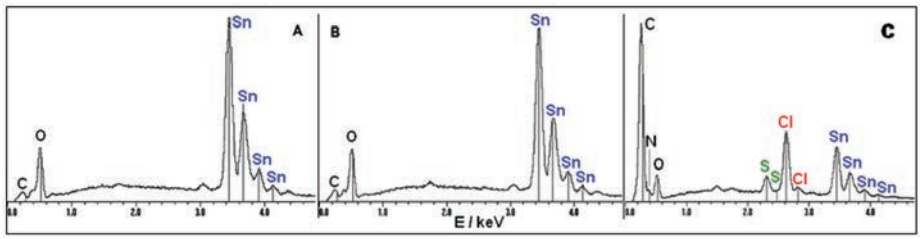


**FIG. 17.19.** – EDS spectra obtained from a $SnO_2$ sample (A) pristine, (B) after immersion for 54 hours at open circuit potential, and (C) after polarization at 1.5 V/SCE for 2 hours, in 1 mg $mL^{-1}$ BSA + 0.5 M NaCl solution (adapted from [48]).

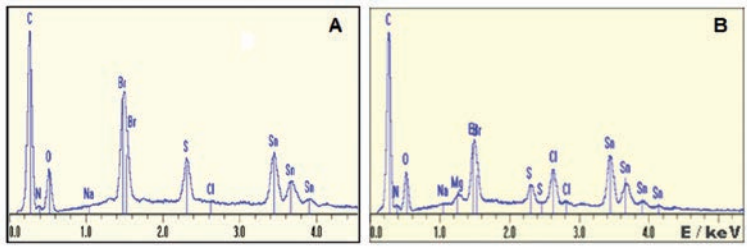


**FIG. 17.20.** – EDS spectra obtained from a $SnO_2$ sample after polarization for 2 hours at (A) 1.3 V/SCE in 0.5 M NaBr solution, (B) 1.5 V/SCE in seawater containing 1 mg $mL^{-1}$ of BSA.

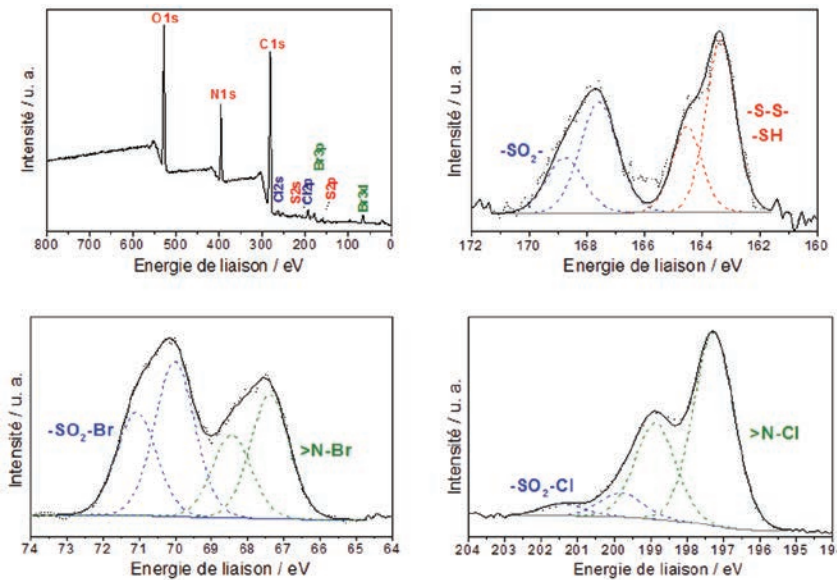


**FIG. 17.21.** – XPS spectra from a $SnO_2$:Sb film after polarization for 2 hours at 1.5 V/SCE in natural seawater containing 1 mg $mL^{-1}$ BSA. Survey, S2p, Br3d and Cl2p spectra (adapted from [49, 50]).

A mechanism has been proposed by the authors on the basis of these observations and results, which implies oxidation of thiol functions (Eq. (17.4)) and disulphide bridges (Eq. (17.5)) by hypobromous and/or hypochlorous acid. These reactions lead to the formation of sulphonyl chloride/bromide and to the substitution of a hydrogen atom bound to a nitrogen one by Cl(+I) or Br(+I) (Eq. (17.6)) [49].

$$R\text{-}SH + 3HOX \rightarrow R\text{-}SO_2\text{-}X + 2X^- + 2H^+ + H_2O \quad (17.4)$$

$$R\text{-}S\text{-}S\text{-}R' + 5HOX \rightarrow R\text{-}SO_2\text{-}X + R'\text{-}SO_2\text{-}X + X^- + 3H^+ + H_2O \quad (17.5)$$

$$RNH_2 + HOX \rightarrow R\text{-}NHX + H_2O \quad (17.6)$$

Furthermore, proteins are polymerized *via* a reaction between a sulphonyl chloride/bromide group and an amine function (Eq. (17.7)).

$$R\text{-}SO_2\text{-}X + H\text{-}NR'R'' \rightarrow R\text{-}SO_2\text{-}NR'R'' + X^- + H^+ \quad (17.7)$$

Globally, it emerges that on the one hand proteins are polymerized and on the other hand they contain haloamine functions which are thought to give the film biocidal properties. The latter ones have been verified by microbiological studies [50, 51], illustrated by figures 17.22 and 17.23 in the case of electrochemically pretreated $SnO_2$:Sb films in the presence of BSA and chloride and/or bromide ions. Indeed, after contact with bacteria (*Escherichia coli*), these films are very few colonized (Fig. 17.22 column on right and Fig. 17.23C) contrary to films without polarization (open circuit, *i.e.*, without chloride/bromide oxidation) (Fig. 17.22 column on left and Fig. 17.23A) or polarized in seawater without BSA added (no presence of amine groups allowing formation of haloamine functions (Eq. (17.6)) (Fig. 17.23B).

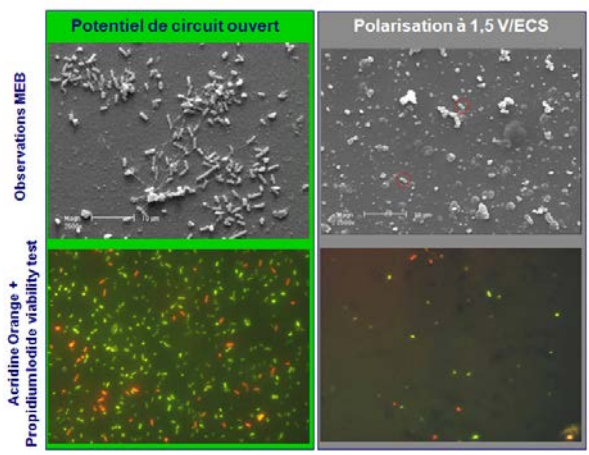


**Fig. 17.22.** – SEM (top) and fluorescence microscopy (bottom) images after 17 hours at 37 °C in contact with 5 $10^7$ *Escherichia coli* $mL^{-1}$ of $SnO_2$ films treated at open circuit potential for 54 hours (left) or under polarization at 1.5 V/SCE for 2 hours (right) in 0.5 M NaCl + 1 mg $mL^{-1}$ BSA solution (adapted from [51]).

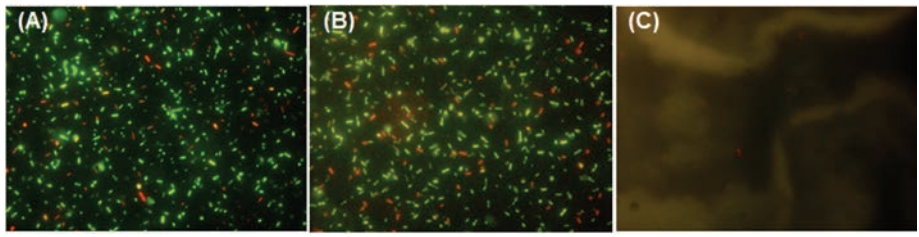


**FIG. 17.23.** – Fluoresence microscopy images of $SnO_2$:Sb films after a pre-treatment and then incubation for 17 hours at 37 °C in a *E. coli* suspension. Pre-treatment: A) 2 hours at open circuit potential; B) and C) polarization for 2 hours at 1.5 V/SCE. Pre-treatment solution: natural seawater (B) containing 1 mg $mL^{-1}$ of BSA (A, C).

Another type of electrode material has been tested, namely a carboneous material: a-$CN_x$ [52, 53]. As evidenced by the SEM micrography in figure 17.24, chloride and bromide ions are oxidized when the a-$CN_x$ electrode is anodically polarized in natural seawater in which BSA was added, in the same way as for $SnO_2$:Sb. An organic and nanostructured film is formed on the a-$CN_x$ electrode surface, composed with the constituent elements of the BSA (C, N, O, S) as well as bromine or chlorine, as shown by the EDS spectrum in figure 17.24 [54].

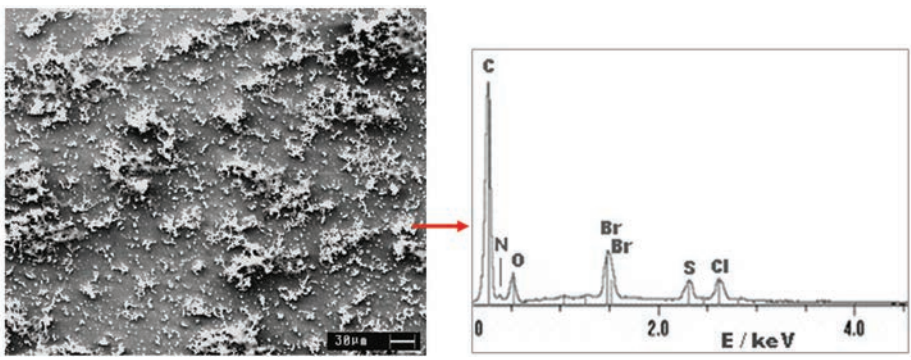


**FIG. 17.24.** – SEM image and EDS spectrum of a a-CNx film polarized for 2 hours at 1.5 V/SCE in natural seawater containing 1 mg $mL^{-1}$ of BSA [54].

Another polymer which, thanks to its chemical structure, is able to fix haloamine functions is chitosan (Figs. 17.12 and 17.25). This polymer can be solubilized in an acetic acid medium, allowing to get a thin film after evaporation. This film can be treated by a sodium hypochlorous solution yielding formation of chloramine functions. Different experiments (Kirby-Bauer test) in the presence of bacteria *E. coli* and *S. aureus* have been performed by Cao and Sun [55]. After seeding (1 mL of a bacterial suspension at $10^8$-$10^9$ CFU $mL^{-1}$) and 4 hours of pre-incubation without the chitosan films, followed by 24 hours of incubation at 37 °C in the presence of the films, an inhibition zone was

observed around the chlorinated chitosan films (Film b – Fig. 17.25). This result shows that Cl (+I) diffusion takes place into the medium, killing bacteria in the vicinity of the polymer.

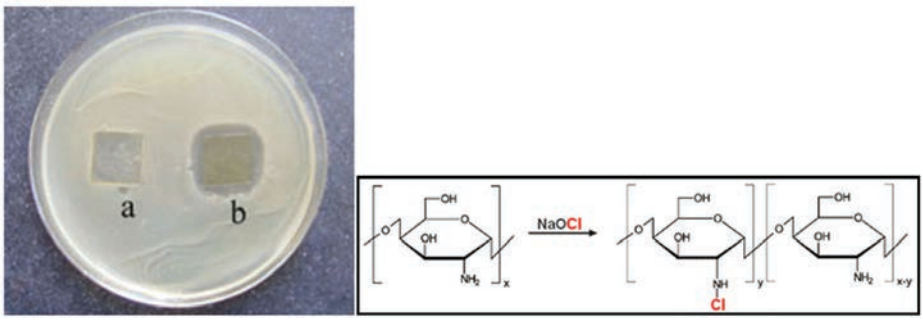


**Fig. 17.25.** – Right: Reaction of chitosan chloration in NaOCl aqueous solution. Left: photo showing the inhibition zone of (a) un-chlorinated chitosan film and (b) chlorinated chitosan film against *S. aureus*, after incubation for 24 hours at 37 °C. Film size: 1 × 1 cm$^2$ (adapted from [55]).

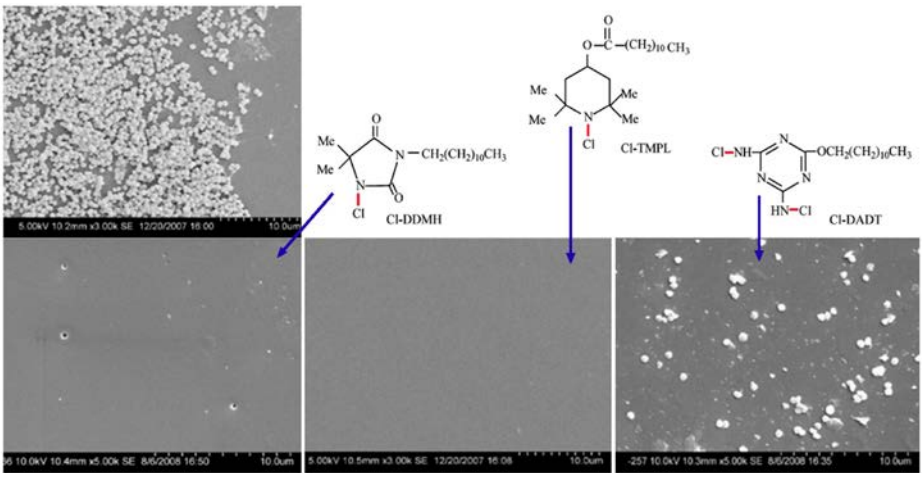


**Fig. 17.26.** – SEM images of a polyurethane film pure (top) or containing 4% Cl-DDMH, 4% Cl- DADT, and 4% Cl-TMPL after immersion in *S. aureus* suspension for 24 hours (adapted from [56]).

The last example presented in this chapter is dealing with a polyurethane coating. The latter contains an additive which is an *N*-halamine compound. Three types of compounds, with the same alkyl chain ($C_{12}$), have been tested: amine (TMPL), amide (DDMH, derived from hydantoin) and melamine (DADT). Their structure is depicted in figure 17.26. SEM micrographies in this

figure clearly show that after contact with a *S. aureus* suspension, there is no colonization of the films containing 4% of a halominated compound, contrary to the unmodified polyurethane film [56].

## 17.4. Conclusion

As the saying goes "Prevention is better than cure", biofilm eradication being a very complicated and difficult task, even unfeasible, it is certain that it is of the upmost importance to protect materials with respect to protein and microorganism adsorption to avoid biofilm formation. Different strategies can be set out, each with specific advantages and drawbacks. A number of criteria have to be taken into account for the purpose of choosing what protection mode to use, for instance life time (implying a possible regeneration), toxicity, easiness of synthesis, action spectrum.

The objective of this chapter was to present a survey of the various strategies that can be used for preparing antimicrobial surfaces. All the strategies are not described in details in this document, but a number of review articles are cited, and the reader interested in will be able to find the required information.

## References

[1] Hasan J. *et al.* (2013) "Antibacterial surfaces: the quest for a new generation of biomaterials." Trends in Biotechnology, 31, 31-40.

[2] Bazaka K. *et al.* (2012) "Efficient surface modification of biomaterial to prevent biofilm formation and the attachment of microorganisms." Applied Microbiology and Biotechnology, 95, 299-311.

[3] Banerjee I. *et al.* (2011) "Antifouling Coatings: Recent developments in the design of surfaces that prevent fouling by proteins, bacteria, and marine organisms." Advanced Materials, 23, 690-718.

[4] Siedenbiedel F., Tiller J.C. (2012) "Antimicrobial polymers in solution and on surfaces: Overview and functional principles." Polymers, 4, 46-71.

[5] Kenawy E.R. *et al.* (2007) "The chemistry and applications of antimicrobial polymers: A state-of-the-art review." Biomacromolecules, 8, 1359-1384.

[6] Hui F., Debiemme-Chouvy C. (2013) "Antimicrobial N-halamine polymers and coatings: a review of their synthesis, characterization, and applications." Biomacromolecules, 14, 585-601.

[7] Ivanova E.P. *et al.* (2013) "Bactericidal activity of black silicon." Nature Communications, 4, 2838, 1-7.

[8] Hasan J. *et al.* (2013) "Selective bactericidal activity of nanopatterned superhydrophobic cicada *Psaltoda claripennis* wing surfaces." Applied Microbiology and Biotechnology, 97, 9257-9262.

[9] Song Ha N. *et al.* (2014) "Natural insect and plant micro-/nanostructsured surfaces: An excellent selection of valuable templates

with superhydrophobic and self-cleaning properties." Molecules, 19, 13614-13630.
[10] Ivanova E.P. *et al.* (2012) "Natural bactericidal surfaces: Mechanical rupture of *Pseudomonas aeruginosa* cells by cicada wings." Small, 8, 2489-2494.
[11] Pogodin S. *et al.* (2013) "Biophysical model of bacterial cell interactions with nanopatterned cicada wing surfaces." Biophysical Journal, 104, 835-840.
[12] Shai Y. (2002) "Mode of action of membrane active antimicrobial peptides." Biopolymers, 66, 236-248.
[13] Melo M.N. *et al.* (2009) "Antimicrobial peptides: linking partition, activity and high membrane-bound concentrations." Nature Reviews Microbiology, 7, 245-250.
[14] Carnicelli V. *et al.* (2013) "Interaction between antimicrobial peptides (AMPs) and their primary target, the biomembranes." Formatex, 1123-1134.
[15] Karal M.A.S. *et al.* (2015) "Stretch-activated pore of the antimicrobial peptide, Magainin 2." Langmuir, 31, 3391-3401.
[16] Nguyen L.T. *et al.* (2011) "The expanding scope of antimicrobial peptide structures and their modes of action." Trends in Biotechnology, 29, 464-472.
[17] Humblot V. *et al.* (2009) "The antibacterial activity of Magainin I immobilized onto mixed thiols self-assembled monolayers." Biomaterials, 30, 3503-3512.
[18] Hequet A. *et al.* (2011) "Optimized grafting of antimicrobial peptides on stainless steel surface and biofilm resistance tests." Colloids and Surfaces B-Biointerfaces, 84, 301-309.
[19] Peyre J. *et al.* (2012) "Co-grafting of amino poly(ethylene glycol) and Magainin I on a $TiO_2$ surface: Tests of antifouling and antibacterial activities." J. Phys. Chem. B, 116, 13839-13847.
[20] Gao G. *et al.* (2011) "The biocompatibility and biofilm resistance of implant coatings based on hydrophilic polymer brushes conjugated with antimicrobial peptides." Biomaterials, 32, 3899-3909.
[21] Onaizi S.A., Leong S.S.J. (2011) "Tethering antimicrobial peptides: Current status and potential challenges." Biotechnology Advances, 29, 67-74.
[22] Salditt T. *et al.* (2006) "Structure of antimicrobial peptides and lipid membranes probed by interface-sensitive X-ray scattering." Biochimica et Biophysica Acta, 1758, 1483-1498.
[23] Kingshott P. *et al.* (2002) "Ultrasensitive probing of the protein resistance of PEG surfaces by secondary ion mass spectrometry." Biomaterials, 23, 4775-4785.
[24] Gour N. *et al.* (2014) "Anti-infectious surfaces achieved by polymer modification." Macromolecular Materials and Engineering, 299, 648-668.
[25] Paladini F. *et al.* (2015) "Metal-based antibacterial substrates for biomedical applications." Biomacromolecules, 16, 1873-1885.

[26] Ivask A. *et al.* (2014) "Mechanisms of toxic action of Ag, ZnO and CuO nanoparticles to selected ecotoxicological test organisms and mammalian cells in vitro: A comparative review." Nanotoxicology, 8, 57-71.
[27] Li M. *et al.* (2011) "Toxicity of ZnO nanoparticles to *Escherichia coli*: mechanism and the influence of medium components." Environmental Science & Technology, 45, 1977-1983.
[28] Ditta I.B. *et al.* (2008) "Photocatalytic antimicrobial activity of thin surface films of $TiO_2$, CuO and $TiO_2$/CuO dual layers on *Escherichia coli* and bacteriophage T4." Applied Microbiology and Biotechnology, 79, 127-133.
[29] Foster H.A. *et al.* (2011) "Photocatalytic disinfection using titanium dioxide: spectrum and mechanism of antimicrobial activity." Applied Microbiology and Biotechnology, 90, 1847-1868.
[30] Li Y. *et al.* (2012) "Mechanism of photogenerated reactive oxygen species and correlation with the antibacterial properties of engineered metal-oxide nanoparticles." ACS Nano, 6, 5164-5173.
[31] Birla S.S. *et al.* (2009) "Fabrication of silver nanoparticles by Phoma glomerata and its combined effect against *Escherichia coli*, *Pseudomonas aeruginosa* and *Staphylococcus aureus*." Letters in Applied Microbiology, 48, 173-179.
[32] Rai M. *et al.* (2009) "Silver nanoparticles as a new generation of antimicrobials." Biotechnology Advances, 27, 76-83.
[33] Saleh N.B. *et al.* (2015) "Mechanistic lessons learned from studies of planktonic bacteria with metallic nanomaterials: implications for interactions between nanomaterials and biofilm bacteria." Frontiers in Microbiology, 6, 677, 1-8.
[34] Chatterjee A.K. *et al.* (2014) "Mechanism of antibacterial activity of copper nanoparticles." Nanotechnology, 25, 135101, 1-12.
[35] Ingle A.P. *et al.* (2014) "Bioactivity, mechanism of action, and cytotoxicity of copper-based nanoparticles: A review." Applied Microbiology and Biotechnology, 98, 1001-1009.
[36] Hajipour M.J. *et al.* (2012) "Antibacterial properties of nanoparticles." Trends in Biotechnology, 30, 499-511.
[37] Amna S. *et al.* (2015) "Review on zinc oxide nanoparticles: antibacterial activity and toxicity mechanism." Nano-Micro Letters, 7, 219-242.
[38] Kumar V. *et al.* (2013) "Development of silver nanoparticle loaded antibacterial polymer mesh using plasma polymerization process." J. Biomed. Mat. Res., Part A, 101, 1121-1132.
[39] Timofeeva L., Kleshcheva N. (2011) "Antimicrobial polymers: mechanism of action, factors of activity, and applications." Applied Microbiology and Biotechnology, 89, 475-492.
[40] Ferreira L., Zumbuehl A. (2009) "Non-leaching surfaces capable of killing microorganisms on contact." Journal of Materials Chemistry, 19, 7796-7806.
[41] Rabea E.I. *et al.* (2003) "Chitosan as antimicrobial agent: Applications and mode of action." Biomacromolecules, 4, 1457-1465.
[42] Cheung R.C.F. *et al.* (2015) "Chitosan: An update on potential biomedical and pharmaceutical applications." Marine Drugs, 13, 5156-5186.

[43] Kong M. *et al.* (2010) "Antimicrobial properties of chitosan and mode of action: A state of the art review." International Journal of Food Microbiology, 144, 51-63.
[44] Shukla S.K. *et al.* (2013) "Chitosan-based nanomaterials: A state-of-the-art review, International." Int. J. Biol. Macromol., 59, 46-58.
[45] Carlson R.P. *et al.* (2008) "Anti-biofilm properties of chitosan-coated surfaces." Journal of Biomaterials Science-Polymer Edition, 19, 1035-1046.
[46] Klibanov A.M. (2007) "Permanently microbiocidal materials coatings." Journal of Materials Chemistry, 17, 2479-2482.
[47] Wei X.Y. *et al.* (2010) "A novel method of surface modification on thin-film-composite reverse osmosis membrane by grafting hydantoin derivative." Journal of Membrane Science, 346, 152-162.
[48] Debiemme-Chouvy C. *et al.* (2007) "An original route to immobilize an organic biocide onto a transparent tin dioxide electrode." Langmuir, 23, 3873-3879.
[49] Debiemme-Chouvy C. *et al.* (2007) "Study by XPS of the chlorination of proteins aggregated onto tin dioxide during electrochemical production of hypochlorous acid." Applied Surface Science, 253, 5506-5510.
[50] Debiemme-Chouvy C. *et al.* (2011) "Electrochemical treatments using tin oxide anode to prevent biofouling." Electrochimica Acta, 56, 10364-10370.
[51] Haskouri S. *et al.* (2006) "First evidence of the antibacterial property of $SnO_2$ surface electrochemically modified in the presence of bovine serum albumin and chloride ions." Electrochemistry Communications, 8, 1115-1118.
[52] Cachet H. *et al.* (2006) "Correlation between electrochemical reactivity and surface chemistry of amorphous carbon nitride films." Surface and Interface Analysis, 38, 719-722.
[53] Benchikh A. *et al.* (2012) "Influence of electrochemical pre-treatment on highly reactive carbon nitride thin films deposited on stainless steel for electrochemical applications." Electrochimica Acta, 75, 131-138.
[54] Debiemme-Chouvy C. (2010) "Electrochemical treatments to prevent biofouling." 61st Annual Meeting ISE, Nice (France), September 27 - October 1 2010.
[55] Cao Z.B., Sun Y.Y. (2008) "N-Halamine-based chitosan: Preparation, characterization, and antimicrobial function." J. Biomed. Mat. Res., Part A, 85A, 99-107.
[56] Sun X.B. *et al.* (2010) "Amine, melamine, and amide N-halamines as antimicrobial additives for polymers." Ind. Eng. Chem. Res., 49, 11206-11213.

# 18 Extracellular microbial substances for cementitious materials

**Nicolas Serres**

## 18.1. Introduction: cementitious materials and admixtures

Concrete, widely used in civil engineering, is an increasingly complex composite material. Indeed, the different components of this material allow it to be adapted to very different uses, ranging from decoration to constructions such as towers, bridges, *etc.* with exceptional mechanical performance and durability.

However, this material is sensitive to aging, induced by various factors, such as microorganisms (bacteria, fungi, foams, *etc.*), which introduce bioalteration. This alteration results from interactions between the components of the cementitious material and the environment to which it is exposed. The material is then subject to aggressions linked to synergies of actions which are more or less strong and prolonged over time. When degradation occurs under the action of biocolonization, the term biodeterioration is used.

The bioreceptivity of a material represents its ability to be colonized by one or more groups of living organisms without necessarily leading to biodeterioration [1]. Different parameters of the material influence its bioreceptivity, such as porosity, roughness, surface energy, chemical composition, and influence the speed of colonization. The durability of cementitious materials is therefore linked to these physicochemical parameters, the resistance to degradation of biological origin depends on several characteristics specific to the material as its composition as well as its porous network distributed on a fairly wide scale.

In order to obtain different performance levels of resistance to the environments, admixtures are usually added during the mixing of the concrete. These admixtures are chemical products whose environmental impact has not been thoroughly studied until now. It appears, however, that a number of them contain pollutants from the chemical industry. It is commonly accepted that products such as admixtures do not constitute a risk of environmental pollution due to release during the period of use, but further studies are necessary to verify what it is involved concerning their demolition and their possible reuse (valorisation). In addition, during a Life Cycle Assessment (LCA), it is essential to validate the non-polluting nature of the manufactured products. It is therefore

advisable to develop biosourced and eco-friendly admixtures which gives better durability properties to concrete – by optimizing the physical and chemical parameters of the cementitious material, for example – making them more environment-friendly, since these admixtures contain only biological substances that are biocompatible with the environment.

## 18.2. Extracellular microbial substances

Biofilm, as defined in Chapter 6, is a living tissue mainly composed of water (98-99%), in which the presence of cells as well as chemical, mineral and extracellular substances are also detectable [2]. These extracellular substances (EPSs) are associated with microorganisms: these are their metabolic products, which contribute to their survival. A biofilm has a reservoir of specific molecules, sometimes unexploited.

Among these molecules, extracellular microbial substances form in a way the "sticky" matrix of organic biofilms that encompasses microorganisms. The EPSs constitute between 85% and 98% of the organic mass of the biofilm. These are mainly highly hydrated polymers of microbial origin in which biofilm organisms are integrated: polysaccharides (soluble and insoluble), proteins, macromolecules (nucleic acids), cell membranes (lipids, glycolipids, phospholipids), humic substances. The EPSs fill and form the space between the cells and determine the morphology of the biofilm. These substances help to fix the organisms of the biofilm together and/or on a support allowing the synergy of the microbial consortium, in other words the "housing" of the cells. The EPSs therefore represent the immediate environment of the biofilm cells and determine their living conditions.

When they are of a cationic polymer nature (polysaccharides), the EPSs intervene in the initial fixation of the cells and in the formation of the biofilm. However, other applications can be envisaged with these products. Indeed, these carbohydrate chains[1] secreted by bacteria living within the biofilm can be used as a traditional admixture following the EN 934-2 standard rules.

For example, EPS 180 are natural polymeric extracellular substances produced by *Lactobacillus reuteri*. This bacterium secretes an enzyme (glucansucrase GTF180), which degrades the sucrose and transforms it into EPS 180 [3]. This type of EPS, obtained in the form of a dried powder, can be diluted in water and incorporated into the mixes of cement pastes or mortars [4]. The EPS 180 showed corrosion-inhibiting properties on steel [5], which are of interest in the case of reinforced concrete.

Among the other functions concerned, maintaining infrastructure in good condition (sustainable structures), avoiding fouling and/or bioalteration,

[1] The extracellular substances consist mainly of carbohydrates (49-50%), but also lipids (39-40%), fatty acids (9-10%) and proteins (> 0.5%).

makes it possible to limit the health risk associated with the development of pathogenic microorganisms and/or alteration of installations in contact with drinking water (pipes, retention basins, *etc.*). On the one hand, environmental issues can be controlled by developing eco-friendly products, with biological antifouling action. Such products may then substitute those subject to REACH [6] in the case (for example) of the replacement of traditional antifouling paints which cause ecological problems in the fauna and aquatic flora [7]. On the other hand, health issues must be respected because biofilms on the surface of concrete can have consequences on health, in the event of the proliferation of pathogenic microorganisms, water pollution phenomena, potentially leading to the development of nosocomial diseases, legionnaires' diseases, *etc.* To combat this bacterial biocontamination, the surface modification induced by a biosourced admixture can inhibit the development of the biofilm and/or favour its detachment from the cementitious surface.

A wide range of extracellular microbial substances is cited in the current literature. These products are used as admixtures or incorporated as additives in the concrete formulations for various expected results. It is always a question of improving the durability of concrete structures, but the declination of the actions is wide-ranging: it is possible to play on the workability, the rheology of fresh concrete, on their compactness, or on their properties in hardened state, such as mechanical properties, or on their surface condition or on their resistance to cracking. The rest of this chapter provides a presentation and discussion of some recent findings.

## 18.3. Influence of the EPSs on mechanical performances

### *18.3.1. Rheological properties*

One of the most important properties of fresh mortars, but also of concrete, is their workability, which not only determines the ease with which they can be installed in the formwork, but also the final quality of the structure.

Microbial polysaccharides, such as curdlan or gellan gum, have been developed in recent years to modify the viscosity of concrete in order to improve its workability [8]. These microbial polysaccharides, which can be applied in cement pastes, mortars or concrete, are particularly useful in the manufacture of concrete, as viscosity modifying admixtures, water reducers or plasticizers.

Extracellular polymeric substances EPS WN9 produced by *Paenibacillus* sp. were used to develop a viscosity modifying admixture [9]. The addition of EPS WN9 in the formulation of a mortar (based on CEM I cement) allows the production of a homogeneous material without segregation. EPS WN9 stabilizes the flow, as the viscosity of mortars containing 0.02% (of the cement mass) of EPS WN9 is reduced by 7% from its initial value after 90 minutes, while in the case of unadmixtured mortars, the decrease is 22% [9]. In addition, a delay of

setting of 1.6 hours can be observed for mortars containing EPS WN9 (0.08% of the cement mass), indicating a plasticizing effect for the product.

Furthermore, the addition of polysaccharides also has a considerable effect on the rheological properties of cement pastes (CEM I), which results in an apparent viscosity increase ranging from 33-40% and 50-155% [10]. This increase is all the more pronounced when the W/C (water-cement) ratio increases and could therefore be explained by a phenomenon of physical absorption of water molecules by the polysaccharides, due to the formation of hydrogen bonds. Moreover, the pseudo-plasticity of the admixture, caused by the entanglement of the long carbon chains, has an important influence on the apparent viscosity.

Slump tests were carried out on admixtured mortars to evaluate their workability as a function of the bioadmixture dosage and the quality of the cement (Fig. 18.1) [11].

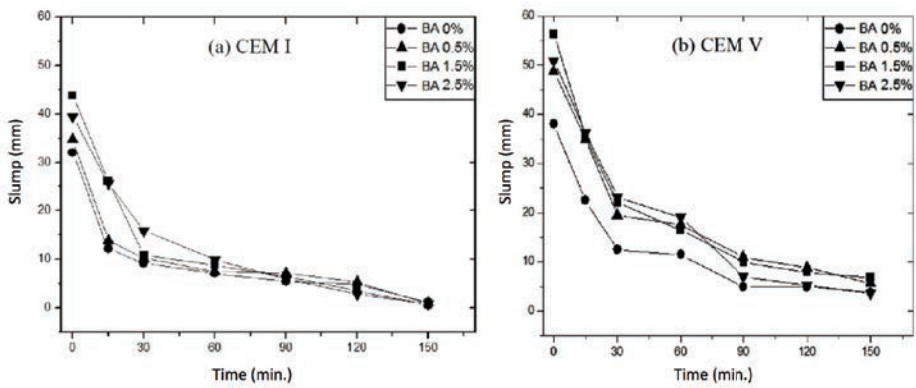


**FIG. 18.1.** – Influence of a bioadmixture (BA) on the slump of CEM I (a) and CEM V (b) mortars as a function of time [11].

If the addition of this bioadmixture, developed under the SEPOLBE project [12], leads to an increase in the slump values of mortars based on CEM V, regardless of the amount of admixture, the results are more nuanced for the CEM I based mortars, where the rate of admixturization seems to have more effect on the workability of this type of mortar since only the mortars with 1.5 and 2.5% of admixture have a significantly greater slump than the mortar without admixture. A dosage of 1.5% of admixture allowed to reach a maximum threshold of initial slump of more than 43 mm for CEM I based mortars and more than 56 mm for CEM V based mortars [11]. This result suggests that the incorporation of the bioadmixture improves the workability of fresh mortar (the workability gain is about 20%) and that its optimum concentration in the mortar is around 1.5%.

The slump values of the two mortars are to be compared with their chemical compositions. The CEM I contains 95% clinker, while the CEM V contains 51%.

Among the constituent phases of the clinker, celite (C3A), which participates mainly in the phenomenon of concrete setting, exhibits a high reactivity with the mixing water and plays a major role in the rheology of the paste. The CEM V mortar contains less C3A (3.64%) than the CEM I (7.6%). However, a high level of C3A tends to reduce slump values. Initially, the slump of the CEM V mortar without admixture is therefore higher than that based on CEM I.

The main function of a concrete is its compressive strength which must comply with standards (EN 196-1) defining minimums according to the age of these and the composition of the cements used. Any incorporation into the concrete formula, whatever the improvement of the desired characteristic, must imperatively satisfy the demand for minimum compressive strength.

### 18.3.2. Compressive strength

Normalized compressive strength (EN 196-1) were carried out on mortars containing an admixture based on extracellular substances [13]. These CEM I based mortars underwent standardized cures of 28 and 120 days in a preservation chamber (T = (23±2) °C, R.H. > 90%). After 28 days of curing, it can be seen (Fig. 18.2) that the results, between 58.5 and 64.6 MPa, are always higher than the minimum required by the EN 196-1 standard for this cementitious grade (52.5 MPa). In contradistinction, if there is no alteration of the mechanical properties of the mortars for bioadmixture contents ranging from 0.5 to 2% (of the cement mass), a decrease is observed for a bioadmixture rate of 2.5%. It seems possible that for this content, the mortar would undergo a modification due to chemical reactions which develop for this high concentration. EPSs can swell and contract, resulting in changes in mechanical pressure on the material.

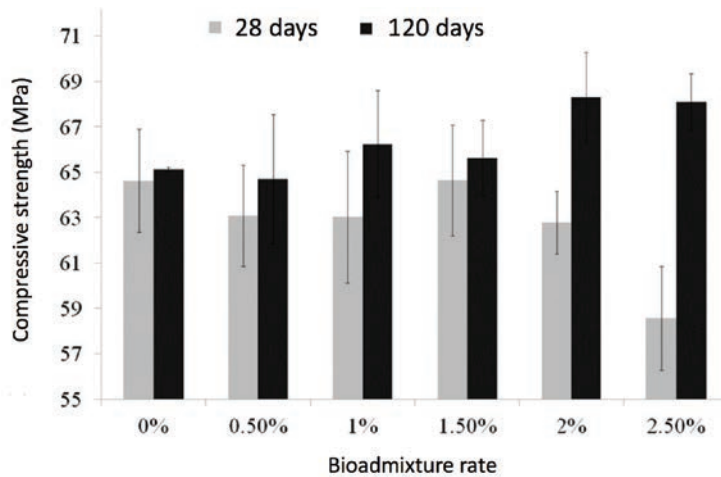


**Fig. 18.2.** – Effect of the bioadmixture content on the compressive strength of mortars (CEM I) as a function of the curing time [13].

A 5 to 16% increase in the compressive strength of mortars is observed with increasing curing time, whatever the bioadmixture content. This increase is only about 2% for unadmixtured mortar. Moreover, after a high curing time of 120 days, the highly admixtured mortars (2 and 2.5% bioadmixture relative to the mass of cement) have higher compressive strength values than the maximum required by EN 196-1 (67 MPa). This strong increase can be mainly due to the formation of C-S-H during the hydration process: the entanglement of the C-S-H gel can create strong cohesion and electrostatic interactions, factors that can increase the mechanical strength.

Further research has focused on the influence of extracellular microbial substances on the mechanical properties of cementitious materials. For example, the compressive strength of CEM I based mortars can be increased by 20% by adding EPS WN9 (0.02% of the cement mass) [9].

The influence of EPSs secreted by microorganisms, isolated from an Indian river (Bakreshwar), of the genus *Shewanella* has been studied [14]. The addition of these EPSs as an admixture in mortars (CEM I) makes it possible to increase the compressive strength 25% after a curing period of 28 days. This improvement is partly explained by the clogging of the pores by the microorganisms, due to an extracellular growth of organic fibres, modifying the porosity and the distribution of the pore size of the mortar. Furthermore, it has been observed, following the addition of *E. coli* in the mix, that the changes in the compressive strength of mortars (CEM I) are negligible (less than 1% whatever the dosage of bacteria). The choice of a microorganism is therefore crucial for improving the compressive strength of a cementitious material. Another bacterial strain of the genus *Bacillus* [15], in the form of cells suspended in a liquid added to the mix, allowed the increase in compressive strength of mortars (CEM I) due to precipitation of calcite, induced by the bacterium, allowing the healing of the microcracks and the reduction of the porosity.

## 18.4. Influence of EPS on physicochemical characteristics

Cementitious materials are heterogeneous composite and porous materials with a high surface roughness. Some recent work deals with the influence of extracellular substances on these physicochemical parameters of the material.

### *18.4.1. Porosity*

It has been demonstrated, by measuring the total porosity to water, that CEM I and CEM V based mortars, with and without EPS 180 admixture, have equivalents porosity rates, as well as apparent densities [4]. Mass surveys of capillary imbibitions have shown that the absorption of water in cement pastes is strongly influenced by the presence of extracellular microbial substances, while they do not influence the absorption of mortars [4]. Indeed, these extracellular

microbial substances do not appear to give rise to any reduction in absorption kinetics when incorporated in mortars. The water absorption in the cement pastes is strongly influenced by the presence of EPS 180 which reduces the imbibition rate by 68% for the CEM I pastes and by 72% for the CEM V, after 5 hours testing. The addition of this bioadmixture to the mix can influence the water transfer within the porous network of the hardened cement by blocking fine porosities such as the capillary pores, which explains why there is no significant influence for larger scale (larger porosities) on the capillary water absorption measurement for mortars.

Another study, conducted with another EPS bioadmixture [16], showed that the porosity of mortars (CEM I) was not influenced by the curing time (28 and 120 days) and retained the same value (approximately 14%) irrespective of the admixture content. Observations by optical microscopy revealed that the distribution of large air voids (Ø ≥ 30 µm) remained stable (with curing time and bioadmixture content), representing between 1.3 and 2.1% of the surface area. SEM observations revealed that the distribution of small air voids (5 ≤ Ø (µm) < 30), between 3.4 and 4.5% of the surface, remained equally stable whatever the curing time and the bioadmixture concentration. In addition, capillary imbibition tests made it possible to establish a relationship between capillary imbibition kinetics, represented by the variation in the amount of water absorbed as a function of time, and the admixture rate (Fig. 18.3).

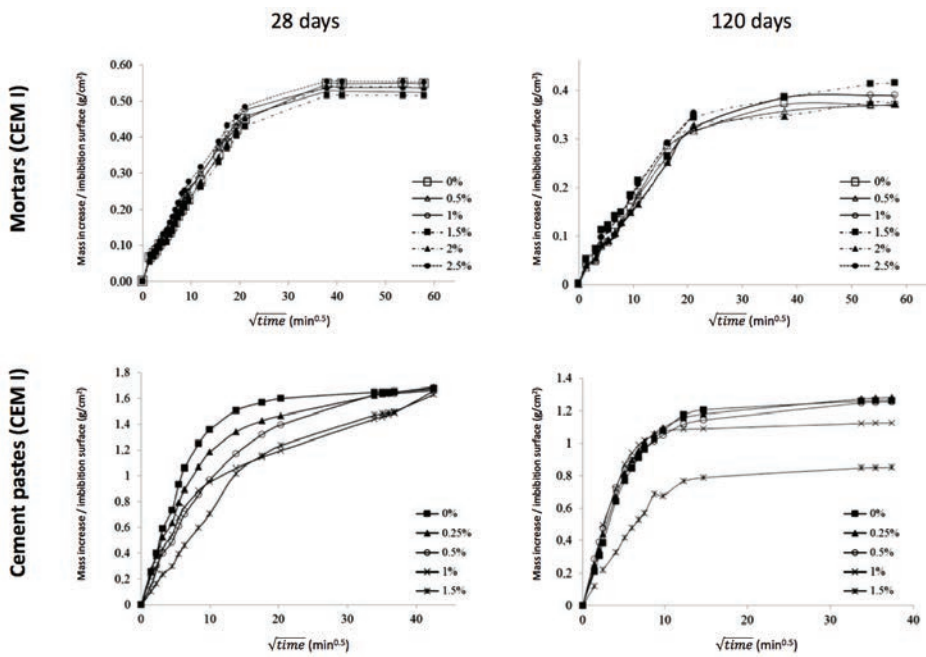


**Fig. 18.3.** – Mass increase of mortars and cement pastes (CEM I) as a function of time after 28 and 120 days of curing in water [16].

The plotting of mass measurements of capillary imbibitions shows that if water absorption in cement pastes is influenced by the presence of a bioadmixture, this is not the case with mortars, where the curves are superimposed (Fig. 18.3). In addition, capillary imbibition tests show that, whatever the curing time, the bioadmixture incorporated in the mixes of the cement pastes substantially reduces the absorption kinetics, due to probable interactions between the bioadmixture and the cementitious matrix.

With the mortars, the presence of sand is at the origin of the formation of an interfacial transition zone (ITZ) between the sand and the cement paste. This specific porosity, whose access thresholds are between 0.1 and 4 μm [17], is not present in cement pastes whose access thresholds for pores are less than one micrometre and mostly less than 0.1 μm [17]. The small amount of bioadmixture added in the mix of the materials thus seems to block the porous network of cement pastes, mainly composed of capillaries, but remains too weak to influence that of the mortars.

The porosity of a cementitious material is an important parameter that determines the surface roughness, but also the amount of water potentially present in the material.

### 18.4.2. Mechanisms of hydration

The cement paste is obtained by a chemical reaction between water and cement. This hydration is a complex process. In the case of Portland cement (CEM I), the main constituents of the clinker react with water to form new compounds which cause the material hardening progressively. For example, the supersaturation of the CaO solution (derived from the calcium silicates belite and alite) precipitates to $Ca(OH)_2$ (portlandite, CH), which crystallizes between the hydrated cement grains (C-S-H), and which represents a reserve of basicity of the cementitious materials.

The kinetics of hydration of the cement may be influenced by the presence of extracellular microbial substances. Cement is indeed a very aggressive alkaline medium, capable of degrading organic molecules. The surface of a heterogeneous cementitious paste presents cracks, pores, hydration products (CH and C-S-H), as well as unhydrated particles (Fig. 18.4).

In the presence of an admixture whose active principles consist of bacterial exoproducts, it has been demonstrated by image analysis that the cement paste (CEM I) surface has fewer unhydrated particles (Table 18.1). A dosage optimum appears to be present at a concentration of 1% of bioadmixture relative to the cement mass. In addition, the morphology and chemical composition of the hydrated calcium silicate (C-S-H) particles in these same cement pastes also evolve with the presence of the bioadmixture (Fig. 18.5). In unadmixtured samples, the C-S-Hs have sizes of about 450 nm, while for bioadmixture concentrations of 1 and 1.5%, these sizes range from 600 to 1450 nm. The C-S-H particles appear to be larger and denser when the bioadmixture content increases in the cement pastes.

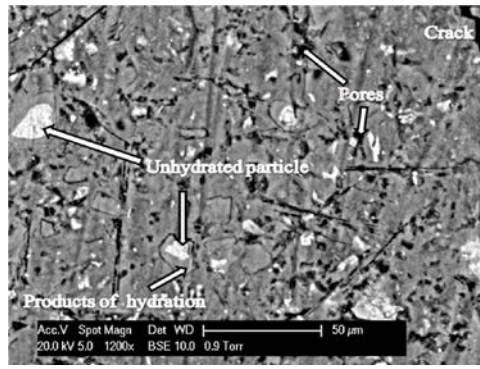


**Fig. 18.4.** – Polished surface of a cement paste (CEM I).

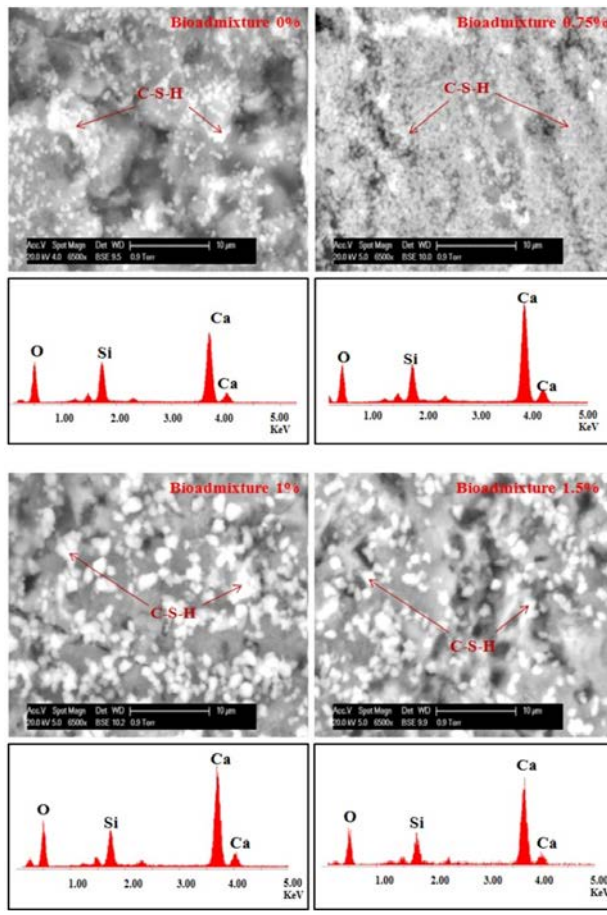


**Fig. 18.5.** – C-S-H observations and EDS analysis on admixtured (or not) surfaces of cement paste (CEM I) [18].

**TABLE 18.1.** – Relationship between the bioadmixture content and the size of the unhydrated particles on the surface of cement pastes (CEM I) [18].

| Bioadmixture rate (% Vs. cement mass) | Average surface area of unhydrated particles (µm²) | Unhydrated cement grains (%) |
|---|---|---|
| 0 | 61.54 | 5.33 |
| 0.25 | 90.68 | 4.27 |
| 0.5 | 58.24 | 3.65 |
| 0.75 | 63.03 | 2.08 |
| 1 | 36.14 | **1.53** |
| 1.5 | 55.22 | 2.04 |

The amount of unhydrated cement particles is a factor affecting several characteristics of the cement pastes, such as their mechanical properties or their roughness. Following a standardized cure, these particles will hydrate and modify the surface roughness.

### *18.4.3. Roughness of cement pastes*

The surface of cement pastes, by definition, has many irregularities, defined by asperities and cavities. All these defects constitute the roughness. A study was carried out on the evolution of the roughness of cement pastes admixtured with extracellular substances [16]. Cement paste (CEM I) containing a bioadmixture at contents ranging from 0.25 to 1.5%, and having undergone normalized cures in water during 28 and 120 days, were analysed by confocal profilometry for extracting values of average roughness (Ra), *i.e.* the arithmetic mean of all deviations of the roughness profile between successive peaks and troughs, according to the EN ISO 4287 standard.

After 28 days curing, the admixtured (or not) cement pastes were polished and exhibited an identical surface state (Ra = 0.08 ± 0.01 µm), whatever the concentration of bioadmixture. These samples were then replaced in a standardized cure up to 120 days, and again analysed by confocal profilometry (without further polishing). It was first found that the curing time changes the surface topography of the cement pastes. Indeed, all surfaces are much more heterogeneous, and have higher peaks after 120 days of curing in water (Fig. 18.6). Moreover, if the topography of the surfaces after a 28 days curing time remains stable and undergoes little modification, this is not the case after 120 days of treatment, when it is possible to observe a decrease in the height of the peaks depending on the bioadmixture content: the bioadmixture appears to smooth the surface of the cement pastes, where the average roughness is (1.72 ± 0.76); (1.39 ± 0.47); (1.31 ± 0.23) and (1.14 ± 0.06) µm for bioadmixture concentrations of 0; 0.25; 0.5 and 1.5%, respectively.

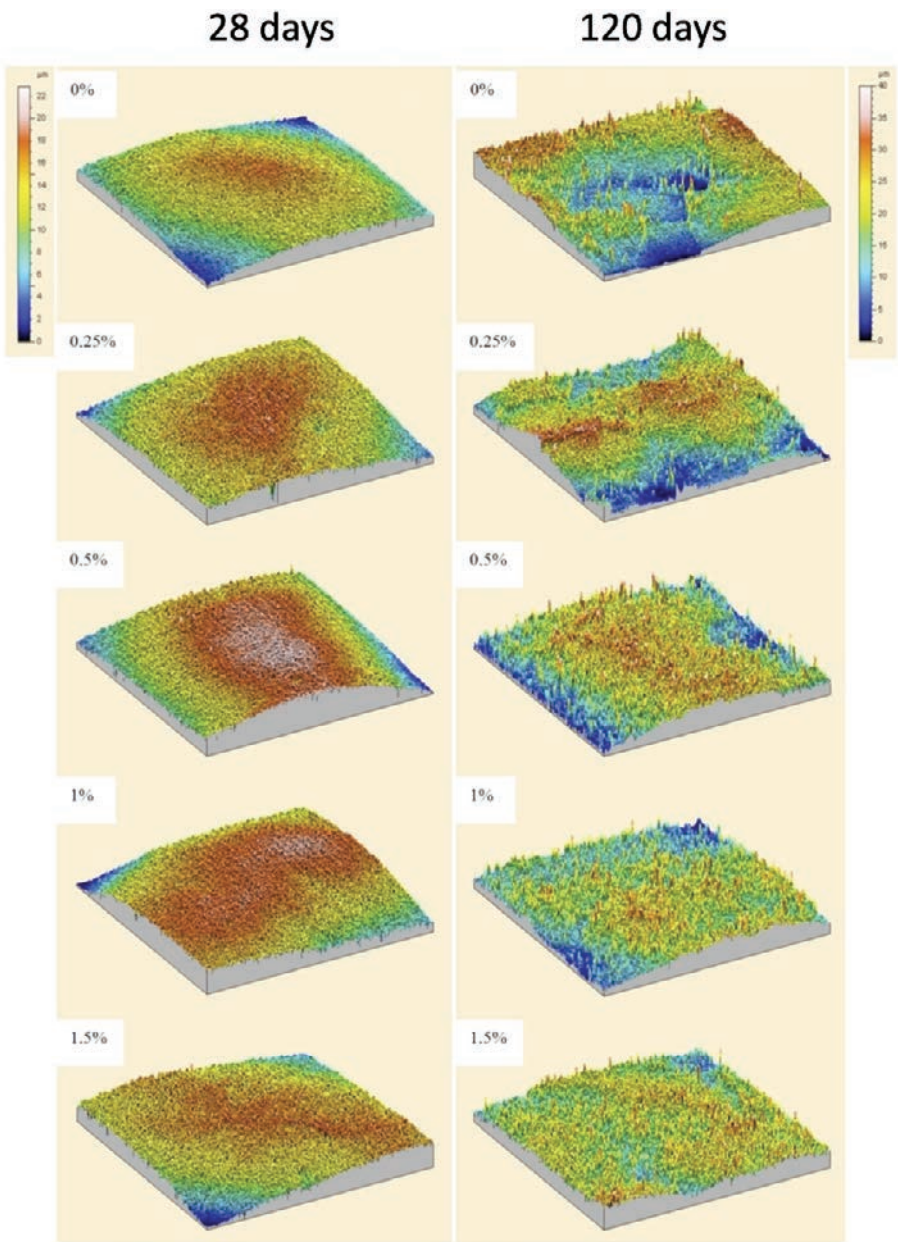


**Fig. 18.6.** – Topographies of cement pastes (CEM I) [18].
The concentration of bioadmixture is specified at the top left of each image; the scale on the left corresponds to the topography of the samples after a cure time of 28 days and that on the right to the topography of the samples after 120 days curing.

This result reflects probable interactions between bioadmixture and cement (CEM I). Hydration of the clinker may be affected by the presence of extracellular substances. Moreover, the structure of the growing C-S-H crystals on the surface appears to depend on the bioadmixture content, as discussed in the previous paragraph.

If the average roughness of the cement pastes decreases, this may involve a change in the bioreceptivity of the materials. A reduction in the roughness of a cement paste can lead to a reduction in shear stresses and thus facilitate the detachment of undesirable bodies on the surface. However, roughness alone does not explain the phenomena of adhesion of biofilm to a surface. The surface energy, affected in this case by the initial polishing that modifies the surface of the crystals (abrasion, cleavage, *etc.*), but also the type of colonizing bacteria and the geometry of these bacteria is to be considered. The possible modification of the biodegradability of the cement pastes can then be explained by a variation in the chemistry of the surface, in addition to the modification of its roughness. In this case, the bioadmixture, of which the dry extract is very low, modifies the behaviour of the water with respect to the cement paste.

The examples discussed above involve extracellular substances that can be added directly into the mix of cementitious materials to make new concretes. For old structures and concrete that require repairs, they can also be surface-brushed, in curative actions.

## 18.5. Interaction between extracellular substances and cementitious materials: curative actions

### *18.5.1. Self-healing concrete*

The formation of cracks is a phenomenon commonly observed on concrete structures. Although microcrack formation has little effect on the structure, setting up a network of microcracks changes the permeability, and may reduce the durability of concrete structures, due to the penetration of aggressive substances, especially in wet environments. Biosourced compounds can be applied to the concrete surface to seal cracks. These substances can be incorporated into porous clay particles, which act as a reservoir of particles. The biomineral formed *via* the bacterial activity leads to the closing of the cracks and to the reduction of the porosity [19]. The cracks are repaired by the calcium carbonate ($CaCO_3$) formed by the bacteria, of the genus *Bacillus* (capable of forming spores), added to the concrete [20]. The combined effect of spore development with calcium lactate (a source of calcium) induces a high precipitation of minerals in cracks: calcite crystals formed *via* bacterial activity allow scarring to maximum crack widths of about 0.4 mm.

### 18.5.2. Permeability of cementitious materials

The ability of concrete to withstand the penetration of chlorides is an essential factor for its long-term performance. A bioproduct formed by bacteria and using urea as a precursor for $CaCO_3$ precipitation has been studied [21]. The bacterial deposit (*Bacillus sphaericus*) of a calcite layer on the surface of a concrete resulted in a decrease in water absorption by capillarity, as well as a reduction in gas permeability. This biodeposition then makes it possible to increase the resistance to carbonation, linked to the nature and connectivity of the pores, due to a modification of the porous network by calcite. This protective effect of biodeposition on carbonation can also be improved by additional treatments, by adding a source of calcium to the bacteria, which increases the concentration of $Ca^{2+}$ ions in the medium.

Finally, the application, by painting or spraying, of EPS 180 on surfaces of cement pastes leads to the same effect as when these substances are incorporated as an admixture into the mix: the same rates of water absorption by capillarity and a strong reduction in the capillary absorption kinetics was observed [22], limiting the capillary rise (reduction of the permeability) and the transfers in aqueous solution.

## 18.6. Conclusion

Among the many challenges associated with cementitious materials (economic, technical, aesthetic, *etc.*), sustainable development and health (environmental and health issues) can be classified as priorities. The development of eco-friendly concretes is nowadays a reality, resulting, for example, in the substitution of clinker, the main constituent of the current cement, and responsible for important $CO_2$ emissions during their production, by ground, granulated blast-furnace slag, now considered a by-product of the steel industry. The development of eco-friendly concretes can also result in the use of admixtures based on extracellular substances.

Extracellular microbial substances (EPSs) are substances of biological origin that contribute to the formation of microbial aggregates: biofilms. In the case of cementitious materials, the active principles of these substances can be used in two ways: either as mass products incorporated in the formulation (admixture) or in the case of curative action (coating, painting, spray, *etc.*).

The action of extracellular microbial substances depends on the type of microorganism from which they are derived, the incorporation technique and the amount of product used. The various examples cited in this chapter illustrate the effects of such additions of products as an admixture on the setting of the cement, its rheology in the fresh state and its mechanical characteristics in the hardened state.

Other physicochemical parameters of the cement materials are also sensitive to the EPS: the capillary properties of the porous network of cement pastes

(CEM I and CEM V) are modified, although there are no notable results for mortars (CEM I and CEM V) due to the presence of sand which modifies the mean scale of the pore size constituting the porosity. Concerning the curative action of the EPS, the precipitation of minerals in the cracks can allow the "healing" of the concrete in order to limit its permeability and to increase resistance to carbonation. Treatments are therefore possible after construction of concrete structures with eco-friendly products, biocompatible with the environment.

The development of biosourced products, in particular made from microbial EPSs, should make it possible to offer a genuinely satisfactory alternative, since they are eco-friendly and safe products for humans. They can considerably improve the durability of concrete structures by giving them special characteristics, including resistance to biocontamination.

## References

[1] Guillitte O. (1995) "Bioreceptivity: A new concept for building ecology studies." Science of the Total Environment, 167, 215-220.

[2] Flemming H.-C., Wingender J. (2010) "The biofilm matrix." Nat. Rev. Microbiol., 8, 623-633.

[3] Van Leeuwen S.S. (2007) "Structural analysis of in vitro produced microbial alpha-D-glucans. Biopolymers synthesised from sucrose by using native and engineered *Lactobacillus reuteri* glucansucrase enzymes." phD thesis, university of Groningen, Groningen, The Netherlands.

[4] Roux S. *et al.* (2011) "Comment améliorer la durabilité de bétons plus éco-respectueux grâce à des polymères bactériens ?." Mat. & Tech., 99, 573-580.

[5] Miqyass M. *et al.* (2008) "Does Exopolysaccharides (EPS) protect steel against corrosion?." COST33 WG3, Obernai, France, May 12-16 2008.

[6] U.E. (2006) Règlement (CE) n° 1907/2006 du 18 décembre 2006 concernant l'enregistrement, l'évaluation et l'autorisation des substances chimiques, ainsi que les restrictions applicables à ces substances (REACH).

[7] Chambers L.D. *et al.* (2006) "Modern approaches to marine antifouling coatings." Surface and Coatings Technology, 201, 3642-3652.

[8] Khayat K.H., Guizani Z. (1997) "Use of viscosity-modifying admixture to enhance stability of concrete." American Concrete Institute Materials Journal, 94, 332-340.

[9] Kahng G.G. *et al.* (2001) "Production of extracellular polysaccharide, EPS WN9, from *Paenibacillus* sp. WN9 KCTC 8951P and its usefulness as a cement mortar admixture." Biotechnology and Bioprocess Engineering, 6, 112-116.

[10] Ghio V.A. *et al.* (1994) "The rheology of fresh cement paste containing polysaccharide gums." Cement and Concrete Research, 24, 243-249.

[11] He H. *et al.* (2013) "Ouvrabilité et performances mécaniques de mortiers contenant un bioadjuvant à base de substances extra-cellulaires." Matériaux & Techniques, 101, 105.

[12] SEPOLBE: Substances Extra-cellulaires POur Les BEtons, http://www.agence-nationale-recherche.fr/,Projet=ANR-12-CDII-0004.
[13] He H. *et al.* (2014) "Workability Tests on Fresh Concrete Formulated with Eco-friendly Admixture." Journal of Civil Engineering and Architecture, 8, 315-321.
[14] Ghosh P. *et al.* (2005) "Use of microorganism to improve the strength of cement mortar." Cem. Concr. Res., 35, 1980-1983.
[15] Ramachandran S.K. *et al.* (2001) "Remediation of concrete using microorganisms." American Concrete Institute Materials Journal, 98, 3-9.
[16] He H. *et al.* (2014) "Influence of a bioadmixture on the mechanical properties of mortars and on the surface roughness of cement pastes." 32es Rencontres de l'AUGC, Orléans, France, June 04-06 2014.
[17] Ollivier J.-P., Torrenti J.-M. (2008) "La structure poreuse des bétons et les propriétés de transfert." In: La durabilité des bétons - Bases scientifiques pour la formulation de bétons durables dans leur environnement". Ollivier J.-P. and Vichot A. Eds, Presses de l'Ecole Nationale des Ponts et Chaussées, Paris, France, IBSN 978-2-85978-434-8, Paris (France), 51-133.
[18] He H. (2015) "Analyse de l'effet d'un adjuvant biosourcé pour élaborer des matériaux cimentaires plus éco-respectueux." PhD thesis, université Louis Pasteur, Strasbourg, France.
[19] Wiktor V., Jonkers H.M. (2013) "Bio-réparation des matériaux cimentaires : les bactéries au service des mortiers fissurés." Mat. & Tech., 101, 401.
[20] Wiktor V., Jonkers H.M. (2011) "Quantification of crack-healing in novel bacteria-based self-healing concrete." Cem. Concr. Comp., 33, 763-770.
[21] De Muynck W. *et al.* (2008) "Bacterial carbonate precipitation as an alternative surface treatment for concrete." Construction and Building Materials, 22, 875-885.
[22] Roux S. *et al.* (2009) "Impact of biofilm on concrete: degradation or protection ?." EUROCORR, Nice, France, September 06-10 2009.

# INTERACTIONS MATERIALS – MICROORGANISMS

## Concretes and Metals more Resistant to Biodeterioration

*Christine Lors, Françoise Feugeas, Bernard Tribollet*

This multidisciplinary book is the result of a collective work synthesizing presentations made by various specialists during the CNRS «BIODEMAT» school, which took place in October 2014 in La Rochelle (France). It is designed for readers of a range of scientific specialties (chemistry, biology, physics, etc.) and examines various industrial problems (e.g., water, sewerage and maintaining building materials).

Metallic, cementitious, polymeric and composite materials age depending on their service and operational environments. In such cases, the presence of microorganisms can lead to biodeterioration. However, microorganisms can also help protect structures, provided their immense possibilities are mastered and put to good use.

This book is divided into five themes related to biocolonization, material biodeterioration, and potential improvements to such materials resulting in better performance levels with respect to biodeterioration:

- physical chemistry of surfaces;
- biofilm implication in biodeterioration;
- biocorrosion of metallic materials;
- biodeterioration of non-metallic materials;
- design and modification of materials.

The affiliations of the authors of the various chapters illustrate the synergy between academic research and its transfer to industry. This demonstrates the essential interaction between the various actors in this complex field: analysing, understanding, and responding to the scientific issues related to biodeterioration.

***Christine LORS**, Professor of Institut Mines Télécom, in charge of research dealing with the interactions between microorganisms and materials in Civil & Environmental Engineering Department of IMT Lille Douai.*

***Françoise FEUGEAS**, Professor at INSA Strasbourg teaches material sciences. She co-heads the Civil and Energy Engineering team at the ICube laboratory in Strasbourg.*

***Bernard TRIBOLLET,** emeritus Director of research at the Interfaces and Electrochemical Systems Laboratory.*

ISBN: 978-2-7598-2200-3 / 75 € TTC
www.edpsciences.org

9 782759 822003

edp sciences

**materials** | biology